RECEIVED
By Docket Room at 2:09 pm, May 15, 2023

UNITED STATES OF AMERICA

DEPARTMENT OF ENERGY

OFFICE OF FOSSIL ENERGY

IN THE MATTER OF	)	
	)	
Alaska LNG Project LLC	)	FE DOCKET NO. 14-96-LNG

REQUEST FOR REHEARING OF ORDER GRANTING AUTHORIZATION OF THE ALASKA LNG PROJECT

Pursuant to Section 19(a) of the Natural Gas Act, 15 U.S.C. § 717r(a), and 10 C.F.R. § 590.501, the Center for Biological Diversity, Cook Inletkeeper, and Sierra Club (Intervenors) hereby request rehearing of the U.S. Department of Energy (DOE or "the Department"), Office of Fossil Energy and Carbon Management's Order Affirming and Amending DOE/FE Order No. 3643-A Following Partial Grant of Rehearing (Order or "Order 3643-C"), DOE/FECM Order No. 3643-C, issued on April 13, 2023, in the above-captioned matter.

Intervenors ask that this order be withdrawn and the underlying application denied, or in the alternative, that the order be withdrawn pending further inquiry and public process regarding the impact of the proposed exports.

DOE granted the Intervenors' respective motions to intervene in these dockets.[1] As such, each Intervenor is a "party" to this proceeding with standing to file this request for rehearing.[2] This request for rehearing is timely, having been filed within 30 days of DOE's Order.[3]

---

[1] Order 3643-C at 21 (granting intervention for Center for Biological Diversity and Cook Inletkeeper); DOE/FE Order No. 3643 at 27 (May 28, 2015) (granting intervention for Sierra Club).
[2] 10 C.F.R. § 590.102(l).
[3] *Id.* § 590.501(a).

Intervenors include citations and other information in footnotes only to enhance the presentation to the reader. Intervenors do not waive any rights with respect to footnotes, and ask that DOE consider all the text of this request equally regardless of whether it appears in a footnote or the body of the request.

STATEMENT OF ERRORS

DOE should withdraw its Order because of the following errors in the Order and final supplemental environmental impact statement (FSEIS) upon which it relies:

I. DOE's determination that the Project's exports are consistent with the public interest was arbitrary and capricious, and violated the Natural Gas Act, because:

A. There is no demonstrated global market need for the Project's exports.

B. DOE ignored the same alleged uncertainties inherent in the Project's benefits. that it used to justify discounting the Project's climate harms.

C. DOE ignored the Project's definite and certain harms.

D. DOE overstated the degree of uncertainty about adverse impacts to the climate.

E. DOE cannot ignore the Project's adverse climate impacts even if the Project substitutes for foreign fossil fuels.

II. DOE's Order rests on an FSEIS that does not comply with the National Environmental Policy Act (NEPA), because:

A. The purpose and need statement does not comply with NEPA.

B. The FSEIS lacks a true no action alternative.

C. The FSEIS does not comply with NEPA regulations regarding missing information.

D. The FSEIS makes unsupported assumptions about byproduct carbon dioxide (CO_2) injection.

E. The FSEIS does not adequately address impacts from proposed carbon storage on the North Slope.

F. The FSEIS does not adequately address methane leakage from the Project.

G. The FSEIS's analysis of overseas impacts is inadequate.

ARGUMENT

I. DOE'S DETERMINATION THAT THE PROJECT'S EXPORTS ARE CONSISTENT WITH THE PUBLIC INTEREST WAS ARBITRARY AND CAPRICIOUS AND VIOLATED THE NATURAL GAS ACT.

Although DOE is required to balance the Alaska LNG Project's ("the Project") costs and benefits against each other to determine whether its liquefied natural gas (LNG) exports are consistent with the public interest, here it has irrationally used the existence of some uncertainty to refuse to meaningfully consider the Project's environmental harms, while effectively giving full weight to the Project's equally-if-not-more uncertain benefits. As a result, its public interest determination is unjustifiably one-sided and amounts to an abdication of DOE's responsibility under the Natural Gas Act.

Numerous problems in DOE's analysis render its public interest determination imbalanced and arbitrary. DOE's analysis of the benefits of the Project ignores the lack of any real market need for additional LNG exports. The LNG export capacity that has already, and will likely, come online before the Project is complete far exceeds the projected global need. DOE tries to have it both ways when it comes to the impact of uncertainties in the LNG market, dismissing climate impacts as unknowable (a position belied by the record) while assuming benefits that are entirely speculative.

Likewise, DOE inappropriately ignores or discounts demonstrable environmental harms that will result from additional gas production on the North Slope—one of the two major reasons

DOE ordered the preparation of a supplemental environmental impact statement. DOE vastly overstates the uncertainties associated with estimating the potential climate impacts from the Project's greenhouse gas emissions. Even if some portion of the Project's output would simply substitute for foreign fossil fuels, DOE still has a duty to consider the greenhouse gas (GHG) impacts from this Project. In short, DOE's approach to evaluating whether the Project's exports would be inconsistent with the public interest is incomplete, incorrect, and biased, and fails entirely to satisfy DOE's legal obligations under the Natural Gas Act.

A. There Is No Demonstrated Global Market Need for the Project's Exports.

The record fails to establish that there will be any real need for the additional exports that the Project will produce if or when it comes online, because DOE already has approved a far greater volume of exports than is needed to cover the projections for international LNG demand through 2050. According to the Energy Information Administration's (EIA) latest predictions, under a high oil price scenario, LNG exports volumes are expected to remain below 15 trillion cubic feet per year by 2050.[4] Under the low oil price scenario, that number is expected to remain closer to the current level of 4 trillion cubic feet.[5] EIA's reference point for LNG export demand in 2050 is 10 trillion cubic feet.[6]

Even those numbers, however, may be high, as one of the big sources of current demand—Europe's need for gas in the wake of Russia's invasion of Ukraine—will likely rapidly diminish. Russia's war in Ukraine has hastened European countries' roll-out of renewables and

[4] EIA, *Annual Energy Outlook 2023*, Fig. 17 (Mar. 16, 2023) (Annual Energy Outlook 2023), https://www.eia.gov/outlooks/aeo/narrative/index.php#InternationalDemandfor.
[5] *Id.*
[6] *Id.*

low-emitting technologies, and the overall demand for gas in Europe fell by 13 percent in 2022.[7] Indeed, the Institute for Energy Economics and Financial Analysis (IEEFA) recently cautioned that, after 2023, "LNG demand is set to decline across Europe."[8] The pace of that decline is likely to only increase as the European Union aims for 45 percent renewable energy by 2030.[9]

The Project's gas exports would likely not go to address any national security needs associated with supporting Ukraine, and are rather destined for four countries—Japan, South Korea, India, and China[10]—all of which have announced plans to expand their renewable energy usage. As DOE recognizes, by 2030, the earliest the Project could come online, Japan is aiming to increase its renewable share to 13 percent;[11] South Korea is aiming to increase its renewable share to 20 percent, with another 30-35 percent by 2040;[12] and India plans to meet 50 percent of its electricity requirements with renewables.[13] China has even earlier goals to account for "40 [percent] of the global growth of renewable capacity between 2019 and 2024."[14] DOE further recognizes that the recommendations in the International Energy Agency's (IEA) "Net Zero by 2050" report will likely be implemented.[15] That report explains that further expansion of global

[7] IEA, *Europe's energy crisis: What factors drove the record fall in natural gas demand in 2022?* (Mar. 14, 2023), https://www.iea.org/commentaries/europe-s-energy-crisis-what-factors-drove-the-record-fall-in-natural-gas-demand-in-2022.
[8] IEEFA, *Over half of Europe's LNG infrastructure assets could be left unused by 2030* (Mar. 21, 2023), https://ieefa.org/articles/over-half-europes-lng-infrastructure-assets-could-be-left-unused-2030.
[9] N. Ferris, *Why LNG's current boom will only accelerate its ultimate demise*, ENERGY MONITOR (Apr. 6, 2023) (Ferris 2023), https://www.energymonitor.ai/sectors/industry/why-lng-market-current-boom-will-only-accelerate-its-ultimate-demise/.
[10] Amended Record of Decision, Order C3643-C at 45.
[11] FSEIS, App. C at 13; IEA, *Japan 2021: Energy Policy Review* (2021), https://www.iea.org/reports/japan-2021.
[12] FSEIS, App. C at 13; IEA, *Korea 2020: Energy Policy Review* (2020), https://www.iea.org/reports/korea-2020.
[13] FSEIS, App. C at 14.
[14] *Id.*
[15] *Id.* at 11-12.

LNG exports and construction of additional LNG export infrastructure cannot be part of the path to net-zero emissions.[16]

Although LNG demand is likely to decline, both globally and in the countries likely to receive exports from the Project, prior to approving the Project, DOE had already authorized more exports to non-free trade countries than the high end of EIA's predicted demand range. The 17.3 trillion cubic feet of LNG exports per year DOE previously approved, which does not include exports to free trade countries or exports from small-scale facilities,[17] is approximately 2 trillion cubic feet per year more export capacity than the maximum level the EIA estimates will be in demand by 2050.[18] Although there is no guarantee that all of that capacity will come online, facilities accounting for 24.19 billion cubic feet per day, or approximately 8.83 trillion cubic feet per year, are currently operating or under construction.[19] That is more than twice the low end of EIA's estimated demand for LNG.[20] There is no evidence to suggest that all of the remaining capacity will fail to come online. If even a relatively small fraction of it does come online, the amount of export DOE will have allowed, even without counting the Project, will easily exceed EIA's reference case levels by trillions of cubic feet per year. Simply put, global realities demonstrate that DOE has authorized more LNG exports than are needed.

Tellingly, the Alaska Gasline Development Corporation's (AGDC) own analysis does not dispute any of the above. Indeed, it confirms that at least a significant portion of the exports from the Project will add to the problem of an over-saturated global market for LNG exports. AGDC's

---

[16] IEA, *Net Zero by 2050: A Roadmap for the Global Energy Sector* at 102 (May 2021) (IEA 2021), https://www.iea.org/reports/net-zero-by-2050.
[17] 88 Fed. Reg. 25,272, 25,274 (Apr. 26, 2023).
[18] *Id.*; Annual Energy Outlook 2023, Fig. 17.
[19] 88 Fed. Reg. at 25,274.
[20] Annual Energy Outlook 2023, Fig. 17.

modeling indicates that, if built, two-thirds of the Project's LNG would add to U.S. export capacity without displacing any other U.S. exports.[21] And although that same modeling seeks to portray the Project's exports as having net-positive economic and other impacts, it assumes total volumes of global LNG exports that are exponentially lower than the amount that is now being produced and that will be produced by terminals that are under construction.[22] Thus, AGDC's analysis does not grapple with the over-supply problem or support the conclusion that the Project's exports are needed when added to the over-supplied market that already exists and certainly will exist when the Project comes online eight years from now.

DOE maintains as a matter of policy that it does not need to find there is a market need for a project's exports to approve them, and that it will let the market, rather than DOE, decide which projects will move forward.[23] However, this is an inappropriate and unlawful abdication of DOE's role under the Natural Gas Act and causes real harm. As DOE itself has acknowledged, when export authorizations get approved but never acted on, it creates an "authorization overhang," which creates a variety of problems with the LNG market.[24] The "overhang obscures an accurate picture of investment-backed commitments involving U.S. LNG," and creates uncertainty that "has become increasingly disruptive to DOE's planning, economic forecasting, and market analysis of the U.S. LNG export market."[25] Further, the

---

[21] AGDC, Application of Alaska LNG Project LLC For Long-Term Authorization to Export Liquefied Natural Gas, App. F: NERA Economic Consulting, Socio-Economic Impact Analysis of Alaska LNG Project at 42 (Jul. 18, 2014) (NFTA Application, App. F) ("As a result of Alaska developing the [North Slope] and exporting 0.93 [trillion cubic feet (Tcf)] of natural gas per year after 2025, total U.S. exports of LNG are approximately 0.6 Tcf higher than in the Baseline.").
[22] *Id.* at 25, Fig. 15 (assuming 1.14 trillion cubic feet by 2048 in its "U.S. LNG Exports—Baseline" and 1.72 trillion cubic feet in its "U.S. LNG Exports—Expected" scenarios).
[23] Order 3643-C at 22 & n.106.
[24] 88 Fed. Reg. at 25,276-77.
[25] *Id.* at 25,277.

overhang causes uncertainty for U.S. trading partners receiving LNG and "may serve to discourage or delay potential new entrants to the U.S. export market—including those that seek to utilize newer technology and to adopt better environmental practices."[26] Though DOE has recently adopted a policy statement to create greater clarity around the ability of approved exporters to extend the life of their DOE export authorizations,[27] the Department arbitrarily refuses to recognize that it should be evaluating applications at the outset to determine if there is a real market need for their export capacity. It simply makes no sense for DOE to acknowledge on the one hand that it has a role to play in preventing the creation of an overly-large export overhang by limiting the availability of extensions of authorizations but denying on the other that it has any role to play in refusing to grant unviable projects export authorizations from the start. Such an approach does not serve the public interest or address any of the market problems DOE seeks to address in its recent policy statement.

Moreover, DOE's refusal to engage in a meaningful inquiry on whether a project's exports are needed and for how long risks causing harms to the environment and communities that are not merely avoidable, but indeed, may be entirely unnecessary. First, while major component parts of unviable projects may never be constructed, DOE's approval sends a powerful signal that may induce construction of supporting infrastructure that causes unnecessary harms. The sheer scope and scale of the infrastructure needed across Alaska to make the Project possible should present a cautionary tale to DOE. Even before the terminal itself is built, countless other impacts—tree felling and wetland conversion for gathering lines, for example—may occur in anticipation of a project that DOE approved, but that will never actually

[26] *Id.*
[27] *Id.* at 25,276-78.

happen. Second, an LNG terminal that is built and then sits un- or under-used, or shuts down well before the end of its useful life, causes extensive harm associated with project construction, while failing to provide any of the purported benefits. As is clear from the glut of import terminals that were built in the 2000s, only to sit idle, markets cannot be blindly trusted to ensure that projects are only actually constructed when there is a need for them.

DOE bears an important responsibility to make decisions that are consistent with the public interest, which includes the responsibility to ensure that its decision is consistent with its obligation to advance environmental justice. The President's Executive Order 14096 on Revitalizing Our Nation's Commitment to Environmental Justice for All mandates that DOE, among other things, "take steps to address disproportionate and adverse human health and environmental effects (including risks) and hazards unrelated to Federal activities, including those related to climate change and cumulative impacts of environmental and other burdens on communities with environmental justice concerns."[28] Although the Federal Energy Regulatory Commission (FERC) bears the primary responsibility for evaluating the effects of the terminals themselves, in deciding whether to approve export infrastructure, FERC consistently argues that need and market demand are demonstrated by DOE's approvals. While it is inappropriate for FERC to defer to decisions DOE has not actually made, DOE has culpably failed to correct FERC on this, and/or failed to actually make a need determination sufficient to inform FERC's decisionmaking on whether construction of LNG infrastructure would be in the public interest. To turn a blind eye to the potential that DOE's approval of exports from an unneeded source would spur construction of a series of massive pieces of infrastructure that will cause significant

[28] *Id.* at 25,253.

harm to the surrounding community and environment amounts to a dereliction of DOE's duty, including the duty to achieve environmental justice as part of its mission.

B. DOE Ignored the Same Alleged Uncertainties Inherent in the Project's Benefits that It Used to Justify Discounting the Project's Climate Harms.

DOE impermissibly employed a highly skewed approach to its public interest balancing test by ignoring that the same uncertainties that caused the Department to refuse to weigh climate impacts apply with equal force and effect to the alleged benefits of the Project's exports.[29] As is discussed in more detail in the following section, DOE is wrong that there is sufficient uncertainty to warrant refusing to seriously weigh the Project's climate impacts. But even if the Department is correct, it cannot arbitrarily use uncertainties about Project costs to dismiss them and then ignore the same uncertainties as they apply to the Project's benefits.

The Department irrationally concluded that, as a result of "substantial uncertainty regarding the magnitude of [the Project's] environmental impacts, particularly GHG emissions and climate impacts. . . . DOE has determined that it cannot draw a definitive conclusion about the magnitude of climate impacts associated with the Project's exports."[30] But DOE's basis for claiming that the climate impacts of the Project were uncertain are that the Department did not know whether the Project's exports would occur, or if they did, how much these exports would lead to increased fossil fuel consumption, rather than merely substituting for LNG exports from the Lower 48 states that would otherwise occur, or for use of foreign fossil fuels.[31]

---

[29] *See* Order 3643-C at 25 (finding there are "compelling public benefits associated with Alaska LNG's exports," and purporting to "weigh[] the acknowledged but highly uncertain climate impacts against the economic and international security benefits of Alaska LNG's approved exports.").
[30] *Id.* at 22.
[31] *Id.* at 22-23 7 n.106.

These same uncertainties apply with equal force to the purported benefits of the Project's exports.[32] In discussing purported benefits, DOE principally relies on economic benefits.[33] Yet, uncertainty about whether the Project will ever actually export LNG, and if so, whether those exports will merely displace LNG exports that would have been produced elsewhere, has just as much impact on whether the Project results in economic benefits as it does climate costs. If the Project does not actually export gas, or insofar as those exports merely substitute for Lower 48 exports that would otherwise occur, the Project provides no "national economic benefits" or increase in "gross domestic product."[34] There is nothing in the record that demonstrates that any economic benefit will result from a project that is never actualized, and DOE has not offered any argument or explanation as to how shifting exports from the Gulf Coast to Alaska, without any net increase in U.S. LNG exports, would benefit the national economy. Similarly, if the Project's exports substitute for Gulf Coast exports, this would provide local and regional economic stimulus in Alaska, but at the cost of comparable local and regional stimulus in the Lower 48.[35]

Beyond economic benefits, DOE asserts that the Project will improve "energy security" for "U.S. allies and trading partners."[36] Again, this purported benefit will only occur if the Project increases U.S. exports, rather than substituting for other U.S. exports that would otherwise occur.

Thus, employing DOE's own logic, the purported benefits of the Project are at least as uncertain as the climate impacts. Moreover, both are correlated with the net increase in U.S.

---

[32] *See* Sierra Club *et al.*, Comments on the Draft Supplemental Environmental Impact Statement for the Alaska LNG Project at 10-11 (Aug. 15, 2022) (DSEIS Comments).
[33] Order 3643-C at 25.
[34] *Id.* (citing Order 3643-A at 30-31).
[35] DSEIS Comments at 10-11.
[36] Order 3643-C at 25.

export volumes; benefits and climate impact will rise and fall together. If the lack of certainty around the Project's fate and the extent to which its exports might substitute exports from elsewhere in the United States was a sufficiently good reason for not being able to weigh climate costs, it is an equally good—if not arguably more compelling—reason to not be able to weigh economic and national security benefits. That DOE failed to apply the same treatment to both sides of its public interest weighing exercise was arbitrary and capricious.

C. DOE Ignored the Alaska LNG Project's Definite and Significant Harms.

Even if there is some uncertainty associated with the magnitude of the Project's climate impacts—which DOE greatly overstates—it is undeniable that the Project, if constructed, will cause significant environmental harm that DOE failed to appropriately evaluate or weigh in its public interest determination. In particular, the Order acknowledges that the FSEIS found that some upstream development impacts of the Project on the North Slope would be significant, including cumulative impacts on permafrost degradation[37] and cumulative impacts from the permanent loss of wetlands,[38] but then effectively dismisses these impacts. With little discussion or analysis, the Order assumes that mitigation conditions,, which are not incorporated into the Order and also may not be incorporated as binding conditions in the Project's other permits, will reduce the wetland and permafrost impacts to an unspecified degree.[39] Even if these mitigation measures were binding on the Project, the record before DOE does not provide any assurance that they will be effective, let alone effective enough to entirely eliminate the harm. Without more in the record, it is inappropriate for DOE to effectively treat the environmental harms that North Slope development will cause as non-existent.

---

[37] Order 3643-C at 14 (citing FSEIS at 4.20-10).
[38] *Id.* at 14-15 (citing FSEIS at 4.20-11).
[39] *Id*.

Even more disturbingly, the Order acknowledges that the Project will have a "disproportionately high and adverse impacts on environmental justice communities, primarily due to potential for impacts to subsistence users of the Kaktovik and Nuiqsut communities,"[40] but summarily concludes that those impacts do not matter, because subsistence users will simply move their activities elsewhere.[41] As is discussed above, DOE is bound by President Biden's Executive Order 14096, which "makes clear that the pursuit of environmental justice is a duty of all executive branch agencies."[42] The Executive Order specifically provides that the Federal government "must recognize, honor, and respect the different cultural practices—including subsistence practices, ways of living, Indigenous Knowledge, and traditions—in communities across America,"[43] a requirement that is utterly contrary to DOE's assumption that the environmental justice community harmed by the Project simply must adapt.

In addition, despite the impacts to the North Slope being one of the two categories of impacts DOE determined required more extensive review when it ordered the FSEIS,[44] DOE does not clearly take these certain North Slope impacts into account in its final public interest determination and ignores additional harms the Department knows will occur if the Project moves forward. The Order merely states that "[i]n weighing the acknowledged but highly uncertain climate impacts against the economic and international security benefits of the Project's approved exports, DOE concludes that the information developed on rehearing does not

---

[40] *Id.* (citing FSEIS at 4.20-11; *id.,* Tbl. S-4 at S-19 to S-20).
[41] *Id.*
[42] The White House, Fact Sheet: President Biden Signs Executive Order to Revitalize Our Nation's Commitment to Environmental Justice for All (Apr. 21, 2023), https://www.whitehouse.gov/briefing-room/statements-releases/2023/04/21/fact-sheet-president-biden-signs-executive-order-to-revitalize-our-nations-commitment-to-environmental-justice-for-all/.
[43] 88 Fed. Reg. at 25,252.
[44] Order 3643-C at 3-4 (citing Order 3643-B).

present a sufficient basis to reach a different conclusion than previously reached."[45] It says nothing about the clear North Slope impacts discussed in the FSEIS or the additional harms already acknowledged in the original EIS, including the 800-mile pipeline bisecting Alaska and adjacent to Denali National Park[46]; the 10,000 acres of impacted wetlands, 8,000 of them permanently;[47] the significant adverse effects on permafrost, wetlands, forests, and caribou; and the potentially significant impacts on the air quality and visibility at several national parks, preserves, and refuges.[48] Mitigation of the impacts to permafrost and wetlands will not reduce those impacts to zero and forcing indigenous hunters to relocate is not a harm-free proposition; and yet the Order effectively treats both sets of impacts as if they did not exist.

There is no question that the definite environmental and community harms that will occur in Alaska from North Slope development will occur as a result of DOE's approval of the exports from the Project and would not occur if LNG production occurred elsewhere in the world. The record does not support a finding that the Project's exports could proceed without DOE's non-free trade agreement (FTA) export approval—no large-scale export project has moved forward solely on the basis of an FTA authorization—and DOE's own order concludes that the gas from the Project is destined for four non-FTA countries: Japan, China, South Korea, and India.[49] Further, DOE has concluded that it is unlikely that another project to export gas from the North

[45] *Id.* at 25.
[46] FSEIS at 1-2, Fig. 1.1-1.
[47] FERC, Order Granting Authorization Under Section 3 of the Natural Gas Act at 35-36, ¶84, 171 FERC ¶ 61,134 (May 21, 2020).
[48] *Id.* at 14, ¶25; *id. at* 57, ¶160; *id.* at 71-73, ¶¶206-08.
[49] Amended Record of Decision, Order 3643-C at 45.

Slope would be constructed if the proposed Project does not move forward.[50] The Department's failure to include these impacts in its public interest determination, therefore, is without justification. Even worse, as is discussed above in Section I.A., because DOE continues to take a laissez-faire approach to its reviews by refusing to take a position "on whether there will, in fact, be market demand for the approved exports,"[51] DOE's authorization of the Project creates a real danger that the North Slope and other infrastructure will be constructed—causing significant environmental harm—but that exports and their purported benefits will never happen. That fact is nowhere acknowledged in DOE's Order and further demonstrates that the Department's conclusion that the exports from the Project are in the public interest is arbitrary and capricious.

D. DOE Overstated the Degree of Uncertainty About Adverse Impacts to the Climate.

DOE discounts the Project's adverse impacts to the climate as highly uncertain but fails to justify its inability to produce any meaningful estimate of those impacts between the best and worst case scenarios, or to reconcile the claim of uncertainty with the Department's reliance on modeled benefits that depend on DOE endorsing more concrete assumptions.

DOE's greenhouse gas analysis purports to address two extreme scenarios: one in which *all* of the Project's exports merely substitute for other gas (a comparison between the Project scenarios and No Action Alternative 1), and one in which *no* substitution occurs, such that the Project's exports are entirely additive (a comparison between the Project scenarios and No

---

[50] *Id.* at 34 ("Concerning the No Action Alternative, DOE reevaluated this conclusion in the Final SEIS and instead determined that, if the Project were not constructed, it is unlikely that another project would be constructed to export natural gas from the North Slope as LNG."); *see also* FSEIS at 2-23 ("The commercial prospects of an alternative project to the Alaska LNG Project are unclear. North Slope natural gas is challenged by the remote location of the gas supply and high estimated cost of bringing the gas to market. . . . [I]f the Alaska LNG Project was not constructed, DOE considers it unlikely that an alternative LNG export project would be constructed to access natural gas reserves on the North Slope in the foreseeable future.").
[51] Order 3643-C at 22, fn. 106 (citing FSEIS at S-7).

Action Alternative 2).[52] DOE suggests that these extremes represent the Project's least possible and greatest possible adverse impacts on the climate, respectively. If No Action Alternative 1 were accurate, DOE estimates there would be no adverse impact on or even a net benefit to the climate.[53] If No Action Alternative 2 were accurate, on the other hand, the climate impacts would be dramatic and adverse, adding between 1,500 and nearly 2,000 MMmt GHGs to the atmosphere.[54] DOE acknowledges that both scenarios are "unlikely,"[55] and therefore the Project's true impacts likely fall somewhere in the middle. However, DOE maintains there is such significant uncertainty about the future of the energy market that the Department is "unable to conclude that either [scenario] . . . is more accurate."[56] This leads DOE to characterize the Project's climate impacts as "highly uncertain," in contrast to the Project's purported benefits.[57]

DOE can do better than merely identify these two extremes and state that the truth is somewhere in the middle. Modeling submitted by the applicant predicts *where* in the middle impacts would likely fall. Specifically, National Economic Research Associates (NERA) predicted that roughly two thirds of Project exports would constitute a net increase in U.S. LNG export totals, and that the remaining third would displace Lower 48 exports.[58] Intervenors submitted comments on the draft supplemental environmental impact statement (DSEIS) pointing out that this modeling could be used to more accurately estimate the Project's GHG

---

[52] *Id.* at 23–24.
[53] *Id.* at 23.
[54] FSEIS at S-9, Tbl. S-2.
[55] Order 3643-C at 24.
[56] Amended Record of Decision, Order 3643-C at 41.
[57] Order 3643-C at 25.
[58] NFTA Application, App. F at 42("As a result of Alaska developing the [North Slope] and exporting 0.93 Tcf of natural gas per year after 2025, total U.S. exports of LNG are approximately 0.6 Tcf higher than in the Baseline.").

emissions.[59] And indeed, DOE has relied on other NERA modeling, using the same tools and methodology, to analyze the macroeconomic impacts of exports from the Lower 48.[60] Yet, DOE failed to explain why this modeling could not offer a more realistic picture of the Project's impacts.

Despite claiming that it cannot conclude either no action alternative is more accurate,[61] DOE states inconsistently, and without any apparent support, that "in DOE's judgment the GHG emissions and related climate impacts associated with Alaska LNG's exports—at the very least, those in the near to medium years of the approximately 33-year export period—are likely to be closer to the difference between No Action Alternative 1 and the Project scenarios."[62] In other words, despite the fact that the FSEIS provides no basis for selecting either extreme, or any point in between, DOE vaguely asserts that the Project's impacts will be closer to the best case scenario than the worst from a climate perspective. This blindly optimistic statement further undercuts DOE's weighing of climate impacts. It is inconsistent with the NERA modeling which predicts more than half the Project's exports would represent a net increase in U.S. LNG exports. And, it endorses without explanation a scenario that is closer to perfect substitution, which courts have rejected as economically unsound.[63]

E. DOE Cannot Ignore the Project's Adverse Climate Impacts Even if the Project Substitutes for Foreign Fossil Fuels.

As the example of the NERA modeling shows, DOE has tools to estimate the extent to which the Project's gas will substitute for other U.S. LNG; even if DOE were to conclude it is

[59] *See* DSEIS Comments at 7-8.
[60] *See, e.g.,* DOE, Office of Fossil Energy, Order and Opinion, *Epcilon LNG, LLC*, DOE/FE Order No. 4629, FE Dkt. No. 20-31-LNG (Dec. 8, 2020), https://www.energy.gov/sites/prod/files/2020/12/f81/ord4629.pdf.
[61] Amended Record of Decision, Order 3643-C at 41.
[62] Order 3643-C at 24-25.
[63] DSEIS Comments at 8-10.

more likely that the Project's gas would instead substitute for foreign fossil fuels, however, the Department could not end its analysis of climate impacts there. DOE would need to account for current global energy trends that increasingly emphasize renewable energy[64] and, especially in Europe, reduce reliance on fossil fuels.[65] And, as with domestic gas, DOE could not assume perfect substitution.

Nor could DOE ignore the Project's substantial direct and upstream GHG emissions that would occur on U.S. soil. These emissions will hinder the ability of the U.S. to attain the Administration's stated emission targets and to comply with international commitments. If the Project substitutes for foreign fossil fuels, then the gas exported would come from what is, from a domestic perspective, new gas production, thereby increasing the U.S.'s domestic GHG emissions at a time when the Administration has committed to achieving a net zero emissions economy by 2050[66] and to reducing GHG emissions to 50–52 percent below 2005 levels by 2030.[67] The U.S. has also made commitments to reduce its territorial GHG emissions under the

[64] FSEIS, App. C at 10-11.
[65] Ferris 2023; K. Abnet, *EU strikes deal to curb energy use by 2030*, REUTERS (Mar. 10, 2023), https://www.reuters.com/business/energy/eu-reaches-agreement-to-reduce-energy-consumption-eu-level-by-117-2030-2023-03-10/; S. Petrequin, *EU climate czar: Putin's war accelerated green transition*, AP NEWS (Feb. 21, 2023), https://apnews.com/article/russia-ukraine-putin-politics-european-union-europe-b38199c0e8410df19274be163906b36f.
[66] The White House, *FACT SHEET: President Biden to Catalyze Global Climate Action through the Major Economies Forum on Energy and Climate* (Apr. 20, 2023), https://www.whitehouse.gov/briefing-room/statements-releases/2023/04/20/fact-sheet-president-biden-to-catalyze-global-climate-action-through-the-major-economies-forum-on-energy-and-climate/
[67] *Id.*; The White House, *FACT SHEET: President Biden Sets 2030 Greenhouse Gas Pollution Reduction Target Aimed at Creating Good-Paying Union Jobs and Securing U.S. Leadership on Clean Energy Technologies* (Apr. 22, 2021), https://www.whitehouse.gov/briefing-room/statements-releases/2021/04/22/fact-sheet-president-biden-sets-2030-greenhouse-gas-pollution-reduction-target-aimed-at-creating-good-paying-union-jobs-and-securing-u-s-leadership-on-clean-energy-technologies/.

Paris and Copenhagen agreements.[68] Additionally, exporting fossil fuels for combustion in other countries is contrary to the goal of assisting other nations in reducing their own GHG emissions. In view of those commitments and international agreements, and in the midst of an undeniable climate crisis, the U.S. should not be enabling additional fossil fuel use or assuming, contrary to basic economic principles, that only demand-side actions will influence global energy use.

II. DOE'S ORDER RESTS ON AN FSEIS THAT DOES NOT COMPLY WITH NEPA.

A. The FSEIS's Purpose and Need Statement Does Not Comply with NEPA.

The FSEIS does not comply with NEPA because DOE adopts the Project applicant's characterization of the purpose and need instead of independently evaluating the Project's purpose in light of the Natural Gas Act.

The purpose and need statement in an EIS drives the selection of alternatives. It cannot be so narrow that only one alternative—the proposed action—will suffice.[69] Such a narrow purpose and need "prevent[s] an agency from considering alternatives that do not meet an applicant's stated goals, but better meet the policies and requirements set forth in NEPA and the agency's

[68] United Nations, Compilation of economy-wide emission reduction targets to be implemented by Parties included in Annex I to the Convention, Framework Convention on Climate Change (June 7, 2011), https://unfccc.int/resource/docs/2011/sb/eng/inf01r01.pdf; United Nations, Paris Agreement to the United Nations Framework Convention on Climate Change, Dec. 12, 2015, T.I.A.S. No 16-1104 (2015), https://unfccc.int/sites/default/files/english_paris_agreement.pdf.
[69] *See, e.g., Citizens Against Burlington, Inc. v. Busey*, 938 F.2d 190, 196 (D.C. Cir. 1991) ("[A]n agency may not define the objectives of its action in terms so unreasonably narrow that only one alternative from among the environmentally benign ones in the agency's power would accomplish the goals of the agency's action, and the EIS would become a foreordained formality.").

statutory authority and goals."[70] Agencies must consider such reasonable alternatives even if those alternatives are outside their jurisdiction.[71]

Here, the purpose and need statement is unlawful because it merely restates the applicant's objective and is crafted so narrowly that the only alternatives that could satisfy it are those with substantially similar components and environmental impacts.[72] As a result, DOE failed to consider reasonable alternatives that would provide similar benefits with different, and potentially less severe, environmental impacts. This approach is "inconsistent with fully informed decision making and sound environmental analysis,"[73] as well as the basic purposes of an EIS.[74]

In particular, the unlawfully narrow purpose and need prevented DOE from including a renewable energy alternative or seriously considering a no action alternative, either of which is far more likely to serve the public interest than the Project itself. For example, DOE rejected the no action alternatives because they did not meet the applicant's objective "to commercialize natural gas resources on the North Slope to bring LNG from Alaska to foreign markets and provide interconnections along the pipeline to allow for in-state gas deliveries."[75] DOE consequently did not adequately consider how authorizing a massive fossil fuel project can possibly be squared with the science that overwhelmingly shows that all Arctic fossil fuel

[70] 87 Fed. Reg. 23,453, 23,459 (Apr. 20, 2022).
[71] *See, e.g.*, *Natural Res. Def. Council v. Morton*, 458 F.2d 827, 834–36 (D.C. Cir. 1972) (holding that the agency's environmental impact statement violated NEPA because it failed to consider alternatives outside of the Department of the Interior's jurisdiction); *Sierra Club v. Lynn*, 502 F.2d 43, 62 (5th Cir. 1974) ("The agency must consider appropriate alternatives which may be outside its jurisdiction or control, and not limit its attention to just those it can provide… .") (citation omitted); 87 Fed. Reg. at 23,459.
[72] FSEIS at 1-7 to 1-8.
[73] 87 Fed. Reg. at 23,458.
[74] 40 C.F.R. § 1502.1.
[75] Amended Record of Decision, Order 3643-C at 38.

reserves must be classified as "unburnable"[76] and that "[a]ny further delay in concerted anticipatory global action on adaptation and mitigation will miss a brief and rapidly closing window of opportunity to secure a liveable and sustainable future for all."[77]

The question of whether a project is consistent with the public interest must be informed by knowledge of what alternatives exist that could serve the same broader policy aims of the Natural Gas Act, which extend far beyond a for-profit applicant's business purpose.[78] NEPA review does not exist in a silo from an agency's substantive decisionmaking under another statute; its purpose in this case is to ensure that DOE's decisionmaking under the Natural Gas Act is fully informed.[79] Unquestioningly adopting an applicant's objective as the purpose and need improperly excludes discussion of alternatives that would help inform the substantive decision the Natural Gas Act charges DOE with making, thereby undercutting NEPA's important informational role and turning environmental review into a formalistic check-the-box exercise.

B. The FSEIS Lacks a True No Action Alternative.

The FSEIS violates NEPA because it does not contain a true no action alternative. Instead, the FSEIS only presents as "different perspectives" the two most extreme possible no action scenarios, both of which DOE acknowledges are unlikely to actually occur.[80] This

---

[76] C. McGlade & P. Ekins, *The geographical distribution of fossil fuels unused when limiting global warming to 2°C*, 517 NATURE 187 (2015).
[77] *Synthesis Report of the IPCC Sixth Assessment Report* at 55, https://report.ipcc.ch/ar6syr/pdf/IPCC_AR6_SYR_LongerReport.pdf.
[78] *See Citizens Against Burlington*, 938 F.2d at 196 ("[A]gencies must look hard at the factors relevant to the definition of purpose," including "the views of Congress . . . in the agency's statutory authorization to act" and then "must define goals for its action that fall somewhere within the range of reasonable choices.); *see also League of Wilderness Defs. v. U.S. Forest Serv.*, 689 F.3d 1060, 1070 (9th Cir. 2012).
[79] *See* 87 Fed. Reg. at 23,458-59.
[80] FSEIS at S-7; Order 3643-C at 24.

precludes DOE from reaching any meaningful conclusion about the Project's impacts on the climate.

Every EIS must contain a no action alternative—an analysis of the world as it would be if the agency did not approve the proposed action.[81] The no action alternative provides a critical baseline without which it is impossible to meaningfully assess a project's environmental impacts.[82] Where an agency has discretion to disapprove a proposed action, the no action alternative also represents a possible outcome that the agency must at least consider choosing.[83]

The FSEIS fails to identify any single no action alternative, and instead presents two admittedly implausible descriptions of what could happen if the Project is not approved. In DOE's No Action Alternative 1, other sources of LNG perfectly substitute for the Project's output.[84] In DOE's No Action Alternative 2, the Project is not built and its output is not substituted by other sources of LNG.[85] DOE admits both scenarios are unlikely; No Action Alternative 1 understates the Project's emissions, while No Action Alternative 2 overstates the Project's emissions.[86] DOE states that it cannot say which is more realistic.[87]

---

[81] 40 C.F.R. § 1502.14(c); 46 Fed. Reg. 18,026, 18,027 (Mar. 23, 1981).
[82] *See Ctr. for Biological Diversity v. U.S. Dep't of Interior*, 623 F.3d 633, 642 (9th Cir. 2010) (*quoting Friends of Southeast's Future v. Morrison*, 153 F.3d 1059, 1065 (9th Cir. 1998)).
[83] *Cf. Anglers of the Au Sable v. U.S. Forest Serv*., 565 F. Supp. 2d 812, 816, 834-36 (E.D. Mich. 2008) (holding that Forest Service arbitrarily and capriciously failed to take a hard look at no action alternative when it "mistakenly considered itself obligated by both policy and by the terms of [an existing] lease to adopt an action alternative").
[84] *See* FSEIS at S-7 (explaining that No Action Alternative 1 "represents the same amount of LNG being supplied to the market"); Order 3643-C at 24.
[85] *See* FSEIS at S-7 (explaining that No Action Alternative 2 "intentionally excludes GHG emissions from energy production . . . to meet equivalent LNG (and crude oil) services"); Order 3643-C at 24.
[86] Order 3643-C at 23-24.
[87] Amended Record of Decision, Order 3643-C at 41 ("Given the complexity of energy markets and the uncertain substitution effects related to the Project's LNG production capacity that could occur in those markets, DOE is unable to conclude that either one of the No Action Alternatives is more accurate.").

DOE's failure to identify any realistic no action alternative, or to adequately explain why one could not be identified, violates NEPA. DOE asserts that providing two unrealistic alternatives "provides decision makers and the public with a wider range of useful information in order to assess potential emissions."[88] However, the only information the no action discussion provides about the Project's life cycle climate impacts is that if the Project is built, its effect on global GHG emissions will fall somewhere between a marginal reduction and a huge addition representing 100 percent of the Project's direct and indirect emissions. This goes no further than identifying the best and worst imaginable scenarios; such a wide range of potential outcomes provides no basis to weigh the Project's climate impacts against its purported benefits.

DOE argues that uncertainty about the future of the energy market is too great to be more specific.[89] However, NEPA does not permit an agency to simply shrug its shoulders in the face of uncertainty.[90] Even if DOE could not reasonably predict a realistic no action scenario, the Department was required to document the reasons that information could not be obtained and make reasonable efforts to estimate the scenario based on generally accepted methods.[91] Intervenors commented on the DSEIS that, at minimum, DOE could use the NERA modeling the applicant submitted as a basis for describing a more realistic no action scenario.[92] As explained *supra* pp. 16-17, DOE relied on that modeling to identify the Project's potential economic benefits, and has a history of relying on NERA modeling in other matters. Yet, DOE did not use the NERA modeling to evaluate a no action scenario and did not provide any reason for failing to

---

[88] *Id.* at 42.
[89] Order 3643-C at 22, 24; FSEIS at 2-24.
[90] *See infra* pp. 25-29.
[91] *Id.*
[92] DSEIS Comments at 10.

use it or any other method to provide a more realistic no action scenario. This was arbitrary and contrary to NEPA.

As Intervenors[93] and U.S. Environmental Protection Agency (EPA) commented[94] on the DSEIS, No Action Alternative 1 violates NEPA because it assumes perfect substitution of the Project's gas for other fossil fuels. Courts have repeatedly, and categorically, rejected agency attempts to rely on perfect substitution to conclude that permitting fossil fuels production or transportation infrastructure will result in no or minimal GHG emissions. Perfect substitution "contradict[s] basic economic principles,"[95] is "illogical," and "places the [agency's] thumb on the scale by inflating the benefits of the action while minimizing its impacts."[96]

To the extent that DOE is continuing to rely on No Action Alternative 1 in its decisionmaking, and is merely obscuring that reliance by also including No Action Alternative 2, its decisionmaking remains as unlawful as if DOE had only included the perfect substitution assumption. While the record of decision (ROD) states "DOE is unable to conclude that either one of the No Action Alternatives is more accurate,"[97] the Order opines without explanation that the GHG and climate impacts "are likely to be closer to the difference between No Action Alternative 1 and the Project scenarios."[98] Aside from being unsupported and inconsistent with the analysis in the FSEIS, [99] DOE's prediction of a scenario closer to perfect substitution

---

[93] *Id.* at 8–10.
[94] FSEIS, App. D at D-86 to D-87, D-89.
[95] *WildEarth Guardians v. Bureau of Land Mgmt.*, 870 F.3d 1222, 1237–38 (10th Cir. 2017).
[96] *Montana Env't Info. Center v. U.S. Office of Surface Mining*, 274 F. Supp. 3d 1074, 1098 (D. Mont. 2017); *see also High Country Conservation Advocs. v. U.S. Forest Service, 52 F. Supp*. 3d 1174, 1197–98 (D. Colo. 2014) (noting that additional supply impacts demand, and fuels that would otherwise be left in the ground will be burned).
[97] Amended Record of Decision, Order 3643-C at 41.
[98] Order 3643-C at 24–25.
[99] *See, e.g.*, FSEIS at 4.19-6 (stating that DOE "takes no position on whether there will be a market demand for the LNG produced by the Alaska LNG Project").

inappropriately minimizes the Project's climate impacts. At best, it is arbitrarily optimistic. At worst, it is an unlawful attempt to circumvent case law that precludes DOE from relying on perfect substitution.

C. The FSEIS Does Not Comply with NEPA Regulations Regarding Missing Information.

The FSEIS does not comply with the requirements in CEQ's regulations addressing how agencies must handle incomplete or unavailable information.[100] When "information relevant to reasonably foreseeable significant adverse impacts" is available, and not unreasonably costly to obtain, an agency preparing an EIS must include that information.[101] If the information cannot be obtained, or is unreasonably expensive to obtain, the agency must include: "a statement that such information is incomplete or unavailable"; a statement of the relevance of that information to evaluating the project's reasonably foreseeable impacts; a summary of existing credible scientific evidence relevant to evaluating those impacts; and the "agency's evaluation of such impacts based upon theoretical approaches or research methods generally accepted in the scientific community."[102] The FSEIS falls short of this requirement.

As discussed above, the FSEIS does not even attempt to make specific projections of the market demand for LNG exports from the Project which could serve as the basis for more precise GHG emissions estimates, instead providing two bookends and stating that it takes "no position" on whether one, the other, or some point in the middle represents reality.[103] DOE ignored the option of relying on the NERA modeling submitted by the applicant, which projected that two-thirds of the Project's exports would represent an increase in overall United States LNG supply

[100] 40 C.F.R. § 1502.21.
[101] *Id*. § 1502.21(b).
[102] *Id*. § 1502.21(c).
[103] FSEIS at 4.19-6.

and one-third would displace other sources.[104] This information was obviously available to DOE, and DOE relied on it to describe the Project's economic benefits, in addition to using NERA modeling in other proceedings.[105] It was arbitrary for DOE not to even consider it as an option.[106] DOE also failed to explain why, in the alternative, it could not complete its own modeling.

In addition, while the FSEIS discloses there is a lack of specific information about planned upstream development on the North Slope, including new pads, wells, access roads, and pipelines[107]—the first step required by CEQ's regulations when information is incomplete or unavailable—it does not adequately discuss the relevance of this information to the Department's decisionmaking, nor does it provide the Department's evaluation of these impacts based on theoretical approaches or generally accepted research methods.[108] The FSEIS was completed without site-specific surveys of water resources,[109] wetlands,[110] or wildlife,[111] and "no floodplain mapping exists for the North Slope."[112] Absent such information, the FSEIS does not adequately explain how DOE was able to evaluate the significance of upstream development impacts or rationally weigh these adverse impacts against the Project's supposed benefits. As discussed above, *see supra* Section I.C, upstream impacts to the North Slope comprise one of the two categories of impacts DOE reviewed in the first instance in the FSEIS, yet DOE's order

---

[104] *See supra* pp. 16-17.
[105] *Id.*
[106] 40 C.F.R. § 1502.21.
[107] FSEIS at 4.21-1 (discussing incomplete and unavailable information); *see also, e.g., id.* at 4.1-2 ("the exact locations of the components of the PTU Expansion Project are unknown at this time").
[108] 40 C.F.R. § 1502.21.
[109] FSEIS at 4.3-4.
[110] *Id.* at 4.4-2.
[111] *Id.* at 4.6-2 to 4.6-3.
[112] *Id.* at 4.3-5.

summarily dismisses these impacts.[113] The FSEIS does not contain an adequate analysis of these impacts to support reasoned decisionmaking.

DOE's FSEIS also does not adequately disclose or analyze the climate forcing effects of the significant black carbon emissions associated with the Project, including upstream infrastructure. Although the FSEIS estimates particulate matter emissions associated with proposed alternatives, it does not disclose any information about what component of those emissions are black carbon or adequately analyze black carbon's climate forcing impacts.

Black carbon impacts the reflectiveness of ice and snow surfaces, increases melting rates, and exacerbates warming.[114] A growing body of scientific literature identifies black carbon, a component of fine particulate matter ($PM_{2.5}$), as a critical climate forcing agent, and suggests that reducing these emissions may be among the most effective near-term strategies for slowing Arctic warming and the melting of sea ice, the Greenland ice sheet, and glaciers and snow pack around the world.[115] It has been estimated that the "soot effect on snow albedo may be responsible for a quarter of observed global warming."[116] One study indicates that the direct warming effect of black carbon on snow can be three times as strong as that due to carbon dioxide during springtime in the Arctic.[117] And scientists have described the average global

---

[113] Amended Record of Decision, Order 3643-C at 44-45, 50.
[114] *See* DSEIS Comments at 27–28.
[115] V. Ramanathan & G. R. Carmichael, *Global and Regional Climate Changes Due to Black Carbon*, NATURE GEOSCIENCE (April 2008).
[116] J. Hansen, & L. Nazarenko, *Soot Climate Forcing Via Snow and Ice Albedos*, 101 PROC. OF THE NAT'L ACAD. OF SCI. 423 (Jan. 13, 2004).
[117] M.G. Flanner *et al*., *Present-day climate forcing and response from black carbon in snow*, 112 J. GEOPHYS. RES. D11202, doi:10.1029/2006JD008003 (2007).

warming potential of black carbon as about 500 times that of carbon dioxide over a 100-year period.[118]

The FSEIS acknowledges that black carbon is harmful to human health and the climate,[119] but does not analyze the magnitude of its impacts in relation to this Project. Black carbon is included in the Project's estimated PM2.5 emissions, but "[b]lack carbon emissions were not separately quantified due to the lack of available emission factors specific to black carbon."[120] The FSEIS asserts "there is considerable uncertainty regarding the climate forcing effects of black carbon, and the [Intergovernmental Panel on Climate Change] and USEPA have not published global warming potential values for black carbon to allow these effects to be quantified."[121] The FSEIS offers no further discussion about the potential magnitude of impacts from this Project due to black carbon.

The mere existence of uncertainty does not excuse FERC from providing information about the magnitude of reasonably foreseeable Project impacts caused by black carbon. FERC's

---

[118] J. Hansen *et al.*, *Dangerous human-made interference with climate: A GISS modelE study*, 7 ATMOS. CHEM. PHYS. 2287-2312 (draft Oct. 13, 2008); *see also* M.S. Reddy & O. Boucher, *Climate impact of black carbon emitted from energy consumption in the world's regions*, 34 GEOPHYS. RES. LETT. L11802, doi:10.1029/2006GLO28904 (2007) (Reddy 2007).
[119] FSEIS at 3.15-4 (describing potential health impacts from black carbon in general terms, but not estimating impacts from this Project); *id.* at 3.19-4 (describing the potential climate change impacts of black carbon in general terms, but not estimating impacts from this Project).
[120] *Id.* at 4.15-6.
[121] *Id.* at 4.19-5.

brief discussion does not satisfy NEPA's requirements for missing information and does not constitute the required hard look at impacts.[122]

D. The FSEIS Makes Unsupported Assertions About Byproduct CO_2 Injection.

The FSEIS makes unsupported assertions about byproduct CO_2 injection and still contains many of the flaws that Intervenors identified in the DSEIS. These flaws conceal and understate the potential for additional emissions resulting from byproduct CO_2.

DOE's estimates of byproduct CO_2 that would be stored continue to ignore the fact that while the same amount of CO_2 will be injected in Scenarios 2 and 3, different amounts will be actually stored.[123] Neither sequestration nor enhanced oil recovery (EOR) permanently stores all of the injected CO_2; in both cases, some CO_2 returns to the atmosphere. As the appendices to the FSEIS recognize, EOR is generally understood to result in a much higher amount of returned CO_2.[124] The FSEIS does not acknowledge this reality, which makes it impossible for the public to understand the true extent that either sequestration or EOR can mitigate the Project's

---

[122] *See* 40 C.F.R. § 1502.21; *Pub. Emps. for Env't Resp. v. Hopper*, 827 F.3d 1077, 1082 (D.C. Cir. 2016); *Gov't of the Province of Man. v. Salazar*, 691 F. Supp. 2d 37, 45 (D.D.C. 2010) ("An agency's primary duty under the NEPA is to 'take a 'hard look' at environmental consequences.'") (*quoting Pub. Utils. Comm'n v. FERC*, 900 F.2d 269, 282 (D.C. Cir. 1990)). In estimating operational emissions, the FSEIS also continues to rely on a resource report prepared by AGDC in 2017 that purports to analyze the "air quality impacts associated with upstream development activities at the [Point Thomson Unit (PTU)] and the [Prudhoe Bay Unit (PBU)]." FSEIS at 4.15-9, Tbl. 4.15-9 (citing AGDC. 2017. Resource Report 9, Air and Noise Quality. Accessed on April 15, 2022 at https://alaskalng.com/regulatory-process/ferc-application-exhibits/resource-reports/). However, that air quality impacts report looks only at emissions associated with injection of byproduct into the PBU, *see* FSEIS at 4.15-2; it does not analyze emissions from Proposed Action Scenarios 2 and 3 at all because those scenarios were not contemplated until the DSEIS was prepared. To foster transparency and informed decisionmaking, the FDSEIS must show its work and present the underlying data for the summary tables in the FDSEIS, including how DOE extrapolated from a study that did not include any equipment, emission factors, or construction timing information for two of the scenarios now under consideration.

[123] FSEIS at 2-21 to 2-22, Tbls. 2.2-1 & 2.2-2.

[124] *See id.*, App. C at 23-24 (Exs. 3-5, 3-6).

emissions. DOE's vague treatment of the issue also makes it unclear whether DOE consistently considered the differences between sequestration and EOR in its own ultimate evaluation.

DOE continues to rely on optimistic and unsupported figures regarding the effectiveness of sequestration and EOR. For the emission rate for EOR, the FSEIS's Appendix C relies on a 2019 publication that just provided a model that could be parameterized with different emission rates; although the model includes a default rate, it does not demonstrate the basis for, or appropriateness of, this default.[125] Appendix C's assumptions about oil produced per kg of CO_2 injected also appear more optimistic than prior work by the same author.[126] Similarly, for sequestration under Scenario 2, the FSEIS's estimate of the amount of injected CO_2 that will return to the surface (1.4 percent, or 13.9 kg per 1000 kg of CO_2 injected) appears to simply be a guess, without any empirical or actual-practice data.[127]

It is also still unclear why the exhibits in Appendix C present inconsistent CO_2-EOR values in the tables for the Japan, South Korea, China, and India analyses.[128]

DOE's adoption of a requirement for certification that no byproduct CO_2 is vented does not alleviate the concerns Intervenors raised about CO_2 venting in their DSEIS comments. DOE's order adopts a new condition, recommended in the FSEIS,[129] requiring that the Project regularly certify gas export "did not result in the venting of byproduct carbon dioxide (CO_2) into

---

[125] *Id.* at 23–24, 72 (citing Jamieson, M. & Skone, T. J., *Carbon Dioxide Enhanced Oil Recovery Life Cycle (CELiC) Model*, National Energy Technology Laboratory (2019)).
[126] Cooney *et al.*, *Evaluating the Climate Benefits of CO2-Enhanced Oil Recovery Using Life Cycle Analysis*, 49 Environ. Sci. Technol. 2015, 7491-7500, DOI: 10.1021/acs.est.5b00700 (2015).
[127] FSEIS, App. C at 23, Ex. 3-5 (citing Littlefield, J. *et al.*, *Life Cycle Analysis of Natural Gas Extraction and Power Generation*, United States: National Energy Technology Laboratory (2019)).
[128] *Id.* at A-18 to A-21 (Exhibits A-17 to A-20),
[129] FSEIS at 4.19-12.

the atmosphere, unless required for emergency, maintenance, or operational exigencies and in compliance with the FERC Order."[130] However, it is unclear that this requirement to avoid venting applies to later steps in the process—the transport, injection, and long-term geologic storage of CO_2—rather than just the steps involving separating the CO_2 from the methane and routing it to a transmission pipeline. If venting occurs at those later stages and is not subject to the certification requirement, the Project's climate impacts could be greater than DOE assumes. In addition, the term "operational exigencies" is so vague that it is impossible to determine how broadly DOE will interpret this exception. For example, this exception might allow venting for years while sequestration or EOR equipment is offline without requiring Project proponents to make necessary repairs, again resulting in greater climate impacts than DOE's analysis assumes and that were disclosed to the public.

E. The FSEIS Does Not Adequately Address Impacts from Proposed Carbon Storage on the North Slope.

The FSEIS treats seismic impacts from carbon storage on the North Slope in a cursory manner and does not adequately address safety issues related to carbon dioxide pipelines.

The FSEIS contains some discussion of seismic impacts, but ultimately dismisses these concerns.[131] The FSEIS asserts that because CO_2 injection for EOR has been happening since 1988 and "the [Kuparuk River Unit (KRU)] and the North Slope are characterized as generally inactive in terms of seismicity" with "good reservoir seals," the potential to induce seismic activity "is low in the KRU."[132] However, DOE does not adequately support that conclusion and ignores relevant information to the contrary. For example, the FSEIS dismisses as irrelevant the studies Intervenors cited in DSEIS comments showing correlation between CO_2 injection for

[130] Order 3643-C at 27; *see also id.* at 6-7, 26.
[131] FSEIS at S-11, 4.1-2, 4.1-5 to 4.1-7.
[132] *Id.* at 4.1-5 to 4.1-6.

EOR and seismic activity or earthquakes. Citing a study Intervenors discussed in their DSEIS comments, DOE states that these studies focused on CO_2 injection into "brittle rocks found within the continental interior, or the region between the Rocky Mountain and Appalachia-Ouachita fronts."[133] However, DOE entirely ignores studies Intervenors pointed to that focused on induced seismicity in Japan and across the globe.[134]

In addition, recent studies from the North Slope show that it is a seismically active region with the capacity for large earthquakes such as the magnitude 6.4 and 6.0 earthquakes in 2018,[135] and that "these earthquakes illustrate the potential for larger, possibly destructive events in a region earmarked for rapid resource development."[136] These studies also note that many faults are still unmapped; for example, the magnitude 6.4 earthquake occurred on a fault whose existence was unknown prior to the event. An array of new seismic monitoring stations installed in northern Alaska in 2014–2017 provide detailed information on earthquake activity in the region. One 2020 study reported that in 2018–2019, more than 4,000 earthquakes between magnitudes 1 and 4.3 were recorded in an earthquake swarm in the Eastern Brooks Range.[137] DOE's cursory dismissal of seismic impacts fails to account for this information and does not constitute a hard look.[138]

---

[133] *Id.* at 4.1-5 (citing Zoback, M.D., & S.M. Gorelick, *Earthquake Triggering and Large-Scale Geologic Storage of Carbon Dioxide*, (2012) 109 PNAS 10164-68).
[134] DSEIS Comments at 33, n.162.
[135] Gaudreau, É. *et al.*, *The August 2018 Kaktovik Earthquakes: Active Tectonics in Northeastern Alaska Revealed With InSAR and Seismology*, 46 Geophys. Res. Let. 14412-14420 (2019); Gibbons, S. *et al.*, *Resolving Northern Alaska Earthquake Sequences Using the Transportable Array and Probabilistic Location Methods*, 91 Seismol. Res. Lett. 3028 (2020); Xu, G. *et al.*, *The Complexity of the 2018 Kaktovik Earthquake Sequence in the Northeast of the Brooks Range, Alaska*, 47 Geophys. Res. Let. e2020GL088012 (2020).
[136] Gaudreau, É. *et al.* at 14412.
[137] Gibbons, S. *et al.* at 3028.
[138] *Pub. Emps. for Env't Resp.*, 827 F.3d at 1082.

The FSEIS also does not adequately address the safety issues related to carbon dioxide pipelines and potential leaks. While the FSEIS does mention the catastrophic CO_2 pipeline leak in Satartia, Mississippi, which sent dozens of people to the hospital and resulted in evacuation of a town in 2020,[139] it fails to fully engage with this risk and the unknowns surrounding CO_2 pipeline engineering.

Pipelines carrying supercritical liquid CO_2 are more susceptible to ductile fractures, and if a CO_2 pipeline's temperature reaches -20 degrees Fahrenheit or lower, there is a risk of catastrophic rupture as the steel becomes brittle.[140] CO_2 is a colorless, odorless gas, so leaks might not be detected quickly and people in the vicinity of a leak that displaces oxygen in the air may not realize they are in danger before they become disoriented. As DOE admits, "[t]he severity of potential accident consequences from CO_2 pipelines are [sic] highly dependent upon the location of a release in proximity to receptors, in addition to the size of the release… [,] atmospheric conditions…, and ultimately the potential for exposure to humans or wildlife."[141] Moreover, "many features of the potential pipelines that would be necessary to conduct a meaningful quantitative exposure analysis" for the Project "are unknown at time."[142] The FSEIS also acknowledges that there are relatively few existing miles of CO_2 pipeline in this country, and that there are no CO_2 pipelines recorded in the Pipelines and Hazardous Materials Safety Administration (PHMSA) 2020 annual report database for Alaska.[143]

---

[139] FSEIS at 3.18-3.
[140] Pipeline Safety Trust, *CO2 Pipelines – Dangerous and Under-Regulated*, (Mar. 30, 2022) (Pipeline Safety Trust 2022), https://pstrust.org/wp-content/uploads/2022/03/CO2-Pipeline-Backgrounder-Final.pdf.
[141] FSEIS, App. D at D-39.
[142] *Id.*
[143] FSEIS at 3.18-2 & Tbl. 3.18-1.

Despite these facts, DOE concludes that the risk of a pipeline rupture is low and that because of the remoteness of the area, there is also a low likelihood that humans or animals would be affected if a leak occurs.[144] This optimistic prediction is not adequately supported and does not constitute a hard look at the risks posed by potential CO_2 pipeline ruptures.[145]

The FSEIS does not disclose how much CO_2 might be released under various scenarios and what that level of exposure would mean for species and the climate in addition to human health. The FSEIS should have provided this basic information, and indeed DOE has previously done so in an EIS that included a health risk assessment to analyze the potential harms associated with a much shorter, 3.36-mile CO_2 pipeline for a proposed project with an EOR component in California.[146]

DOE also cannot satisfy its obligations under NEPA by relying on the regulations and judgments of other agencies. This is especially true in the case of CO_2 pipelines: PHMSA recently announced that it will start a new rulemaking process because its current safety requirements are inadequate to prevent and respond to emergencies related to CO_2 pipelines.[147] This announcement follows a report by the Pipeline Safety Trust, which concluded that existing federal regulations do not allow for the safe transportation of CO_2 via pipelines due to the unique

---

[144] *Id.*, App. D at D-39.
[145] *Pub. Emps. for Env't Resp.*, 827 F.3d at 1082.
[146] *See* Office of Fossil Energy & Carbon Mgmt., *Hydrogen Energy California Project draft Environmental Impact Statement* (June 30, 2013); Stantec, Hydrogen Energy Center Application for Certification Amendment –Attachment D: Hazards Assessment of CO2 Supply Line at 6-7 (Apr. 12, 2011).
[147] Pipeline & Hazardous Materials Safety Admin., PHMSA Announces New Safety Measures to Protect Americans From Carbon Dioxide Pipeline Failures After Satartia, MS Leak (May 26, 2022).

risks associated with transporting compressed CO_2 and the gaps in jurisdiction for pipelines carrying CO_2 at certain concentrations and states.[148]

F. The FSEIS Does Not Adequately Address Methane Leakage from the Project.

DOE's analysis of methane leakage is inadequate because it relies on EPA data that undercounts methane emissions and because it does not clearly account for methane emissions from all life cycle stages. DOE's conclusion that different methane emission rates have only a modest impact on overall Project GHG emissions is based on a sensitivity analysis that does not clearly encompass the realistic range of leakage rates.

The EPA Greenhouse Gas Reporting Program data on which DOE relies has been demonstrated to consistently underestimate methane emissions. One study found national emissions from pipeline mains to be five times greater than EPA's estimate,[149] and another study found U.S. oil and gas supply chain emissions to be 60 percent higher than EPA's figure, likely due to EPA's failure to account for abnormal operating conditions.[150] Another recent study found that mean methane emissions from U.S. oil and gas production during the period from 2010 to 2019 were about 70 percent higher than EPA's emissions inventory estimates.[151]

As Intervenors noted in comments on the DSEIS, DOE does not provide information about the basis for its methane leakage analysis. The FSEIS contains neither the methane

---

[148] Pipeline Safety Trust 2022 (citing Accufacts Inc., *Accufacts' Perspectives on the State of Federal Carbon Dioxide Transmission Pipeline Safety Regulations as it Relates to Carbon Capture, Utilization, and Sequestration within the U.S.* (2022)).
[149] Weller, Z. D. *et al.*, *A National Estimate of Methane Leakage from Pipeline Mains in Natural Gas Local Distribution Systems*, 54 Environ. Sci. Technol. 8958 (2020).
[150] Alvarez, R. A. *et al.*, *Assessment of methane emissions from the U.S. oil and gas supply chain*, 361 Science 186 (June 21, 2018) (Alvarez 2018).
[151] Lu, X. *et al.*, *Observation-derived 2010-2019 trends in methane emissions and intensities from US oil and gas fields tied to activity metrics*, Proceedings of the National Academy of Sciences (Apr. 17, 2023), https://doi.org/10.1073/pnas.2217900120.

emissions factors for each stage of the supply chain nor any other data on which the estimates are based.[152] Therefore, there is no clear explanation of how the life cycle analysis reached its estimates of methane leakage rates. DOE's analysis does not clearly account for methane emissions from each stage examined—gas extraction to pipeline transport, to liquefaction, to ocean transport, to power plant operations—because the potential for fugitive methane emissions is not discussed in each stage.[153] Methane emissions are still not listed as a key parameter in the production stage of the lifecycle analysis for the PBU,[154] despite the fact that roughly 85 percent of national methane emissions from the oil and gas supply chain are estimated to come from production, gathering, and processing,[155] while the appendix to the life cycle analysis includes emissions associated with extraction. The FSEIS therefore does not adequately disclose to the public the basis for DOE's estimates, and it is not possible to determine whether these estimates are reasonable.

The FSEIS's conclusion that variations in the methane leak rate have only a "modest" impact on total life cycle GHG emissions[156] remains unsupported because, as discussed above, it is unclear how the estimated leakage rates were reached and therefore remains unclear whether the sensitivity analysis considered a wide enough range of methane leak rates to capture the likely real-world emissions. The sensitivity analysis examined changes of ± 5 percent in methane emissions and found that "[f]or each of the countries [examined,] the total GHG emissions vary about 1.5 to 5 kg CO_2e/MWh electricity produced and 53 kg of crude-oil products consumed in either direction. This difference is representative of about 0.2 – 0.7 percent of total life cycle

---

[152] DSEIS Comments at 35.
[153] FSEIS, App. C.
[154] *Id.* at 20, Ex. 3-1.
[155] Alvarez 2018.
[156] FSEIS, App. C at 68.

GHG emissions."[157] DOE's response to Intervenors' critique of that analysis range does not actually address Intervenors' point that actual methane emissions could likely be much more than 5 percent higher than the numbers DOE analyzed. DOE responds that the purpose of selecting the ± 5 percent change was only to understand the effect of an arbitrary change in methane emissions on the results, and that the choice was "not intended to imply a known range of direct methane emissions uncertainty within the study."[158] However, just because DOE intended the 5 percent range to be arbitrary does not mean it is a valid basis for DOE to draw conclusions about the real-world impact of variations in the methane leak rate, which might be much greater than 5 percent. If the methane leak variation rate DOE selected is arbitrarily modest, it stands to reason that its effect on total lifecycle emissions would likewise be arbitrarily modest. DOE must evaluate a realistic range of methane leak rates or explain why it would be prohibitively costly to do so.[159]

G. The FSEIS's Analysis of Overseas Impacts is Inadequate.

In evaluating the Project's lifecycle emissions, DOE's analysis of overseas impacts in is inadequate because it relies on unfounded assumptions about the identity of the destination countries, about whether those countries would use LNG with or without the Project, and about the use and efficacy of carbon capture equipment on power plants in those countries.

DOE still does not support the assumption carried over from the DSEIS that only Japan, South Korea, China, and India would receive exports from the Project. The FSEIS merely adds text noting that:

> These four countries were chosen to represent geographically proximate delivery destinations from Alaska that, at the time of study initiation, were known or expected to be significant LNG

---

157 *Id.*
158 *Id.*
159 *See supra* pp. 25-29; 40 C.F.R. § 1502.21.

> importers. Note that the range of shipping distances to these specific countries (5,000 to 10,000 miles from Alaska) closely approximate those to other emerging LNG importers such as in Europe (about 10,000 miles away via the Panama Canal).[160]

In 2022, the U.S. exported LNG by vessel to 38 countries, including countries in South America, the Caribbean, Europe, Asia, and the Middle East.[161] If LNG was exported to a country farther away than the four analyzed—shipped to Pakistan instead of India, or to Bangladesh, Indonesia, or Singapore instead of Japan, South Korea, and China—emissions associated with shipping would be higher than those that were analyzed.

For purposes of No Action Alternative 1, the FSEIS also does not support DOE's assumption that if these destination countries did not import Alaskan LNG, they would import gas from the Lower 48 or a location that is sufficiently similar in shipping distances and overall emissions that the Lower 48 is a reasonable proxy. In analyzing No Action Alternative 1, "DOE assumed the energy demand from foreign markets would remain and would be fulfilled by an alternate source of LNG from the global market. DOE modeled GHG emissions associated with the alternative source of LNG using the U.S. average production from the Lower 48 as a representative proxy."[162] This approach may inflate the overall emissions of No Action Alternative 1, making the Project's emissions seem more favorable by comparison. Even though DOE admits No Action Alternative 1 is unlikely, DOE expects the Project's climate impacts will likely be "closer to" the difference between No Action Alternative 1 and Project impacts.[163] Therefore, this unsupported assumption in No Action Alternative 1 may have skewed DOE's decisionmaking.

---

[160] FSEIS at 4.19-2.
[161] U.S. EIA, *U.S. Natural Gas Exports and Re-Exports by Country*, https://www.eia.gov/dnav/ng/NG_MOVE_EXPC_S1_A.htm (last visited May 11, 2023).
[162] FSEIS at 4.19-2.
[163] Order 3643-C at 24-25.

DOE provides two scenarios relevant to end use carbon capture and sequestration (CCS)—that it either is, or is not, used on gas-fired power plants in destination countries—but its use scenario is entirely unrealistic. DOE concludes that using CCS would cut total lifecycle emissions approximately in half for each of the three Project scenarios,[164] an extreme underestimate of emissions that is based on unfounded assumptions about CCS capture rates, a failure to account for all the emissions associated with CCS, and wildly optimistic views about deployment of CCS in destination countries. DOE bases its emissions modeling on an idealized 90 percent carbon capture rate for gas combined cycle power plants in destination countries.[165]

Real-world experience shows that much lower capture rates are typically achieved, however. For example, in July 2021, Chevron, operator of Australia's only commercial-scale CCS project, admitted that its self-described "world's biggest" CCS project failed to meet its five-year capture target rate of 80 percent CO_2, and is now seeking a deal with regulators on how to make up for millions of tons of CO_2 emitted.[166] Shell's Quest project in Alberta, Canada, promised a rate of 90 percent and delivered just 48 percent.[167] In the United States, the Petra Nova coal-fired power plant in Texas achieved only a 65-70 percent CO_2 capture rate compared to the 90 percent promised,[168] before being shut down indefinitely for being uneconomic.

Additionally, a proper accounting of emissions from carbon capture would account for full lifecycle emissions—including combustion emissions from the gas or other fuel to power the

---

164 FSEIS at 2-21, Tbl. 2.2-1.
165 *Id.*, App. D at D-24.
166 Mazengarb, M., Chevron admits failure of $3 billion CCS facility in Western Australia, IEEFA (July 19, 2021).
167 Meredith, S., *Shell's massive carbon capture facility in Canada emits far more than it captures, study says*, CNBC (Jan. 24, 2022).
168 Schlissel, D., *Reality of carbon capture not even close to proponents' wishful thinking*, IEEFA (Aug. 8, 2019).

CCS equipment, and upstream emissions from producing that fuel—something DOE does not appear to have done. For example, a Stanford study of the lifecycle emissions associated with Petra Nova power plant CCS project found that "the [CCS] equipment captured the equivalent of only 10-11 percent of the emissions they produced, averaged over 20 years."[169] This study also determined that when factoring in the resulting air pollution, potential health problems, economic costs, and climate change impacts, carbon capture created social costs as high or higher than a fossil fuel plant *without* carbon capture, concluding "it is always better to use the renewable electricity instead to replace coal or natural gas electricity or to do nothing."[170] Capturing CO_2 is energy intensive, and power plants using carbon capture require approximately 15 to 25 percent more energy to produce the same amount of power they would without carbon capture.[171] In addition to higher electricity costs, this additional fuel combustion can mean greater emissions of non-CO_2 air pollutants such as fine particulate matter, ammonia, hazardous volatile organic compounds, and other toxic pollutants that threaten the health of nearby communities.[172] The energy required to capture, transport, and inject carbon underground for sequestration reduces the net benefit of carbon capture. Injecting captured carbon to boost oil extraction through EOR

---

[169] Kubota, T., *Stanford study casts doubt on carbon capture*, Stanford News (Oct. 25, 2019) (citing Jacobson, M. Z., *The health and climate impacts of carbon capture and direct air capture*, 12 Energy Envt. Sci. 3567 (2019)).

[170] *Id.* (also concluding "that the social cost of coal with carbon capture powered by natural gas was about 24 percent higher, over 20 years, than the coal without carbon capture," and that "[o]nly when wind replaced coal itself did social costs decrease.").

[171] Climate Action Network International, Position: Carbon Capture, Storage and Utilisation at 9 (Jan. 2021); European Environment Agency, *Carbon capture and storage could also impact air pollution* (last modified Nov. 23, 2020) (European Environment Agency 2020).

[172] *See, e.g.*, European Environment Agency 2020 (citing European Environment Agency, Air pollution impacts from carbon capture and storage (CCS), EEA Technical report No 14/2011 (2011))..

would further increase emissions; one modeling study estimated a coal-fired power plant using CCS with EOR would emit 3.7 to 4.7 times as much CO_2 as it removes.[173]

It is also unrealistic to assume full deployment of CCS in the near term. The FSEIS itself admits that "[t]he technical viability of sequestering carbon from power generation in each destination country was also not evaluated as part of this study" and that "commercial deployment of carbon capture technology is new, with demonstration projects currently being supported by the U.S. Government."[174] The FSEIS therefore concludes that "end use results without CCS are more likely to reflect existing electricity generating plants today, and the results with CCS are likely to be more representative of future electricity generation, with lower GHG emissions."[175] Nonetheless, the FSEIS bases its low-end estimates for lifecycle GHGs from all three scenarios on this assumption, providing significant under-estimates of the Project's emissions impacts.

The FSEIS briefly acknowledges that it does "not evaluate destination country geologic storage potential" for captured carbon.[176] It also completely fails to evaluate current or projected CCS capacity in these countries. Instead, the FSEIS vaguely states that "[t]here are movements within each of the countries to pursue the technology" and "CCS can reduce the impacts from existing infrastructure by retrofitting the existing fossil based power and industrial plants, or in the integrated design of new fossil plants, to capture the CO_2 emissions from these large point

[173] Jaramillo, P. *et al.*, *Life Cycle Inventory of CO_2 in an Enhanced Oil Recovery System*, 43 Environ. Sci. and Technol. 8027, 8030 (2009).
[174] FSEIS at 4.19-4.
[175] *Id.*
[176] *Id.*, App. C at 15.

source emitters."[177] The FSEIS also briefly points to the IEA "Net Zero by 2050" report to assert that carbon capture on gas-fired power plants is expected to increase.[178]

However, current and projected CCS deployment on power plants indicates that assuming full deployment of CCS in the near-term is unfounded. CCS industry data shows that as of 2021, were no operational commercial gas-fired power plants with CCS anywhere in the world.[179] Further, three of the four destination countries—Japan, South Korea, and India—had no operating commercial CCS facilities of any type—on gas-fired power plants or otherwise. The entire country of China had only three operating commercial CCS facilities—none on a gas-fired power plant—that combined have a CO_2 capture capacity of 570,000 to 820,000 tons per year, with all captured CO_2 being used for EOR instead of geologic storage.[180] In addition, the IEA "Net Zero by 2050" report cited by the FSEIS projects a rapidly declining role for fossil fuels, including fossil gas, in the global power sector over the Project's lifetime, signaling that the DOE's assumption of a prominent, ongoing role for fossil gas, with or without CCS, is unfounded. In the power sector, the IEA projects that the share of renewables increases from 29 percent in 2020 to over 60 percent in 2030 to nearly 90 percent in 2050.[181] As a share of total energy supply, fossil fuel use falls from 80 percent in 2020 to just over 20 percent in 2050.[182] In short, based on current status and projected trends, there is no basis for the FSEIS to assume that

[177] *Id.*
[178] *Id.* at 11.
[179] Global CCS Institute, Global Status of CCS 2021: CCS Accelerating to Net Zero at 62-63 (5.1 COMMERCIAL CCS FACILITES AND PROJECTS) (Oct. 2021), https://www.globalccsinstitute.com/wp-content/uploads/2021/10/2021-Global-Status-of-CCS-Report_Global_CCS_Institute.pdf.
[180] *Id.* at 62.
[181] IEA 2021 at 114.
[182] *Id.* at 57.

gas-fired power plants in the destination countries will be retrofitted with costly CCS equipment, making its lifecycle estimates using CCS unreliable.

COMMUNICATIONS

Pursuant to 10 C.F.R. § 590.107, all communications regarding this request should be addressed to and served upon the following:

For Center for Biological Diversity:

Elizabeth Jones, Staff Attorney
Kristen Monsell, Senior Attorney
CENTER FOR BIOLOGICAL DIVERSITY
1212 Broadway, St. #800
Oakland, CA 94612
E: ljones@biologicaldiversity.org
E: kmonsell@biologicaldiversity.org

Jason Rylander, Senior Attorney
CENTER FOR BIOLOGICAL DIVERSITY
1411 K Street NW, Suite 1300
Washington, DC 20005
E: jrylander@biologicaldiversity.org

For Cook Inletkeeper:

Sue Mauger, Science & Executive Director
Cook Inletkeeper
3734 Ben Walters Lane
Homer, AK 99603
E: sue@inletkeeper.org

Erin Colón, Senior Attorney
Sarah Saunders, Litigation Paralegal
EARTHJUSTICE
325 Fourth Street
Juneau, AK 99801
E: ecolon@earthjustice.org
E: ssaunders@earthjustice.org

Moneen Nasmith, Senior Attorney
EARTHJUSTICE
48 Wall Street, 15th Floor
New York, NY 10005-2903

For Sierra Club:

Nathan Matthews, Senior Attorney
Meral Basit, Legal Assistant
SIERRA CLUB
2101 Webster St., Suite 1300
Oakland, CA 94612
E: nathan.matthews@sierraclub.org
E: meral.basit@sierraclub.org

E: mnasmith@earthjustice.org

Ann Jaworski, Associate Attorney
EARTHJUSTICE
311 S. Wacker Dr., Suite 1400
Chicago, IL 60606
E: ajaworski@earthjustice.org

CONCLUSION

For the foregoing reasons, Intervenors respectfully request that this order be withdrawn and the underlying application denied, or in the alternative, that the order be withdrawn pending further inquiry and public process regarding the impact of the proposed exports.

Respectfully submitted this 15th day of May, 2023,

s/
Elizabeth Jones, Staff Attorney
Kristen Monsell, Senior Attorney
CENTER FOR BIOLOGICAL DIVERSITY
1212 Broadway, St. #800
Oakland, CA 94612
E: ljones@biologicaldiversity.org
E: kmonsell@biologicaldiversity.org

Jason Rylander, Senior Attorney
CENTER FOR BIOLOGICAL DIVERSITY
1411 K Street NW, Suite 1300
Washington, DC 20005
E: jrylander@biologicaldiversity.org

s/
Erin Colón, Senior Attorney
EARTHJUSTICE
325 Fourth Street
Juneau, AK 99801
E: ecolon@earthjustice.org

Moneen Nasmith, Senior Attorney
EARTHJUSTICE
48 Wall Street, 15th Floor
New York, NY 10005-2903
E: mnasmith@earthjustice.org

Ann Jaworski, Associate Attorney
EARTHJUSTICE
311 S. Wacker Dr., Suite 1400
Chicago, IL 60606
E: ajaworski@earthjustice.org

s/
Nathan Matthews, Senior Attorney
SIERRA CLUB
2101 Webster St., Suite 1300
Oakland, CA 94612
E: nathan.matthews@sierraclub.org

TABLE OF ATTACHMENTS

Abnet, K., *EU strikes deal to curb energy use by 2030*, REUTERS (Mar. 10, 2023)

Ferris, N., *Why LNG's current boom will only accelerate its ultimate demise*, ENERGY MONITOR (Apr. 6, 2023)

Gaudreau, É. *et al.*, *The August 2018 Kaktovik earthquakes: Active tectonics in northeastern Alaska revealed with InSAR and seismology*, 46 Geophysical Research Letters (2019)

Gibbons, S. *et al.*, *Resolving Northern Alaska earthquake sequences using the transportable array and probabilistic location methods*, 91 Seismol. Res. Lett. 3028 (2020)

Intergovernmental Panel on Climate Change, *Synthesis Report of the IPCC Sixth Assessment Report*

International Energy Agency (IEA), *Europe's energy crisis: What factors drove the record fall in natural gas demand in 2022?* (Mar. 14, 2023)

Institute for Energy Economics and Financial Analysis (IEEFA), *Over half of Europe's LNG infrastructure assets could be left unused by 2030* (Mar. 21, 2023)

Lu, X. *et al.*, *Observation-derived 2010-2019 trends in methane emissions and intensities from US oil and gas fields tied to activity metrics*, Proceedings of the National Academy of Sciences (Apr. 17, 2023)

Petrequin, S., *EU climate czar: Putin's war accelerated green transition*, AP NEWS (Feb. 21, 2023)

The White House, *FACT SHEET: President Biden Sets 2030 Greenhouse Gas Pollution Reduction Target Aimed at Creating Good-Paying Union Jobs and Securing U.S. Leadership on Clean Energy Technologies* (Apr. 22, 2021)

The White House, *Fact Sheet: President Biden Signs Executive Order to Revitalize Our Nation's Commitment to Environmental Justice for All* (Apr. 21, 2023)

The White House, *FACT SHEET: President Biden to Catalyze Global Climate Action through the Major Economies Forum on Energy and Climate* (Apr. 20, 2023)

U.S. Energy Information Administration (EIA), *Annual Energy Outlook 2023* (Mar. 16, 2023)

EIA, *U.S. Natural Gas Exports and Re-Exports by Country*

Xu, G. *et al.*, *The complexity of the 2018 Kaktovik earthquake sequence in the northeast of the Brooks Range, Alaska*, 47 Geophysical Research Letters e2020GL088012 (2020)

UNITED STATES OF AMERICA

DEPARTMENT OF ENERGY

OFFICE OF FOSSIL ENERGY

IN THE MATTER OF	)	
	)	
Alaska LNG Project LLC	)	FE DOCKET NO. 14-96-LNG

VERIFICATION FOR CENTER FOR BIOLOGICAL DIVERSITY

Pursuant to 10 C.F.R. § 590.103(b), I, Elizabeth Jones, hereby verify under penalty of perjury that I am authorized to execute this verification, that I have read the foregoing document, and that the facts stated therein are true and correct to the best of my knowledge.

Executed on May 15, 2023,

s/

Elizabeth Jones, Staff Attorney
CENTER FOR BIOLOGICAL DIVERSITY
1212 Broadway, Ste. 800
Oakland, CA 94612
T: 310.365.9281
E: ljones@biologicaldiversity.org

UNITED STATES OF AMERICA

DEPARTMENT OF ENERGY

OFFICE OF FOSSIL ENERGY

IN THE MATTER OF	)	
	)	
Alaska LNG Project LLC	)	FE DOCKET NO. 14-96-LNG

VERIFICATION FOR COOK INLETKEEPER

Pursuant to 10 C.F.R. § 590.103(b), I, Erin Colón, as authorized representative for Cook Inletkeeper, affirm that I have read and have knowledge of the facts alleged within the foregoing REQUEST FOR REHEARING OF ORDER GRANTING AUTHORIZATION OF THE ALASKA LNG PROJECT.

Executed on May 15, 2023,

s/
Erin Colón,
Senior Attorney
EARTHJUSTICE
325 Fourth Street
Juneau, AK 99801
T: 907.586.2751
E: ecolon@earthjustice.org

UNITED STATES OF AMERICA

DEPARTMENT OF ENERGY

OFFICE OF FOSSIL ENERGY

IN THE MATTER OF	)	
	)	
Alaska LNG Project LLC	)	FE DOCKET NO. 14-96-LNG

VERIFICATION FOR SIERRA CLUB

Pursuant to 10 C.F.R. § 590.103(b), I, Nathan Matthews, as authorized representative for Sierra Club, affirm that I have read and have knowledge of the facts alleged within the foregoing REQUEST FOR REHEARING OF ORDER GRANTING AUTHORIZATION OF THE ALASKA LNG PROJECT.

Executed on May 15, 2023,

s/

Nathan Matthews, Senior Attorney
SIERRA CLUB
2101 Webster St., Suite 1300
Oakland, CA 94612
E: nathan.matthews@sierraclub.org

UNITED STATES OF AMERICA

DEPARTMENT OF ENERGY

OFFICE OF FOSSIL ENERGY

IN THE MATTER OF	)	
	)	
Alaska LNG Project LLC	)	FE DOCKET NO. 14-96-LNG

CERTIFICATE OF SERVICE

Pursuant to 10 C.F.R. § 590.107, I hereby certify that on May 15, 2023, I caused the foregoing REQUEST FOR REHEARING OF ORDER GRANTING AUTHORIZATION OF THE ALASKA LNG PROJECT to be served on the applicant and all other parties by electronic mail.

Respectfully submitted this 15th day of May, 2023

s/

Erin Colón
EARTHJUSTICE
325 Fourth Street
Juneau, AK 99801
T: 907.586.2751
E: ecolon@earthjustice.org

Gas Fuel Oil Sustainable Markets Climate Change Climate Solutions

2 minute read · March 10, 2023 3:45 AM AKST · Last Updated 2 months ago

My View Following Saved

[1/2] The cooling tower of Bouchain power station, a 585-megawatt (MW) gas-fired power plant is seen during sunset in Bouchain, northen France, France, December 12, 2022. REUTERS/Pascal Rossignol

1 2

Aa

BRUSSELS, March 10 (Reuters) - The European Union struck a deal on Friday to cut final energy consumption across the bloc by 11.7% by 2030, a goal lawmakers said would help fight climate change and curb Europe's use of Russian fossil fuels.

The deal was agreed after all-night talks between negotiators from EU countries and the European Parliament.

Hitting the targets will require countries to renovate millions of draughty buildings to waste less energy. With most European buildings heated by fossil fuels, the policy is crucial to the EU's efforts to combat climate change.

"This will mean real change for the benefit of the climate and disadvantage of Putin," said Niels Fuglsang, Parliament's lead negotiator.

Negotiators agreed that energy consumed by end-users in the bloc such as households and factories in 2030 should be 11.7% lower than expected use by that date.

But the deal fell short of the 13% target the European Commission last year said the EU would need to help wean countries off Russian fossil fuels faster after Moscow invaded Ukraine.

"It improves the current energy efficiency directive, but not to the extent needed to meet the REPowerEU objectives," Arianna Vitali, Secretary General of the non-profit Coalition for Energy Savings, referring to the EU's targets to quit Russian fossil fuels by 2027.

The EU Parliament had wanted a higher goal of 14%, while some EU countries pushed for a lower 9% - the original EU proposal from 2021, which it changed following Russia's invasion.

The target will be legally binding. Countries will set their own non-binding national goals - but if they do not add up to the 11.7% goal, the European Commission will correct them.

From 2024 to 2030, countries will have to save an average of 1.49% of final energy consumption per year. Countries will have to speed up renovations of publicly-owned buildings, renovating at least 3% of such buildings' total floor area each year.

The deal will now go to the European Parliament and EU countries for a final vote, which is usually a formality that approves the law with no changes.

Reporting by Benoit Van Overstraeten, Charlotte Van Campenhout, Kate Abnett; Editing by Toby Chopra

Our Standards: **The Thomson Reuters Trust Principles.**

Read Next

Transport Fuels
Oil prices fall on stronger dollar, demand fears
11:23 AM AKDT

Exploration & Production
US weekly natgas rig count falls by most since 2016 -Baker Hughes
9:46 AM AKDT

Energy Monitor

Industry April 6, 2023

Why LNG's current boom will only accelerate its ultimate demise

A tight market is putting emerging markets off LNG – and Europe's energy transition may push the continent off gas faster than anticipated.

By Nick Ferris

Nick Ferris
@nichferris

A liquefied natural gas (LNG) tanker approaches port. (Photo by Kiyoshi Ota/Bloomberg via Getty Images)

Russia's invasion of Ukraine triggered extreme tightness in the global liquefied natural gas (LNG) market, as Europe scrambled to secure shipments of the fuel once Russian pipeline gas exports were shut off. European countries ended up importing 121 million tonnes of LNG in 2022, an increase of 60% compared to 2021.

"The huge decline in Russian pipeline gas exports to Europe has effectively shrunk the amount of supply available to the global market, because that gas hasn't got anywhere else to go now," explains Jack Sharples, from the Oxford Institute for Energy Studies. "We are unlikely to see a substantial rebound in pipeline gas supplies from Russia in the next five years, meaning that the market will likely remain tight for some time."

RWE AG

Gunvor SA

View all

The energy policy response to this new status quo means that there are 32 LNG projects that are either under construction or in the planning stage around Europe (with certain facilities claiming they will be able to transport hydrogen by the end of the decade). These facilities are set to be added to the 31 operational LNG import terminals that currently exist in Europe, according to the Institute for Energy Economics and Financial Analysis (IEEFA), a think tank.

There is a similar boom in new facilities on the liquefaction side of the industry, with two multi-billion dollar final investment decisions announced on major US LNG export projects in March 2023 alone. Data tracked by IEEFA anticipates there being vast liquefaction capacity added in the next five years, led by the US and Qatar.

The next few years will see global liquefact

Forecast liquefaction capacity additions, 2023-7 (mtpa)

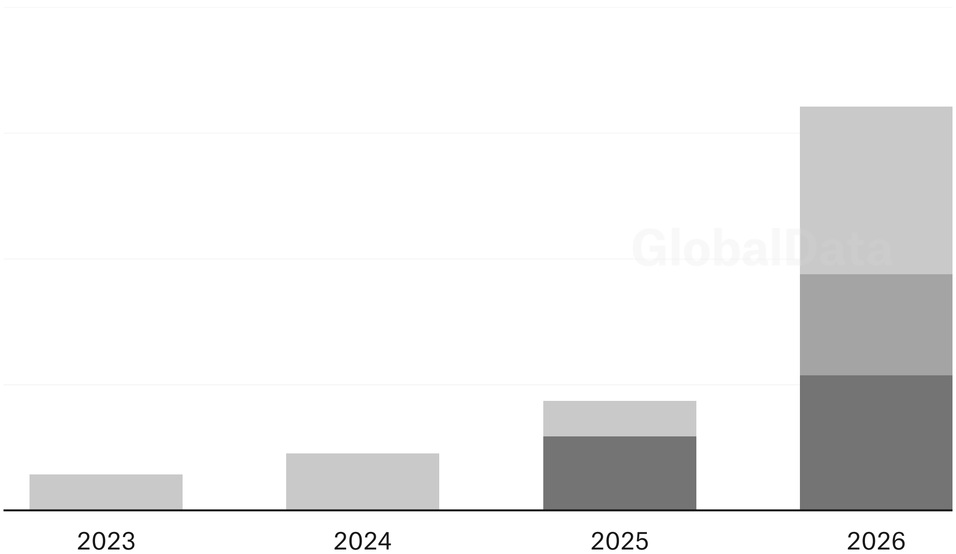

Source: IEEFA

LNG oversupply

With the boom in new LNG project announcements, some experts are beginning to voice the possibility that Europe will soon be oversupplied.

“It is dawning on us that there is likely to be too many LNG facilities in development,” says Henning Gloystein, director of energy, climate and resources at the Eurasia Group, a political risk consultancy. “There’s going to be an enormous glut of facilities in Europe, because so many governments want to have their own facilities to ensure they have security of supply.”

Russia's invasion of Ukraine prompted a flurry of new LNG announcements in Europe

Planned LNG facilities in Europe, February 2023

Regasification Liquefaction

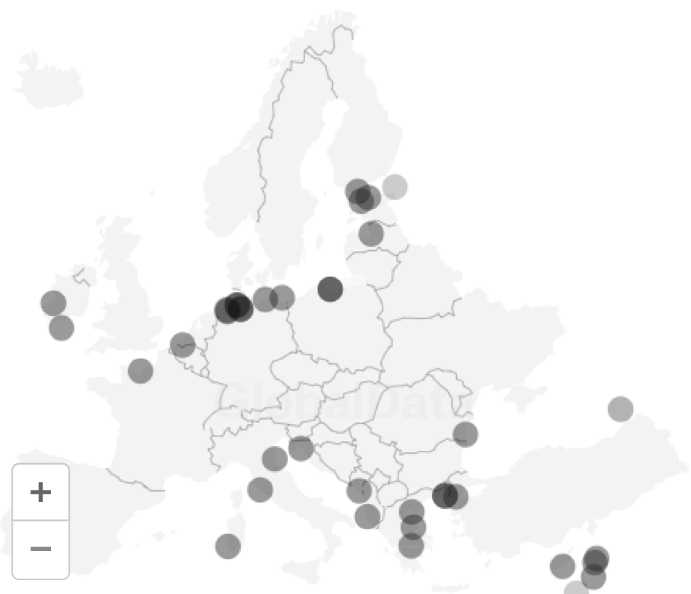

Source: GlobalData

A number of outlets have modelled how big this 'glut' might be. In a March 2023 policy briefing, IEEFA points out that Europe's LNG terminal import capacity could grow from 270 billion cubic metres (bcm) at the end of 2022 to 400bcm by 2030, based on current plans. European demand for LNG is, however, expected to be between 150bcm (IEEFA) and 190bcm (S&P Global Commodity Insights); in other words, less than half of what Europe's import capacity would be.

Elsewhere, a March 2023 report from the NGO Global Energy Monitor highlights Europe's "uncoordinated and costly" LNG build-out, which would "increase the LNG import capacity into the EU by 136% of its current maximum capacity".

"The EU has a gas addiction, and the treatment for this disease is not to build more gas import infrastructure," said Baird Langenbrunner, research analyst for Global Energy Monitor, in a press statement. "The EU needs to reduce fossil fuel demand by continuing to scale up efficiency measures and renewables."

Francesca Gregory, an analyst at *Energy Monitor's* parent company GlobalData, says the current build-out of new LNG facilities "raises concerns about sunken assets".

European LNG demand and import capacity is set to diverge

Europe's LNG imports vs demand (billion cubic metres)

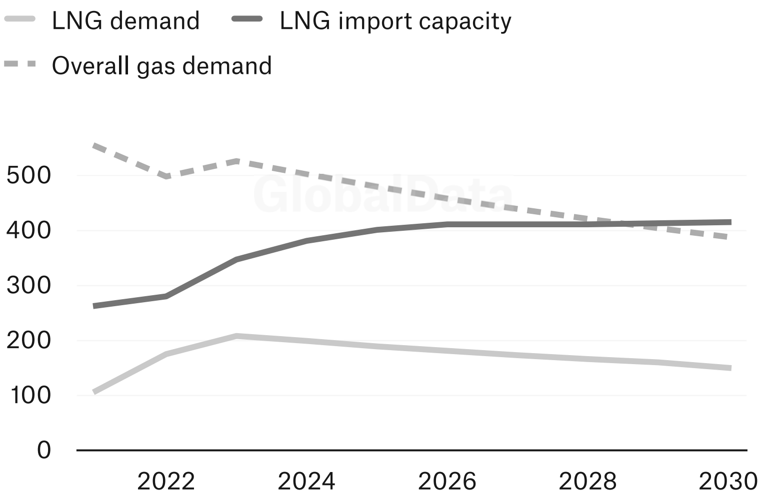

Source: Sources: BP, Dukes, Eurostat, Statista, IEEFA assumptions

On the liquefaction side, Ben Cahill, a senior fellow at US think tank the Center for Strategic and International Studies (CSIS), says "there is definitely a risk that we are overbuilding, with a lot of capacity in the United States and Qatar that might not be used in five years, if you have a rapid diversion away from gas". He points out that in 2022, use rates at liquefaction plants globally remained significantly below full capacity.

Europe: sooner-than-expected fall in LNG demand

Warnings of overcapacity are not only due to an overzealous LNG terminal build-out, but also as a result of the roll-out of low-carbon technologies in Europe, which have been catalysed by Russia's war in Ukraine. The REPowerEU policy package announced in the wake of the invasion aims for 45% European renewable energy by 2030. In practice, this translates into 69% renewable electricity, 32% renewable transport and 60% renewable energy in buildings.

This renewed ambition is already delivering results. Last year, wind and solar generated a record fifth of EU electricity (22%), overtaking natural gas for the first time (20%). Growth in rooftop solar increased by nearly 50% in 2022 year-on-year, while European heat pump sales hit three million units in 2022, representing growth of 41% year-on-year.

"European gas demand was down significantly in 2022, and I think that this trend is only going to continue as currently there are such strong incentives and subsidies for clean technologies and reducing energy consumption," Gloystein says.

Overall European gas demand fell by 13% in 2022

Estimated drivers of change in natural gas demand in power, buildings and industry in the EU, 2022 versus 2021 (%)

Renewables growth Other avoided demand Fuel switching
Weather Energy efficiency gains Production curtailment
Less hydropower Less nuclear

−20 0 20

Power

Buildings

Industry

Source: IEA

It is true that many analysts maintain a bullish market outlook for LNG in Europe even if gas demand declines. Xi Nan, a senior vice president on Rystad Energy's markets research team, says the war in Ukraine has led Rystad to revise down overall European gas demand in 2040 from 410bcm to 330bcm. However, LNG demand in 2040 has been revised up, from 70bcm to 160bcm.

Nan acknowledges that this picture would change, however, if European countries enhance policy sufficiently to meet their long-term net-zero targets.

European clean energy installations have boomed since Russia invaded Ukraine

Growth in heat pump sales, 2022 vs 2021 (%)

Poland	102
Czechia	99
Netherlands	80
Belgium	66
Sweden	60
Austria	59
Germany	53
Finland	52
UK	40
Italy	37
Norway	25
Switzerland	22
Spain	21
Denmark	20
France	20
Portugal	17

Source: European Heat Pump Associaton

The boom in low-carbon technologies in Europe has led other analysts to consider whether LNG demand may actually fall sooner. "It is clear that up to the late 2020s we are going to have a tight LNG market, but after that it really depends how successful Europe is in its energy transition," says Sharples.

IEEFA, meanwhile, is forecasting LNG demand in Europe to increase in 2023, as it did last year, but then begin decreasing straight after.

Lisa Fischer, from the think tank E3G, adds that Europe's [illegible]gy crisis response plan envisages a 50% drop in gas [illegible]nd by 2030. She says that on the current trajectory, Europe would cut 30% of demand, but trends "in the heat pump and solar market are expected to be exponential not linear". This means it is reasonable to expect a significant overshoot of that 30%, to the point that the entire shortfall of former Russian gas supply is accounted for, and there is no room for more LNG growth in Europe.

LNG markets outside Europe

Even if the long-term future of LNG in Europe remains uncertain, the events of the past year have proved highly disruptive to other LNG markets, bringing into doubt the long-term prospects of the fuel in countries like Pakistan and Bangladesh.

"Forecasts for global LNG before the war in Ukraine are characterised by this expectation that we are in the golden age of gas," says Sharples. "Everything was indicating that markets like Pakistan, India and Bangladesh would all grow strongly. There was an understanding that if you are a developing economy, and you are trying to meet climate targets in the medium term, then LNG would be a good option."

In January 2021, for example, Morgan Stanley projected LNG demand in India would grow at 5% per year through 2025, while Southeast Asian demand would grow at an astonishing 13% per year over the same period. Similarly, in 2019 consultancy McKinsey & Company called Asia the "engine for growth in gas demand" globally, forecasting that China, Southeast Asia and South Asia would account for 95% of global LNG demand growth through 2035.

"These and similar projections came on the heels of several years of low and relatively stable LNG prices," explains Clark Williams-Derry from IEEFA. "During that time – roughly 2018–2020 – the global LNG market was wrestling with oversupply. With global LNG supplies seemingly abundant and prices seemingly slated to stay low, many forecasters assumed that strong Asian demand growth was all but guaranteed."

The last two years, however, have seen sky-high LNG prices, earning LNG a reputation as "the globe's most expensive and unreliable energy commodity", says Williams-Derry. Europe has been outbidding key "growth markets" for LNG cargoes, which has caused problems for nations such as Pakistan and Bangladesh that were relying on spot markets for much of their gas.

Most emerging markets in Asia recorded steep declines in LNG imports in 2022 as they switched to cheaper fuels, with a notable exception in the highly gas-dependent economy of Thailand, which was forced to buy expensive LNG from the spot market as it grappled with declining domestic gas production.

High LNG prices in 2022 caused imports to fall in Asian markets

Change in annual LNG imports, 2021 to 2022 (%)

Source: IEEFA

Williams-Derry adds that Asian governments have taken long-term steps to reduce LNG demand and de-emphasise LNG in their national energy plans. Pakistan, for example, recently executed a "U-turn" on its prior energy import policy, with officials asserting: "The nation won't build new power plants that rely on imported coal, LNG or fuel oil over the next decade." Similarly, the Philippines has accelerated policies to improve the investment environment for domestic renewable energy, specifically due to high and volatile fossil fuel commodity prices.

Even Japan and South Korea – who have long been two of the biggest global consumers of LNG – are responding to high LNG prices by turning to other energy sources, says Williams-Derry, with a notable new push for nuclear power.

China – a country which for most of the past decade has ... the engine of global LNG demand growth – showed its willingness to switch fuels in 2022, with LNG imports slumping by 20%.

"China is quite highly spot [price]-reliant and looked at the price and said no thanks," says Gloystein. He adds that the country's energy security strategy now seems to be firmly back in the realms of coal, rather than gas. Indeed, recent analysis from E3G shows that China's coal project pipeline resurged by nearly 50% in the last six months of 2022, taking the total to 250GW.

More generally, China is "shifting to a slower rate of economic growth which is less commodity-dependent", says CSIS's Cahill, making it unlikely that China will return to being a big LNG growth market any time soon.

Long-term contracts insignificant

The surge in LNG prices since 2021 has sparked a trend whereby buyers secure more long-term contracts. "Long-term contracts provide some certainty for both buyers and sellers, by reducing exposure to spot price volatility," explains Cahill. In November 2022, China signed a $60bn, 27-year deal for LNG to be supplied by Qatar, while recent months have also seen a flurry of long-term contracts signed by EU buyers including Engie, Ineos and RWE.

But long-term contracts do not necessarily mean that buyers are locked into their LNG supplies for decades to come. "Long-term contracts mean that you are guaranteed your supply, but they do not guarantee price, which can be tied to gas hub pricing, or the crude oil market," says Sharples. "Over the last year, when the price oo high in India, Pakistan, Bangladesh and China, these countries began reselling their cargos back into the market on a spot basis, which European buyers then acquired."

In effect, then, countries are not obligated to use their contracted supplies because they can copy LNG 'portfolio players' like BP, Shell and Gunvor and sell LNG at whatever price the market is asking for. In that sense, just because more LNG supplies are signed for, does not mean countries are locking themselves into gas for decades to come.

Of course, if LNG demand does fall more rapidly in Europe than many analysts are expecting, there might be a renewed business case for emerging markets to reinvest. "If the market falls back into some kind of balance by the late 2020s, then it could stimulate developing economies to come back into the market in a more serious way," says Sharples.

But the rapid pace at which clean energy technologies are being installed, and the plummeting prices of energy transition technologies like battery storage, means that even in that instance, there is a chance that investing in new LNG infrastructure may no longer have a strong business case.

Poll

1.How will renewable energy companies react to the EU's move to mobilize state aid and sovereign funds for renewable energy companies within the new Net-Zero Industry Act?

- Establish domestic production facilities
- Continue sourcing from other countries
- Increase project investments

Submit

Share this article

M... e Relevant

Features Comment Electrification

its green
credentials

Will Saudi Arabia ever make good on its solar ambitions?

Opinion: Finance is not the choke point to accelerating the energy transition in the Global South

Should Europe mine more to secure its clean energy future?

Inside the global transition to net zero

About Us

Advertise with us

License our content

Contact us

Newsletters

Our marketing solutions

Privacy policy

Terms and conditions

Powered by

AGU100 ADVANCING EARTH AND SPACE SCIENCE

Geophysical Research Letters

RESEARCH LETTER
10.1029/2019GL085651

Key Points:
- The largest earthquakes recorded in northern Alaska (M_w 6.4 and M_w 6.0) occurred on previously unknown active faults
- InSAR and calibrated hypocenter relocations indicate that the faults are conjugate to the Canning displacement zone
- The Canning displacement zone involves a complex fault network and vertical-axis block rotations

Supporting Information:
- Figure S1
- Table S1
- Table S2

Correspondence to:
É. Gaudreau,
gaudreau@uvic.ca

Citation:
Gaudreau, É., Nissen, E. K., Bergman, E. A., Benz, H. M., Tan, F., & Karasözen, E. (2019). The August 2018 kaktovik earthquakes: Active tectonics in northeastern alaska revealed with InSAR and seismology. *Geophysical Research Letters*, *46*, 14,412–14,420. https://doi.org/10.1029/2019GL085651

Received 1 OCT 2019
Accepted 25 NOV 2019
Accepted article online 5 DEC 2019
Published online 23 DEC 2019

The August 2018 Kaktovik Earthquakes: Active Tectonics in Northeastern Alaska Revealed With InSAR and Seismology

É. Gaudreau[1], E. K. Nissen[1], E. A. Bergman[2], H. M. Benz[3], F. Tan[1], and E. Karasözen[4]

[1]School of Earth and Ocean Sciences, University of Victoria, Victoria, British Columbia, Canada, [2]Global Seismological Services, Golden, CO, USA, [3]U.S. Geological Survey, Golden, CO, USA, [4]Department of Geophysics, Colorado School of Mines, Golden, CO, USA

Abstract The largest earthquakes recorded in northern Alaska (M_w 6.4 and M_w 6.0) occurred ~6 hr apart on 12 August 2018, in the northeastern Brooks Range. The earthquakes were captured by Sentinel-1 interferometric synthetic aperture radar (InSAR) satellites and Earthscope Transportable Array seismic data, giving insight into the little-known active tectonic processes of Arctic Alaska, obscured until recently by sparse data availability. In this study, InSAR modeling, teleseismic back projections, calibrated hypocentral relocations, and regional moment tensor solutions resolve two previously unknown, SSW dipping right-lateral fault segments. These are the first active faults identified as conjugate to the NE trending sinistral Canning displacement zone directly to the west, which is therefore a more complex zone of diffuse faulting than previously thought. The northeastern Brooks Range has been characterized as an area of low to moderate seismic hazard, but these earthquakes illustrate the potential for larger, possibly destructive events in a region earmarked for rapid resource development.

Plain Language Summary The largest earthquakes recorded in northern Alaska (magnitude 6.4 and magnitude 6.0) occurred ~6 hr apart on 12 August 2018. Few active faults are mapped in this region despite widespread seismicity, and the current tectonic setting remains unclear due to limited available data and the remote location. We use satellite radar images and seismic data to resolve two previously unknown fault segments, along which the magnitude 6.4 earthquake ruptured unilaterally eastward. This fault geometry demonstrates that the Canning displacement zone, the main tectonic feature in the area, is a more complex zone of diffuse faulting than previously thought. These results are also important for reassessing seismic hazard by illustrating the potential for damaging earthquakes on seemingly aseismic faults.

1. Introduction

The M_w 6.4 earthquake that occurred on 12 August 2018, ~80 km SW of Kaktovik, Alaska, is the largest ever recorded in the Brooks Range or its foreland basin to the north (Figure 1). The second largest earthquake in this region, a M_w 6.0 aftershock, occurred ~6 hr later, ~35 km to the east (Figure 1b). More than 6,000 aftershocks recorded within 1 year of the mainshock form a WNW-ESE striking trend at the northern margin of the eastern Brooks Range, beneath the Sadlerochit Mountains (Ruppert & West, 2020). The only known faults in this area are mapped as pre-Quaternary and do not align with the 2018 seismicity (Koehler, 2013).

Despite widespread seismicity in Arctic Alaska, few active faults are mapped, and currently published GPS velocities are sparse (Snay et al., 2016). The current tectonic setting is equivocal (Finzel et al., 2015; Fuis et al., 2008; Haeussler, 2008; Koehler, 2013; Leonard et al., 2008; Mazzotti et al., 2008), but a relatively recent increase in seismic and geodetic data available from this area, with the deployment of the USArray in Alaska since 2014 and launch of the Sentinel-1 satellite pair in 2014 and 2016, permit a more detailed characterization of active tectonics in the Brooks Range.

We use Sentinel-1 interferometric synthetic aperture radar (InSAR) data and elastic dislocation modeling to characterize the fault geometry and slip distribution of the 2018 Kaktovik sequence, which are the most northerly earthquakes ever imaged in this way. We use seismic back projections, calibrated hypocentral relocations and regional moment tensors (RMTs) to map the mainshock rupture and aftershock activity over time and space. These new constraints are used to reassess regional tectonics and provide new information for seismic hazard assessments in an area of keen interest to the petroleum industry for oil drilling.

10.1029/2019GL085651

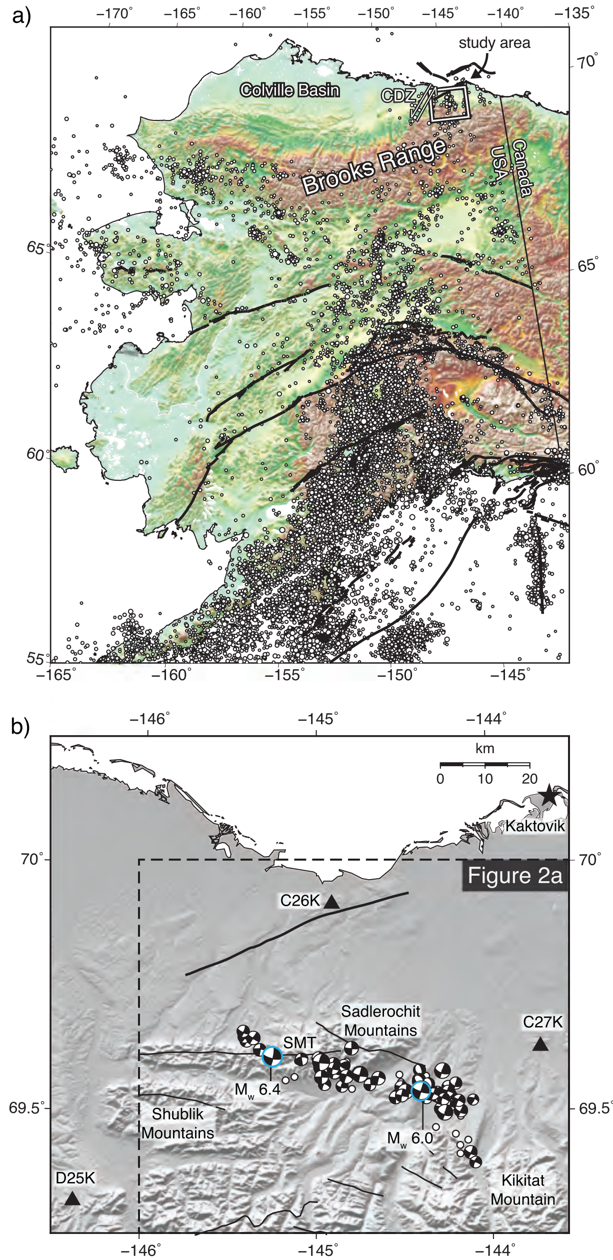

Figure 1. (a) Digital elevation model (DEM) of Alaska (USGS 30 ARC-second Global Elevation Data, GTOPO30; https://doi.org/10.5066/F7DF6PQS) with location of epicenters prior to the 2018 Kaktovik sequence in USGS Comcat Catalog (white circles; https://earthquake.usgs.gov/earthquakes/search/) and Quaternary faults are bold black lines (Koehler, 2013). Study area is located in the white rectangle. CDZ: Canning displacement zone. (b) Shaded-relief DEM (Porter et al., 2018) with regional moment tensor solutions for the 2018 Kaktovik mainshock and M_w 3.5+ aftershocks from the following 5 months plotted at the relocated epicenter locations. White circles represent additional relocated epicenters. Pre-Quaternary faults are thin black lines (Koehler, 2013). SMT: south dipping Sadlerochit Mountains thrust. Location of closest seismic stations used for calibrated relocations are indicated by black triangles.

2. Geologic and Tectonic Setting

The Brooks Range (Figure 1a) is underlain by a thick crustal root where the Moho is mapped to depths of ~50 km (compared to ~30–35 km in central Alaska) and the lithosphere is up to ~200 km thick (Fuis et al., 1997; Jiang et al., 2018; Miller et al., 2018; O'Driscoll & Miller, 2015; Ward and Lin, 2018). Mantle flow or northward motion of the Yakutat indentor are thought to be driving current tectonic activity (Finzel et al., 2015; Mazzotti & Hyndman, 2002; Mazzotti et al., 2008). According to moment tensor solutions, the northeastern Brooks Range is currently dominated by a transtensional tectonic regime, in contrast to transpression south of the Brooks Range, where the lithosphere is weaker and deforming at a faster rate (Jiang et al., 2018; Leonard et al., 2008; O'Driscoll & Miller, 2015). The main mapped tectonic feature in the northeastern Brooks Range is the Canning displacement zone (CDZ), a NE-SW left-lateral diffuse deformation zone first identified by Grantz et al. (1983) located between the northeastern Brooks Range and the North Slope Deep Magnetic High (Figure 1a), a domain of mechanically strong crust to the west (Saltus et al., 1999).

The Brooks Range is composed of multiple arc and continental margin terranes, which accreted onto the North American margin at the onset of the Brookian orogeny in the latest Jurassic-Cretaceous (Moore, 1992; Moore et al., 1997). The first phase of the Brookian orogeny resulted in thin-skinned deformation in the Brooks Range south of the study area (Moore & Box, 2016) and was followed by middle-Late Cretaceous extension at the southern margin of the Brooks Range (Amato & Miller, 2004; Hannula et al., 1995). A Paleogene episode of thick-skinned deformation formed large-scale duplex structures in the northeastern Brooks Range and is coeval with accretionary deformation in the forearc in southern Alaska and right-lateral strike-slip faulting in the interior (Fuis et al., 2008; Wallace, 1992). This synchronicity suggests that these structures may be linked by a detachment (Moore & Box, 2016).

The 2018 Kaktovik earthquakes occurred beneath the Sadlerochit Mountains, at the northern margin of the northeastern Brooks Range (Figure 1). The geology of these mountains is dominated by Neoproterozoic dolomite overlain by Cambrian to Ordovician limestone (Molenaar et al., 1987, and references therein). Most of the mapped tectonic features in this area formed during the later reactivation of the Brookian orogeny in the Paleogene, expressed on the surface as north vergent listric thrusts and east-west trending folds in the Sadlerochit Mountains and adjacent Kikitat and Shublik Mountains (Moore et al., 1997; O'Sullivan et al., 1993; Wallace & Hanks, 1990).

3. InSAR Analysis

3.1. InSAR Data

The European Space Agency's Sentinel-1 satellites captured the coseismic surface deformation of the 2018 Kaktovik earthquakes. Two 12-day descending track interferograms and one 42-day ascending track interferogram (the shortest repeat time available on ascending orbits) were used in this study, obtained from the automated SARVIEWS program (Meyer et al., 2016) (Figure 2a). Since available interferogram pairs capture the coseismic deformation from both the M_w 6.4 and M_w 6.0 events, in this section we discuss the cumulative coseismic deformation without specifying the causative earthquake.

The radar line-of-sight (LOS) coseismic deformation appears as three lobes in the ascending and descending track interferograms, with one northern lobe and two southern ones (Figure 2a). In all interferograms, peak displacements are greatest in the southern lobes, which are LOS range increase in descending interferograms and range decrease in the ascending interferogram. The northern lobes exhibit the opposite sense of motion, consistent with right-lateral faulting along an approximately E-W trend.

3.2. InSAR Modeling

To characterize the causative faulting, the LOS displacements were downsampled using a quadtree algorithm (Jónsson et al., 2002) and the reduced data were inverted for slip on rectangular dislocations embedded within a uniform elastic half-space with Lamé parameters $\mu = \lambda = 3.2 \times 10^{10}$ Pa (Okada, 1985; Wright et al., 1999). The single ascending data set was given equal weighting to the two descending data sets in the inversion. We used Powell's algorithm (Press et al., 1992) to solve for the best-fit fault strike, dip, rake, slip, surface projection center point, length, and top and bottom depths, avoiding local minima by repeating the inversion 500 times with starting parameters sampled randomly from the ranges given in supporting information Table S1 (Wright et al., 1999).

Our preferred slip model was determined using the two-step methodology outlined by Elliott et al. (2012). In the first step, fault geometry was established using a small number of rectangular, uniform slip model faults. A single rectangular fault cannot reproduce the three-lobed fringe pattern (supporting information Table S2 and Figure S1); however, two faults provide a good visual fit (root-mean-square residual displacements of 1.20×10^{-2} m). Both en echelon segments strike ESE, involve right-lateral slip, and dip toward the SSW, explaining the greater deformation observed in the southern lobes of the interferograms (supporting information Figure S2 and Table S3). The ~15 km-long western segment is steeper (82°) than the ~12 km-long eastern segment (64°). Uncertainties in these uniform slip parameters were estimated using

10.1029/2019GL085651

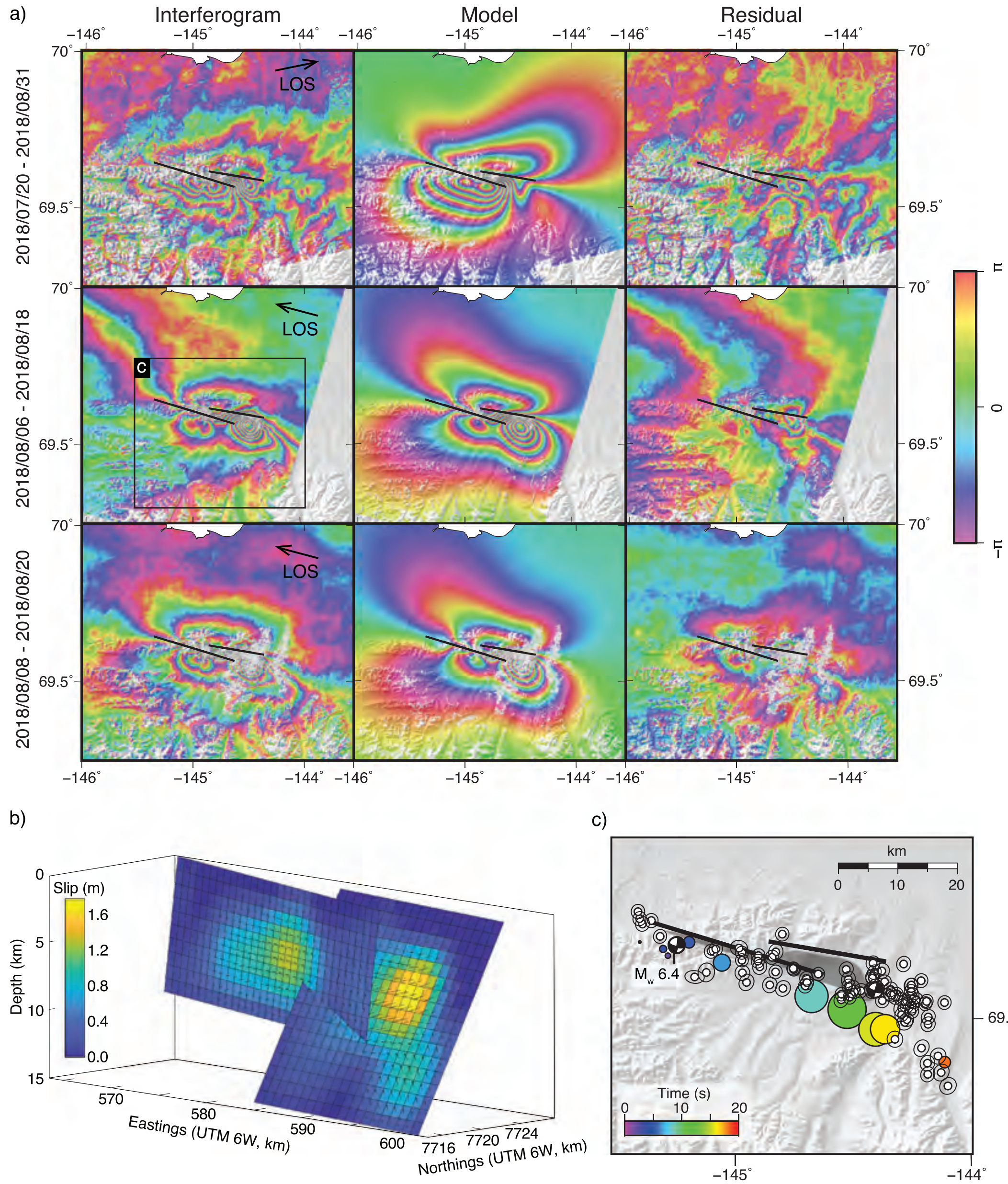

Figure 2. (a) Sentinel-1 interferograms, models based on distributed slip with variable rake on two fault planes, and residuals superimposed onto topography from ArcticDEM (Porter et al., 2018). Surface projections of the modeled, buried fault segments are in black. (b) Slip distribution on the fault planes with variable rake. Each fault segment measures 1 km × 1 km. (c) The model slip area is shaded, with the mainshock and aftershocks superimposed (white circles with 95% confidence ellipses). Colored circles represent back projected 0.2- to 2-Hz energy for the M_w 6.4 mainshock, colored by time since rupture initiation and scaled by relative energy. The average rupture velocity is 2.6 km/s.

Monte Carlo inversions of 100 data sets perturbed with realistic noise (Elliott et al., 2012). Strike, rake, length, and center point easting and northing are well constrained for both faults, with relative standard deviations <9% (supporting information Figures S3 and S4). Dip is less well constrained for the eastern fault, but a shallower angle than that of the western fault is resolved. The results also show that the rupture did not reach the surface; thus, slip, fault width, minimum depth, maximum depth, and seismic moment are less well constrained (relative standard deviations >20%) due to strong trade-offs between these parameters. We also explored the possibility of a listric fault—as the Sadlerochit Mountains thrust is believed to be (O'Sullivan & Wallace, 2002)—which would extend the rupture area farther south. Listric slip models were created using a steeper slip plane near the surface and a deeper segment with a shallower dip; the results were very similar for each model that was created, one such model is described in supporting information Tables S5 and S6. In all cases, slip predominantly occurs on the steeper fault segments near the surface; thus, the slip does not extend farther south in the listric models. Therefore, slip on two steep fault segments remains our preferred model.

In the second step, we solved for the distribution of slip and rake across the two fault planes (Funning et al., 2005). The western and eastern fault lengths were increased to 30 and 20 km, respectively; their bottom depths increased to 10 and 15 km and were subdivided into 1-km × 1-km patches. We solved for the rake and slip magnitude of each patch using a Laplacian smoothing operator to ensure realistic slip gradients (Figure 2). Allowing for distributed slip and rake reduced the root-mean-square residual displacements to 1.066×10^{-2} m, though notable residuals remain between the two faults and at the eastern termination of the eastern fault (Figure 2a). Rake is consistently right lateral on both faults. Slip is concentrated between depths of 2.7 and 11.0 km on the eastern fault, peaking at 1.8 m at 6-km depth. Slip is concentrated between 1.5 and 9.5 km of slip on the western fault, peaking at 1.3 m at 4-km depth.

The InSAR moments for the western and eastern faults are 2.798×10^{18} and 3.259×10^{18} N m, respectively, and the combined moment magnitude from slip on both faults is 6.5. For comparison, the U.S. Geological Survey W-phase moment magnitude for this event is estimated at 6.4.

4. Seismological Constraints

4.1. Calibrated Earthquake Relocations

We reevaluated hypocenter locations of the Kaktovik mainshock and 109 of the best-recorded aftershocks using the *mloc* calibrated earthquake relocation technique (Bergman & Solomon, 1990; Walker et al., 2011). This minimizes location bias by assuming that raypaths of events clustered in space and recorded at common stations sample roughly the same portion of Earth, such that travel time differences more likely reflect the relative epicenter locations within the cluster rather than the 3-D velocity structure. The *mloc* method splits the relocation into two independent steps, each utilizing a specific, tailored set of arrival time data (Jordan & Sverdrup, 1981). First, relative locations of each hypocenter within the cluster are estimated from differences in arrival times picked at common stations at all distances. Second, the absolute location of the hypocentroid—the geometric mean of the cluster—is calculated based on the observed travel times at local distances, since nearby stations will have accumulated less travel time error. This step is a direct calibration—an indirect calibration (i.e., using an independent data set to constrain the absolute location of the hypocentroid) may be used in the event that a cluster of events cannot be reliably calibrated using travel times. The azimuthal coverage is not ideal in this case since only one regional station (C26K) is located north of the cluster.

Using a direct calibration, the relocated mainshock hypocenter lies ~7 km south of the western model fault plane, as do most aftershocks. Three hypotheses for this discrepancy were explored: (1) a timing error at the only station north of the cluster (C26K), exerting a strong influence on the latitude of the relocated cluster; (2) lateral heterogeneities in crustal seismic velocity, notably those north of the cluster in the Colville basin (Fuis et al., 1997; Moore et al., 1994); and (3) the fault that ruptured was listric; thus, the true slip patch could extend farther south than that shown in Figure 2c. As described in section 3.2, listric fault models were tested; however, the slip in these models is concentrated on the steep parts of the fault, which would not extend the slip patch farther south. On the other hand, the InSAR data are mostly sensitive to shallow slip, thus it is possible that some unresolvable component of slip occurred on deeper parts of the faults that have a shallower dip. As for the possibility of a timing error, clock quality at station C26K was assessed using the IRIS timeseries Web Service (https://service.iris.edu/irisws/timeseries/docs/). From these data, we conclude that time errors are not large enough to affect the location of the calibrated cluster. Moreover, an unreasonably large timing error of 1.2 s at station C26K is required to shift the cluster northward to correct the discrepancy with the InSAR model; thus, a heterogeneous crust is a more likely explanation.

An indirect calibration was performed using the InSAR model faults due to the likelihood of strong lateral heterogeneities in the crust biasing the epicenters ~7 km to the south (Fuis et al., 1997). The mainshock and M_w 6.0 aftershock were used as calibration events (Figure 2c and supporting information Table S7). The origin times for calibration were set so that the arrival times at the local station in the Brooks Range, D25K, agreed with a typical crustal model. The M_w6.4 mainshock nucleated close to the western end of the western model fault, implying that it ruptured unilaterally eastward. The M_w6.0 aftershock hypocenter is near the eastern end of the eastern model fault, among a concentration of smaller events.

There was also an increase in seismic activity southwest of the study area starting in late July 2018 and peaking in October 2018 (Ruppert & West, 2020). These events will be referred to as the Niviak cluster, after the nearby Niviak Pass. Some of these events cluster in multiple NW-SE trends similar to the Kaktovik cluster, while others form more diffuse groups. We investigate whether both clusters are related to the larger-scale left-lateral motion of the CDZ by relocating the 155 best-recorded earthquakes in this area using a direct calibration (supporting information Figure S5).

4.2. RMTs

RMT solutions were calculated for the mainshock and 87 best-recorded aftershocks. The RMTs were computed using the same Green's functions, fit function, and filtering strategy found in Herrmann et al. (2011). Unlike the grid search approach of Herrmann et al. (2011), we used a linear inversion to solve for the moment tensor components and assumed a pure double-couple source. For events M_w 4.0 or smaller, waveform filtering is typically done in the passband 16–50 s, while for larger events waveform filtering is typically done in the passband 20–50 s. For all events, we used the central U.S. velocity model of Herrmann et al. (2011), an observational distance range 0–500 km, and three-component waveforms that included body waves and surface waves. RMT solutions were computed in the depth range 2–24 km in increments of 1 km. The RMT solution for each event is the one with the best fit as a function of depth. All RMT solutions were computed using the single event locations found in the U.S. Geological Survey earthquake catalog (https://earthquake.usgs.gov/earthquakes/map/). Given the good azimuthal distribution of stations surrounding the source region and longer period signals used in the inversion, we expect little differences in computed mechanisms whether using the single or multiple locations in this study.

The large majority of RMTs are consistent with E-W right-lateral strike-slip motion. The southward dips (mostly >60°) of the E-W nodal planes are in agreement with the dips of the modeled fault segments (Figures 1b and S6 and Table S8). Centroid depths range from 0–22.7 km, with most <10 km. The mainshock has a centroid depth of 2.2 km.

4.3. Teleseismic Back Projection

We applied a phase-weighted relative back projection method (Tan et al., 2019) to track the rupture energy in time and space. This provides a measure of relative energy release, rather than true moment release, since the amplitudes are normalized and the phases are used as a weighting factor. The phase-weighted stacking emphasizes both large amplitudes and the coherency of the signal, reducing biases introduced by incoherent signals with large amplitudes.

We performed back projections for both the M_w 6.4 mainshock and M_w 6.0 aftershock using teleseismic stations from the contiguous United States, and the teleseismic travel times are estimated using the IASP91 reference model (Kennett & Engdahl, 1991). The 10-s window that was used gave rise to artifacts in the form of multiple energy radiators at the same latitude and longitude, but with slightly different source times. Of the energy radiators at the same coordinates, the result with the median source time was chosen and the rest discarded. Other array configurations were considered; however, they had less suitable distance and azimuth ranges (Tan et al., 2019). Relocated epicenters from section 4.1 were used to constrain the location of each rupture. For the mainshock, the back projection indicates linear rupture propagation from WNW to ESE at an average velocity of 2.6 km/s (Figures 2c and S7a and Table S9). Coherent back projected energy encompasses the full length of the InSAR model faults, with peak energy release occurring after ~10 s on the eastern fault. Though close to the limit of what a back projection can resolve, the M_w 6.0 aftershock also seems to have propagated from WNW to ESE and thus likely occurred on the same eastern fault segment rather than on a conjugate fault (supporting information Figure S7b and Table S9).

5. Discussion

5.1. Faulting in the 2018 Kaktovik Sequence

The InSAR modeling suggests rupture of two en echelon, ESE striking right-lateral faults within the Sadlerochit Mountains (Figure 2a). This is supported by distributions of back projected energy and aftershocks, which are both oriented WNW-ESE, and their RMT solutions (Figures 1b and 2c). The lack of decorrelation between the northern and southern lobes in the 6–18 August 2018 interferogram (Figure 2a) suggests

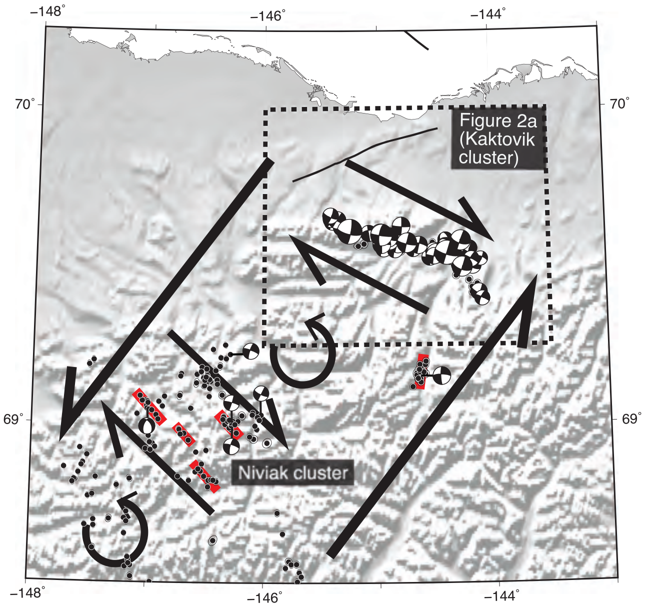

Figure 3. Relocated epicenters for the Kaktovik mainshock and best-recorded aftershocks from the following 12 months. The Niviak cluster includes the seismic events southwest of the Kaktovik sequence. Some of these events potentially highlight similar conjugate structures to the CDZ (highlighted in red). The arrows demonstrate a simplified version of the block rotation model for northeastern Alaska where the primary faults are NE-SW oriented left lateral, and the secondary faults are NW-SE-oriented right lateral.

that neither segment ruptured to the surface, in agreement with our InSAR slip model. The mainshock centroid depth of 2.2 km is much shallower than both the relocated focal depth of 11 km and most of the slip in the InSAR model (Figure 2b). The hypocenter depth is located near the bottom of the rupture, as is often the case (Karasözen et al., 2016). We interpret that this discrepancy reflects uncertainties of ∼5 km in RMT centroid depths (Herman et al., 2014).

Back projection results indicate that the M_w 6.4 mainshock ruptured both faults, with greater relative energy release on the eastern segment, consistent with the high slip patch in the InSAR slip model (Figure 2). Relative energy mapped at 18 s is located ∼15 km SE of the modeled rupture area (Figure 2c), and this most likely constitutes a "swimming artifact" since this is approximately the same azimuth as the seismic stations used in the contiguous United States (Koper et al., 2012), though we cannot rule out an off-fault, near-instantaneous aftershock (Fan & Shearer, 2016). The M_w 6.0 aftershock probably enlarged the eastern slip patch or ruptured a shallower part of the fault (supporting information Figure S7). Smaller aftershocks concentrate in this same area, with a number located farther east and south, a spatial bias in the direction of mainshock rupture propagation that may indicate a component of dynamic triggering (Gomberg et al., 2003).

The western fault cuts obliquely across the Paleogene Sadlerochit Mountains thrust, mapped as a south dipping listric thrust in this area (O'Sullivan & Wallace, 2002). However, the eastern fault (strike 98°) is parallel to the eastern segment of the Sadlerochit Mountains thrust; thus, it is possible that the steep, shallower part of this listric fault was reactivated. The 2018 Kaktovik earthquakes may have ruptured a combination of unknown and known faults. The steep, southward nodal plane dip angles in nearly all of the Kaktovik focal mechanisms also hint that the structural fabric of the Sadlerochit Mountains may have influenced the geometry of the strike-slip rupture plane.

5.2. Regional Tectonics

The Kaktovik earthquakes exposed the first known active faults in the northeastern Brooks Range that are conjugate to the NE-SW left-lateral CDZ directly to the west (Figures 1a and 2). Previous moment tensor solutions have been interpreted as representing NNE-SSW left-lateral faulting based on the known slip sense of the CDZ. However, diffuse zones of shearing are often associated with conjugate strike-slip faults (Cunningham, 2005; Ghods et al., 2015; Soumaya et al., 2018), and the faults in the Sadlerochit Mountains are optimally oriented with respect to the local maximum horizontal principal stress for right-lateral slip (Hanks et al., 2000).

To explore whether faulting of this orientation may be widespread within the eastern Brooks Range, we performed an additional relocation of the Niviak cluster (Figure 3). The results highlight several discrete concentrations of events along similar NW-SE trends, which presumably represent similar faults conjugate to the CDZ. These right-lateral faults must rotate counterclockwise around vertical axes in order to accommodate overall left-lateral motion along the main CDZ trend (Kim et al., 2004).

The northeastern Brooks Range exhibits low seismic deformation rates and is underlain by a thick Moho (∼50-km depth) and thick and strong lithosphere (Fuis et al., 2008; Jiang et al., 2018; Leonard et al., 2008; O'Driscoll & Miller, 2015). We interpret that faults involved in the Kaktovik sequence and the CDZ compose a diffuse zone of active faulting that accommodates slow strain between two mechanically strong lithospheric domains: the NE Brooks Range to the east and the North Slope Deep Magnetic High to the west (Jiang et al., 2018; O'Driscoll & Miller, 2015; Saltus et al., 1999). This has parallels with other diffuse deformation zones such as in northwestern Iran (Ghods et al., 2015), the Mongolian Altai (Cunningham, 2005), and the Alboran-Rif domain in northwestern Africa (Soumaya et al., 2018), many of which exhibit low levels of instrumental seismicity, and low strain rates, but are capable of hosting large earthquakes. The

Kaktovik earthquakes thus highlight the importance of reassessing the seismic hazard of areas of low internal deformation.

6. Conclusion

The 12 August 2018 M_w 6.4 and M_w 6.0 Kaktovik earthquakes occurred on previously unknown active right-lateral faults that are conjugate to the CDZ, striking ESE. The M_w 6.4 mainshock nucleated on the western fault and propagated unilaterally eastward onto the eastern fault, where most of the slip and energy release occurred. The M_w 6.0 aftershock likely further extended the slip area of the mainshock. A direct calibration results in hypocenters systematically biased to the south by >7 km, possibly due to the 1-D velocity model and less-than-ideal azimuthal coverage used in the relocations. Using an indirect calibration, relocated mainshock and aftershock hypocenters lie on the rupture area of the InSAR-derived model faults. These earthquakes are the largest-magnitude events recorded in northern Alaska and the first determined as conjugate to the CDZ. Other areas with potential NW-SE right-lateral faulting have been identified from relocated earthquake trends south of the study area. Together, these right-lateral faults may accommodate the overall left-lateral motion of the CDZ by rotating about vertical axes. The relatively low seismicity and deformation rates in the northeastern Brooks Range reflect its thickened crust and lithosphere, but the Kaktovik earthquakes nevertheless highlight the potential for damaging earthquakes on seemingly aseismic faults.

Acknowledgments

É. G. was supported through a Graduate Scholarship from the University of Victoria and an Alexander Graham Bell Canada Graduate Scholarship from the Natural Sciences and Engineering Research Council of Canada (NSERC). E. N. was supported through NSERC Discovery Grant 201704029, a Canada Research Chair, and grants from the Canada Foundation for Innovation and B. C. SAR interferograms were made using European Space Agency Copernicus Sentinel data [2018] and the University of Alaska Fairbanks SARVIEWS web portal (Meyer et al. 2017; http://sarviews-hazards.alaska.edu/Earthquakes/), which is funded by the National Aeronautics and Space Administration (NASA). Seismic back projection data were obtained from Incorporated Research Institutions for Seismology (https://ds.iris.edu/wilber3/find&urluscore;event) and data used in the relocations and regional moment tensors were gathered from the U.S. Geological Survey (USGS) National Earthquake Information Center (NEIC; https://earthquake.usgs.gov/earthquakes/map/). Computer programs used in the paper are available from the references cited in the text. We also thank two anonymous reviewers and Morgan Moschetti (USGS) for helpful comments.

References

Amato, J., & Miller, E. (2004). Geologic map and summary of the evolution of the Kigluiak Mountains gneiss dome, Seward Peninsula, Alaska. In D. L. Whitney, C. Teyssier, & C. S. Siddoway (Eds.), *Gneiss domes in orogeny*, Geological Society of America Special Paper 380 (Vol. 380, pp. 295–306). Boulder, CO: Geological Society of America.

Bergman, E. A., & Solomon, S. C. (1990). Earthquake swarms on the Mid-Atlantic Ridge: Products of magmatism or extensional tectonics. *Journal of Geophysical Research*, *95*(B4), 4943–4965. https://doi.org/10.1029/JB095iB04p04943

Cunningham, D. (2005). Active intracontinental transpressional mountain building in the Mongolian Altai: Defining a new class of orogen. *Earth and Planetary Science Letters*, *240*, 436–444. https://doi.org/10.1016/j.epsl.2005.09.013

Elliott, J. R., Nissen, E. K., England, P. C., Jackson, J. A., Lamb, S., Li, Z., et al. (2012). Slip in the 2010-2011 Canterbury earthquakes, New Zealand. *Journal of Geophysical Research: Solid Earth*, *117*, B03401. https://doi.org/10.1029/2011JB008868

Fan, W., & Shearer, P. M. (2016). Local near instantaneously dynamically triggered aftershocks of large earthquakes. *Science*, *353*, 1133–1136.

Finzel, E. S., Flesch, L. M., Ridgway, K. D., Holt, W. E., & Ghosh, A. (2015). Surface motions and intraplate continental deformation in Alaska driven by mantle flow. *Geophysical Research Letters*, *42*, 4350–4358. https://doi.org/10.1002/2015GL063987

Fuis, G. S., Moore, T. E., Plafker, G., Brocher, T. M., Fisher, M. A., Mooney, W. D., et al. (2008). Trans-Alaska Crustal Transect and continental evolution involving subduction underplating and synchronous foreland thrusting. *Geology*, *36*(3), 267–270. https://doi.org/10.1130/G24257A.1

Fuis, G. S., Murphy, J. M., Lutter, W. J., Moore, T. E., Bird, K. J., & Christensen, N. I. (1997). Deep seismic structure and tectonics of northern Alaska: Crustal-scale duplexing with deformation extending into the upper mantle. *Journal of Geophysical Research*, *102*(B9), 20,873–20,896. https://doi.org/10.1029/96JB03959

Funning, G. J., Parsons, B., Wright, T. J., Jackson, J. A., & Fielding, E. J. (2005). Surface displacements and source parameters of the 2003 Bam (Iran) earthquake from Envisat advanced synthetic aperture radar imagery. *Journal of Geophysical Research: Solid Earth*, *110*, B09406. https://doi.org/10.1029/2004JB003338

Ghods, A., Shabanian, E., Bergman, E., Faridi, M., Donner, S., Mortezanejad, G., & Aziz-Zanjani, A. (2015). The Varzaghan-Ahar, Iran, Earthquake Doublet (M_w 6.4, 6.2): implications for the geodynamics of northwest Iran. *Geophysical Journal International*, *203*(1), 522–540. https://doi.org/10.1093/gji/ggv306

Gomberg, J., Bodin, P., & Reasenberg, P. A. (2003). Observing earthquakes triggered in the near field by dynamic deformations. *Bulletin of the Seismological Society of America*, *93*, 118–138.

Grantz, A., Dinter, D. A., & Biswas, N. N. (1983). Map, cross sections, and chart showing late Quaternary faults, folds, and earthquake epicenters on the Alaskan Beaufort Shelf, U.S. Geological Survey Miscellaneous Investigations Series Map I-1182-C, 1:500,000 scale.

Haeussler, P. J. (2008). An overview of the neotectonics of interior Alaska: Far-field deformation from the Yakutat Microplate collision. *Washington DC American Geophysical Union Geophysical Monograph Series*, *179*, 83–108. https://doi.org/10.1029/179GM05

Hanks, C., Parker, M., & Jemison, E. (2000). *Borehole breakouts and implications for regional in situ stress patterns of the northeastern North Slope, Alaska*, Alaska Division of Geological & Geophysical Surveys Professional Report 119C. https://doi.org/10.14509/2685.

Hannula, K. A., Miller, E. L., Dumitru, T. A., Lee, J., & Rubin, C. M. (1995). Structural and metamorphic relations in the southwest Seward Peninsula, Alaska: Crustal extension and the unroofing of blueschists. *Geological Society of America Bulletin*, *107*(5), 536–553. https://doi.org/10.1130/0016-7606(1995)107<0536:SAMRIT>2.3.CO;2

Herman, M. W., Herrmann, R. B., Benz, H. M., & Furlong, K. P. (2014). Using regional moment tensors to constrain the kinematics and stress evolution of the 2010–2013 Canterbury earthquake sequence, South Island, New Zealand. *Tectonophysics*, *633*, 1–15.

Herrmann, R. B., Benz, H., & Ammon, C. J. (2011). Monitoring the earthquake source process in North America. *Bulletin of the Seismological Society of America*, *101*(6), 2609–2625.

Jiang, C., Schmandt, B., Ward, K. M., Lin, F.-C., & Worthington, L. L. (2018). Upper Mantle Seismic Structure of Alaska From Rayleigh and S Wave Tomography. *Geophysical Research Letters*, *45*(19), 10,350–10,359. https://doi.org/10.1029/2018GL079406

Jónsson, S., Zebker, H., Segall, P., & Amelung, F. (2002). Fault slip distribution of the 1999 M_w 7.1 Hector Mine, California, earthquake, estimated from satellite radar and GPS measurements. *Bulletin of the Seismological Society of America*, *92*(4), 1377–1389.

Jordan, T. H., & Sverdrup, K. A. (1981). Teleseismic location techniques and their application to earthquake clusters in the south-central Pacific. *Bulletin of the Seismological Society of America*, *71*(4), 1105–1130.

Karasözen, E., Nissen, E., Bergman, E. A., Johnson, K. L., & Walters, R. J. (2016). Normal faulting in the Simav graben of western Turkey reassessed with calibrated earthquake relocations. *Journal of Geophysical Research: Solid Earth*, *121*, 4553–4574. https://doi.org/10.1002/2016JB012828

Kennett, B. L. N., & Engdahl, E. R. (1991). Traveltimes for global earthquake location and phase identification. *Geophysical Journal International*, *105*, 429–465. https://doi.org/10.1111/j.1365-246X.1991.tb06724.x

Kim, Y.-S., Peacock, D. C. P., & Sanderson, D. J. (2004). Fault damage zones. *Journal of Structural Geology*, *26*(3), 503–517. https://doi.org/10.1016/j.jsg.2003.08.002

Koehler, R. (2013). Quaternary faults and folds (QFF), http://maps.dggs.alaska.gov/qff. http://doi.org/10.14509/24956.

Koper, K. D., Hutko, A. R., Lay, T., & Sufri, O. (2012). Imaging short-period seismic radiation from the 27 February 2010 Chile (M_w 8.8) earthquake by back-projection of P, PP, and PKIKP waves. *Journal of Geophysical Research: Solid Earth*, *117*, B02308. https://doi.org/10.1029/2011JB008576

Leonard, L. J., Mazzotti, S., & Hyndman, R. D. (2008). Deformation rates estimated from earthquakes in the northern Cordillera of Canada and eastern Alaska. *Journal of Geophysical Research: Solid Earth*, *113*, B08406. https://doi.org/10.1029/2007JB005456

Mazzotti, S., & Hyndman, R. D. (2002). Yakutat collision and strain transfer across the northern Canadian Cordillera. *Geology*, *30*, 495. https://doi.org/10.1130/0091-7613(2002)030<0495:YCASTA>2.0.CO;2

Mazzotti, S., Leonard, L. J., Hyndman, R. D., & Cassidy, J. F. (2008). Tectonics, dynamics, and seismic hazard in the Canada-Alaska Cordillera. *Washington DC American Geophysical Union Geophysical Monograph Series*, *179*, 297–319. https://doi.org/10.1029/179GM17

Meyer, F. J., Webley, P. W., Dehn, J., Arko, S. A., McAlpin, D. B., & Gong, W. (2016). The SARVIEWS project: Automated SAR processing in support of operational near real-time volcano monitoring. In *AGU Fall Meeting Abstracts*. San Francisco, CA: American Geophysical Union.

Miller, M. S., O'Driscoll, L. J., Porritt, R. W., & Roeske, S. M. (2018). Multiscale crustal architecture of Alaska inferred from P receiver functions. *Lithos*, *10*(2), 267–278. https://doi.org/10.1130/L701.1

Molenaar, C., Mull, C., & Swauger, D. (1987). Geologic features of Ignek Valley and adjacent mountains, northeastern Alaska. In M. L. Hill (Ed.), *Centennial Field Guide* (Vol. 1, pp. 473–478). Boulder, CO: Cordilleran Section of the Geological Society of America.

Moore, T. (1992). The Arctic Alaska superterrane. In D. Bradley & C. Dusel-Bacon (Eds.), *Geologic studies in Alaska by the U.S. Geological Survey, 1991: Geological Survey Bulletin, Geological Survey Bulletin* (Vol. 2041, pp. 238–244). Washington, DC: U.S. Geological Survey.

Moore, T. E., & Box, S. E. (2016). Age, distribution and style of deformation in Alaska north of 60° N: Implications for assembly of Alaska. *Tectonophysics*, *691*, 133–170. https://doi.org/10.1016/j.tecto.2016.06.025

Moore, T. E., Wallace, W. K., Bird, K. J., Karl, S. M., Mull, C. G., & Dillon, J. T. (1994). *Geology of northern Alaska, The Geology of North America* (Vol. G-1, pp. 49–140). Geological Society of America: Boulder, CO.

Moore, T. E., Wallace, W. K., Mull, C. G., Adams, K. E., Plafker, G., & Nokleberg, W. J. (1997). Crustal implications of bedrock geology along the Trans-Alaska Crustal Transect (TACT) in the Brooks Range, northern Alaska. *Journal of Geophysical Research: Solid Earth*, *102*(B9), 20,645–20,684. https://doi.org/10.1029/96JB03733

O'Driscoll, L. J., & Miller, M. S. (2015). Lithospheric discontinuity structure in Alaska, thickness variations determined by Sp receiver functions. *Tectonics*, *34*(4), 694–714. https://doi.org/10.1002/2014TC003669

O'Sullivan, P., Green, P., Bergman, S. C., Decker, J., Duddy, I., et al. (1993). Multiple phases of Tertiary uplift and erosion in the Arctic Wildlife Refuge, Alaska, revealed by apatite fission track analysis. *AAPG Bulletin*, *77*(3), 359–385.

O'Sullivan, P. B., & Wallace, W. K. (2002). Out-of-sequence, basement-involved structures in the Sadlerochit Mountains region of the Arctic National Wildlife Refuge, Alaska: Evidence and implications from fission-track thermochronology. *Geological Society of America Bulletin*, *114*(11), 1356–1378. https://doi.org/10.1130/0016-7606(2002)114<1356:OOSBIS>2.0.CO;2

Okada, Y. (1985). Surface deformation due to shear and tensile faults in a half-space. *Bulletin of the Seismological Society of America*, *75*(4), 1135–1154.

Porter, C., Morin, P., Howat, I., Noh, M.-J., Bates, B., Peterman, K., et al. (2018). ArcticDEM, doi: https://doi.org/10.7910/DVN/OHHUKH, accessed 5 December 2018.

Press, W. H., Teukolsky, S. A., Vetterling, W. T., & Flannery, B. P. (1992). *Numerical recipes in C: The art of scientific computing*. Cambridge: Cambridge University Press.

Ruppert, N. A., & West, M. E. (2020). The impact of USArray on earthquake monitoring in Alaska. *Seismological Research Letters*. https://doi.org/10.1785/0220190227

Saltus, R. W., Hudson, T. L., & Connard, G. G. (1999). A new magnetic view of Alaska. *GSA Today*, *9*(3), 1–6.

Snay, R. A., Freymueller, J. T., Craymer, M. R., Pearson, C. F., & Saleh, J. (2016). Modeling 3-D crustal velocities in the United States and Canada. *Journal of Geophysical Research: Solid Earth*, *121*, 5365–5388. https://doi.org/10.1002/2016JB012884

Soumaya, A., Ben Ayed, N., Rajabi, M., Meghraoui, M., Delvaux, D., Kadri, A., et al. (2018). Active faulting geometry and stress pattern near complex strike-slip systems along the Maghreb Region: Constraints on active convergence in the western Mediterranean. *Tectonics*, *37*(9), 3148–3173. https://doi.org/10.1029/2018TC004983

Tan, F., Ge, Z., Kao, H., & Nissen, E. (2019). Validation of the 3-D phase-weighted relative back projection technique and its application to the 2016 M_w 7.8 Kaikōura earthquake. *Geophysical Journal International*, *217*(1), 375–388. https://doi.org/10.1093/gji/ggz032

Walker, R. T., Bergman, E. A., Szeliga, W., & Fielding, E. J. (2011). Insights into the 1968-1997 Dasht-e-Bayaz and Zirkuh earthquake sequences, eastern Iran, from calibrated relocations, InSAR and high-resolution satellite imagery. *Geophysical Journal International*, *187*(3), 1577–1603. https://doi.org/10.1111/j.1365-246X.2011.05213.x

Wallace, W. (1992). *Detachment folds above a passive-roof duplex: An example from the northeastern Brooks Range, Alaska*. Alaska Division of Geological & Geophysical Surveys - Public Data File 92-9. Fairbanks, AK. https://doi.org/10.14509/1533

Wallace, W., & Hanks, C. (1990). Structural provinces of the Northeastern Brooks Range, Arctic National Wildlife Refuge, Alaska. *AAPG Bulletin*, *74*(7), 1100–1118.

Ward, K. M., & Lin, F.-C. (2018). Lithospheric structure across the Alaskan cordillera from the joint inversion of surface waves and receiver functions. *Journal of Geophysical Research: Solid Earth*, *123*, 8780–8797. https://doi.org/10.1029/2018JB015967

Wright, T. J., Parsons, B. E., Jackson, J. A., Haynes, M., Fielding, E. J., England, P. C., & Clarke, P. J. (1999). Source parameters of the 1 October 1995 Dinar (Turkey) earthquake from SAR interferometry and seismic bodywave modelling. *Earth and Planetary Science Letters*, *172*, 23–37.

Resolving Northern Alaska Earthquake Sequences Using the Transportable Array and Probabilistic Location Methods

Steven J. Gibbons*[1], Natalia A. Ruppert[2], Ezgi Karasözen[2], Kasey Aderhold[3], and Ian Dickson[4]

Abstract

Between 2014 and 2017, almost 200 new seismic stations were installed in Alaska and northwestern Canada as part of the EarthScope USArray Transportable Array. These stations currently provide an unprecedented capability for the detection and location of seismic events in regions with otherwise relatively sparse station coverage. Two interesting earthquake sequences in 2018 and 2019 in the northeastern Brooks Range were exceptionally well recorded because of this deployment. First is the aftershock sequence of the M_w 6.4 and M_w 6.0 Kaktovik earthquakes of 12 August 2018, the largest earthquakes recorded to date in the region. The second is the Niviak swarm, southwest of the Kaktovik sequence. Since July 2018, >4000 earthquakes between magnitudes 1 and 4.3 have been recorded across a region exceeding 5000 km^2. We explore how the Bayesloc probabilistic multiple seismic-event location algorithm can better resolve features of these two sequences, exploiting the large numbers of readings that the improved station coverage provides from events down to magnitudes below 2. The Bayesloc calculations consistently move events in the Kaktovik sequence a few kilometers to the northeast, providing an almost linear east-southeast-striking southern limit to the aftershock zone. Analysis of the Bayesloc joint probability distribution of corrections to travel-time predictions indicate that anomalously fast wave propagation to the southwest is likely the most significant contribution to the seismic-event mislocation. The joint relocations are more consistent with Interferometric Synthetic Aperture Radar–inferred coseismic displacement than the network location estimates. The Bayesloc relocation of the Niviak events confirms that the earthquakes are distributed between many distinct clusters of seismicity that have clearer spatial separation following the relocation. The probabilistic relocations motivate both double-difference studies to better resolve clustered seismicity at the smallest spatial scales and systematic multiple event relocation studies to calculate structure and travel-time corrections over larger scales.

Cite this article as Gibbons, S. J., N. A. Ruppert, E. Karasözen, K. Aderhold, and I. Dickson (2020). Resolving Northern Alaska Earthquake Sequences Using the Transportable Array and Probabilistic Location Methods, *Seismol. Res. Lett.* **91**, 3028–3038, doi: 10.1785/0220200142.

Introduction

Between 2004 and 2015, the EarthScope USArray Transportable Array (TA) of ~400 digital broadband seismometers was deployed from west to east across the "lower 48" states, with stations remaining in place for 1.5–2 yr before being moved to a new location to the east. Deployment in Alaska and northwest Canada began in 2014 after initial test installs, and the full network was operational by the end of the 2017 field season. A comprehensive review of the deployment is provided by Busby and Aderhold (2020). Whereas the permanent networks are concentrated in the most seismically active regions of Alaska, the TA provides a remarkably uniform coverage of the remaining territory. Ruppert and West (2020) discuss the lowering of the seismic detection thresholds that the additional stations provide and draw attention to two extensive seismic sequences in the relatively aseismic regions, which could only be characterized to the degree they are because of the TA presence. The first is the aftershock sequence of the 12 August 2018 M_w 6.4 Kaktovik earthquake; the second is the 2018–2019 eastern Brooks Range sequence (Fig. 1).

Seismicity in northeastern Alaska is distributed over an ~200-kilometer-wide, ~500-kilometer-long zone that trends

1. Norges Geotekniske Institutt, Oslo, Norway; 2. Alaska Earthquake Center, Geophysical Institute, University of Alaska Fairbanks, Fairbanks, Alaska, U.S.A.; 3. Kasey Aderhold, IRIS, Washington, D.C., U.S.A.; 4. University of Colorado Denver, Denver, Colorado, U.S.A.

*Corresponding author: steven.gibbons@ngi.no

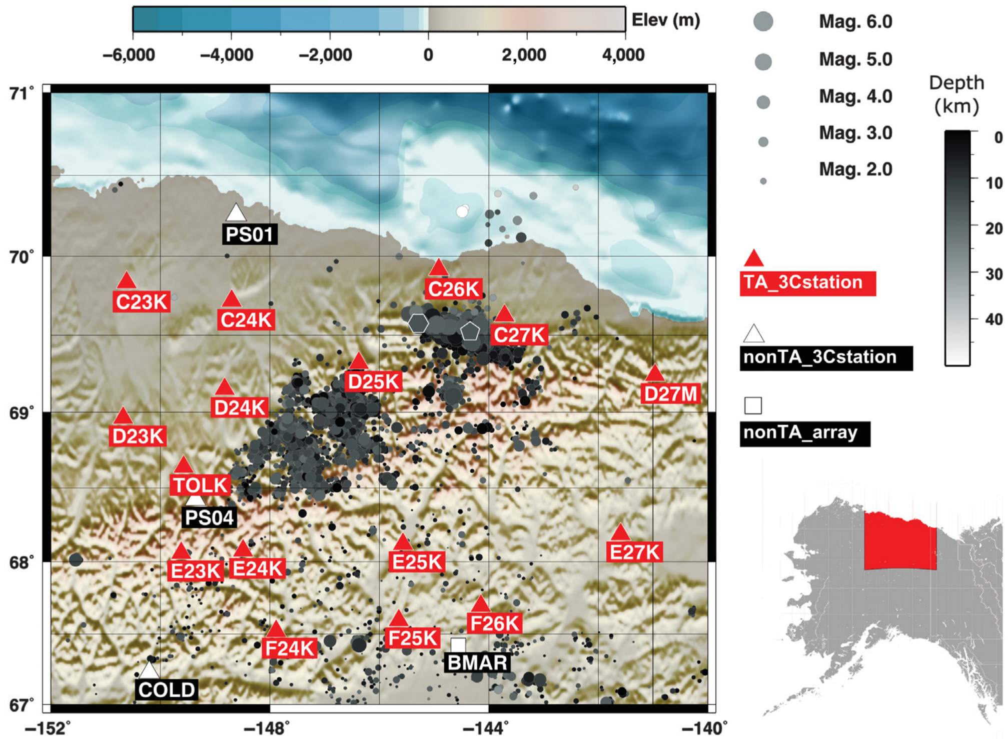

Figure 1. Subset of the earthquake catalog from the Alaska Earthquake Center (AEC; 2017–2019), including the aftershocks of the 12 August 2018 Kaktovik sequence and the 2018 eastern Brooks Range swarm together with the closest available stations. BMAR is the Burnt Mountain seismic array, consisting of five short-period vertical-component seismometers within an aperture of ~5 km. The M_w 6.0 and M_w 6.4 earthquakes on 12 August 2018 are marked with five- and six-sided polygons, respectively.

southwest to northeast. Whereas the northern limit of this zone extends into the Beaufort Sea, its southern end is truncated by the Tintina fault, a major right-lateral strike-slip fault that extends eastward into Canada. Earthquakes have been recorded in this region since regional monitoring began in the early 1970s (Gedney *et al.*, 1977; Estabrook *et al.*, 1988). Although the seismic record until recently has been poor, moderate-size earthquakes have been recorded in the region for decades, albeit with highly variable accuracy. There has been one magnitude ≥5 earthquake every few years on average. The earthquakes have occurred throughout the entire region, generally do not follow well-defined linear trends, and sometimes present swarm-like behavior for months to years before returning to its previous state.

There are no mapped active faults between the Tintina fault to the south and the offshore faults in the Beaufort Sea to the north (Koehler *et al.*, 2012). Given the extensive seismicity in the area, however, this apparent lack of active faults may be attributed to limited geologic field mapping, which is due in large part to the remoteness of the area and the challenges this presents for undertaking geologic mapping studies. Crustal seismicity of northeastern Alaska has long been recognized as an earthquake hazard; it has been attributed to far-field deformation from the subduction of the Pacific plate compounded by collision of the Yakutat block by a variety of studies (e.g., Mazzotti and Hyndman, 2002; Leonard *et al.*, 2008; Mazzotti *et al.*, 2008).

Gaudreau *et al.* (2019) provide a thorough study of the August 2018 earthquake and aftershock sequence both with seismological and Interferometric Synthetic Aperture Radar (InSAR) data. They find that seismological location estimates of the mainshock and numerous aftershocks are a few kilometers to the south of the InSAR-inferred fault plane and discuss hypotheses for the discrepancy. These include the possibility of instrumental timing errors, which could be significant given the unfavorable azimuthal station coverage. They conclude that heterogeneous velocity structure in the crust is a more likely explanation. In this study, we try to resolve the issue by applying the Bayesloc probabilistic multiple-event location algorithm (Myers *et al.*, 2007), which has been shown to provide improved locations for clustered seismicity, partly by mitigating the influence of velocity heterogeneity. This procedure provides both probabilistic hypocenter and origin-time estimates for the earthquakes and estimates of bias and uncertainty in travel-time predictions. We present Bayesloc relocations of earthquakes in both sequences and provide justification as to why we can have confidence in the results.

Aftershocks of the 12 August 2018 M_w 6.4 Kaktovik Earthquake

Figure 2a displays locations of events in the Alaska Earthquake Center (AEC) catalog likely to be associated with the 12 August 2018 Kaktovik earthquake sequence based on location and time. Earthquakes in this catalog are located by automatic detection algorithms and later reviewed event by event by human analysts who correct erroneous autopicks and add more phase picks that the autodetectors may have missed. We apply Bayesloc, which locates multiple events simultaneously in a probabilistic framework, to see if structure can be identified in the aftershock distribution not found in the network locations. The motivation

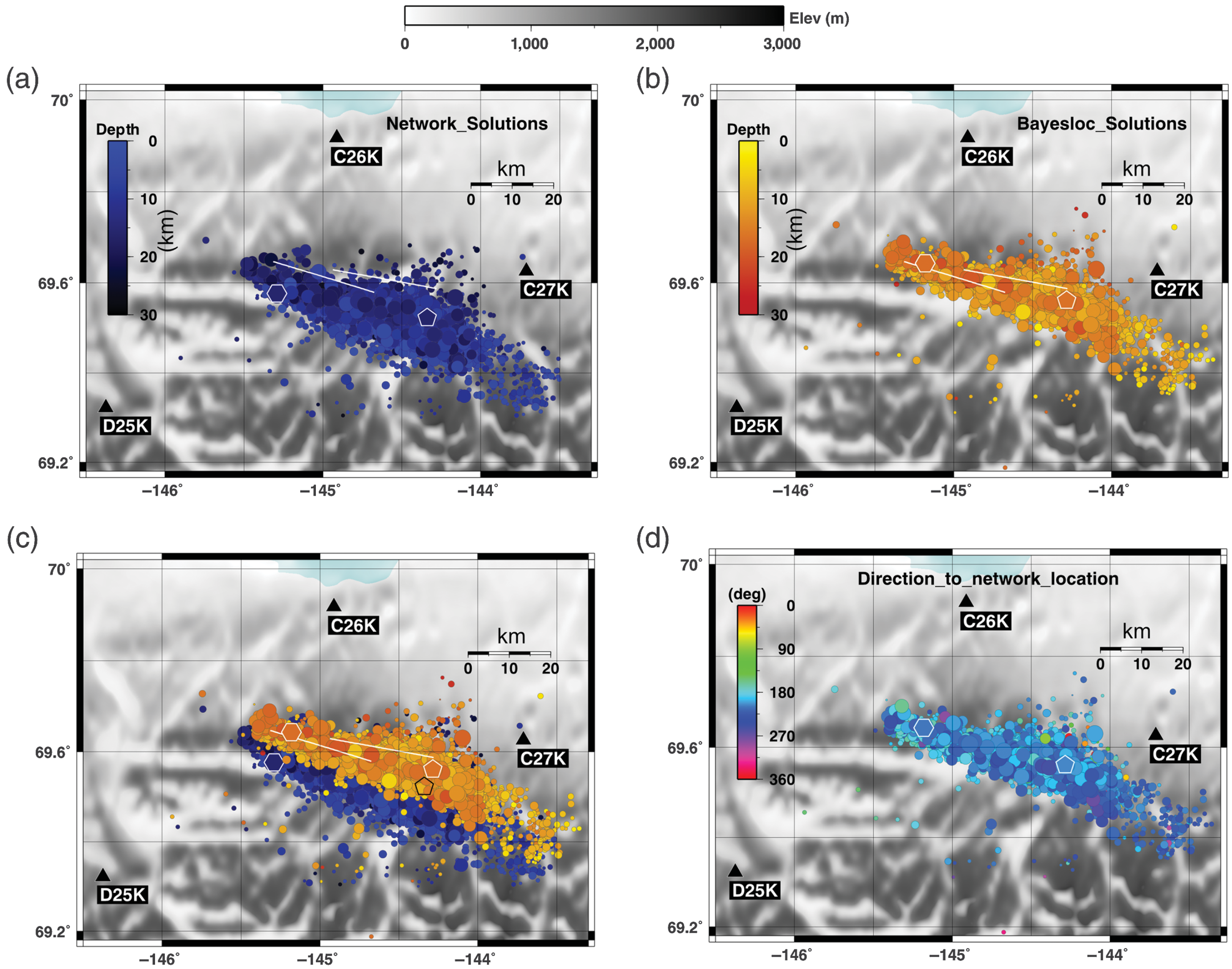

Figure 2. All events in the catalog of the AEC for the region displayed in the time period 2018–2019 (a) as reported in the AEC catalog, (b) as relocated by Bayesloc using only the arrival picks from the AEC catalog, and (c) with the relocated hypocenters plotted over the catalog hypocenters with the same color scales. The symbols in (d) are drawn at the locations of the relocated hypocenters with a color indicating the direction from the relocated epicenter to the catalog epicenter. Blue colors indicate that the catalog locations for almost all events lie to the southwest of the relocated events. The M_w 6.0 and M_w 6.4 earthquakes on 12 August 2018 are marked with five- and six-sided polygons, respectively. In (c), the catalog location of the M_w 6.0 earthquake is marked with a black pentagon outline. White lines in (a–c) indicate the surface projections of the Interferometric-Synthetic-Aperture-Radar-modeled buried fault segments from Gaudreau *et al.* (2019).

is that Bayesloc seeks a joint probability distribution of all event hypocenters, origin times, arrival-time uncertainty, and corrections to travel-time predictions and may be able to compensate for geologic heterogeneity and consequent deficiencies in the underlying velocity model used. In contrast, the network solutions are forced to assume zero-mean Gaussian distributions for all uncertainties and are therefore unable to identify bias in any parameters common to multiple events. Gibbons and Kværna (2017) applied Bayesloc to the aftershocks of the October 2005 Kashmir earthquake and found far more structured event clusters than could be resolved in the single-event network solutions. In that case study, the primary cause of mislocation in the network solutions was deemed likely to be anomalous travel times to stations at regional distances. The probabilistic estimates for travel-time corrections transformed the clouds of aftershocks to align convincingly with the strike of the surface rupture. Bayesloc was applied by Hayes *et al.* (2015) for accurate relocations of aftershocks from the April 2015 M_w 7.8 Gorkha, Nepal, earthquake by Nealy *et al.* (2017) to constrain the 2008 Wells, Nevada, sequence, and by Pyle *et al.* (2015) to provide accurate event locations for seismicity in Rock Valley, Nevada.

Whereas the relocation of the Kashmir aftershocks involved a significant repicking of arrivals from raw waveform data, it is important to note here that all Bayesloc solutions presented use exactly the same set of arrivals as the AEC network location estimates. A 1D velocity model was prescribed based on profiles presented in Fuis *et al.* (1997), and travel-time tables were calculated for *Pg*, *Pn*, *Pb*, *Sg*, *Sn*, and *Sb* phases (see Storchak *et al.*, 2003) for distances up to around 15°, as applicable, for input to the Bayesloc program. Additional travel-timetables containing the travel time for the first-arriving *P* and first-arriving *S* phases were also calculated and labeled *P*1 and *S*1. Following the practice of Gibbons *et al.* (2017), relocating seismicity along the North Atlantic spreading ridge, we performed a parallel calculation using a different basis velocity model (in this case, ak135, Kennett *et al.*, 1995) to confirm that the final joint probability distribution of event hypocenters was largely stable to small changes in the underlying 1D velocity model. As seen in Figure 1, there are stations ranging from a few tens of kilometers to many hundreds of kilometers, so the identification of the first-arriving phase will change with distance. There may be uncertainty regarding the identification of the first-arriving phase in some regions. All first *P* and *S* arrivals from the AEC bulletin were initially labeled *P*1 and *S*1, and we exploit the Bayesloc probabilistic identification of phase labels (Myers *et al.*, 2009) to attribute the most likely label to each arrival given the most probable location.

Figure 2b shows the distribution of mean event hypocenters from a run of Bayesloc with no priors on the event locations and a total of 40,000 iterations. The diffuse southern boundary of the network solutions becomes a sharper edge with an east-southeast strike direction, a few kilometers north of the southernmost epicenters from the AEC catalog. The contrast between the two sets of event locations is more easily seen in Figure 2c in which the relocations are plotted on top of the catalog location estimates. The northern boundary of the aftershock cloud remains diffuse and largely unchanged in the relocations. We display the surface projections of the InSAR-modeled western and eastern fault segments from Gaudreau *et al.* (2019) in each of panels (a–c). In panel (a), the network location estimates almost all lie to the south of these two lines. In panel (b), the southern extent of the relocated events is approximately parallel to the western fault, and the northern extent of the relocated events is approximately parallel to the eastern fault. In Figure 2d, we illustrate how the events in different regions of the aftershock zone are moved. Essentially, all events are shifted in a northeasterly direction. Events in the western part of the aftershock zone may be relocated more in a northerly direction and events in the eastern part of the aftershock zone in a more easterly direction, although the pattern is quite consistent. The relocations obtained using the ak135 model as a basis are essentially identical to those displayed in Figure 2.

In Figure 3, we display both the distance and direction of each relocation. The majority of the larger events are relocated to the northeast by between 2 and 10 km. Events that are relocated in a significantly different direction are low-magnitude events and may be subject to far poorer location constraints to begin with due to fewer phase-arrival readings and poorer azimuthal coverage. Figure 3 demonstrates that although the overall change of shape of the aftershock cloud is significant, the relocations of the individual events are modest. Given the station geometry, the relocated epicenters lie well within the formal uncertainty ellipses of the AEC catalog locations. The elliptical distribution of the relocation vector end points provides an indication of consistency between the two sets of location estimates. Whereas an identical set of phase-arrival times is used to construct both sets of origin estimates, the two location procedures are entirely independent; no information about the catalog event locations is used as prior information for the Bayesloc calculation.

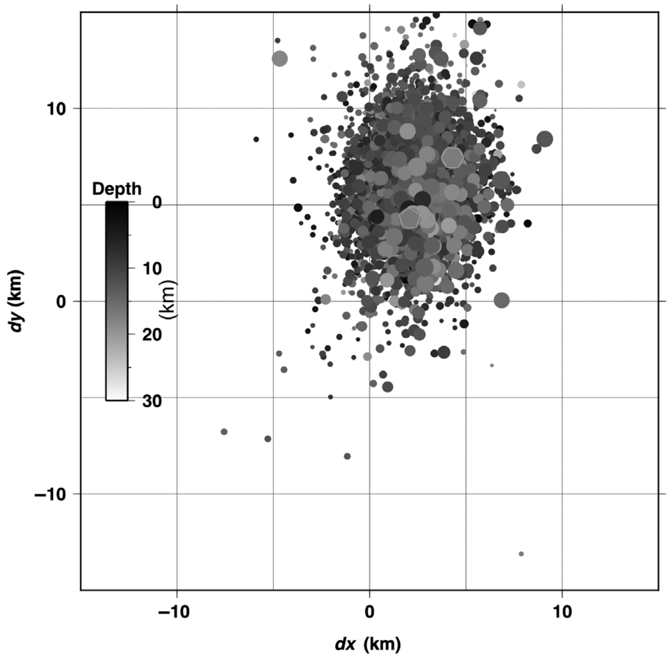

Figure 3. Relocation vectors for all events displayed in Figure 2. We define the catalog location of each event to be at the origin and plot the relocated hypocenter relative to the catalog hypocenter. The size of the symbol is proportional to the event magnitude. The M_w 6.0 and M_w 6.4 earthquakes on 12 August 2018 are marked with five- and six-sided polygons, respectively.

Validating and Interpreting Probabilistic Earthquake Relocations

The underlying algorithm in Bayesloc is iterative. It is instructive to examine the progress of the solution from start to end understand why the resulting pattern of hypocenter estimates may provide a higher confidence image of the seismicity. The latitude, longitude, depth, and origin times of the events; the uncertainties associated with the arrival-time estimates; and

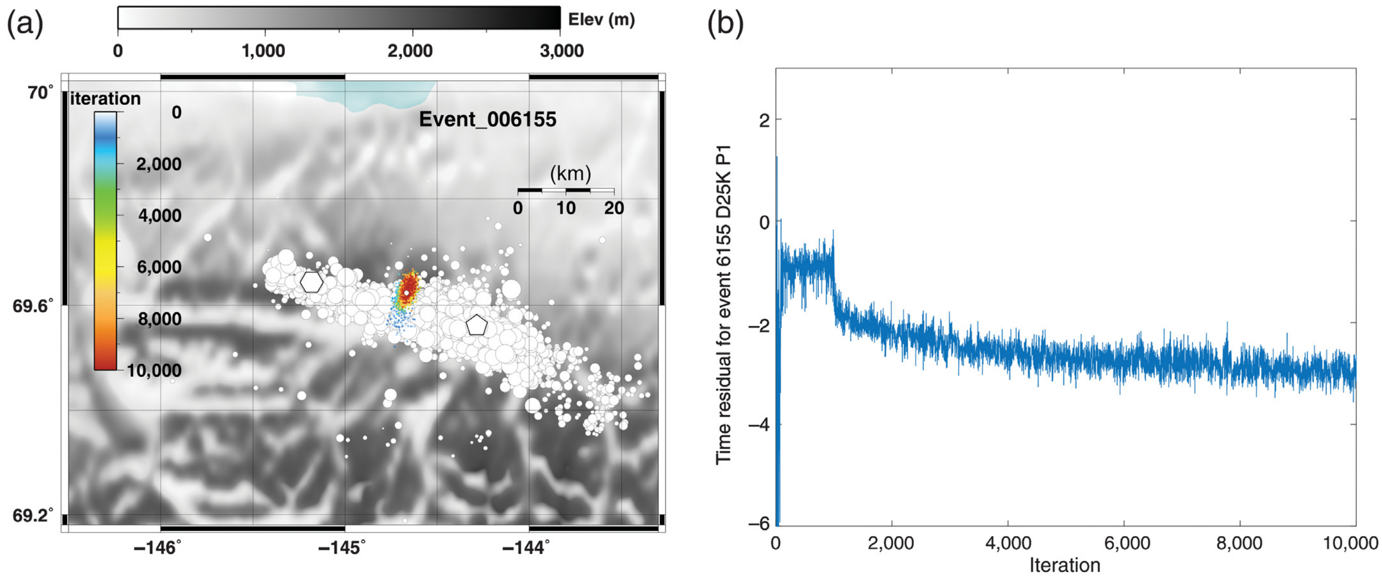

Figure 4. Evolution of the location estimate for a single earthquake in the sequence as a function of iteration number in the Monte Carlo Markov chains of the Bayesloc program. White symbols in (a) display the mean epicenters for all events in the sequence, and small colored symbols indicate the epicenter location for event 6155 colored according to the iteration. (b) The observed minus predicted travel-time residual with respect to the 1D velocity model for the first *P* arrival at station D25K. The M_w 6.0 and M_w 6.4 earthquakes on 12 August 2018 are marked with five- and six-sided polygons, respectively.

corrections to the travel-time estimates for each of the arrivals form a large parameter space for a given input. The Monte Carlo Markov chains in the Bayesloc algorithm explore this parameter space to try to converge to a solution that best supports the full set of observations. The process starts with no knowledge of the true parameters (unless prior information is available and provided) and probes stochastically through different alternatives, identifying favorable choices.

In Figure 4a, we see as plain white symbols the final mean epicenters of all the events. Superimposed onto this image are the location estimates at each iteration for a single selected event, displayed as small colored dots to indicate the iteration number. (Only the first 10,000 iterations are displayed because changes in the epicenter estimates do not change significantly beyond that number.) Blue dots in Figure 4a indicate trial epicenters for this event in the earlier iterations, and red dots indicate trial epicenters toward the end. The most important features in the model parameter space in the presence of geologic or velocity structure heterogeneity are the corrections to travel-time predictions. Gibbons *et al.* (2017) demonstrated very large travel-time residuals for individual regional station and phase combinations that were consistent from event-to-event over wide geographical regions: biases far larger than the uncertainty in the arrival-time estimates themselves. This is why we plot (in Fig. 4b) the observed minus predicted travel-time residual of a given phase arrival at a given station for every hypocenter and origin-time estimate for this event as a function of the iteration number. The convergence (or otherwise) of this parameter and the corresponding parameters for other phase and station combinations provide an indicator as to whether the process has converged on a solution. This offers an insight into how the event locations might relate to local velocity structure.

The station and phase combination displayed in Figure 4b is the first *P*-arrival at station D25K, the closest station southwest of the aftershock zone. Before describing the evolution of this time residual with iteration number, it is worth taking the time to consider what values of this parameter would imply about the velocity structure between the aftershock zone and this station. How would the values be affected by an analyst reading error, or a clock error? If we assume that the analyst placed the arrival-time estimate very accurately, and that the instrumental time stamp is correct, then a zero value of the observed minus predicted travel-time residual means that our baseline 1D velocity model provides an accurate representation of the geologic structure along these paths. A negative value of this residual would mean that the picked arrival time is before the predicted arrival time and therefore that the seismic waves travel faster along the path than the model predicts. Similarly, a positive value would imply slower rock than the model predicts. If the analyst placed the arrival-time estimate too late on the seismogram, this would move the curve up uniformly; this offset would be constant for all hypocenter and origin-time estimates. A too-early arrival-time estimate would move the curve down uniformly. We have a corresponding curve for every event in our dataset for which a first *P*-arrival at station D25K has been picked: potentially several thousand such curves. The travel-time prediction correction for this phase and station combination, as part of the final joint probability distribution, would consider all the curves generated.

A timing error on the station would lift the *P*- and *S*-time residuals for the station up or down by the same amount. It is important to note that the earthquakes relocated in these two sequences occurred over time intervals of many months (see Ruppert and West, 2020, for details). A timing error typically covers a limited time span or is very variable with time and would likely be detected.

At the very start of the Bayesloc run, the time residual in Figure 4b takes on extreme values (often greatly exceeding the actual travel time from the true event location to the station) because the trial hypocenters and origin times for the event lie far from the true values. Few iterations pass before epicenter estimates begin to stabilize in the region of the map where the blue dots in Figure 4a are observed. The time residuals in Figure 4b oscillate around a mean value of around −0.8 s. At iteration 1000, corrections to model-based travel-time predictions are activated within Bayesloc. At this point, a rapid change in the evolution of this travel-time residual is observed, decreasing to around −2 s. The corresponding trial hypocenters move northeast. A more negative observed minus predicted time residual means that the seismic wavefront is traveling farther than the basis model expects in a given time, and the event hypocenter moves farther away from the station to accommodate this. The time residuals for stations in other locations will evolve in different ways. Over the next 9000 iterations, the D25K-*P* time residual continues to decrease but flattens off to a value of around −2.8 s. The spread of time-residual estimates for different trial hypocenters and origin times does not appear to decrease further. Similarly, the cloud of trial hypocenters for the later iterations (the red dots in Fig. 4a) cover an elliptical region about 4 by 7 km, elongated in a direction with a north-northeast strike. The size of this ellipse and the spread in the time residuals provide a visual uncertainty estimate for the event displayed.

Figure 4b displays the time residual for the one event for every single trial hypocenter and origin time. The most typically used parameters from Bayesloc output are the mean values for latitude, longitude, depth, and origin time (once the so-called burn-in phase, in which the location estimates may be qualitatively different to the end solutions, is removed). In Figure 5, we instead evaluate the time residual for mean hypocenter and origin time for each event for the six station and phase combinations indicated. This plot indicates both the internal consistency within the aftershock zone of the travel-time residual for a given phase and how the values vary from station to station. We see in Figure 5e that the large negative time residual we converge toward in Figure 4b is typical for almost all events in the cluster and would confirm the hypothesis of fast crust to the southwest of the aftershock zone. The consistency of this residual term over the full population of events, covering many months, essentially eliminates the hypothesis of a timing error on the station. The variability of *S*-wave travel-time residuals is generally somewhat higher than for *P*-wave travel-time residuals. This is likely related to the increased difficulty in picking the arrival time for the secondary phases.

The output from Bayesloc provides uncertainty statistics for the hypocenter distributions both laterally and in depth. Whereas the median over Kaktovik events of the standard deviation for location in the east–west direction was 4.2 km, the median standard deviation in the north–south direction was 6.2 km. This is consistent with the distribution of trial hypocenters displayed for the event in Figure 4 and is a function of the network geometry. The median standard deviation in the depth was 3.8 km, and the median standard deviation in the origin time was 0.65 s. The travel time from hypocenter to station has a trade-off with depth and the travel-time residuals, as displayed in Figure 5, are relatively insensitive to depth.

We focus here on the three closest stations to the aftershock zone to give maximum insight into the northeasterly shift of the hypocenters. The Bayesloc solutions include all arrivals used in the AEC catalog and therefore many hundreds of stations at far larger distances; the time residuals farther from the source are discussed later. The parallel calculation using a different baseline 1D velocity model is a valuable check on robustness of the hypocenters. We increase the confidence in the spatial distribution of hypocenters obtained if essentially the same distribution is obtained using a somewhat different set of travel-time tables; if the solution is robust, the solutions obtained from the different baseline models should differ primarily only in the correction terms to travel-time predictions. We note also that only stations within regional distances are used in the AEC bulletin. Given the magnitude distribution of the Kaktovik events (Ruppert and West, 2020), many aftershocks will be well recorded with good global coverage at teleseismic distances. Teleseismic travel times are less susceptible to crustal heterogeneity (e.g., Myers *et al.*, 2015), and augmenting the bulletin with high-quality teleseismic phases with a wide azimuthal distribution for the largest events may provide additional constraints and reduce the sensitivity of the hypocenters to local geologic heterogeneity.

The 2018 and 2019 Eastern Brooks Range Earthquake Swarm

To the southwest of the aftershock zone considered is a distinct earthquake swarm, referred to by Gaudreau *et al.* (2019) as the Niviak cluster. Ruppert and West (2020) describe the temporal and magnitude distributions of both sequences; the Niviak cluster consists only of events below magnitude 4.5 but is more enigmatic given the spatial distribution, the long duration, and the absence of a causative mainshock. The swarm intensified in July 2018 (shortly prior to the large Kaktovik earthquakes and their aftershocks) and reached a peak in October 2018 before decreasing over the fall of 2018. A new intensification of seismicity started in July and August 2019.

Figure 6a displays the locations of the events throughout 2018 and 2019 from the AEC bulletin. We have better

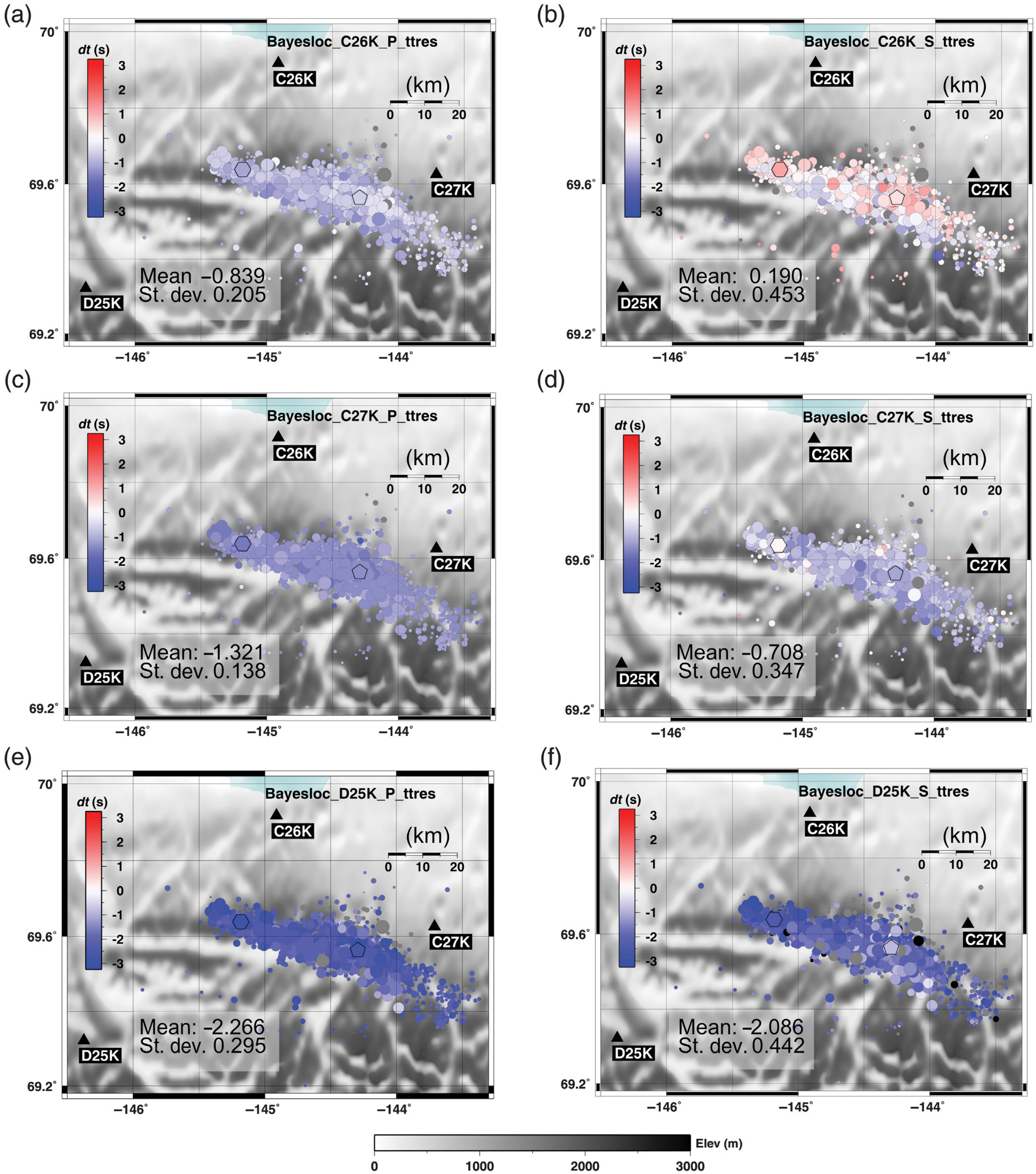

azimuthal coverage for recording this swarm than for the Kaktovik earthquakes, with multiple stations observing the sequence in all directions. This is especially true to the north, where the Kaktovik sequence relied on a single station, C26K. Bayesloc was run using the same arrivals as were used to compile the AEC catalog; the results are displayed in Figure 6b. The

Figure 5. Observed minus predicted travel-time residuals for relocated events in the Kaktovik sequence for (a) C26K *P* phase, (b) C26K *S*, (c) C27K *P*, (d) C27K *S*, (e) D25K *P*, and (f) D25K *S* relative to the 1D velocity model used to locate the events. The M_w 6.0 and M_w 6.4 earthquakes on 12 August 2018 are marked with five- and six-sided polygons, respectively. St. dev., standard deviation.

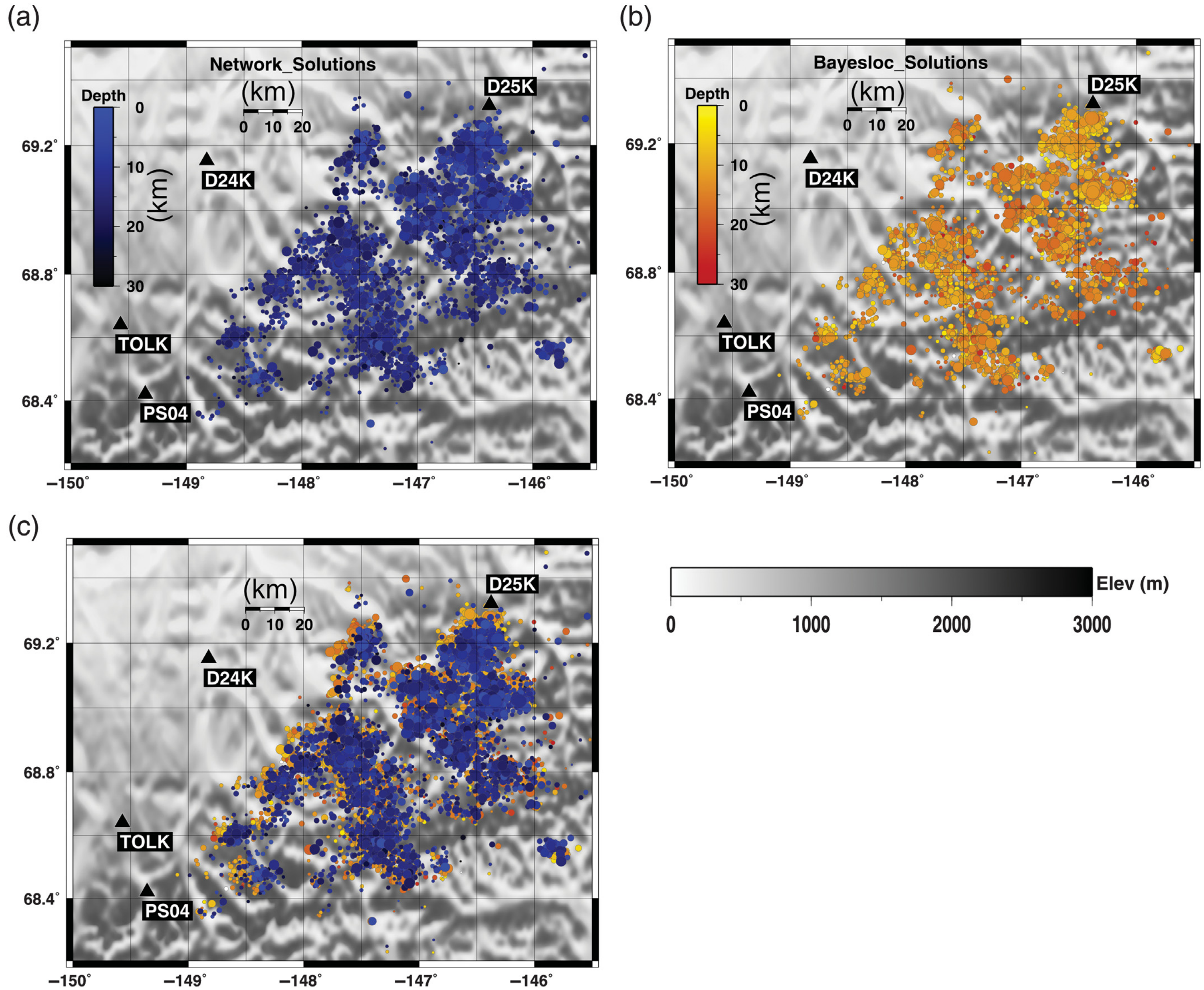

Figure 6. Locations of earthquakes in the eastern Brooks Range swarm (a) from the catalog of the AEC, (b) from the Bayesloc relocations, and (c) with the two sets of hypocenters superimposed with the same color code.

large-scale features are unchanged, although many features can be identified that appear better resolved or more cleanly separated in the multiple event location estimates. The most southeasterly cluster at 68.55° N, −145.5° E becomes significantly more compact in the relocations. A double cluster in the AEC network solutions at 68.8° N, −148.2° E resolves into two distinct clusters elongated in the direction of the topographic features. The cluster at 69.2° N, −147.5° E migrates a few kilometers to the northwest and appears to split into two; the change is easier to identify in Figure 6c in which the relocated event positions are superimposed on top of the network solutions. The spatial separation between each of the clusters in the northeast is a little more pronounced in the relocations than in the AEC catalog.

Given the fine structures and complex cluster patterns visible in the relocations, there is motivation to perform full-waveform cluster analysis using cross correlation or other signal semblance analysis. A given arrival measurement can contribute to a location error in two ways: error in travel-time prediction and error in the arrival-time measurement. Bayesloc mitigates the first of these in a way that event-by-event network solutions cannot, although we are still only using analyst arrival picks in this study and are still vulnerable to the uncertainty in the human-estimated arrival times. Using relative time-delay measurements and double-difference location methods (e.g., Shearer, 1997; Waldhauser and Ellsworth, 2000) may reveal geometrical structure at finer spatial scales not resolvable using only absolute arrival-time estimates; however, such a study is beyond the scope of this article. Given that the maximum event magnitude is <4.5, we are unlikely to be able to exploit teleseismic data to improve location accuracy.

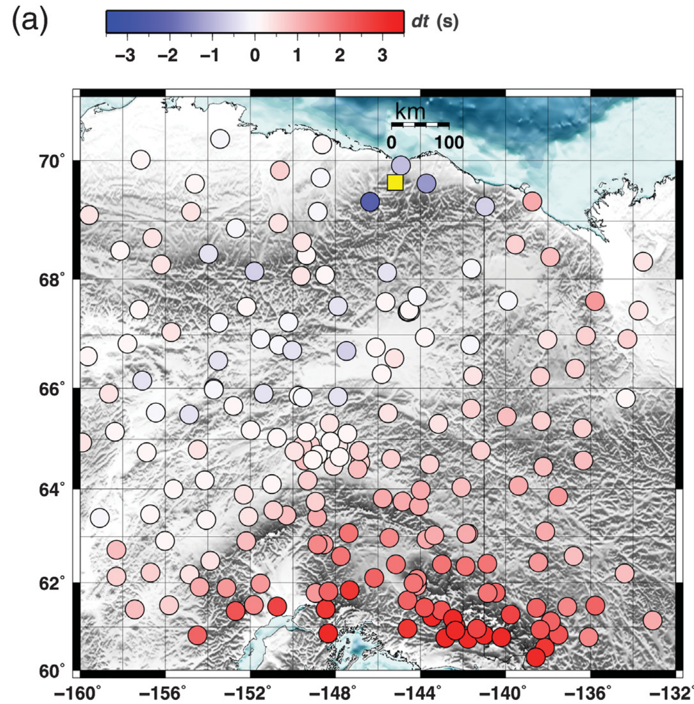

Figure 7. Median observed minus predicted travel-time residuals for (a) first *P* and (b) first *S* arrivals from events in the Kaktovik aftershock sequence given the hypocenters and origin times from the Bayesloc relocation. Blue symbols indicate an earlier than predicted arrival, and red symbols indicate a later than predicted arrival. The yellow square indicates the location of the largest earthquake on 12 August 2018. A symbol indicates that the phase and station combination appeared in the catalog of the AEC for at least 25 events in the sequence.

Discussion and Future Perspectives

We have applied the probabilistic multiple event location algorithm Bayesloc to two seismic sequences in northern Alaska for which most of the phase arrivals were provided by stations of the EarthScope USArray TA. In the first, aftershocks of the 12 August 2018 Kaktovik earthquakes, Bayesloc made a small but significant relocation of the entire cluster. The relocated event cluster has a far sharper southernmost boundary with a strike angle consistent with nonseismological constraints on the fault plane. In the second, the Niviak cluster, the probabilistic event locations are significantly more clustered and indicate clearer separation between localized zones of seismicity. Without the TA stations, we would not have the detection threshold or the station coverage to be able to resolve these sequences.

Full-waveform cluster analysis, using correlation methods to measure both signal similarity and enhanced time-delay estimates, is likely to provide improved local scale resolution of the seismicity in both sequences. The feature of Bayesloc that appears to be most powerful in these cases is the ability to solve for corrections to travel-time predictions for given paths. The exploitation of readings from multiple events to account for or to eliminate bias in travel-time estimates is a cornerstone of many advanced seismic-event location algorithms (e.g., Douglas, 1967; Richards-Dinger and Shearer, 2000; Nooshiri *et al.*, 2017). The solutions obtained using Bayesloc indicate that failure to account for anomalously fast propagation to the southwest of the Kaktovik aftershock is the primary reason that the network locations in many cases lie to the south of the InSAR-inferred fault line.

In Figure 5, we display spatially consistent time residuals for *P* and *S* phases at the three stations closest to the Kaktovik aftershocks. In Figure 7, instead of a single travel-time residual per event for a given phase, we display the median travel-time residual for all events in the Kaktovik sequence for *P* and *S* arrivals at each station. The blue symbols to the southwest of the earthquakes (the yellow square) are of similar colors to the symbols in Figure 5e,f and indicate the faster propagation along these paths. It should be noted that the geological heterogeneity over this short path is not necessarily more extreme than elsewhere in Alaska. The waves arriving at more distant stations from the Kaktovik earthquakes have traveled longer paths over which the contribution to the travel time from regions with anomalously fast propagation will cancel with the contributions from regions with anomalously slow propagation.

The travel-time residuals displayed in Figure 7 are relative to one specific 1D velocity model. However, the location calculations were repeated using alternative velocity models, and we confirm that the large-scale features of the relocated clusters of seismicity are largely unchanged. The travel-time residual plots for ak135 (corresponding to Figs. 5 and 7) look somewhat different as different corrections are required to compensate for the deficiencies of the baseline model along the different paths. Relative insensitivity to the details of the underlying 1D model was also demonstrated by Gibbons *et al.* (2017). Another feature of Figure 7 that increases our confidence that the residuals are related to 3D geologic properties and not a simple inapplicability of the underlying 1D model is the distribution of high positive *P*-wave time residuals for stations to the south of the map. The size of the residuals does not increase simply with distance from the source; the highest residuals are found to the south of the Chugach Mountains and indicate slow propagation along these specific paths.

Repeating the procedure applied here to clusters of seismicity across Alaska would generate corresponding maps that could be used to validate existing 3D tomographic images and provide input for large-scale evaluations of 3D velocity maps. Similar studies have been performed both globally and regionally (e.g., Myers *et al.*, 2011; Simmons *et al.*, 2012), and applying such a procedure to Alaska now would benefit from the recently improved station coverage. There is no limit, in principle, as to how large the datasets for the Bayesloc program can be. In practice, the computational cost of calculating the joint probability distributions increases greatly with the number of events and phases; the 40,000-iteration calculation for the Kaktovik aftershock sequence with 4192 events and 109,905 phases took approximately 11.5 hr on a high-end Linux workstation. Simply covering all historical seismicity over all of Alaska and adding new events with all readings as they occur is not a viable strategy for near-real-time event location with current technology. Bayesloc, however, can take prior information regarding both uncertainty in event hypocenters and origin times and travel-time predictions; results from previous runs can be used to constrain subsequent runs without needing to include all the raw inputs. Whereas only a subset of Alaska TA stations will be transitioned into longer-term operation, the contribution of any of the TA stations that are removed will always be valuable in the framework of probabilistic multiple event location algorithms.

Data and Resources

All maps generated by the Generic Mapping Tools (GMT) package, Wessel and Smith (1995) (GMT: https://www.soest.hawaii.edu/gmt/). Original earthquake hypocenters and phase picks are from the Alaska Earthquake Center catalog. Earthquake relocations were performed using the Bayesloc program, available for download from https://www-gs.llnl.gov/nuclear-threat-reduction/nuclear-explosion-monitoring/bayesloc. The website of the EarthScope USArray is www.usarray.org. All websites were last accessed in June 2020.

Acknowledgments

This research was supported in part by the Geophysical Institute – University of Alaska Fairbanks and Office of Alaska State Seismologist (N. A. R. and E. K.).

The facilities of Incorporated Research Institutions for Seismology (IRIS) Data Services, specifically the IRIS Data Management Center, were used for access to waveforms, related metadata, and derived products used in this study. IRIS Data Services are funded through the Seismological Facilities for the Advancement of Geoscience (SAGE) Award of the National Science Foundation under Cooperative Service Agreement EAR-1851048.

Data from the Transportable Array (TA) network (IRIS TA, 2003) were made freely available as part of the EarthScope USArray facility, operated by IRIS and supported by the National Science Foundation, under Cooperative Agreements EAR-1261681.

The authors are very grateful to Geoffrey Abers, Steve Myers, and an anonymous reviewer for very constructive comments and suggestions that led to a significant improvement in this article.

References

Busby, R. W., and K. Aderhold (2020). The Alaska Transportable Array: As built, *Seismol. Res. Lett.* doi: 10.1785/0220200154 (this issue).

Douglas, A. (1967). Joint epicentre determination, *Nature* **215,** 47–48, doi: 10.1038/215047a0.

Estabrook, C., D. B. Stone, and J. N. Davies (1988). Seismotectonics of northern Alaska, *J. Geophys. Res.* **93,** no. B10, 12,026–12,040, doi: 10.1029/JB093iB10p12026.

Fuis, G. S., J. M. Murphy, W. J. Lutter, T. E. Moore, K. J. Bird, and N. I. Christensen (1997). Deep seismic structure and tectonics of northern Alaska: Crustal-scale duplexing with deformation extending into the upper mantle, *J. Geophys. Res.* **102,** no. B9, 20,873–20,896, doi: 10.1029/96jb03959.

Gaudreau, É., E. K. Nissen, E. A. Bergman, H. M. Benz, F. Tan, and E. Karasözen (2019). The August 2018 Kaktovik earthquakes: Active tectonics in Northeastern Alaska revealed with InSAR and seismology, *Geophys. Res. Lett.* **46,** doi: 10.1029/2019GL085651.

Gedney, L., N. Biswas, P. Huang, S. Estes, and C. Pearson (1977). Seismicity of Northeast Alaska, *Geophys. Res. Lett.* **4,** no. 5, 175–177, doi: 10.1029/GL004i005p00175.

Gibbons, S. J., and T. Kværna (2017). Illuminating the seismicity pattern of the October 8, 2005, M = 7.6 Kashmir earthquake aftershocks, *Phys. Earth Planet. In.* **270,** 1–8, doi: 10.1016/j.pepi.2017.06.008.

Gibbons, S. J., D. B. Harris, T. Dahl-Jensen, T. Kværna, T. B. Larsen, B. Paulsen, and P. H. Voss (2017). Locating seismicity on the Arctic plate boundary using multiple-event techniques and empirical signal processing, *Geophys. J. Int.* **211,** no. 3, 1613–1627, doi: 10.1093/GJI/GGX398.

Hayes, G. P., R. W. Briggs, W. D. Barnhart, W. L. Yeck, D. E. McNamara, D. J. Wald, J. L. Nealy, H. M. Benz, R. D. Gold, K. S. Jaiswal, *et al.* (2015). Rapid characterization of the 2015 M_w 7.8 Gorkha, Nepal, earthquake sequence and its seismotectonic context, *Seismol. Res. Lett.* **86,** no. 6, 1557–1567, doi: 10.1785/0220150145.

Incorporated Research Institutions for Seismology (IRIS) Transportable Array (2003). USArray Transportable Array, International Federation of Digital Seismograph Networks, Dataset/Seismic Network, doi: 10.7914/SN/TA.

Kennett, B. L. N., E. R. Engdahl, and R. Buland (1995). Constraints on seismic velocities in the Earth from travel times, *Geophys. J. Int.* **122,** 108–124, doi: 10.1111/j.1365-246x.1995.tb03540.x.

Koehler, R. D., R.-E. Farrell, P. A. C. Burns, and R. A. Combellick (2012). Quaternary faults and folds in Alaska: A digital database, 1:3,700,000, 31 pp., 1 sheet, Alaska Division of Geological & Geophysical Surveys Digital Data Series 3, Fairbanks, Alaska, doi: 10.14509/23944.

Leonard, L. J., S. Mazzotti, and R. D. Hyndman (2008). Deformation rates from earthquakes in the northern Cordillera of Canada and eastern Alaska, *J. Geophys. Res.* **113,** no. B08406, doi: 10.1029/2007JB005456.

Mazzotti, S., and R. D. Hyndman (2002). Yakutat collision and strain transfer across the northern Canadian Cordillera, *Geology* **30,** 495–498, doi: 10.1130/0091-7613(2002)030<0495:YCASTA>2.0.CO;2.

Mazzotti, S., L. J. Leonard, R. D. Hyndman, and J. F. Cassidy (2008). Tectonics, dynamics, and seismic hazard in the Canada–Alaska Cordillera, active tectonics and seismic potential of Alaska, *AGU Geophysical Monograph Series* 179, doi: 10.1029/179GM17.

Myers, S. C., G. Johannesson, and W. Hanley (2007). A Bayesian hierarchical method for multiple-event seismic location, *Geophys. J. Int.* **171,** 1049–1063, doi: 10.1111/j.1365-246x.2007.03555.x.

Myers, S. C., G. Johannesson, and W. Hanley (2009). Incorporation of probabilistic seismic phase labels into a Bayesian multiple-event seismic locator, *Geophys. J. Int.* **177,** no. 1, 193–204, doi: 10.1111/j.1365-246x.2008.04070.x.

Myers, S. C., G. Johannesson, and N. A. Simmons (2011). Global-scale *P* wave tomography optimized for prediction of teleseismic and regional travel times for Middle East events: 1. Data set development, *J. Geophys. Res.* **116,** no. B04304, doi: 10.1029/2010jb007967.

Myers, S. C., N. A. Simmons, G. Johannesson, and E. Matzel (2015). Improved regional and teleseismic *P*-wave travel-time prediction and event location using a global 3D velocity model, *Bull. Seismol. Soc. Am.* **105,** 1642–1660, doi: 10.1785/0120140272.

Nealy, J. L., H. M. Benz, G. P. Hayes, E. A. Bergman, and W. D. Barnhart (2017). The 2008 Wells, Nevada, earthquake sequence: Source constraints using calibrated multiple-event relocation and InSAR, *Bull. Seismol. Soc. Am.* **107,** 1107–1117, doi: 10.1785/0120160298.

Nooshiri, N., J. Saul, S. Heimann, F. Tilmann, and T. Dahm (2017). Revision of earthquake hypocentre locations in global bulletin data sets using source-specific station terms, *Geophys. J. Int.* **208,** 589–602, doi: 10.1093/gji/ggw405.

Pyle, M. L., S. C. Myers, W. R. Walter, and K. D. Smith (2015). Accurate local event locations in Rock Valley, Nevada, using a Bayesian multiple-event method, *Bull. Seismol. Soc. Am.* **105,** 706–718, doi: 10.1785/0120140251.

Richards-Dinger, K. B., and P. M. Shearer (2000). Earthquake locations in southern California obtained using source-specific station terms, *J. Geophys. Res.* **105,** 10,939–10,960, doi: 10.1029/2000jb900014.

Ruppert, N. A., and M. E. West (2020). The impact of USArray on earthquake monitoring in Alaska, *Seismol. Res. Lett.* **91,** no. 2A, 601–610, doi: 10.1785/0220190227.

Shearer, P. M. (1997). Improving local earthquake locations using the L1 norm and waveform cross correlation: Application to the Whittier Narrows, California, aftershock sequence, *J. Geophys. Res.* **102,** 8269–8283, doi: 10.1029/96jb03228.

Simmons, N. A., S. C. Myers, G. Johannesson, and E. Matzel (2012). LLNL-G3Dv3: Global *P* wave tomography model for improved regional and teleseismic travel time prediction, *J. Geophys. Res.* **117,** no. B10302, doi: 10.1029/2012jb009525.

Storchak, D. A., J. Schweitzer, and P. Bormann (2003). The IASPEI standard seismic phase list, *Seismol. Res. Lett.* **74,** no. 6, 761–772.

Waldhauser, F., and W. L. Ellsworth (2000). A double-difference earthquake location algorithm: Method and application to the Northern Hayward fault, California, *Bull. Seismol. Soc. Am.* **90,** 1353–1368, doi: 10.1785/0120000006.

Wessel, P., and W. H. F. Smith (1995). New version of the Generic Mapping Tools released, *Eos Trans. AGU* **76,** no. 33, 329.

Manuscript received 14 April 2020
Published online 22 July 2020

Europe’s energy crisis: What factors drove the record fall in natural gas demand in 2022?

Peter Zeniewski, WEO Energy Analyst
Gergely Molnar, Energy Analyst – Natural Gas
Paul Hugues, Energy Modeller
Commentary — 14 March 2023

Cite Share

In the wake of Russia’s invasion of Ukraine and a surge in energy prices, natural gas demand in the European Union fell in 2022 by 55 bcm, or 13%, its steepest drop in history. The decline is the equivalent to the amount of gas needed to supply over 40 million homes. What were the main drivers behind this decline? In this commentary we assess how changes in the energy mix, economic activity, weather, behavioural changes and other factors were responsible for this dramatic shift in natural gas consumption.

Milder winter temperatures certainly played a role. However, not all weather effects reduced gas use – low rainfall in southern Europe led to a very poor year for hydropower and increased the call on gas-fired power. Policy-driven changes were vital, most notably record additions of wind and solar capacity. High prices also played a considerable role in bringing down demand, especially in gas-intensive industrial sectors. However, the extent to which they led to permanent demand reductions remains unclear.

Change in natural gas demand by European Union member state, 2022 vs 2021

Open

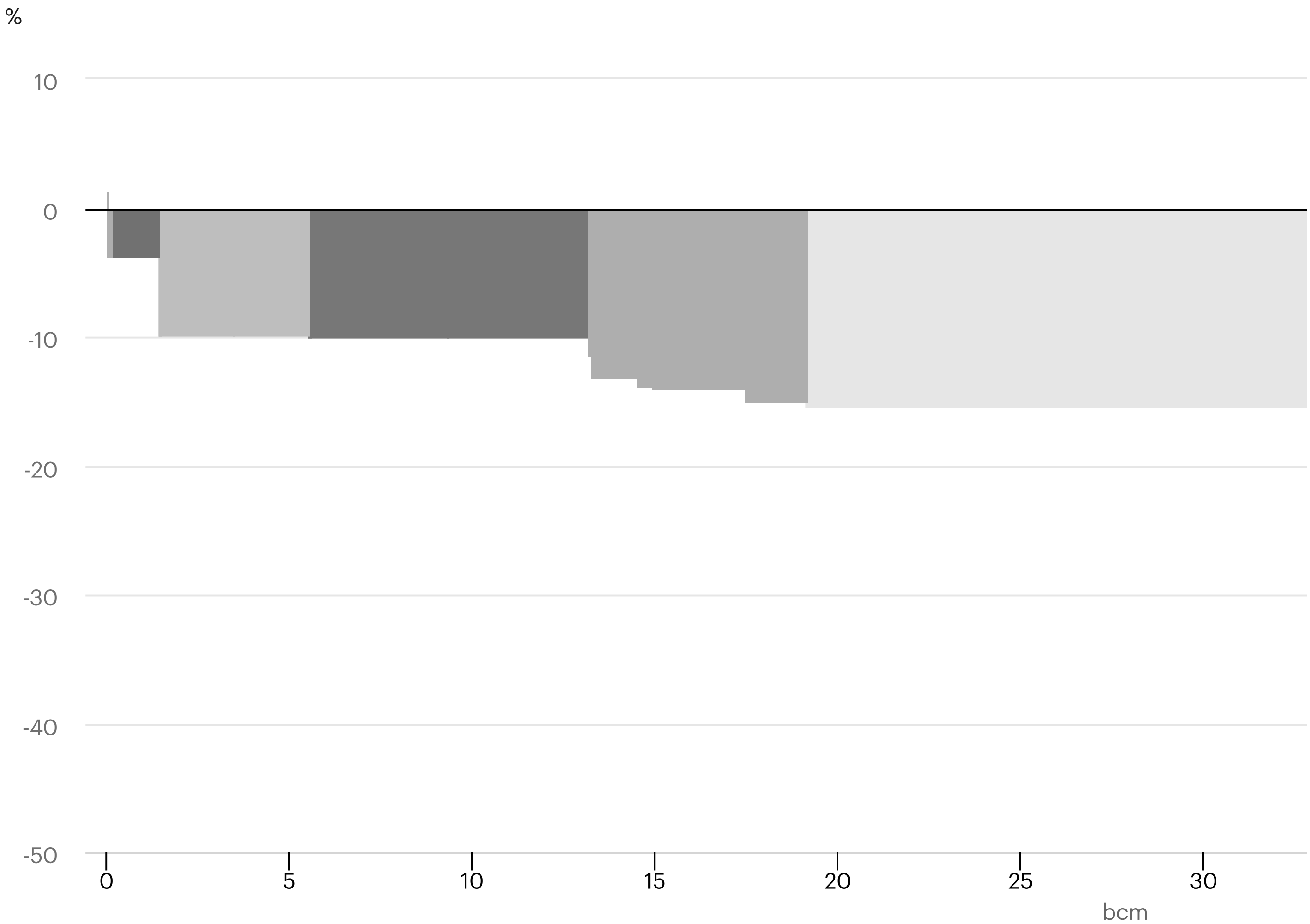

Other Spain France Italy Germany Netherlands Finland

As noted by IEA Executive Director Fatih Birol, it is important to credit governments for how they responded to this large and complex energy crisis. Policy measures – such as renewable support schemes, grants and preferential loans for housing retrofits and heat pump installations, alongside campaigns to encourage behavioural change – all played a part in moderating gas demand. Rapid adjustment to lower Russian gas exports and higher prices was also possible thanks to decades of reforms and policy initiatives, which enabled large consumers to lower their consumption, pursue import substitution and draw on alternative supplies across a well-meshed European gas grid. Nonetheless, there remains a vigorous debate about what weight should be assigned to each factor in reducing gas demand.

Estimated drivers of change in natural gas demand in power, buildings and industry in the European Union, 2022 versus 2021 **Open**

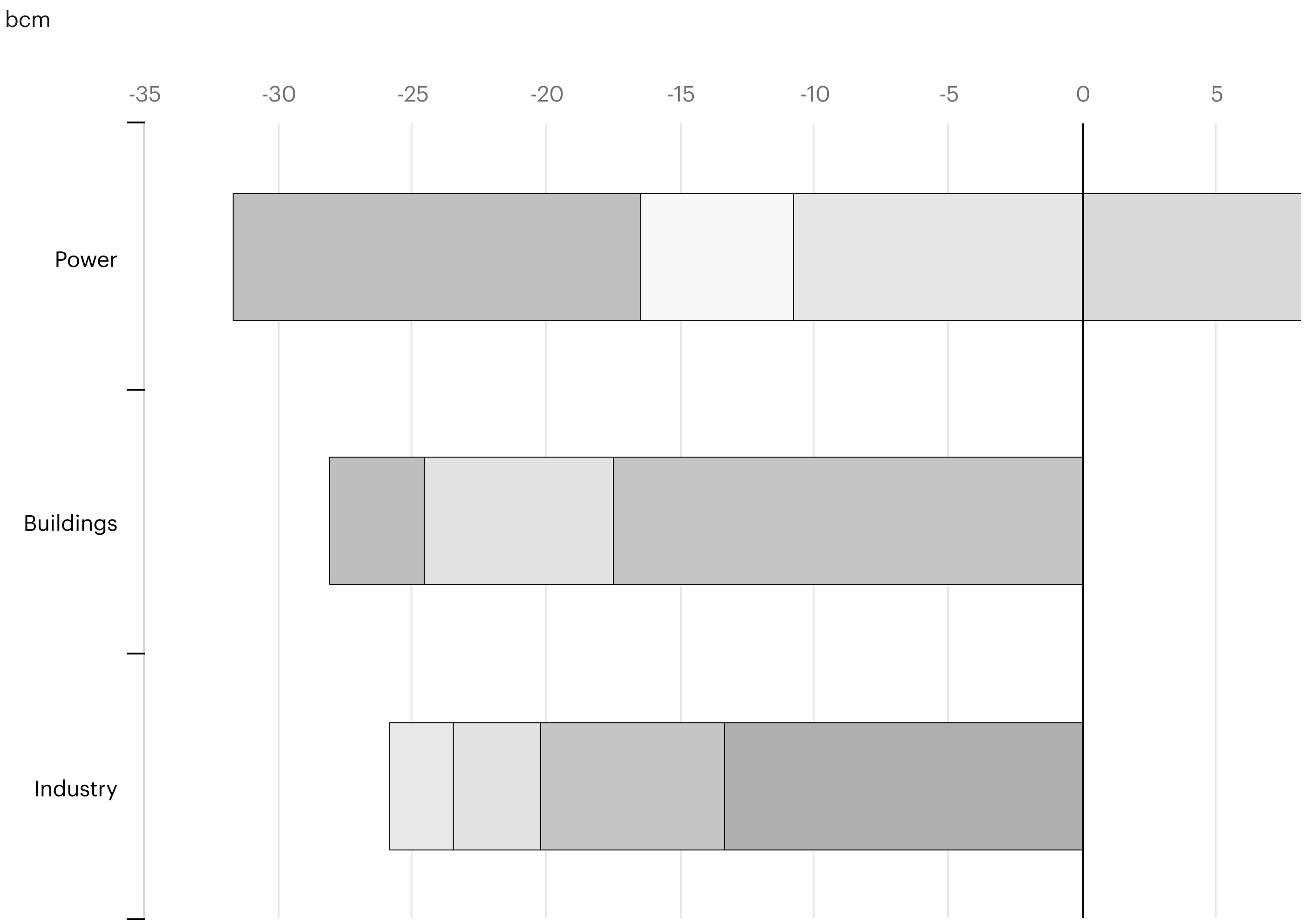

- Production curtailment
- Fuel switching
- Efficiency
- Other avoided demand
- Weather
- Behaviour and fuel switching
- Efficiency
- More renewables
- Less hydro
- Less nuclear
- More coal
- Other avoided demand

Power was the only sector in which gas demand rose above 2021 levels, with some of the notable changes caused by:

- **Renewables, especially wind and solar.** Thanks to ongoing policy support for renewables, around 50 GW of wind and solar was installed in the European Union in 2022, a record high. These additions avoided the need for around 11 bcm of natural gas in the power sector – the single largest structural driver of reduced natural gas demand.
- **Nuclear and hydro.** The sharp year-on-year declines in both nuclear and hydropower output pushed up demand for gas-fired power, leading to a small overall net increase in gas demand in the power sector.
- **Lower electricity demand**. EU electricity demand fell by around 3% in 2022. This meant that around 14 bcm of gas demand was avoided. Weather played a part in reducing electricity demand, even though higher summer temperatures and drought conditions drove up gas-fired power generation in parts of Europe.

The **buildings** sector, which comprises both households and public and commercial spaces, used 28 bcm less natural gas than in 2021, a drop of almost 20%:

- **Weather effects**. Heating Degree Days – a measure of how much energy is required to heat a building due to colder weather – across the European Union were 12% lower on average in 2022 than in 2021, lowering space heating requirements. There are different ways to attribute gas demand changes to weather effects, but this could explain up to 18 bcm of the drop in natural gas consumption in buildings.
- **Behaviour and fuel switching**. In a high-price environment, we estimate that behavioural changes, rising fuel poverty and fuel-switching in the residential and commercial sectors reduced natural gas demand in buildings by at least 7 bcm. Data from a sampling of smart thermostat providers suggests that consumers adjusted their thermostats lower by an average of around 0.6 °C. Such adjustments were, in part, a response to government-led campaigns to reduce energy demand (as per the IEA’s 10-Point Plan). Additional

savings arose from efforts to reduce heating and hot water usage in commercial and public buildings. **Fuel poverty** was another factor: many vulnerable consumers reduced consumption because they could not afford the higher bills, leading to cold homes or a shift to cheaper and sometimes more polluting fuels such as wood pellets, charcoal, waste or low-quality fuel oil.

- **Efficiency, including heat pumps.** Improved energy performance of buildings, including efficiency retrofits as well as boiler replacements, are estimated to have reduced natural gas demand by around 3.5 bcm. These structural reductions in natural gas use during seasonal peaks will carry over into future years. Around 2.8 million heat pumps were installed over the course of 2022, accounting for around 1.4 bcm of savings. There were also efficiency gains in industry as well as in the power sector, where the efficiency of the gas-fired power plant fleet was marginally higher than in 2021.

In the **industry** sector gas use fell by 25 bcm, or around 25%:

- **Production curtailment.** Energy-intensive industries were the first to respond to gas price shocks in the European Union. Several plants reduced production, and in some cases imported finished products from outside the EU instead of manufacturing them domestically at higher cost. This reduced the need for around 13 bcm of natural gas, with the fertiliser industry accounting for nearly half of this volume. Some industries also reduced their gas needs by increasing imports of intermediate gas-intensive goods, enabling overall output of final products to remain largely unchanged. This explains why industrial production in gas-intensive sectors – such as fertilisers, steel and aluminium – fell on average by around 8% in 2022 in the EU, less than the corresponding reduction in their gas consumption.
- **Fuel switching**. We estimate that around 7 bcm of gas-to-oil switching occurred in the industrial sector.

Overall, all these factors together contributed to a 13% drop in natural gas demand in a single year. The largest reductions in percentage terms occurred in Northern and Northwest European EU member states, where gas use declined across industry, buildings and power. Some of these factors can be considered cyclical or temporary – such as price-sensitive fuel switching or weather effects. Others, such as renewable capacity additions, efficiency improvements and sales of heat pumps, are structural – laying the foundation for lasting reductions in gas demand. There are also less desirable structural changes, such as permanent closures of factories or businesses. In the middle are changes such as voluntary actions to reduce demand or import substitutions to manage higher prices, which may not endure if gas markets rebalance and prices revert to historical averages.

Despite this historic drop in demand, the EU's gas import bill ran close to EUR 400 billion in 2022 – more than three times the level in 2021. Russia's share of total EU natural gas demand fell from 40% in 2021 to below 10% by the end of 2022, but the sharp increase in prices nonetheless ensured significant income for Russia over the course of 2022. Gas prices have come off recent highs and, according to Russia's Ministry of Finance, natural gas revenues dropped by over 40% over the first two months of 2023 compared with the same period in 2022.

Export revenues by key natural gas suppliers to the European Union, 2021 estimates **Open**

% of total revenue

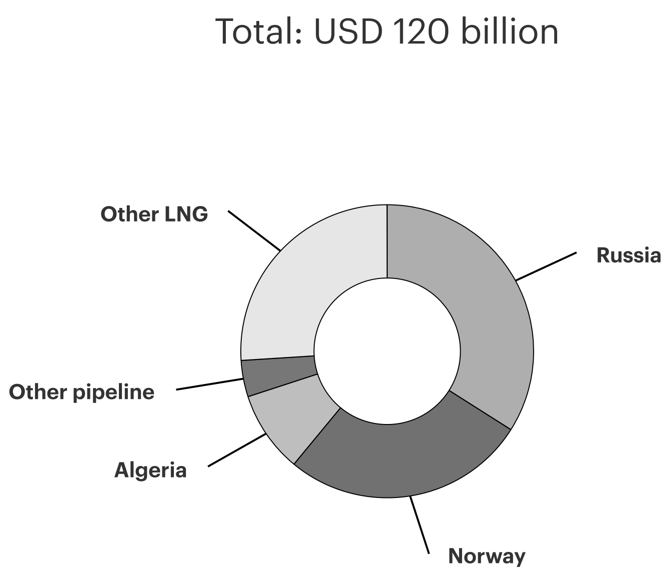

Export revenues by key natural gas suppliers to the European Union, 2022 estimates **Open**

% of total revenue

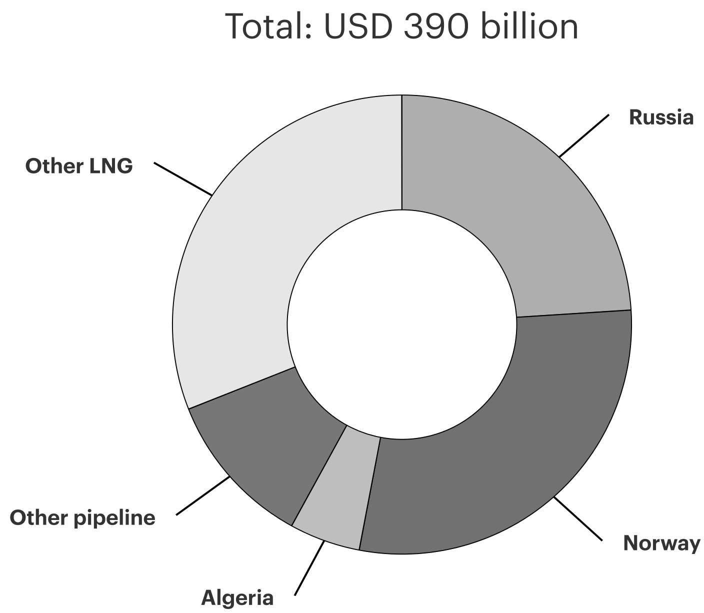

As we move into 2023, tensions in Europe's gas market have significantly moderated due to favourable weather conditions and timely policy actions. However, gas supply is set to remain tight in 2023 with an unusually wide range of uncertainties and risk. These include the possibility of a complete cessation of Russian pipeline gas deliveries to the European Union, as well as potentially tighter LNG supply as China's LNG imports recover. Weather-related factors – such a dry summer or a cold winter later in 2023 – could put further pressure on gas markets. Continuing the strong momentum in renewables growth seen in 2022 would also need sustained policy efforts.

Acknowledging these risks, the IEA hosted a Special Ministerial in mid-February. Forty governments took part, discussing how to foster gas supply security and highlighting the need for structural gas demand reduction and enhanced dialogue between consumers and responsible gas producers.

Such efforts are essential to manage ongoing supply risks without harming economic activity or compromising climate targets. Global CO_2 emissions from natural gas fell in 2022 by 115 million tonnes, with the European Union alone accounting for more than 100 million tonnes of this reduction. This was more than offset by the uptick in coal and oil-related emissions, but the rise in overall energy-related CO_2 emissions worldwide would have been three times higher without 2022's rapid rate of clean energy deployment. Spurred on by additional government support and even more favourable economics, the amount of added renewable power capacity worldwide rose by about a quarter in 2022; global electric car sales leaped by close to 60% and investments in energy efficiency were sharply higher. Fostering these lasting solutions to the global energy crisis – both in Europe and further afield – needs to remain a cornerstone of European energy and climate policy.

LNG Stranded Assets Europe

Over half of Europe’s LNG infrastructure assets could be left unused by 2030

March 21, 2023

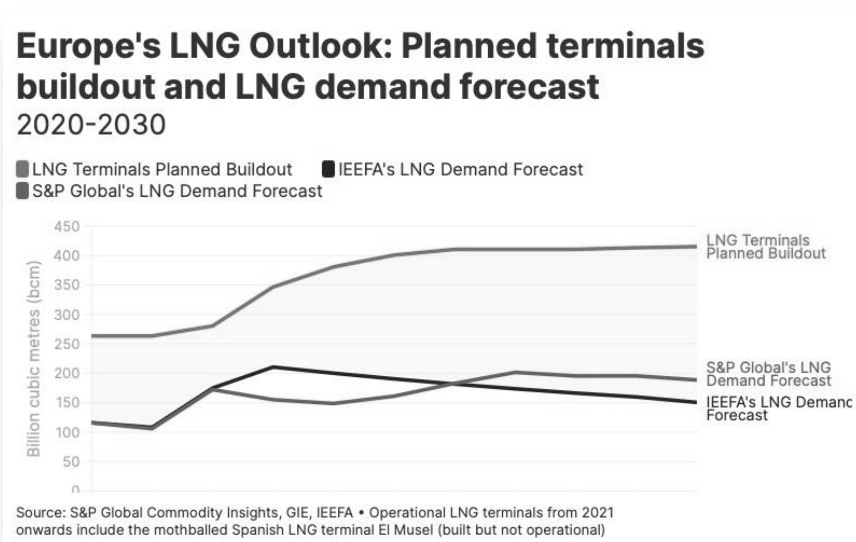

operation by 2030, but demand for LNG is unlikely to exceed 190 bcm.

Key Takeaways:

Europe’s LNG terminal capacity could exceed 400 billion cubic metres by 2030, based on current infrastructure buildout plans. This is up from 270 billion cubic metres at the end of 2022.

However, demand for LNG in 2030 is forecasted to range between 150 bcm according to IEEFA, and 190 bcm according to S&P Global Commodity Insights.

This leaves a significant gap of up to 250 bcm of unused capacity—over half the EU's total gas consumption in 2021, which was 413 bcm.

Europe's LNG capacity in 2030 will be more than the total forecasted demand for gas, including both LNG and pipeline gas. IEEFA forecasts gas demand in Europe in 2030 will be about 390 bcm.

London, 22 March 2023 | Today, IEEFA launched its European LNG Tracker, the first fully publicly accessible interactive data set to visualise Europe's rampant LNG buildout.

Europe's appetite for new LNG projects is pushing the continent to boost its import capacity by one-third, but the mismatch between future LNG demand and import facilities might result in 200-250 billion cubic metres (bcm) of unused capacity by 2030. This is equivalent to around half the EU's total gas demand in 2021, which was 413 bcm.

Europe's LNG terminal capacity could exceed 400 billion cubic metres in 2030 based on current infrastructure plans. Demand for LNG by 2030 will range between 150 bcm according to IEEFA forecast, and 190 bcm according to S&P Global Commodity Insights forecast.

There is a significant discrepancy between regasification infrastructure being built, and planned and forecasted

(14 bcm), Italy (10 bcm), and Germany (9 bcm) in 2030.

Several countries have announced new LNG projects or expansion to existing ones in a bid to cut Russian ties, including Germany (3 onshore and 6 FSRUs), Italy (2 FSRUs), Greece (2 FSRUs), Netherlands (1 FSRU), and France (1 FSRU).

By 2030, IEEFA forecasts a 36% utilisation rate of Europe's LNG terminals, including those that are currently being planned and being built.

"This is the world's most expensive and unnecessary insurance policy. Europe must carefully balance its gas and LNG systems, and avoid tipping the scale from reliability to redundancy. Boosting Europe's LNG infrastructure will not necessarily increase reliability—there's a tangible risk that assets could become stranded," says Ana Maria Jaller Makarewicz, author of the analysis and Energy Analyst for IEEFA Europe.

"Over-engineered networks are expensive to build and maintain. Decisions to expand Europe's LNG infrastructure must be based on future demand needs, and take into account that the EU is planning to reduce gas demand by at least one-third by 2030."

Europe's dependency on Russian LNG is deepening

While flows of Russian piped gas significantly decreased in 2022 compared to 2021, LNG imports increased to 20.2 bcm in 2022, up from 18 bcm in 2021. Q3 2022

The biggest importers of Russian LNG in 2022 were France (7.4 bcm), Spain (5.2 bcm), and Belgium (3.0 bcm). Imports of LNG from Russia increased by 58% in France and Belgium, and 50% in Spain compared to the previous year.

LNG demand is set to decline across Europe

LNG imports into Europe increased by 60% in 2022 compared to 2021, mostly from the top-three exporters: United States (+143%), Qatar (+23%) and Russia (+12%).

In 2022, the largest importers of LNG were France (35.7 bcm), Spain (29.5 bcm), and the United Kingdom (26.5 bcm), followed by the Netherlands (17.1bcm), Türkiye (15.5 bcm), Italy (14.8 bcm), and Belgium (12.9 bcm).

Belgium had the biggest increase of LNG imports in 2022 compared with 2021 (136%), followed by France (96%), Netherlands (94%), Lithuania (88%) and UK (71%).

Demand for LNG is expected to increase in 2023 and then reduce in the following years, mainly due to forecasted gas demand reductions across EU countries.

Read the report: European LNG Tracker

About IEEFA

The Institute for Energy Economics and Financial Analysis (IEEFA) examines issues related to energy markets, trends and policies. The Institute's mission is to accelerate the

Media contact

Sofia Russi | srussi@ieefa.org | +393493229728

World Energy News

BNP Paribas to stop financing new oil and gas projects

May 12, 2023
Reuters

World Energy News

Turkey to receive $110 million loan in support of wind investments

May 12, 2023
Renewables Now

World Energy News

Invenergy, Chinese manufacturer look to build largest U.S. solar factory

May 12, 2023
Reuters

World Energy News

Ireland awards contracts for 3 gigawatts of offshore wind

May 12, 2023
Irish Times

Join our newsletter

Keep up to date with all the latest from IEEFA

Newsroom Research About **Explore** Subscribe

Newsroom

All News

Press Releases

World Energy News

IEEFA in the Media

Media Inquiries

Research

All Research

Reports

Analysis

Explore

About

What We Do

Who We Are

Conference

Employment

Get in Touch

Contact Us

Subscribe

Contact us

INSTITUTE FOR ENERGY ECONOMICS AND FINANCIAL ANALYSIS

14900 Detroit Avenue Suite 206 Lakewood, OH 44107

T: 216-712-6612
E: staff@ieefa.org

Data & T&C's
Privacy policy
Site by 89up

SYNTHESIS REPORT
OF THE IPCC SIXTH ASSESSMENT REPORT (AR6)

Longer Report

Core Writing Team: Hoesung Lee (Chair), Katherine Calvin (USA), Dipak Dasgupta (India/USA), Gerhard Krinner (France/Germany), Aditi Mukherji (India), Peter Thorne (Ireland/United Kingdom), Christopher Trisos (South Africa), José Romero (Switzerland), Paulina Aldunce (Chile), Ko Barrett (USA), Gabriel Blanco (Argentina), William W. L. Cheung (Canada), Sarah L. Connors (France/United Kingdom), Fatima Denton (The Gambia), Aïda Diongue-Niang (Senegal), David Dodman (Jamaica/United Kingdom/Netherlands), Matthias Garschagen (Germany), Oliver Geden (Germany), Bronwyn Hayward (New Zealand), Christopher Jones (United Kingdom), Frank Jotzo (Australia), Thelma Krug (Brazil), Rodel Lasco (Philippines), June-Yi Lee (Republic of Korea), Valérie Masson-Delmotte (France), Malte Meinshausen (Australia/Germany), Katja Mintenbeck (Germany), Abdalah Mokssit (Morocco), Friederike E. L. Otto (United Kingdom/Germany), Minal Pathak (India), Anna Pirani (Italy), Elvira Poloczanska (UK/Australia), Hans-Otto Pörtner (Germany), Aromar Revi (India), Debra C. Roberts (South Africa), Joyashree Roy (India/Thailand), Alex C. Ruane (USA), Jim Skea (United Kingdom), Priyadarshi R. Shukla (India), Raphael Slade (United Kingdom), Aimée Slangen (The Netherlands), Youba Sokona (Mali), Anna A. Sörensson (Argentina), Melinda Tignor (USA/Germany), Detlef van Vuuren (The Netherlands), Yi-Ming Wei (China), Harald Winkler (South Africa), Panmao Zhai (China), Zinta Zommers (Latvia)

Extended Writing Team: Jean-Charles Hourcade (France), Francis X. Johnson (Thailand/Sweden), Shonali Pachauri (Austria/India), Nicholas P. Simpson (South Africa/Zimbabwe), Chandni Singh (India), Adelle Thomas (Bahamas), Edmond Totin (Benin)

Contributing Authors: Andrés Alegría (Germany/Honduras), Kyle Armour (USA), Birgit Bednar-Friedl (Austria), Kornelis Blok (The Netherlands) Guéladio Cissé (Switzerland/Mauritania/France), Frank Dentener (EU/Netherlands), Siri Eriksen (Norway), Erich Fischer (Switzerland), Gregory Garner (USA), Céline Guivarch (France), Marjolijn Haasnoot (The Netherlands), Gerrit Hansen (Germany), Matthias Hauser (Switzerland), Ed Hawkins (UK), Tim Hermans (The Netherlands), Robert Kopp (USA), Noëmie Leprince-Ringuet (France), Debora Ley (Mexico/Guatemala), Jared Lewis (Australia/New Zealand), Chloé Ludden (Germany/France), Zebedee Nicholls (Australia), Leila Niamir (Iran/The Netherlands/Austria), Shreya Some (India/Thailand), Sophie Szopa (France), Blair Trewin (Australia), Kaj-Ivar van der Wijst (The Netherlands), Gundula Winter (The Netherlands/Germany), Maximilian Witting (Germany)

Review Editors: Paola Arias (Colombia), Mercedes Bustamante (Brazil), Ismail Elgizouli (Sudan), Gregory Flato (Canada), Mark Howden (Australia), Carlos Méndez (Venezuela), Joy Pereira (Malaysia), Ramón Pichs-Madruga (Cuba), Steven K Rose (USA), Yamina Saheb (Algeria/France), Roberto Sánchez (Mexico), Diana Ürge-Vorsatz (Hungary), Cunde Xiao (China), Noureddine Yassaa (Algeria)

Scientific Steering Committee: Hoesung Lee (Chair, IPCC), Amjad Abdulla (Maldives), Edvin Aldrian (Indonesia), Ko Barrett (United States of America), Eduardo Calvo (Peru), Carlo Carraro (Italy), Fatima Driouech (Morocco), Andreas Fischlin (Switzerland), Jan Fuglestvedt (Norway), Diriba Korecha Dadi (Ethiopia), Thelma Krug (Brazil), Nagmeldin G.E. Mahmoud (Sudan), Valérie Masson-Delmotte (France), Carlos Méndez (Venezuela), Joy Jacqueline Pereira (Malaysia), Ramón Pichs-Madruga (Cuba), Hans-Otto Pörtner (Germany), Andy Reisinger (New Zealand), Debra Roberts (South Africa), Sergey Semenov (Russian Federation), Priyadarshi Shukla (India), Jim Skea (United Kingdom), Youba Sokona (Mali), Kiyoto Tanabe (Japan), Muhammad IrfanTariq (Pakistan), Diana Ürge-Vorsatz (Hungary), Carolina Vera (Argentina), Pius Yanda (United Republic of Tanzania), Noureddine Yassaa (Algeria), Taha M. Zatari (Saudi Arabia), Panmao Zhai (China)

Visual Conception and Information Design: Arlene Birt (USA), Meeyoung Ha (Republic of Korea)

Notes: SFs Compiled Version

Table of Contents

Section 1: Introduction

1. Introduction

This Synthesis Report (SYR) of the IPCC Sixth Assessment Report (AR6) summarises the state of knowledge of climate change, its widespread impacts and risks, and climate change mitigation and adaptation, based on the peer-reviewed scientific, technical and socio-economic literature since the publication of the IPCC's Fifth Assessment Report (AR5) in 2014.

The assessment is undertaken within the context of the evolving international landscape, in particular, developments in the UN Framework Convention on Climate Change (UNFCCC) process, including the outcomes of the Kyoto Protocol and the adoption of the Paris Agreement. It reflects the increasing diversity of those involved in climate action.

This report integrates the main findings of the AR6 Working Group reports[1] and the three AR6 Special Reports[2]. It recognizes the interdependence of climate, ecosystems and biodiversity, and human societies; the value of diverse forms of knowledge; and the close linkages between climate change adaptation, mitigation, ecosystem health, human well-being and sustainable development. Building on multiple analytical frameworks, including those from the physical and social sciences, this report identifies opportunities for transformative action which are effective, feasible, just and equitable using concepts of systems transitions and resilient development pathways[3]. Different regional classification schemes[4] are used for physical, social and economic aspects, reflecting the underlying literature.

After this introduction, Section 2, '*Current Status and Trends*', opens with the assessment of observational evidence for our changing climate, historical and current drivers of human-induced climate change, and its impacts. It assesses the current implementation of adaptation and mitigation response options. Section 3, '*Long-Term Climate and Development Futures*', provides a long-term assessment of climate change to 2100 and beyond in a broad range of socio-economic futures. It considers long-term characteristics, impacts, risks and costs in adaptation and mitigation pathways in the context of sustainable development. Section 4, '*Near-Term Responses in a Changing Climate*', assesses opportunities for scaling up effective action in the period up to 2040, in the context of climate pledges, and commitments, and the pursuit of sustainable development.

Based on scientific understanding, key findings can be formulated as statements of fact or associated with an assessed level of confidence using the IPCC calibrated language[5]. The scientific findings are drawn from the underlying reports and arise from their Summary for Policymakers (hereafter SPM), Technical Summary (hereafter TS), and underlying chapters and are indicated by {} brackets. Figure 1.1 shows the Synthesis Report Figures Key, a guide to visual icons that are used across multiple figures within this report.

---

[1] The three Working Group contributions to AR6 are: Climate Change 2021: The Physical Science Basis; Climate Change 2022: Impacts, Adaptation and Vulnerability; and Climate Change 2022: Mitigation of Climate Change, respectively. Their assessments cover scientific literature accepted for publication respectively by 31 January 2021, 1 September 2021 and 11 October 2021.

[2] The three Special Reports are : Global Warming of 1.5°C (2018): an IPCC Special Report on the impacts of global warming of 1.5°C above pre-industrial levels and related global greenhouse gas emission pathways, in the context of strengthening the global response to the threat of climate change, sustainable development, and efforts to eradicate poverty (SR1.5); Climate Change and Land (2019): an IPCC Special Report on climate change, desertification, land degradation, sustainable land management, food security, and greenhouse gas fluxes in terrestrial ecosystems (SRCCL); and The Ocean and Cryosphere in a Changing Climate (2019) (SROCC). The Special Reports cover scientific literature accepted for publication respectively by 15 May 2018, 7 April 2019 and 15 May 2019.

[3] The Glossary (Annex I) includes definitions of these, and other terms and concepts used in this report drawn from the AR6 joint Working Group Glossary.

[4] Depending on the climate information context, geographical regions in AR6 may refer to larger areas, such as sub-continents and oceanic regions, or to typological regions, such as monsoon regions, coastlines, mountain ranges or cities. A new set of standard AR6 WGI reference land and ocean regions have been defined {1.4.5, 10.1, 11.9, 12.1–12.4, Atlas.1.3.3–1.3.4}. WGIII allocates countries to geographical regions, based on the UN Statistics Division Classification {Annex II, WG III}.

[5] Each finding is grounded in an evaluation of underlying evidence and agreement. A level of confidence is expressed using five qualifiers: very low, low, medium, high and very high, and typeset in italics, for example, *medium confidence*. The following terms have been used to indicate the assessed likelihood of an outcome or result: virtually certain 99–100% probability; very likely 90–100%; likely 66–100%; more likely than not >50-100%; about as likely as not 33–66%; unlikely 0–33%; very unlikely 0–10%; and exceptionally unlikely 0–1%. Additional terms (extremely likely 95–100%; more likely than not >50–100%; and extremely unlikely 0–5%) are also used when appropriate. Assessed likelihood also is typeset in italics: for example, *very likely*. This is consistent with AR5. In this Report, unless stated otherwise, square brackets [x to y] are used to provide the assessed *very likely* range, or 90% interval.

Figure 1.1: The Synthesis Report figures key.

Section 2: Current Status and Trends

2.1 Observed Changes, Impacts and Attribution

Human activities, principally through emissions of greenhouse gases, have unequivocally caused global warming, with global surface temperature reaching 1.1°C above 1850-1900 in 2011-2020. Global greenhouse gas emissions have continued to increase over 2010-2019, with unequal historical and ongoing contributions arising from unsustainable energy use, land use and land-use change, lifestyles and patterns of consumption and production across regions, between and within countries, and between individuals (*high confidence*). Human-caused climate change is already affecting many weather and climate extremes in every region across the globe. This has led to widespread adverse impacts on food and water security, human health and on economies and society and related losses and damages[6] to nature and people (*high confidence*). Vulnerable communities who have historically contributed the least to current climate change are disproportionately affected (*high confidence*).

2.1.1 Observed Warming and its Causes

Global surface temperature was around 1.1°C above 1850–1900 in 2011–2020 (1.09°C [0.95°C–1.20°C])[7], with larger increases over land (1.59 [1.34 to 1.83]°C) than over the ocean (0.88°C [0.68°C–1.01°C])[8]. Observed warming is human-caused, with warming from greenhouse gases (GHG), dominated by CO_2 and methane (CH_4), partly masked by aerosol cooling (Figure 2.1). Global surface temperature in the first two decades of the 21st century (2001-2020) was 0.99 [0.84 to 1.10]°C higher than 1850-1900. Global surface temperature has increased faster since 1970 than in any other 50-year period over at least the last 2000 years (*high confidence*). The *likely* range of total human-caused global surface temperature increase from 1850–1900 to 2010–2019[9] is 0.8°C to 1.3°C, with a best estimate of 1.07°C. It is *likely* that well-mixed GHGs[10] contributed a warming of 1.0°C–2.0°C, and other human drivers (principally aerosols) contributed a cooling of 0.0°C–0.8°C, natural (solar and volcanic) drivers changed global surface temperature by ±0.1°C and internal variability changed it by ±0.2°C. {WGI SPM A.1, WGI SPM A.1.2, WGI SPM A.1.3, WGI SPM A.2.2, WGI Figure SPM.2; SRCCL TS.2}

Observed increases in well-mixed GHG concentrations since around 1750 are unequivocally caused by GHG emissions from human activities. Land and ocean sinks have taken up a near-constant proportion (globally about 56% per year) of CO_2 emissions from human activities over the past six decades, with regional differences (*high confidence*). In 2019, atmospheric CO_2 concentrations reached 410 parts per million (ppm), CH_4 reached 1866 parts per billion (ppb) and nitrous oxide (N_2O) reached 332 ppb[11]. Other major contributors to warming are tropospheric ozone (O_3) and halogenated gases. Concentrations of CH_4 and N_2O have increased to levels unprecedented in at least 800,000 years (*very high confidence*), and there is *high confidence* that current CO_2 concentrations are higher than at any time over at least the past two million years. Since 1750, increases in CO_2 (47%) and CH_4 (156%) concentrations far exceed – and increases in N_2O (23%) are similar to – the natural multi-millennial changes between glacial and interglacial periods over at least the past 800,000

[6] In this report, the term 'losses and damages' refers to adverse observed impacts and/or projected risks and can be economic and/or non-economic. (See Annex I: Glossary)

[7] The estimated increase in global surface temperature since AR5 is principally due to further warming since 2003–2012 (+0.19 [0.16 to 0.22] °C). Additionally, methodological advances and new datasets have provided a more complete spatial representation of changes in surface temperature, including in the Arctic. These and other improvements have also increased the estimate of global surface temperature change by approximately 0.1°C, but this increase does not represent additional physical warming since AR5 {WGI SPM A1.2 and footnote 10}

[8] For 1850–1900 to 2013–2022 the updated calculations are 1.15°C [1.00°C–1.25°C] for global surface temperature, 1.65°C [1.36°C–1.90°C] for land temperatures and 0.93°C [0.73°C–1.04°C] for ocean temperatures above 1850–1900 using the exact same datasets (updated by 2 years) and methods as employed in WGI.

[9] The period distinction with the observed assessment arises because the attribution studies consider this slightly earlier period. The observed warming to 2010–2019 is 1.06°C [0.88°C–1.21°C]. {WGI SPM footnote 11}

[10] Contributions from emissions to the 2010-2019 warming relative to 1850-1900 assessed from radiative forcing studies are: CO2 0.8 [0.5 to 1.2]°C; methane 0.5 [0.3 to 0.8]°C; nitrous oxide 0.1 [0.0 to 0.2]°C and fluorinated gases 0.1 [0.0 to 0.2]°C.

[11] For 2021 (the most recent year for which final numbers are available) concentrations using the same observational products and methods as in AR6 WGI are: 415 ppm CO_2; 1896 ppb CH_4; and 335 ppb N_2O. Note that the CO_2 is reported here using the WMO-CO2-X2007 scale to be consistent with WGI. Operational CO_2 reporting has since been updated to use the WMO-CO2-X2019 scale.

years (*very high confidence*). The net cooling effect which arises from anthropogenic aerosols peaked in the late 20th century (*high confidence*). {WGI SPM A1.1, WGI SPM A1.3, WGI SPM A.2.1, WGI Figure SPM.2, WGI TS 2.2, WGI 2ES, WGI Figure 6.1}

[START FIGURE 2.1 HERE]

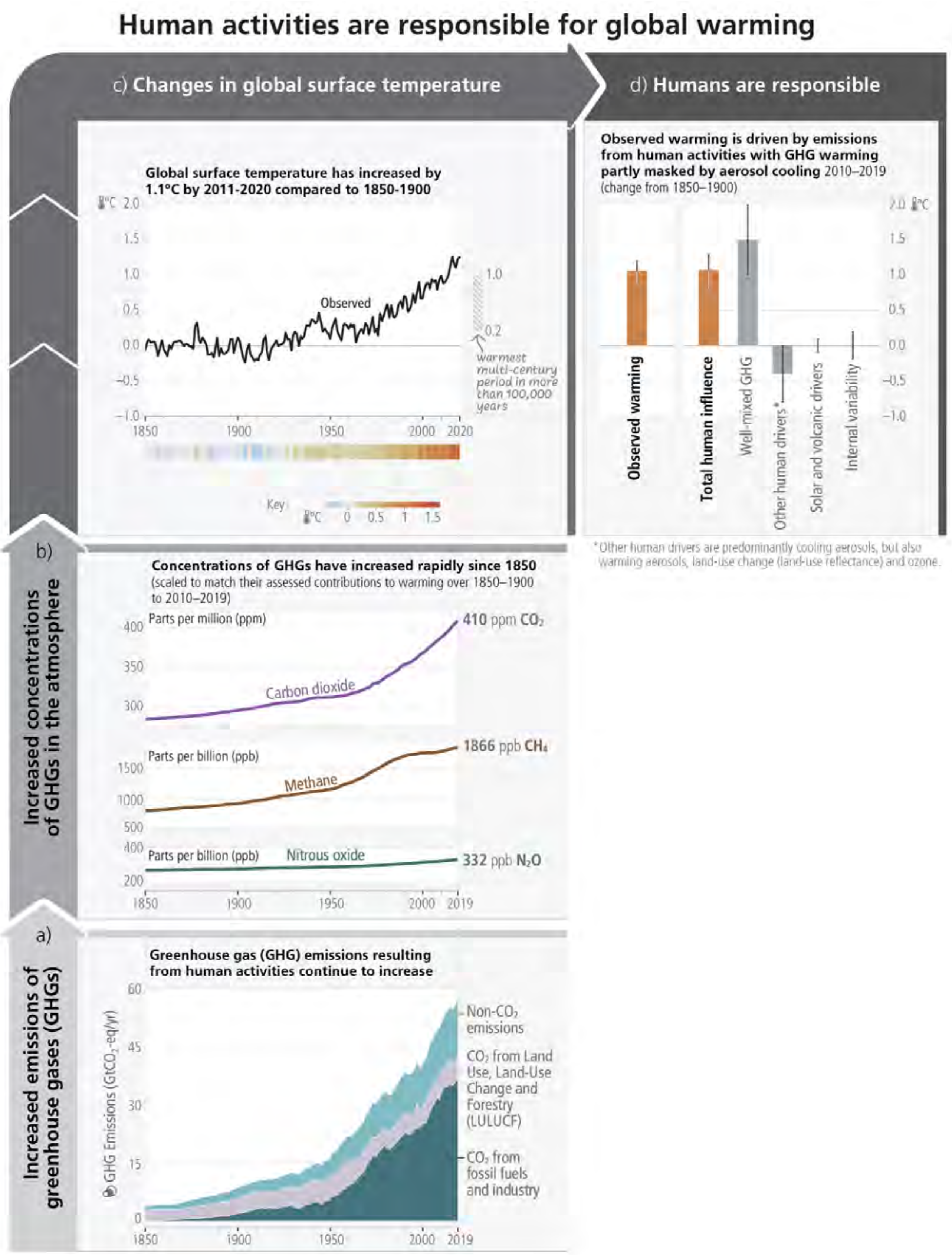

Figure 2.1: The causal chain from emissions to resulting warming of the climate system. Emissions of GHG have increased rapidly over recent decades (**panel (a)**). Global net anthropogenic GHG emissions include CO_2 from fossil fuel combustion and industrial processes (CO_2-FFI) (dark green); net CO_2 from land use, land-use change and forestry (CO_2-LULUCF) (green); CH_4; N_2O; and fluorinated gases (HFCs, PFCs, SF_6, NF_3) (light blue). These emissions have led to increases in the atmospheric concentrations of several GHGs including the three major well-mixed GHGs CO_2, CH_4 and N_2O (**panel (b)**, annual values). To indicate their relative importance each subpanel's vertical extent for CO_2, CH_4 and N_2O is scaled to match the assessed individual direct effect (and, in the case of CH_4 indirect effect via atmospheric chemistry impacts on tropospheric ozone) of historical emissions on temperature change from 1850–1900 to 2010–2019. This estimate arises from an assessment of effective radiative forcing and climate sensitivity. The global surface temperature (shown as annual anomalies from a 1850–1900 baseline) has increased by around 1.1°C since 1850–1900 (**panel (c)**). The vertical bar on the right shows the estimated temperature (*very likely* range) during the warmest multi-century period in at least the last 100,000 years, which occurred around 6500 years ago during the current interglacial period (Holocene). Prior to that, the next most recent warm period was about 125,000 years ago, when the assessed multi-century temperature range [0.5°C–1.5°C] overlaps the observations of the most recent decade. These past warm periods were caused by slow (multi-millennial) orbital variations. Formal detection and attribution studies synthesise information from climate models and observations and show that the best estimate is that all the warming observed between 1850–1900 and 2010–2019 is caused by humans (**panel (d)**). The panel shows temperature change attributed to: total human influence; its decomposition into changes in GHG concentrations and other human drivers (aerosols, ozone and land-use change (land-use reflectance)); solar and volcanic drivers; and internal climate variability. Whiskers show *likely* ranges. {WGI SPM A.2.2, WGI Figure SPM.1, WGI Figure SPM.2, WGI TS2.2, WGI 2.1; WGIII Figure SPM.1, WGIII A.III.II.2.5.1}

[END FIGURE 2.1 HERE]

Average annual GHG emissions[12] during 2010–2019 were higher than in any previous decade, but the rate of growth between 2010 and 2019 (1.3% yr^{-1}) was lower than that between 2000 and 2009 (2.1% yr^{-1}). Historical cumulative net CO_2 emissions from 1850 to 2019 were 2400 ±240 $GtCO_2$. Of these, more than half (58%) occurred between 1850 and 1989 [1400 ±195 $GtCO_2$], and about 42% between 1990 and 2019 [1000 ±90 $GtCO_2$]. Global net anthropogenic GHG emissions have been estimated to be 59±6.6 $GtCO_2$-eq in 2019, about 12% (6.5 $GtCO_2$-eq) higher than in 2010 and 54% (21 $GtCO_2$-eq) higher than in 1990. By 2019, the largest growth in gross emissions occurred in CO_2 from fossil fuels and industry (CO_2-FFI) followed by CH_4, whereas the highest relative growth occurred in fluorinated gases (F-gases), starting from low levels in 1990. (*high confidence*) {WGIII SPM B1.1, WGIII SPM B.1.2, WGIII SPM B.1.3, WGIII Figure SPM.1, WGIII Figure SPM.2}

[START FIGURE 2.2 HERE]

[12] GHG emission metrics are used to express emissions of different GHGs in a common unit. Aggregated GHG emissions in this report are stated in CO_2-equivalents (CO_2-eq) using the Global Warming Potential with a time horizon of 100 years (GWP100) with values based on the contribution of Working Group I to the AR6. The AR6 WGI and WGIII reports contain updated emission metric values, evaluations of different metrics with regard to mitigation objectives, and assess new approaches to aggregating gases. The choice of metric depends on the purpose of the analysis and all GHG emission metrics have limitations and uncertainties, given that they simplify the complexity of the physical climate system and its response to past and future GHG emissions. {WGI SPM D.1.8, WGI 7.6; WGIII SPM B.1, WGIII Cross-Chapter Box 2.2} (Annex I: Glossary)

Emissions have grown in most regions but are distributed unevenly, both in the present day and cumulatively since 1850

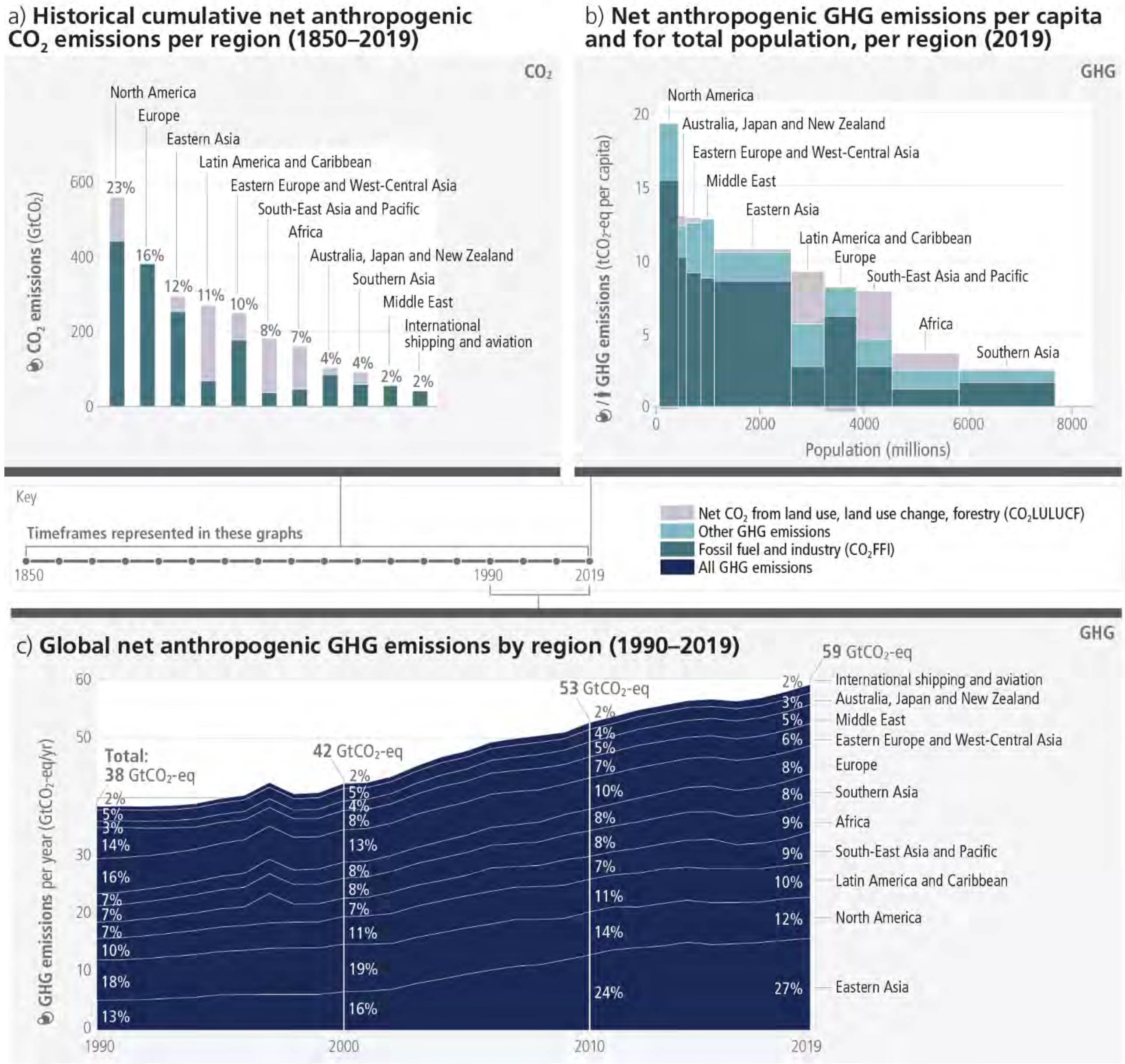

d) **Regional indicators (2019) and regional production vs consumption accounting (2018)**

	Africa	Australia, Japan, New Zealand	Eastern Asia	Eastern Europe, West-Central Asia	Europe	Latin America and Caribbean	Middle East	North America	South-East Asia and Pacific	Southern Asia
Population (million persons, 2019)	1292	157	1471	291	620	646	252	366	674	1836
GDP per capita ($USD1000_{PPP}$ 2017 per person) [1]	5.0	43	17	20	43	15	20	61	12	6.2
Net GHG 2019 [2] (production basis)										
GHG emissions intensity (tCO_2-eq / $USD1000_{PPP}$ 2017)	0.78	0.30	0.62	0.64	0.18	0.61	0.64	0.31	0.65	0.42
GHG per capita (tCO_2-eq per person)	3.9	13	11	13	7.8	9.2	13	19	7.9	2.6
CO_2FFI, 2018, per person										
Production-based emissions (tCO_2FFI per person, based on 2018 data)	1.2	10	8.4	9.2	6.5	2.8	8.7	16	2.6	1.6
Consumption-based emissions (tCO_2FFI per person, based on 2018 data)	0.84	11	6.7	6.2	7.8	2.8	7.6	17	2.5	1.5

[1] GDP per capita in 2019 in USD2017 currency purchasing power basis.
[2] Includes CO_2FFI, CO_2LULUCF and Other GHGs, excluding international aviation and shipping.

The regional groupings used in this figure are for statistical purposes only and are described in WGIII Annex II, Part I.

Figure 2.2: Regional GHG emissions, and the regional proportion of total cumulative production-based CO_2 emissions from 1850 to 2019. Panel (a) shows the share of historical cumulative net anthropogenic CO_2 emissions per region from 1850 to 2019 in $GtCO_2$. This includes CO_2-FFI and CO_2-LULUCF. Other GHG emissions are not included. CO_2-LULUCF emissions are subject to high uncertainties, reflected by a global uncertainty estimate of ±70% (90%

confidence interval). **Panel (b)** shows the distribution of regional GHG emissions in tonnes CO_2-eq per capita by region in 2019. GHG emissions are categorised into: CO_2-FFI; net CO_2-LULUCF; and other GHG emissions (CH_4, N_2O, fluorinated gases, expressed in CO_2-eq using GWP100-AR6). The height of each rectangle shows per capita emissions, the width shows the population of the region, so that the area of the rectangles refers to the total emissions for each region. Emissions from international aviation and shipping are not included. In the case of two regions, the area for CO_2-LULUCF is below the axis, indicating net CO_2 removals rather than emissions. **Panel (c)** shows global net anthropogenic GHG emissions by region (in $GtCO_2$-eq yr^{-1} (GWP100-AR6)) for the time period 1990–2019. Percentage values refer to the contribution of each region to total GHG emissions in each respective time period. The single-year peak of emissions in 1997 was due to higher CO_2-LULUCF emissions from a forest and peat fire event in South East Asia. Regions are as grouped in Annex II of WGIII. **Panel (d)** shows population, GDP per person, emission indicators by region in 2019 for total GHG per person, and total GHG emissions intensity, together with production-based and consumption-based CO_2-FFI data, which is assessed in this report up to 2018. Consumption-based emissions are emissions released to the atmosphere in order to generate the goods and services consumed by a certain entity (e.g., region). Emissions from international aviation and shipping are not included. {WGIII Figure SPM.2}

[END FIGURE 2.2 HERE]

Regional contributions to global human-caused GHG emissions continue to differ widely. Historical contributions of CO_2 emissions vary substantially across regions in terms of total magnitude, but also in terms of contributions to CO_2-FFI (1650 ± 73 $GtCO_2$-eq) and net CO_2-LULUCF (760 ± 220 $GtCO_2$-eq) emissions (Figure 2.2). Variations in regional and national per capita emissions partly reflect different development stages, but they also vary widely at similar income levels. Average per capita net anthropogenic GHG emissions in 2019 ranged from 2.6 tCO_2-eq to 19 tCO_2-eq across regions (Figure 2.2). Least developed countries (LDCs) and Small Island Developing States (SIDS) have much lower per capita emissions (1.7 tCO2-eq and 4.6 tCO2-eq, respectively) than the global average (6.9 tCO_2-eq), excluding CO_2-LULUCF. Around 48% of the global population in 2019 lives in countries emitting on average more than 6 tCO_2-eq per capita, 35% of the global population live in countries emitting more than 9 tCO_2-eq per capita[13] (excluding CO_2-LULUCF) while another 41% live in countries emitting less than 3 tCO_2-eq per capita. A substantial share of the population in these low-emitting countries lack access to modern energy services. (*high confidence*) {WGIII SPM B.3, WGIII SPM B3.1, WGIII SPM B.3.2, WGIII SPM B.3.3}

Net GHG emissions have increased since 2010 across all major sectors (*high confidence*). In 2019, approximately 34% (20 $GtCO_2$-eq) of net global GHG emissions came from the energy sector, 24% (14 $GtCO_2$-eq) from industry, 22% (13 $GtCO_2$-eq) from AFOLU, 15% (8.7 $GtCO_2$-eq) from transport and 6% (3.3 $GtCO_2$-eq) from buildings[14] (*high confidence*). Average annual GHG emissions growth between 2010 and 2019 slowed compared to the previous decade in energy supply (from 2.3% to 1.0%) and industry (from 3.4% to 1.4%) but remained roughly constant at about 2% yr^{-1} in the transport sector (*high confidence*). About half of total net AFOLU emissions are from CO_2 LULUCF, predominantly from deforestation (*medium confidence*). Land overall constituted a net sink of –6.6 (±4.6) $GtCO_2$ yr^{-1} for the period 2010–2019[15] (*medium confidence*). {WGIII SPM B.2, WGIII SPM B.2.1, WGIII SPM B.2.2, WGIII TS 5.6.1}

Human-caused climate change is a consequence of more than a century of net GHG emissions from energy use, land-use and land use change, lifestyle and patterns of consumption, and production. Emissions reductions in CO_2 from fossil fuels and industrial processes (CO2-FFI), due to improvements in energy intensity of GDP and carbon intensity of energy, have been less than emissions increases from rising global activity levels in industry, energy supply, transport, agriculture and buildings. The 10% of households with the highest per capita emissions contribute 34–45% of global consumption-based household GHG emissions, while the middle 40% contribute 40–53%, and the bottom 50% contribute 13–15%. An increasing share of emissions can be attributed to urban areas (a rise from about 62% to 67–72% of the global share between 2015 and 2020). The drivers of urban GHG emissions[16] are complex and include population size,

[13] Territorial emissions

[14] GHG emission levels are rounded to two significant digits; as a consequence, small differences in sums due to rounding may occur {WGIII SPM footnote 8}

[15] Comprising a gross sink of -12.5 (±3.2) $GtCO_2$ yr^{-1} resulting from responses of all land to both anthropogenic environmental change and natural climate variability, and net anthropogenic CO_2- LULUCF emissions +5.9 (±4.1) $GtCO_2$ yr^{-1} based on book-keeping models {WGIII SPM Footnote 14}.

[16] This estimate is based on consumption-based accounting, including both direct emissions from within urban areas, and indirect emissions from outside urban areas related to the production of electricity, goods and services consumed in cities. These estimates

income, state of urbanisation and urban form. (*high confidence*). {WGIII SPM B.2, WGIII SPM B.2.3, WGIII SPM B.3.4, WGIII SPM D.1.1}

2.1.2 Observed Climate System Changes and Impacts to Date

It is unequivocal that human influence has warmed the atmosphere, ocean and land. Widespread and rapid changes in the atmosphere, ocean, cryosphere and biosphere have occurred (Table 2.1). The scale of recent changes across the climate system as a whole and the present state of many aspects of the climate system are unprecedented over many centuries to many thousands of years. It is *very likely* that GHG emissions were the main driver[17] of tropospheric warming and *extremely likely* that human-caused stratospheric ozone depletion was the main driver of stratospheric cooling between 1979 and the mid-1990s. It is *virtually certain* that the global upper ocean (0-700m) has warmed since the 1970s and *extremely likely* that human influence is the main driver. Ocean warming accounted for 91% of the heating in the climate system, with land warming, ice loss and atmospheric warming accounting for about 5%, 3% and 1%, respectively (*high confidence*). Global mean sea level increased by 0.20 [0.15–0.25] m between 1901 and 2018. The average rate of sea level rise was 1.3 [0.6 to 2.1]mm yr-1 between 1901 and 1971, increasing to 1.9 [0.8 to 2.9] mm yr-1 between 1971 and 2006, and further increasing to 3.7 [3.2 to –4.2] mm yr-1 between 2006 and 2018 (*high confidence*). Human influence was very likely the main driver of these increases since at least 1971 (Figure 3.4). Human influence is *very likely* the main driver of the global retreat of glaciers since the 1990s and the decrease in Arctic sea ice area between 1979–1988 and 2010–2019. Human influence has also *very likely* contributed to decreased Northern Hemisphere spring snow cover and surface melting of the Greenland ice sheet. It is *virtually certain* that human-caused CO_2 emissions are the main driver of current global acidification of the surface open ocean. {WGI SPM A.1, WGI SPM A.1.3, WGI SPM A.1.5, WGI SPM A.1.6, WG1 SPM A1.7, WGI SPM A.2, WG1.SPM A.4.2; SROCC SPM.A.1, SROCC SPM A.2}

[START TABLE 2.1 HERE]

Table 2.1: Assessment of observed changes in large-scale indicators of mean climate across climate system components, and their attribution to human influence. The colour coding indicates the assessed confidence in / likelihood[18] of the observed change and the human contribution as a driver or main driver (specified in that case) where available (see colour key). Otherwise, explanatory text is provided. {WGI Table TS.1}

include all CO_2 and CH_4 emission categories except for aviation and marine bunker fuels, land-use change, forestry and agriculture {WGIII SPM footnote 15}

[17] 'Main driver' means responsible for more than 50% of the change {WGI SPM footnote 12}.

[18] Based on scientific understanding, key findings can be formulated as statements of fact or associated with an assessed level of confidence indicated using the IPCC calibrated language.

Change in indicator		Observed change assessment	Human contribution assessment
Atmosphere and water cycle	Warming of global mean surface air temperature since 1850-1900		*likely* range of human contribution ([0.8-1.3°C]) encompasses the *very likely* range of observed warming ([0.9-1.2°C])
	Warming of the troposphere since 1979		Main driver
	Cooling of the lower stratosphere since the mid-20th century		Main driver 1979 - mid-1990s
	Large-scale precipitation and upper troposphere humidity changes since 1979		
	Expansion of the zonal mean Hadley Circulation since the 1980s		Southern Hemisphere
Ocean	Ocean heat content increase since the 1970s		Main driver
	Salinity changes since the mid-20th century		
	Global mean sea level rise since 1970		Main driver
Cryosphere	Arctic sea ice loss since 1979		Main driver
	Reduction in Northern Hemisphere springtime snow cover since 1950		
	Greenland ice sheet mass loss since 1990s		
	Antarctic ice sheet mass loss since 1990s		*Limited evidence & medium agreement*
	Retreat of glaciers		Main driver
Carbon cycle	Increased amplitude of the seasonal cycle of atmospheric CO_2 since the early 1960s		Main driver
	Acidification of the global surface ocean		Main driver
Land climate	Mean surface air temperature over land (about 40% larger than global mean warming)		Main driver
Synthesis	**Warming of the global climate system since preindustrial times**		

Key: *medium confidence*; *likely / high confidence*; *very likely*; *extremely likely*; *virtually certain*; fact

[END TABLE 2.1 HERE]

Human-caused climate change is already affecting many weather and climate extremes in every region across the globe. Evidence of observed changes in extremes such as heatwaves, heavy precipitation, droughts, and tropical cyclones, and, in particular, their attribution to human influence, has strengthened since AR5 (Figure 2.3). It is *virtually certain* that hot extremes (including heatwaves) have become more frequent and more intense across most land regions since the 1950s (Figure 2.3), while cold extremes (including cold waves) have become less frequent and less severe, with *high confidence* that human-caused climate change is the main driver of these changes. Marine heatwaves have approximately doubled in frequency since the 1980s *(high confidence)*, and human influence has *very likely* contributed to most of them since at least 2006. The frequency and intensity of heavy precipitation events have increased since the 1950s over most land areas for which observational data are sufficient for trend analysis (*high confidence*), and human-caused climate change is *likely* the main driver (Figure 2.3). Human-caused climate change has contributed to increases in agricultural and ecological droughts in some regions due to increased land evapotranspiration (*medium confidence*) (Figure 2.3). It is *likely* that the global proportion of major (Category 3–5) tropical cyclone occurrence has increased over the last four decades. {WGI SPM A.3, WGI SPM A3.1, WGI SPM A3.2; WGI SPM A3.4; SRCCL SPM.A.2.2; SROCC SPM. A.2}

[START FIGURE 2.3 HERE]

Climate change has impacted human and natural systems across the world with those who have generally least contributed to climate change being most vulnerable

a) **Synthesis of assessment of observed change in hot extremes, heavy precipitation and drought, and confidence in human contribution to the observed changes in the world's regions**

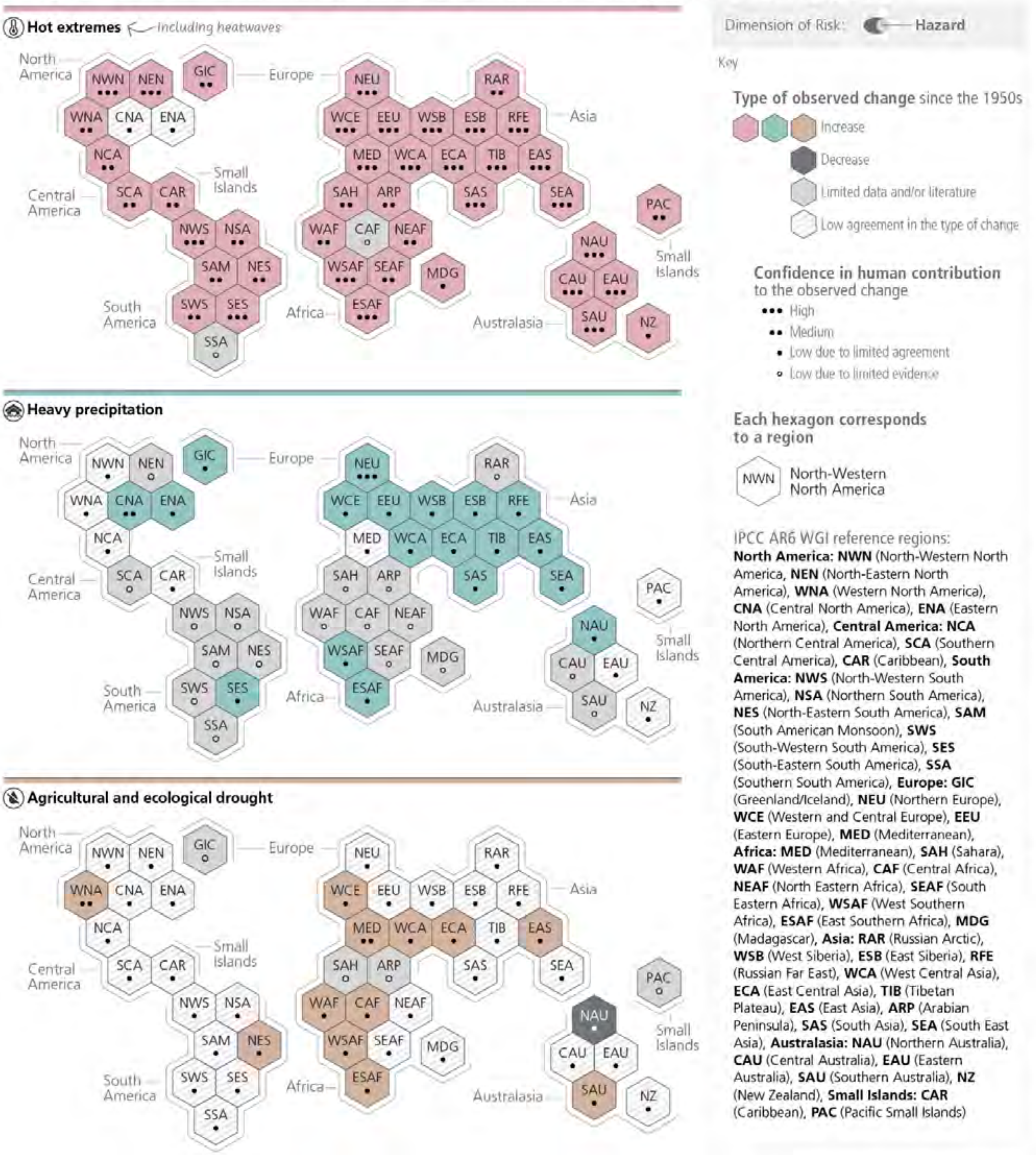

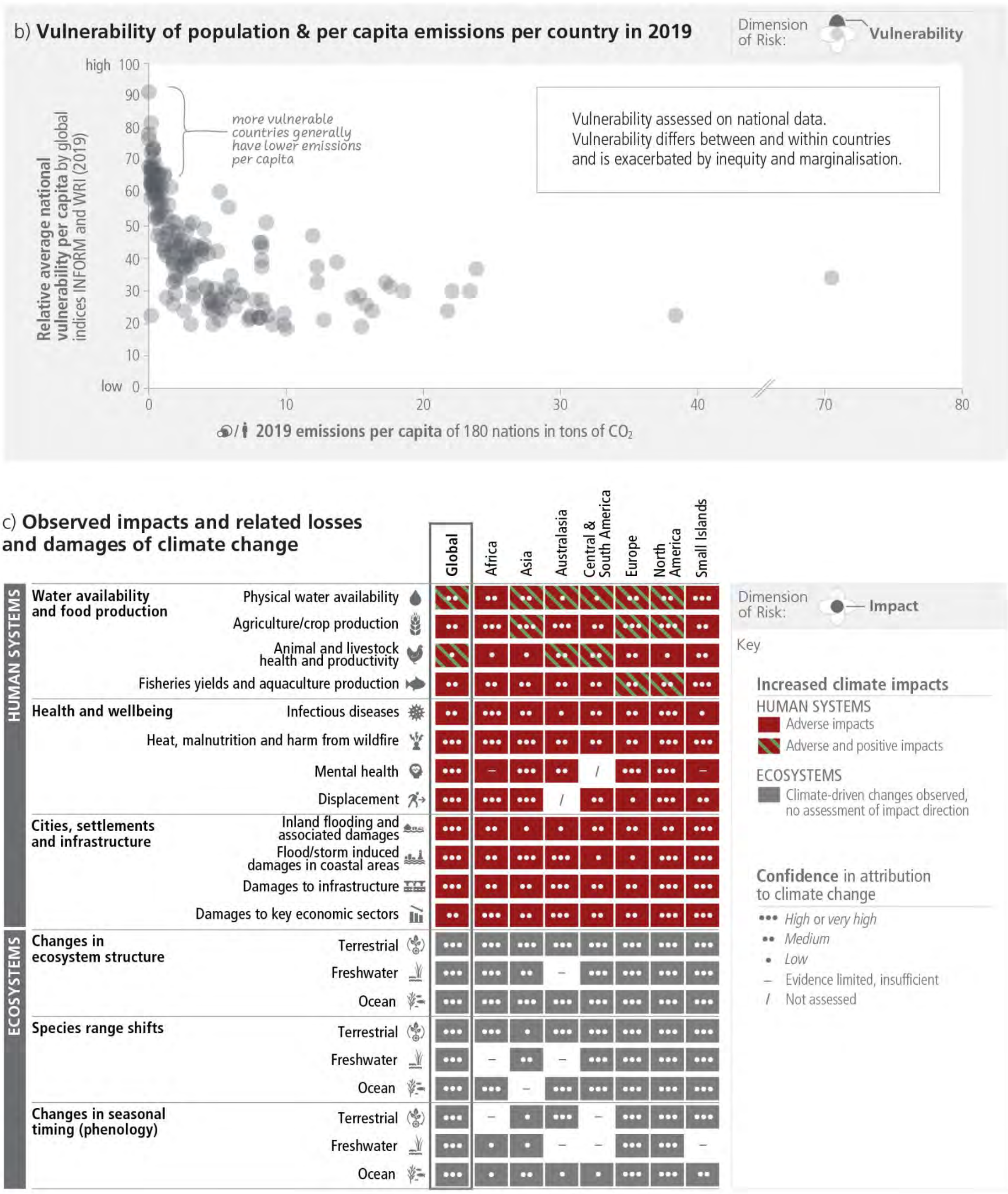

Figure 2.3: Both vulnerability to current climate extremes and historical contribution to climate change are highly heterogeneous with many of those who have least contributed to climate change to date being most vulnerable to its impacts. Panel (a) The IPCC AR6 WGI inhabited regions are displayed as hexagons with identical size in their approximate geographical location (see legend for regional acronyms). All assessments are made for each region as a whole and for the 1950s to the present. Assessments made on different time scales or more local spatial scales might differ from what is shown in the figure. The colours in each panel represent the four outcomes of the assessment on observed changes. Striped hexagons (white and light-grey) are used where there is *low agreement* in the type of change for the region as a whole, and grey hexagons are used when there is limited data and/or literature that prevents an assessment of the region as a whole. Other colours indicate at least *medium confidence* in the observed change. The confidence level for the human influence on these observed changes is based on assessing trend detection and attribution and event attribution literature, and it is indicated by the number of dots: three dots for *high confidence*, two dots for *medium confidence* and one dot for *low confidence* (single, filled dot: *limited agreement*; single, empty dot: *limited evidence*). For hot extremes, the evidence is mostly drawn from changes in metrics based on daily maximum temperatures; regional studies using other indices (heatwave duration, frequency and intensity) are used in addition. For heavy precipitation, the evidence is mostly drawn from changes in indices based on one-day or five-day precipitation amounts

using global and regional studies. Agricultural and ecological droughts are assessed based on observed and simulated changes in total column soil moisture, complemented by evidence on changes in surface soil moisture, water balance (precipitation minus evapotranspiration) and indices driven by precipitation and atmospheric evaporative demand. **Panel (b)** shows the average level of vulnerability amongst a country's population against 2019 CO_2-FFI emissions per- capita per country for the 180 countries for which both sets of metrics are available. Vulnerability information is based on two global indicator systems, namely INFORM and World Risk Index. Countries with a relatively low average vulnerability often have groups with high vulnerability within their population and vice versa. The underlying data includes, for example, information on poverty, inequality, health care infrastructure or insurance coverage. **Panel (c)** Observed impacts on ecosystems and human systems attributed to climate change at global and regional scales. Global assessments focus on large studies, multi-species, meta-analyses and large reviews. Regional assessments consider evidence on impacts across an entire region and do not focus on any country in particular. For human systems, the direction of impacts is assessed and both adverse and positive impacts have been observed e.g., adverse impacts in one area or food item may occur with positive impacts in another area or food item (for more details and methodology see WGII SMTS.1). Physical water availability includes balance of water available from various sources including ground water, water quality and demand for water. Global mental health and displacement assessments reflect only assessed regions. Confidence levels reflect the assessment of attribution of the observed impact to climate change. {WGI Figure SPM.3, Table TS.5, Interactive Atlas; WGII Figure SPM.2, WGII SMTS.1, WGII 8.3.1, Figure 8.5; WGIII 2.2.3}

[END FIGURE 2.3 HERE]

Climate change has caused substantial damages, and increasingly irreversible[19] losses, in terrestrial, freshwater, cryospheric and coastal and open ocean ecosystems (*high confidence*). The extent and magnitude of climate change impacts are larger than estimated in previous assessments (*high confidence*). Approximately half of the species assessed globally have shifted polewards or, on land, also to higher elevations (*very high confidence*). Biological responses including changes in geographic placement and shifting seasonal timing are often not sufficient to cope with recent climate change (*very high confidence*). Hundreds of local losses of species have been driven by increases in the magnitude of heat extremes (*high confidence*) and mass mortality events on land and in the ocean (*very high confidence*). Impacts on some ecosystems are approaching irreversibility such as the impacts of hydrological changes resulting from the retreat of glaciers, or the changes in some mountain (*medium confidence*) and Arctic ecosystems driven by permafrost thaw (*high confidence*). Impacts in ecosystems from slow-onset processes such as ocean acidification, sea level rise or regional decreases in precipitation have also been attributed to human-caused climate change (*high confidence*). Climate change has contributed to desertification and exacerbated land degradation, particularly in low lying coastal areas, river deltas, drylands and in permafrost areas (*high confidence*). Nearly 50% of coastal wetlands have been lost over the last 100 years, as a result of the combined effects of localised human pressures, sea level rise, warming and extreme climate events (*high confidence*). {WGII SPM B.1.1, WGII SPM B.1.2, WGII Figure SPM.2.A, WGII TS.B.1; SRCCL SPM A.1.5, SRCCL SPM A.2, SRCCL SPM A.2.6, SRCCL Figure SPM.1; SROCC SPM A.6.1, SROCC SPM, A.6.4, SROCC SPM A.7}

Climate change has reduced food security and affected water security due to warming, changing precipitation patterns, reduction and loss of cryospheric elements, and greater frequency and intensity of climatic extremes, thereby hindering efforts to meet Sustainable Development Goals (*high confidence*). Although overall agricultural productivity has increased, climate change has slowed this growth in agricultural productivity over the past 50 years globally (*medium confidence*), with related negative crop yield impacts mainly recorded in mid- and low latitude regions, and some positive impacts in some high latitude regions (*high confidence*). Ocean warming in the 20th century and beyond has contributed to an overall decrease in maximum catch potential (*medium confidence*), compounding the impacts from overfishing for some fish stocks (*high confidence*). Ocean warming and ocean acidification have adversely affected food production from shellfish aquaculture and fisheries in some oceanic regions (*high confidence*). Current levels of global warming are associated with moderate risks from increased dryland water scarcity (*high confidence*). Roughly half of the world's population currently experiences severe water scarcity for at least some part of the year due to a combination of climatic and non-climatic drivers (*medium confidence*) (Figure 2.3). Unsustainable agricultural expansion, driven in part by unbalanced diets[20], increases ecosystem and human

[19] See Annex I: Glossary.
[20] Balanced diets feature plant-based foods, such as those based on coarse grains, legumes fruits and vegetables, nuts and seeds, and animal-source foods produced in resilient, sustainable and low-GHG emissions systems, as described in SRCCL. {WGII SPM Footnote 32}

vulnerability and leads to competition for land and/or water resources (*high confidence*). Increasing weather and climate extreme events have exposed millions of people to acute food insecurity[21] and reduced water security, with the largest impacts observed in many locations and/or communities in Africa, Asia, Central and South America, LDCs, Small Islands and the Arctic, and for small-scale food producers, low-income households and Indigenous Peoples globally *(high confidence*). {WGII SPM B.1.3, WGII SPM.B.2.3, WGII Figure SPM.2, WGII TS B.2.3, WGII TS Figure TS. 6; SRCCL SPM A.2.8, SRCCL SPM A.5.3; SROCC SPM A.5.4., SROCC SPM A.7.1, SROCC SPM A.8.1, SROCC Figure SPM.2}

In urban settings, climate change has caused adverse impacts on human health, livelihoods and key infrastructure (*high confidence*). Hot extremes including heatwaves have intensified in cities *(high confidence)*, where they have also worsened air pollution events *(medium confidence*) and limited functioning of key infrastructure (*high confidence*). Urban infrastructure, including transportation, water, sanitation and energy systems have been compromised by extreme and slow-onset events[22], with resulting economic losses, disruptions of services and impacts to well-being *(high confidence)*. Observed impacts are concentrated amongst economically and socially marginalised urban residents, e.g., those living in informal settlements *(high confidence)*. Cities intensify human-caused warming locally (*very high confidence*), while urbanisation also increases mean and heavy precipitation over and/or downwind of cities (*medium confidence*) and resulting runoff intensity (*high confidence*). {WGI SPM C.2.6; WGII SPM B.1.5, WGII Figure TS.9, WGII 6 ES}

Climate change has adversely affected human physical health globally and mental health in assessed regions (*very high confidence*), and is contributing to humanitarian crises where climate hazards interact with high vulnerability (*high confidence*). In all regions increases in extreme heat events have resulted in human mortality and morbidity (*very high confidence*). The occurrence of climate-related food-borne and water-borne diseases has increased (*very high confidence*). The incidence of vector-borne diseases has increased from range expansion and/or increased reproduction of disease vectors (*high confidence*). Animal and human diseases, including zoonoses, are emerging in new areas (*high confidence*). In assessed regions, some mental health challenges are associated with increasing temperatures (*high confidence*), trauma from extreme events (*very high confidence*), and loss of livelihoods and culture (*high confidence*) (Figure 2.3). Climate change impacts on health are mediated through natural and human systems, including economic and social conditions and disruptions (*high confidence*). Climate and weather extremes are increasingly driving displacement in Africa, Asia, North America (*high confidence*), and Central and South America (*medium confidence*) (Figure 2.3) , with small island states in the Caribbean and South Pacific being disproportionately affected relative to their small population size (*high confidence*). Through displacement and involuntary migration from extreme weather and climate events, climate change has generated and perpetuated vulnerability (*medium confidence*). {WGII SPM B.1.4, WGII SPM B.1.7}

Human influence has *likely* increased the chance of compound extreme events[23] since the 1950s. Concurrent and repeated climate hazards have occurred in all regions, increasing impacts and risks to health, ecosystems, infrastructure, livelihoods and food (*high confidence*). Compound extreme events include increases in the frequency of concurrent heatwaves and droughts (*high confidence*); fire weather in some regions (*medium confidence*); and compound flooding in some locations (*medium confidence*). Multiple risks interact, generating new sources of vulnerability to climate hazards, and compounding overall risk (*high confidence*). Compound climate hazards can overwhelm adaptive capacity and substantially increase damage *(high confidence)*. {WGI SPM A.3.5; WGII SPM. B.5.1, WGII TS.C.11.3}

Economic impacts attributable to climate change are increasingly affecting peoples' livelihoods and are causing economic and societal impacts across national boundaries *(high confidence)*. Economic damages from climate change have been detected in climate-exposed sectors, with regional effects to agriculture, forestry, fishery, energy, and tourism, and through outdoor labour productivity (*high confidence*) with some exceptions of positive impacts in regions with low energy demand and comparative advantages in agricultural

[21] Acute food insecurity can occur at any time with a severity that threatens lives, livelihoods or both, regardless of the causes, context or duration, as a result of shocks risking determinants of food security and nutrition, and is used to assess the need for humanitarian action {WGII SPM, footnote 30}.
[22] Slow-onset events are described among the climatic-impact drivers of the WGI AR6 and refer to the risks and impacts associated with e.g., increasing temperature means, desertification, decreasing precipitation, loss of biodiversity, land and forest degradation, glacial retreat and related impacts, ocean acidification, sea level rise and salinization {WGII SPM footnote 29}
[23] See Annex 1: Glossary.

markets and tourism (*high confidence*). Individual livelihoods have been affected through changes in agricultural productivity, impacts on human health and food security, destruction of homes and infrastructure, and loss of property and income, with adverse effects on gender and social equity (*high confidence*). Tropical cyclones have reduced economic growth in the short-term (*high confidence*). Event attribution studies and physical understanding indicate that human-caused climate change increases heavy precipitation associated with tropical cyclones (*high confidence*). Wildfires in many regions have affected built assets, economic activity, and health (*medium* to *high confidence*). In cities and settlements, climate impacts to key infrastructure are leading to losses and damages across water and food systems, and affect economic activity, with impacts extending beyond the area directly impacted by the climate hazard (*high confidence*). {WGI SPM A.3.4, WGII SPM B.1.6, WGII SPM B.5.2, WGII SPM B.5.3}

Climate change has caused widespread adverse impacts and related losses and damages to nature and people (*high confidence*). Losses and damages are unequally distributed across systems, regions and sectors (*high confidence*). Cultural losses, related to tangible and intangible heritage, threaten adaptive capacity and may result in irrevocable losses of sense of belonging, valued cultural practices, identity and home, particularly for Indigenous Peoples and those more directly reliant on the environment for subsistence (*medium confidence*). For example, changes in snow cover, lake and river ice, and permafrost in many Arctic regions, are harming the livelihoods and cultural identity of Arctic residents including Indigenous populations (*high confidence*). Infrastructure, including transportation, water, sanitation and energy systems have been compromised by extreme and slow-onset events, with resulting economic losses, disruptions of services and impacts to wellbeing (*high confidence*). {WGII SPM B.1; WGII SPM B.1.2, WGII SPM.B.1.5, WGII SPM C.3.5, WGII TS.B.1.6; SROCC SPM A.7.1}

Across sectors and regions, the most vulnerable people and systems have been disproportionately affected by the impacts of climate change (*high confidence*). LDCs and SIDS who have much lower per capita emissions (1.7 tCO_2-eq, 4.6 tCO_2-eq, respectively) than the global average (6.9 tCO_2-eq) excluding CO_2-LULUCF, also have high vulnerability to climatic hazards, with global hotspots of high human vulnerability observed in West-, Central- and East Africa, South Asia, Central and South America, SIDS and the Arctic (*high confidence*). Regions and people with considerable development constraints have high vulnerability to climatic hazards (*high confidence*). Vulnerability is higher in locations with poverty, governance challenges and limited access to basic services and resources, violent conflict and high levels of climate-sensitive livelihoods (e.g., smallholder farmers, pastoralists, fishing communities) (*high confidence*). Vulnerability at different spatial levels is exacerbated by inequity and marginalisation linked to gender, ethnicity, low income or combinations thereof (*high confidence*), especially for many Indigenous Peoples and local communities (*high confidence*). Approximately 3.3 to 3.6 billion people live in contexts that are highly vulnerable to climate change (*high confidence*). Between 2010 and 2020, human mortality from floods, droughts and storms was 15 times higher in highly vulnerable regions, compared to regions with very low vulnerability (*high confidence*). In the Arctic and in some high mountain regions, negative impacts of cryosphere change have been especially felt among Indigenous Peoples (*high confidence*). Human and ecosystem vulnerability are interdependent (*high confidence*). Vulnerability of ecosystems and people to climate change differs substantially among and within regions (*very high confidence*), driven by patterns of intersecting socio-economic development, unsustainable ocean and land use, inequity, marginalisation, historical and ongoing patterns of inequity such as colonialism, and governance[24] (*high confidence*). {WGII SPM B.1, WGII SPM B.2, WGII SPM B.2.4; WGIII SPM B.3.1; SROCC SPM A.7.1, SROCC SPM A.7.2}

[24] Governance: The structures, processes and actions through which private and public actors interact to address societal goals. This includes formal and informal institutions and the associated norms, rules, laws and procedures for deciding, managing, implementing and monitoring policies and measures at any geographic or political scale, from global to local. {WGII SPM Footnote 31}

2.2 Responses Undertaken to Date

International climate agreements, rising national ambitions for climate action, along with rising public awareness are accelerating efforts to address climate change at multiple levels of governance. Mitigation policies have contributed to a decrease in global energy and carbon intensity, with several countries achieving GHG emission reductions for over a decade. Low-emission technologies are becoming more affordable, with many low or zero emissions options now available for energy, buildings, transport, and industry. Adaptation planning and implementation progress has generated multiple benefits, with effective adaptation options having the potential to reduce climate risks and contribute to sustainable development. Global tracked finance for mitigation and adaptation has seen an upward trend since AR5, but falls short of needs. (*high confidence*)

2.2.1 Global Policy Setting

The United Nations Framework Convention on Climate Change (UNFCCC), Kyoto Protocol, and Paris Agreement are supporting rising levels of national ambition and encouraging the development and implementation of climate policies at multiple levels of governance *(high confidence)*. The Kyoto Protocol led to reduced emissions in some countries and was instrumental in building national and international capacity for GHG reporting, accounting and emissions markets (*high confidence*). The Paris Agreement, adopted under the UNFCCC, with near universal participation, has led to policy development and target-setting at national and sub-national levels, particularly in relation to mitigation but also for adaptation, as well as enhanced transparency of climate action and support (*medium confidence*). Nationally Determined Contributions (NDCs), required under the Paris Agreement, have required countries to articulate their priorities and ambition with respect to climate action. {WGII 17.4, WGIII SPM B.5.1, WGIII SPM E.6, WGII TS D.1.1}

Loss & Damage[25] was formally recognized in 2013 through establishment of the *Warsaw International Mechanism on Loss and Damage* (WIM), and in 2015, Article 8 of the Paris Agreement provided a legal basis for the WIM. There is improved understanding of both economic and non-economic losses and damages, which is informing international climate policy and which has highlighted that losses and damages are not comprehensively addressed by current financial, governance and institutional arrangements, particularly in vulnerable developing countries (*high confidence*). {WGII SPM C.3.5, WGII Cross-Chapter Box LOSS}

Other recent global agreements that influence responses to climate change include the Sendai Framework for Disaster Risk Reduction (2015–2030), the finance-oriented Addis Ababa Action Agenda (2015) and the New Urban Agenda (2016), and the Kigali Amendment to the Montreal Protocol on Substances that Deplete the Ozone Layer (2016), among others. In addition, the 2030 Agenda for Sustainable Development, adopted in 2015 by UN member states, sets out 17 Sustainable Development Goals (SDGs) and seeks to align efforts globally to prioritise ending extreme poverty, protect the planet and promote more peaceful, prosperous and inclusive societies. If achieved, these agreements would reduce climate change, and the impacts on health, wellbeing, migration, and conflict, among others (*very high confidence*). {WGII TS.A.1, WGII 7 ES}

Since AR5, rising public awareness and an increasing diversity of actors, have overall helped accelerate political commitment and global efforts to address climate change (*medium confidence*). Mass social movements have emerged as catalysing agents in some regions, often building on prior movements including Indigenous Peoples-led movements, youth movements, human rights movements, gender activism, and climate litigation, which is raising awareness and, in some cases, has influenced the outcome and ambition of climate governance (*medium confidence*). Engaging Indigenous Peoples and local communities using just-transition and rights-based decision-making approaches, implemented through collective and participatory decision-making processes has enabled deeper ambition and accelerated action in different ways, and at all scales, depending on national circumstances (*medium confidence*). The media helps shape the public discourse about climate change. This can usefully build public support to accelerate climate action (*medium evidence, high agreement)*. In some instances, public discourses of media and organised counter movements have impeded climate action, exacerbating helplessness and disinformation and fuelling polarisation, with negative implications for climate action (*medium confidence*). {WGII SPM C.5.1, WGII SPM D.2, WGII TS.D.9, WGII

[25] See Annex I: Glossary.

TS.D.9.7, WGII TS.E.2.1, WGII 18.4; WGIII SPM D.3.3, WGIII SPM E.3.3, WGIII TS.6.1, WGIII 6.7, WGIII 13 ES, WGIII Box.13.7}

2.2.2 Mitigation Actions to Date

There has been a consistent expansion of policies and laws addressing mitigation since AR5 (*high confidence*). Climate governance supports mitigation by providing frameworks through which diverse actors interact, and a basis for policy development and implementation (*medium confidence*). Many regulatory and economic instruments have already been deployed successfully (*high confidence*). By 2020, laws primarily focussed on reducing GHG emissions existed in 56 countries covering 53% of global emissions (*medium confidence*). The application of diverse policy instruments for mitigation at the national and sub-national levels has grown consistently across a range of sectors (*high confidence*). Policy coverage is uneven across sectors and remains limited for emissions from agriculture, and from industrial materials and feedstocks (*high confidence*). {WGIII SPM B.5, WGIII SPM B.5.2, WGIII SPM E.3, WGIII SPM E.4}

Practical experience has informed economic instrument design and helped to improve predictability, environmental effectiveness, economic efficiency, alignment with distributional goals, and social acceptance (*high confidence*). Low-emission technological innovation is strengthened through the combination of technology-push policies, together with policies that create incentives for behaviour change and market opportunities (*high confidence*) (Section 4.8.3). Comprehensive and consistent policy packages have been found to be more effective than single policies (*high confidence*). Combining mitigation with policies to shift development pathways, policies that induce lifestyle or behaviour changes, for example, measures promoting walkable urban areas combined with electrification and renewable energy can create health co-benefits from cleaner air and enhanced active mobility (*high confidence*). Climate governance enables mitigation by providing an overall direction, setting targets, mainstreaming climate action across policy domains and levels, based on national circumstances and in the context of international cooperation. Effective governance enhances regulatory certainty, creating specialised organisations and creating the context to mobilise finance *(medium confidence)*. These functions can be promoted by climate-relevant laws, which are growing in number, or climate strategies, among others, based on national and sub-national context (*medium confidence*). Effective and equitable climate governance builds on engagement with civil society actors, political actors, businesses, youth, labour, media, Indigenous Peoples and local communities (*medium confidence*). {WGIII SPM E.2.2, WGIII SPM E.3, WGIII SPM E.3.1, WGIII SPM E.4.2, WGIII SPM E.4.3, WGIII SPM E.4.4}

The unit costs of several low-emission technologies, including solar, wind and lithium-ion batteries, have fallen consistently since 2010 (Figure 2.4). Design and process innovations in combination with the use of digital technologies have led to near-commercial availability of many low or zero emissions options in buildings, transport and industry. From 2010 to 2019, there have been sustained decreases in the unit costs of solar energy (by 85%), wind energy (by 55%), and lithium-ion batteries (by 85%), and large increases in their deployment, e.g., >10× for solar and >100× for electric vehicles (EVs), albeit varying widely across regions (Figure 2.4). Electricity from PV and wind is now cheaper than electricity from fossil sources in many regions, electric vehicles are increasingly competitive with internal combustion engines, and large-scale battery storage on electricity grids is increasingly viable. In comparison to modular small-unit size technologies, the empirical record shows that multiple large-scale mitigation technologies, with fewer opportunities for learning, have seen minimal cost reductions and their adoption has grown slowly. Maintaining emission-intensive systems may, in some regions and sectors, be more expensive than transitioning to low emission systems. (*high confidence*) {WGIII SPM B.4, WGIII SPM B.4.1, WGIII SPM C.4.2, WGIII SPM C.5.2, WGIII SPM C.7.2, WGIII SPM C.8, WGIII Figure SPM.3, WGIII Figure SPM.3}

For almost all basic materials – primary metals, building materials and chemicals – many low- to zero-GHG intensity production processes are at the pilot to near-commercial and in some cases commercial stage but they are not yet established industrial practice. Integrated design in construction and retrofit of buildings has led to increasing examples of zero energy or zero carbon buildings. Technological innovation made possible the widespread adoption of LED lighting. Digital technologies including sensors, the internet of things, robotics, and artificial intelligence can improve energy management in all sectors; they can increase energy efficiency, and promote the adoption of many low-emission technologies, including decentralised renewable energy, while creating economic opportunities. However, some of these climate change mitigation gains can be reduced or counterbalanced by growth in demand for goods and services due to the use of digital devices. Several mitigation options, notably solar energy, wind energy, electrification of urban systems, urban green infrastructure, energy efficiency, demand side management, improved forest- and crop/grassland management, and reduced food waste and loss, are technically viable, are becoming increasingly cost effective and are generally supported by the public, and this enables expanded deployment in many regions. (*high confidence*) {WGIII SPM B.4.3, WGIII SPM C.5.2, WGIII SPM C.7.2, WGIII SPM E.1.1, WGIII TS.6.5}

[START FIGURE 2.4 HERE]

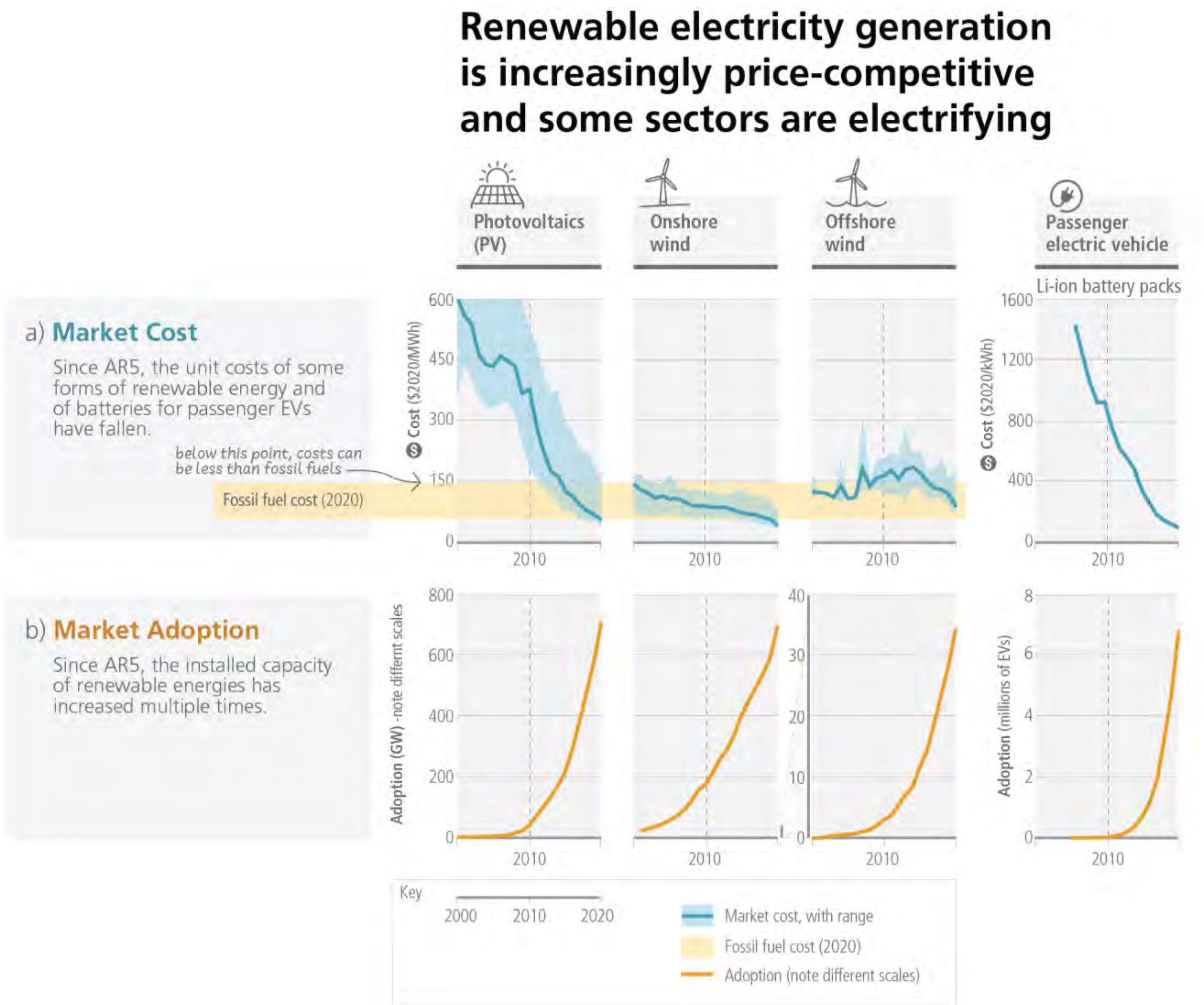

Figure 2.4: **Unit cost reductions and use in some rapidly changing mitigation technologies.** The **top panel (a)** shows global costs per unit of energy (USD per MWh) for some rapidly changing mitigation technologies. Solid blue lines indicate average unit cost in each year. Light blue shaded areas show the range between the 5th and 95th percentiles in each year. Yellow shading indicates the range of unit costs for new fossil fuel (coal and gas) power in 2020 (corresponding to USD55–148 per MWh). In 2020, the levelised costs of energy (LCOE) of the three renewable energy technologies could compete with fossil fuels in many places. For batteries, costs shown are for 1 kWh of battery storage capacity; for the others, costs are LCOE, which includes installation, capital, operations, and maintenance costs per MWh of electricity produced. The literature uses LCOE because it allows consistent comparisons of cost trends across a diverse set of energy technologies to be made. However, it does not include the costs of grid integration or climate impacts. Further, LCOE does not take into account other environmental and social externalities that may modify the overall (monetary and non-monetary) costs of technologies and alter their deployment. The **bottom panel (b)** shows cumulative global adoption for each technology, in GW of installed capacity for renewable energy and in millions of vehicles for battery-electric vehicles. A vertical dashed line is placed in 2010 to indicate the change over the past decade. The electricity production share reflects different capacity factors; for example, for the same amount of installed capacity, wind produces about twice as

much electricity as solar PV {WGIII 2.5, 6.4}. Renewable energy and battery technologies were selected as illustrative examples because they have recently shown rapid changes in costs and adoption, and because consistent data are available. Other mitigation options assessed in the WGIII report are not included as they do not meet these criteria. {WGIII Figure SPM.3}

[END FIGURE 2.4 HERE]

The magnitude of global climate finance flows has increased and financing channels have broadened (*high confidence*). Annual tracked total financial flows for climate mitigation and adaptation increased by up to 60% between 2013/14 and 2019/20, but average growth has slowed since 2018 (*medium confidence*) and most climate finance stays within national borders (*high confidence*). Markets for green bonds, environmental, social and governance and sustainable finance products have expanded significantly since AR5 (*high confidence*). Investors, central banks, and financial regulators are driving increased awareness of climate risk to support climate policy development and implementation (*high confidence*). Accelerated international financial cooperation is a critical enabler of low-GHG and just transitions (*high confidence*). {WGIII SPM B.5.4, WGIII SPM E.5, WGIII TS.6.3, WGIII TS.6.4}

Economic instruments have been effective in reducing emissions, complemented by regulatory instruments mainly at the national and also sub-national and regional level (*high confidence*). By 2020, over 20% of global GHG emissions were covered by carbon taxes or emissions trading systems, although coverage and prices have been insufficient to achieve deep reductions (*medium confidence*). Equity and distributional impacts of carbon pricing instruments can be addressed by using revenue from carbon taxes or emissions trading to support low-income households, among other approaches (*high confidence*). The mix of policy instruments which reduced costs and stimulated adoption of solar energy, wind energy and lithium-ion batteries includes public R&D, funding for demonstration and pilot projects, and demand pull instruments such as deployment subsidies to attain scale (*high confidence*) (Figure 2.4). {WGIII SPM B.4.1, WGIII SPM B.5.2, WGIII SPM E.4.2, WG III TS.3}

Mitigation actions, supported by policies, have contributed to a decrease in global energy and carbon intensity between 2010 and 2019, with a growing number of countries achieving absolute GHG emission reductions for more than a decade (*high confidence*). While global net GHG emissions have increased since 2010, global energy intensity (total primary energy per unit GDP) decreased by 2% yr^{-1} between 2010 and 2019. Global carbon intensity (CO_2-FFI per unit primary energy) also decreased by 0.3% yr^{-1}, mainly due to fuel switching from coal to gas, reduced expansion of coal capacity, and increased use of renewables, and with large regional variations over the same period. In many countries, policies have enhanced energy efficiency, reduced rates of deforestation and accelerated technology deployment, leading to avoided and in some cases reduced or removed emissions (*high confidence*). At least 18 countries have sustained production-based CO_2 and GHG and consumption-based CO_2 absolute emission reductions for longer than 10 years since 2005 through energy supply decarbonization, energy efficiency gains, and energy demand reduction, which resulted from both policies and changes in economic structure (*high confidence*). Some countries have reduced production-based GHG emissions by a third or more since peaking, and some have achieved reduction rates of around 4% yr^{-1} for several years consecutively (*high confidence*). Multiple lines of evidence suggest that mitigation policies have led to avoided global emissions of several $GtCO_2$-eq yr^{-1} (*medium confidence*). At least 1.8 $GtCO_2$-eq yr^{-1} of avoided emissions can be accounted for by aggregating separate estimates for the effects of economic and regulatory instruments (*medium confidence*). Growing numbers of laws and executive orders have impacted global emissions and are estimated to have resulted in 5.9 $GtCO_2$-eq yr^{-1} of avoided emissions in 2016 (*medium confidence*). These reductions have only partly offset global emissions growth (*high confidence*) {WGIII SPM B.1, WGIII SPM B.2.4, WGIII SPM B.3.5, WGIII SPM B.5.1, WGIII SPM B.5.3, WGIII 1.3.2, WGIII 2.2.3}

2.2.3 Adaptation Actions to Date

Progress in adaptation planning and implementation has been observed across all sectors and regions, generating multiple benefits (*very high confidence*). The ambition, scope and progress on adaptation have risen among governments at the local, national and international levels, along with businesses, communities and civil society (*high confidence*). Various tools, measures and processes are available that can enable, accelerate and sustain adaptation implementation (*high confidence*). Growing public and political awareness of climate impacts and risks has resulted in at least 170 countries and many cities including adaptation in their climate policies and planning processes (*high confidence*). Decision support tools and climate services are increasingly being used (*very high confidence*) and pilot projects and local experiments are being implemented in different sectors (*high confidence*). {WGII SPM C.1, WGII SPM.C.1.1, WGII TS.D.1.3, WGII TS.D.10}

Adaptation to water-related risks and impacts make up the majority (~60%) of all documented[26] adaptation (*high confidence*). A large number of these adaptation responses are in the agriculture sector and these include on-farm water management, water storage, soil moisture conservation, and irrigation. Other adaptations in agriculture include cultivar improvements, agroforestry, community-based adaptation and farm and landscape diversification among others (*high confidence*). For inland flooding, combinations of non-structural measures like early warning systems, enhancing natural water retention such as by restoring wetlands and rivers, and land use planning such as no build zones or upstream forest management, can reduce flood risk (*medium confidence*). Some land-related adaptation actions such as sustainable food production, improved and sustainable forest management, soil organic carbon management, ecosystem conservation and land restoration, reduced deforestation and degradation, and reduced food loss and waste are being undertaken, and can have mitigation co-benefits (*high confidence*). Adaptation actions that increase the resilience of biodiversity and ecosystem services to climate change include responses like minimising additional stresses or disturbances, reducing fragmentation, increasing natural habitat extent, connectivity and heterogeneity, and protecting small-scale refugia where microclimate conditions can allow species to persist (*high confidence*). Most innovations in urban adaptation have occurred through advances in disaster risk management, social safety nets and green/blue infrastructure (*medium confidence*). Many adaptation measures that benefit health and wellbeing are found in other sectors (e.g., food, livelihoods, social protection, water and sanitation, infrastructure) (*high confidence*). {WGII SPM C.2.1, WGII SPM C.2.2, WGII TS.D.1.2, WGII TS.D.1.4, WGII TS.D.4.2, WGII TS.D.8.3, WGII 4 ES; SRCCL SPM B.1.1}

Adaptation can generate multiple additional benefits such as improving agricultural productivity, innovation, health and well-being, food security, livelihood, and biodiversity conservation as well as reduction of risks and damages (*very high confidence*). {WGII SPM C1.1}

Globally tracked adaptation finance has shown an upward trend since AR5, but represents only a small portion of total climate finance, is uneven and has developed heterogeneously across regions and sectors (*high confidence*). Adaptation finance has come predominantly from public sources, largely through grants, concessional and non-concessional instruments (*very high confidence*). Globally, private-sector financing of adaptation from a variety of sources such as commercial financial institutions, institutional investors, other private equity, non-financial corporations, as well as communities and households has been limited, especially in developing countries (*high confidence*). Public mechanisms and finance can leverage private sector finance for adaptation by addressing real and perceived regulatory, cost and market barriers, for example via public-private partnerships (*high confidence*). Innovations in adaptation and resilience finance, such as forecast-based/anticipatory financing systems and regional risk insurance pools, have been piloted and are growing in scale (*high confidence*). {WGII SPM C.3.2, WGII SPM C.5.4; WGII TS.D.1.6, WGII Cross-Chapter Box FINANCE; WGIII SPM E.5.4}

There are adaptation options which are effective[27] in reducing climate risks[28] for specific contexts, sectors and regions and contribute positively to sustainable development and other societal goals. In the agriculture sector, cultivar improvements, on-farm water management and storage, soil moisture conservation, irrigation[29], agroforestry, community-based adaptation, and farm and landscape level diversification, and sustainable land management approaches, provide multiple benefits and reduce climate risks. Reduction of food loss and waste, and adaptation measures in support of balanced diets contribute to nutrition, health, and biodiversity benefits. (*high confidence*) {WGII SPM C.2, WGII SPM C.2.1, WGII SPM C.2.2; SRCCL B.2, SRCCL SPM C.2.1}

[26] Documented adaptation refers to published literature on adaptation policies, measures and actions that has been implemented and documented in peer reviewed literature, as opposed to adaptation that may have been planned, but not implemented.
[27] Effectiveness refers here to the extent to which an adaptation option is anticipated or observed to reduce climate-related risk.
[28] See Annex I: Glossary.
[29] Irrigation is effective in reducing drought risk and climate impacts in many regions and has several livelihood benefits, but needs appropriate management to avoid potential adverse outcomes, which can include accelerated depletion of groundwater and other water sources and increased soil salinization (*medium confidence*).

Ecosystem-based Adaptation[30] approaches such as urban greening, restoration of wetlands and upstream forest ecosystems reduce a range of climate change risks, including flood risks, urban heat and provide multiple co-benefits. Some land-based adaptation options provide immediate benefits (e.g., conservation of peatlands, wetlands, rangelands, mangroves and forests); while afforestation and reforestation, restoration of high-carbon ecosystems, agroforestry, and the reclamation of degraded soils take more time to deliver measurable results. Significant synergies exist between adaptation and mitigation, for example through sustainable land management approaches. Agroecological principles and practices and other approaches that work with natural processes support food security, nutrition, health and well-being, livelihoods and biodiversity, sustainability and ecosystem services. (*high confidence*) {WGII SPM C.2.1, WGII SPM C.2.2, WGII SPM C.2.5, WGII TS.D.4.1; SRCCL SPM B.1.2, SRCCL SPM.B.6.1; SROCC SPM C.2}

Combinations of non-structural measures like early warning systems and structural measures like levees have reduced loss of lives in case of inland flooding (*medium confidence*) and early warning systems along with flood-proofing of buildings have proven to be cost-effective in the context of coastal flooding under current sea level rise (*high confidence*). Heat Health Action Plans that include early warning and response systems are effective adaptation options for extreme heat (*high confidence*). Effective adaptation options for water, food and vector-borne diseases include improving access to potable water, reducing exposure of water and sanitation systems to extreme weather events, and improved early warning systems, surveillance, and vaccine development (*very high confidence*). Adaptation options such as disaster risk management, early warning systems, climate services and social safety nets have broad applicability across multiple sectors (*high confidence*). {WGII SPM C.2.1, WGII SPM C.2.5, WGII SPM C.2.9, WGII SPM C.2.11, WGII SPM C.2.13; SROCC SPM C.3.2}

Integrated, multi-sectoral solutions that address social inequities, differentiate responses based on climate risk and cut across systems, increase the feasibility and effectiveness of adaptation in multiple sectors (*high confidence*). {WGII SPM C.2}

2.3 Current Mitigation and Adaptation Actions and Policies are not Sufficient

At the time of the present assessment[31] there are gaps between global ambitions and the sum of declared national ambitions. These are further compounded by gaps between declared national ambitions and current implementation for all aspects of climate action. For mitigation, global GHG emissions in 2030 implied by NDCs announced by October 2021 would make it *likely* that warming will exceed 1.5°C during the 21st century and would make it harder to limit warming below 2°C.[32] Despite progress, adaptation gaps[33] persist, with many initiatives prioritising short-term risk reduction, hindering transformational adaptation. Hard and soft limits to adaptation are being reached in some sectors and regions, while maladaptation is also increasing and disproportionately affecting vulnerable groups. Systemic barriers such as funding, knowledge, and practice gaps, including lack of climate literacy and data hinders adaptation progress. Insufficient financing, especially for adaptation, constraints climate action in particular in developing countries. (*high confidence*)

2.3.1 The Gap Between Mitigation Policies, Pledges and Pathways that Limit Warming to 1.5 or Below 2°C

Global GHG emissions in 2030 associated with the implementation of NDCs announced prior to COP26[34] would make it *likely* that warming will exceed 1.5°C during the 21st century and would make

[30] EbA is recognised internationally under the Convention on Biological Diversity (CBD14/5). A related concept is Nature-based Solutions (NbS), see Annex I: Glossary
[31] The timing of various cut-offs for assessment differs by WG report and the aspect assessed. See footnote 1 in Section 1.
[32] See CSB.2 for a discussion of scenarios and pathways.
[33] See Annex I: Glossary.
[34] NDCs announced prior to COP26 refer to the most recent NDCs submitted to the UNFCCC up to the literature cut-off date of the WGIII report, 11 October 2021, and revised NDCs announced by China, Japan and the Republic of Korea prior to October 2021 but

it harder to limit warming below 2°C – if no additional commitments are made or actions taken (Figure 2.5, Table 2.2). A substantial 'emissions gap' exists as global GHG emissions in 2030 associated with the implementation of NDCs announced prior to COP26 would be similar to or only slightly below 2019 emission levels and higher than those associated with modelled mitigation pathways that limit warming to 1.5°C (>50%) with no or limited overshoot or to 2°C (>67%), assuming immediate action, which implies deep, rapid and sustained global GHG emission reductions this decade (*high confidence*) (Table 2.2, Table 3.1, 4.1).[35] The magnitude of the emissions gap depends on the global warming level considered and whether only unconditional or also conditional elements of NDCs[36] are considered (*high confidence*) (Table 2.2). Modelled pathways that are consistent with NDCs announced prior to COP26 until 2030 and assume no increase in ambition thereafter have higher emissions, leading to a median global warming of 2.8 [2.1–3.4]°C by 2100 (*medium confidence*). If the 'emission gap' is not reduced, global GHG emissions in 2030 consistent with NDCs announced prior to COP26 make it *likely* that warming will exceed 1.5°C during the 21st century, while limiting warming to 2°C (>67%) would imply an unprecedented acceleration of mitigation efforts during 2030–2050 (*medium confidence*) (see Section 4.1, CSB2). {WGIII SPM B.6, WGIII SPM B.6.1, WGIII SPM B.6.3, WGIII SPM B.6.4, WGIII SPM C.1.1}.

Policies implemented by the end of 2020 are projected to result in higher global GHG emissions in 2030 than those implied by NDCs, indicating an 'implementation gap'[37] (*high confidence*) (Table 2.2, Figure 2.5). Projected global emissions implied by policies implemented by the end of 2020 are 57 (52–60) $GtCO_2$-eq in 2030 (Table 2.2). This points to an implementation gap compared with the NDCs of 4–7 $GtCO_2$-eq in 2030 (Table 2.2); without a strengthening of policies, emissions are projected to rise, leading to a median global warming of 2.2°C–3.5°C (*very likely* range) by 2100 (*medium confidence*) (see Section 3.1.1). {WGIII SPM B.6.1, WGIII SPM C.1}

Projected cumulative future CO_2 emissions over the lifetime of existing fossil fuel infrastructure without additional abatement[38] exceed the total cumulative net CO_2 emissions in pathways that limit warming to 1.5°C (>50%) with no or limited overshoot. They are approximately equal to total cumulative net CO_2 emissions in pathways that limit warming to 2°C with a likelihood of 83%[39] (see Figure 3.5). Limiting warming to 2°C (>67%) or lower will result in stranded assets. About 80% of coal, 50% of gas, and 30% of oil reserves cannot be burned and emitted if warming is limited to 2°C. Significantly more reserves are expected to remain unburned if warming is limited to 1.5°C. (*high confidence*) {WGIII SPM B.7, WGIII Box. 6.13}

[**START TABLE 2.2 HERE**]

Table 2.2 Projected global emissions in 2030 associated with policies implemented by the end of 2020 and NDCs announced prior to COP26, and associated emissions gaps. Emissions projections for 2030 and gross differences in emissions are based on emissions of 52–56 $GtCO_2$-eq yr^{-1} in 2019 as assumed in underlying model studies[40]. (*medium confidence*) {WGIII Table SPM.1} (Table 3.1, CSB.2)

---

only submitted thereafter. 25 NDC updates were submitted between 12 October 2021 and the start of COP26. {WGIII SPM footnote 24}

[35] Immediate action in modelled global pathways refers to the adoption between 2020 and at latest before 2025 of climate policies intended to limit global warming to a given level. Modelled pathways that limit warming to 2°C (>67%) based on immediate action are summarised in category C3a in Table 3.1. All assessed modelled global pathways that limit warming to 1.5°C (>50%) with no or limited overshoot assume immediate action as defined here (Category C1 in Table 3.1). {WGIII SPM footnote 26)

[36] In this report, 'unconditional' elements of NDCs refer to mitigation efforts put forward without any conditions. 'Conditional' elements refer to mitigation efforts that are contingent on international cooperation, for example bilateral and multilateral agreements, financing or monetary and/or technological transfers. This terminology is used in the literature and the UNFCCC's NDC Synthesis Reports, not by the Paris Agreement. {WGIII SPM footnote 27}

[37] Implementation gaps refer to how far currently enacted policies and actions fall short of reaching the pledges. The policy cut-off date in studies used to project GHG emissions of 'policies implemented by the end of 2020' varies between July 2019 and November 2020. {WGIII Table 4.2, WGIII SPM footnote 25}

[38] Abatement here refers to human interventions that reduce the amount of GHGs that are released from fossil fuel infrastructure to the atmosphere. {WGIII SPM footnote 34}

[39] WGI provides carbon budgets that are in line with limiting global warming to temperature limits with different likelihoods, such as 50%, 67% or 83% {WGI Table SPM.2}.

[40] The 2019 range of harmonised GHG emissions across the pathways [53–58 $GtCO_2$-eq] is within the uncertainty ranges of 2019 emissions assessed in WGIII Chapter 2 [53–66 $GtCO_2$-eq]

Emission and implementation gaps associated with projected global emissions in 2030 under Nationally Determined Contributions (NDCs) and implemented policies

	Implied by policies implemented by the end of 2020 ($GtCO_2$-eq/yr)	Implied by Nationally Determined Contributions (NDCs) announced prior to COP26	
		Unconditional elements ($GtCO_2$-eq/yr)	Including conditional elements ($GtCO_2$-eq/yr)
Median projected global emissions (min–max)*	57 [52–60]	53 [50–57]	50 [47–55]
Implementation gap between implemented policies and NDCs (median)	–	4	7
Emissions gap between NDCs and pathways that limit warming to 2°C (>67%) with immediate action	–	10–16	6–14
Emissions gap between NDCs and pathways that limit warming to 1.5°C (>50%) with no or limited overshoot with immediate action	–	19–26	16–23

*Emissions projections for 2030 and gross differences in emissions are based on emissions of 52–56 $GtCO_2$-eq/yr in 2019 as assumed in underlying model studies. (*medium confidence*)

[END TABLE 2.2 HERE]

[START FIGURE 2.5 HERE]

Projected global GHG emissions from NDCs announced prior to COP26 would make it *likely* that warming will exceed 1.5°C and also make it harder after 2030 to limit warming to below 2°C

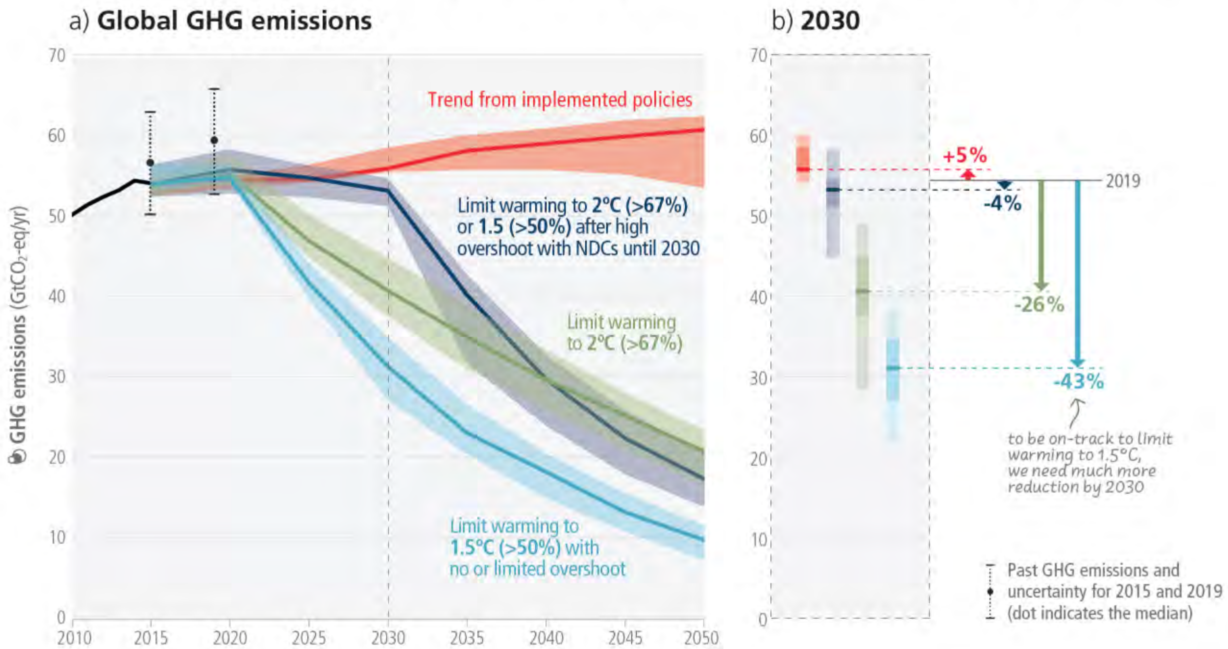

Figure 2.5 Global GHG emissions of modelled pathways (funnels in Panel a), and projected emission outcomes from near-term policy assessments for 2030 (Panel b). Panel a shows global GHG emissions over 2015–2050 for four types of assessed modelled global pathways:

– Trend from implemented policies: Pathways with projected near-term GHG emissions in line with policies implemented until the end of 2020 and extended with comparable ambition levels beyond 2030 (29 scenarios across categories C5–C7, WGIII Table SPM.2);

– Limit to 2°C (>67%) or return warming to 1.5°C (>50%) after a high overshoot, NDCs until 2030: Pathways with GHG emissions until 2030 associated with the implementation of NDCs announced prior to COP26, followed by accelerated

emissions reductions *likely* to limit warming to 2°C (C3b, WGIII Table SPM.2) or to return warming to 1.5°C with a probability of 50% or greater after high overshoot (subset of 42 scenarios from C2, WGIII Table SPM.2).
– Limit to 2°C (>67%) with immediate action: Pathways that limit warming to 2°C (>67%) with immediate action after 2020 (C3a, WGIII Table SPM.2).
– Limit to 1.5°C (>50%) with no or limited overshoot: Pathways limiting warming to 1.5°C with no or limited overshoot (C1, WGIII Table SPM.2 C1).
All these pathways assume immediate action after 2020. Past GHG emissions for 2010–2015 used to project global warming outcomes of the modelled pathways are shown by a black line. **Panel b** shows a snapshot of the GHG emission ranges of the modelled pathways in 2030 and projected emissions outcomes from near-term policy assessments in 2030 from WGIII Chapter 4.2 (Tables 4.2 and 4.3; median and full range). GHG emissions are CO_2-equivalent using GWP100 from AR6 WGI. {WGIII Figure SPM.4, WGIII 3.5, 4.2, Table 4.2, Table 4.3, Cross-Chapter Box 4 in Chapter 4} (Table 3.1, CSB.2)

[END FIGURE 2.5 HERE]

[START CROSS-SECTION BOX.1 HERE]

Cross-Section Box.1: Understanding Net Zero CO_2 and Net Zero GHG Emissions

Limiting human-caused global warming to a specific level requires limiting cumulative CO_2 emissions, reaching net zero or net negative CO_2 emissions, along with strong reductions in other GHG emissions (see 3.3.2). Future additional warming will depend on future emissions, with total warming dominated by past and future cumulative CO_2 emissions {WGI SPM D.1.1, WGI Figure SPM.4; SR1.5 SPM A.2.2}.

Reaching net zero CO_2 emissions is different from reaching net zero GHG emissions. The timing of net zero for a basket of GHGs depends on the emissions metric, such as global warming potential over a 100-year period, chosen to convert non-CO_2 emissions into CO_2-equivalent (*high confidence*). However, for a given emissions pathway, the physical climate response is independent of the metric chosen (*high confidence*) {WGI SPM D.1.8; WGIII Box TS.6, WGIII Cross-chapter box 2}.

Achieving global net zero GHG emissions requires all remaining CO_2 and metric-weighted[41] non-CO_2 GHG emissions to be counterbalanced by durably stored CO_2 removals (*high confidence*). Some non-CO_2 emissions, such as CH_4 and N_2O from agriculture, cannot be fully eliminated using existing and anticipated technical measures {WGIII SPM C.2.4, WGIII SPM C.11.4, Cross-Chapter Box 3}.

Global net zero CO_2 or GHG emissions can be achieved even if some sectors and regions are net emitters, provided that others reach net negative emissions (see Figure 4.1). The potential and cost of achieving net zero or even net negative emissions vary by sector and region. If and when net zero emissions for a given sector or region are reached depends on multiple factors, including the potential to reduce GHG emissions and undertake carbon dioxide removal, the associated costs, and the availability of policy mechanisms to balance emissions and removals between sectors and countries. (*high confidence*) {WGIII Box TS.6, WGIII Cross-Chapter Box 3}.

The adoption and implementation of net-zero emission targets by countries and regions also depend on equity and capacity considerations (*high confidence*). The formulation of net zero pathways by countries will benefit from clarity on scope, plans-of-action, and fairness. Achieving net zero emission targets relies on policies, institutions, and milestones against which to track progress. Least-cost global modelled pathways have been shown to distribute the mitigation effort unevenly, and the incorporation of equity principles could change the country-level timing of net zero (*high confidence*). The Paris Agreement also recognizes that peaking of emissions will occur later in developing countries than developed countries (Article 4.1) {WGIII Box TS.6, WGIII Cross-Chapter Box 3, WGIII 14.3}.

More information on country-level net zero pledges is provided in S2.3.1, on the timing of global net zero emissions in S3.3.2, and on sectoral aspects of net zero in S4.1.

[41] See footnote 12 above.

[END CROSS-SECTION BOX.1 HERE]

Many countries have signalled an intention to achieve net-zero GHG or net-zero CO_2 emissions by around mid-century (Cross-Section Box 1). More than 100 countries have either adopted, announced or are discussing net zero GHG or net zero CO_2 emissions commitments, covering more than two-thirds of global GHG emissions. A growing number of cities are setting climate targets, including net-zero GHG targets. Many companies and institutions have also announced net zero emissions targets in recent years. The various net zero emission pledges differ across countries in terms of scope and specificity, and limited policies are to date in place to deliver on them. {WGIII SPM C.6.4, WGIII TS.4.1, WGIII Table TS.1, WGIII 13.9, WGIII 14.3, WGIII 14.5}

All mitigation strategies face implementation challenges, including technology risks, scaling, and costs (*high confidence*). Almost all mitigation options also face institutional barriers that need to be addressed to enable their application at scale (*medium confidence*). Current development pathways may create behavioural, spatial, economic and social barriers to accelerated mitigation at all scales (*high confidence*). Choices made by policymakers, citizens, the private sector and other stakeholders influence societies' development pathways (*high confidence*). Structural factors of national circumstances and capabilities (e.g., economic and natural endowments, political systems and cultural factors and gender considerations) affect the breadth and depth of climate governance (*medium confidence*). The extent to which civil society actors, political actors, businesses, youth, labour, media, Indigenous Peoples, and local communities are engaged influences political support for climate change mitigation and eventual policy outcomes (*medium confidence*). {WGIII SPM C.3.6, WGIII SPM E.1.1, WGIII SPM E.2.1, WGIII SPM E.3.3}

The adoption of low-emission technologies lags in most developing countries, particularly least developed ones, due in part to weaker enabling conditions, including limited finance, technology development and transfer, and capacity (*medium confidence*). In many countries, especially those with limited institutional capacity, several adverse side-effects have been observed as a result of diffusion of low-emission technology, e.g., low-value employment, and dependency on foreign knowledge and suppliers (*medium confidence*). Low-emission innovation along with strengthened enabling conditions can reinforce development benefits, which can, in turn, create feedbacks towards greater public support for policy (*medium confidence*). Persistent and region-specific barriers also continue to hamper the economic and political feasibility of deploying AFOLU mitigation options (*medium confidence*). Barriers to implementation of AFOLU mitigation include insufficient institutional and financial support, uncertainty over long-term additionality and trade-offs, weak governance, insecure land ownership, low incomes and the lack of access to alternative sources of income, and the risk of reversal (*high confidence*). {WGIII SPM B.4.2, WGIII SPM C.9.1, WGIII SPM C.9.3}

2.3.2 Adaptation Gaps and Barriers

Despite progress, adaptation gaps exist between current levels of adaptation and levels needed to respond to impacts and reduce climate risks (*high confidence*). While progress in adaptation implementation is observed across all sectors and regions (*very high confidence*), many adaptation initiatives prioritise immediate and near-term climate risk reduction, e.g., through hard flood protection, which reduces the opportunity for transformational adaptation[42] (*high confidence*). Most observed adaptation is fragmented, small in scale, incremental, sector-specific, and focused more on planning rather than implementation (*high confidence*). Further, observed adaptation is unequally distributed across regions and the largest adaptation gaps exist among lower population income groups (*high confidence*). In the urban context, the largest adaptation gaps exist in projects that manage complex risks, for example in the food–energy–water–health nexus or the inter-relationships of air quality and climate risk (*high confidence*). Many funding, knowledge and practice gaps remain for effective implementation, monitoring and evaluation and current adaptation efforts are not expected to meet existing goals (*high confidence*). At current rates of adaptation planning and implementation the adaptation gap will continue to grow (*high confidence*). {WGII SPM C.1, WGII SPM C.1.2, WGII SPM C.4.1, WGII TS.D.1.3, WGII TS.D.1.4}

[42] See Annex I: Glossary.

Soft and hard adaptation limits[43] have already been reached in some sectors and regions, in spite of adaptation having buffered some climate impacts (*high confidence*). Ecosystems already reaching hard adaptation limits include some warm water coral reefs, some coastal wetlands, some rainforests, and some polar and mountain ecosystems (*high confidence*). Individuals and households in low lying coastal areas in Australasia and Small Islands and smallholder farmers in Central and South America, Africa, Europe and Asia have reached soft limits (*medium confidence*), resulting from financial, governance, institutional and policy constraints and can be overcome by addressing these constraints (*high confidence*). Transitioning from incremental to transformational adaptation can help overcome soft adaptation limits (*high confidence*). {WGII SPM C.3, WGII SPM C.3.1, WGII SPM C.3.2, WGII SPM C.3.3, WGII SPM.C.3.4, WGII 16 ES}

Adaptation does not prevent all losses and damages, even with effective adaptation and before reaching soft and hard limits. Losses and damages are unequally distributed across systems, regions and sectors and are not comprehensively addressed by current financial, governance and institutional arrangements, particularly in vulnerable developing countries. (*high confidence*) {WGII SPM.C.3.5}

There is increased evidence of maladaptation[44] in various sectors and regions. Examples of maladaptation are observed in urban areas (e.g., new urban infrastructure that cannot be adjusted easily or affordably), agriculture (e.g., using high-cost irrigation in areas projected to have more intense drought conditions), ecosystems (e.g. fire suppression in naturally fire-adapted ecosystems, or hard defences against flooding) and human settlements (e.g. stranded assets and vulnerable communities that cannot afford to shift away or adapt and require an increase in social safety nets). Maladaptation especially affects marginalised and vulnerable groups adversely (e.g., Indigenous Peoples, ethnic minorities, low-income households, people living in informal settlements), reinforcing and entrenching existing inequities. Maladaptation can be avoided by flexible, multi-sectoral, inclusive and long-term planning and implementation of adaptation actions with benefits to many sectors and systems. (*high confidence*) {WGII SPM C.4, WGII SPM C.4.3, WGII TS.D.3.1}

Systemic barriers constrain the implementation of adaptation options in vulnerable sectors, regions and social groups (*high confidence*). Key barriers include limited resources, lack of private-sector and civic engagement, insufficient mobilisation of finance, lack of political commitment, limited research and/or slow and low uptake of adaptation science and a low sense of urgency. Inequity and poverty also constrain adaptation, leading to soft limits and resulting in disproportionate exposure and impacts for most vulnerable groups (*high confidence*). The largest adaptation gaps exist among lower income population groups (*high confidence*). As adaptation options often have long implementation times, long-term planning and accelerated implementation, particularly in this decade, is important to close adaptation gaps, recognising that constraints remain for some regions (*high confidence*). Prioritisation of options and transitions from incremental to transformational adaptation are limited due to vested interests, economic lock-ins, institutional path dependencies and prevalent practices, cultures, norms and belief systems (*high confidence*). Many funding, knowledge and practice gaps remain for effective implementation, monitoring and evaluation of adaptation (*high confidence*), including, lack of climate literacy at all levels and limited availability of data and information (*medium confidence*); for example for Africa, severe climate data constraints and inequities in research funding and leadership reduce adaptive capacity (*very high confidence*). {WGII SPM C.1.2, WGII SPM C.3.1, WGII TS.D.1.3, WGII TS.D.1.5, TS.D.2.4}

2.3.3 Lack of Finance as a Barrier to Climate Action

Insufficient financing, and a lack of political frameworks and incentives for finance, are key causes of the implementation gaps for both mitigation and adaptation (*high confidence*). Financial flows remained heavily focused on mitigation, are uneven, and have developed heterogeneously across regions and sectors (*high confidence*). In 2018, public and publicly mobilised private climate finance flows from developed to developing countries were below the collective goal under the UNFCCC and Paris Agreement to

[43] Adaptation limit: The point at which an actor's objectives (or system needs) cannot be secured from intolerable risks through adaptive actions. Hard adaptation limit - No adaptive actions are possible to avoid intolerable risks. Soft adaptation limit - Options are currently not available to avoid intolerable risks through adaptive action.

[44] Maladaptation refers to actions that may lead to increased risk of adverse climate-related outcomes, including via increased greenhouse gas emissions, increased or shifted vulnerability to climate change, more inequitable outcomes, or diminished welfare, now or in the future. Most often, maladaptation is an unintended consequence. See Annex I: Glossary.

mobilise USD 100 billion per year by 2020 in the context of meaningful mitigation action and transparency on implementation (*medium confidence*). Public and private finance flows for fossil fuels are still greater than those for climate adaptation and mitigation (*high confidence*). The overwhelming majority of tracked climate finance is directed towards mitigation (*very high confidence*). Nevertheless, average annual modelled investment requirements for 2020 to 2030 in scenarios that limit warming to 2°C or 1.5°C are a factor of three to six greater than current levels, and total mitigation investments (public, private, domestic and international) would need to increase across all sectors and regions (*medium confidence*). Challenges remain for green bonds and similar products, in particular around integrity and additionality, as well as the limited applicability of these markets to many developing countries (*high confidence*). {WGII SPM C.3.2, WGII SPM C.5.4; WGIII SPM B.5.4, WGIII SPM E5.1}

Current global financial flows for adaptation including from public and private finance sources, are insufficient for and constrain implementation of adaptation options, especially in developing countries (*high confidence*). There are widening disparities between the estimated costs of adaptation and the documented finance allocated to adaptation (*high confidence*). Adaptation finance needs are estimated to be higher than those assessed in AR5, and the enhanced mobilisation of and access to financial resources are essential for implementation of adaptation and to reduce adaptation gaps (*high confidence*). Annual finance flows targeting adaptation for Africa, for example, are billions of USD less than the lowest adaptation cost estimates for near-term climate change (*high confidence*). Adverse climate impacts can further reduce the availability of financial resources by causing losses and damages and impeding national economic growth, thereby further increasing financial constraints for adaptation particularly for developing countries and LDCs (*medium confidence*). {WGII SPM C.1.2, WGII SPM C.3.2, WGII SPM C.5.4, WGII TS.D.1.6}

Without effective mitigation and adaptation, losses and damages will continue to disproportionately affect the poorest and most vulnerable populations. Accelerated financial support for developing countries from developed countries and other sources is a critical enabler to enhance mitigation action {WGIII SPM. E.5.3}. Many developing countries lack comprehensive data at the scale needed and lack adequate financial resources needed for adaptation for reducing associated economic and non-economic losses and damages. (*high confidence)* {WGII Cross-Chapter Box LOSS, WGII SPM C.3.1, WGII SPM C.3.2, WGII TS.D.1.3, WGII TS.D.1.5; WGIII SPM E.5.3}

There are barriers to redirecting capital towards climate action both within and outside the global financial sector. These barriers include: the inadequate assessment of climate-related risks and investment opportunities, regional mismatch between available capital and investment needs, home bias factors, country indebtedness levels, economic vulnerability, and limited institutional capacities. Challenges from outside the financial sector include: limited local capital markets; unattractive risk-return profiles, in particular due to missing or weak regulatory environments that are inconsistent with ambition levels; limited institutional capacity to ensure safeguards; standardisation, aggregation, scalability and replicability of investment opportunities and financing models; and, a pipeline ready for commercial investments. *(high confidence)* {WGII SPM C.5.4; WGIII SPM E.5.2; SR15 SPM D.5.2}

[START CROSS-SECTION BOX.2 HERE]

Cross-Section Box.2: Scenarios, Global Warming Levels, and Risks

Modelled scenarios and pathways[45] are used to explore future emissions, climate change, related impacts and risks, and possible mitigation and adaptation strategies and are based on a range of assumptions, including socio-economic variables and mitigation options. These are quantitative projections and are neither predictions nor forecasts. Global modelled emission pathways, including those based on cost effective approaches contain regionally differentiated assumptions and outcomes, and have to be assessed with the careful recognition of these assumptions. Most do not make explicit assumptions about global equity, environmental justice or intra-regional income distribution. IPCC is neutral with regard to the assumptions underlying the scenarios in the

[45] In the literature, the terms pathways and scenarios are used interchangeably, with the former more frequently used in relation to climate goals. WGI primarily used the term scenarios and WGIII mostly used the term modelled emissions and mitigation pathways. The SYR primarily uses scenarios when referring to WGI and modelled emissions and mitigation pathways when referring to WGIII. {WGI Box SPM.1; WGIII footnote 44}

literature assessed in this report, which do not cover all possible futures.[46] {SROCC Box SPM.1; SRCCL Box SPM.1; WGI Box SPM.1; WGII Box SPM.1; WGIII Box SPM.1}.

Socio-economic Development, Scenarios, and Pathways

The five Shared Socio-economic Pathways (SSP1 to SSP5) were designed to span a range of challenges to climate change mitigation and adaptation. For the assessment of climate impacts, risk and adaptation, the SSPs are used for future exposure, vulnerability and challenges to adaptation. Depending on levels of GHG mitigation, modelled emissions scenarios based on the SSPs can be consistent with low or high warming levels[47]. There are many different mitigation strategies that could be consistent with different levels of global warming in 2100 (see Figure 4.1). {WGI Box SPM.1; WGII Box SPM.1; WGIII Box SPM.1, WGIII Box TS.5, WGIII Annex III; SRCCL Box SPM.1, Figure SPM.2}

WGI assessed the climate response to five illustrative scenarios based on SSPs[48] that cover the range of possible future development of anthropogenic drivers of climate change found in the literature. These scenarios combine socio-economic assumptions, levels of climate mitigation, land use and air pollution controls for aerosols and non-CH_4 ozone precursors. The high and very high GHG emissions scenarios (SSP3-7.0 and SSP5-8.5) have CO_2 emissions that roughly double from current levels by 2100 and 2050, respectively[49]. The intermediate GHG emissions scenario (SSP2-4.5) has CO_2 emissions remaining around current levels until the middle of the century. The very low and low GHG emissions scenarios (SSP1-1.9 and SSP1-2.6) have CO_2 emissions declining to net zero around 2050 and 2070, respectively, followed by varying levels of net negative CO_2 emissions. In addition, Representative Concentration Pathways (RCPs)[50] were used by WGI and WGII to assess regional climate changes, impacts and risks. {WGI Box SPM.1} (Cross-Section Box.2, Figure 1)

In WGIII, a large number of global modelled emissions pathways were assessed, of which 1202 pathways were categorised based on their projected global warming over the 21st century, with categories ranging from pathways that limit warming to 1.5°C with more than 50% likelihood[51] with no or limited overshoot (C1) to pathways that exceed 4°C (C8). Methods to project global warming associated with the modelled pathways were updated to ensure consistency with the AR6 WGI assessment of the climate system response[52]. {WGIII Box SPM.1, WGIII Table 3.1} (Table 3.1, Cross-Section Box.2, Figure 1)

Global Warming Levels (GWLs)

For many climate and risk variables, the geographical patterns of changes in climatic impact-drivers[53] and climate impacts for a level of global warming[54] are common to all scenarios considered and independent of timing when that level is reached. This motivates the use of GWLs as a dimension of integration. {WGI Box SPM.1.4, WGI TS.1.3.2; WGII Box SPM.1} (Figure 3.1, Figure 3.2)

[46] Around half of all modelled global emissions pathways assume cost-effective approaches that rely on least-cost mitigation/abatement options globally. The other half look at existing policies and regionally and sectorally differentiated actions. The underlying population assumptions range from 8.5 to 9.7 billion in 2050 and 7.4 to 10.9 billion in 2100 (5–95th percentile) starting from 7.6 billion in 2019. The underlying assumptions on global GDP growth range from 2.5 to 3.5% per year in the 2019–2050 period and 1.3 to 2.1% per year in the 2050–2100 (5–95th percentile). {WGIII Box SPM.1}.

[47] High mitigation challenges, for example, due to assumptions of slow technological change, high levels of global population growth, and high fragmentation as in the Shared Socio-economic Pathway SSP3, may render modelled pathways that limit warming to 2°C (> 67%) or lower infeasible (*medium confidence*) {SRCCL Box SPM.1; WGIII SPM C.1.4}.

[48] SSP-based scenarios are referred to as SSPx-y, where 'SSPx' refers to the Shared Socioeconomic Pathway describing the socioeconomic trends underlying the scenarios, and 'y' refers to the level of radiative forcing (in watts per square metre, or Wm-2) resulting from the scenario in the year 2100. {WGI SPM footnote 22}

[49] Very high emission scenarios have become less likely but cannot be ruled out. Temperature levels > 4C may result from very high emission scenarios, but can also occur from lower emission scenarios if climate sensitivity or carbon cycle feedbacks are higher than the best estimate.

[50] RCP-based scenarios are referred to as RCPy, where 'y' refers to the approximate level of radiative forcing (in watts per square metre, or Wm^{-2}) resulting from the scenario in the year 2100. {WGII SPM footnote 21}

[51] Denoted '>50%' in this report.

[52] The climate response to emissions is investigated with climate models, paleoclimatic insights and other lines of evidence. The assessment outcomes are used to categorise thousands of scenarios via simple physically-based climate models (emulators) {WGI TS.1.2.2}.

[53] See Annex I: Glossary

[54] See Annex I: Glossary. Here, global warming is the 20-year average global surface temperature relative to 1850–1900. The assessed time of when a certain global warming level is reached under a particular scenario is defined here as the mid-point of the first 20-year running average period during which the assessed average global surface temperature change exceeds the level of global warming. {WGI SPM footnote 26, Cross-Section Box TS.1}

Risks
Dynamic interactions between climate-related hazards, exposure and vulnerability of the affected human society, species, or ecosystems result in risks arising from climate change. AR6 assesses key risks across sectors and regions as well as providing an updated assessment of the Reasons for Concern (RFCs) – five globally aggregated categories of risk that evaluate risk accrual with increasing global surface temperature. Risks can also arise from climate change mitigation or adaptation responses when the response does not achieve its intended objective, or when it results in adverse effects for other societal objectives. {WGII SPM A, WGII Figure SPM.3, WGII Box TS.1, WGII Figure TS.4; SR1.5 Figure SPM.2; SRCCL Figure SPM.2; SROCC Errata Figure SPM.3} (3.1.2, Cross-Section Box.2, Figure 1; Figure 3.3)

[START CROSS-SECTION BOX.2, FIGURE 1 HERE]

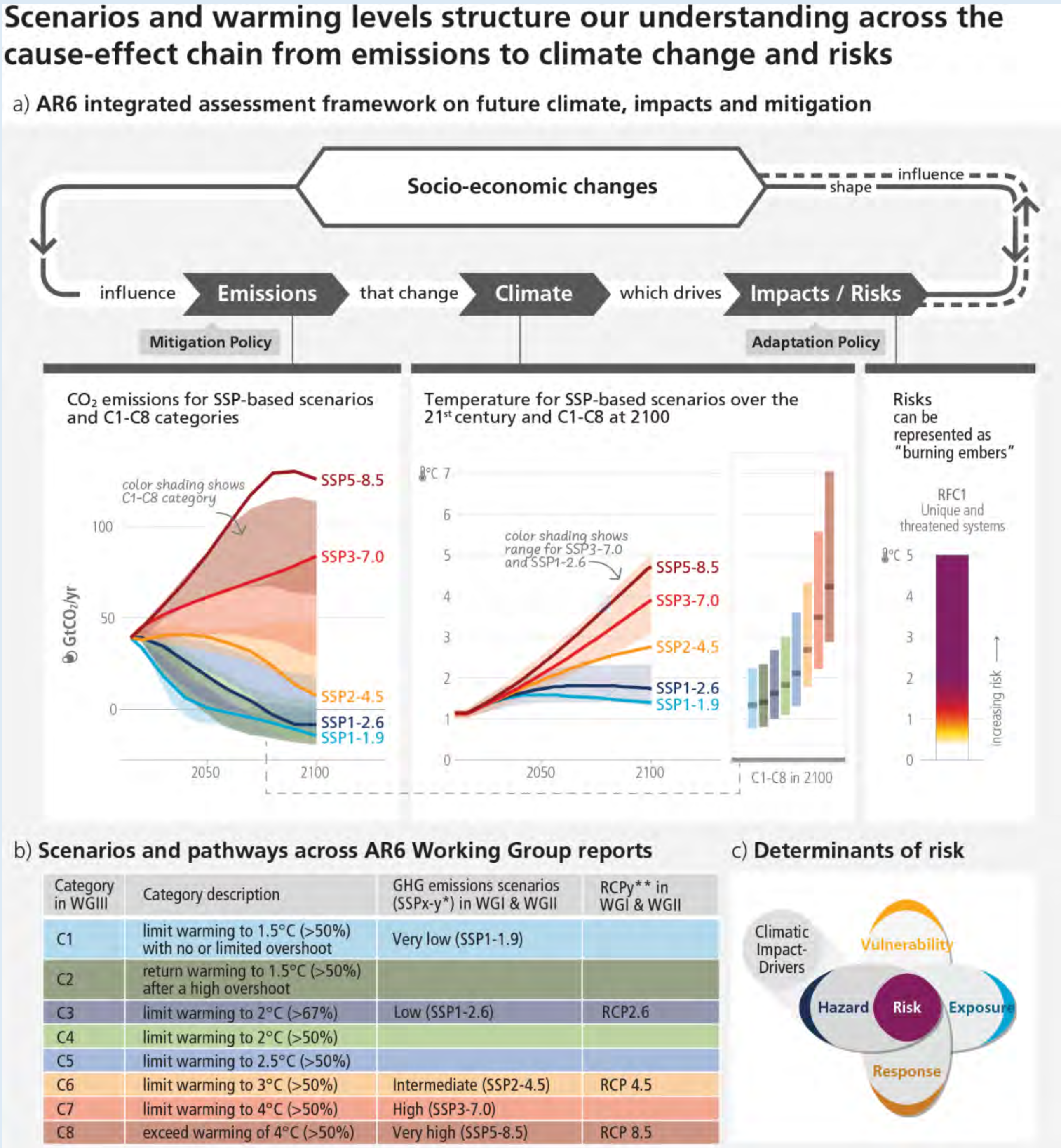

Category in WGIII	Category description	GHG emissions scenarios (SSPx-y*) in WGI & WGII	RCPy** in WGI & WGII
C1	limit warming to 1.5°C (>50%) with no or limited overshoot	Very low (SSP1-1.9)	
C2	return warming to 1.5°C (>50%) after a high overshoot		
C3	limit warming to 2°C (>67%)	Low (SSP1-2.6)	RCP2.6
C4	limit warming to 2°C (>50%)		
C5	limit warming to 2.5°C (>50%)		
C6	limit warming to 3°C (>50%)	Intermediate (SSP2-4.5)	RCP 4.5
C7	limit warming to 4°C (>50%)	High (SSP3-7.0)	
C8	exceed warming of 4°C (>50%)	Very high (SSP5-8.5)	RCP 8.5

* The terminology SSPx-y is used, where 'SSPx' refers to the Shared Socio-economic Pathway or 'SSP' describing the socio-economic trends underlying the scenario, and 'y' refers to the approximate level of radiative forcing (in watts per square metre, or W m^{-2}) resulting from the scenario in the year 2100.

** The AR5 scenarios (RCPy), which partly inform the AR6 WGI and WGII assessments, are indexed to a similar set of approximate 2100 radiative forcing levels (in Wm^{-2}). The SSP scenarios cover a broader range of GHG and air pollutant futures than the RCPs. They are similar but not identical, with differences in concentration trajectories for different GHGs. The overall radiative forcing tends to be higher for the SSPs compared to the RCPs with the same label (*medium confidence*). {WGI TS.1.3.1}
*** Limited overshoot refers to exceeding 1.5°C global warming by up to about 0.1°C, high overshoot by 0.1°C-0.3°C, in both cases for up to several decades.

Cross-Section Box.2, Figure 1: Schematic of the AR6 framework for assessing future greenhouse gas emissions, climate change, risks, impacts and mitigation. Panel (**a**) The integrated framework encompasses socio-economic development and policy, emissions pathways and global surface temperature responses to the five scenarios considered by WGI (SSP1-1.9, SSP1-2.6, SSP2-4.5, SSP3-7.0, and SSP5-8.5) and eight global mean temperature change categorisations (C1–C8) assessed by WGIII, and the WGII risk assessment. The dashed arrow indicates that the influence from impacts/risks to socio-economic changes is not yet considered in the scenarios assessed in the AR6. Emissions include GHGs, aerosols, and ozone precursors. CO_2 emissions are shown as an example on the left. The assessed global surface temperature changes across the 21st century relative to 1850–1900 for the five GHG emissions scenarios are shown as an example in the centre. *Very likely* ranges are shown for SSP1-2.6 and SSP3-7.0. Projected temperature outcomes at 2100 relative to 1850–1900 are shown for C1 to C8 categories with median (line) and the combined *very likely* range across scenarios (bar). On the right, future risks due to increasing warming are represented by an example 'burning ember' figure (see 3.1.2 for the definition of RFC1). **Panel** (**b**) Description and relationship of scenarios considered across AR6 Working Group reports. **Panel** (**c**) Illustration of risk arising from the interaction of hazard (driven by changes in climatic impact-drivers) with vulnerability, exposure and response to climate change. {WGI TS1.4, Figure 4.11; WGII Figure 1.5, WGII Figure 14.8; WGIII Table SPM.2, Figure 3.11}

[END CROSS-SECTION BOX.2 FIGURE 1 HERE]

[END CROSS-SECTION BOX.2 HERE]

Section 3: Long-Term Climate and Development Futures

3.1 Long-Term Climate Change, Impacts and Related Risks

Future warming will be driven by future emissions and will affect all major climate system components, with every region experiencing multiple and co-occurring changes. Many climate-related risks are assessed to be higher than in previous assessments, and projected long-term impacts are up to multiple times higher than currently observed. Multiple climatic and non-climatic risks will interact, resulting in compounding and cascading risks across sectors and regions. Sea level rise, as well as other irreversible changes, will continue for thousands of years, at rates depending on future emissions. (*high confidence*)

3.1.1 Long-term Climate Change

The uncertainty range on assessed future changes in global surface temperature is narrower than in the AR5. For the first time in an IPCC assessment cycle, multi-model projections of global surface temperature, ocean warming and sea level are constrained using observations and the assessed climate sensitivity. The *likely* range of equilibrium climate sensitivity has been narrowed to 2.5°C–4.0°C (with a best estimate of 3.0°C) based on multiple lines of evidence[55], including improved understanding of cloud feedbacks. For related emissions scenarios, this leads to narrower uncertainty ranges for long-term projected global temperature change than in AR5. {WGI A.4, WGI Box SPM.1, WGI TS.3.2, WGI 4.3}

Future warming depends on future greenhouse gas (GHG) emissions, with cumulative net CO_2 dominating. The assessed best estimates and *very likely* ranges of warming for 2081–2100 with respect to 1850–1900 vary from 1.4°C [1.0-1.8°C] in the very low GHG emissions scenario (SSP1-1.9) to 2.7°C [2.1°C–3.5°C] in the intermediate GHG emissions scenario (SSP2-4.5) and 4.4°C [3.3°C–5.7°C] in the very high GHG emissions scenario (SSP5-8.5)[56]. {WGI SPM B.1.1, WGI Table SPM.1, WGI Figure SPM.4} (Cross-Section Box.2, Figure 1)

Modelled pathways consistent with the continuation of policies implemented by the end of 2020 lead to global warming of 3.2 [2.2-3.5]°C (5–95% range) by 2100 (*medium confidence*) (see also Section 2.3.1). Pathways of >4°C (≥50%) by 2100 would imply a reversal of current technology and/or mitigation policy trends (*medium confidence*). However, such warming could occur in emissions pathways consistent with policies implemented by the end of 2020 if climate sensitivity or carbon cycle feedbacks are higher than the best estimate (*high confidence*). {WGIII SPM C.1.3}

Global warming will continue to increase in the near term in nearly all considered scenarios and modelled pathways. Deep, rapid and sustained GHG emissions reductions, reaching net zero CO_2 emissions and including strong emissions reductions of other GHGs, in particular CH_4, are necessary to limit warming to 1.5°C (>50%) or less than 2°C (>67%) by the end of century (*high confidence*). The best estimate of reaching 1.5°C of global warming lies in the first half of the 2030s in most of the considered scenarios and modelled pathways[57]. In the very low GHG emissions scenario (SSP1-1.9), CO_2 emissions reach net zero around 2050 and the best-estimate end-of-century warming is 1.4°C, after a temporary overshoot (see Section 3.3.4) of no more than 0.1°C above 1.5°C global warming. Global warming of 2°C will be exceeded during the 21st century unless deep reductions in CO_2 and other GHG emissions occur in the coming decades.

[55] Understanding of climate processes, the instrumental record, paleoclimates and model-based emergent constraints (see Annex I: Glossary). {WGI SPM footnote 21}

[56] The best estimates [and *very likely* ranges] for the different scenarios are: 1.4°C [1.0°C–1.8°C] (SSP1-1.9); 1.8°C [1.3°C–2.4°C] (SSP1-2.6); 2.7°C [2.1°C–3.5°C] (SSP2-4.5); 3.6°C [2.8°C–4.6°C] (SSP3-7.0); and 4.4°C [3.3°C–5.7°C] (SSP5-8.5). {WGI Table SPM.1} (CSB.2)

[57] In the near term (2021–2040), the 1.5°C global warming level is *very likely* to be exceeded under the very high GHG emissions scenario (SSP5-8.5), *likely* to be exceeded under the intermediate and high GHG emissions scenarios (SSP2-4.5, SSP3-7.0), *more likely than not* to be exceeded under the low GHG emissions scenario (SSP1-2.6) and *more likely than not* to be reached under the very low GHG emissions scenario (SSP1-1.9). In all scenarios considered by WGI except the very high emissions scenario, the midpoint of the first 20-year running average period during which the assessed global warming reaches 1.5°C lies in the first half of the 2030s. In the very high GHG emissions scenario, this mid-point is in the late 2020s. Median five-year interval at which a 1.5°C global warming level is reached (50% probability) in categories of modelled pathways considered in WGIII is 2030-2035. {WGI SPM B.1.3, WGI Cross-Section Box TS.1, WGIII Table 3.2} (Cross-Section Box.2)

Deep, rapid and sustained reductions in GHG emissions would lead to improvements in air quality within a few years, to reductions in trends of global surface temperature discernible after around 20 years, and over longer time periods for many other climate impact-drivers[58] (*high confidence*). Targeted reductions of air pollutant emissions lead to more rapid improvements in air quality compared to reductions in GHG emissions only, but in the long term, further improvements are projected in scenarios that combine efforts to reduce air pollutants as well as GHG emissions (*high confidence*)[59]. {WGI SPM B.1, WGI SPM B.1.3, WGI SPM D.1, WGI SPM D.2, WGI Figure SPM.4, WGI Table SPM.1, WGI Cross-Section Box TS.1; WGIII SPM C.3, WGIII Table SPM.2, WGIII Figure SPM.5, WGIII Box SPM.1 Figure 1, WGIII Table 3.2} (Table 3.1, Cross-Section Box 2, Figure 1)

Changes in short-lived climate forcers (SLCF) resulting from the five considered scenarios lead to an additional net global warming in the near and long term (*high confidence*). Simultaneous stringent climate change mitigation and air pollution control policies limit this additional warming and lead to strong benefits for air quality (*high confidence*). In high and very high GHG emissions scenarios (SSP3-7.0 and SSP5-8.5), combined changes in SLCF emissions, such as CH_4, aerosol and ozone precursors, lead to a net global warming by 2100 of *likely* 0.4°C–0.9°C relative to 2019. This is due to projected increases in atmospheric concentration of CH_4, tropospheric ozone, hydrofluorocarbons and, when strong air pollution control is considered, reductions of cooling aerosols. In low and very low GHG emissions scenarios (SSP1-1.9 and SSP1-2.6), air pollution control policies, reductions in CH_4 and other ozone precursors lead to a net cooling, whereas reductions in anthropogenic cooling aerosols lead to a net warming (*high confidence*). Altogether, this causes a *likely* net warming of 0.0°C–0.3°C due to SLCF changes in 2100 relative to 2019 and strong reductions in global surface ozone and particulate matter (*high confidence*). {WGI SPM D.1.7, WGI Box TS.7} (CSB.2)

Continued GHG emissions will further affect all major climate system components, and many changes will be irreversible on centennial to millennial time scales. Many changes in the climate system become larger in direct relation to increasing global warming. With every additional increment of global warming, changes in extremes continue to become larger. Additional warming will lead to more frequent and intense marine heatwaves and is projected to further amplify permafrost thawing and loss of seasonal snow cover, glaciers, land ice and Arctic sea ice (*high confidence*). Continued global warming is projected to further intensify the global water cycle, including its variability, global monsoon precipitation[60], and very wet and very dry weather and climate events and seasons (*high confidence*). The portion of global land experiencing detectable changes in seasonal mean precipitation is projected to increase (*medium confidence*) with more variable precipitation and surface water flows over most land regions within seasons (*high confidence*) and from year to year (*medium confidence*). Many changes due to past and future GHG emissions are irreversible[61] on centennial to millennial time scales, especially in the ocean, ice sheets and global sea level (see 3.1.3). Ocean acidification (*virtually certain*), ocean deoxygenation (*high confidence*) and global mean sea level (*virtually certain*) will continue to increase in the 21st century, at rates dependent on future emissions. {WGI SPM B.2, WGI SPM B.2.2, WGI SPM B.2.3, WGI SPM B.2.5, WGI SPM B.3, WGI SPM B.3.1, WGI SPM B.3.2, WGI SPM B.4, WGI SPM B.5, WGI SPM B.5.1, WGI SPM B.5.3, WGI Figure SPM.8} (Figure 3.1)

With further global warming, every region is projected to increasingly experience concurrent and multiple changes in climatic impact-drivers. Increases in hot and decreases in cold climatic impact-drivers, such as temperature extremes, are projected in all regions (*high confidence*). At 1.5°C global warming, heavy precipitation and flooding events are projected to intensify and become more frequent in most regions in Africa, Asia (*high confidence*), North America (*medium to high confidence*) and Europe (*medium confidence*). At 2°C or above, these changes expand to more regions and/or become more significant (*high confidence*), and more frequent and/or severe agricultural and ecological droughts are projected in Europe, Africa, Australasia and North, Central and South America (*medium* to *high confidence*). Other projected regional changes include intensification of tropical cyclones and/or extratropical storms (*medium confidence*), and increases in aridity and fire weather[62] (*medium* to *high confidence*). Compound heatwaves and droughts

[58] See Cross-Section Box.2.
[59] Based on additional scenarios.
[60] Particularly over South and South East Asia, East Asia and West Africa apart from the far west Sahel {WGI SPM B.3.3}
[61] See Annex I: Glossary.
[62] See Annex I: Glossary.

become *likely* more frequent, including concurrently at multiple locations (*high confidence*). {WGI SPM C.2, WGI SPM C.2.1, WGI SPM C.2.2, WGI SPM C.2.3, WGI SPM C.2.4, WGI SPM C.2.7}

[START FIGURE 3.1 HERE]

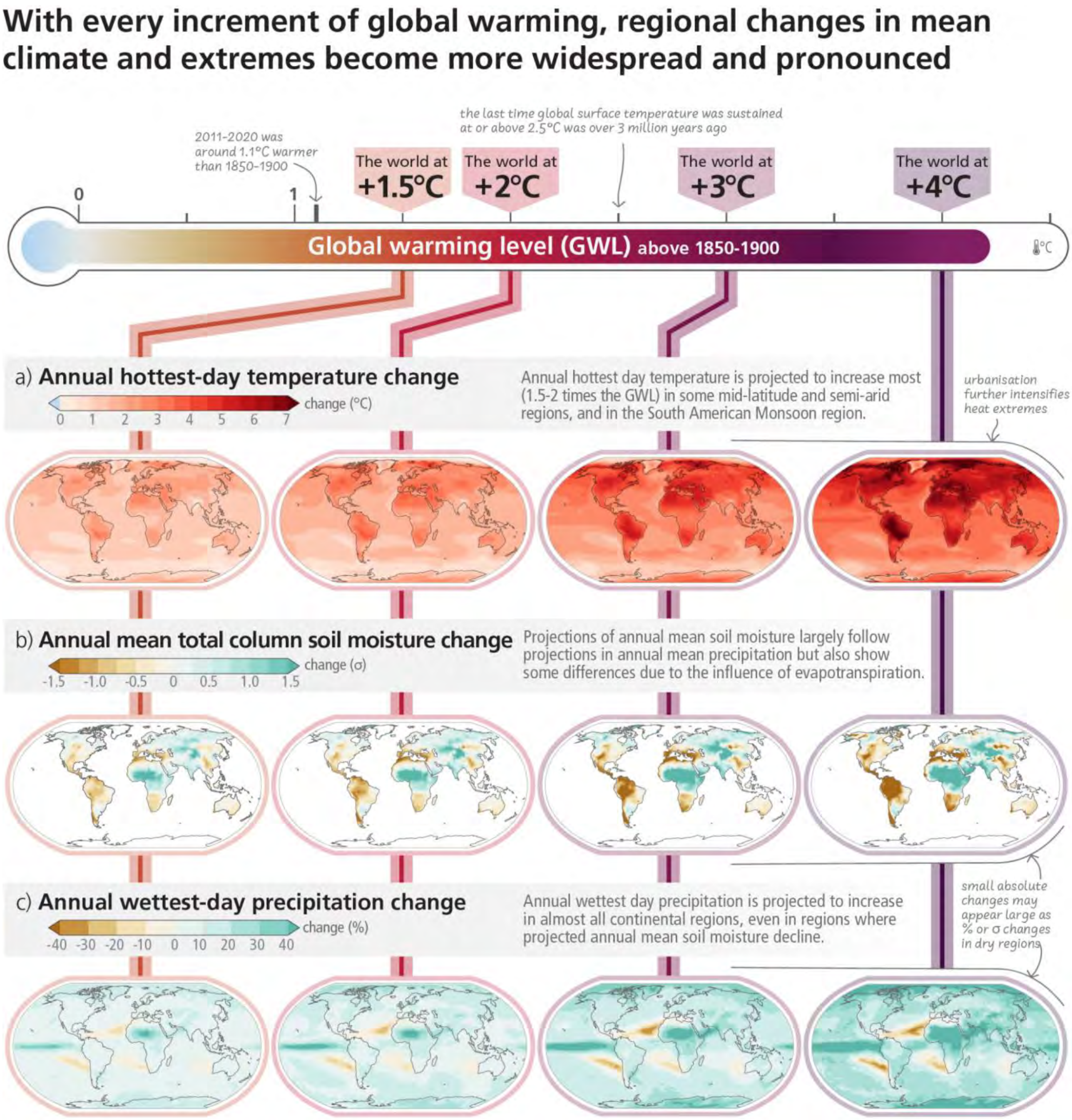

Figure 3.1: Projected changes of annual maximum daily temperature, annual mean total column soil moisture CMIPand annual maximum daily precipitation at global warming levels of 1.5°C, 2°C, 3°C, and 4°C relative to 1850–1900. Simulated (**a**) annual maximum temperature change (°C), (**b**) annual mean total column soil moisture (standard deviation), (**c**) annual maximum daily precipitation change (%). Changes correspond to CMIP6 multi-model median changes. In panels (b) and (c), large positive relative changes in dry regions may correspond to small absolute changes. In panel (b), the unit is the standard deviation of interannual variability in soil moisture during 1850–1900. Standard deviation is a widely used metric in characterising drought severity. A projected reduction in mean soil moisture by one standard deviation corresponds to soil moisture conditions typical of droughts that occurred about once every six years during 1850–1900. The WGI Interactive Atlas (https://interactive-atlas.ipcc.ch/) can be used to explore additional changes in the climate system across the range of global warming levels presented in this figure. {WGI Figure SPM.5, WGI Figure TS.5, WGI Figure 11.11, WGI Figure 11.16, WGI Figure 11.19} (CSB.2)

[END FIGURE 3.1 HERE]

3.1.2 Impacts and Related Risks

For a given level of warming, many climate-related risks are assessed to be higher than in AR5 (*high confidence*). Levels of risk[63] for all Reasons for Concern[64] (RFCs) are assessed to become high to very high at lower global warming levels compared to what was assessed in AR5 (*high confidence*). This is based upon recent evidence of observed impacts, improved process understanding, and new knowledge on exposure and vulnerability of human and natural systems, including limits to adaptation. Depending on the level of global warming, the assessed long-term impacts will be up to multiple times higher than currently observed (*high confidence*) for 127 identified key risks, e.g., in terms of the number of affected people and species. Risks, including cascading risks (see 3.1.3) and risks from overshoot (see 3.3.4), are projected to become increasingly severe with every increment of global warming (*very high confidence*). {WGII SPM B.3.3, WGII SPM B.4, WGII SPM B.5, WGII 16.6.3; SRCCL SPM A5.3} (Figure 3.2, Figure 3.3)

Climate-related risks for natural and human systems are higher for global warming of 1.5°C than at present (1.1°C) but lower than at 2°C (*high confidence*) (see Section 2.1.2)**.** Climate-related risks to health, livelihoods, food security, water supply, human security, and economic growth are projected to increase with global warming of 1.5°C. In terrestrial ecosystems, 3–14% of the tens of thousands of species assessed will *likely* face a very high risk of extinction at a GWL of 1.5°C. Coral reefs are projected to decline by a further 70–90% at 1.5°C of global warming (*high confidence*). At this GWL, many low-elevation and small glaciers around the world would lose most of their mass or disappear within decades to centuries (*high confidence*). Regions at disproportionately higher risk include Arctic ecosystems, dryland regions, small island development states and Least Developed Countries (*high confidence*). {WGII SPM B.3, WGII SPM B.4.1, WGII TS.C.4.2; SR1.5 SPM A.3, SR1.5 SPM B.4.2, SR1.5 SPM B.5, SR1.5 SPM B.5.1} (Figure 3.3)

At 2°C of global warming, overall risk levels associated with the unequal distribution of impacts (RFC3), global aggregate impacts (RFC4) and large-scale singular events (RFC5) would be transitioning to high (*medium confidence*), those associated with extreme weather events (RFC2) would be transitioning to very high (*medium confidence*), and those associated with unique and threatened systems (RFC1) would be very high (*high confidence*) (Figure 3.3, panel a). With about 2°C warming, climate-related changes in food availability and diet quality are estimated to increase nutrition-related diseases and the number of undernourished people, affecting tens (under low vulnerability and low warming) to hundreds of millions of people (under high vulnerability and high warming), particularly among low-income households in low- and middle-income countries in sub-Saharan Africa, South Asia and Central America (*high confidence*). For example, snowmelt water availability for irrigation is projected to decline in some snowmelt dependent river basins by up to 20% (*medium confidence*). Climate change risks to cities, settlements and key infrastructure will rise sharply in the mid- and long-term with further global warming, especially in places already exposed to high temperatures, along coastlines, or with high vulnerabilities (*high confidence*). {WGII SPM B.3.3, WGII SPM B.4.2, WGII SPM B.4.5, WGII TS C.3.3, WGII TS.C.12.2} (Figure 3.3)

---

[63] Undetectable risk level indicates no associated impacts are detectable and attributable to climate change; moderate risk indicates associated impacts are both detectable and attributable to climate change with at least *medium confidence*, also accounting for the other specific criteria for key risks; high risk indicates severe and widespread impacts that are judged to be high on one or more criteria for assessing key risks; and very high risk level indicates very high risk of severe impacts and the presence of significant irreversibility or the persistence of climate-related hazards, combined with limited ability to adapt due to the nature of the hazard or impacts/risks. {WGII Figure SPM.3}

[64] The Reasons for Concern (RFC) framework communicates scientific understanding about accrual of risk for five broad categories {WGII Figure SPM.3}. RFC1: Unique and threatened systems: ecological and human systems that have restricted geographic ranges constrained by climate-related conditions and have high endemism or other distinctive properties. Examples include coral reefs, the Arctic and its Indigenous Peoples, mountain glaciers and biodiversity hotspots. RFC2: Extreme weather events: risks/impacts to human health, livelihoods, assets and ecosystems from extreme weather events such as heatwaves, heavy rain, drought and associated wildfires, and coastal flooding. RFC3: Distribution of impacts: risks/impacts that disproportionately affect particular groups due to uneven distribution of physical climate change hazards, exposure or vulnerability. RFC4: Global aggregate impacts: impacts to socio-ecological systems that can be aggregated globally into a single metric, such as monetary damages, lives affected, species lost or ecosystem degradation at a global scale. RFC5: Large-scale singular events: relatively large, abrupt and sometimes irreversible changes in systems caused by global warming, such as ice sheet instability or thermohaline circulation slowing. Assessment methods include a structured expert elicitation based on the literature described in WGII SM16.6 and are identical to AR5 but are enhanced by a structured approach to improve robustness and facilitate comparison between AR5 and AR6. For further explanations of global risk levels and Reasons for Concern, see WGII TS.AII. {WGII Figure SPM.3}

At global warming of 3°C, additional risks in many sectors and regions reach high or very high levels, implying widespread systemic impacts, irreversible change and many additional adaptation limits (see Section 3.2) (*high confidence*). For example, very high extinction risk for endemic species in biodiversity hotspots is projected to increase at least tenfold if warming rises from 1.5°C to 3°C (*medium confidence*). Projected increases in direct flood damages are higher by 1.4–2 times at 2°C and 2.5–3.9 times at 3°C, compared to 1.5°C global warming without adaptation (*medium confidence*). {WGII SPM B.4.1, WGII SPM B.4.2, WGII Figure SPM.3, WGII TS Appendix AII, WGII Atlas Fig.AI.46} (Figure 3.2, Figure 3.3)

Global warming of 4°C and above is projected to lead to far-reaching impacts on natural and human systems (*high confidence*). Beyond 4°C of warming, projected impacts on natural systems include local extinction of ~50% of tropical marine species (*medium confidence*) and biome shifts across 35% of global land area (*medium confidence*). At this level of warming, approximately 10% of the global land area is projected to face both increasing high and decreasing low extreme streamflow, affecting, without additional adaptation, over 2.1 billion people (*medium confidence*) and about 4 billion people are projected to experience water scarcity (*medium confidence*). At 4°C of warming, the global burned area is projected to increase by 50–70% and the fire frequency by ~30% compared to today (*medium confidence*). {WGII SPM B.4.1, WGII SPM B.4.2, WGII TS.C.1.2, WGII TS.C.2.3, WGII TS.C.4.1, WGII TS.C.4.4} (Figure 3.2, Figure 3.3)

Projected adverse impacts and related losses and damages from climate change escalate with every increment of global warming (*very high confidence*), but they will also strongly depend on socio-economic development trajectories and adaptation actions to reduce vulnerability and exposure (*high confidence*). For example, development pathways with higher demand for food, animal feed, and water, more resource-intensive consumption and production, and limited technological improvements result in higher risks from water scarcity in drylands, land degradation and food insecurity (*high confidence*). Changes in, for example, demography or investments in health systems have effect on a variety of health-related outcomes including heat-related morbidity and mortality (Figure 3.3 Panel d). {WGII SPM B.3, WGII SPM B.4, WGII Figure SPM.3; SRCCL SPM A.6}

With every increment of warming, climate change impacts and risks will become increasingly complex and more difficult to manage. Many regions are projected to experience an increase in the probability of compound events with higher global warming, such as concurrent heatwaves and droughts, compound flooding and fire weather. In addition, multiple climatic and non-climatic risk drivers such as biodiversity loss or violent conflict will interact, resulting in compounding overall risk and risks cascading across sectors and regions. Furthermore, risks can arise from some responses that are intended to reduce the risks of climate change, e.g., adverse side effects of some emission reduction and carbon dioxide removal (CDR) measures (see 3.4.1). (*high confidence*) {WGI SPM C.2.7, WGI Figure SPM.6, WGI TS.4.3; WGII SPM B.1.7, WGII B.2.2, WGII SPM B.5, WGII SPM B.5.4, WGII SPM C.4.2, WGII SPM B.5, WGII CCB2}

Solar Radiation Modification (SRM) approaches, if they were to be implemented, introduce a widespread range of new risks to people and ecosystems, which are not well understood. SRM has the potential to offset warming within one or two decades and ameliorate some climate hazards but would not restore climate to a previous state, and substantial residual or overcompensating climate change would occur at regional and seasonal scales (*high confidence*). Effects of SRM would depend on the specific approach used[65], and a sudden and sustained termination of SRM in a high CO_2 emissions scenario would cause rapid climate change (*high confidence*). SRM would not stop atmospheric CO_2 concentrations from increasing nor reduce resulting ocean acidification under continued anthropogenic emissions (*high confidence*). Large uncertainties and knowledge gaps are associated with the potential of SRM approaches to reduce climate change risks. Lack of robust and formal SRM governance poses risks as deployment by a limited number of states could create international tensions. {WGI 4.6; WGII SPM B.5.5; WGIII 14.4.5.1; Cross-WG box SRM; SR1.5 SPM C.1.4}

[START FIGURE 3.2 HERE]

[65] Several SRM approaches have been proposed, including stratospheric aerosol injection, marine cloud brightening, ground-based albedo modifications, and ocean albedo change. See Annex I: Glossary.

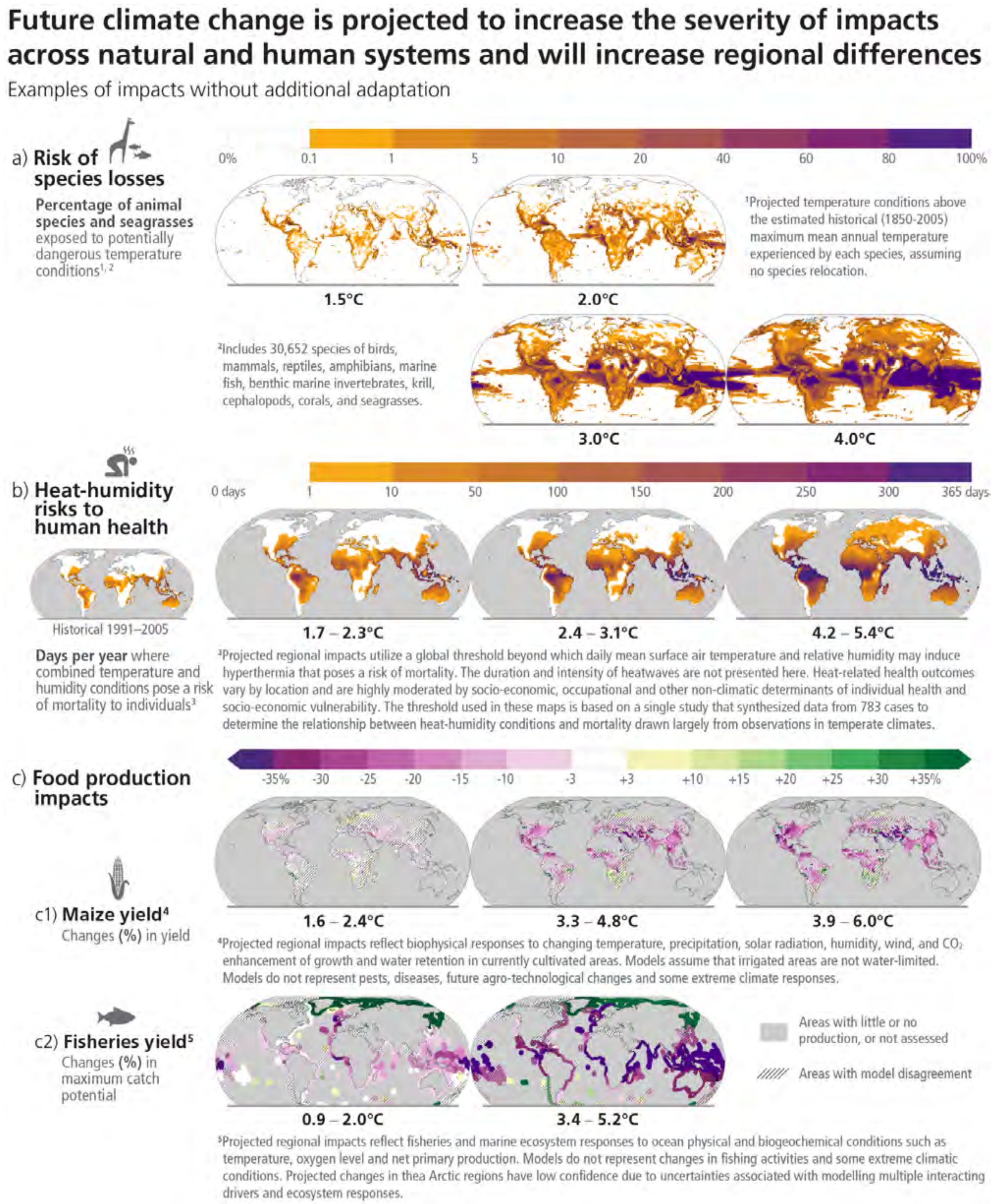

Figure 3.2: Projected risks and impacts of climate change on natural and human systems at different global warming levels (GWLs) relative to 1850–1900 levels. Projected risks and impacts shown on the maps are based on outputs from different subsets of Earth system models that were used to project each impact indicator without additional adaptation. WGII provides further assessment of the impacts on human and natural systems using these projections and additional lines of evidence. **(a)** Risks of species losses as indicated by the percentage of assessed species exposed to potentially dangerous temperature conditions, as defined by conditions beyond the estimated historical (1850-2005) maximum mean annual temperature experienced by each species, at GWLs of 1.5°C, 2°C, 3°C and 4°C. Underpinning projections of temperature are from 21 Earth system models and do not consider extreme events impacting ecosystems such as the Arctic. **(b)** Risk to human health as indicated by the days per year of population exposure to hypothermic conditions that pose a risk of mortality from surface air temperature and humidity conditions for historical period (1991-2005) and at GWLs of 1.7°C–2.3°C (mean = 1.9°C; 13 climate models), 2.4°C–3.1°C (2.7°C; 16 climate models) and 4.2°C–5.4°C (4.7°C; 15 climate models). Interquartile ranges of WGLs by 2081-2100 under RCP2.6, RCP4.5 and

RCP8.5. The presented index is consistent with common features found in many indices included within WGI and WGII assessments. **(c)** Impacts on food production: (c1) Changes in maize yield at projected GWLs of 1.6°C–2.4ºC (2.0°C), 3.3°C–4.8ºC (4.1°C) and 3.9°C–6.0ºC (4.9°C). Median yield changes from an ensemble of 12 crop models, each driven by bias-adjusted outputs from 5 Earth system models from the Agricultural Model Intercomparison and Improvement Project (AgMIP) and the Inter-Sectoral Impact Model Intercomparison Project (ISIMIP). Maps depict 2080–2099 compared to 1986–2005 for current growing regions (>10 ha), with the corresponding range of future global warming levels shown under SSP1-2.6, SSP3-7.0 and SSP5-8.5, respectively. Hatching indicates areas where <70% of the climate-crop model combinations agree on the sign of impact. (c2) Changes in maximum fisheries catch potential by 2081–2099 relative to 1986–2005 at projected GWLs of 0.9°C–2.0°C (1.5°C) and 3.4°C–5.2°C (4.3°C). GWLs by 2081–2100 under RCP2.6 and RCP8.5. Hatching indicates where the two climate-fisheries models disagree in the direction of change. Large relative changes in low yielding regions may correspond to small absolute changes. Biodiversity and fisheries in Antarctica were not analysed due to data limitations. Food security is also affected by crop and fishery failures not presented here {WGII Fig. TS.5, WGII Fig TS.9, WGII Annex I: Global to Regional Atlas Figure AI.15, Figure AI.22, Figure AI.23, Figure AI.29; WGII 7.3.1.2, 7.2.4.1, SROCC Figure SPM.3} (3.1.2, Cross-Section Box.2)

[END FIGURE 3.2 HERE]

[START FIGURE 3.3 HERE]

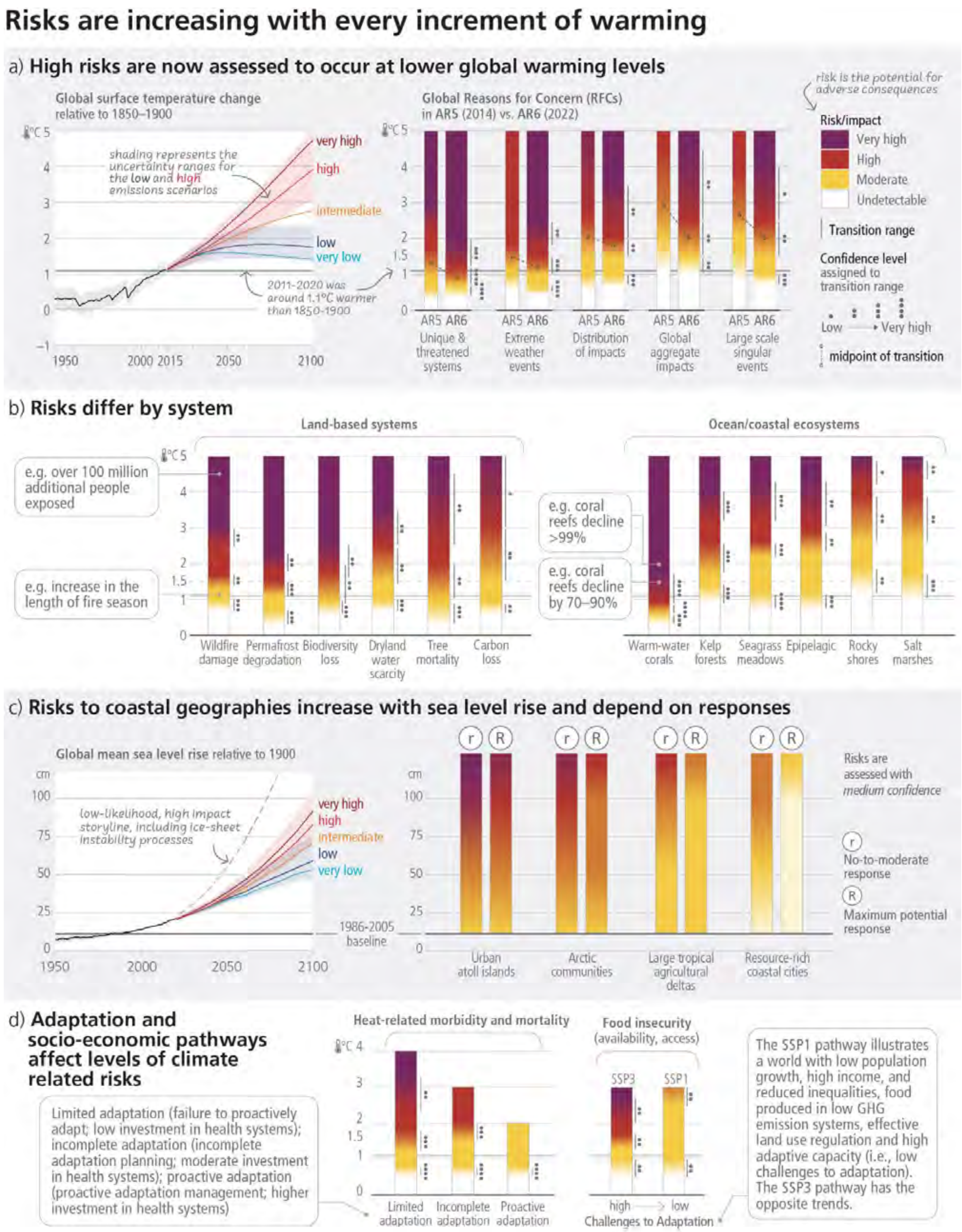

Risks are increasing with every increment of warming
a) High risks are now assessed to occur at lower global warming levels
Global surface temperature change relative to 1850–1900
shading represents the uncertainty ranges for the low and high emissions scenarios
very high
high
intermediate
low
very low
2011-2020 was around 1.1°C warmer than 1850-1900
Global Reasons for Concern (RFCs) in AR5 (2014) vs. AR6 (2022)
AR5 AR6
Unique & threatened systems
Extreme weather events
Distribution of impacts
Global aggregate impacts
Large scale singular events
risk is the potential for adverse consequences
Risk/impact
Very high
High
Moderate
Undetectable
Transition range
Confidence level assigned to transition range
Low
Very high
midpoint of transition
b) Risks differ by system
Land-based systems
Ocean/coastal ecosystems
e.g. over 100 million additional people exposed
e.g. increase in the length of fire season
Wildfire damage
Permafrost degradation
Biodiversity loss
Dryland water scarcity
Tree mortality
Carbon loss
e.g. coral reefs decline >99%
e.g. coral reefs decline by 70–90%
Warm-water corals
Kelp forests
Seagrass meadows
Epipelagic
Rocky shores
Salt marshes
c) Risks to coastal geographies increase with sea level rise and depend on responses
Global mean sea level rise relative to 1900
low-likelihood, high impact storyline, including ice-sheet instability processes
1986-2005 baseline
Urban atoll islands
Arctic communities
Large tropical agricultural deltas
Resource-rich coastal cities
Risks are assessed with medium confidence
No-to-moderate response
Maximum potential response
d) Adaptation and socio-economic pathways affect levels of climate related risks
Limited adaptation (failure to proactively adapt; low investment in health systems); incomplete adaptation (incomplete adaptation planning; moderate investment in health systems); proactive adaptation (proactive adaptation management; higher investment in health systems)
Heat-related morbidity and mortality
Limited adaptation
Incomplete adaptation
Proactive adaptation
Food insecurity (availability, access)
SSP3
SSP1
high
low
Challenges to Adaptation
The SSP1 pathway illustrates a world with low population growth, high income, and reduced inequalities, food produced in low GHG emission systems, effective land use regulation and high adaptive capacity (i.e., low challenges to adaptation). The SSP3 pathway has the opposite trends.

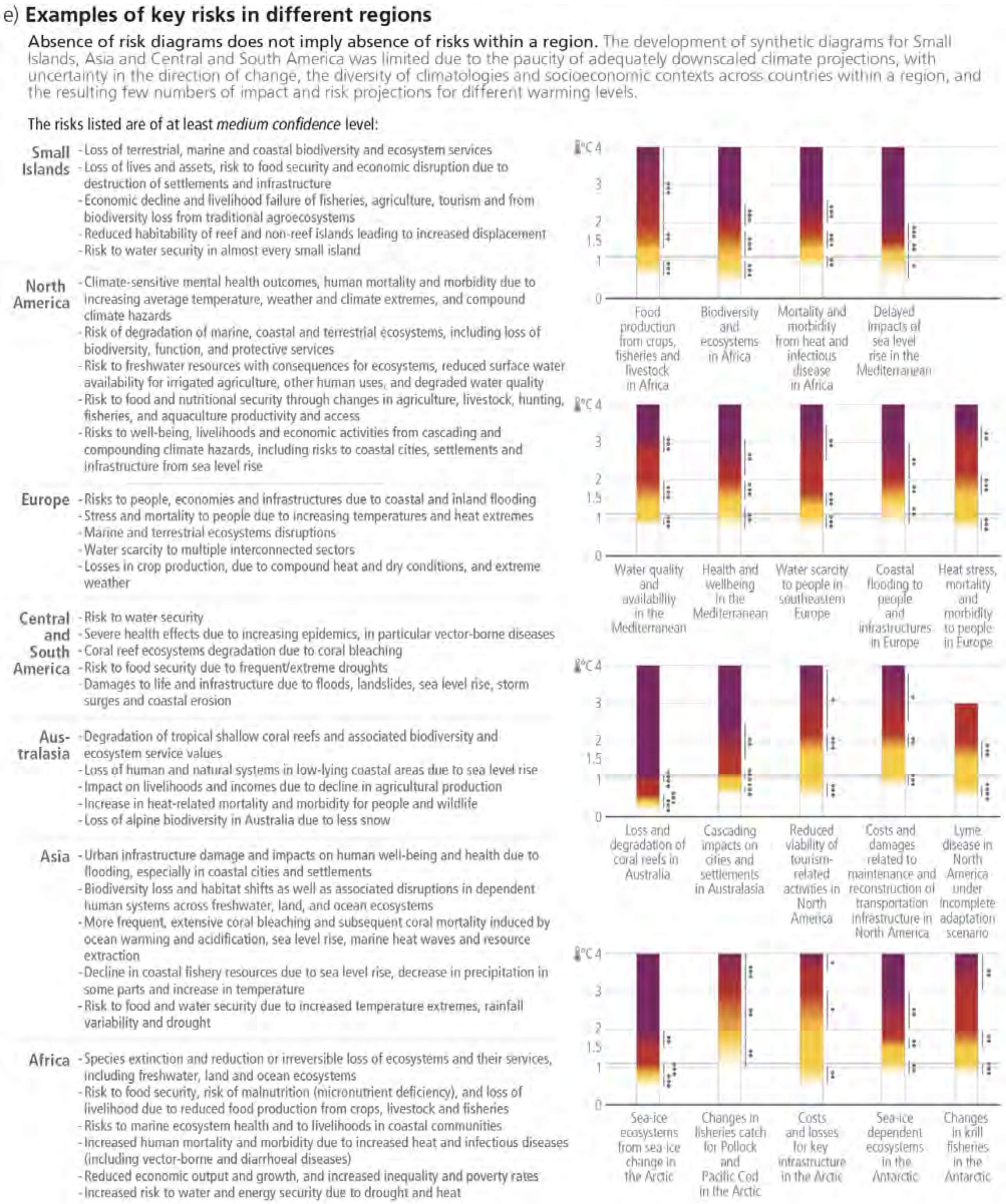

Figure 3.3: Synthetic risk diagrams of global and sectoral assessments and examples of regional key risks. The burning embers result from a literature based expert elicitation. **Panel (a)**: **Left** - Global surface temperature changes in °C relative to 1850–1900. These changes were obtained by combining CMIP6 model simulations with observational constraints based on past simulated warming, as well as an updated assessment of equilibrium climate sensitivity. *Very likely* ranges are shown for the low and high GHG emissions scenarios (SSP1-2.6 and SSP3-7.0); **Right** - Global Reasons for Concern, comparing AR6 (thick embers) and AR5 (thin embers) assessments. Diagrams are shown for each RFC, assuming low to no adaptation (i.e., adaptation is fragmented, localised and comprises incremental adjustments to existing practices). However, the transition to a very high risk level has an emphasis on irreversibility and adaptation limits. The horizontal line denotes the present global warming of 1.1°C which is used to separate the observed, past impacts below the line from the future projected risks above it. Lines connect the midpoints of the transition from moderate to high risk across AR5 and AR6. **Panel (b)**: Risks for land-based systems and ocean/coastal ecosystems. Diagrams shown for each

risk assume low to no adaptation. Text bubbles indicate examples of impacts at a given warming level. **Panel (c): Left** - Global mean sea level change in centimetres, relative to 1900. The historical changes (black) are observed by tide gauges before 1992 and altimeters afterwards. The future changes to 2100 (coloured lines and shading) are assessed consistently with observational constraints based on emulation of CMIP, ice-sheet, and glacier models, and *likely* ranges are shown for SSP1-2.6 and SSP3-7.0. **Right** - Assessment of the combined risk of coastal flooding, erosion and salinization for four illustrative coastal geographies in 2100, due to changing mean and extreme sea levels, under two response scenarios, with respect to the SROCC baseline period (1986–2005) and indicating the IPCC AR6 baseline period (1995–2014). The assessment does not account for changes in extreme sea level beyond those directly induced by mean sea level rise; risk levels could increase if other changes in extreme sea levels were considered (e.g., due to changes in cyclone intensity). "No-to-moderate response" describes efforts as of today (i.e., no further significant action or new types of actions). "Maximum potential response" represents a combination of responses implemented to their full extent and thus significant additional efforts compared to today, assuming minimal financial, social and political barriers. The assessment criteria include exposure and vulnerability (density of assets, level of degradation of terrestrial and marine buffer ecosystems), coastal hazards (flooding, shoreline erosion, salinization), in-situ responses (hard engineered coastal defences, ecosystem restoration or creation of new natural buffers areas, and subsidence management) and planned relocation. Planned relocation refers to managed retreat or resettlement. Forced displacement is not considered in this assessment. The term response is used here instead of adaptation because some responses, such as retreat, may or may not be considered to be adaptation. **Panel (d)**: **Left** - Heat-sensitive human health outcomes under three scenarios of adaptation effectiveness. The diagrams are truncated at the nearest whole ºC within the range of temperature change in 2100 under three SSP scenarios. **Right** - Risks associated with food security due to climate change and patterns of socio-economic development. Risks to food security include availability and access to food, including population at risk of hunger, food price increases and increases in disability adjusted life years attributable to childhood underweight. Risks are assessed for two contrasted socio-economic pathways (SSP1 and SSP3) excluding the effects of targeted mitigation and adaptation policies. **Panel (e)**: Examples of regional key risks. Risks identified are of at least *medium confidence* level. Key risks are identified based on the magnitude of adverse consequences (pervasiveness of the consequences, degree of change, irreversibility of consequences, potential for impact thresholds or tipping points, potential for cascading effects beyond system boundaries); likelihood of adverse consequences; temporal characteristics of the risk; and ability to respond to the risk, e.g., by adaptation. {WGI Figure SPM.8; WGII SPM B.3.3, WGII Figure SPM.3, WGII SM 16.6, WGII SM 16.7.4; SRCCL Figure SPM.2; SROCC Figure SPM.3d; SROCC SPM.5a; SROCC 4SM; SRCCL 7.3.1; SRCCL 7SM} (CSB.2)

[END FIGURE 3.3 HERE]

3.1.3 The Likelihood and Risks of Abrupt and Irreversible Change

The likelihood of abrupt and irreversible changes and their impacts increase with higher global warming levels (*high confidence*). As warming levels increase, so do the risks of species extinction or irreversible loss of biodiversity in ecosystems such as forests (*medium confidence*), coral reefs (*very high confidence*) and in Arctic regions (*high confidence*). Risks associated with large-scale singular events or tipping points, such as ice sheet instability or ecosystem loss from tropical forests, transition to high risk between 1.5°C–2.5°C (*medium confidence*) and to very high risk between 2.5°C–4°C (*low confidence*). The response of biogeochemical cycles to anthropogenic perturbations can be abrupt at regional scales and irreversible on decadal to century time scales (*high confidence*). The probability of crossing uncertain regional thresholds increases with further warming (*high confidence*). {WGI SPM C.3.2, WGI Box TS.9, WGI TS.2.6; WGII Figure SPM.3, WGII SPM B.3.1, WGII SPM B.4.1, WGII SPM B.5.2, WGII Table TS.1, WGII TS.C.1, WGII TS.C.13.3; SROCC SPM B.4}

Sea level rise is unavoidable for centuries to millennia due to continuing deep ocean warming and ice sheet melt, and sea levels will remain elevated for thousands of years (*high confidence*). Global mean sea level rise will continue in the 21st century (*virtually certain*), with projected regional relative sea level rise within 20% of the global mean along two-thirds of the global coastline (*medium confidence*). The magnitude, the rate, the timing of threshold exceedances, and the long-term commitment of sea level rise depend on emissions, with higher emissions leading to greater and faster rates of sea level rise. Due to relative sea level rise, extreme sea level events that occurred once per century in the recent past are projected to occur at least annually at more than half of all tide gauge locations by 2100 and risks for coastal ecosystems, people and infrastructure will continue to increase beyond 2100 (*high confidence*). At sustained warming levels between 2°C and 3°C, the Greenland and West Antarctic ice sheets will be lost almost completely and irreversibly over multiple millennia (*limited evidence*). The probability and rate of ice mass loss increase with higher global surface temperatures (*high confidence*). Over the next 2000 years, global mean sea level will rise by about 2–3 m if warming is limited to 1.5°C and 2–6 m if limited to 2°C (*low confidence*). Projections of multi-millennial global mean sea level rise are consistent with reconstructed levels during past warm climate periods: global mean sea level was *very likely* 5–25 m higher than today roughly 3 million years ago, when global temperatures were 2.5°C–4°C higher than 1850–1900 (*medium confidence*). Further examples of unavoidable changes in the climate system due to multi-decadal or longer response timescales include continued glacier melt (*very high confidence*) and permafrost carbon loss (*high confidence*). {WGI SPM B.5.2, WGI SPM B.5.3, WGI SPM B.5.4, WGI SPM C.2.5, WGI Box TS.4, WGI Box TS.9, WGI 9.5.1; WGII TS C.5; SROCC SPM B.3, SROCC SPM B.6, SROCC SPM B.9} (Figure 3.4)

The probability of low-likelihood outcomes associated with potentially very large impacts increases with higher global warming levels (*high confidence*). Warming substantially above the assessed *very likely* range for a given scenario cannot be ruled out, and there is *high confidence* this would lead to regional changes greater than assessed in many aspects of the climate system. Low-likelihood, high-impact outcomes could occur at regional scales even for global warming within the *very likely* assessed range for a given GHG emissions scenario. Global mean sea level rise above the *likely* range – approaching 2 m by 2100 and in excess of 15 m by 2300 under a very high GHG emissions scenario (SSP5-8.5) (*low confidence*) – cannot be ruled out due to deep uncertainty in ice-sheet processes[66] and would have severe impacts on populations in low elevation coastal zones. If global warming increases, some compound extreme events[67] will become more frequent, with higher likelihood of unprecedented intensities, durations or spatial extent (*high confidence*). The Atlantic Meridional Overturning Circulation is *very likely* to weaken over the 21st century for all considered scenarios (*high confidence*), however an abrupt collapse is not expected before 2100 (*medium confidence*). If such a low probability event were to occur, it would *very likely* cause abrupt shifts in regional weather patterns and water cycle, such as a southward shift in the tropical rain belt, and large impacts on ecosystems and human activities. A sequence of large explosive volcanic eruptions within decades, as have occurred in the past, is a low-likelihood high-impact event that would lead to substantial cooling globally and regional climate perturbations over several decades {WGI SPM B.5.3, WGI SPM C.3, WGI SPM C.3.1, WGI SPM C.3.2, WGI SPM C.3.3, WGI SPM C.3.4, WGI SPM C.3.5, WGI Figure SPM.8, WGI Box TS.3, WGI Figure TS.6, WGI Box 9.4; WGII SPM B.4.5, WGII SPM C.2.8; SROCC SPM B.2.7}. (Figure 3.4, Cross-Section Box.2)

3.2 Long-term Adaptation Options and Limits

With increasing warming, adaptation options will become more constrained and less effective. At higher levels of warming, losses and damages will increase, and additional human and natural systems will reach adaptation limits. Integrated, cross-cutting multi-sectoral solutions increase the effectiveness of adaptation. Maladaptation can create lock-ins of vulnerability, exposure and risks but can be avoided by long-term planning and the implementation of adaptation actions that are flexible, multi-sectoral and inclusive. (*high confidence*)

The effectiveness of adaptation to reduce climate risk is documented for specific contexts, sectors and regions (*high confidence*) and will decrease with increasing warming (*high confidence*)[68]. For example, common adaptation responses in agriculture – adopting improved cultivars and agronomic practices, and changes in cropping patterns and crop systems – will become less effective from 2°C to higher levels of warming (*high confidence*). The effectiveness of most water-related adaptation options to reduce projected risks declines with increasing warming (*high confidence*). Adaptations for hydropower and thermo-electric power generation are effective in most regions up to 1.5°C–2°C, with decreasing effectiveness at higher levels of warming (*medium confidence*). Ecosystem-based Adaptation is vulnerable to climate change impacts, with effectiveness declining with increasing global warming (*high confidence*). Globally, adaptation options related to agroforestry and forestry have a sharp decline in effectiveness at 3°C, with a substantial increase in residual risk (*medium confidence*). {WGII SPM C.2, WGII SPM C.2.1, WGII SPM C.2.5, WGII SPM C.2.10, WGII Figure TS.6 Panel (e), 4.7.2}

[66] This outcome is characterised by deep uncertainty: Its likelihood defies quantitative assessment but is considered due to its high potential impact. {WGI Box TS.1; WGII Cross-Chapter Box DEEP}
[67] See Annex I: Glossary. Examples of compound extreme events are concurrent heatwaves and droughts or compound flooding. {WGI SPM Footnote 18}
[68] There are limitations to assessing the full scope of adaptation options available in the future since not all possible future adaptation responses can be incorporated in climate impact models, and projections of future adaptation depend on currently available technologies or approaches. {WGII 4.7.2}

With increasing global warming, more limits to adaptation will be reached (*high confidence*) and losses and damages, strongly concentrated among the poorest vulnerable populations, will increase (*high confidence*). Already below 1.5°C, autonomous and evolutionary adaptation responses by terrestrial and aquatic ecosystems will increasingly face hard limits (*high confidence*) (Section 2.1.2). Above 1.5°C, some ecosystem-based adaptation measures will lose their effectiveness in providing benefits to people as these ecosystems will reach hard adaptation limits (*high confidence*). Adaptation to address the risks of heat stress, heat mortality and reduced capacities for outdoor work for humans face soft and hard limits across regions that become significantly more severe at 1.5°C, and are particularly relevant for regions with warm climates (*high confidence*). Above 1.5°C global warming level, limited freshwater resources pose potential hard limits for Small Islands and for regions dependent on glacier and snow melt (*medium confidence*). By 2°C, soft limits are projected for multiple staple crops, particularly in tropical regions (*high confidence*). By 3°C, soft limits are projected for some water management measures for many regions, with hard limits projected for parts of Europe (*medium confidence*). {WGII SPM C.3, WGII SPM C.3.3, WGII SPM C.3.4, WGII SPM C.3.5, WGII TS.D.2.2, WGII TS.D.2.3; SR1.5 SPM B.6; SROCC SPM C.1}

Integrated, cross-cutting multi-sectoral solutions increase the effectiveness of adaptation. For example, inclusive, integrated and long-term planning at local, municipal, sub-national and national scales, together with effective regulation and monitoring systems and financial and technological resources and capabilities foster urban and rural system transition. There are a range of cross-cutting adaptation options, such as disaster risk management, early warning systems, climate services and risk spreading and sharing that have broad applicability across sectors and provide greater benefits to other adaptation options when combined. Transitioning from incremental to transformational adaptation, and addressing a range of constraints, primarily in the financial, governance, institutional and policy domains, can help overcome soft adaptation limits. However, adaptation does not prevent all losses and damages, even with effective adaptation and before reaching soft and hard limits. (*high confidence*) {WGII SPM C.2, WGII SPM C.2.6, WGII SPM.C.2.13, WGII SPM C.3.1, WGII SPM.C.3.4, WGII SPM C.3.5, WGII Figure TS.6 Panel (e)}

Maladaptive responses to climate change can create lock-ins of vulnerability, exposure and risks that are difficult and expensive to change and exacerbate existing inequalities. Actions that focus on sectors and risks in isolation and on short-term gains often lead to maladaptation. Adaptation options can become maladaptive due to their environmental impacts that constrain ecosystem services and decrease biodiversity and ecosystem resilience to climate change or by causing adverse outcomes for different groups, exacerbating inequity. Maladaptation can be avoided by flexible, multi-sectoral, inclusive and long-term planning and implementation of adaptation actions with benefits to many sectors and systems. (*high confidence*) {WGII SPM C.4, WGII SPM.C.4.1, WGII SPM C.4.2, WGII SPM C.4.3}

Sea level rise poses a distinctive and severe adaptation challenge as it implies both dealing with slow onset changes and increases in the frequency and magnitude of extreme sea level events (*high confidence*). Such adaptation challenges would occur much earlier under high rates of sea level rise (*high confidence*). Responses to ongoing sea level rise and land subsidence include protection, accommodation, advance and planned relocation (*high confidence*). These responses are more effective if combined and/or sequenced, planned well ahead, aligned with sociocultural values and underpinned by inclusive community engagement processes (*high confidence*). Ecosystem-based solutions such as wetlands provide co-benefits for the environment and climate mitigation, and reduce costs for flood defences (*medium confidence*), but have site-specific physical limits, at least above 1.5ºC of global warming (*high confidence)* and lose effectiveness at high rates of sea level rise beyond 0.5–1 cm/yr (*medium confidence*). Seawalls can be maladaptive as they effectively reduce impacts in the short term but can also result in lock-ins and increase exposure to climate risks in the long term unless they are integrated into a long-term adaptive plan (*high confidence*). {WGI SPM C.2.5; WGII SPM C.2.8, WGII SPM C.4.1; WGII 13.10, WGII Cross-Chapter Box SLR; SROCC SPM B.9, SROCC SPM C.3.2, SROCC Figure SPM.4, SROCC Figure SPM.5c} (Figure 3.4)

[START FIGURE 3.4 HERE]

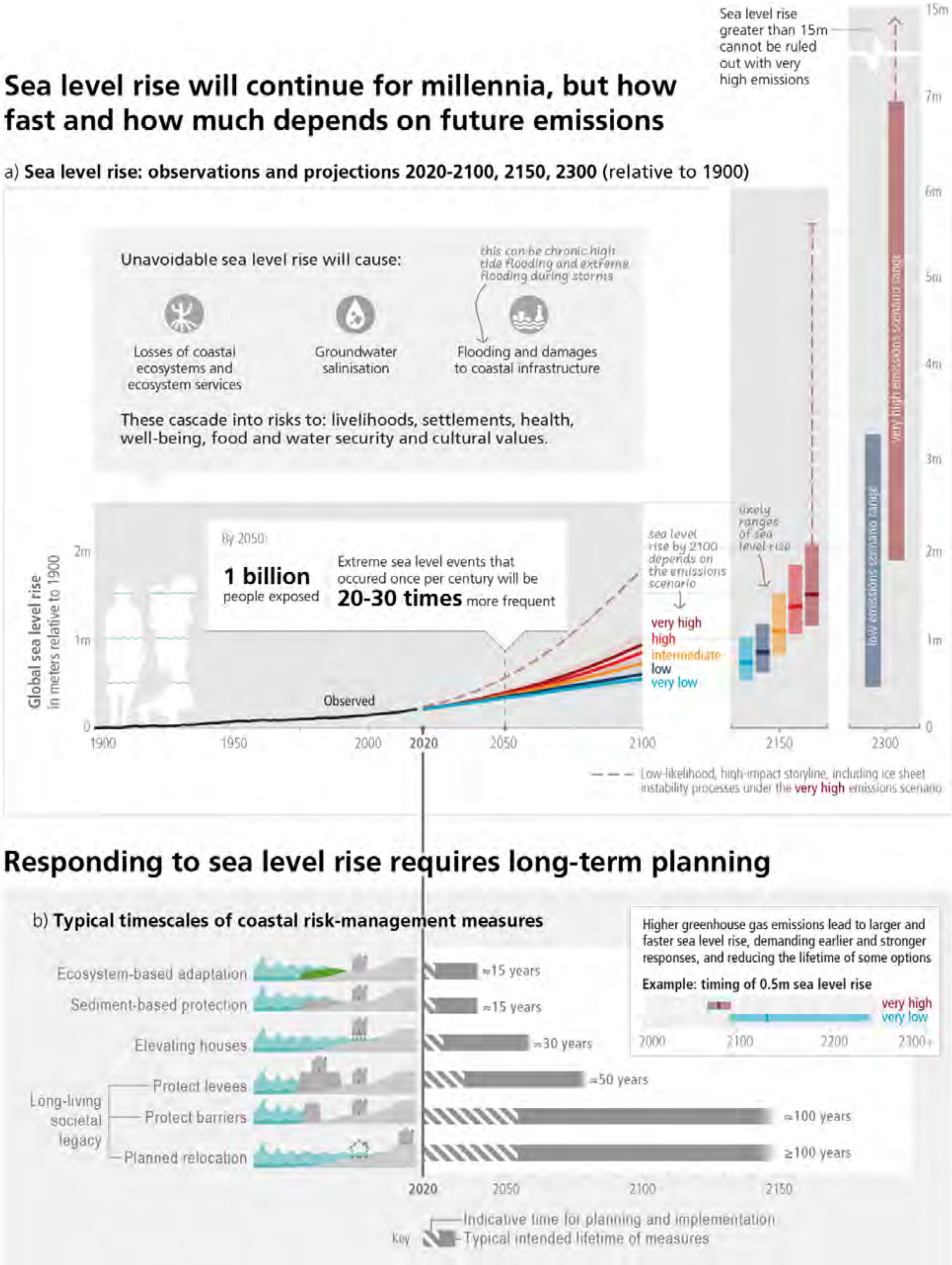

Figure 3.4: Observed and projected global mean sea level change and its impacts, and time scales of coastal risk management. Panel (a): Global mean sea level change in metres relative to 1900. The historical changes (black) are observed by tide gauges before 1992 and altimeters afterwards. The future changes to 2100 and for 2150 (coloured lines and shading) are assessed consistently with observational constraints based on emulation of CMIP, ice-sheet, and glacier models, and median values and *likely* ranges are shown for the considered scenarios. Relative to 1995–2014, the *likely* global mean sea level rise by 2050 is between 0.15–0.23 m in the very low GHG emissions scenario (SSP1-1.9) and 0.20–0.29 m in the very high GHG emissions scenario (SSP5-8.5); by 2100 between 0.28–0.55 m under SSP1-1.9 and 0.63–1.01 m under SSP5-8.5; and by 2150 between 0.37–0.86 m under SSP1-1.9 and 0.98–1.88 m under SSP5-8.5 (*medium*

confidence). Changes relative to 1900 are calculated by adding 0.158 m (observed global mean sea level rise from 1900 to 1995–2014) to simulated changes relative to 1995–2014. The future changes to 2300 (bars) are based on literature assessment, representing the 17th–83rd percentile range for SSP1-2.6 (0.3–3.1 m) and SSP5-8.5 (1.7–6.8 m). Red dashed lines: Low-likelihood, high-impact storyline, including ice sheet instability processes. These indicate the potential impact of deeply uncertain processes, and show the 83rd percentile of SSP5-8.5 projections that include low-likelihood, high-impact processes that cannot be ruled out; because of *low confidence* in projections of these processes, this is not part of a *likely* range. IPCC AR6 global and regional sea level projections are hosted at https://sealevel.nasa.gov/ipcc-ar6-sea-level-projection-tool. The low-lying coastal zone is currently home to around 896 million people (nearly 11% of the 2020 global population), projected to reach more than one billion by 2050 across all five SSPs. **Panel (b)**: Typical time scales for the planning, implementation (dashed bars) and operational lifetime of current coastal risk-management measures (blue bars). Higher rates of sea level rise demand earlier and stronger responses and reduce the lifetime of measures (inset). As the scale and pace of sea level rise accelerates beyond 2050, long-term adjustments may in some locations be beyond the limits of current adaptation options and for some small islands and low-lying coasts could be an existential risk. {WGI SPM B.5, C.2.5, Figure SPM.8, 9.6; WGII SPM B.4.5, B.5.2, C.2.8, D.3.3, TS.D.7, Cross-Chapter Box SLR} (CSB.2)

[END FIGURE 3.4 HERE]

3.3 Mitigation Pathways

Limiting human-caused global warming requires net zero anthropogenic CO_2 emissions. Pathways consistent with 1.5°C and 2°C carbon budgets imply rapid, deep, and in most cases immediate GHG emission reductions in all sectors (*high confidence*). Exceeding a warming level and returning (i.e. overshoot) implies increased risks and potential irreversible impacts; achieving and sustaining global net negative CO_2 emissions would reduce warming (*high confidence*).

3.3.1 Remaining Carbon Budgets

Limiting global temperature increase to a specific level requires limiting cumulative net CO_2 emissions to within a finite carbon budget[69], along with strong reductions in other GHGs. For every 1000 $GtCO_2$ emitted by human activity, global mean temperature rises by *likely* 0.27°C–0.63°C (best estimate of 0.45°C). This relationship implies that there is a finite carbon budget that cannot be exceeded in order to limit warming to any given level. {WGI SPM D.1, WGI SPM D.1.1; SR1.5 SPM C.1.3} (Figure 3.5)

The best estimates of the remaining carbon budget (RCB) from the beginning of 2020 for limiting warming to 1.5°C with a 50% likelihood[70] is estimated to be 500 $GtCO_2$; for 2°C (67% likelihood) this is 1150 $GtCO_2$.[71] Remaining carbon budgets have been quantified based on the assessed value of TCRE and its uncertainty, estimates of historical warming, climate system feedbacks such as emissions from thawing permafrost, and the global surface temperature change after global anthropogenic CO_2 emissions reach net zero, as well as variations in projected warming from non-CO_2 emissions due in part to mitigation action. The stronger the reductions in non-CO_2 emissions the lower the resulting temperatures are for a given RCB or the larger RCB for the same level of temperature change. For instance, the RCB for limiting warming to 1.5°C with a 50% likelihood could vary between 300 to 600 $GtCO_2$ depending on non-CO_2 warming[72]. Limiting warming to 2°C with a 67% (or 83%) likelihood would imply a RCB of 1150 (900) $GtCO_2$ from the beginning

[69] See Annex 1: Glossary.
[70] This likelihood is based on the uncertainty in transient climate response to cumulative net CO_2 emissions and additional Earth system feedbacks and provides the probability that global warming will not exceed the temperature levels specified. {WGI Table SPM.1}
[71] Global databases make different choices about which emissions and removals occurring on land are considered anthropogenic. Most countries report their anthropogenic land CO_2 fluxes including fluxes due to human-caused environmental change (e.g., CO_2 fertilisation) on 'managed' land in their National GHG inventories. Using emissions estimates based on these inventories, the remaining carbon budgets must be correspondingly reduced. {WGIII SPM Footnote 9, WGIII TS.3, WGIII Cross-Chapter Box 6}
[72] The central case RCB assumes future non-CO_2 warming (the net additional contribution of aerosols and non-CO_2 GHG) of around 0.1°C above 2010–2019 in line with stringent mitigation scenarios. If additional non-CO_2 warming is higher, the RCB for limiting warming to 1.5°C with a 50% likelihood shrinks to around 300 $GtCO_2$. If, however, additional non-CO_2 warming is limited to only 0.05°C (via stronger reductions of CH_4 and N_2O through a combination of deep structural and behavioural changes, e.g., dietary changes), the RCB could be around 600 $GtCO_2$ for 1.5°C warming. {WGI Table SPM.2, WGI Box TS.7; WGIII Box 3.4}

of 2020. To stay below 2°C with a 50% likelihood, the RCB is higher, i.e., 1350 $GtCO_2$[73]. {WGI SPM D.1.2, WGI Table SPM.2; WGIII Box SPM.1, WGIII Box 3.4; SR1.5 SPM C.1.3}

If the annual CO_2 emissions between 2020-2030 stayed, on average, at the same level as 2019, the resulting cumulative emissions would almost exhaust the remaining carbon budget for 1.5°C (50%), and exhaust more than a third of the remaining carbon budget for 2°C (67%) (Figure 3.5). Based on central estimates only, historical cumulative net CO_2 emissions between 1850 and 2019 (2400 ±240 GtCO2) amount to about four-fifths[74] of the total carbon budget for a 50% probability of limiting global warming to 1.5°C (central estimate about 2900 GtCO2) and to about two-thirds[75] of the total carbon budget for a 67% probability to limit global warming to 2°C (central estimate about 3550 GtCO2). {WGI Table SPM.2; WGIII SPM B.1.3, WGIII Table 2.1}

In scenarios with increasing CO_2 emissions, the land and ocean carbon sinks are projected to be less effective at slowing the accumulation of CO_2 in the atmosphere (*high confidence*). While natural land and ocean carbon sinks are projected to take up, in absolute terms, a progressively larger amount of CO_2 under higher compared to lower CO_2 emissions scenarios, they become less effective, that is, the proportion of emissions taken up by land and ocean decreases with increasing cumulative net CO_2 emissions (*high confidence*). Additional ecosystem responses to warming not yet fully included in climate models, such as GHG fluxes from wetlands, permafrost thaw, and wildfires, would further increase concentrations of these gases in the atmosphere *(high confidence*). In scenarios where CO_2 concentrations peak and decline during the 21st century, the land and ocean begin to take up less carbon in response to declining atmospheric CO_2 concentrations (*high confidence*) and turn into a weak net source by 2100 in the very low GHG emissions scenario (*medium confidence*)[76]. {WGI SPM B.4, WGI SPM B.4.1, WGI SPM B.4.2, WGI SPM B.4.3}

[START FIGURE 3.5 HERE]

[73] When adjusted for emissions since previous reports, these RCB estimates are similar to SR1.5 but larger than AR5 values due to methodological improvements. {WGI SPM D.1.3}
[74] Uncertainties for total carbon budgets have not been assessed and could affect the specific calculated fractions.
[75] See footnote 77.
[76] These projected adjustments of carbon sinks to stabilisation or decline of atmospheric CO_2 concentrations are accounted for in calculations of remaining carbon budgets. {WGI SPM footnote 32}

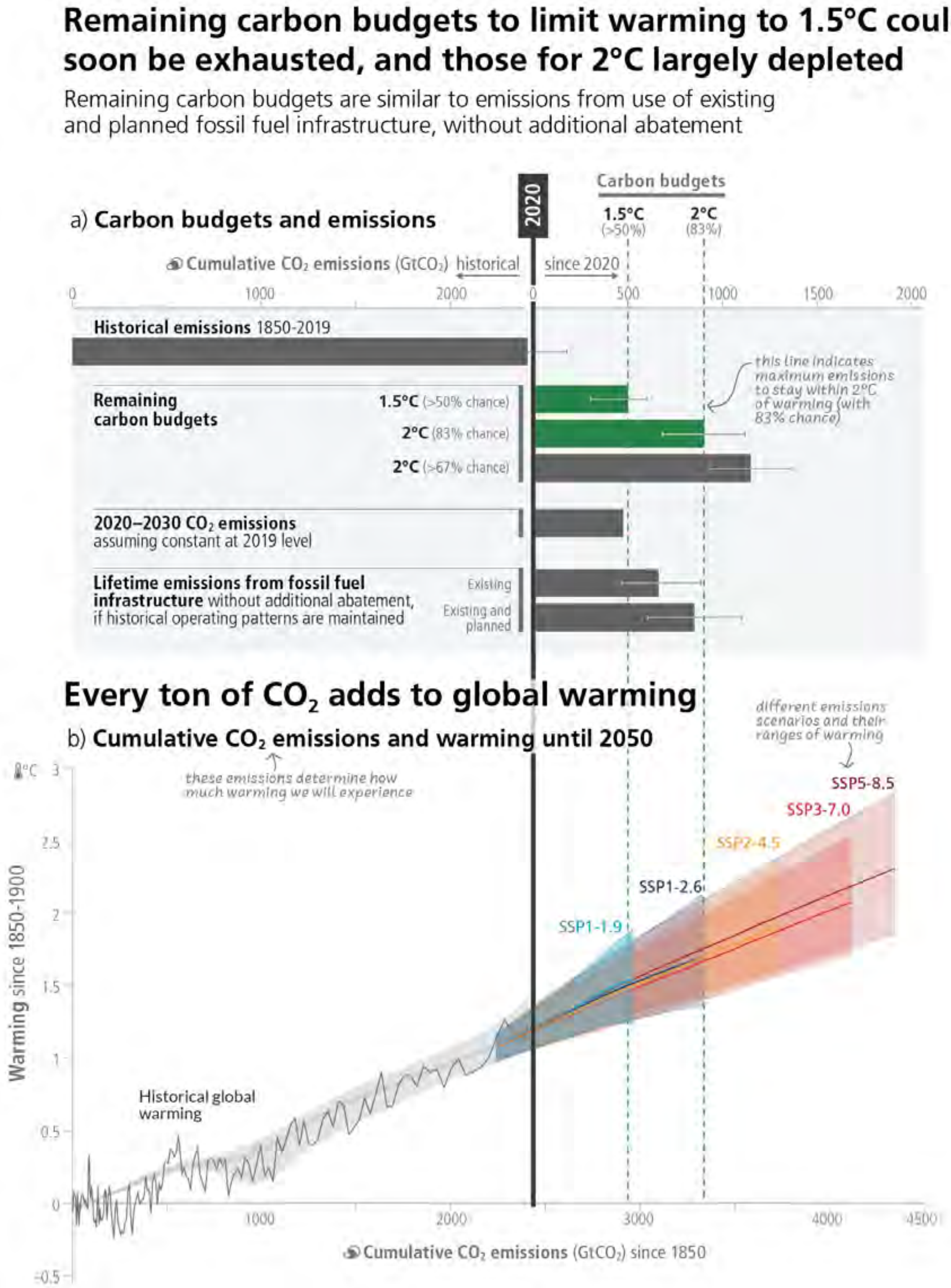

Figure 3.5: Cumulative past, projected, and committed emissions, and associated global temperature changes. Panel (a) Assessed remaining carbon budgets to limit warming *more likely than not* to 1.5°C, below 2°C with a 83% and 67% likelihood, compared to cumulative emissions corresponding to constant 2019 emissions until 2030, existing and planned fossil fuel infrastructures (in $GtCO_2$). For remaining carbon budgets, thin lines indicate the uncertainty due to the contribution of non-CO_2 warming. For lifetime emissions from fossil fuel infrastructure, thin lines indicate the assessed sensitivity range. **Panel (b)** Relationship between cumulative CO_2 emissions and the increase in global surface temperature. Historical data (thin black line) shows historical CO_2 emissions versus observed global surface temperature increase relative to the period 1850–1900. The grey range with its central line shows a corresponding estimate of the human-caused share of historical warming. Coloured areas show the assessed *very likely* range of global surface temperature projections, and thick coloured central lines show the median estimate as a function of cumulative CO_2 emissions for the selected scenarios SSP1-1.9, SSP1-2.6, SSP2-4.5, SSP3-7.0, and SSP5-8.5. Projections until 2050 use the cumulative CO_2 emissions of each respective scenario, and the projected global warming includes the contribution from all anthropogenic forcers. {WGI SPM D.1, WGI Figure SPM.10, WGI Table SPM.2; WGIII SPM B.1, WGIII SPM B.7, WGIII 2.7; SR1.5 SPM C.1.3}

[END FIGURE 3.5 HERE]

[START TABLE 3.1 HERE]

Table 3.1: Key characteristics of the modelled global emissions pathways. Summary of projected CO_2 and GHG emissions, projected net-zero timings and the resulting global warming outcomes. Pathways are categorised (columns), according to their likelihood of limiting warming to different peak warming levels (if peak temperature occurs before 2100) and 2100 warming levels. Values shown are for the median [p50] and 5th–95th percentiles [p5–p95], noting that not all pathways achieve net-zero CO_2 or GHGs. {WGIII Table SPM.2}

p50 [p5-p95] (1)												
	Category (2) [# pathways]	Modelled global emissions pathways categorised by projected global warming levels (GWL). Detailed likelihood definitions are provided in SPM Box1. The five illustrative scenarios (SSPx-yy) considered by AR6 WGI and the Illustrative (Mitigation) Pathways assessed in WGIII are aligned with the temperature categories and are indicated in a separate column. Global emission pathways contain regionally differentiated information. This assessment focuses on their global characteristics.	C1 [97]	C1a [50]	C1b [47]	C2 [133]	C3 [311]	C3a [204]	C3b [97]	C4 [159]	C5 [212]	C6 [97]
	Category/ subset label		limit warming to 1.5°C (>50%) with no or limited overshoot	… with net zero GHGs	… without net zero GHGs	return warming to 1.5°C (>50%) after a high overshoot	limit warming to 2°C (>67%)	… with action starting in 2020	… NDCs until 2030	limit warming to 2°C (>50%)	limit warming to 2.5°C (>50%)	limit warming to 3°C (>50%)
GHG emissions reductions from 2019 (%) (3)	2030	Projected median GHG emissions reductions of pathways in the year across the scenarios compared to modelled 2019, with the 5th-95th percentile in brackets. Negative numbers indicate increase in emissions compared to 2019	43 [34-60]	41 [31-59]	48 [35-61]	23 [0-44]	21 [1-42]	27 [13-45]	5 [0-14]	10 [0-27]	6 [-1 to 18]	2 [-10 to 11]
	2040		69 [58-90]	66 [58-89]	70 [62-87]	55 [40-71]	46 [34-63]	47 [35-63]	46 [34-63]	31 [20-5]	18 [4-33]	3 [-14 to 14]
	2050		84 [73-98]	85 [72-100]	84 [76-93]	75 [62-91]	64 [53-77]	63 [52-76]	68 [56-83]	49 [35-65]	29 [11-48]	5 [-2 to 18]
Emissions milestones (4)	Net zero CO_2 (% net zero pathways)	Median 5-year intervals at which projected CO_2 & GHG emissions of pathways in this category reach net-zero, with the 5th-95th percentile interval in square brackets. Percentage of net zero pathways is denoted in round brackets. Three dots (…) denotes net zero not reached for that percentile.	2050-2055 (100%) [2035-2070]			2055-2060 (100%) [2045-2070]	2070-2075 (93%) [2055-…]	2070-2075 (91%) [2055-…]	2065-2070 (97%) [2055-2090]	2080-2085 (86%) [2065-…]	…-… (41%) [2080-…]	no net-zero
	Net zero GHGs (5) (% net zero pathways)		2095-2100 (52%) [2050-…]	2070-2075 (100%) [2050-2090]	…-… (0%) […-…]	2070-2075 (87%) [2055-…]	…-… (30%) [2075-…]	…-… (24%) [2080-…]	…-… (41%) [2075-…]	…-… (31%) [2075-…]	…-… (12%) [2090-…]	no net-zero
Cumulative CO_2 emissions [Gt CO_2] (6)	2020 to net zero CO_2	Median cumulative net CO_2 emissions across the projected scenarios in this category until reaching net-zero or until 2100, with the 5th-95th percentile interval in square brackets.	510 [330-710]	550 [340-760]	460 [320-590]	720 [530-930]	890 [640-1160]	860 [640-1180]	910 [720-1150]	1210 [970-1490]	1780 [1400-2360]	no net-zero
	2020–2100		320 [-210-570]	160 [-220-620]	360 [10-540]	400 [-90-620]	800 [510-1140]	790 [480-1150]	800 [560-1050]	1160 [700-1490]	1780 [1260-2360]	2790 [2440-3520]
Global mean temperature changes 50% probability (°C)	at peak warming	Projected temperature change of pathways in this category (50% probability across the range of climate uncertainties), relative to 1850-1900, at peak warming and in 2100, for the median value across the scenarios and the 5th-95th percentile interval in square brackets.	1.6 [1.4-1.6]	1.6 [1.4-1.6]	1.6 [1.5-1.6]	1.7 [1.5-1.8]	1.7 [1.6-1.8]	1.7 [1.6-1.8]	1.8 [1.6-1.8]	1.9 [1.7-2.0]	2.2 [1.9-2.5]	no peaking by 2100
	2100		1.3 [1.1-1.5]	1.2 [1.1-1.4]	1.4 [1.3-1.5]	1.4 [1.2-1.5]	1.6 [1.5-1.8]	1.6 [1.5-1.8]	1.6 [1.5-1.7]	1.8 [1.5-2.0]	2.1 [1.9-2.5]	2.7 [2.4-2.9]
Likelihood of peak global warming staying below (%)	<1.5°C	Median likelihood that the projected pathways in this category stay below a given global warming level, with the 5th-95th percentile interval in square brackets.	38 [33-58]	38 [34-60]	37 [33-56]	24 [15-42]	20 [13-41]	21 [14-42]	17 [12-35]	11 [7-22]	4 [0-10]	0 [0-0]
	<2.0°C		90 [86-97]	90 [85-97]	89 [87-96]	82 [71-93]	76 [68-91]	78 [69-91]	73 [67-87]	59 [50-77]	37 [18-59]	8 [2-18]
	<3.0°C		100 [99-100]	100 [99-100]	100 [99-100]	100 [99-100]	99 [98-100]	100 [98-100]	99 [98-99]	98 [95-99]	91 [83-98]	71 [53-88]

1 Detailed explanations on the Table are provided in WGIII Box SPM.1 and WGIII Table SPM.2. The relationship between the temperature categories and SSP/RCPs is discussed in Cross-Section Box 2. Values in the table refer to the 50th and [5th–95th] percentile values across the pathways falling within a given category as defined in WGIII Box SPM.1. The three dots (…) sign denotes that the value cannot be given (as the value is after 2100 or, for net zero, net-zero is not reached). Based on the assessment of climate emulators in AR6 WG I (Chapter 7, Box 7.1), two climate emulators were used for the probabilistic assessment of the resulting warming of the pathways. For the 'Temperature Change' and 'Likelihood' columns, the non-bracketed values represent the 50th percentile across the pathways in that category and the median [50th percentile] across the warming estimates of the probabilistic MAGICC climate model emulator. For the bracketed ranges in the "likelihood" column, the median warming for every pathway in that category is calculated for each of the two climate model emulators (MAGICC and FaIR). These ranges cover both the uncertainty of the emissions pathways as well as the climate emulators' uncertainty. All global warming levels are relative to 1850–1900.

2 C3 pathways are sub-categorised according to the timing of policy action to match the emissions pathways in WGIII Figure SPM.4.

3 Global emission reductions in mitigation pathways are reported on a pathway-by-pathway basis relative to harmonised modelled global emissions in 2019 rather than the global emissions reported in WGIII SPM Section B and WGIII Chapter 2; this ensures internal consistency in assumptions about emission sources and activities, as well as consistency with temperature projections based on the physical climate science assessment by WGI (see WGIII SPM Footnote 49). Negative values (e.g., in C5, C6) represent an increase in emissions. The modelled GHG emissions in 2019 are 55 [53–58] $GtCO_2$-eq, thus within the uncertainty ranges of estimates for 2019 emissions [53-66] $GtCO_2$-eq (see 2.1.1).

4 Emissions milestones are provided for 5-year intervals in order to be consistent with the underlying 5-year time-step data of the modelled pathways. Ranges in square brackets underneath refer to the range across the pathways, comprising the lower bound of the 5th percentile 5-year interval and the upper bound of the 95th percentile 5-year interval. Numbers in round brackets signify the fraction of pathways that reach specific milestones over the 21st century. Percentiles reported across all pathways in that category include those that do not reach net zero before 2100.

5 For cases where models do not report all GHGs, missing GHG species are infilled and aggregated into a Kyoto basket of GHG emissions in CO_2-eq defined by the 100-year global warming potential. For each pathway, reporting of CO_2, CH_4, and N_2O emissions was the minimum required for the assessment of the climate response and the assignment to a climate category. Emissions pathways without climate assessment are not included in the ranges presented here. See WGIII Annex III.II.5.

6 Cumulative emissions are calculated from the start of 2020 to the time of net zero and 2100, respectively. They are based on harmonised net CO_2 emissions, ensuring consistency with the WG I assessment of the remaining carbon budget. {WGIII Box 3.4, WGIII SPM Footnote 50}

[END TABLE 3.1 HERE]

3.3.2 Net Zero Emissions: Timing and Implications

From a physical science perspective, limiting human-caused global warming to a specific level requires limiting cumulative CO_2 emissions, reaching net zero or net negative CO_2 emissions, along with strong reductions of other GHG emissions (see Cross-Section Box 1). Global modelled pathways that reach and sustain net zero GHG emissions are projected to result in a gradual decline in surface temperature (*high confidence*). Reaching net zero GHG emissions primarily requires deep reductions in CO_2, methane, and other GHG emissions, and implies net-negative CO2 emissions[77]. Carbon dioxide removal (CDR) will be necessary to achieve net-negative CO2 emissions[78]. Achieving global net zero CO_2 emissions, with remaining anthropogenic CO_2 emissions balanced by durably stored CO_2 from anthropogenic removal, is a requirement to stabilise CO_2-induced global surface temperature increase (see 3.3.3) (*high confidence*). This is different from achieving net zero GHG emissions, where metric-weighted anthropogenic GHG emissions (see Cross-Section Box 1) equal CO_2 removal (*high confidence*). Emissions pathways that reach and sustain net zero GHG emissions defined by the 100-year global warming potential imply net-negative CO_2 emissions and are projected to result in a gradual decline in surface temperature after an earlier peak (*high confidence*). While reaching net-zero CO_2 or net-zero GHG emissions requires deep and rapid reductions in gross emissions, the deployment of CDR to counterbalance hard-to-abate residual emissions (e.g., some emissions from agriculture, aviation, shipping, and industrial processes) is unavoidable (*high confidence*). {WGI SPM D.1, WGI SPM D.1.1, WGI SPM D.1.8; WGIII SPM C.2, WGIII SPM C.3, WGIII SPM C.11, WGIII Box TS.6; SR1.5 SPM A.2.2}

In modelled pathways, the timing of net-zero CO_2 emissions, followed by net-zero GHG emissions, depends on several variables, including the desired climate outcome, the mitigation strategy and the gases covered (*high confidence*). Global net zero CO_2 emissions are reached in the early 2050s in pathways that limit warming to 1.5°C (>50%) with no or limited overshoot, and around the early 2070s in pathways that limit warming to 2°C (>67%). While non-CO_2 GHG emissions are strongly reduced in all pathways that limit warming to 2°C (>67%) or lower, residual emissions of CH_4 and N_2O and F-gases of about 8 [5–11] $GtCO_2$-eq/yr remain at the time of net zero GHG, counterbalanced by net negative CO_2 emissions. As a result, net zero CO_2 would be reached before net zero GHGs (*high confidence*). {WGIII SPM C.2, WGIII SPM C.2.3, WGIII SPM C.2.4, WGIII Table SPM.2, WGIII 3.3} (Figure 3.6)

[77] Net zero GHG emissions defined by the 100-year global warming potential. See footnote 12.
[78] See section 3.3.3 and 3.4.1

[START FIGURE 3.6 HERE]

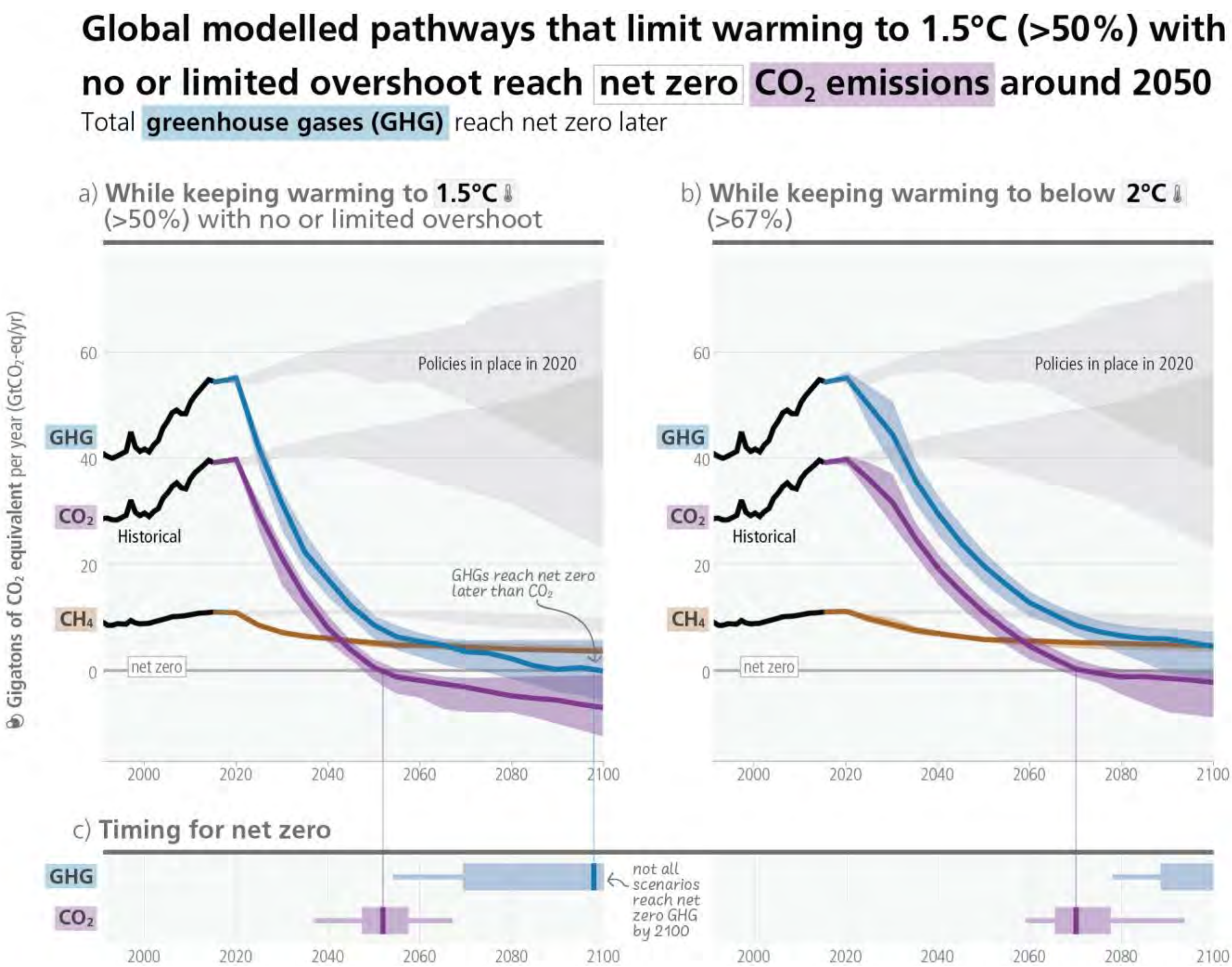

Figure 3.6: Total GHG, CO_2 and CH_4 emissions and timing of reaching net-zero in different mitigation pathways. Top row: GHG, CO_2 and CH_4 emissions over time (in $GtCO_2eq$) with historical emissions, projected emissions in line with policies implemented until the end of 2020 (grey), and pathways consistent with temperature goals in colour (blue, purple, and brown, respectively); **Panel (a) (left)** shows pathways that limit warming to 1.5°C (>50%) with no or limited overshoot (C1) and **Panel (b) (right)** shows pathways that limit warming to 2°C (>66%) (C3). **Bottom row: Panel (c)** shows *median* (vertical line), *likely* (bar) and *very likely* (thin lines) timing of reaching net-zero GHG and CO_2 emissions for global modelled pathways that limit warming to 1.5°C (>50%) with no or limited overshoot (C1) (left) or 2°C (>67%) (C3) (right). {WGIII Figure SPM.5}

[END FIGURE 3.6 HERE]

3.3.3 Sectoral Contributions to Mitigation

All global modelled pathways that limit warming to 2°C (>67%) or lower by 2100 involve rapid and deep and in most cases immediate GHG emissions reductions in all sectors (see also 4.1, 4.5). Reductions in GHG emissions in industry, transport, buildings, and urban areas can be achieved through a combination of energy efficiency and conservation and a transition to low-GHG technologies and energy carriers (see also 4.5, Figure 4.4). Socio-cultural options and behavioural change can reduce global GHG emissions of end-use sectors, with most of the potential in developed countries, if combined with improved infrastructure design and access. (*high confidence*) {WGIII SPM C.3, WGIII SPM C.5, WGIII SPM C.6, WGIII SPM C.7.3, WGIII SPM C.8, WGIII SPM C.10.2}

Global modelled mitigation pathways reaching net zero CO2 and GHG emissions include transitioning from fossil fuels without carbon capture and storage (CCS) to very low- or zero-carbon energy sources, such as renewables or fossil fuels with CCS, demand-side measures and improving efficiency, reducing non-CO2 GHG emissions, and CDR.[79] In global modelled pathways that limit warming to 2°C or below, almost all electricity is supplied from zero or low-carbon sources in 2050, such as renewables or fossil fuels with CO_2 capture and storage, combined with increased electrification of energy demand. Such pathways meet energy service demand with relatively low energy use, through e.g., enhanced energy efficiency and behavioural changes and increased electrification of energy end use. Modelled global pathways limiting global warming to 1.5°C (>50%) with no or limited overshoot generally implement such changes faster than pathways limiting global warming to 2°C (>67%). (*high confidence*) {WGIII SPM C.3, WGIII SPM C.3.2, WGIII SPM C.4, WGIII TS.4.2; SR1.5 SPM C.2.2}

AFOLU mitigation options, when sustainably implemented, can deliver large-scale GHG emission reductions and enhanced CO_2 removal; however, barriers to implementation and trade-offs may result from the impacts of climate change, competing demands on land, conflicts with food security and livelihoods, the complexity of land ownership and management systems, and cultural aspects (see 3.4.1). All assessed modelled pathways that limit warming to 2°C (>67%) or lower by 2100 include land-based mitigation and land-use change, with most including different combinations of reforestation, afforestation, reduced deforestation, and bioenergy. However, accumulated carbon in vegetation and soils is at risk from future loss (or sink reversal) triggered by climate change and disturbances such as flood, drought, fire, or pest outbreaks, or future poor management. (*high confidence*) {WGI SPM B.4.3; WGII SPM B.2.3, WGII SPM B.5.4; WGIII SPM C.9, WGIII SPM C.11.3, WGIII SPM D.2.3, WGIII TS.4.2, 3.4; SR1.5 SPM C.2.5; SRCCL SPM B.1.4, SRCCL SPM B.3, SRCCL SPM B.7}

In addition to deep, rapid, and sustained emission reductions, CDR can fulfil three complementary roles: lowering net CO_2 or net GHG emissions in the near term; counterbalancing 'hard-to-abate' residual emissions (e.g., some emissions from agriculture, aviation, shipping, industrial processes) to help reach net zero CO_2 or GHG emissions, and achieving net negative CO_2 or GHG emissions if deployed at levels exceeding annual residual emissions (*high confidence*). CDR methods vary in terms of their maturity, removal process, time scale of carbon storage, storage medium, mitigation potential, cost, co-benefits, impacts and risks, and governance requirements (*high confidence*). Specifically, maturity ranges from lower maturity (e.g., ocean alkalinisation) to higher maturity (e.g., reforestation); removal and storage potential ranges from lower potential (<1 Gt CO_2/yr, e.g., blue carbon management) to higher potential (>3 Gt CO_2/yr, e.g., agroforestry); costs range from lower cost (e.g., –45 to 100 USD/tCO_2 for soil carbon sequestration) to higher cost (e.g., 100–300 USD/tCO_2 for direct air carbon dioxide capture and storage) (*medium confidence*). Estimated storage timescales vary from decades to centuries for methods that store carbon in vegetation and through soil carbon management, to ten thousand years or more for methods that store carbon in geological formations (*high confidence*). Afforestation, reforestation, improved forest management, agroforestry and soil carbon sequestration are currently the only widely practiced CDR methods (*high confidence*). Methods and levels of CDR deployment in global modelled mitigation pathways vary depending on assumptions about costs, availability and constraints (*high confidence*). {WGIII SPM C.3.5, WGIII SPM C.11.1, WGIII SPM C.11.4}

[79] CCS is an option to reduce emissions from large-scale fossil-based energy and industry sources provided geological storage is available. When CO2 is captured directly from the atmosphere (DACCS), or from biomass (BECCS), CCS provides the storage component of these CDR methods. CO2 capture and subsurface injection is a mature technology for gas processing and enhanced oil recovery. In contrast to the oil and gas sector, CCS is less mature in the power sector, as well as in cement and chemicals production, where it is a critical mitigation option. The technical geological storage capacity is estimated to be on the order of 1000 GtCO2, which is more than the CO2 storage requirements through 2100 to limit global warming to 1.5°C, although the regional availability of geological storage could be a limiting factor. If the geological storage site is appropriately selected and managed, it is estimated that the CO2 can be permanently isolated from the atmosphere. Implementation of CCS currently faces technological, economic, institutional, ecological environmental and socio-cultural barriers. Currently, global rates of CCS deployment are far below those in modelled pathways limiting global warming to 1.5°C to 2°C. Enabling conditions such as policy instruments, greater public support and technological innovation could reduce these barriers. (*high confidence*) {WGIII SPM C.4.6}

3.3.4 Overshoot Pathways: Increased Risks and Other Implications

Exceeding a specific remaining carbon budget results in higher global warming. Achieving and sustaining net negative global CO_2 emissions could reverse the resulting temperature exceedance (*high confidence*). Continued reductions in emissions of short-lived climate forcers, particularly methane, after peak temperature has been reached, would also further reduce warming (*high confidence*). Only a small number of the most ambitious global modelled pathways limit global warming to 1.5°C (>50%) without overshoot. {WGI SPM D.1.1, WGI SPM D.1.6, WGI SPM D.1.7; WGIII TS.4.2}

Overshoot of a warming level results in more adverse impacts, some irreversible, and additional risks for human and natural systems compared to staying below that warming level, with risks growing with the magnitude and duration of overshoot (*high confidence*). Compared to pathways without overshoot, societies and ecosystems would be exposed to greater and more widespread changes in climatic impact-drivers, such as extreme heat and extreme precipitation, with increasing risks to infrastructure, low-lying coastal settlements, and associated livelihoods *(high confidence*). Overshooting 1.5°C will result in irreversible adverse impacts on certain ecosystems with low resilience, such as polar, mountain, and coastal ecosystems, impacted by ice-sheet glacier melt, or by accelerating and higher committed sea level rise (*high confidence*). Overshoot increases the risks of severe impacts, such as increased wildfires, mass mortality of trees, drying of peatlands, thawing of permafrost and weakening natural land carbon sinks; such impacts could increase releases of GHGs making temperature reversal more challenging (*medium confidence*). {WGI SPM C.2, WGI SPM C.2.1, WGI SPM C.2.3; WGII SPM B.6, WGII SPM B.6.1, WGII SPM B.6.2; SR1.5 3.6}

The larger the overshoot, the more net negative CO_2 emissions needed to return to a given warming level (*high confidence*). Reducing global temperature by removing CO_2 would require net negative emissions of 220 $GtCO_2$ (best estimate, with a *likely* range 160-370 $GtCO_2$) for every tenth of a degree (*medium confidence*). Modelled pathways that limit warming to 1.5°C (>50%) with no or limited overshoot reach median values of cumulative net-negative emissions of 220 $GtCO_2$ by 2100, pathways that return warming to 1.5°C (>50%) after high overshoot reach median values of 360 $GtCO_2$ (*high confidence*).[80] More rapid reduction in CO_2 and non-CO_2 emissions, particularly methane, limits peak warming levels and reduces the requirement for net negative CO_2 emissions and CDR, thereby reducing feasibility and sustainability concerns, and social and environmental risks (*high confidence*). {WGI SPM D.1.1; WGIII SPM B.6.4, WGIII SPM C.2, WGIII SPM C.2.2, WGIII Table SPM.2}

3.4 Long-Term Interactions Between Adaptation, Mitigation and Sustainable Development

Mitigation and adaptation can lead to synergies and trade-offs with sustainable development (*high confidence*). Accelerated and equitable mitigation and adaptation bring benefits from avoiding damages from climate change and are critical to achieving sustainable development (*high confidence*). Climate resilient development[81] pathways are progressively constrained by every increment of further warming (*very high confidence*). There is a rapidly closing window of opportunity to secure a liveable and sustainable future for all (*very high confidence*).

3.4.1 Synergies and trade-offs, costs and benefits

Mitigation and adaptation options can lead to synergies and trade-offs with other aspects of sustainable development (see also Section 4.6, Figure 4.4). Synergies and trade-offs depend on the pace and magnitude of changes and the development context including inequalities, with consideration of climate justice. The potential or effectiveness of some adaptation and mitigation options decreases as climate change intensifies (see also Sections 3.2, 3.3.3, 4.5). (*high confidence*) {WGII SPM C.2, WGII Figure SPM.4b; WGIII SPM D.1, WGIII SPM D.1.2, WGIII TS.5.1, WGIII Figure SPM.8; SR1.5 SPM D.3, SR1.5 SPM D.4; SRCCL SPM B.2, SRCCL SPM B.3, SRCCL SPM D.3.2, SRCCL Figure SPM.3}

[80] Limited overshoot refers to exceeding 1.5°C global warming by up to about 0.1°C, high overshoot by 0.1°C-0.3°C, in both cases for up to several decades. {WGIII Box SPM.1}

[81] See Annex I: Glossary.

In the energy sector, transitions to low-emission systems will have multiple co-benefits, including improvements in air quality and health. There are potential synergies between sustainable development and, for instance, energy efficiency and renewable energy. (*high confidence*) {WGIII SPM C.4.2, WGIII SPM D.1.3}

For agriculture, land, and food systems, many land management options and demand-side response options (e.g., dietary choices, reduced post-harvest losses, reduced food waste) can contribute to eradicating poverty and eliminating hunger while promoting good health and wellbeing, clean water and sanitation, and life on land (*medium confidence*). In contrast, certain adaptation options that promote intensification of production, such as irrigation, may have negative effects on sustainability (e.g., for biodiversity, ecosystem services, groundwater depletion, and water quality) (*high confidence*). {WGII TS.D.5.5; WGIII SPM D.10; SRCCL SPM B.2.3}

Reforestation, improved forest management, soil carbon sequestration, peatland restoration and coastal blue carbon management are examples of CDR methods that can enhance biodiversity and ecosystem functions, employment and local livelihoods, depending on context.[82] However, afforestation or production of biomass crops for bioenergy with carbon dioxide capture and storage or biochar can have adverse socio-economic and environmental impacts, including on biodiversity, food and water security, local livelihoods and the rights of Indigenous Peoples, especially if implemented at large scales and where land tenure is insecure. (*high confidence*) {WGII SPM B.5.4, WGII SPM C.2.4; WGIII SPM C.11.2; SR1.5 SPM C.3.4, SR1.5 SPM C.3.5; SRCCL SPM B.3, SRCCL SPM B.7.3, SRCCL Figure SPM.3}

Modelled pathways that assume using resources more efficiently or shift global development towards sustainability include fewer challenges, such as dependence on CDR and pressure on land and biodiversity, and have the most pronounced synergies with respect to sustainable development (*high confidence*). {WGIII SPM C.3.6; SR1.5 SPM D.4.2}

Strengthening climate change mitigation action entails more rapid transitions and higher up-front investments, but brings benefits from avoiding damages from climate change and reduced adaptation costs. The aggregate effects of climate change mitigation on global GDP (excluding damages from climate change and adaptation costs) are small compared to global projected GDP growth. Projected estimates of global aggregate net economic damages and the costs of adaptation generally increase with global warming level. (*high confidence*) {WGII SPM B.4.6, WGII TS.C.10; WGIII SPM C.12.2, WGIII SPM C.12.3}

Cost-benefit analysis remains limited in its ability to represent all damages from climate change, including non-monetary damages, or to capture the heterogeneous nature of damages and the risk of catastrophic damages (*high confidence*). Even without accounting for these factors or for the co-benefits of mitigation, the global benefits of limiting warming to 2°C exceed the cost of mitigation (*medium confidence*). This finding is robust against a wide range of assumptions about social preferences on inequalities and discounting over time (*medium confidence*). Limiting global warming to 1.5°C instead of 2°C would increase the costs of mitigation, but also increase the benefits in terms of reduced impacts and related risks (see 3.1.1, 3.1.2) and reduced adaptation needs (*high confidence*)[83]. {WGII SPM B.4, WGII SPM B.6; WGIII SPM C.12, WGIII SPM C.12.2, WGIII SPM C.12.3 WGIII Box TS.7; SR1.5 SPM B.3, SR1.5 SPM B.5, SR1.5 SPM B.6}

Considering other sustainable development dimensions, such as the potentially strong economic benefits on human health from air quality improvement, may enhance the estimated benefits of mitigation (*medium confidence*). The economic effects of strengthened mitigation action vary across regions and countries, depending notably on economic structure, regional emissions reductions, policy design and level of international cooperation (*high confidence*). Ambitious mitigation pathways imply large and sometimes disruptive changes in economic structure, with implications for near-term actions (Section 4.2), equity (Section 4.4), sustainability (Section 4.6), and finance (Section 4.8) (*high confidence*). {WGIII SPM C.12.2, WGIII SPM D.3.2, WGIII TS.4.2}

[82] The impacts, risks, and co-benefits of CDR deployment for ecosystems, biodiversity and people will be highly variable depending on the method, site-specific context, implementation and scale (*high confidence*). {WGIII SPM C.11.2}
[83] The evidence is too limited to make a similar robust conclusion for limiting warming to 1.5°C. {WGIII SPM FOOTNOTE 68}

3.4.2 Advancing Integrated Climate Action for Sustainable Development

An inclusive, equitable approach to integrating adaptation, mitigation and development can advance sustainable development in the long term *(high confidence)*. Integrated responses can harness synergies for sustainable development and reduce trade-offs (*high confidence*)}. Shifting development pathways towards sustainability and advancing climate resilient development is enabled when governments, civil society and the private sector make development choices that prioritise risk reduction, equity and justice, and when decision-making processes, finance and actions are integrated across governance levels, sectors and timeframes (*very high confidence*) (see also Figure 4.2). Inclusive processes involving local knowledge and Indigenous Knowledge increase these prospects (*high confidence*). However, opportunities for action differ substantially among and within regions, driven by historical and ongoing patterns of development (*very high confidence*). Accelerated financial support for developing countries is critical to enhance mitigation and adaptation action (*high confidence*). {WGII SPM C.5.4, WGII SPM D.1, WGII SPM D.1.1, WGII SPM D.1.2, WGII SPM D.2, WGII SPM D.3, WGII SPM D.5, WGII SPM D.5.1, WGII SPM D.5.2; WGIII SPM D.1, WGIII SPM D.2, WGIII SPM D.2.4, WGIII SPM E.2.2, WGIII SPM E.2.3, WGIII SPM E.5.3, WGIII Cross-Chapter Box 5}

Policies that shift development pathways towards sustainability can broaden the portfolio of available mitigation and adaptation responses (*medium confidence*). Combining mitigation with action to shift development pathways, such as broader sectoral policies, approaches that induce lifestyle or behaviour changes, financial regulation, or macroeconomic policies can overcome barriers and open up a broader range of mitigation options (*high confidence*). Integrated, inclusive planning and investment in everyday decision-making about urban infrastructure can significantly increase the adaptive capacity of urban and rural settlements. Coastal cities and settlements play an important role in advancing climate resilient development due to the high number of people living in the Low Elevation Coastal Zone, the escalating and climate compounded risk that they face, and their vital role in national economies and beyond (*high confidence*). {WGII SPM.D.3, WGII SPM D.3.3; WGIII SPM E.2, WGIII SPM E.2.2; SR1.5 SPM D.6}

Observed adverse impacts and related losses and damages, projected risks, trends in vulnerability, and adaptation limits demonstrate that transformation for sustainability and climate resilient development action is more urgent than previously assessed (*very high confidence*). Climate resilient development integrates adaptation and GHG mitigation to advance sustainable development for all. Climate resilient development pathways have been constrained by past development, emissions and climate change and are progressively constrained by every increment of warming, in particular beyond 1.5°C (*very high confidence*). Climate resilient development will not be possible in some regions and sub-regions if global warming exceeds 2°C (*medium confidence*). Safeguarding biodiversity and ecosystems is fundamental to climate resilient development, but biodiversity and ecosystem services have limited capacity to adapt to increasing global warming levels, making climate resilient development progressively harder to achieve beyond 1.5°C warming (*very high confidence*). {WGII SPM D.1, WGII SPM D.1.1, WGII SPM D.4, WGII SPM D.4.3, WGII SPM D.5.1; WGIII SPM D.1.1}

The cumulative scientific evidence is unequivocal: climate change is a threat to human well-being and planetary health (*very high confidence*). Any further delay in concerted anticipatory global action on adaptation and mitigation will miss a brief and rapidly closing window of opportunity to secure a liveable and sustainable future for all (*very high confidence*). Opportunities for near-term action are assessed in the following section. {WGII SPM D.5.3; WGIII SPM D.1.1}

Section 4: Near-Term Responses in a Changing Climate

4.1 The Timing and Urgency of Climate Action

Deep, rapid and sustained mitigation and accelerated implementation of adaptation reduces the risks of climate change for humans and ecosystems. In modelled pathways that limit warming to 1.5°C (>50%) with no or limited overshoot and in those that limit warming to 2°C (>67%) and assume immediate action, global GHG emissions are projected to peak in the early 2020s followed by rapid and deep reductions. As adaptation options often have long implementation times, accelerated implementation of adaptation, particularly in this decade, is important to close adaptation gaps. (*high confidence*)

The magnitude and rate of climate change and associated risks depend strongly on near-term mitigation and adaptation actions (*very high confidence*). Global warming is *more likely than not* to reach 1.5°C between 2021 and 2040 even under the very low GHG emission scenarios (SSP1-1.9), and *likely* or *very likely* to exceed 1.5°C under higher emissions scenarios[84]. Many adaptation options have medium or high feasibility up to 1.5°C (*medium to high confidence*, depending on option), but hard limits to adaptation have already been reached in some ecosystems and the effectiveness of adaptation to reduce climate risk will decrease with increasing warming (*high confidence*). Societal choices and actions implemented in this decade determine the extent to which medium- and long-term pathways will deliver higher or lower climate resilient development (*high confidence*). Climate resilient development prospects are increasingly limited if current greenhouse gas emissions do not rapidly decline, especially if 1.5°C global warming is exceeded in the near-term (*high confidence*). Without urgent, effective and equitable adaptation and mitigation actions, climate change increasingly threatens the health and livelihoods of people around the globe, ecosystem health, and biodiversity, with severe adverse consequences for current and future generations (*high confidence*). {WGI SPM B.1.3, WGI SPM B.5.1, WGI SPM B.5.2; WGII SPM A, WGII SPM B.4, WGII SPM C.2, WGII SPM C.3.3, WGII Figure SPM.4, WGII SPM D.1, WGII SPM D.5, WGIII SPM D.1.1 SR1.5 SPM D.2.2}. (Cross-Section Box.2, Figure 2.1, Figure 2.3)

In modelled pathways that limit warming to 1.5°C (>50%) with no or limited overshoot and in those that limit warming to 2°C (>67%), assuming immediate actions, global GHG emissions are projected to peak in the early 2020s followed by rapid and deep GHG emissions reductions (*high confidence*) [85]. In pathways that limit warming to 1.5°C (>50%) with no or limited overshoot, net global GHG emissions are projected to fall by 43% [34–60%][86] below 2019 levels by 2030,60% [49–77%] by 2035, 69% [58-90%] by 2040 and 84% [73-98%] (*high confidence*) (Section 2.3.1, Table 2.2, Figure 2.5, Table 3.1)[87]. Global modelled pathways that limit warming to 2°C (>67%) have reductions in GHG emissions below 2019 levels of 21% [1–42]% by 2030, 35% [22–55%] by 2035, 46% [34-63%] by 2040 and 64% [53-77%] by 2050 [88](*high confidence*). Global GHG emissions associated with NDCs announced prior to COP26 would make it *likely* that warming would exceed 1.5°C (*high confidence*) and limiting warming to 2°C (>67%) would then imply a rapid acceleration of emission reductions during 2030–2050, around 70% faster than in pathways where immediate action is taken to limit warming to 2°C (>67%) (*medium confidence*) (Section 2.3.1) Continued investments in unabated high-emitting infrastructure[89] and limited development and deployment of low-emitting alternatives prior to 2030 would act as barriers to this acceleration and increase feasibility risks (*high confidence*). {WGIII SPM B.6.3, WGIII Chapter 3.5.2, WGIII SPM B.6, WGIII SPM B.6., WGIII SPM C.1, WGIII SPM C1.1, Table SPM.2} (Cross-Section Box.2)

---

[84]In the near term (2021–2040), the 1.5°C global warming level is *very likely* to be exceeded under the very high GHG emissions scenario (SSP5-8.5), *likely* to be exceeded under the intermediate and high GHG emissions scenarios (SSP2-4.5, SSP3-7.0), *more likely than not* to be exceeded under the low GHG emissions scenario (SSP1-2.6) and *more likely than not* to be reached under the very low GHG emissions scenario (SSP1-1.9). The best estimates [and *very likely* ranges] of global warming for the different scenarios in the near-term are: 1.5°C [1.2°C–1.7°C] (SSP1-1.9); 1.5°C [1.2°C–1.8°C] (SSP1-2.6); 1.5°C [1.2°C–1.8°C] (SSP2-4.5); 1.5°C [1.2°C–1.8°C] (SSP3-7.0); and 1.6°C [1.3°C–1.9°C] (SSP5-8.5). {WGI SPM B.1.3, WGI Table SPM.1} (Cross-Section Box.2)

[85] Values in parentheses indicate the likelihood of limiting warming to the level specified (see Cross-Section Box.2).

[86] Median and *very likely* range [5th to 95th percentile] {WGIII SPM footnote 30}.

[87] These numbers for CO2 are 48% [36-69] in 2030, 65% [50-96%] in 2035, 80% [61-109%] in 2040 and 99 [79-119%] in 2050.

[88] These numbers for CO2 are 22% [1-44] in 2030, 37% [21-59%] in 2035, 51% [36-70%] in 2040 and 73 [55-90%] in 2050

[89] In this context, 'unabated fossil fuels' refers to fossil fuels produced and used without interventions that substantially reduce the amount of GHG emitted throughout the life cycle; for example, capturing 90% or more CO_2 from power plants, or 50–80% of fugitive methane emissions from energy supply {WGIII SPM footnote 54}.

All global modelled pathways that limit warming to 2°C (>67%) or lower by 2100 involve reductions in both net CO_2 emissions and non-CO_2 emissions (see Figure 3.6) (*high confidence*). For example, in pathways that limit warming to 1.5°C (>50%) with no or limited overshoot, global CH_4 (methane) emissions are reduced by 34% [21–57%] below 2019 levels by 2030 and by 44% [31–63%] in 2040 (*high confidence*). Global CH_4 emissions are reduced by 24% [9–53%] below 2019 levels by 2030 and by 37% [20–60%] in 2040 in modelled pathways that limit warming to 2°C with action starting in 2020 (>67%) (*high confidence*). {WGIII SPM C1.2, WGIII Table SPM.2, WGIII Chapter 3.3; SR1.5 SPM C.1, SR1.5 SPM C.1.2} (Cross-Section Box.2)

All global modelled pathways that limit warming to 2°C (>67%) or lower by 2100 involve GHG emission reductions in all sectors (*high confidence*). The contributions of different sectors vary across modelled mitigation pathways. In most global modelled mitigation pathways, emissions from land-use, land-use change and forestry, via reforestation and reduced deforestation, and from the energy supply sector reach net zero CO_2 emissions earlier than the buildings, industry and transport sectors (Figure 4.1). Strategies can rely on combinations of different options (Figure 4.1, Section 4.5), but doing less in one sector needs to be compensated by further reductions in other sectors if warming is to be limited. (*high confidence*) {WGIII SPM C.3, WGIII SPM C.3.1, WGIII SPM 3.2, WGIII SPM C.3.3} (Cross-Section Box.2)

Without rapid, deep and sustained mitigation and accelerated adaptation actions, losses and damages will continue to increase, including projected adverse impacts in Africa, LDCs, SIDS, Central and South America[90], Asia and the Arctic, and will disproportionately affect the most vulnerable populations (*high confidence*). {WGII SPM C.3.5; WGII SPM B.2.4; WGII Global to Regional Atlas Annex A1.15, A1.27; WGII 12.2; WGII 10. Box 10.6; WGII TS D.7.5; WGII CCB6 ES; SR1.5 SPM B.5.3; SR 1.5 SPM B.5.7; SRCCL A.5.6} (Figure 3.2; Figure 3.3)

[START FIGURE 4.1 HERE]

[90] The southern part of Mexico is included in the climatic subregion South Central America (SCA) for WGI. Mexico is assessed as part of North America for WGII. The climate change literature for the SCA region occasionally includes Mexico, and in those cases WGII assessment makes reference to Latin America. Mexico is considered part of Latin America and the Caribbean for WGIII. {WGII 12.1.1, WGIII AII.1.1}

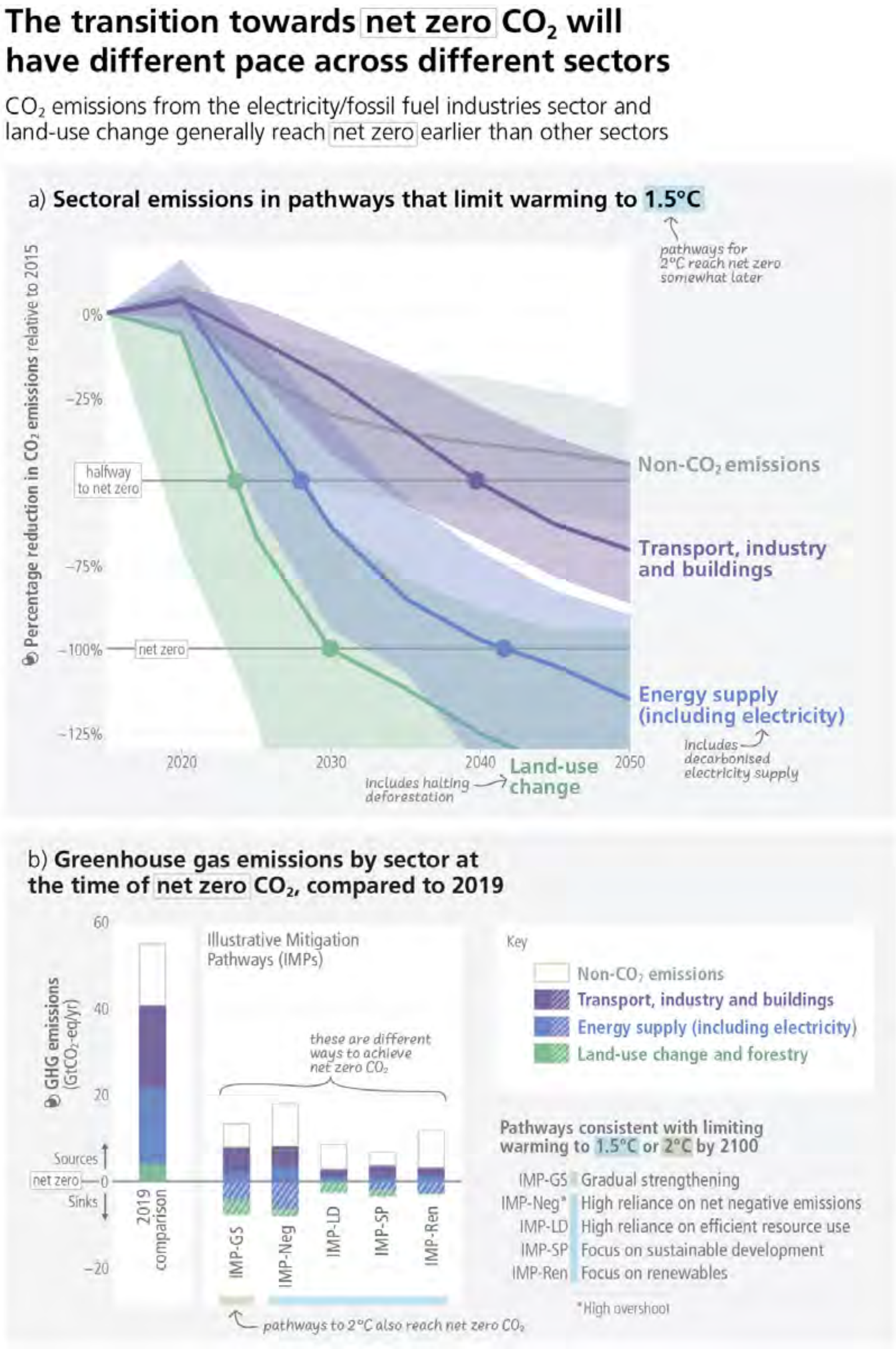

Figure 4.1: Sectoral emissions in pathways that limit warming to 1.5°C. Panel (a) shows sectoral CO_2 and non-CO_2 emissions in global modelled pathways that limit warming to 1.5°C (>50%) with no or limited overshoot. The horizontal lines illustrate halving 2015 emissions (base year of the pathways) (dashed) and reaching net-zero emissions (solid line). The range shows the 5–95th percentile of the emissions across the pathways. The timing strongly differs by sector, with the CO_2 emissions from the electricity/fossil fuel industries sector and land-use change generally reaching net zero earlier. Non-CO_2 emissions from agriculture are also substantially reduced compared to pathways without climate policy but do not typically reach zero. **Panel (b)** Although all pathways include strongly reduced emissions, there are different pathways as indicated by the illustrative mitigation pathways used in IPCC WGIII. The pathways emphasise routes consistent with limiting warming to 1.5°C with a high reliance on net negative emissions (IMP-Neg), high resource efficiency (IMP-LD), a focus on sustainable development (IMP-SP) or renewables (IMP-Ren) and consistent with 2°C

based on a less rapid introduction of mitigation measures followed by a subsequent gradual strengthening (IMP-GS). Positive (solid filled bars) and negative emissions (hatched bars) for different illustrative mitigation pathways are compared to GHG emissions from the year 2019. The category "energy supply (including electricity)" includes bioenergy with carbon capture and storage and direct air carbon capture and storage. {WGIII Box TS.5, 3.3, 3.4, 6.6, 10.3, 11.3} (Cross-Section Box 2)

[END FIGURE 4.1 HERE]

4.2 Benefits of Strengthening Near-Term Action

Accelerated implementation of adaptation will improve well-being by reducing losses and damages, especially for vulnerable populations. Deep, rapid and sustained mitigation actions would reduce future adaptation costs and losses and damages, enhance sustainable development co-benefits, avoid locking-in emission sources, and reduce stranded assets and irreversible climate changes. These near-term actions involve higher up-front investments and disruptive changes, which can be moderated by a range of enabling conditions and removal or reduction of barriers to feasibility. *(high confidence)*

Accelerated implementation of adaptation responses will bring benefits to human well-being (*high confidence*) (Section 4.3). As adaptation options often have long implementation times, long-term planning and accelerated implementation, particularly in this decade, is important to close adaptation gaps, recognising that constraints remain for some regions. The benefits to vulnerable populations would be high (see Section 4.4). (*high confidence)* {WGI SPM B.1, WGI SPM B.1.3, WGI SPM B.2.2, WGI SPM B.3; WGII SPM C.1.1, WGII SPM C.1.2, WGII SPM C.2, WGII SPM C.3.1, WGII SPM Figure SPM.4b; SROCC SPM C.3.4, SROCC Figure 3.4, SROCC SPM Figure 5}

Near-term actions that limit global warming to close to 1.5°C would substantially reduce projected losses and damages related to climate change in human systems and ecosystems, compared to higher warming levels, but cannot eliminate them all (*very high confidence*). The magnitude and rate of climate change and associated risks depend strongly on near-term mitigation and adaptation actions, and projected adverse impacts and related losses and damages escalate with every increment of global warming (*very high confidence*). Delayed mitigation action will further increase global warming which will decrease the effectiveness of many adaptation options, including Ecosystem-based Adaptation and many water-related options, as well as increasing mitigation feasibility risks, such as for options based on ecosystems (*high confidence*). Comprehensive, effective, and innovative responses integrating adaptation and mitigation can harness synergies and reduce trade-offs between adaptation and mitigation, as well as in meeting requirements for financing (*very high confidence*) (see Section 4.5, 4.6, 4.8 and 4.9) {WGII SPM B.3, WGII SPM B.4, WGII SPM B.6.2, WGII SPM C.2, WGII SPM C.3, WGII SPM D.1, WGII SPM D.4.3, WGII SPM D.5, WG II TS D.1.4, WG II TS.D.5, WGII TS D.7.5, WGIII SPM B.6.3,WGIII SPM B.6.4, WGIII SPM C.9, WGIII SPM D.2, WGIII SPM E.13, SR1.5 SPM C.2.7, SR1.5 D.1.3, SR1.5 D.5.2}.

Mitigation actions will have other sustainable development co-benefits (*high confidence*). Mitigation will improve air quality and human health in the near-term notably because many air pollutants are co-emitted by GHG emitting sectors and because methane emissions leads to surface ozone formation (*high confidence*) The benefits from air quality improvement include prevention of air pollution-related premature deaths, chronic diseases and damages to ecosystems and crops. The economic benefits for human health from air quality improvement arising from mitigation action can be of the same order of magnitude as mitigation costs, and potentially even larger (*medium confidence*). As methane has a short lifetime but is a potent GHG, strong, rapid and sustained reductions in methane emissions can limit near-term warming and improve air quality by reducing global surface ozone (*high confidence*). {WGI SPM D.1.7, WGI SPM D.2.2, WGI Chapter 6.7, WGI TS Box TS.7, WGI Chapter 6 Box 6.2, WGI Figures 6.3, 6.16, 6.17, WGII TS.D.8.3, WGII Cross-Chapter Box HEALTH, WGII Chapter 5 ES, WGII Chapter 7 ES; WGII Chapter 7.3.1.2; WGIII Figure SPM.8, WGIII SPM C.2.3, WGIII SPM C.4.2, WGIII TS.4.2}

Challenges from delayed adaptation and mitigation actions include the risk of cost escalation, lock-in of infrastructure, stranded assets, and reduced feasibility and effectiveness of adaptation and mitigation options (*high confidence*). The continued installation of unabated fossil fuel[91] infrastructure will 'lock-in' GHG emissions (*high confidence*). Limiting global warming to 2°C or below will leave a substantial amount of fossil fuels unburned and could strand considerable fossil fuel infrastructure (*high confidence*), with globally discounted value projected to be around USD1–4 trillion from 2015 to 2050 (*medium confidence*). Early actions would limit the size of these stranded assets, whereas delayed actions with continued investments in unabated high-emitting infrastructure and limited development and deployment of low-emitting alternatives prior to 2030 would raise future stranded assets to the higher end of the range – acting as barriers and increase political economy feasibility risks that may jeopardise efforts to limit global warming (*high confidence*). {WGIII SPM B.6.3, WGIII SPM C.4, WGIII Box TS.8}.

Scaling-up near-term climate actions (Section 4.1) will mobilise a mix of low-cost and high-cost options. High-cost options, as in energy and infrastructure, are needed to avoid future lock-ins, foster innovation and initiate transformational changes (Figure 4.4). Climate resilient development pathways in support of sustainable development for all are shaped by equity, and social and climate justice (*very high confidence*). Embedding effective and equitable adaptation and mitigation in development planning can reduce vulnerability, conserve and restore ecosystems, and enable climate resilient development. This is especially challenging in localities with persistent development gaps and limited resources. (*high confidence*) {WGII SPM C.5, WGII SPM D1; WGIII TS.5.2, WGIII Section 8.3.1, WGIII Section 8.3.4, WGIII Section 8.4.1, WGIII Section 8.6}.

Scaling-up climate action may generate disruptive changes in economic structure with distributional consequences and need to reconcile divergent interests, values and worldviews, within and between countries. Deeper fiscal, financial, institutional and regulatory reforms can offset such adverse effects and unlock mitigation potentials. Societal choices and actions implemented in this decade will determine the extent to which medium and long-term development pathways will deliver higher or lower climate resilient development outcomes. (*high confidence*) {WGII SPM D.2, WGII SPM D.5, WGII Box TS.8; WGIII SPM D.3, WGIII SPM E.2, WGIII SPM E.3, WGIII SPM E.4, WGIII TS.2, WGIII TS.4.1, WGIII TS.6.4, WGIII Chapter 15.2, WGIII Chapter 15.6,}

Enabling conditions would need to be strengthened in the near-term and barriers reduced or removed to realise opportunities for deep and rapid adaptation and mitigation actions and climate resilient development *(high confidence)* (Figure 4.2). These enabling conditions are differentiated by national, regional and local circumstances and geographies, according to capabilities, and include: equity and and inclusion in climate action (see Section 4.4), rapid and far-reaching transitions in sectors and system (see Section 4.5), measures to achieve synergies and reduce trade-offs with sustainable development goals (see Section 4.6), governance and policy improvements (see Section 4.7), access to finance, improved international cooperation and technology improvements (see Section 4.8), and integration of near-term actions across sectors, systems and regions (see Section 4.9). {WGII SPM D.2, WGIII SPM E.1, WGIII SPM E.2}

Barriers to feasibility would need to be reduced or removed to deploy mitigation and adaptation options at scale. Many limits to feasibility and effectiveness of responses can be overcome by addressing a range of barriers, including economic, technological, institutional, social, environmental and geophysical. The feasibility and effectiveness of options increase with integrated, multi-sectoral solutions that differentiate responses based on climate risk, cut across systems and address social inequities. Strengthened near-term actions in modelled cost-effective pathways that limit global warming to 2°C or lower, reduce the overall risk to the feasibility of the system transitions, compared to modelled pathways with delayed or uncoordinated action. (*high confidence*) {WGII SPM C.2, WGII SPM C.3, WGII SPM C.5; WGIII SPM E.1, WGIII SPM E.1.3}.

[91] In this context, 'unabated fossil fuels' refers to fossil fuels produced and used without interventions that substantially reduce the amount of GHG emitted throughout the life cycle; for example, capturing 90% or more CO_2 from power plants, or 50–80% of fugitive methane emissions from energy supply {WGIII SPM footnote 54}.

[START FIGURE 4.2 HERE]

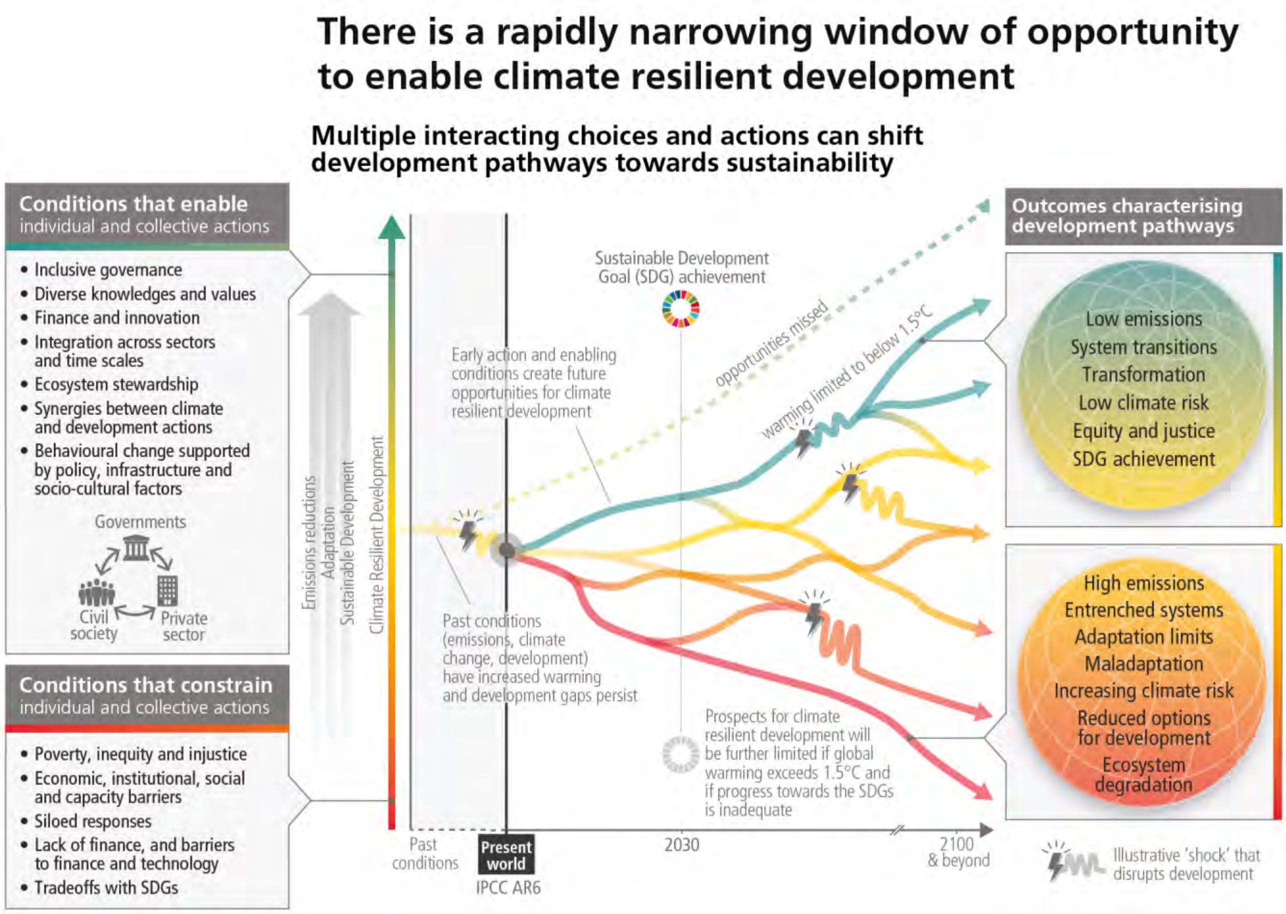

Figure 4.2: The illustrative development pathways (red to green) and associated outcomes (right panel) show that there is a rapidly narrowing window of opportunity to secure a liveable and sustainable future for all. Climate resilient development is the process of implementing greenhouse gas mitigation and adaptation measures to support sustainable development. Diverging pathways illustrate that interacting choices and actions made by diverse government, private sector and civil society actors can advance climate resilient development, shift pathways towards sustainability, and enable lower emissions and adaptation. Diverse knowledges and values include cultural values, Indigenous Knowledge, local knowledge, and scientific knowledge. Climatic and non-climatic events, such as droughts, floods or pandemics, pose more severe shocks to pathways with lower climate resilient development (red to yellow) than to pathways with higher climate resilient development (green). There are limits to adaptation and adaptive capacity for some human and natural systems at global warming of 1.5°C, and with every increment of warming, losses and damages will increase. The development pathways taken by countries at all stages of economic development impact GHG emissions and hence shape mitigation challenges and opportunities, which vary across countries and regions. Pathways and opportunities for action are shaped by previous actions (or inactions and opportunities missed, dashed pathway), and enabling and constraining conditions (left panel), and take place in the context of climate risks, adaptation limits and development gaps. The longer emissions reductions are delayed, the fewer effective adaptation options. {WGI SPM B.1, WGII SPM B.1-B.5, WGII SPM C.2-5, WGII SPM D.1-5, WGII Figure SPM.3; WGII Figure SPM.4, WGII Figure SPM.5; WGII TS.D.5, WGII Chapter 3.1, WGII Chapter 3.2, WGII Chapter 3.4; WGII Chapter 4.2, WGII Figure 4.4, WGII Chapter 4.5, WGII Chapter 4.6, WGII Chapter 4.9, WGIII SPM A, WGIII SPM B1, WGIII SPM B.3, WGIII SPM B.6, WGIII SPM C.4, WGIII SPM D1-3, WGIII SPM E.1, WGIII SPM E.2, WGIII SPM E.4, WGIII SPM E.5, WGIII FigureTS.1, TS.7, Box TS. 3, Box TS.8, Cross-Working Group Box 1, WGIII Cross-Chapter Box 5 in Chapter 4, SR1.5 SPM D1-6, SRCCL SPM D.3}

[END FIGURE 4.2 HERE]

Integrating ambitious climate actions with macroeconomic policies under global uncertainty would provide benefits (*high confidence*). This encompasses three main directions: (a) economy-wide mainstreaming packages supporting options to improved sustainable low-emission economic recovery, development and job creation programs (Sections 4.4, 4.5, 4.6, 4.8, 4.9) (b) safety nets and social protection in the transition (Section 4.4, 4.7); and (c) broadened access to finance, technology and capacity-building and coordinated support to low-emission infrastructure ('leap-frog' potential), especially in developing regions, and under debt stress (*high confidence*). (Section 4.8) {WGII SPM C.2, WGII SPM C.4.1, WGII SPM D.1.3, WGII SPM D.2, WGII SPM D.3.2, WGII SPM E.2.2, WGII SPM E.4, WGII SPM TS.2, WGII SPM TS.5.2, WGII TS.6.4, WGII TS.15, WGII TS Box TS.3 WGIII SPM B.4.2, WGIII SPM C.5.4, WGIII SPM C.6.2, WGIII SPM C.12.2, WGIII SPM D.3.4, WGIII SPM E.4.2, WGIII SPM E.4.5, WGIII SPM E.5.2, WGIII SPM E.5.3, WGIII TS.1, WGIII Box TS.15, WGIII Chapter 15.2, WGIII Cross-Chapter Box 1 on COVID in Chapter 1}

4.3 Near-Term Risks

Many changes in the climate system, including extreme events, will become larger in the near term with increasing global warming (*high confidence*). Multiple climatic and non-climatic risks will interact, resulting in increased compounding and cascading impacts becoming more difficult to manage (*high confidence*). Losses and damages will increase with increasing global warming (*very high confidence*), while strongly concentrated among the poorest vulnerable populations (*high confidence*). Continuing with current unsustainable development patterns would increase exposure and vulnerability of ecosystems and people to climate hazards (*high confidence*).

Global warming will continue to increase in the near term (2021–2040) mainly due to increased cumulative CO_2 emissions in nearly all considered scenarios and pathways. In the near term, every region in the world is projected to face further increases in climate hazards (*medium to high confidence*, depending on region and hazard), increasing multiple risks to ecosystems and humans (*very high confidence*). In the near-term, natural variability[92] will modulate human-caused changes, either attenuating or amplifying projected changes, especially at regional scales, with little effect on centennial global warming. Those modulations are important to consider in adaptation planning. Global surface temperature in any single year can vary above or below the long-term human-induced trend, due to natural variability. By 2030, global surface temperature in any individual year could exceed 1.5oC relative to 1850–1900 with a probability between 40% and 60%, across the five scenarios assessed in WGI (medium confidence). The occurrence of individual years with global surface temperature change above a certain level does not imply that this global warming level has been reached. If a large explosive volcanic eruption were to occur in the near-term[93] , it would temporarily and partially mask human-caused climate change by reducing global surface temperature and precipitation, especially over land, for one to three years (*medium confidence*). {WGI SPM B.1.3, WGI SPM B.1.4, WGI SPM C.1, WGI SPM C.2, WGI Cross-Section Box TS.1, WGI Cross-Chapter Box 4.1; WGII SPM B.3, WGII SPM B.3.1; WGIII Box SPM.1 Figure 1}.

The level of risk for humans and ecosystems will depend on near-term trends in vulnerability, exposure, level of socio-economic development and adaptation (*high confidence*). In the near-term, many climate-associated risks to natural and human systems depend more strongly on changes in these systems' vulnerability and exposure than on differences in climate hazards between emissions scenarios (*high confidence*). Future exposure to climatic hazards is increasing globally due to socio-economic development trends including growing inequality, and when urbanisation or migration increase exposure (*high confidence*). Urbanisation increases hot extremes (*very high confidence*) and precipitation runoff intensity (*high confidence*). Increasing urbanisation in low-lying and coastal zones will be a major driver of increasing exposure to extreme riverflow events and sea level rise hazards, increasing risks (*high confidence*) (Figure 4.3). Vulnerability will also rise rapidly in low-lying Small Island Developing States and atolls in the context of sea level rise (*high confidence*) (see Figure 3.4 and Figure 4.3). Human vulnerability will concentrate in informal settlements and rapidly growing smaller settlements; and vulnerability in rural areas will be heightened by reduced habitability and

[92] See Annex I: Glossary. The main internal variability phenomena include El Niño–Southern Oscillation, Pacific Decadal Variability and Atlantic Multi-decadal Variability through their regional influence {WGI SPM footnote 37}. The internal variability of global surface temperature in any single year is estimated to be about ±0.25°C (5–95% range, *high confidence)* {WGI SPM footnote 29}.
[93] Based on 2500-year reconstructions, eruptions with a radiative forcing more negative than -1 Wm^{-2}, related to the radiative effect of volcanic stratospheric aerosols in the literature assessed in this report, occur on average twice per century. {WGI SPM footnote 38}

high reliance on climate-sensitive livelihoods (*high confidence*). Human and ecosystem vulnerability are interdependent (*high confidence*). Vulnerability to climate change for ecosystems will be strongly influenced by past, present, and future patterns of human development, including from unsustainable consumption and production, increasing demographic pressures, and persistent unsustainable use and management of land, ocean, and water (*high confidence*). Several near-term risks can be moderated with adaptation (*high confidence*). (see Section 4.5 and 3.2) {WGI SPM C.2.6; WGII SPM B.2, WGII SPM B.2.3, WGII SPM B.2.5, WGII SPM B.3, WGII SPM B.3.2, WGII TS.C.5.2}

Principal hazards and associated risks expected in the near-term (at 1.5°C global warming) are:

- Increased intensity and frequency of hot extremes and dangerous heat-humidity conditions, with increased human mortality, morbidity, and labour productivity loss (*high confidence*) {WGI SPM B.2.2, WGI TS Figure TS.6; WGII SPM B.1.4, WGII SPM B.4.4, WGII SPM Figure SPM.2}.
- Increasing frequency of marine heatwaves will increase risks of biodiversity loss in the oceans, including from mass mortality events (*high confidence*) {WGI SPM B.2.3; WGII SPM B.1.2, WGII SPM Figure SPM.2; SROCC SPM B.5.1}
- Near-term risks for biodiversity loss are moderate to high in forest ecosystems (*medium confidence*) and kelp and seagrass ecosystems (*high to very high confidence*) and are high to very high in Arctic sea-ice and terrestrial ecosystems (*high confidence*) and warm-water coral reefs (*very high confidence*) {WGII SPM B.3.1}.
- More intense and frequent extreme rainfall and associated flooding in many regions including coastal and other low-lying cities (*medium to high confidence*), and increased proportion of and peak wind speeds of intense tropical cyclones (*high confidence*) {WGI SPM B.2.4, WGI SPM C.2.2, WGI SPM C.2.6, WGI Chapter 11.7}.
- High risks from dryland water scarcity, wildfire damage, and permafrost degradation (*medium confidence*) {SRCCL SPM A.5.3.}.
- Continued sea level rise and increased frequency and magnitude of extreme sea level events encroaching on coastal human settlements and damaging coastal infrastructure (*high confidence)*, committing low-lying coastal ecosystems to submergence and loss (*medium confidence*), expanding land salinization (*very high confidence*), with cascading to risks to livelihoods, health, well-being, cultural values, food and water security (*high confidence*) (Figure 3.4, 4.3). {WGI SPM C.2.5, WGI SPM C.2.6; WGII SPM B.3.1, WGII SPM B.5.2; SRCCL SPM A.5.6; SROCC SPM B.3.4, SROCC SPM 3.6, SROCC SPM B.9.1}.
- Climate change will significantly increase ill health and premature deaths from the near- to long-term (*high confidence*). Further warming will increase climate-sensitive food-borne, water-borne, and vector-borne disease risks (*high confidence*), and mental health challenges including anxiety and stress (*very high confidence*). {WGII SPM B.4.4}
- Cryosphere-related changes in floods, landslides, and water availability have the potential to lead to severe consequences for people, infrastructure and the economy in most mountain regions (high confidence). {WGII TS C.4.2}
- The projected increase in frequency and intensity of heavy precipitation (high confidence) will increase rain-generated local flooding (medium confidence). {WGI Figure SPM.6; WGI SPM B.2.2; WGII TS C.4.5}

Multiple climate change risks will increasingly compound and cascade in the near term (*high confidence*). Many regions are projected to experience an increase in the probability of compound events with higher global warming (*high confidence*) including concurrent heatwaves and drought. Risks to health and food production will be made more severe from the interaction of sudden food production losses from heat and drought, exacerbated by heat-induced labour productivity losses (*high confidence*) (Figure 4.3). These interacting impacts will increase food prices, reduce household incomes, and lead to health risks of malnutrition and climate-related mortality with no or low levels of adaptation, especially in tropical regions (*high confidence*). Concurrent and cascading risks from climate change to food systems, human settlements, infrastructure and health will make these risks more severe and more difficult to manage, including when interacting with non-climatic risk drivers such as competition for land between urban expansion and food production, and pandemics (*high confidence*). Loss of ecosystems and their services has cascading and long-term impacts on people globally, especially for Indigenous Peoples and local communities who are directly dependent on ecosystems, to meet basic needs (*high confidence*). Increasing transboundary risks are projected across the food, energy and water sectors as impacts from weather and climate extremes propagate through supply-chains, markets, and natural resource flows (*high confidence*) and may interact with impacts from other crises such as pandemics. Risks also arise from some responses intended to reduce the risks of climate change, including risks from maladaptation and adverse side effects of some emissions reduction and carbon dioxide removal measures, such as afforestation of naturally unforested land or poorly implemented bioenergy compounding climate-related risks to biodiversity, food and water security, and livelihoods (*high confidence*). (see Section 3.4.1 and 4.5) {WGI SPM.2.7; WGII SPM B.2.1, WGII SPM B.5, WGII SPM B.5.1, WGII SPM B.5.2, WGII SPM B.5.3, WGII SPM B.5.4, WGII Cross-Chapter Box COVID in Chapter 7; WGIII SPM C.11.2; SRCCL SPM A.5, SRCCL SPM A.6.5} (Figure 4.3)

With every increment of global warming losses and damages will increase (*very high confidence*), become increasingly difficult to avoid and be strongly concentrated among the poorest vulnerable populations (*high confidence*). Adaptation does not prevent all losses and damages, even with effective adaptation and before reaching soft and hard limits. Losses and damages will be unequally distributed across systems, regions and sectors and are not comprehensively addressed by current financial, governance and institutional arrangements, particularly in vulnerable developing countries. *(high confidence).* {WGII SPM B.4, WGII SPM C.3, WGII SPM C.3.5}

[START FIGURE 4.3 HERE]

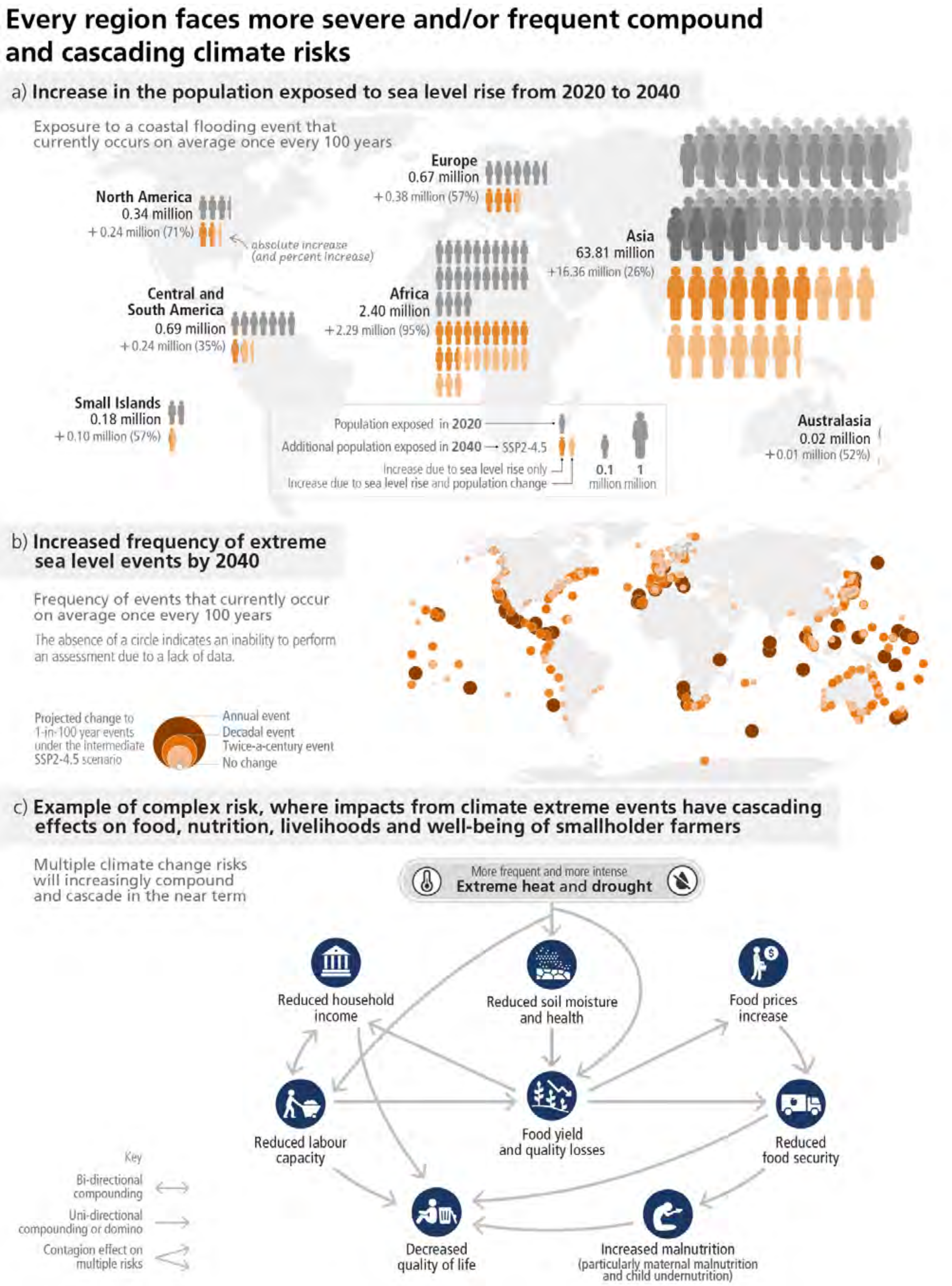

Figure 4.3: Every region faces more severe or frequent compound and/or cascading climate risks in the near term. Changes in risk result from changes in the degree of the hazard, the population exposed, and the degree of vulnerability of people, assets, or ecosystems. **Panel (a)** Coastal flooding events affect many of the highly populated regions of the world where large percentages of the population are exposed. The panel shows near-term projected increase of population exposed to 100-year flooding events depicted as the increase from the year 2020 to 2040 (due to sea level rise and

population change), based on the intermediate GHG emissions scenario (SSP2-4.5) and current adaptation measures. Out-migration from coastal areas due to future sea level rise is not considered in the scenario. **Panel (b)** projected median probability in the year 2040 for extreme water levels resulting from a combination of mean sea level rise, tides and storm surges, which have a historical 1% average annual probability. A peak-over-threshold (99.7%) method was applied to the historical tide gauge observations available in the Global Extreme Sea Level Analysis version 2 database, which is the same information as WGI Figure 9.32, except here the panel uses relative sea level projections under SSP2-4.5 for the year 2040 instead of 2050 The absence of a circle indicates an inability to perform an assessment due to a lack of data, but does not indicate absence of increasing frequencies.
Panel (c) Climate hazards can initiate risk cascades that affect multiple sectors and propagate across regions following complex natural and societal connections. This example of a compound heat wave and a drought event striking an agricultural region shows how multiple risks are interconnected and lead to cascading biophysical, economic, and societal impacts even in distant regions, with vulnerable groups such as smallholder farmers, children and pregnant women particularly impacted. {WGI Figure 9.32; WGII SPM B4.3, WGII SPM B1.3, WGII SPM B.5.1, WGII TS Figure TS.9, WGII TS Figure TS.10 (c), WGII Fig 5.2, WGII TS.B.2.3, WGII TS.B.2.3, WGII TS.B.3.3, WGII 9.11.1.2}

[END FIGURE 4.3 HERE]

4.4 Equity and Inclusion in Climate Change Action

Actions that prioritise equity, climate justice, social justice and inclusion lead to more sustainable outcomes, co-benefits, reduce trade-offs, support transformative change and advance climate resilient development. Adaptation responses are immediately needed to reduce rising climate risks, especially for the most vulnerable. Equity, inclusion and just transitions are key to progress on adaptation and deeper societal ambitions for accelerated mitigation. (*high confidence*)

Adaptation and mitigation actions, across scales, sectors and regions, that prioritise equity, climate justice, rights-based approaches, social justice and inclusivity, lead to more sustainable outcomes, reduce trade-offs, support transformative change and advance climate resilient development (*high confidence*). Redistributive policies across sectors and regions that shield the poor and vulnerable,, social safety nets, equity, inclusion and just transitions, at all scales can enable deeper societal ambitions and resolve trade-offs with sustainable development goals.(SDGs), particularly education, hunger, poverty, gender and energy access (*high confidence*). Mitigation efforts embedded within the wider development context can increase the pace, depth and breadth of emission reductions (*medium confidence*). Equity, inclusion and just transitions at all scales enable deeper societal ambitions for accelerated mitigation, and climate action more broadly (*high confidence*). The complexity in risk of rising food prices, reduced household incomes, and health and climate-related malnutrition (particularly maternal malnutrition and child undernutrition) and mortality increases with little or low levels of adaptation (*high confidence*). {WGII SPM B.5.1, WGII SPM C.2.9, WGII SPM D.2.1, WGII TS Box TS.4; WGIII SPM D.3, WGIII SPM D.3.3, WGIII SPM WGIII SPM E.3, SR1.5 SPM D.4.5} (Figure 4.3c)

Regions and people with considerable development constraints have high vulnerability to climatic hazards. Adaptation outcomes for the most vulnerable within and across countries and regions are enhanced through approaches focusing on equity, inclusivity, and rights-based approaches, including 3.3 to 3.6 billion people living in contexts that are highly vulnerable to climate change (*high confidence*). Vulnerability is higher in locations with poverty, governance challenges and limited access to basic services and resources, violent conflict and high levels of climate-sensitive livelihoods (e.g., smallholder farmers, pastoralists, fishing communities) (*high confidence*). Several risks can be moderated with adaptation (*high confidence*). The largest adaptation gaps exist among lower income population groups (*high confidence*) and adaptation progress is unevenly distributed with observed adaptation gaps (*high confidence*). Present development challenges causing high vulnerability are influenced by historical and ongoing patterns of inequity such as colonialism, especially for many Indigenous Peoples and local communities (*high confidence*). Vulnerability is exacerbated by inequity and marginalisation linked to gender, ethnicity, low income or combinations thereof, especially for many Indigenous Peoples and local communities (*high confidence*). {WGII SPM B.2, WGII SPM B.2.4, WGII SPM B.3.2, WGII SPM B.3.3, WGII SPM C.1, WGII SPM C.1.2, WGII SPM C.2.9}

Meaningful participation and inclusive planning, informed by cultural values, Indigenous Knowledge, local knowledge, and scientific knowledge can help address adaptation gaps and avoid maladaptation (*high confidence*). Such actions with flexible pathways may encourage low-regret and timely actions (*very high confidence*). Integrating climate adaptation into social protection programmes, including cash transfers and public works programmes, would increase resilience to climate change, especially when supported by basic services and infrastructure (*high confidence*). {WGII SPM C.2.3, WGII SPM C.4.3, WGII SPM C.4.4, WGII SPM C.2.9, WGII WPM D.3}

Equity, inclusion, just transitions, broad and meaningful participation of all relevant actors in decision making at all scales enable deeper societal ambitions for accelerated mitigation, and climate action more broadly, and build social trust, support transformative changes and an equitable sharing of benefits and burdens (*high confidence*). Equity remains a central element in the UN climate regime, notwithstanding shifts in differentiation between states over time and challenges in assessing fair shares. Ambitious mitigation pathways imply large and sometimes disruptive changes in economic structure, with significant distributional consequences, within and between countries, including shifting of income and employment during the transition from high to low emissions activities (*high confidence*). While some jobs may be lost, low-emissions development can also open up opportunities to enhance skills and create jobs (*high confidence*). Broadening equitable access to finance, technologies and governance that facilitate mitigation, and consideration of climate justice can help equitable sharing of benefits and burdens, especially for vulnerable countries and communities. {WGIII SPM D.3, WGIII SPM D.3.2, WGIII SPM D.3.3, WGIII SPM D.3.4, WGIII TS Box TS.4}

Development priorities among countries also reflect different starting points and contexts, and enabling conditions for shifting development pathways towards increased sustainability will therefore differ, giving rise to different needs (*high confidence*). Implementing just transition principles through collective and participatory decision-making processes is an effective way of integrating equity principles into policies at all scales depending on national circumstances, while in several countries just transition commissions, task forces and national policies have been established (*medium confidence*). {WGIII SPM D.3.1, WGIII SPM D.3.3}

Many economic and regulatory instruments have been effective in reducing emissions and practical experience has informed instrument design to improve them while addressing distributional goals and social acceptance (*high confidence*). The design of behavioural interventions, including the way that choices are presented to consumers work synergistically with price signals, making the combination more effective (*medium confidence*). Individuals with high socio-economic status contribute disproportionately to emissions, and have the highest potential for emissions reductions, e.g., as citizens, investors, consumers, role models, and professionals (*high confidence*). There are options on design of instruments such as taxes, subsidies, prices, and consumption-based approaches, complemented by regulatory instruments to reduce high-emissions consumption while improving equity and societal well-being (*high confidence*). Behaviour and lifestyle changes to help end-users adopt low-GHG-intensive options can be supported by policies, infrastructure and technology with multiple co-benefits for societal well-being (*high confidence*). Broadening equitable access to domestic and international finance, technologies and capacity can also act as a catalyst for accelerating mitigation and shifting development pathways in low-income contexts (*high confidence*). Eradicating extreme poverty, energy poverty, and providing decent living standards to all in these regions in the context of achieving sustainable development objectives, in the near-term, can be achieved without significant global emissions growth (*high confidence*). Technology development, transfer, capacity building and financing can support developing countries/ regions leapfrogging or transitioning to low-emissions transport systems thereby providing multiple co-benefits (*high confidence*). Climate resilient development is advanced when actors work in equitable, just and enabling ways to reconcile divergent interests, values and worldviews, toward equitable and just outcomes (*high confidence*) {WGII D.2.1, WGIII SPM B.3.3, WGIII SPM.C.8.5, WGIII SPM C.10.2, WGIII SPM C.10.4, WGIII SPM D.3.4, WGIII SPM E.4.2, WGIII TS.5.1, WGIII Chapter 5.4, WGIII Chapter 5.8, WGIII Chapter 15.2}

4.5 Near-Term Mitigation and Adaptation Actions

Rapid and far-reaching transitions across all sectors and systems are necessary to achieve deep and sustained emissions reductions and secure a liveable and sustainable future for all. These system transitions involve a significant upscaling of a wide portfolio of mitigation and adaptation options. Feasible, effective and low-cost options for mitigation and adaptation are already available, with differences across systems and regions. (*high confidence*)

Rapid and far-reaching transitions across all sectors and systems are necessary to achieve deep emissions reductions and secure a liveable and sustainable future for all (*high confidence*). System transitions[94] consistent with pathways that limit warming to 1.5°C (>50%) with no or limited overshoot are more rapid and pronounced in the near-term than in those that limit warming to 2°C (>67%) (*high confidence*). Such a systemic change is unprecedented in terms of scale, but not necessarily in terms of speed (*medium confidence*). The system transitions make possible the transformative adaptation required for high levels of human health and well-being, economic and social resilience, ecosystem health, and planetary health. {WGII SPM A, WGII SPM Figure SPM.1; WGIII SPM C.3; SR1.5 SPM C.2, SR1.5 SPM C.2.1, SR1.5 SPM C.2, SR1.5 SPM C.5}

Feasible, effective and low-cost options for mitigation and adaptation are already available (*high confidence*) (Figure 4.4). Mitigation options costing USD100 per tCO_2-eq or less could reduce global GHG emissions by at least half the 2019 level by 2030 (options costing less than USD20 $tCO_2\text{-eq}^{-1}$ are estimated to make up more than half of this potential) (*high confidence*) (Figure 4.4). The availability, feasibility[95] and potential of mitigation or effectiveness of adaptation options in the near-term differ across systems and regions (*very high confidence*). {WGII SPM C.2; WGIII SPM C.12, WGIII SPM E.1.1; SR1.5 SPM B.6}

Demand-side measures and new ways of end-use service provision can reduce global GHG emissions in end-use sectors by 40–70% by 2050 compared to baseline scenarios, while some regions and socioeconomic groups require additional energy and resources. Demand-side mitigation encompasses changes in infrastructure use, end-use technology adoption, and socio-cultural and behavioural change. (*high confidence*) (Figure 4.4) {WGIII SPM C.10}

[START FIGURE 4.4 HERE]

[94] System transitions involve a wide portfolio of mitigation and adaptation options that enable deep emissions reductions and transformative adaptation in all sectors. This report has a particular focus on the following system transitions: energy; industry; cities, settlements and infrastructure; land, ocean, food and water; health and nutrition; and society, livelihood and economies { WGII SPM A., WGII SPM Figure SPM.1, WGII SPM Figure SPM.4; SR1.5 SPM C.2,}

[95] See Annex I: Glossary.

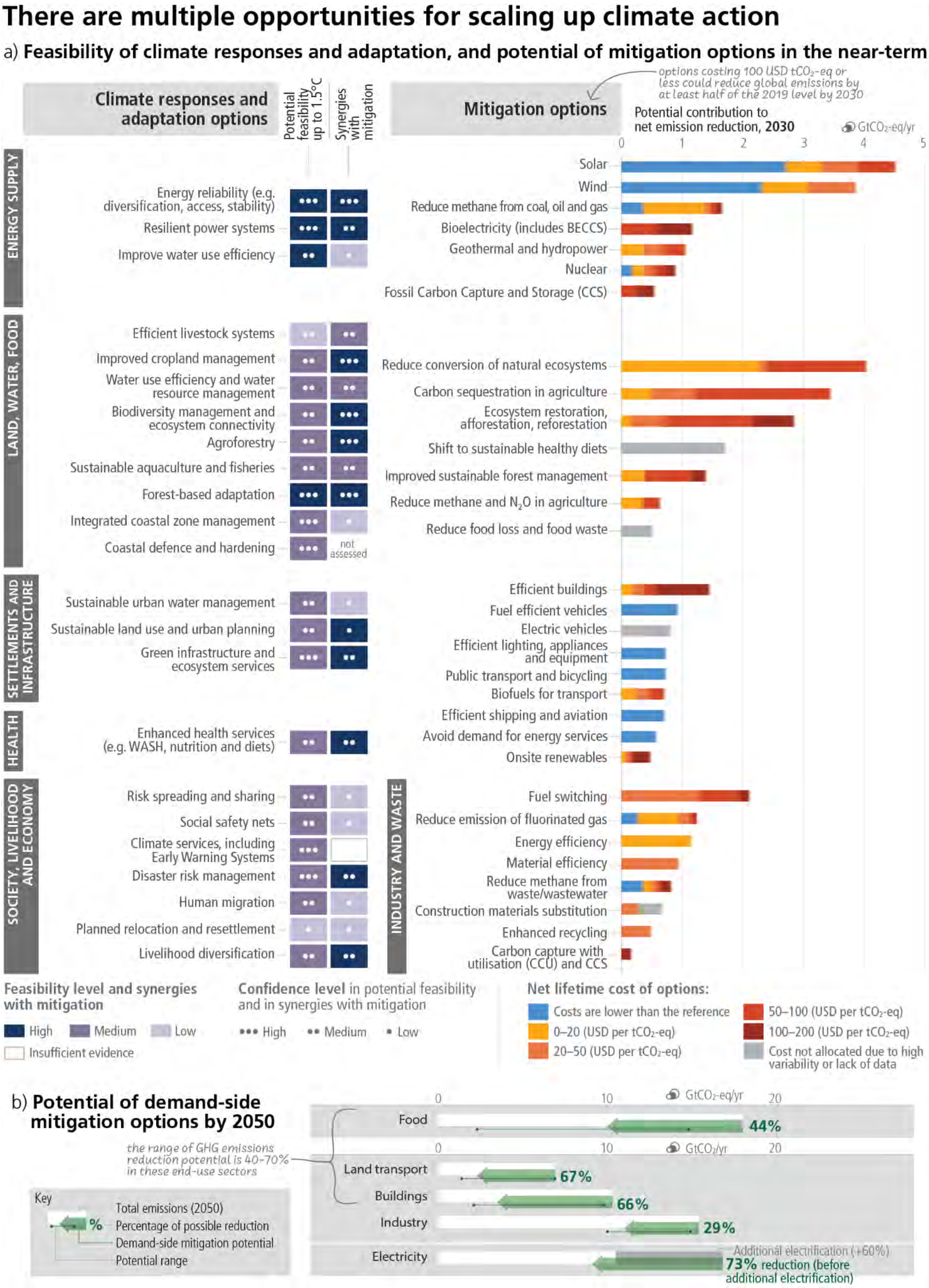
There are multiple opportunities for scaling up climate action
a) Feasibility of climate responses and adaptation, and potential of mitigation options in the near-term
Climate responses and adaptation options
Potential feasibility up to 1.5°C
Synergies with mitigation
Mitigation options
options costing 100 USD tCO2-eq or less could reduce global emissions by at least half of the 2019 level by 2030
Potential contribution to net emission reduction, 2030
GtCO2-eq/yr
0 1 2 3 4 5
ENERGY SUPPLY
Energy reliability (e.g. diversification, access, stability)
Resilient power systems
Improve water use efficiency
Solar
Wind
Reduce methane from coal, oil and gas
Bioelectricity (includes BECCS)
Geothermal and hydropower
Nuclear
Fossil Carbon Capture and Storage (CCS)
LAND, WATER, FOOD
Efficient livestock systems
Improved cropland management
Water use efficiency and water resource management
Biodiversity management and ecosystem connectivity
Agroforestry
Sustainable aquaculture and fisheries
Forest-based adaptation
Integrated coastal zone management
Coastal defence and hardening
not assessed
Reduce conversion of natural ecosystems
Carbon sequestration in agriculture
Ecosystem restoration, afforestation, reforestation
Shift to sustainable healthy diets
Improved sustainable forest management
Reduce methane and N2O in agriculture
Reduce food loss and food waste
SETTLEMENTS AND INFRASTRUCTURE
Sustainable urban water management
Sustainable land use and urban planning
Green infrastructure and ecosystem services
Efficient buildings
Fuel efficient vehicles
Electric vehicles
Efficient lighting, appliances and equipment
Public transport and bicycling
Biofuels for transport
Efficient shipping and aviation
Avoid demand for energy services
Onsite renewables
HEALTH
Enhanced health services (e.g. WASH, nutrition and diets)
SOCIETY, LIVELIHOOD AND ECONOMY
Risk spreading and sharing
Social safety nets
Climate services, including Early Warning Systems
Disaster risk management
Human migration
Planned relocation and resettlement
Livelihood diversification
INDUSTRY AND WASTE
Fuel switching
Reduce emission of fluorinated gas
Energy efficiency
Material efficiency
Reduce methane from waste/wastewater
Construction materials substitution
Enhanced recycling
Carbon capture with utilisation (CCU) and CCS
Feasibility level and synergies with mitigation
High Medium Low
Insufficient evidence
Confidence level in potential feasibility and in synergies with mitigation
••• High •• Medium • Low
Net lifetime cost of options:
Costs are lower than the reference
0–20 (USD per tCO2-eq)
20–50 (USD per tCO2-eq)
50–100 (USD per tCO2-eq)
100–200 (USD per tCO2-eq)
Cost not allocated due to high variability or lack of data
b) Potential of demand-side mitigation options by 2050
the range of GHG emissions reduction potential is 40-70% in these end-use sectors
Key
Total emissions (2050)
Percentage of possible reduction
Demand-side mitigation potential
Potential range
0 10 GtCO2-eq/yr 20
Food 44%
0 10 GtCO2/yr 20
Land transport 67%
Buildings 66%
Industry 29%
Electricity
Additional electrification (+60%)
73% reduction (before additional electrification)

Figure 4.4: Multiple Opportunities for scaling up climate action. **Panel (a)** presents selected mitigation and adaptation options across different systems. The left hand side of panel (a) shows climate responses and adaptation options assessed for their multidimensional feasibility at global scale, in the near term and up to 1.5°C global warming. As literature above 1.5°C is limited, feasibility at higher levels of warming may change, which is currently not possible to assess robustly. The term response is used here in addition to adaptation because some responses, such as migration, relocation and resettlement may or may not be considered to be adaptation. Migration, when voluntary, safe and orderly, allows reduction of risks to climatic and non-climatic stressors. Forest based adaptation includes sustainable forest management, forest conservation and restoration, reforestation and afforestation. WASH refers to water, sanitation and hygiene. Six feasibility dimensions (economic, technological, institutional, social, environmental and geophysical) were used to calculate the potential feasibility of climate responses and adaptation options, along with their synergies with mitigation. For potential feasibility and feasibility dimensions, the figure shows high, medium, or low feasibility. Synergies with mitigation are identified as high, medium, and low. The right hand side of panel (a) provides an overview of selected mitigation options and their estimated costs and potentials in 2030. Relative potentials and costs will vary by place, context and time and in the longer term compared to 2030. Costs are net lifetime discounted monetary costs of avoided greenhouse gas emissions calculated relative to a reference technology. The potential (horizontal axis) is the quantity of net GHG emission reduction that can be achieved by a given mitigation option relative to a specified emission baseline. Net GHG emission reductions are the sum of reduced emissions and/or enhanced sinks. The baseline used consists of current policy (around 2019) reference scenarios from the AR6 scenarios database (25/75 percentile values). The mitigation potentials are assessed independently for each option and are not necessarily additive. Health system mitigation options are included mostly in settlement and infrastructure (e.g., efficient healthcare buildings) and cannot be identified separately. Fuel switching in industry refers to switching to electricity, hydrogen, bioenergy and natural gas. The length of the solid bars represents the mitigation potential of an option. Potentials are broken down into cost categories, indicated by different colours (see legend). Only discounted lifetime monetary costs are considered. Where a gradual colour transition is shown, the breakdown of the potential into cost categories is not well known or depends heavily on factors such as geographical location, resource availability, and regional circumstances, and the colours indicate the range of estimates. The uncertainty in the total potential is typically 25–50%. When interpreting this figure, the following should be taken into account: (1) The mitigation potential is uncertain, as it will depend on the reference technology (and emissions) being displaced, the rate of new technology adoption, and several other factors; (2) Different options have different feasibilities beyond the cost aspects, which are not reflected in the figure; and (3) Costs for accommodating the integration of variable renewable energy sources in electricity systems are expected to be modest until 2030, and are not included.

Panel (b) displays the indicative potential of demand-side mitigation options for 2050. Potentials are estimated based on approximately 500 bottom-up studies representing all global regions. The baseline (white bar) is provided by the sectoral mean GHG emissions in 2050 of the two scenarios (IEA-STEPS and IP_ModAct) consistent with policies announced by national governments until 2020. The green arrow represents the demand-side emissions reductions potentials. The range in potential is shown by a line connecting dots displaying the highest and the lowest potentials reported in the literature. Food shows demand-side potential of socio-cultural factors and infrastructure use, and changes in land-use patterns enabled by change in food demand. Demand-side measures and new ways of end-use service provision can reduce global GHG emissions in end-use sectors (buildings, land transport, food) by 40–70% by 2050 compared to baseline scenarios, while some regions and socioeconomic groups require additional energy and resources. The last row shows how demand-side mitigation options in other sectors can influence overall electricity demand. The dark grey bar shows the projected increase in electricity demand above the 2050 baseline due to increasing electrification in the other sectors. Based on a bottom-up assessment, this projected increase in electricity demand can be avoided through demand-side mitigation options in the domains of infrastructure use and socio-cultural factors that influence electricity usage in industry, land transport, and buildings (green arrow).

{WGII SPM Figure SPM 4, WGII Cross-Chapter Box FEASIB in Chapter 18; WGIII SPM C.10, WGIII Chapter 12.2.1, WGIII Chapter 12.2.2, WGIII Figure SPM 6, WGIII SPM Figure SPM 7}

[END FIGURE 4.4 HERE]

4.5.1 Energy Systems

Rapid and deep reductions in GHG emissions require major energy system transitions (*high confidence*). Adaptation options can help reduce climate-related risks to the energy system (*very high confidence*). Net zero CO_2 energy systems entail: a substantial reduction in overall fossil fuel use, minimal use of unabated fossil fuels[96], and use of Carbon Capture and Storage in the remaining fossil fuel systems;

[96] In this context, 'unabated fossil fuels' refers to fossil fuels produced and used without interventions that substantially reduce the amount of GHG emitted throughout the life cycle; for example, capturing 90% or more CO_2 from power plants, or 50–80% of fugitive methane emissions from energy supply {WGIII SPM footnote 54}.

electricity systems that emit no net CO_2; widespread electrification; alternative energy carriers in applications less amenable to electrification; energy conservation and efficiency; and greater integration across the energy system (*high confidence*). Large contributions to emissions reductions can come from options costing less than USD20 $tCO_2\text{-eq}^{-1}$, including solar and wind energy, energy efficiency improvements, and CH_4 (methane) emissions reductions (from coal mining, oil and gas, and waste) (*medium confidence*).[97] Many of these response options are technically viable and are supported by the public (*high confidence*). Maintaining emission-intensive systems may, in some regions and sectors, be more expensive than transitioning to low emission systems (*high confidence*) {WGII SPM C.2.10; WGIII SPM C.4.1, WGIII SPM C.4.2, WGIII SPM C.12.1, WGIII SPM E.1.1, WGIII TS.5.1}.

Climate change and related extreme events will affect future energy systems, including hydropower production, bioenergy yields, thermal power plant efficiencies, and demands for heating and cooling (*high confidence*). The most feasible energy system adaptation options support infrastructure resilience, reliable power systems and efficient water use for existing and new energy generation systems (*very high confidence*). Adaptations for hydropower and thermo-electric power generation are effective in most regions up to 1.5°C to 2°C, with decreasing effectiveness at higher levels of warming (*medium confidence*). Energy generation diversification (e.g., wind, solar, small-scale hydroelectric) and demand side management (e.g., storage and energy efficiency improvements) can increase energy reliability and reduce vulnerabilities to climate change, especially in rural populations (*high confidence*). Climate responsive energy markets, updated design standards on energy assets according to current and projected climate change, smart-grid technologies, robust transmission systems and improved capacity to respond to supply deficits have high feasibility in the medium- to long-term, with mitigation co-benefits (*very high confidence*). {WGII SPM B.5.3, WGII SPM C.2.10; WGIII TS.5.1}

4.5.2 Industry

There are several options to reduce industrial emissions that differ by type of industry; many industries are disrupted by climate change, especially from extreme events (*high confidence*). Reducing industry emissions will entail coordinated action throughout value chains to promote all mitigation options, including demand management, energy and materials efficiency, circular material flows, as well as abatement technologies and transformational changes in production processes (*high confidence*). Light industry and manufacturing can be largely decarbonized through available abatement technologies (e.g., material efficiency, circularity), electrification (e.g., electrothermal heating, heat pumps), and switching to low- and zero-GHG emitting fuels (e.g., hydrogen, ammonia, and bio-based and other synthetic fuels) (*high confidence*), while deep reduction of cement process emissions will rely on cementitious material substitution and the availability of Carbon Capture and Storage (CCS) until new chemistries are mastered (*high confidence*). Reducing emissions from the production and use of chemicals would need to rely on a life cycle approach, including increased plastics recycling, fuel and feedstock switching, and carbon sourced through biogenic sources, and, depending on availability, Carbon Capture and Utilisation (CCU), direct air CO_2 capture, as well as CCS (*high confidence*). Action to reduce industry sector emissions may change the location of GHG-intensive industries and the organisation of value chains, with distributional effects on employment and economic structure (*medium confidence*). {WGII TS.B.9.1, WGII Chapter 16.5.2 WGIII SPM C.5, WGIII SPM C.5.2, WGIII SPM C.5.3, WGIII TS.5.5}

Many industrial and service sectors are negatively affected by climate change through supply and operational disruptions, especially from extreme events (*high confidence*), and will require adaptation efforts. Water intensive industries (e.g., mining) can undertake measures to reduce water stress, such as water recycling and reuse, using brackish or saline sources, working to improve water use efficiency. However, residual risks will remain, especially at higher levels of warming (*medium confidence*). (Section 3.2) {WGII TS.B.9.1, WGII Chapter 16.5.2, WGII Chapter 4.6.3}

[97] The mitigation potentials and mitigation costs of individual technologies in a specific context or region may differ greatly from the provided estimates (*medium confidence*) {WGIII SPM C.12.1}.

4.5.3 Cities, Settlements and Infrastructure

Urban systems are critical for achieving deep emissions reductions and advancing climate resilient development, particularly when this involves integrated planning that incorporates physical, natural and social infrastructure (*high confidence*). Deep emissions reductions and integrated adaptation actions are advanced by: integrated, inclusive land use planning and decision-making; compact urban form by co-locating jobs and housing; reducing or changing urban energy and material consumption; electrification in combination with low emissions sources; improved water and waste management infrastructure; and enhancing carbon uptake and storage in the urban environment (e.g. bio-based building materials, permeable surfaces and urban green and blue infrastructure). Cities can achieve net-zero emissions if emissions are reduced within and outside of their administrative boundaries through supply chains, creating beneficial cascading effects across other sectors. (*high confidence*). {WGII SPM C.5.6, WGII SPM D.1.3, WGII SPM D.3; WGIII SPM C.6, WGIII SPM C.6.2, WGIII TS 5.4, SR1.5 SPM C.2.4}

Considering climate change impacts and risks (e.g., through climate services) in the design and planning of urban and rural settlements and infrastructure is critical for resilience and enhancing human well-being. Effective mitigation can be advanced at each of the design, construction, retrofit, use and disposal stages for buildings. Mitigation interventions for buildings include: at the construction phase, low-emission construction materials, highly efficient building envelope and the integration of renewable energy solutions; at the use phase, highly efficient appliances/equipment, the optimisation of the use of buildings and their supply with low-emission energy sources; and at the disposal phase, recycling and re-using construction materials. Sufficiency[98] measures can limit the demand for energy and materials over the lifecycle of buildings and appliances. (*high confidence*) {WGII SPM C.2.5; WGIII SPM C.7.2}.

Transport-related GHG emissions can be reduced by demand-side options and low-GHG emissions technologies. Changes in urban form, reallocation of street space for cycling and walking, digitalisation (e.g., teleworking) and programs that encourage changes in consumer behaviour (e.g. transport, pricing) can reduce demand for transport services and support the shift to more energy efficient transport modes (*high confidence*). Electric vehicles powered by low-emissions electricity offer the largest decarbonisation potential for land-based transport, on a life cycle basis (*high confidence*). Costs of electrified vehicles are decreasing and their adoption is accelerating, but they require continued investments in supporting infrastructure to increase scale of deployment (*high confidence*). The environmental footprint of battery production and growing concerns about critical minerals can be addressed by material and supply diversification strategies, energy and material efficiency improvements, and circular material flows (*medium confidence*). Advances in battery technologies could facilitate the electrification of heavy-duty trucks and compliment conventional electric rail systems (*medium confidence*). Sustainable biofuels can offer additional mitigation benefits in land-based transport in the short and medium term (*medium confidence*). Sustainable biofuels, low-emissions hydrogen, and derivatives (including synthetic fuels) can support mitigation of CO_2 emissions from shipping, aviation, and heavy-duty land transport but require production process improvements and cost reductions (*medium confidence*). Key infrastructure systems including sanitation, water, health, transport, communications and energy will be increasingly vulnerable if design standards do not account for changing climate conditions (*high confidence*) {WGII SPM B.2.5; WGIII SPM C.6.2, WGIII SPM C.8, WGIII SPM C.8.1, WGIII SPM C.8.2, WGIII SPM C.10.2, WGIII SPM C.10.3, WGIII SPM C.10.4}.

Green/natural and blue infrastructure such as urban forestry, green roofs, ponds and lakes, and river restoration can mitigate climate change through carbon uptake and storage, avoided emissions, and reduced energy use while reducing risk from extreme events such as heatwaves, heavy precipitation and droughts, and advancing co-benefits for health, wellbeing and livelihoods (*medium confidence*). Urban greening can provide local cooling (*very high confidence*). Combining green/natural and grey/physical infrastructure adaptation responses has potential to reduce adaptation costs and contribute to flood control, sanitation, water resources management, landslide prevention and coastal protection (*medium confidence*). Globally, more financing is directed at grey/physical infrastructure than green/natural infrastructure and social infrastructure (*medium confidence*), and there is limited evidence of investment in informal settlements (*medium to high confidence*). The greatest gains in well-being in urban areas can be achieved by prioritising finance to reduce climate risk

[98] A set of measures and daily practices that avoid demand for energy, materials, land and water while delivering human well-being for all within planetary boundaries {WGIII Annex I}

for low-income and marginalised communities including people living in informal settlements (*high confidence*). {WGII SPM C.2.5, WGII SPM C.2.6, WGII SPM C.2.7, WGII SPM D.3.2, WGII TS.E.1.4, WGII Cross-Chapter Box FEAS; WGIII SPM C.6, WGIII SPM C.6.2, WGIII SPM D.1.3, WGIII SPM D.2.1}

Responses to ongoing sea level rise and land subsidence in low-lying coastal cities and settlements and small islands include protection, accommodation, advance and planned relocation. These responses are more effective if combined and/or sequenced, planned well ahead, aligned with sociocultural values and development priorities, and underpinned by inclusive community engagement processes. (*high confidence*) {WGII SPM C.2.8}

4.5.4 Land, Ocean, Food, and Water

There is substantial mitigation and adaptation potential from options in agriculture, forestry and other land use, and in the oceans, that could be upscaled in the near term across most regions (*high confidence*) (Figure 4.5). Conservation, improved management, and restoration of forests and other ecosystems offer the largest share of economic mitigation potential, with reduced deforestation in tropical regions having the highest total mitigation potential. Ecosystem restoration, reforestation, and afforestation can lead to trade-offs due to competing demands on land. Minimizing trade-offs required integrated approaches to meet multiple objectives including food security. Demand-side measures (shifting to sustainable healthy diets and reducing food loss/waste) and sustainable agricultural intensification can reduce ecosystem conversion and CH_4 and N_2O emissions, and free up land for reforestation and ecosystem restoration. Sustainably sourced agriculture and forest products, including long-lived wood products, can be used instead of more GHG-intensive products in other sectors. Effective adaptation options include cultivar improvements, agroforestry, community-based adaptation, farm and landscape diversification, and urban agriculture. These AFOLU response options require integration of biophysical, socioeconomic and other enabling factors. The effectiveness of ecosystem-based adaptation and most water-related adaptation options declines with increasing warming (see 3.2). (*high confidence*). {WGII SPM C.2.1, WGII SPM C.2.2, WGII SPM C.2.5 WGIII SPM C.9.1; SRCCL SPM B.1.1, SRCCL SPM B.5.4, SRCCL SPM D.1; SROCC SPM C}

Some options, such as conservation of high-carbon ecosystems (e.g., peatlands, wetlands, rangelands, mangroves and forests), have immediate impacts while others, such as restoration of high-carbon ecosystems, reclamation of degraded soils or afforestation, take decades to deliver measurable results (*high confidence*). Many sustainable land management technologies and practices are financially profitable in three to ten years (*medium confidence*). {SRCCL SPM B.1.2, SRCCL SPM D.2.2}

Maintaining the resilience of biodiversity and ecosystem services at a global scale depends on effective and equitable conservation of approximately 30–50% of Earth's land, freshwater and ocean areas, including currently near-natural ecosystems (*high confidence*). The services and options provided by terrestrial, freshwater, coastal and ocean ecosystems can be supported by protection, restoration, precautionary ecosystem-based management of renewable resource use, and the reduction of pollution and other stressors (*high confidence*). {WGII SPM C.2.4, WGII SPM D.4; SROCC SPM C.2}

Large-scale land conversion for bioenergy, biochar, or afforestation can increase risks to biodiversity, water and food security. In contrast, restoring natural forests and drained peatlands, and improving sustainability of managed forests enhances the resilience of carbon stocks and sinks and reduces ecosystem vulnerability to climate change. Cooperation, and inclusive decision making, with local communities and Indigenous Peoples, as well as recognition of inherent rights of Indigenous Peoples, is integral to successful adaptation across forests and other ecosystems. (*high confidence*). {WGII SPM B.5.4, WGII SPM C.2.3, WGII SPM C.2.4; WGIII SPM D.2.3; SRCCL B.7.3, SRCCL SPM C.4.3, SRCCL TS.7}

Natural rivers, wetlands and upstream forests reduce flood risk in most circumstances (*high confidence*). Enhancing natural water retention such as by restoring wetlands and rivers, land use planning such as no build zones or upstream forest management, can further reduce flood risk (*medium confidence*). For inland flooding, combinations of non-structural measures like early warning systems and structural measures like levees have reduced loss of lives (*medium confidence*), but hard defences against flooding or sea level rise can also be maladaptive (*high confidence*). {WGII SPM C.2.1, WGII SPM C.4.1, WGII SPM C.4.2, WGII SPM C.2.5}

Protection and restoration of coastal 'blue carbon' ecosystems (e.g., mangroves, tidal marshes and seagrass meadows) could reduce emissions and/or increase carbon uptake and storage (*medium confidence*). Coastal wetlands protect against coastal erosion and flooding (*very high confidence*). Strengthening precautionary approaches, such as rebuilding overexploited or depleted fisheries, and responsiveness of existing fisheries management strategies reduces negative climate change impacts on fisheries, with benefits for regional economies and livelihoods (*medium confidence*). Ecosystem-based management in fisheries and aquaculture supports food security, biodiversity, human health and well-being (*high confidence*). {WGII SPM C.2.2, WGII SPM C.2; SROCC SPM C2.3, SROCC SPM C.2.4}

4.5.5 Health and Nutrition

Human health will benefit from integrated mitigation and adaptation options that mainstream health into food, infrastructure, social protection, and water policies (*very high confidence*). Balanced and sustainable healthy diets[99] and reduced food loss and waste present important opportunities for adaptation and mitigation while generating significant co-benefits in terms of biodiversity and human health (*high confidence*). Public health policies to improve nutrition, such as increasing the diversity of food sources in public procurement, health insurance, financial incentives, and awareness-raising campaigns, can potentially influence food demand, reduce food waste, reduce healthcare costs, contribute to lower GHG emissions and enhance adaptive capacity (*high confidence*). Improved access to clean energy sources and technologies, and shifts to active mobility (e.g., walking and cycling) and public transport can deliver socioeconomic, air quality and health benefits, especially for women and children (*high confidence*). {WGII SPM C.2.2, WGII SPM C.2.11, WGII Cross-Chapter Box HEALTH; WGIII SPM C.2.2, WGIII SPM C.4.2, WGIII SPM C.9.1, WGIII SPM C.10.4, WGIII SPM D.1.3, WGIII SPM Figure SPM6, WGIII SPM Figure SPM.8; SRCCL SPM B.6.2, SRCCL SPM B.6.3, SRCCL B.4.6, SRCCL SPM C.2.4}

Effective adaptation options exist to help protect human health and wellbeing (*high confidence*). Health Action Plans that include early warning and response systems are effective for extreme heat (*high confidence*). Effective options for water-borne and food-borne diseases include improving access to potable water, reducing exposure of water and sanitation systems to flooding and extreme weather events, and improved early warning systems (*very high confidence*). For vector-borne diseases, effective adaptation options include surveillance, early warning systems, and vaccine development (*very high confidence*). Effective adaptation options for reducing mental health risks under climate change include improving surveillance and access to mental health care, and monitoring of psychosocial impacts from extreme weather events (*high confidence*). A key pathway to climate resilience in the health sector is universal access to healthcare (*high confidence*) {WGII SPM C.2.11, WGII Chapter 7.4.6}

4.5.6 Society, Livelihoods, and Economies

Enhancing knowledge on risks and available adaptation options promotes societal responses, and behaviour and lifestyle changes supported by policies, infrastructure and technology can help reduce global GHG emissions (*high confidence*). Climate literacy and information provided through climate services and community approaches, including those that are informed by Indigenous Knowledge and local knowledge, can accelerate behavioural changes and planning (*high confidence*). Educational and information programmes, using the arts, participatory modelling and citizen science can facilitate awareness, heighten risk perception, and influence behaviours (*high confidence*). The way choices are presented can enable adoption of low GHG intensive socio-cultural options, such as shifts to balanced, sustainable healthy diets, reduced food waste, and active mobility (*high confidence*). Judicious labelling, framing, and communication of social norms can increase the effect of mandates, subsidies, or taxes (*medium confidence*) {WGII SPM C.5.3, WGII TS.D.10.1; WGIII SPM C.10, WGIII SPM C.10.2, WGIII SPM C.10.3, WGIII SPM E.2.2, WGIII Figure SPM.6, WGIII TS.6.1, 5.4; SR1.5 SPM D.5.6; SROCC SPM C.4}.

[99] Balanced diets refer to diets that feature plant-based foods, such as those based on coarse grains, legumes, fruits and vegetables, nuts and seeds, and animal-sourced food produced in resilient, sustainable and low-GHG emission systems, as described in SRCCL.

A range of adaptation options, such as disaster risk management, early warning systems, climate services and risk spreading and sharing approaches, have broad applicability across sectors and provide greater risk reduction benefits when combined (*high confidence*). Climate services that are demand-driven and inclusive of different users and providers can improve agricultural practices, inform better water use and efficiency, and enable resilient infrastructure planning (*high confidence*). Policy mixes that include weather and health insurance, social protection and adaptive safety nets, contingent finance and reserve funds, and universal access to early warning systems combined with effective contingency plans, can reduce vulnerability and exposure of human systems (*high confidence*). Integrating climate adaptation into social protection programs, including cash transfers and public works programs, is highly feasible and increases resilience to climate change, especially when supported by basic services and infrastructure (*high confidence*). Social safety nets can build adaptive capacities, reduce socioeconomic vulnerability, and reduce risk linked to hazards (*robust evidence, medium agreement*). {WGII SPM C.2.9, WGII SPM C.2.13, WGII Cross-Chapter Box FEASIB in Chapter 18; SRCCL SPM C.1.4, SRCCL SPM D.1.2}.

Reducing future risks of involuntary migration and displacement due to climate change is possible through cooperative, international efforts to enhance institutional adaptive capacity and sustainable development (*high confidence*). Increasing adaptive capacity minimises risk associated with involuntary migration and immobility and improves the degree of choice under which migration decisions are made, while policy interventions can remove barriers and expand the alternatives for safe, orderly and regular migration that allows vulnerable people to adapt to climate change (*high confidence*). {WGII SPM C.2.12, WGII TS.D.8.6, WGII Cross-Chapter Box MIGRATE in Chapter 7}

Accelerating commitment and follow-through by the private sector is promoted for instance by building business cases for adaptation, accountability and transparency mechanisms, and monitoring and evaluation of adaptation progress (*medium confidence*). Integrated pathways for managing climate risks will be most suitable when so-called 'low-regret' anticipatory options are established jointly across sectors in a timely manner and are feasible and effective in their local context, and when path dependencies and maladaptations across sectors are avoided (*high confidence*). Sustained adaptation actions are strengthened by mainstreaming adaptation into institutional budget and policy planning cycles, statutory planning, monitoring and evaluation frameworks and into recovery efforts from disaster events (*high confidence*). Instruments that incorporate adaptation such as policy and legal frameworks, behavioural incentives, and economic instruments that address market failures, such as climate risk disclosure, inclusive and deliberative processes strengthen adaptation actions by public and private actors (*medium confidence*). {WGII SPM C.5.1, WGII SPM C.5.2, WGII TS.D.10.4}

4.6 Co-Benefits of Adaptation and Mitigation for Sustainable Development Goals

Mitigation and adaptation actions have more synergies than trade-offs with Sustainable Development Goals (SDGs). Synergies and trade-offs depend on context and scale of implementation. Potential trade-offs can be compensated or avoided with additional policies, investments and financial partnerships. (*high confidence*)

Many mitigation and adaptation actions have multiple synergies with Sustainable Development Goals (SDGs), but some actions can also have trade-offs. Potential synergies with SDGs exceed potential trade-offs. Synergies and trade-offs are context specific and depend on: means and scale of implementation, intra- and inter-sectoral interactions, cooperation between countries and regions, the sequencing, timing and stringency of actions, governance, and policy design. Eradicating extreme poverty, energy poverty, and providing decent living standards to all, consistent with near-term sustainable development objectives, can be achieved without significant global emissions growth. (*high confidence*) (Figure 4.5) {WGII SPM C.2.3, WGII SPM Figure SPM.4b; WGIII SPM B.3.3, WGIII SPM C.9.2, WGIII SPM D.1.2, WGIII SPM D.1.4, WGIII SPM Figure SPM.8}

Several mitigation and adaptation options can harness near-term synergies and reduce trade-offs to advance sustainable development in energy, urban and land systems (Figure 4.5) (*high confidence*). Clean energy supply systems have multiple co-benefits, including improvements in air quality and health. Heat Health Action Plans that include early warning and response systems, approaches that mainstream health into food, livelihoods, social protection, water and sanitation benefit health and well-being. There are potential synergies between multiple Sustainable Development Goals and sustainable land use and urban planning with more green spaces, reduced air pollution, and demand-side mitigation including shifts to balanced, sustainable healthy diets. Electrification combined with low-GHG energy, and shifts to public transport can enhance health, employment, and can contribute to energy security and deliver equity. Conservation, protection and restoration of terrestrial, freshwater, coastal and ocean ecosystems, together with targeted management to adapt to unavoidable impacts of climate change can generate multiple additional benefits, such as agricultural productivity, food security, and biodiversity conservation. (*high confidence*). {WGII SPM C.1.1, WGII C.2.4, WGII SPM D.1, WGII SPM Figure SPM.4, WGII Cross-Chapter Box HEALTH in Chapter 17, WGII Cross-Chapter Box FEASIB in Chapter 18; WGIII SPM C.4.2, WGIII SPM D.1.3, WGIII SPM D.2, WGIII SPM Figure SPM.8; SRCCL SPM B.4.6}

When implementing mitigation and adaptation together, and taking trade-offs into account, multiple co-benefits and synergies for human well-being as well as ecosystem and planetary health can be realised (*high confidence*). There is a strong link between sustainable development, vulnerability and climate risks. Social safety nets that support climate change adaptation have strong co-benefits with development goals such as education, poverty alleviation, gender inclusion and food security. Land restoration contributes to mitigation and adaptation with synergies via enhanced ecosystem services and with economically positive returns and co-benefits for poverty reduction and improved livelihoods. Trade-offs can be evaluated and minimised by giving emphasis to capacity building, finance, technology transfer, investments; governance, development, context specific gender-based and other social equity considerations with meaningful participation of Indigenous Peoples, local communities and vulnerable populations. (*high confidence*). {WGII SPM C.2.9, WGII SPM C.5.6, WGII SPM D.5.2, WGII Cross-Chapter Box on Gender in Chapter 18; WGIII SPM C.9.2, WGIII SPM D.1.2, WGIII SPM D.1.4, WGIII SPM D.2; SRCCL SPM D.2.2, SRCCL TS.4}

Context relevant design and implementation requires considering people's needs, biodiversity, and other sustainable development dimensions (*very high confidence*). Countries at all stages of economic development seek to improve the well-being of people, and their development priorities reflect different starting points and contexts. Different contexts include but are not limited to social, economic, environmental, cultural, or political circumstances, resource endowment, capabilities, international environment, and prior development. n regions with high dependency on fossil fuels for, among other things, revenue and employment generation, mitigating risks for sustainable development requires policies that promote economic and energy sector diversification and considerations of just transitions principles, processes and practices (*high confidence*). For individuals and households in low-lying coastal areas, in Small Islands, and smallholder farmers transitioning from incremental to transformational adaptation can help overcome soft adaptation limits (*high confidence*). Effective governance is needed to limit trade-offs of some mitigation options such as large scale afforestation and bioenergy options due to risks from their deployment for food systems, biodiversity, other ecosystem functions and services, and livelihoods (*high confidence*). Effective governance requires adequate institutional capacity at all levels (*high confidence*) {WGII SPM B.5.4, WGII SPM C.3.1, WGII SPM C.3.4; WGIII SPM D.1.3, WGIII SPM E.4.2; SR1.5 SPM C.3.4, SR1.5 SPM C.3.5, SR1.5 SPM Figure SPM.4, SR1.5 SPM D.4.3, SR1.5 SPM D.4.4}

[START FIGURE 4.5]

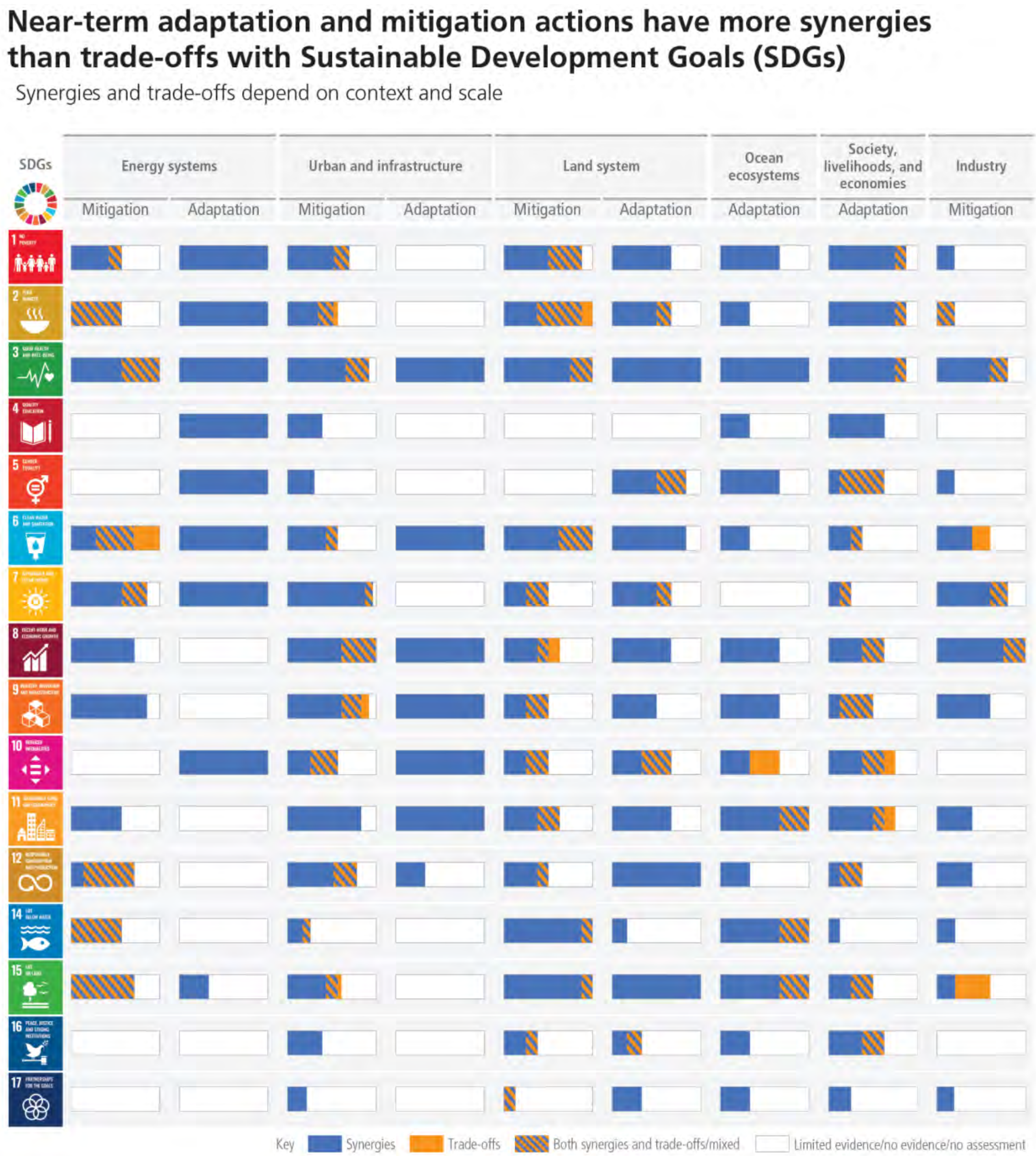

Figure 4.5: Potential synergies and trade-offs between the portfolio of climate change mitigation and adaptation options and the Sustainable Development Goals (SDGs). This figure presents a high-level summary of potential synergies and trade-offs assessed in WGII Figure SPM.4b and WGIII Figure SPM.8, based on the qualitative and quantitative assessment of each individual mitigation or option. The SDGs serve as an analytical framework for the assessment of different sustainable development dimensions, which extend beyond the time frame of 2030 SDG targets. Synergies and trade-offs across all individual options within a sector/system are aggregated into sector/system potentials for the whole mitigation or adaptation portfolio.

The length of each bar represents the total number of mitigation or adaptation options under each system/sector. The number of adaptation and mitigation options vary across system/sector, and have been normalised to 100% so that bars are comparable across mitigation, adaptation, system/sector, and SDGs. Positive links shown in WGII Figure SPM 4b and WGIII Figure SPM 8 are counted and aggregated to generate the percentage share of synergies, represented here by the blue proportion within the bars. Negative links shown in WGII Figure SPM 4b and WGIII Figure SPM 8 are counted and aggregated to generate the percentage share of trade-offs and is represented by orange proportion within the bars. 'Both synergies and trade-offs' shown in WGII Figure SPM 4b WGIII Figure SPM 8 are counted and aggregated to generate the percentage share of 'both synergies and trade-off', represented by the striped proportion within the bars. The 'white' proportion within the bar indicates limited evidence/ no evidence/ not assessed.

Energy systems comprise all mitigation options listed in WGIII Figure SPM.8 and WGII Figure SPM.4b for adaptation. Urban and infrastructure comprises all mitigation options listed in WGIII Figure SPM.8 under Urban systems, under Buildings and under Transport and adaptation options listed in WGII Figure SPM.4b under Urban and infrastructure systems. Land system comprises mitigation options listed in WGIII Figure SPM.8 under AFOLU and adaptation options listed in WGII Figure SPM.4b under Land and ocean systems: forest-based adaptation, agroforestry, biodiversity management and ecosystem connectivity, improved cropland management, efficient livestock management, water use efficiency and water resource management. Ocean ecosystems comprises adaptation options listed in WGII Figure SPM.4b under Land and ocean systems: coastal defence and hardening, integrated coastal zone management and sustainable aquaculture and fisheries. Society, livelihood and economies comprises adaptation options listed in WGII Figure SPM.4b under Cross-sectoral; Industry comprises all those mitigation options listed in WGIII Figure SPM.8 under Industry.

SDG 13 (Climate Action) is not listed because mitigation/ adaptation is being considered in terms of interaction with SDGs and not vice versa (SPM SR1.5 Figure SPM.4 caption). The bars denote the strength of the connection and do not consider the strength of the impact on the SDGs. The synergies and trade-offs differ depending on the context and the scale of implementation. Scale of implementation particularly matters when there is competition for scarce resources. For the sake of uniformity, we are not reporting the confidence levels because there is knowledge gap in adaptation option wise relation with SDGs and their confidence level which is evident from WGII fig SPM 4b. {WGII Figure SPM.4b; WGIII Figure SPM.8}

[END FIGURE 4.5 HERE]

4.7 Governance and Policy for Near-Term Climate Change Action

Effective climate action requires political commitment, well-aligned multi-level governance and institutional frameworks, laws, policies and strategies. It needs clear goals, adequate finance and financing tools, coordination across multiple policy domains, and inclusive governance processes. Many mitigation and adaptation policy instruments have been deployed successfully, and could support deep emissions reductions and climate resilience if scaled up and applied widely, depending on national circumstances. Adaptation and mitigation action benefits from drawing on diverse knowledge. (*high confidence*)

Effective climate governance enables mitigation and adaptation by providing overall direction based on national circumstances, setting targets and priorities, mainstreaming climate action across policy domains and levels, based on national circumstances and in the context of international cooperation. Effective governance enhances monitoring and evaluation and regulatory certainty, prioritising inclusive, transparent and equitable decision-making, and improves access to finance and technology (*high confidence*). These functions can be promoted by climate-relevant laws and plans, which are growing in number across sectors and regions, advancing mitigation outcomes and adaptation benefits (*high confidence*). Climate laws have been growing in number and have helped deliver mitigation and adaptation outcomes (*medium confidence*). {WGII SPM C.5, WGII SPM C.5.1, WGII SPM C5.4, WGII SPM C.5.6; WGIII SPM B.5.2, WGIII SPM E.3.1}

Effective municipal, national and sub-national climate institutions, such as expert and co-ordinating bodies, enable co-produced, multi-scale decision-processes, build consensus for action among diverse interests, and inform strategy settings (*high confidence*). This requires adequate institutional capacity at all levels (*high confidence*). Vulnerabilities and climate risks are often reduced through carefully designed and implemented laws, policies, participatory processes, and interventions that address context specific inequities such as based on gender, ethnicity, disability, age, location and income (*high confidence*). Policy support is influenced by Indigenous Peoples, businesses, and actors in civil society, including, youth, labour, media, and local communities, and effectiveness is enhanced by partnerships between many different groups in society (*high confidence*).Climate-related litigation is growing, with a large number of cases in some developed countries and with a much smaller number in some developing countries, and in some cases has influenced the outcome and ambition of climate governance (*medium confidence*). {WGII SPM C2.6, WGII SPM C.5.2, WGII SPM C.5.5, WGII SPM C.5.6, WGII SPM D.3.1; WGIII SPM E3.2, WGIII SPM E.3.3}

Effective climate governance is enabled by inclusive decision processes, allocation of appropriate resources, and institutional review, monitoring and evaluation (*high confidence*). Multi-level, hybrid and cross-sector governance facilitates appropriate consideration for co-benefits and trade-offs, particularly in land sectors where decision processes range from farm level to national scale (*high confidence*). Consideration of climate justice can help to facilitate shifting development pathways towards sustainability. {WGII SPM C.5.5, WGII SPM C.5.6, WGII SPM D.1.1, WGII SPM D.2, WGII SPM D.3.2; SRCCL SPM C.3, SRCCL TS.1}

Drawing on diverse knowledge and partnerships, including with women, youth, Indigenous Peoples, local communities, and ethnic minorities can facilitate climate resilient development and has allowed locally appropriate and socially acceptable solutions (*high confidence*). {WGII SPM D.2, D.2.1}

Many regulatory and economic instruments have already been deployed successfully. These instruments could support deep emissions reductions if scaled up and applied more widely. Practical experience has informed instrument design and helped to improve predictability, environmental effectiveness, economic efficiency, and equity. (*high confidence*) {WGII SPM E.4; WGIII SPM E.4.2}.

Scaling up and enhancing the use of regulatory instruments, consistent with national circumstances, can improve mitigation outcomes in sectoral applications (*high confidence*), and regulatory instruments that include flexibility mechanisms can reduce costs of cutting emissions (*medium confidence*). {WGII SPM C.5.4; WGIII SPM E.4.1}

Where implemented, **carbon pricing instruments have incentivized low-cost emissions reduction measures, but have been less effective, on their own and at prevailing prices during the assessment period, to promote higher-cost measures necessary for further reductions *(medium confidence)*.** Revenue from carbon taxes or emissions trading can be used for equity and distributional goals, for example to support low-income households, among other approaches (*high confidence*). There is no consistent evidence that current emission trading systems have led to significant emissions leakage (*medium confidence*). {WGIII SPM E4.2, WGIII SPM E.4.6}

Removing fossil fuel subsidies would reduce emissions, improve public revenue and macroeconomic performance, and yield other environmental and sustainable development benefits such as improved public revenue, macroeconomic and sustainability performance; subsidy removal can have adverse distributional impacts especially on the most economically vulnerable groups which, in some cases, can be mitigated by measures such as re-distributing revenue saved, and depend on national circumstances (*high confidence*). Fossil fuel subsidy removal is projected by various studies to reduce global CO_2 emissions by 1–4%, and GHG emissions by up to 10% by 2030, varying across regions (*medium confidence*). {WGIII SPM E.4.2}

National policies to support technology development, and participation in international markets for emission reduction, can bring positive spillover effects for other countries (*medium confidence*), although reduced demand for fossil fuels as a result of climate policy could result in costs to exporting countries (*high confidence*). Economy-wide packages can meet short-term economic goals while reducing emissions and shifting development pathways towards sustainability (*medium confidence*). Examples are public spending commitments; pricing reforms; and investment in education and training, R&D and infrastructure (*high confidence*). Effective policy packages would be comprehensive in coverage, harnessed to a clear vision for change, balanced across objectives, aligned with specific technology and system needs, consistent in terms of design and tailored to national circumstances (*high confidence*). {WGIII SPM E4.4, WGIII SPM 4.5, WGIII SPM 4.6}

4.8 Strengthening the Response: Finance, International Cooperation and Technology

Finance, international cooperation and technology are critical enablers for accelerated climate action. If climate goals are to be achieved, both adaptation and mitigation financing would have to increase many-fold. There is sufficient global capital to close the global investment gaps but there are barriers to redirect capital to climate action. Barriers include institutional, regulatory and market access barriers, are reduced and address the needs and opportunities, economic vulnerability and indebtedness in many developing countries. Enhancing international cooperation is possible through multiple channels. Enhancing technology innovation systems is key to accelerate the widespread adoption of technologies and practices. (*high confidence*)

4.8.1 Finance for Mitigation and Adaptation Actions

Improved availability and access to finance[100] will enable accelerated climate action (*very high confidence*). Addressing needs and gaps and broadening equitable access to domestic and international finance, when combined with other supportive actions, can act as a catalyst for accelerating mitigation and shifting development pathways *(high confidence)*. Climate resilient development is enabled by increased international cooperation including improved access to financial resources, particularly for vulnerable regions, sectors and groups, and inclusive governance and coordinated policies *(high confidence)*. Accelerated international financial cooperation is a critical enabler of low-GHG and just transitions, and can address inequities in access to finance and the costs of, and vulnerability to, the impacts of climate change (*high confidence*). {WGII SPM C.1.2, WGII SPM C.3.2, WGII SPM C.5, WGII SPM C.5.4, WGII SPM D.2, WGII SPM D.3.2, WGII SPM D.5, WGII SPM D.5.2; WGIII SPM B.4.2,WGIII SPM B.5, WGIII SPM B.5.4, WGIII SPM C.4.2, WGIII SPM C.7.3, WGIII SPM C.8.5, WGIII SPM D.1.2, WGIII SPM D.2.4, WGIII SPM D.3.4, WGIII SPM E.2.3, WGIII SPM E.3.1, WGIII SPM E.5, WGIII SPM E.5.1, WGIII SPM E.5.2, WGIII SPM E.5.3, WGIII SPM E.5.4, WGIII SPM E.6.2}

Both adaptation and mitigation finance need to increase many-fold, to address rising climate risks and to accelerate investments in emissions reduction (*high confidence*). Increased finance would address soft limits to adaptation and rising climate risks while also averting some related losses and damages, particularly in vulnerable developing countries (*high confidence*). Enhanced mobilisation of and access to finance, together with building capacity, are essential for implementation of adaptation actions and to reduce adaptation gaps given rising risks and costs, especially for the most vulnerable groups, regions and sectors (*high confidence*). Public finance is an important enabler of adaptation and mitigation, and can also leverage private finance (*high confidence*). Adaptation funding predominately comes from public sources, and public mechanisms and finance can leverage private sector finance by addressing real and perceived regulatory, cost and market barriers, for instance via public-private partnerships (*high confidence*). Financial and technological resources enable effective and ongoing implementation of adaptation, especially when supported by institutions with a strong understanding of adaptation needs and capacity (*high confidence*). Average annual modelled mitigation investment requirements for 2020 to 2030 in scenarios that limit warming to 2°C or 1.5°C are a factor of three to six greater than current levels, and total mitigation investments (public, private, domestic and international) would need to increase across all sectors and regions (*medium confidence*). Even if extensive global mitigation efforts are implemented, there will be a large need for financial, technical, and human resources for adaptation *(high confidence)* (Section 2.3.2, 2.3.3, 4.4, Figure 4.6) {WGII SPM C.1.2, WGII SPM C2.11, WGII SPM C.3, WGII SPM C.3.2, WGII SPM C3.5, WGII SPM C.5, WGII SPM C.5.4, WGII SPM D.1, WGII SPM D.1.1, WGII SPM D.1.2, WGII SPM C.5.4; WGIII SPM D.2.4,WGIII SPM E.5, WGIII SPM E.5.1,WGIII Chapter 15.2}

There is sufficient global capital and liquidity to close global investment gaps, given the size of the global financial system, but there are barriers to redirect capital to climate action both within and outside the global financial sector and in the context of economic vulnerabilities and indebtedness facing many

[100] Finance can originate from diverse sources, singly or in combination: public or private, local, national or international, bilateral or multilateral, and alternative sources (e.g., philanthropic, carbon offsets). It can be in the form of grants, technical assistance, loans (concessional and non-concessional), bonds, equity, risk insurance and financial guarantees (of various types).

developing countries (*high confidence*). For shifts in private finance, options include better assessment of climate-related risks and investment opportunities within the financial system, reducing sectoral and regional mismatches between available capital and investment needs, improving the risk-return profiles of climate investments, and developing institutional capacities and local capital markets. Macroeconomic barriers include, amongst others, indebtedness and economic vulnerability of developing regions. (*high confidence*). {WGII SPM C.5.4; WGIII SPM E.4.2, WGIII SPM E.5, WGIII SPM E.5.2, WGIII SPM E.5.3}

Scaling up financial flows requires clear signalling from governments and the international community. Tracked financial flows fall short of the levels needed for adaptation and to achieve mitigation goals across all sectors and regions. These gaps create many opportunities and the challenge of closing gaps is largest in developing countries. This includes a stronger alignment of public finance, lowering real and perceived regulatory, cost and market barriers, and higher levels of public finance to lower the risks associated with low-emission investments. Up-front risks deter economically sound low carbon projects, and developing local capital markets are an option. Investors, financial intermediaries, central banks and financial regulators can shift the systemic underpricing of climate-related risks. A robust labelling of bonds and transparency is needed to attract savers. (*high confidence*). {WGII SPM C.5.4; WGIII SPM B.5.4, WGIII SPM E.4, WGIII SPM E.5.4, WGIII Section 15.2, 15.6.1, 15.6.2, 15.6.7}

[START FIGURE 4.6 HERE]

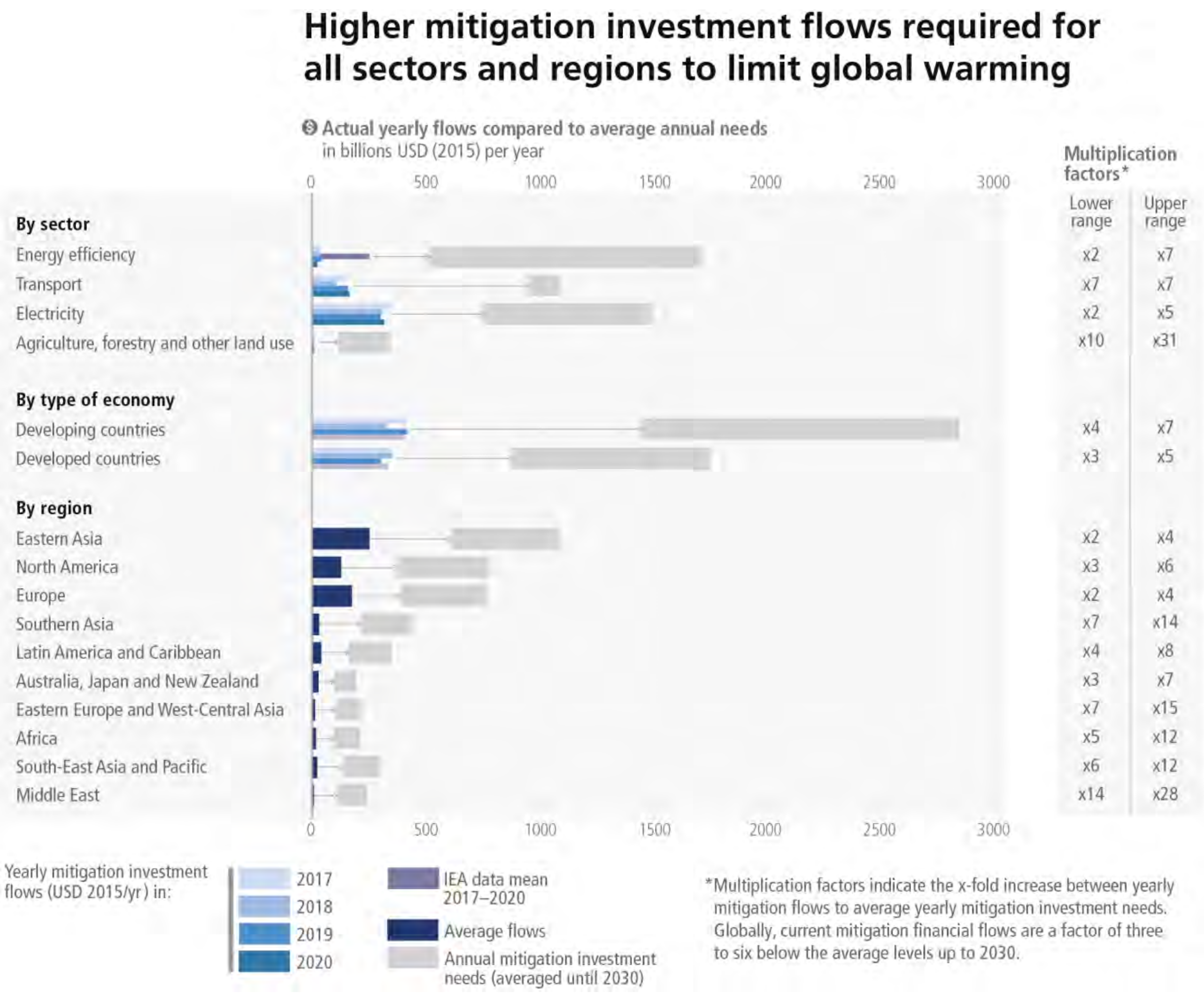

Figure 4.6: Breakdown of average mitigation investment flows and investment needs until 2030 (USD billion). Mitigation investment flows and investment needs by sector (energy efficiency, transport, electricity, and agriculture,

forestry and other land use), by type of economy, and by region (see WGIII Annex II Part I Section 1 for the classification schemes for countries and areas).
The blue bars display data on mitigation investment flows for four years: 2017, 2018, 2019 and 2020 by sector and by type of economy. For the regional breakdown, the annual average mitigation investment flows for 2017–2019 are shown. The grey bars show the minimum and maximum level of global annual mitigation investment needs in the assessed scenarios. This has been averaged until 2030. The multiplication factors show the ratio of global average early mitigation investment needs (averaged until 2030) and current yearly mitigation flows (averaged for 2017/18–2020). The lower multiplication factor refers to the lower end of the range of investment needs. The upper multiplication factor refers to the upper range of investment needs.
Given the multiple sources and lack of harmonised methodologies, the data can be considered only if indicative of the size and pattern of investment needs. {WGIII Figure TS.25, WGIII Sections 15.3, 15.4, 15.5, Table 15.2, Table 15.3, Table 15.4}

[END FIGURE 4.6 HERE]

The largest climate finance gaps and opportunities are in developing countries (*high confidence*). Accelerated support from developed countries and multilateral institutions is a critical enabler to enhance mitigation and adaptation action and can address inequities in finance, including its costs, terms and conditions, and economic vulnerability to climate change. Scaled-up public grants for mitigation and adaptation funding for vulnerable regions, e.g., in Sub-Saharan Africa, would be cost-effective and have high social returns in terms of access to basic energy. Options for scaling up mitigation and adaptation in developing regions include: increased levels of public finance and publicly mobilised private finance flows from developed to developing countries in the context of the USD 100 billion-a-year goal of the Paris Agreement; increase the use of public guarantees to reduce risks and leverage private flows at lower cost; local capital markets development; and building greater trust in international cooperation processes. A coordinated effort to make the post-pandemic recovery sustainable over the long term through increased flows of financing over this decade can accelerate climate action, including in developing regions facing high debt costs, debt distress and macroeconomic uncertainty. (*high confidence*) {WGII SPM C.5.2, WGII SPM C.5.4, WGII SPM C.6.5, WGII SPM D.2, WGII TS.D.10.2; WGIII SPM E.5, WGIII SPM E.5.3, WGIII TS.6.4, WGIII Box TS.1, WGIII Chapter 15.2, WGIII Chapter 15.6}

4.8.2 International Cooperation and Coordination

International cooperation is a critical enabler for achieving ambitious climate change mitigation goals and climate resilient development (*high confidence*). Climate resilient development is enabled by increased international cooperation including mobilising and enhancing access to finance, particularly for developing countries, vulnerable regions, sectors and groups and aligning finance flows for climate action to be consistent with ambition levels and funding needs (*high confidence*). While agreed processes and goals, such as those in the UNFCCC, Kyoto Protocol and Paris Agreement, are helping (Section 2.2.1), international financial, technology and capacity building support to developing countries will enable greater implementation and more ambitious actions (*medium confidence*). By integrating equity and climate justice, national and international policies can help to facilitate shifting development pathways towards sustainability, especially by mobilising and enhancing access to finance for vulnerable regions, sectors and communities (*high confidence*). International cooperation and coordination, including combined policy packages, may be particularly important for sustainability transitions in emissions-intensive and highly traded basic materials industries that are exposed to international competition (*high confidence*). The large majority of emission modelling studies assume significant international cooperation to secure financial flows and address inequality and poverty issues in pathways limiting global warming. There are large variations in the modelled effects of mitigation on GDP across regions, depending notably on economic structure, regional emissions reductions, policy design and level of international cooperation (*high confidence*). Delayed global cooperation increases policy costs across regions (*high confidence*). {WGII SPM D.2, WGII SPM D.3.1, WGII SPM D.5.2; WGIII SPM D.3.4, WGIII SPM C5.4, WGIII SPM C.12.2, WGIII SPM E.6, WGIII SPM E.6.1, WGIII E.5.4, WGIII TS.4.2, WGIII TS.6.2; SR1.5 SPM D.6.3, SR1.5 SPM D.7, SR1.5 SPM D.7.3}.

The transboundary nature of many climate change risks (e.g., for supply chains, markets and natural resource flows in food, fisheries, energy and water, and potential for conflict) increases the need for climate-informed transboundary management, cooperation, responses and solutions through multi-national or regional governance processes (*high confidence*). Multilateral governance efforts can help reconcile contested interests, world views and values about how to address climate change. International environment and sectoral agreements, and initiatives in some cases, may help to stimulate low GHG investment and reduce emissions (such as ozone depletion, transboundary air pollution and atmospheric emissions of mercury). Improvements to national and international governance structures would further enable the decarbonisation of shipping and aviation through deployment of low-emissions fuels, for example through stricter efficiency and carbon intensity standards. Transnational partnerships can also stimulate policy development, low-emissions technology diffusion, emission reductions and adaptation, by linking sub-national and other actors, including cities, regions, non-governmental organisations and private sector entities, and by enhancing interactions between state and non-state actors, though uncertainties remain over their costs, feasibility, and effectiveness. International environmental and sectoral agreements, institutions, and initiatives are helping, and in some cases may help, to stimulate low GHG emissions investment and reduce emissions. (*medium confidence*) {WGII SPM B.5.3, WGII SPM C.5.6, WGII TS.E.5.4, WGII TS.E.5.5, WGIII SPM C.8.4, WGIII SPM E.6.3, WGIII SPM E.6.4, WGIII SPM E.6.4, WGIII TS.5.3}

4.8.3 Technology Innovation, Adoption, Diffusion and Transfer

Enhancing technology innovation systems can provide opportunities to lower emissions growth and create social and environmental co-benefits. Policy packages tailored to national contexts and technological characteristics have been effective in supporting low-emission innovation and technology diffusion. Support for successful low-carbon technological innovation includes public policies such as training and R&D, complemented by regulatory and market-based instruments that create incentives and market opportunities such as appliance performance standards and building codes. (*high confidence*) {WGIII SPM B.4, WGIII SPM B.4.4, WGIII SPM E.4.3, WGIII SPM E4.4}.

International cooperation on innovation systems and technology development and transfer, accompanied by capacity building, knowledge sharing, and technical and financial support can accelerate the global diffusion of mitigation technologies, practices and policies and align these with other development objectives (*high confidence*). Choice architecture can help end-users adopt technology and low-GHG-intensive options (*high confidence*). Adoption of low-emission technologies lags in most developing countries, particularly least developed ones, due in part to weaker enabling conditions, including limited finance, technology development and transfer, and capacity building (*medium confidence*). {WGIII SPM B.4.2, WGIII SPM E.6.2, WGIII SPM C.10.4, WGIII Chapter 16.5}

International cooperation on innovation works best when tailored to and beneficial for local value chains, when partners collaborate on an equal footing, and when capacity building is an integral part of the effort (*medium confidence*). {WGIII SPM E.4.4, WGIII SPM E.6.2}.

Technological innovation can have trade-offs that include externalities such as new and greater environmental impacts and social inequalities; rebound effects leading to lower net emission reductions or even emission increases; and overdependence on foreign knowledge and providers (*high confidence*). Appropriately designed policies and governance have helped address distributional impacts and rebound effects (*high confidence*). For example, digital technologies can promote large increases in energy efficiency through coordination and an economic shift to services (*high confidence*). However, societal digitalization can induce greater consumption of goods and energy and increased electronic waste as well as negatively impacting labour markets and worsening inequalities between and within countries (*medium confidence*). Digitalisation requires appropriate governance and policies in order to enhance mitigation potential (*high confidence*) . Effective policy packages can help to realise synergies, avoid trade-offs and/or reduce rebound effects: these might include a mix of efficiency targets, performance standards, information provision, carbon pricing, finance and technical assistance (*high confidence*). {WGIII SPM B.4.2, WGIII SPM B.4.3, WGIII SPM E.4.4, WGIII TS 6.5, WGIII Cross-Chapter Box 11 on Digitalization in Chapter 16}

Technology transfer to expand use of digital technologies for land use monitoring, sustainable land management, and improved agricultural productivity supports reduced emissions from deforestation and land use change while also improving GHG accounting and standardisation (*medium confidence*) {SRCCL SPM C.2.1, SRCCL SPM D.1.2, SRCCL SPM D.1.4, SRCCL Chapter 7.4.4, SRCCL Chapter 7.4.6}.

4.9 Integration of Near-Term Actions Across Sectors and Systems

The feasibility, effectiveness and benefits of mitigation and adaptation actions are increased when multi-sectoral solutions are undertaken that cut across systems. When such options are combined with broader sustainable development objectives, they can yield greater benefits for human well-being, social equity and justice, and ecosystem and planetary health. (*high confidence*)

Climate resilient development strategies that treat climate, ecosystems and biodiversity, and human society as parts of an integrated system are the most effective (*high confidence*). Human and ecosystem vulnerability are interdependent (*high confidence*). Climate resilient development is enabled when decision-making processes and actions are integrated across sectors (*very high confidence*). Synergies with and progress towards the Sustainable Development Goals enhance prospects for climate resilient development. Choices and actions that treat humans and ecosystems as an integrated system build on diverse knowledge about climate risk, equitable, just and inclusive approaches, and ecosystem stewardship. {WGII SPM B.2, WGII Figure SPM.5, WGII SPM D.2, WGII SPM D2.1, WGII SPM 2.2, WGII SPM D4, WGII SPM D4.1, WGII SPM D4.2, WGII SPM D5.2, WGII SPM Figure SPM.5}.

Approaches that align goals and actions across sectors provide opportunities for multiple and large-scale benefits and avoided damages in the near-term. **Such measures can also achieve greater benefits through cascading effects across sectors (*medium confidence*).** For example, the feasibility of using land for both agriculture and centralised solar production can increase when such options are combined (*high confidence*). Similarly, integrated transport and energy infrastructure planning and operations can together reduce the environmental, social, and economic impacts of decarbonising the transport and energy sectors (*high confidence*). The implementation of packages of multiple city-scale mitigation strategies can have cascading effects across sectors and reduce GHG emissions both within and outside a city's administrative boundaries (*very high confidence*). Integrated design approaches to the construction and retrofit of buildings provide increasing examples of zero energy or zero carbon buildings in several regions. To minimise maladaptation, multi-sectoral, multi-actor and inclusive planning with flexible pathways encourages low-regret and timely actions that keep options open, ensure benefits in multiple sectors and systems and suggest the available solution space for adapting to long-term climate change (*very high confidence*). Trade-offs in terms of employment, water use, land-use competition and biodiversity, as well as access to, and the affordability of, energy, food, and water can be avoided by well-implemented land-based mitigation options, especially those that do not threaten existing sustainable land uses and land rights, with frameworks for integrated policy implementation *(high confidence)*{WGII SPM C.2, WGII SPM C.2.1–2.13, WGII SPM C.4.4; WGIII SPM C.6.3, WGIII SPM C.6, WGIII SPM C.7.2, WGIII SPM C.8.5, WGIII SPM D.1.2, WGIII SPM D.1.5, WGIII SPM E.1.2}

Mitigation and adaptation when implemented together, and combined with broader sustainable development objectives, would yield multiple benefits for human well-being as well as ecosystem and planetary health (*high confidence*). The range of such positive interactions is significant in the landscape of near-term climate policies across regions, sectors and systems. For example, AFOLU mitigation actions in land-use change and forestry, when sustainably implemented, can provide large-scale GHG emission reductions and removals that simultaneously benefit biodiversity, food security, wood supply and other ecosystem services but cannot fully compensate for delayed mitigation action in other sectors. Adaptation measures in land, ocean and ecosystems similarly can have widespread benefits for food security, nutrition, health and well-being, ecosystems and biodiversity. Equally, urban systems are critical, interconnected sites for climate resilient development; urban policies that implement multiple interventions can yield adaptation or mitigation gains with equity and human well-being. Integrated policy packages can improve the ability to integrate considerations of equity, gender equality and justice. Coordinated cross-sectoral policies and planning can maximise synergies and avoid or reduce trade-offs between mitigation and adaptation. Effective action in all of the above areas will require near-term political commitment and follow-through, social cooperation, finance, and more integrated cross-sectoral policies and support and actions. (*high confidence*). (3.4, 4.4) {WGII SPM C.1, WG II SPM C.2, WGII SPM C.2, WGII SPM C.5, WGII SPM D.2, WGII SPM D.3.2, WGII SPM D.3.3, WGII SPM Figure SPM.4; WGIII SPM C.6.3, WGIII SPM C.8.2, WGIII SPM C.9, WGIII SPM C.9.1, WGIII SPM C.9.2, WGIII SPM D.2, WGIII SPM D.2.4, WGIII SPM D.3.2, WGIII SPM E.1, WGIII SPM E.2.4, WGIII SPM Figure SPM.8, WGIII TS.7, WGIII TS Figure TS.29: SRCCL ES Section 7.4.8, SRCCL SPM B.6}

Samuel Petrequin
Petrequin is covering European news and sports.
sampetrequin
spetrequin@ap.org

Click to copy

RELATED TOPICS

Russia-Ukraine war
Vladimir Putin
Science
Politics
World News
Business
European Union
Europe
Climate and environment

EU climate czar: Putin's war accelerated green transition

By SAMUEL PETREQUIN February 21, 2023

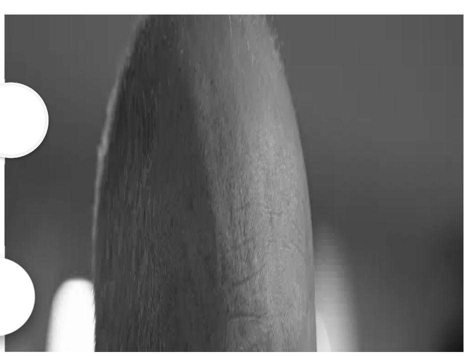

BRUSSELS (AP) — Russian President Vladimir Putin unwittingly accelerated the European Union's green transition with his war in Ukraine, with the 27-nation bloc reducing its dependency on Russian fossil fuels and increasing its renewable energy use over the past year, the EU's climate czar said Tuesday.

"The European Union now

energy

renewables because we have very little gas left, we have almost no coal left, and we have no oil, Frans Timmermans, the commissioner in charge of the European Green Deal, said.

Speaking during an interview with The Associated Press ahead of Friday's one-year anniversary of the Russian invasion, Timmermans said Putin completely underestimated the EU's resilience when Moscow cut off most natural gas flows to Europe amid the war, a called energy blackmail

"He's been saying publicly that this winter Europeans would freeze and starve," Timmermans said. "Well, we neither froze nor starved because our food production was at high levels. There were no shortages. And our energy: We weapon in the effective way."

however, fueled an energy price crisis in the EU that sent the bills of households and businesses through the roof.

CLIMATE AND ENVIRONMEN

Early heat wave in Pacific Northwest could break records

New Mexico regulators grilled over oilfield spills, lack of enforceme

Largest US public utility switching from coal to gas, despite proposed EPA carbon pollution limits

Stragglers pack up as Swiss village is evacuated under rockslide threat

"Our citizens did have to bear the brunt of his manipulations," Timmermans added. "But he he certainly didn't get us

In response to reduced supplies of Russian energy, the EU introduced last year counter measures that included launching a nearly 300 billion-euro ($320 billion) program to promote more efficient fuel use and a faster rollout of renewable power.

The EU also introduced embargoes on Russian coal and oil, accompanied by a price cap on Russian oil exports. In addition, the bloc diversified its energy sources by sealing deals for liquefied natural gas to compensate stocks for the winter while ... electricity.

As Putin continues to justify his invasion of Ukraine by accusing Western countries of threatening Russia, Timmermans said the Russian leader's use of energy as a weapon has backfired. In January, gas prices on the European spot market were back to their prewar level.

"He's losing a lot of income because of this," and cut prices to India and

sale of gas. He thought he could use that as a weapon. But the weapon turned against him, and it has sped up."

Some EU member countries reduced their natural gas consumption by more than 20% this year, Timmermans said. The war "is changing the way we relate to energy and it's helping us understand that we need to move quicker in terms of renewable energy," he added.

According to the bloc's data, gas consumption in the EU dropped by

2023, compared with

for the same months between 2017 and 2022.

To meet the EU's goal of becoming climate neutral by 2050, the European Commission supports a target of 45% renewable energy sources in the bloc's energy mix by 2030 as countries look to wind and solar power to bolster their energy security.

According to a review by global energy

up in clean

and solar in 2022 generated a record 22% of the bloc's electricity and for the first time overtook gas, which accounted for 20%. Coal power accounted for 16%.

"We have a unique opportunity to move toward clean technologies that will need no emissions, that will be circular, so you don't have to keep digging up primary materials," Timmermans said. "If we move in that direction, clean growth is possible. I am optimistic about the potential of that, but we now."

time is running out to keep average global temperatures from rising 1.5 degrees Celsius (2.7 degrees Fahrenheit) above pre-industrial levels. That target, laid down in the 2015 Paris climate accord, appears increasingly doubtful as temperatures have already increased by more than 1.1 C.

"And we need to make sure that our

degrees of temperature

continue with the policies of today, we will overshoot 2 degrees and we will be in a completely different territory."

Follow AP's coverage of the war in Ukraine at https://apnews.com/l ukraine and of tje climate and environment at https://apnews.com/l and-environment

Annual Energy Outlook 2023

with projections to 2050

Narrative Figures

U.S. Energy Information Administration

#AEO2023

March 16, 2023
www.eia.gov/aeo

You can access chart data by right-clicking the chart.

Figure 1

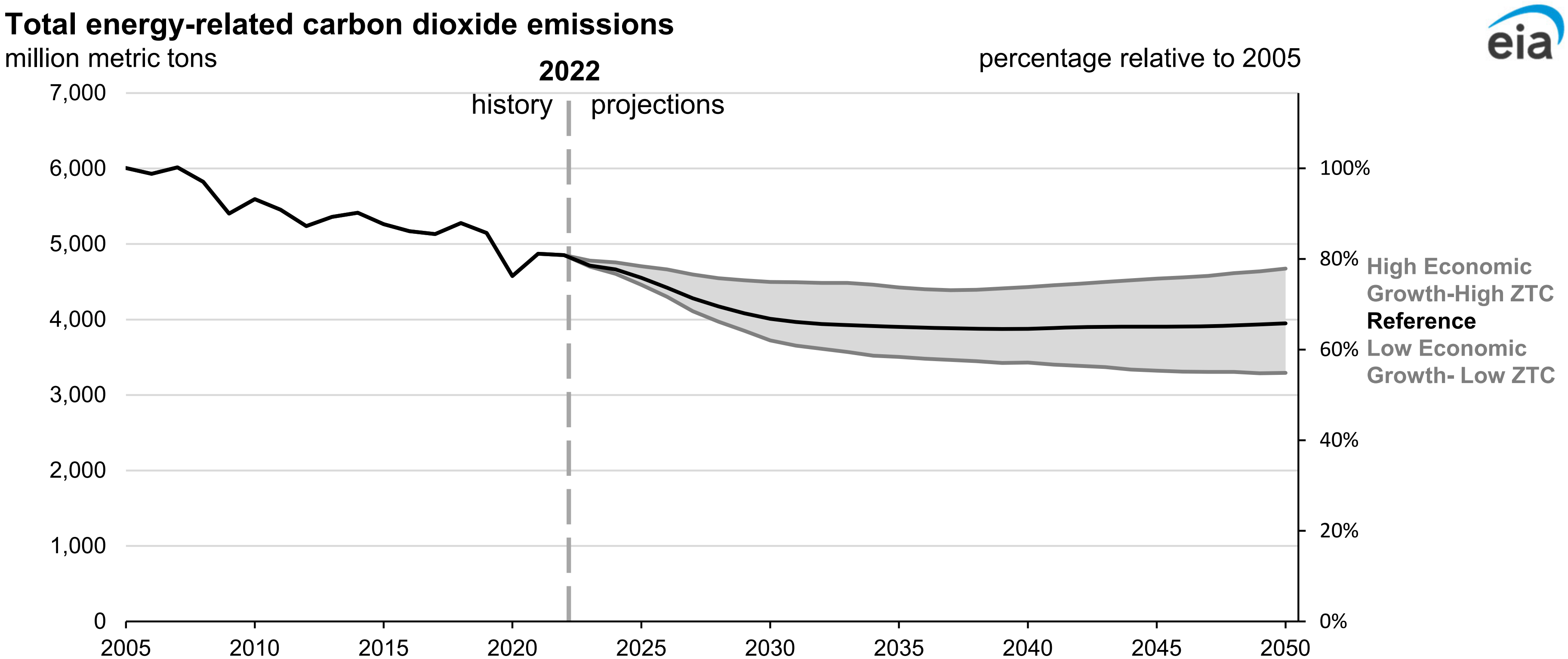

Data source: U.S. Energy Information Administration, *Annual Energy Outlook 2023* (AEO2023)
Note: Shaded regions represent maximum and minimum values for each projection year across the AEO2023 Reference case and side cases. ZTC=Zero-Carbon Technology Cost.

Figure 2

U.S. electricity generation by select technologies for all cases
billion kilowatthours

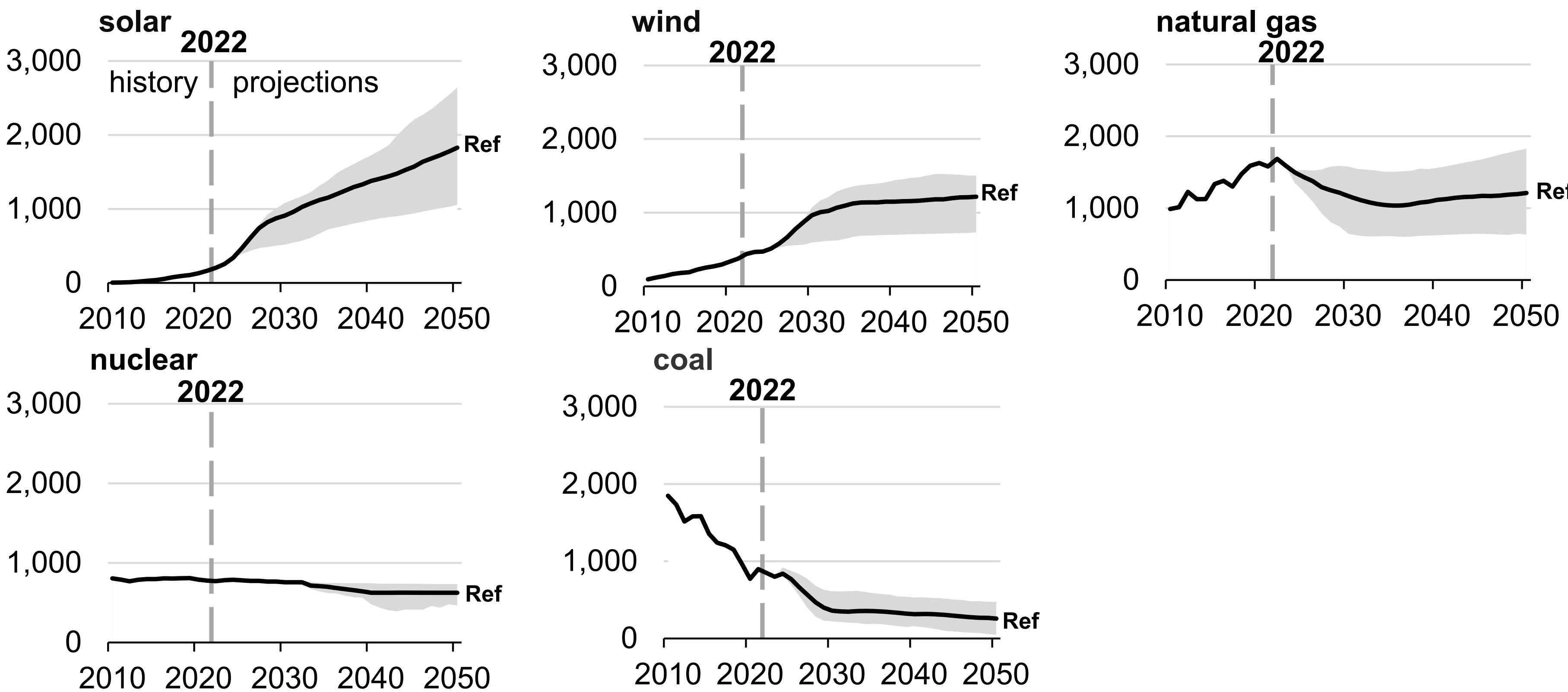

Data source: U.S. Energy Information Administration, *Annual Energy Outlook 2023* (AEO2023)
Note: Shaded regions represent maximum and minimum values for each projection year across the AEO2023 Reference case and side cases. Ref=Reference case.

Figure 3

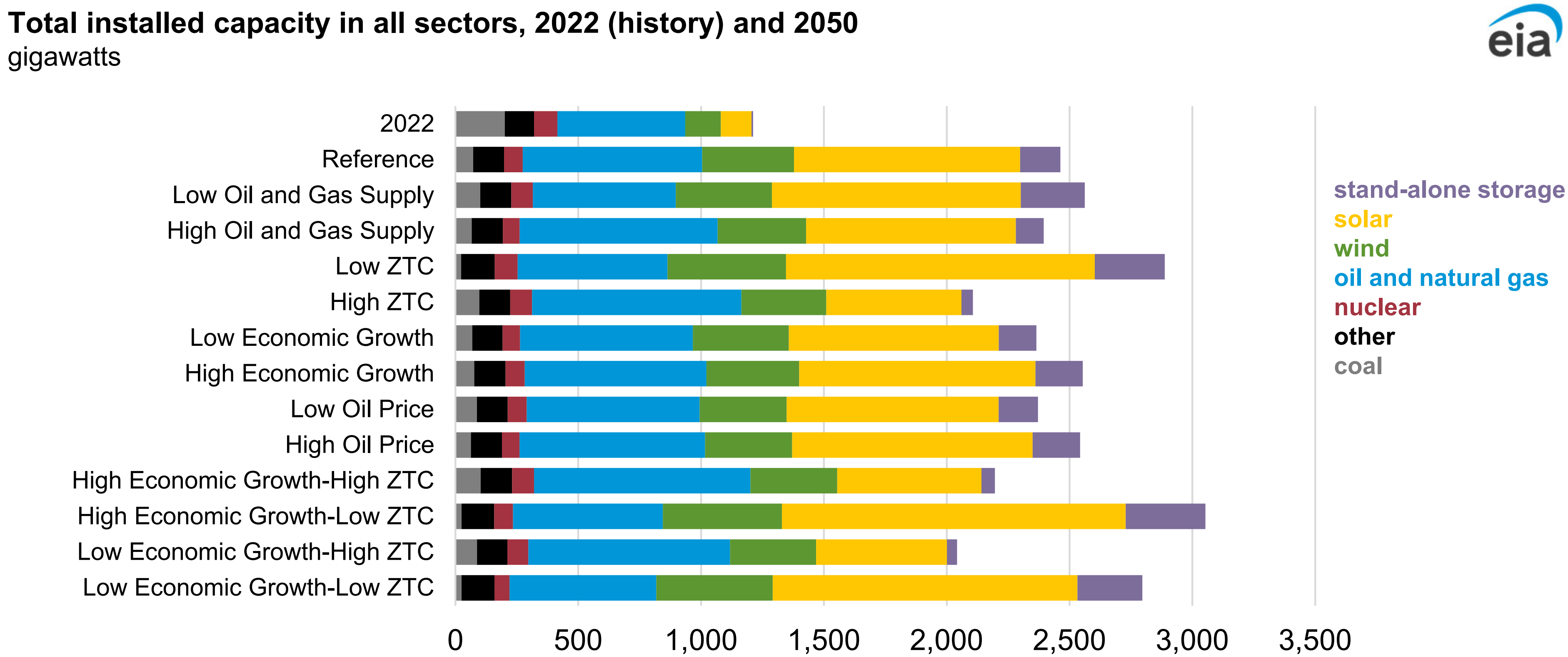

Data source: U.S. Energy Information Administration, *Annual Energy Outlook 2023* (AEO2023)

Note: ZTC=Zero-Carbon Technology Cost; other=geothermal, biomass, municipal waste, fuel cells, hydroelectric, pumped hydro storage.

Figure 4

Total renewables capacity in all sectors, 2022 (history) and 2050
gigawatts

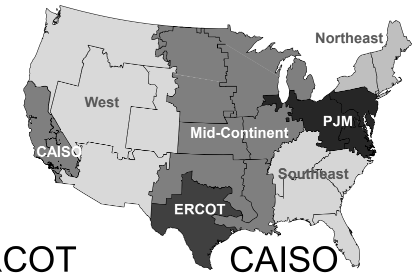

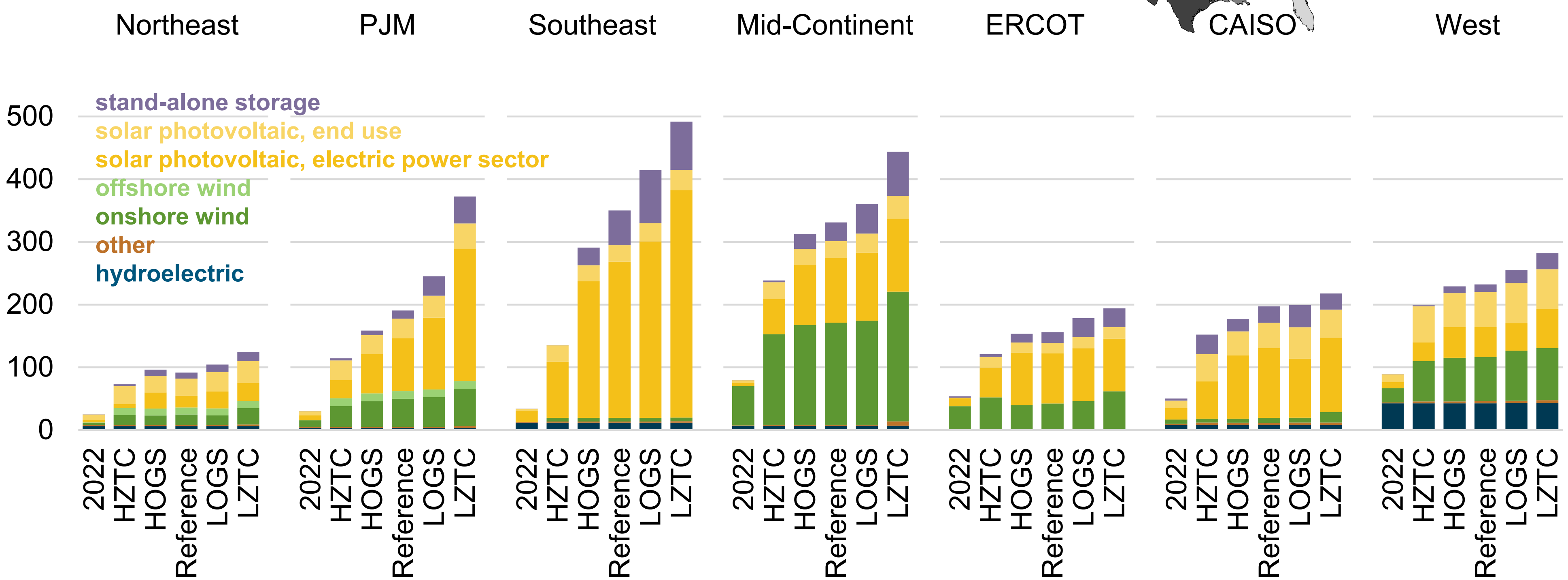

Data source: U.S. Energy Information Administration, *Annual Energy Outlook 2023* (AEO2023)

Note: HZTC=High Zero-Carbon Technology Cost; LZTC=Low Zero-Carbon Technology Cost; HOGS=High Oil & Gas Supply; LOGS=Low Oil & Gas Supply; other=geothermal, biomass, municipal waste.

Figure 5

Hourly U.S. electricity generation and load by fuel for selected cases and representative years
billion kilowatthours

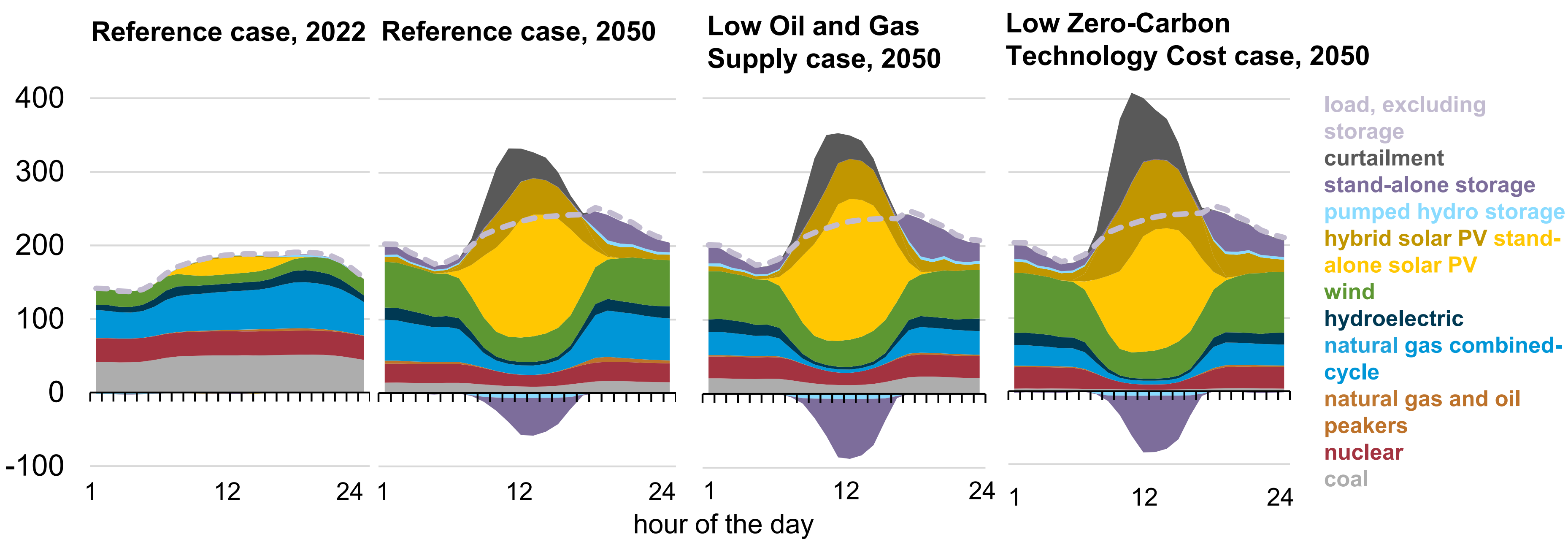

Data source: U.S. Energy Information Administration, *Annual Energy Outlook 2023* (AEO2023)
Note: Negative generation represents charging of energy storage technologies such as pumped hydro storage and battery storage. Hourly dispatch estimates are illustrative and are developed to determine curtailment and storage operations; final dispatch estimates are developed separately and may differ from total utilization as this figure shows. Standalone solar photovoltaic (PV) includes both utility-scale and end-use PV electricity generation.

Technical Note 1: Renewable costs and deployment

Overnight installation cost

Reference case
2022 dollars per kilowatt

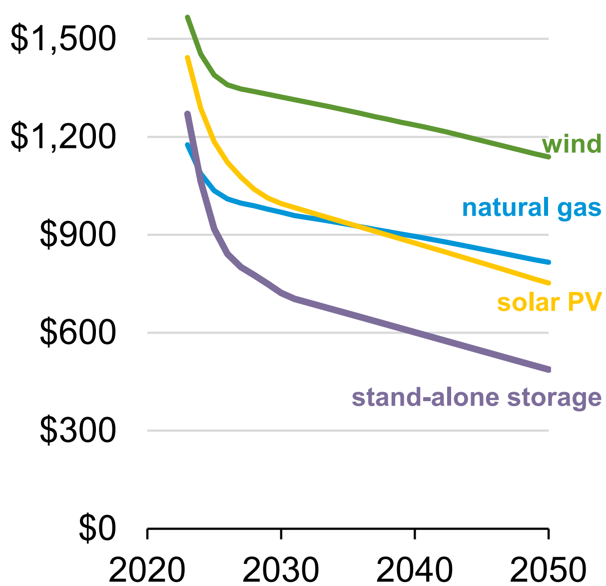

Low Zero-Carbon Technology Cost case
2022 dollars per kilowatt

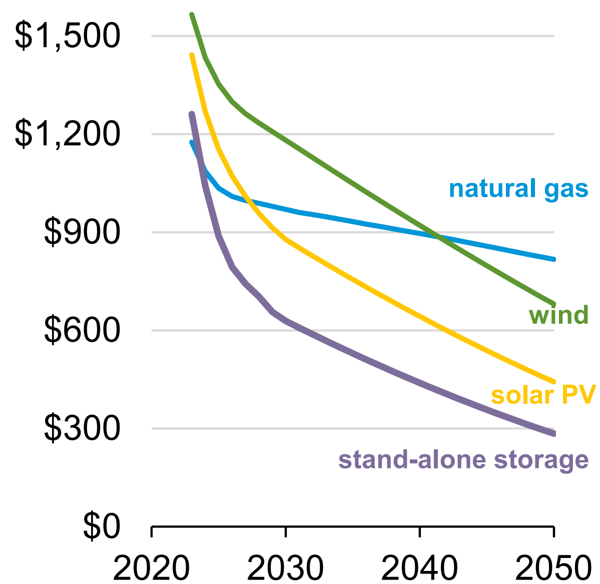

High Zero-Carbon Technology Cost case
2022 dollars per kilowatt

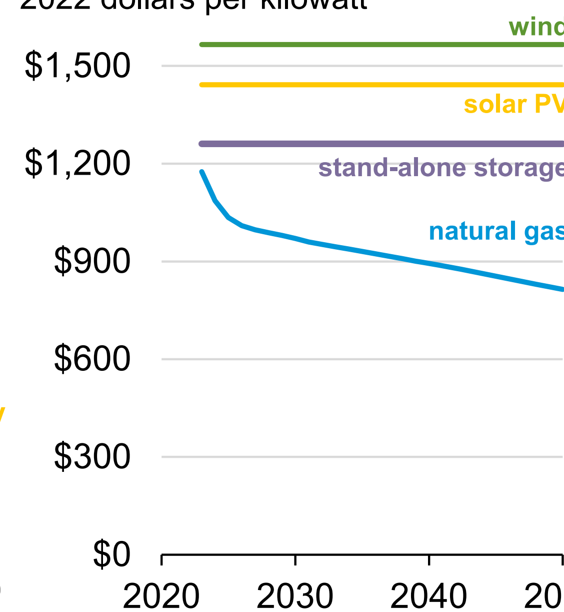

Data source: U.S. Energy Information Administration, *Annual Energy Outlook 2023* (AEO2023)
Note: Series in all charts begin in 2023. Overnight installation cost for natural gas refers to combined-cycle, multi-shaft technologies. Nuclear costs decline in the Reference and Low Zero-Carbon Technology cases, but they are not shown given the large differences in absolute cost compared with renewables. In the Reference case, nuclear begins at $7,900 per kilowatt (kW) and declines to $5,000/kW in 2050. In the Low Zero-Carbon Technology case, the cost of nuclear declines to $3,000/kW in 2050. Solar PV= stand-alone solar photovoltaic.

Figure 6

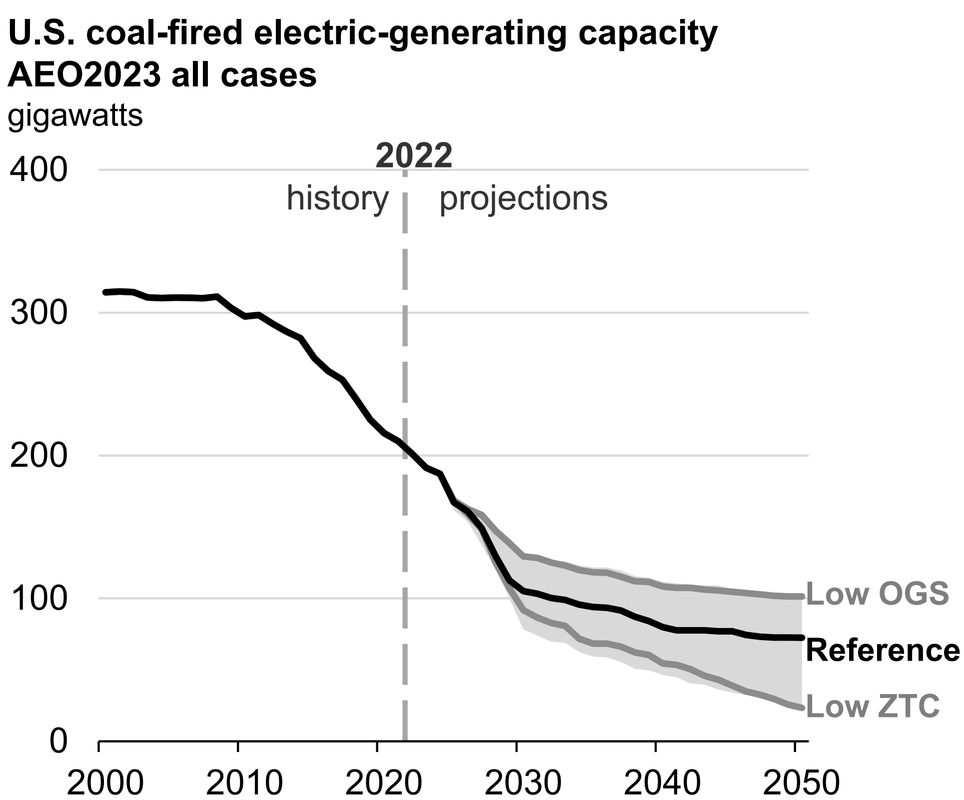

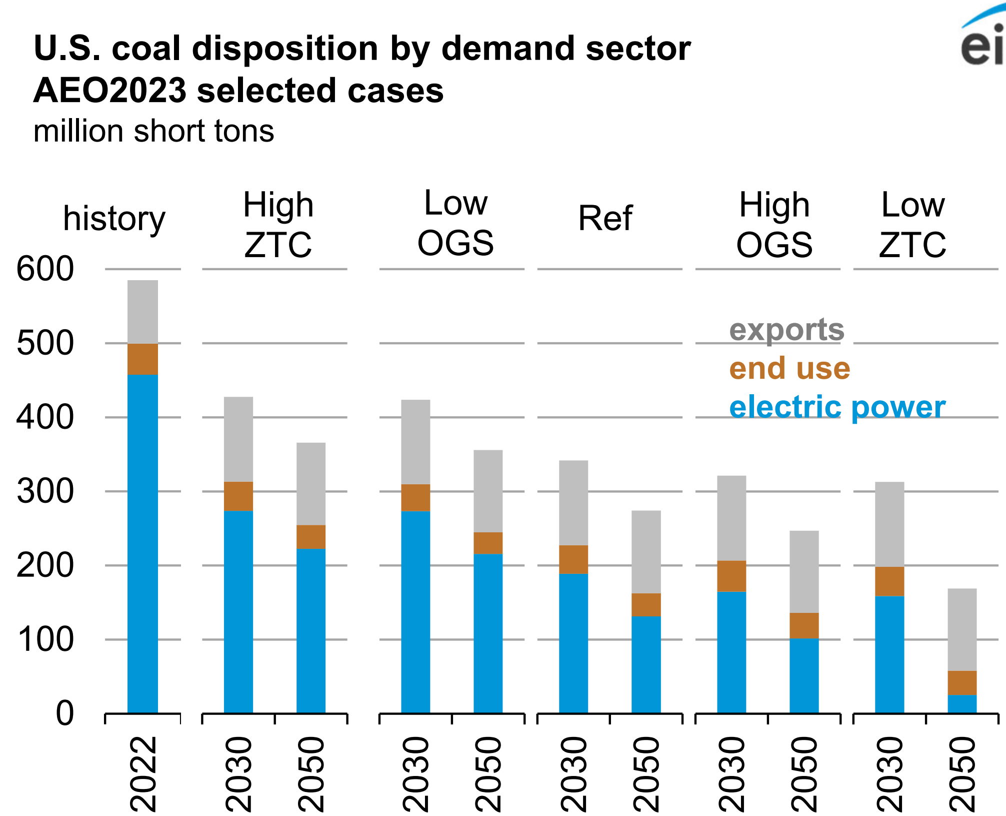

Data source: U.S. Energy Information Administration, *Annual Energy Outlook 2023* (AEO2023)
Note: Shaded regions represent maximum and minimum values for each projection year across the AEO2023 Reference case and side cases.
ZTC=Zero-Carbon Technology Cost; Ref=Reference case; OGS=Oil and Gas Supply.

Figure 7

Total energy consumption by end-use sector
quadrillion British thermal units

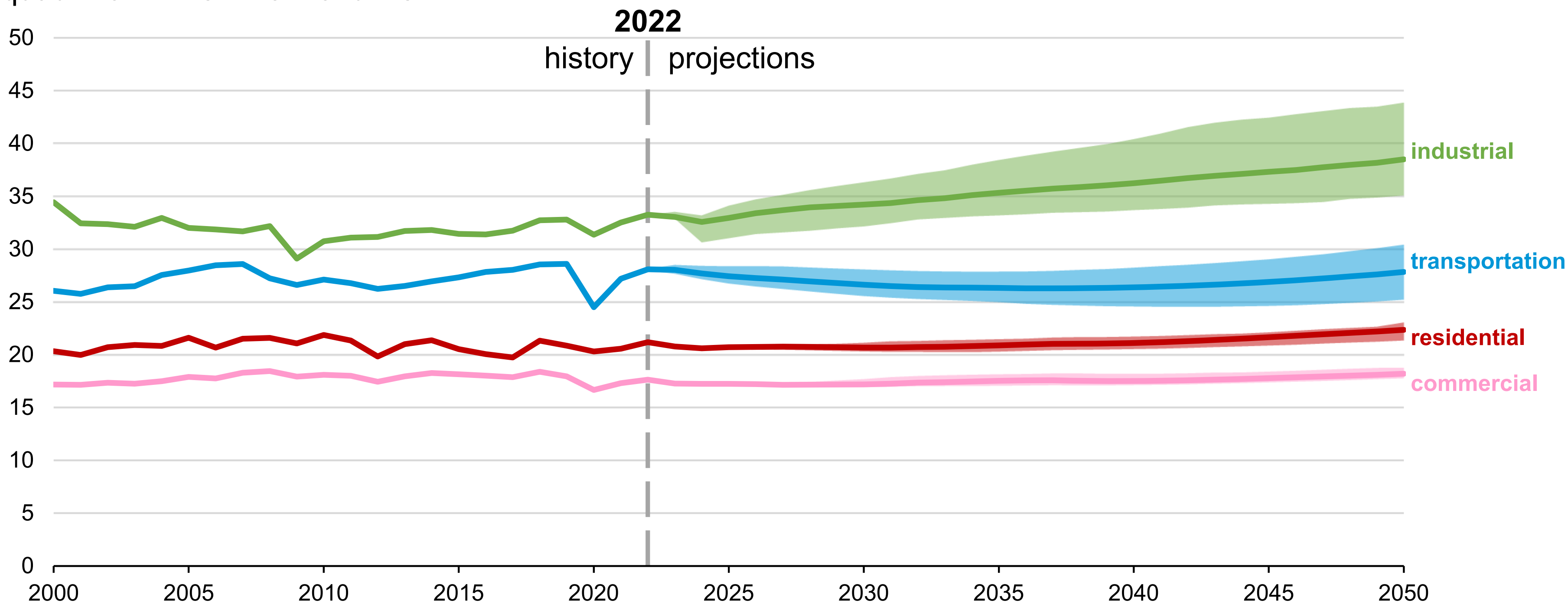

Data source: U.S. Energy Information Administration, *Annual Energy Outlook 2023* (AEO2023)
Note: Total consumption in end-use sectors includes purchased electricity and electricity-related losses. Each line represents AEO2023 Reference case projections. Shaded regions represent maximum and minimum values for each projection year across the AEO2023 Reference case and side cases.

Figure 8

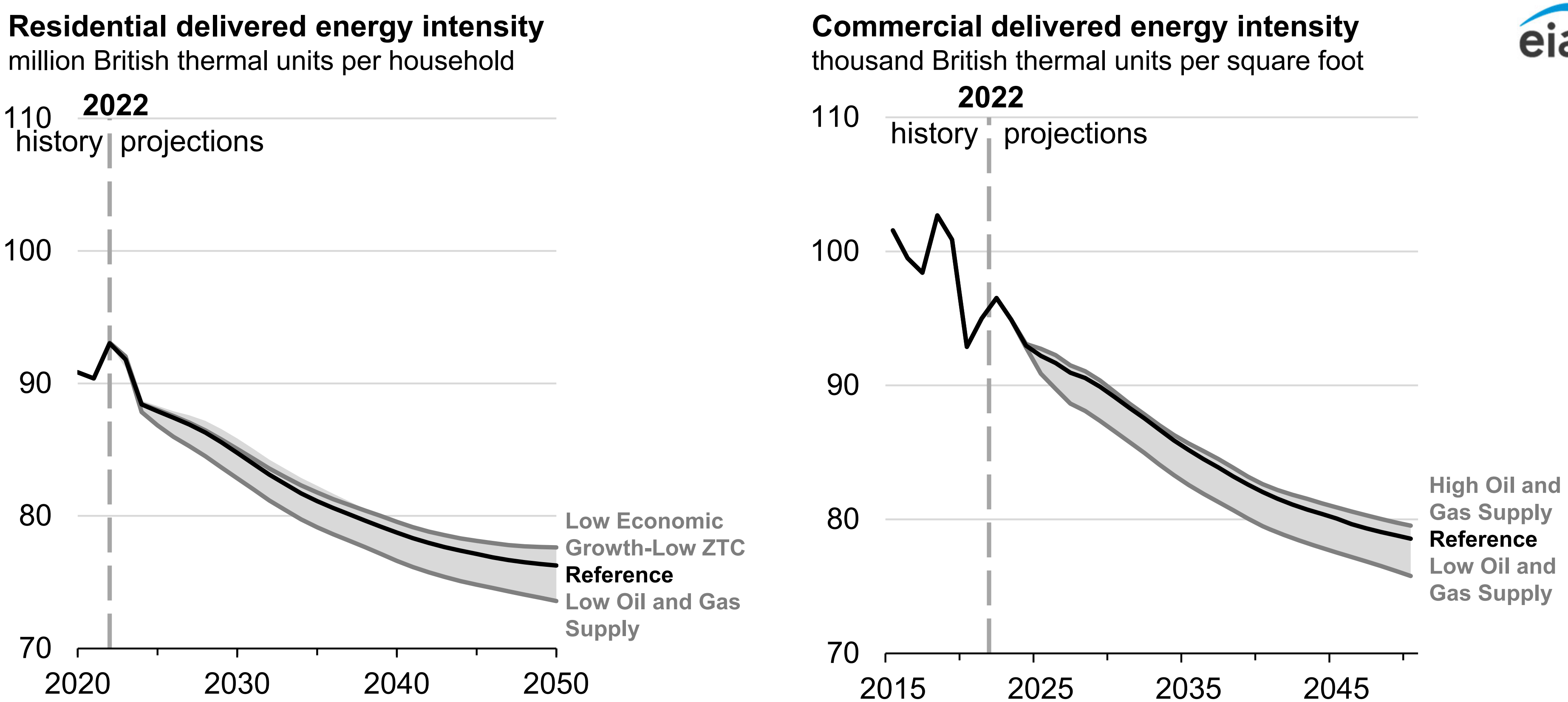

Data source: U.S. Energy Information Administration, *Annual Energy Outlook 2023* (AEO2023)
Note: Shaded regions represent maximum and minimum values for each projection year across the AEO2023 Reference case and side cases.
ZTC=Zero-Carbon Technology Cost.

Figure 9

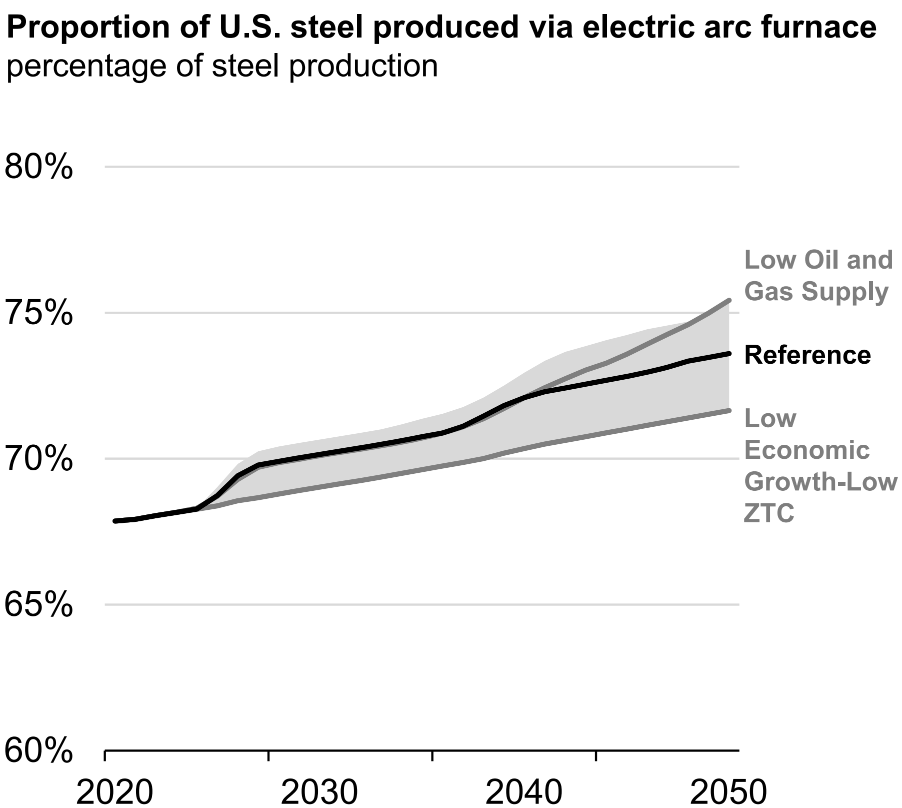

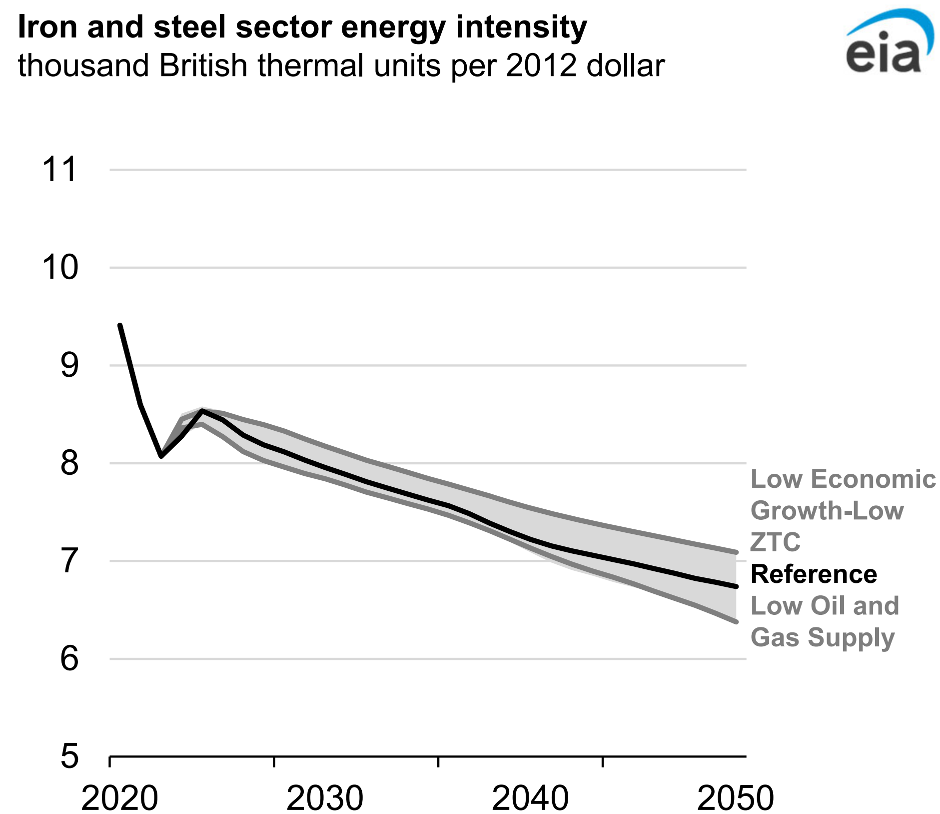

Data source: U.S. Energy Information Administration, *Annual Energy Outlook 2023* (AEO2023)
Note: All displayed data are projections. Shaded regions represent maximum and minimum values for each projection year across the AEO2023 Reference case and side cases. ZTC=Zero-Carbon Technology Cost.

Figure 10

Light-duty vehicle average fuel economy
miles per gallon gasoline equivalent

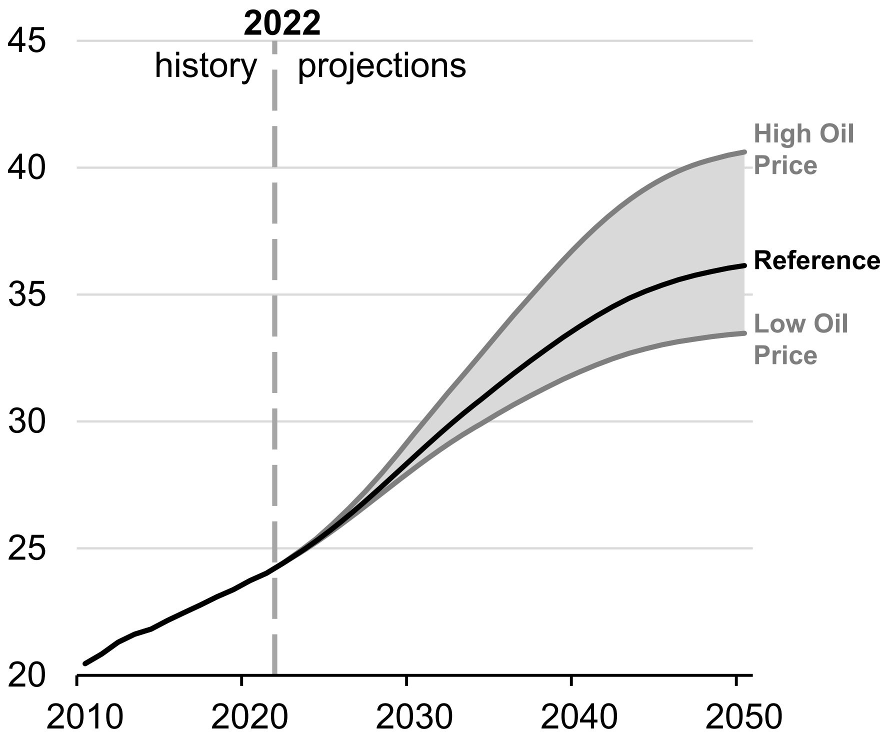

Market share of electric light-duty vehicles*
percentage of sales

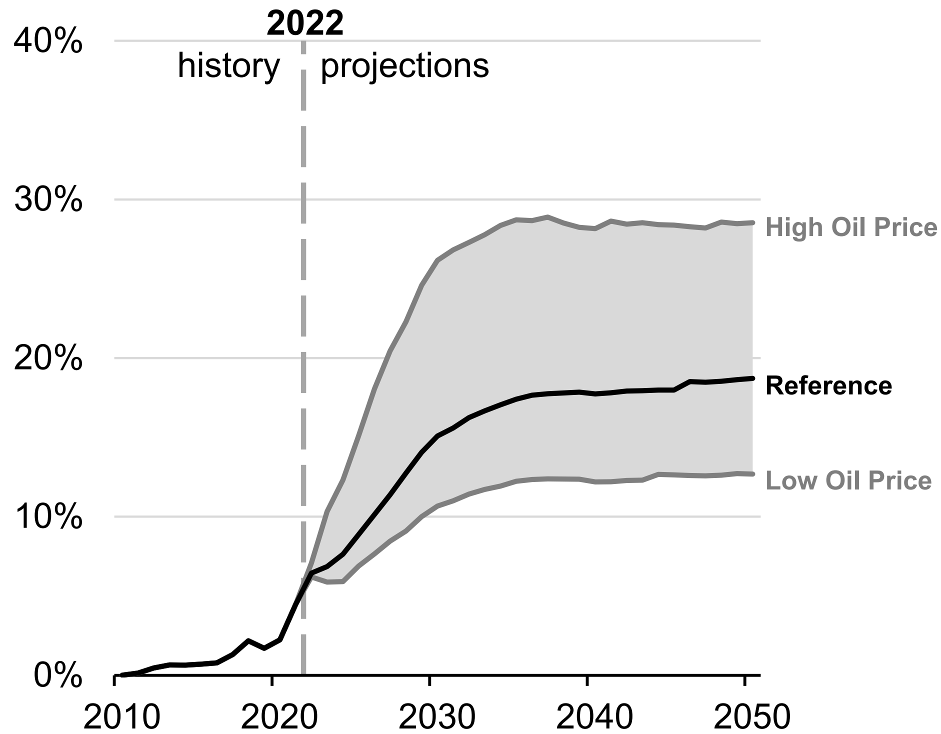

Data source: U.S. Energy Information Administration, *Annual Energy Outlook 2023* (AEO2023)
Note: *Includes battery electric and plug-in hybrid electric vehicles. Shaded regions represent maximum and minimum values for each projection year across the AEO2023 Reference case and side cases.

Figure 11

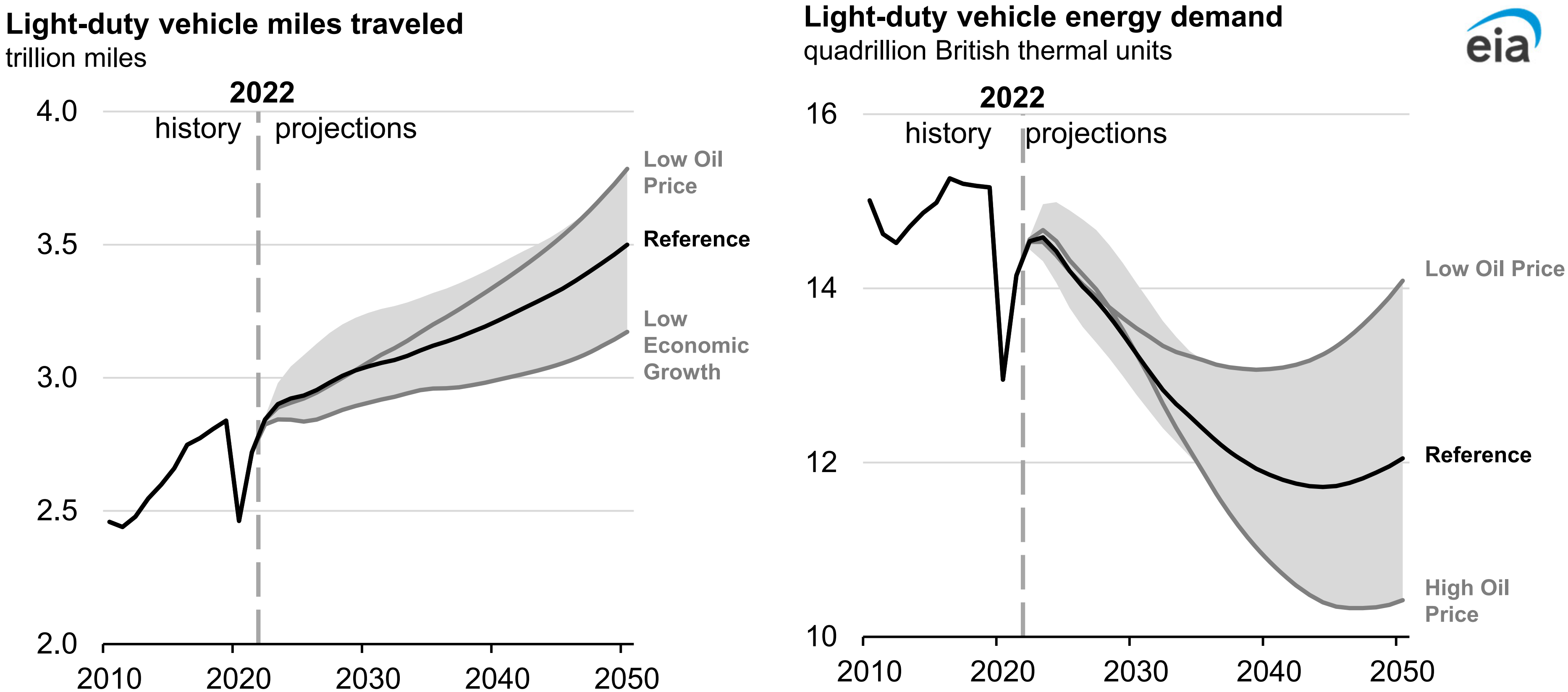

Data source: U.S. Energy Information Administration, *Annual Energy Outlook 2023* (AEO2023)
Note: Shaded regions represent maximum and minimum values for each projection year across the AEO2023 Reference case and side cases. Right hand chart includes delivered energy, specifically energy consumed on board the vehicle; it does not include losses between car and charger.

Figure 12

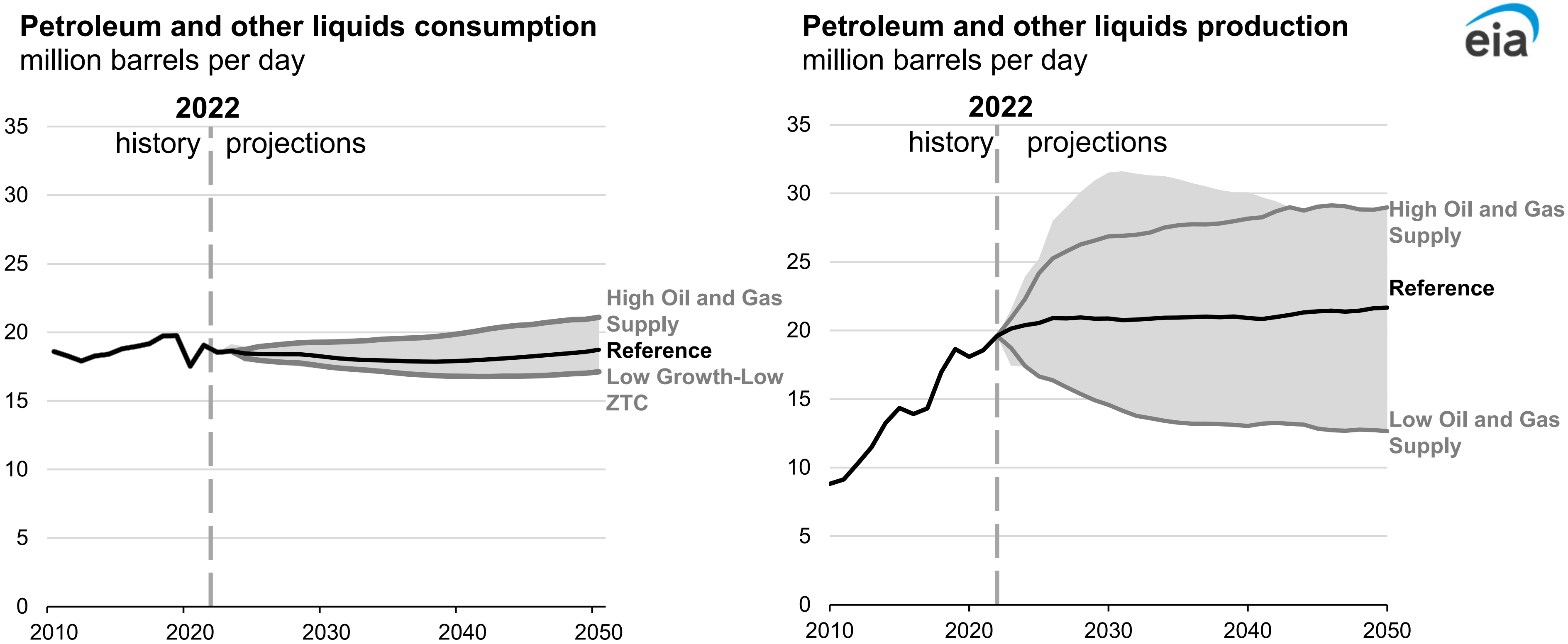

Data source: U.S. Energy Information Administration, *Annual Energy Outlook 2023* (AEO2023)
Note: Biofuels are not included in *petroleum and other liquids* production or consumption. Shaded regions represent maximum and minimum values for each projection year across the AEO2023 Reference case and side cases. ZTC=Zero-Carbon Technology Cost.

Figure 13

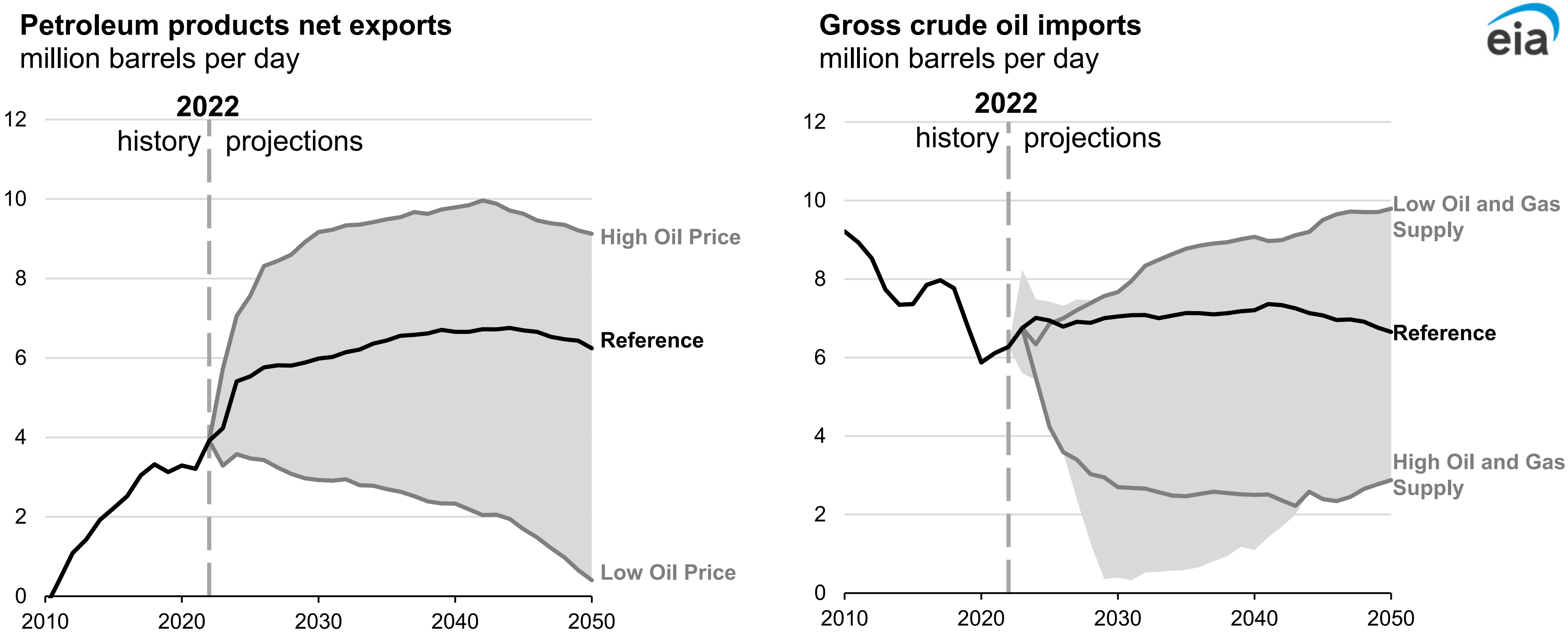

Data source: U.S. Energy Information Administration, *Annual Energy Outlook 2023* (AEO2023)
Note: Shaded regions represent maximum and minimum values for each projection year across the AEO2023 Reference case and side cases.

Figure 14

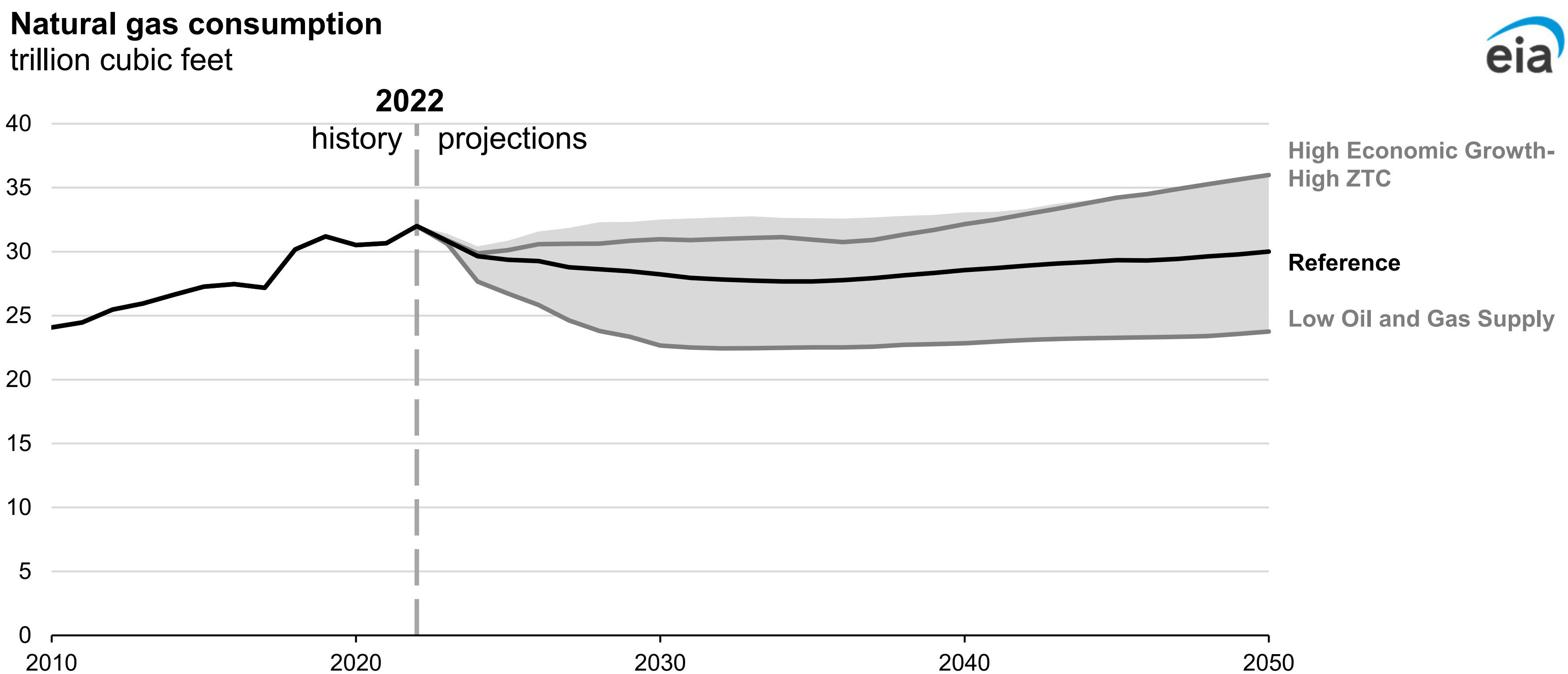

Data source: U.S. Energy Information Administration, *Annual Energy Outlook 2023* (AEO2023)
Note: Shaded regions represent maximum and minimum values for each projection year across the AEO2023 Reference case and side cases. ZTC=Zero-Carbon Technology Cost.

Figure 15

Natural gas consumption in industrial sector
trillion cubic feet

Natural gas consumption in electric power sector
trillion cubic feet

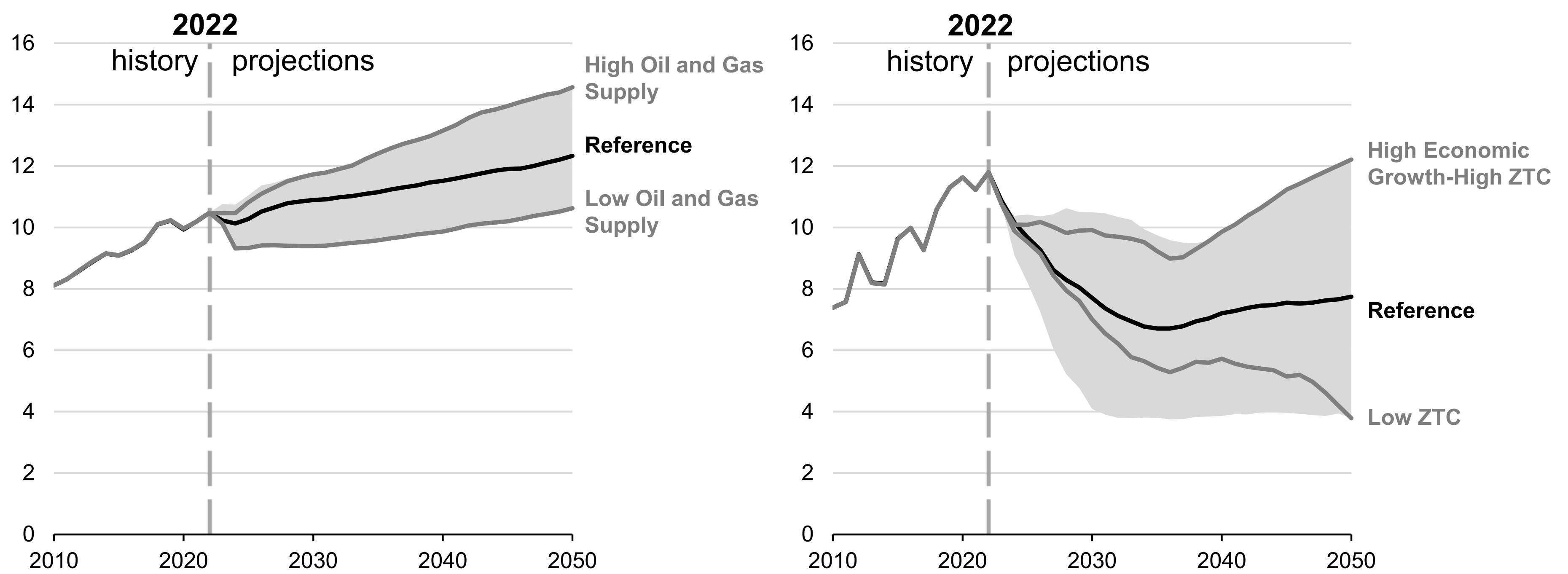

Data source: U.S. Energy Information Administration, *Annual Energy Outlook 2023* (AEO2023)
Note: Shaded regions represent maximum and minimum values for each projection year across the AEO2023 Reference case and side cases. ZTC=Zero-Carbon Technology Cost.

Figure 16

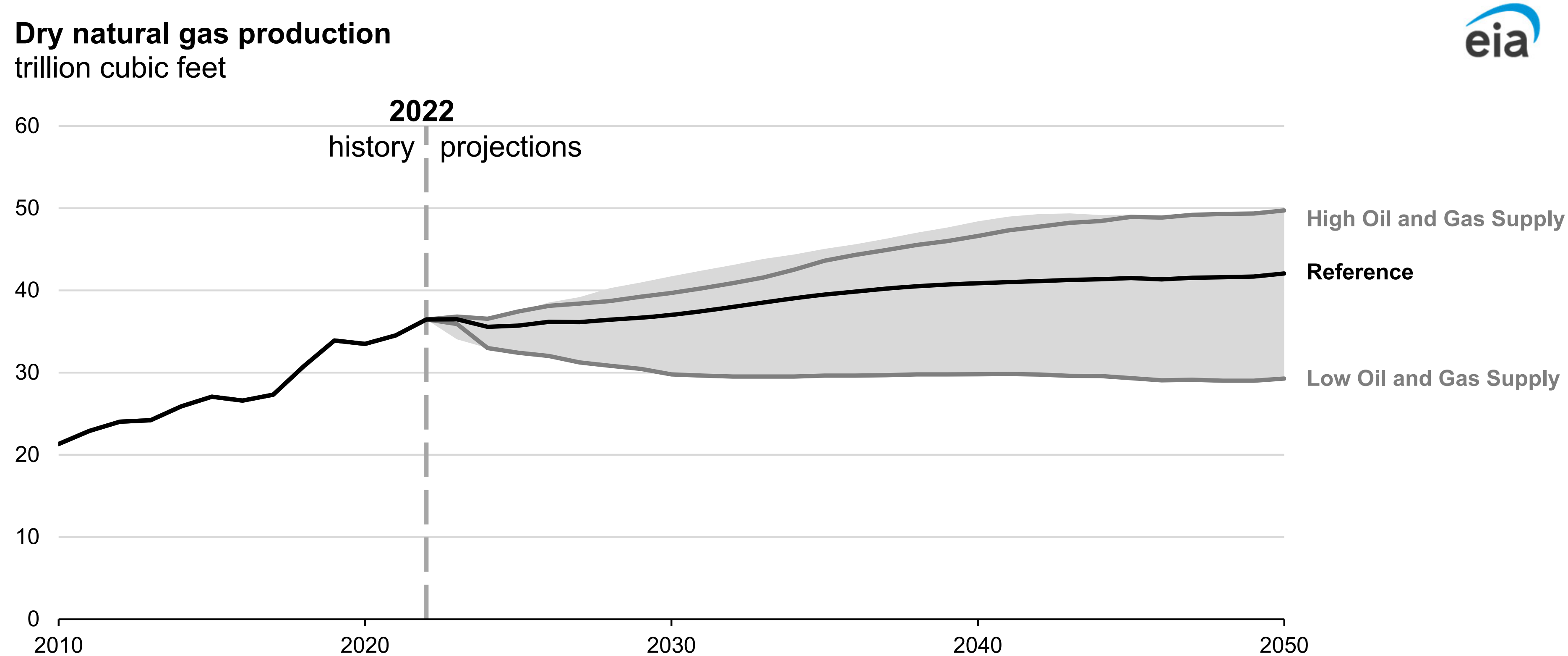

Data source: U.S. Energy Information Administration, *Annual Energy Outlook 2023* (AEO2023)
Note: Shaded regions represent maximum and minimum values for each projection year across the AEO2023 Reference case and side cases.

Figure 17

Liquefied natural gas exports
trillion cubic feet

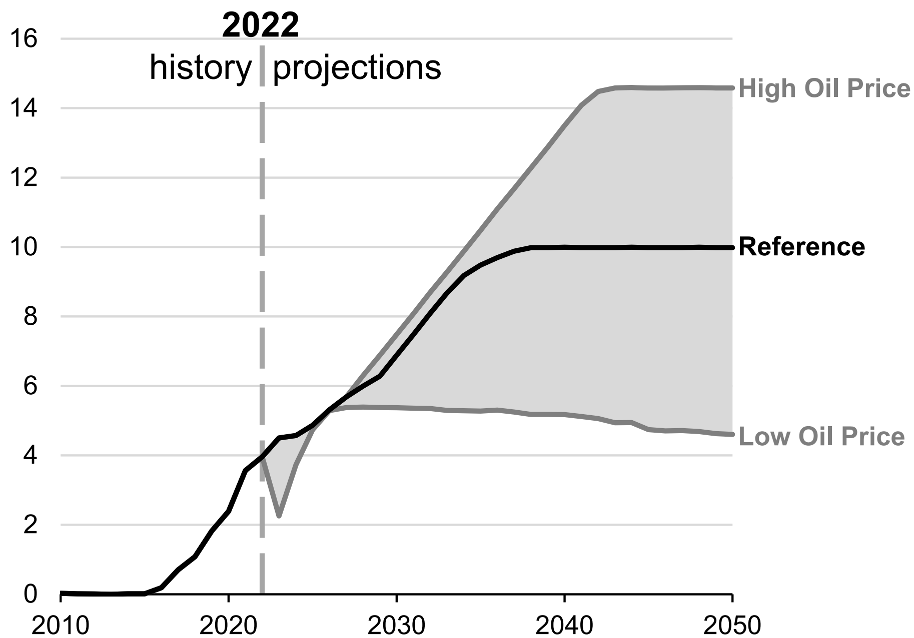

Ratio of Brent price to natural gas price at Henry Hub
Brent price/Henry Hub price (energy-equivalent terms)

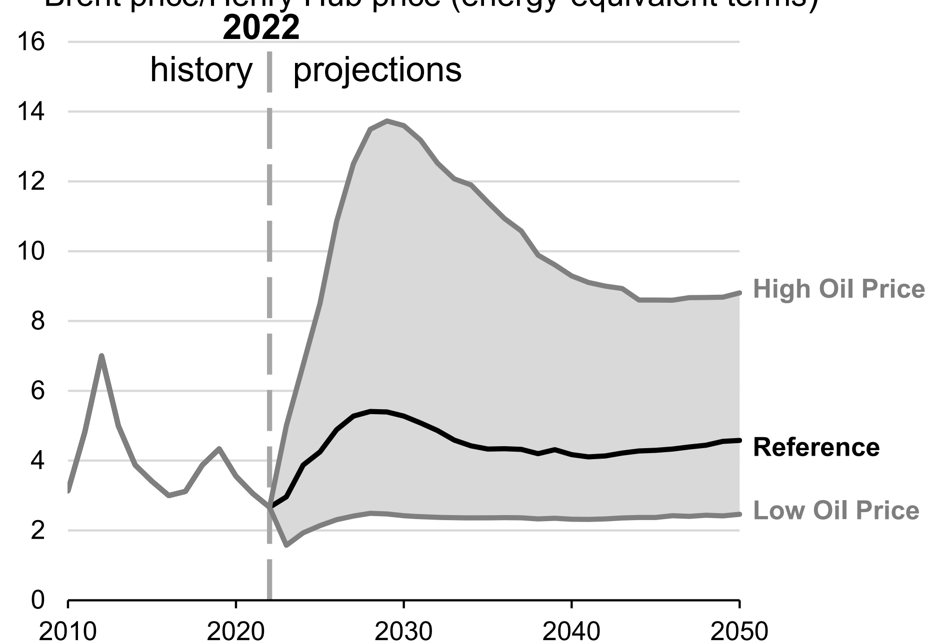

Data source: U.S. Energy Information Administration, *Annual Energy Outlook 2023* (AEO2023)
Note: Shaded regions represent maximum and minimum values for each projection year across the AEO2023 Reference case and side cases.

Figure 18

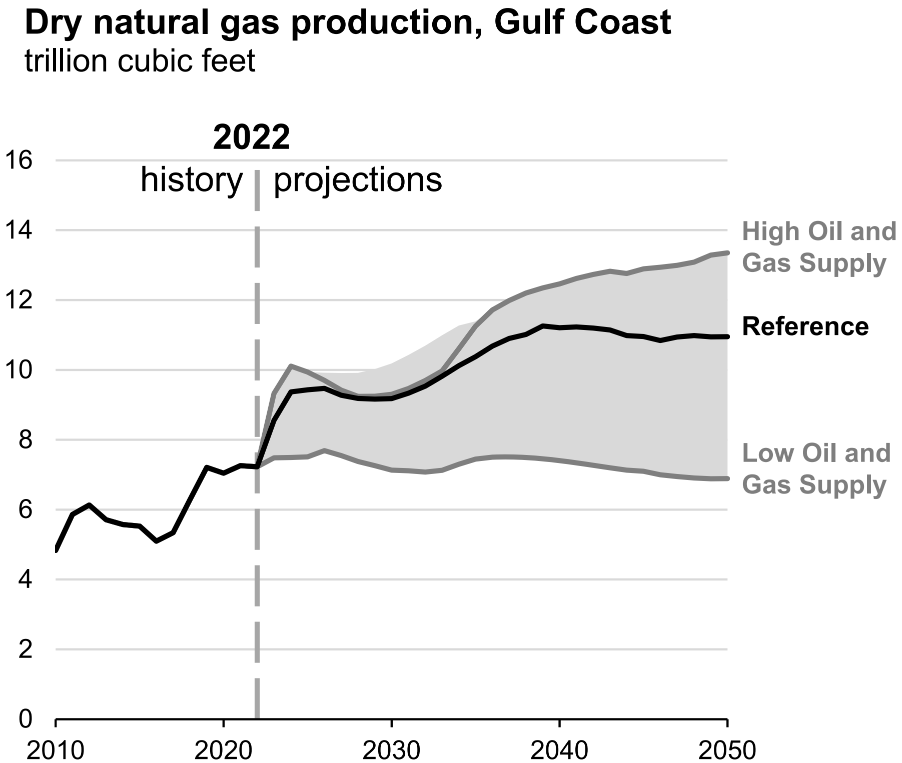

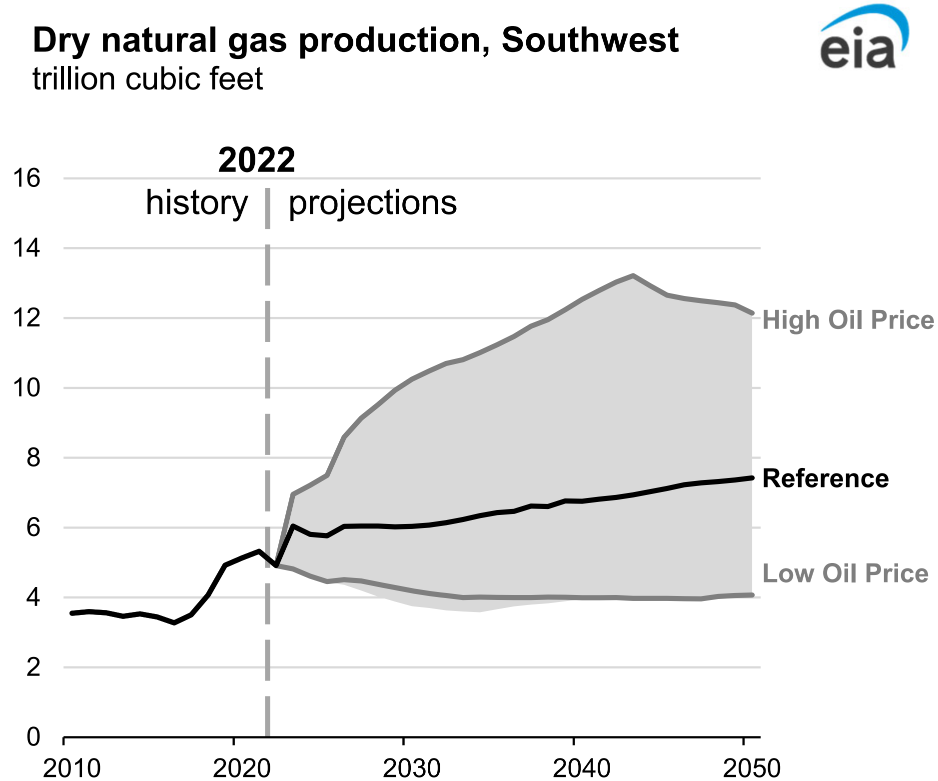

Data source: U.S. Energy Information Administration, *Annual Energy Outlook 2023* (AEO2023)
Note: Shaded regions represent maximum and minimum values for each projection year across the AEO2023 Reference case and side cases.

Figure 19

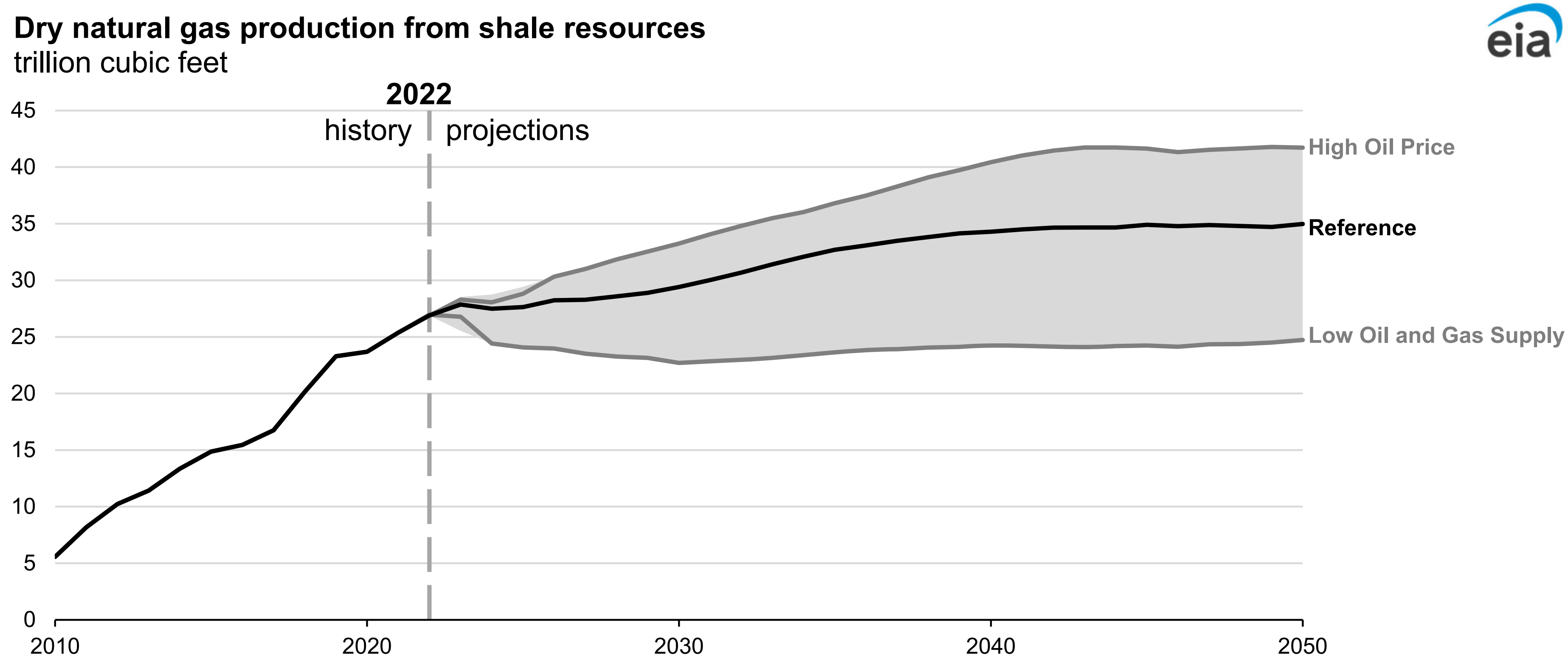

Data source: U.S. Energy Information Administration, *Annual Energy Outlook 2023* (AEO2023)
Note: Shaded regions represent maximum and minimum values for each projection year across the AEO2023 Reference case and side cases.

Figure 20

Total energy-related carbon dioxide emissions
million metric tons

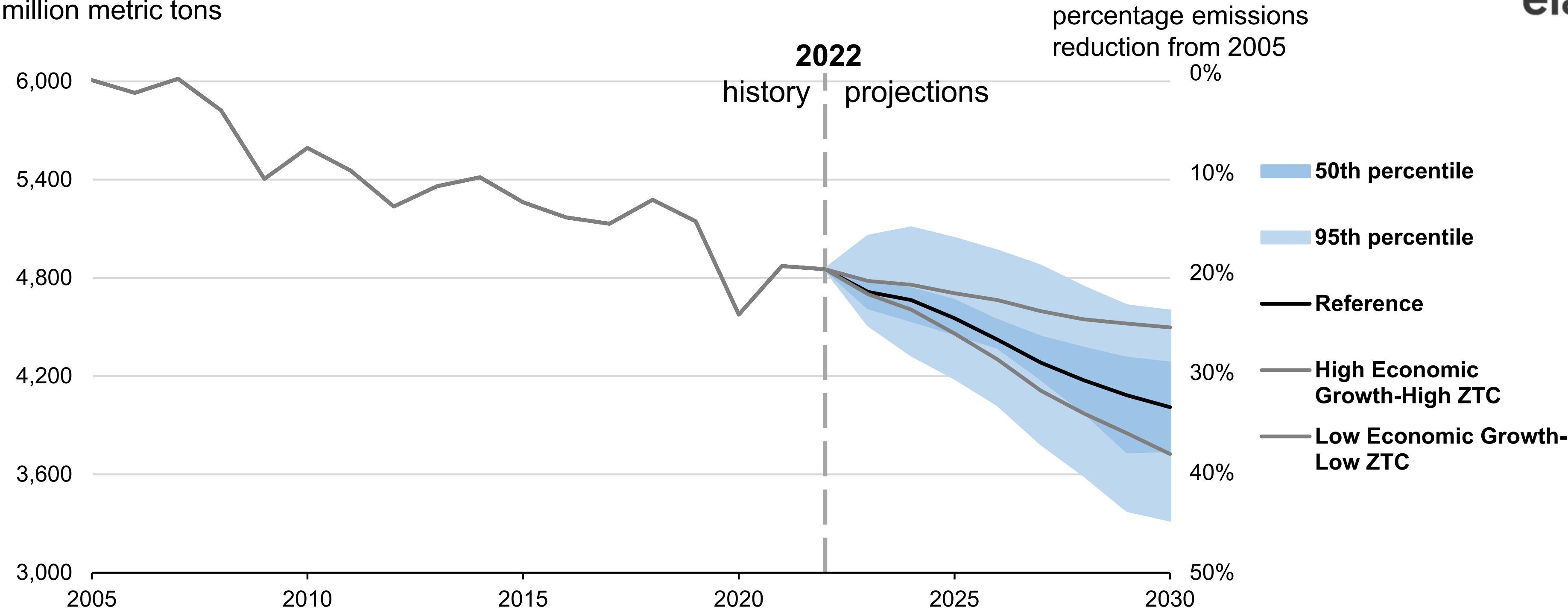

Data source: U.S. Energy Information Administration, *Annual Energy Outlook 2023* (AEO2023)
Note: Cone of uncertainty associated with total energy-related CO_2 emissions using empirical projection intervals. Historical values and AEO2023 Reference case are displayed as solid black line. The projection error density forecast by blue shaded areas. The different shades correspond to the 50th and 95th percentiles. AEO2023 envelope side cases are in solid grey lines. ZTC=Zero-Carbon Technology Cost.

Independent Statistics and Analysis
U.S. Energy Information Administration

Annual Energy Outlook

AEO2023

The U.S. Energy Information Administration (EIA), the statistical and analytical agency within the U.S. Department of Energy (DOE), prepared this report. By law, our data, analyses, and forecasts are independent of approval by any other officer or employee of the U.S. Government. The views in this report do not represent those of DOE or any other federal agencies.

Table of Contents

Table of Figures

Administrator's Foreword

After a 23-year hiatus, I am reintroducing the Administrator's Foreword as part of the *Annual Energy Outlook* (AEO). The Foreword affords me an opportunity to provide context and outline future directions for one of our flagship products.

The U.S. energy system is rapidly changing. In recent years, technology innovation has accelerated the deployment of renewable energy, expanded markets for electric vehicles, and established record-high levels of petroleum and natural gas production. Heightened geopolitical risks have also influenced the energy system. And this year, recent federal legislation authorizes historic levels of investment in clean energy technology.

Ideally, we would model these dynamics to produce precise numerical forecasts that demonstrate how energy prices, technology deployment, and emissions will shift over time. Unfortunately, such precise forecasts are not possible. The 30-year decision landscape we model is too complex and uncertain. Thus, our objective must be to identify robust insights rather than precise numbers—think ranges and trends, not predictions and point estimates.

The AEO includes a series of projections—which we refer to as *cases*—each with different input assumptions that represent alternative views of how uncertainty may be resolved in the future. The Reference case represents our best guess under nominal conditions, which presumes no new policy or laws over the modeled time horizon. It's best to think of the Reference case as the experimental control: a baseline against which we can judge the other cases. Although the Reference case serves as an important benchmark, judgments about energy futures should never be based on a single projection. The AEO side cases represent plausible variations in key input assumptions that tend to drive the largest changes in projected outputs from the Reference case. This year's AEO narrative focuses on the full set of modeled cases in order to derive insights about our collective energy future.

Among the uncertainties we must confront, the timing, structure, and targets associated with yet-to-be-developed policy are the most uncertain. We only consider current laws and regulations across all modeled cases in this AEO. For some readers, this approach may be unsatisfying because policy rarely remains static for long periods. But this AEO should be considered part of an iterative policymaking process rather than apart from it; it gives decision-makers an opportunity to peer into a future without new policy. If the projected outcomes are undesirable from their viewpoint, they can effect change.

Changes to This Year's Edition

This year's edition of the *Annual Energy Outlook* includes three enhancements that improve the characterization of future uncertainty and provide more technical details on the model results.

Combination cases

Although the AEO core side cases address key uncertainties, each case represents a one-factor change to the Reference case. But, real energy markets often surprise us in more ways than one, particularly over the decades-long timeframes modeled in the AEO. In this year's edition, we include cases that combine assumptions from our macroeconomic and zero-carbon technology cost cases. These new cases reflect a combination of demand-side changes (macroeconomic growth affecting energy demand) and supply-side changes (renewables costs affecting generating capacity deployment) to expand the range of projections in the *Annual Energy Outlook*.

Visualizing uncertainty

Running a set of cases is not enough: how we present and discuss them within the report affects the insights that our readers draw from the analysis. Although the Reference case is an important benchmark, each case represents a possible alternative. So, in each of the figures in this report, you will see shaded areas that represent the range of results obtained across the modeled cases. Uncertainty can be characterized in many other ways beyond the analysis of multiple cases. One way, presented in the discussion section, uses deviations between realized and projected values drawn from previous AEO editions to derive a cone of uncertainty for future energy-related CO_2 emissions. Looking ahead, you should expect to see more innovation in how we treat uncertainty.

Technical notes

The narrative tends to focus on model-based results. We recognize that some readers want a deeper technical explanation around key issues. Although we describe our modeling approach elsewhere, how the model formulation and input assumptions influence the results is not always clear. To better explain key results, we included a series of technical notes in the narrative that focus on heat pump deployment, cost projections for renewables, electric vehicle deployment, and crude oil trade.

Future Work

At EIA, we are also pursuing broader changes to our long-term modeling efforts. I would like to highlight three such efforts.

Open-source code

One of our priorities at EIA is to make our data and model-based analysis as transparent and accessible as possible. We are working to make the National Energy Modeling System (NEMS) publicly available in GitHub under a permissive, open-source license, and we hope to complete this effort later this year. Making our models open source allows users to examine, reuse, and redistribute our code under clear legal guidelines. Giving you this kind of access is important to the learning and discovery process associated with energy modeling.

Expanded scenario range

Building on the combination cases in this year's AEO, we are expanding our capability to model a wider range of future scenarios using NEMS. In particular, decision makers need objective and rigorous assessments of net zero emissions pathways to inform ongoing policy discussions. We are working to incorporate novel fuel and technology pathways into NEMS and to appropriately treat uncertainty around technologies with limited commercial deployment.

A next-generation, open-source modeling framework

Although regularly updated, we have been using NEMS to produce the AEO since 1994—a span of nearly three decades that has born witness to significant changes in the real energy system, energy modeling methods, and software development practices. Moving forward, we need a flexible, next-generation modeling framework that can rapidly assess the cost, emissions, reliability, security, and community-level impacts associated with a number of contemporary energy issues. Some of these issues include pathways to a net-zero energy system, supply chain risks, rapid technology innovation, and shifting trade patterns. This modeling system will also be open source to promote transparency and encourage innovation within the modeling community. We've begun discussing this new framework, and I look forward to sharing our progress throughout my tenure as EIA Administrator.

In Closing

I'd like to thank our long-term modelers for their willingness to take on new directions and their tremendous effort to produce this year's AEO. I am very excited by the future work outlined above, and I feel privileged to help lead such a talented team of energy modelers.

Executive Summary

Our *Annual Energy Outlook* 2023 (AEO2023) explores long-term energy trends in the United States. Since last year's AEO, much has changed, most notably the passage of the Inflation Reduction Act (IRA), Public Law 117–169, which altered the policy landscape we use to develop our projections.

Energy-related CO_2 emissions fall across all AEO2023 cases because of increased electrification, higher equipment efficiencies, and more zero-carbon electricity generation.

We project that U.S. energy-related CO_2 emissions drop 25% to 38% below the 2005 level by 2030. For reference, the United States' *nationally determined contribution* (NDC), submitted as part of the Paris Agreement, calls for a target of 50% to 52% of net greenhouse gas emissions below the 2005 level by 2030.[1] We only consider energy-related CO_2 emissions, which does not cover the full NDC scope. Total energy-related CO_2 emissions in 2050 declined by 17% in this year's Reference case compared with last year's. Some of the primary factors that contributed to the change in our base case include the IRA, updates to technology costs and performance across the energy system, and changes in the macroeconomic outlook. All AEO2023 cases assume current laws and regulations, and compared with last year's AEO, there is a significant shift toward lower future emissions. The IRA represents a complex piece of legislation, and we could not model all provisions given model structure and uncertainty over select implementation details. The appendix includes a detailed accounting of IRA provisions and how we addressed them. To further explore possible emissions reductions, we also derive a cone of uncertainty based on an empirical analysis of our past projections and find that the energy-related CO_2 emissions reduction can be as high as 45% below 2005 levels in 2030.

Overall, our lower projected U.S. energy-related CO_2 emissions is driven by increased electrification, equipment efficiency, and renewable technologies for electricity generation. However, emissions reductions are limited by longer-term growth in U.S. transportation and industrial activity. As a result, these projected emissions reductions are most sensitive to our assumptions regarding economic growth and the cost of zero-carbon generation technology.

[1] The *nationally determined contribution* (NDC) is a formal submission to the United Nations Framework Convention on Climate Change. The United States submitted, "To achieve an economy-wide target of reducing its net greenhouse gas emissions by 50-52 percent below 2005 levels in 2030."

In AEO2023, we see stable growth in U.S. electric power demand through 2050 in all cases we considered because of increasing electrification and ongoing economic growth. The combination of declining capital costs and government subsidies, including IRA initiatives, drive rising renewable technologies for electricity generation, such as solar and wind. Once built and when the resource is available, wind and solar are the least cost resources to operate to meet electricity demand because they have zero fuel costs. Over time, the combined investment and operating cost advantage increases the share of zero-carbon electricity generation. As a result, in AEO2023, we see renewable generating capacity growing in all regions of the United States in all cases. Across all cases, compared with 2022, solar generating capacity grows by about 325% to 1019% by 2050, and wind generating capacity grows by about 138% to 235%. We see growth in installed battery capacity in all cases to support this growth in renewables. Across the span of AEO cases, relative to 2022, natural gas generating capacity ranges from an increase of between 20% to 87% through 2050.

Renewable generating capacity grows in all regions of the United States in all AEO2023 cases, supported by growth in installed battery capacity.

Technological advancements and electrification drive projected decreases in demand-side energy intensity.

Not only is the U.S. electric power sector's composition changing, but we see increased electrification in the end-use sectors. We project more heat pumps and electric vehicles, as well as electric arc furnaces increasingly deployed in the iron and steel industry. In the residential and commercial sectors, higher equipment efficiencies and stricter building codes extend ongoing declines in energy intensity. Despite the growth in adopting heat pumps, natural gas-fired heating equipment, including furnaces and boilers, continue to account for the largest share of energy consumption for space heating in U.S. residential and commercial buildings across all cases through 2050. In the transportation sector, light-duty vehicle energy demand declines through 2045 as more electric vehicles are deployed and stricter Corporate Average Fuel Economy (CAFE) standards largely offset the continued growth in travel demand. The energy demand then increases as rising travel overcomes increasing efficiency. Across all cases, light-duty vehicle energy demand decreases by 3% to 28% in 2050 relative to 2022.

High international demand leads to continued growth in U.S. production, and combined with relatively little growth in domestic consumption, allows the United States to remain a net exporter of petroleum products and natural gas through 2050 in all AEO2023 cases.

Despite no significant change in domestic petroleum and other liquids consumption through 2040 across most AEO2023 cases, we expect U.S. production to remain historically high as exports of finished products grow in response to growing international demand. Despite the shift toward renewable sources and batteries in electricity generation, domestic natural gas consumption remains relatively stable—ending recent growth in most cases. Natural gas production, however, in some cases continues to grow in response to international demand for liquefied natural gas, supported by associated natural gas produced along with crude oil. Given the combination of relatively little growth in domestic consumption and continued growth in production, we project that the United States will remain a net exporter of petroleum products and natural gas through 2050 in all AEO2023 cases.

Introduction

The *Annual Energy Outlook* 2023 (AEO2023) explores long-term energy trends in the United States. Since we released the last AEO in early 2022, passage of the Inflation Reduction Act (IRA), Public Law 117–169, altered the policy landscape we use to develop our projections. The Appendix in this report explains our assumptions around IRA implementation and how we implemented the IRA in our AEO2023 cases. We are also releasing a separate *Issues in Focus* paper that explores how these assumptions affect our model-based projections. We have seen significant national and international short-term market volatility associated with economic growth as the world reemerges from the COVID-19 pandemic and political instability associated with Russia's full-scale invasion of Ukraine. We continuously monitor such developments and consider how they may affect our long-term projections.

AEO2023 includes a Reference case and 12 side cases that explore key areas of uncertainty about how energy markets will develop. We retooled our graphs to emphasize the range of results, denoted by shaded areas, across the full suite of modeled cases. We derive our key analytical insights by assessing the results across cases and examining how overall trends may vary under different assumptions. This year, we've added a discussion section focused on sources of uncertainty in the AEO2023 projections. We also now derive a cone of uncertainty associated with future energy-related CO_2 emissions using deviations between past projections and realized values.

By 2030, energy-related CO_2 emissions fall 25% to 38% below 2005 levels, depending on case assumptions

Under the Paris Agreement, the United States set a goal to reduce economy-wide greenhouse gas emissions by 50% to 52% of 2005 levels by 2030. We only consider energy-related CO_2 emissions, which does not cover the full NDC scope. We project lower U.S. energy-related CO_2 emissions in 2030 relative to 2005 in the AEO2023 Reference case and all side cases (Figure 1). CO_2 emissions are most sensitive to economic growth and assumptions related to the cost of zero-carbon generation technology. Combinations of these two sets of assumptions form the upper and lower bounds of projected CO_2 emissions. Emissions decrease by 25% in 2030 relative to 2005 under the combined high economic growth and high zero-carbon technology cost assumptions and by as much as 38% under low economic growth and low zero-carbon technology cost assumptions. Both of these cases hinge on specific assumptions regarding the relationship between economic growth and zero-carbon technology development.[2] In the High Economic Growth case, emissions fall initially and then begin to increase

[2] The purpose of the combination cases was to explore a wider range of outcomes. We did not explicitly consider the correlation or interaction between zero-carbon technology costs and economic growth. The High Economic Growth and High Zero-Carbon Technology Cost case assume this higher growth rate takes place without declining zero-carbon technology costs. Similarly, slower economic growth accompanies declining technology costs in the Low Economic Growth and Low Zero-Carbon Technology Cost case.

again in 2040 as industrial activity and travel (measured in vehicle miles traveled) increase, surpassing emissions reductions from the electric power sector.

Figure 1.

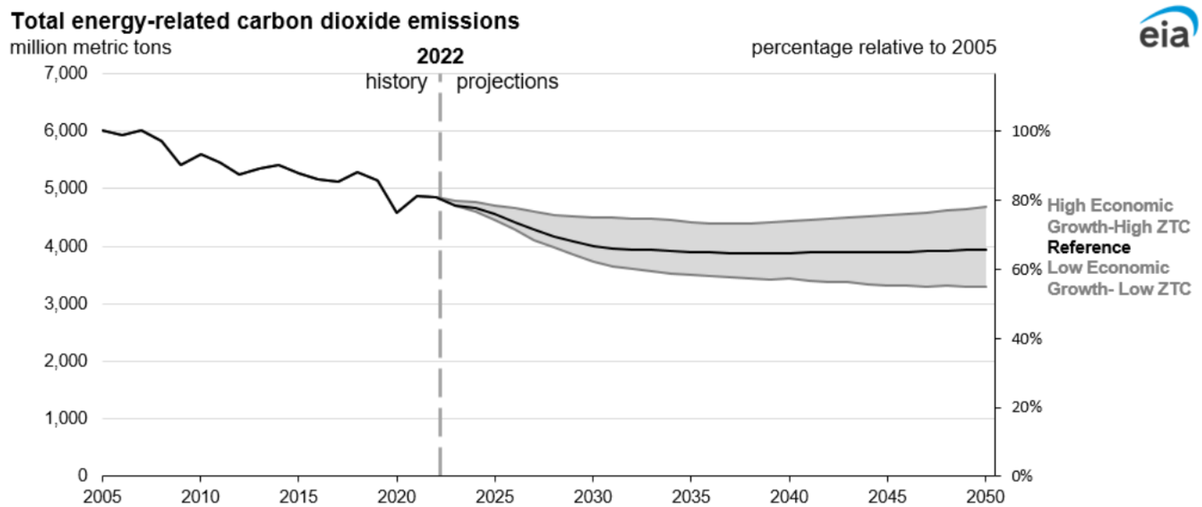

Data source: U.S. Energy Information Administration, *Annual Energy Outlook 2023* (AEO2023)
Note: Shaded regions represent maximum and minimum values for each projection year across the AEO2023 Reference case and side cases. ZTC=Zero-Carbon Technology Cost.

The largest variations in projected U.S. CO_2 emissions across cases occur in the electric power, transportation, and industrial sectors. Although economic growth assumptions affect consumption and, in turn, projected CO_2 emissions in all sectors, different case-specific assumptions affect sectors differently. For example, emissions from the electric power sector are particularly responsive to assumptions about the cost of zero-carbon technologies, and transportation sector emissions are sensitive to assumptions about fossil fuel supply and cost, particularly oil and petroleum products.

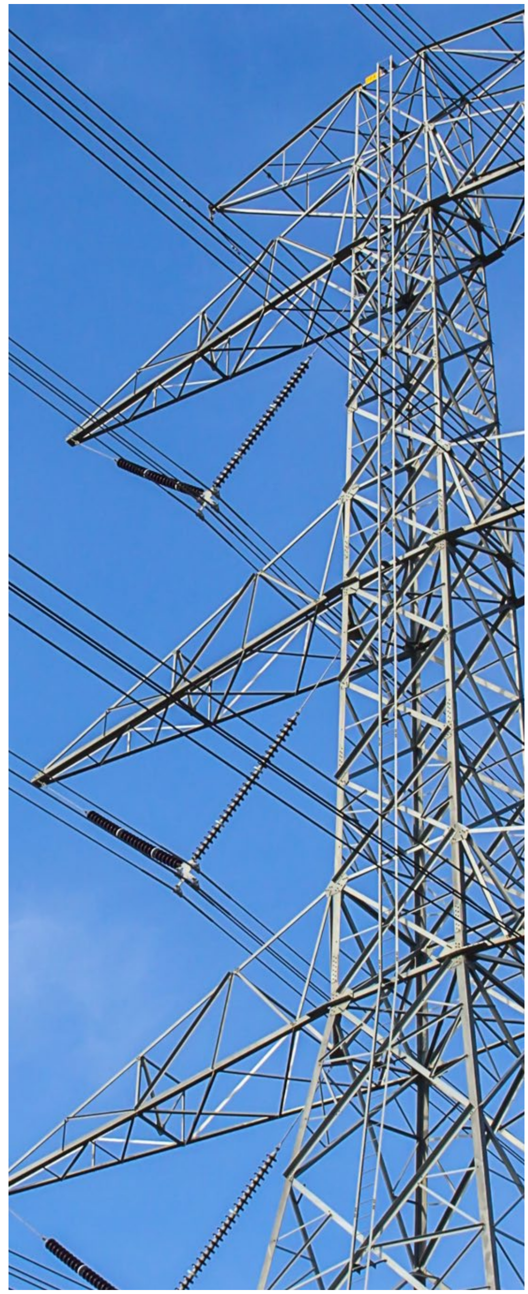

1

The Electricity Mix in the United States Shifts from Fossil Fuels to Renewables

In this section, we discuss renewables displacing fossil fuels in the electric power sector.

Renewables displace fossil fuels in the electric power sector due to declining renewable technology costs and rising subsidies for renewable power

Economic growth paired with increasing electrification in end-use sectors results in stable growth in U.S. electric power demand through 2050 in all cases. Declining capital costs for solar panels, wind turbines, and battery storage, as well as government subsidies such as those included in the IRA, result in renewables becoming increasingly cost effective compared with the alternatives when building new power capacity.

> Power demand is increasingly met by renewables throughout the projection period.

Renewables are increasingly meeting power demand throughout the projection period (Figure 2). Natural gas, coal, and nuclear generation shares decline. Renewable power outcompetes nuclear power, even in the Low Zero-Carbon Technology Cost (ZTC) case, which evaluates the impact of more aggressive cost declines for nuclear and renewables than the Reference case. Most natural gas-fired generation comes from combined-cycled power plants as opposed to simple-cycle combustion turbines. Uncertainty in natural gas prices across cases leads to various projections for combined-cycle units in the short term, but in the long term, natural gas demand from the electric power sector stabilizes across all cases.

Figure 2.

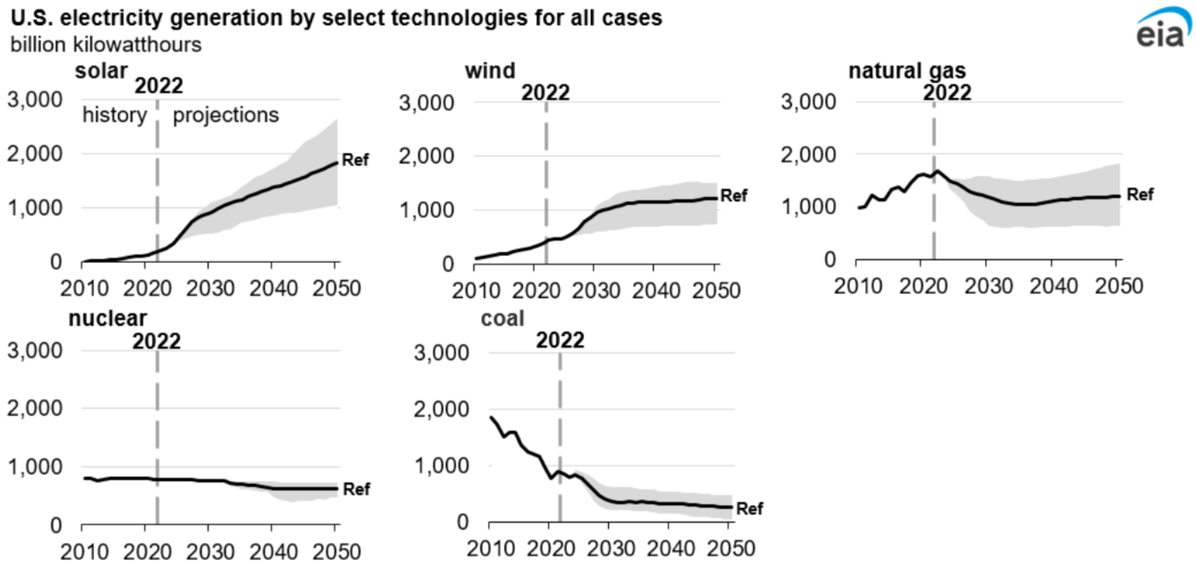

Data source: U.S. Energy Information Administration, *Annual Energy Outlook 2023* (AEO2023)
Note: Shaded regions represent maximum and minimum values for each projection year across the AEO2023 Reference case and side cases. Ref=Reference case.

In order to meet increasing demand for electric power throughout the projection, total installed power capacity close to doubles across most cases, even in the Low Economic Growth case (Figure 3). Cases with a higher share of renewables in the generation mix have higher total grid capacity due to the inherently lower capacity factors of solar and wind compared with coal, nuclear, and combined-cycle plants.

Figure 3.

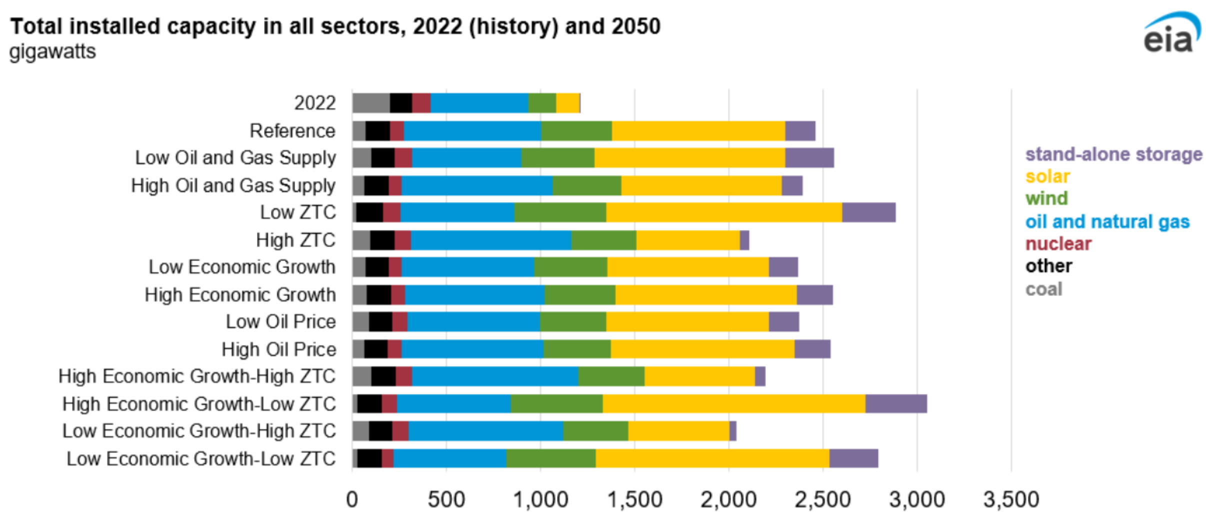

Data source: U.S. Energy Information Administration, *Annual Energy Outlook 2023* (AEO2023)
Note: ZTC=Zero-Carbon Technology Cost; other=geothermal, biomass, municipal waste, fuel cells, hydroelectric, pumped hydro storage.

We project that renewable power capacity will increase in all regions of the United States in all AEO2023 cases, although regional resource availability results in varying renewable resource mixes across regions (Figure 4). Across all cases, between 40%-60% of the renewable power capacity in the Mid-Continent region in 2050 comes from wind, and the Southeast and the region managed by the California

Independent System Operator (CAISO) have large shares of solar and a small amount of wind power capacity in all cases.

Figure 4.

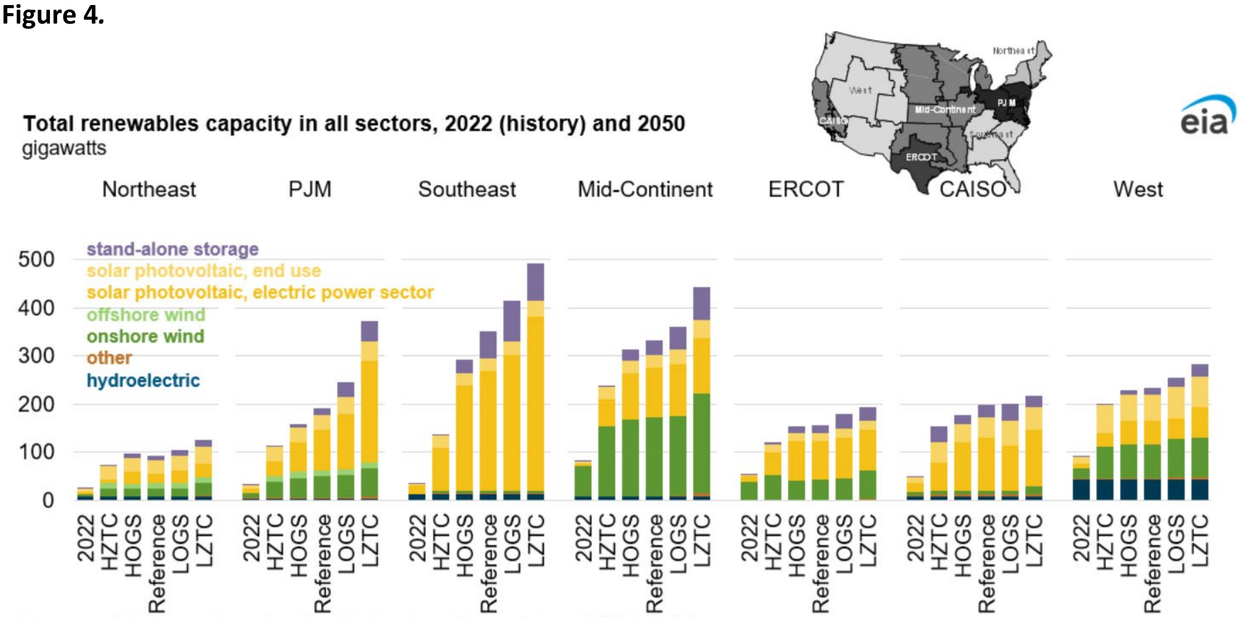

Data source: U.S. Energy Information Administration, *Annual Energy Outlook 2023* (AEO2023)
Note: HZTC=High Zero-Carbon Technology Cost; LZTC=Low Zero-Carbon Technology Cost; HOGS=High Oil & Gas Supply; LOGS=Low Oil & Gas Supply; other=geothermal, biomass, municipal waste.

Once built and when the resource is available, wind and solar generation outcompete other technologies for system dispatch because they have zero fuel costs. Across all AEO2023 cases, some renewable generation is left unused and curtailed, typically midday when solar generation can exceed demand in some regions and seasons. Battery capacity is built in all cases to store and dispatch some of this otherwise unused generation in later hours, decreasing reliance on fossil fuel capacity, such as natural gas-fired peaking units or load-following combined-cycle units (Figure 5). Battery storage is also used to replace natural gas-fired capacity to provide reserve capacity. In the Reference case in 2050, 160 gigawatts (GW) of standalone battery storage capacity will be deployed, and deployment varies between 40 GW and 260 GW in the other cases.

Figure 5.

Hourly U.S. electricity generation and load by fuel for selected cases and representative years
billion kilowatthours

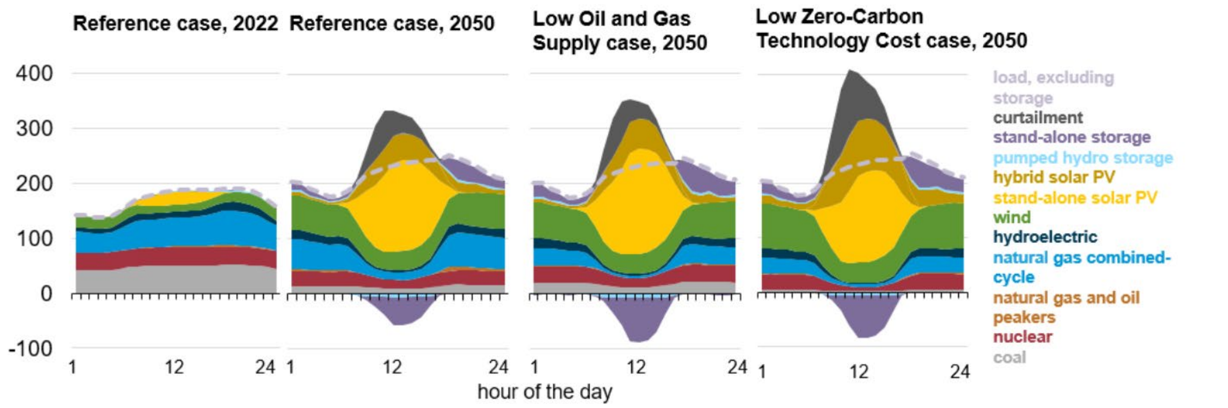

Data source: U.S. Energy Information Administration, *Annual Energy Outlook 2023* (AEO2023)
Note: Negative generation represents charging of energy storage technologies such as pumped hydro storage and battery storage. Hourly dispatch estimates are illustrative and are developed to determine curtailment and storage operations; final dispatch estimates are developed separately and may differ from total utilization as this figure shows. Standalone solar photovoltaic (PV) includes both utility-scale and end-use PV electricity generation.

Technical Note 1: Renewable costs and deployment

Continued decline of renewable technology costs relative to natural gas-fired generating technologies contributes to the change in generation mix in our projection period. In addition to recent policies that also favor renewables in the generation mix, we use learning factors to represent learning by doing, which reduces capital costs. Learning factors are calculated independently for each of the major design components of the technology, and they increase based on how much new capacity is deployed. For details on renewable costs in the ZTC cases, please see the Appendix. New, untested components decrease at a more rapid initial rate than mature components or conventional designs. More details can be found in the NEMS Electricity Market Module documentation.

Overnight installation cost

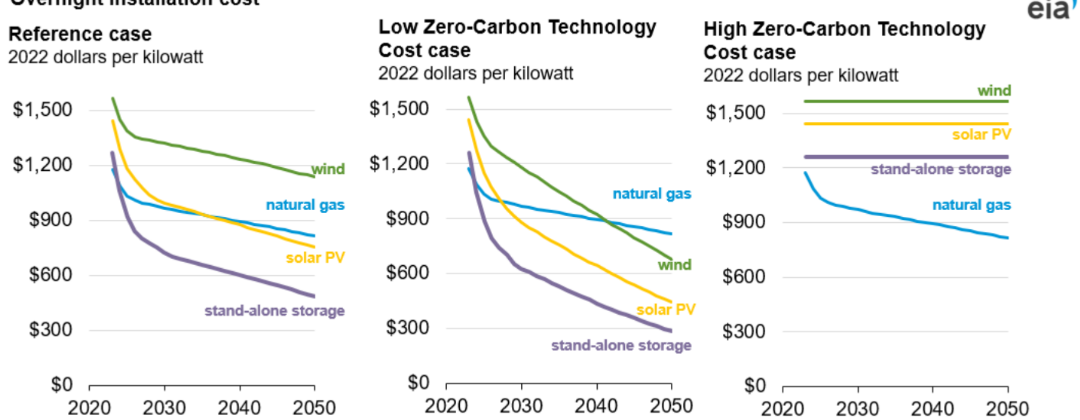

Data source: U.S. Energy Information Administration, *Annual Energy Outlook 2023* (AEO2023)
Note: Series in all charts begin in 2023. Overnight installation cost for natural gas refers to combined-cycle, multi-shaft technologies. Nuclear costs decline in the Reference and Low Zero-Carbon Technology cases, but they are not shown given the large differences in absolute cost compared with renewables. In the Reference case, nuclear begins at $7,900 per kilowatt (kW) and declines to $5,000/kW in 2050. In the Low Zero-Carbon Technology case, the cost of nuclear declines to $3,000/kW in 2050. Solar PV=stand-alone solar photovoltaic.

As a result of renewables growth, we project that U.S. coal-fired generation capacity will decline sharply by 2030 to about 50% of current levels (about 200 GW) with a more gradual decline thereafter. We project between 23 GW and 103 GW of coal-fired capacity operating in 2050 (Figure 6). The IRA provides additional incentives to wind and solar power generation, which accelerates the near-term decline of electric power sector coal-fired generating capacity and hastens the timeline for retirement in the U.S. coal fleet.

Figure 6.

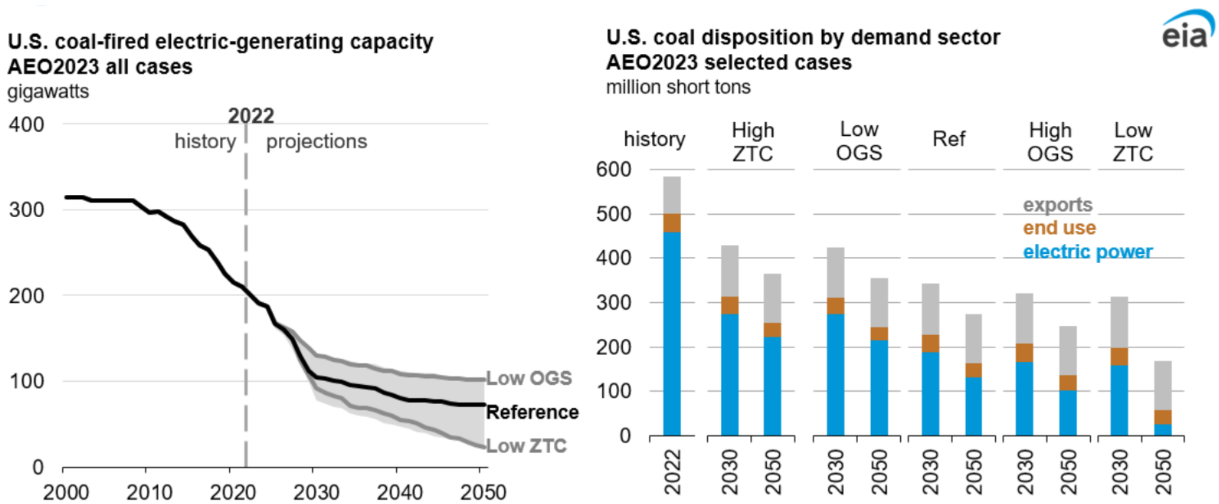

Data source: U.S. Energy Information Administration, *Annual Energy Outlook 2023* (AEO2023)
Note: Shaded regions represent maximum and minimum values for each projection year across the AEO2023 Reference case and side cases.
ZTC=Zero-Carbon Technology Cost; Ref=Reference case; OGS=Oil and Gas Supply.

Coal consumption in the U.S. electric power sector in the Reference case drops to 189 million short tons (MMst) in 2030 and to 131 MMst in 2050 from 458 MMst in 2022. Coal disposition, which includes exports and consumption by the electric power sector and other end-use sectors, declines to a low of 170 MMst in 2050 in the Low ZTC case. In a high natural gas price environment, such as in the Low Oil and Gas Supply case, coal disposition could remain as high as 350 MMst in 2050. In all cases, annual coal exports average about 110 MMst in 2050, and end-use coal demand averages about 36 MMst. The ratio of coal exports to domestic coal consumption generally increases through the projection period in all cases. The majority of domestically produced coal is exported by 2050 in the Low ZTC case, 45% is exported in the High Oil and Gas supply case, which are the two cases that have the least coal demand from the electric power sector. Even in cases with more aggressive retirement of coal-fired power plants, such as the Low ZTC case, some of the relatively newer and more efficient coal power plants remain online across the United States because they can provide cheap dispatchable power to the grid.

The electric power sector is also decreasing its reliance on natural gas in favor of renewables, which we will discuss in Section 3.

2

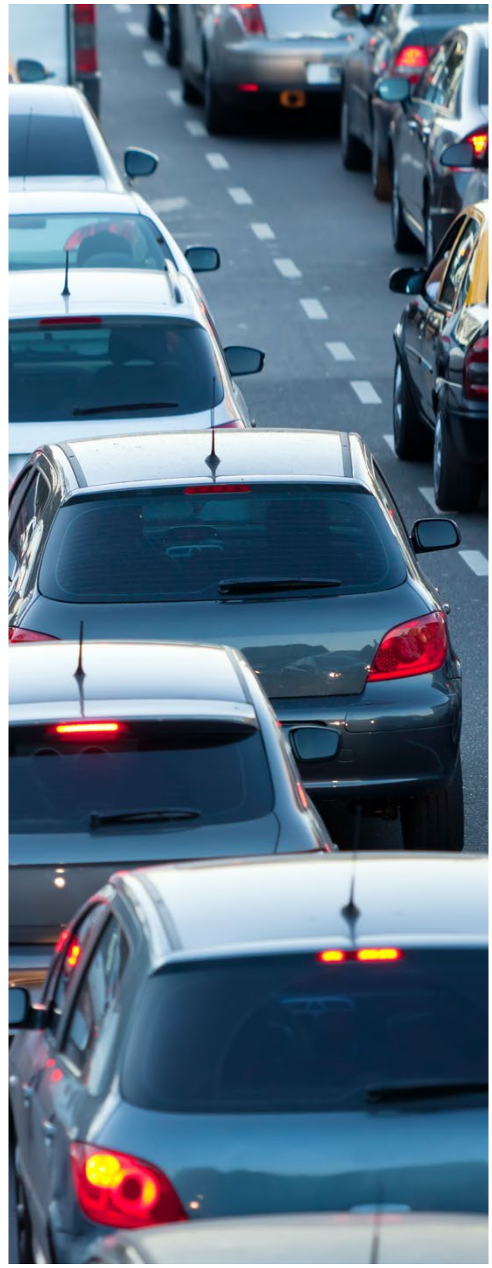

Technological Advancements and Electrification Decrease Demand-Side Energy Intensity

Moderate growth in U.S. energy consumption is the result of economic growth, population growth, and increased travel offsetting continued energy efficiency improvements. Demand-side energy intensity—the measure of energy consumed per household or per square foot of commercial floorspace—decreases as a result of changes in technology, policy, consumer behavior, demographics, and fuel mix. In this section, we quantify the decreases in CO_2 emissions intensity and demand-side energy intensity, and we discuss equipment changes in the buildings sector, electrification in iron and steel production, and technological advancements and government standards in the transportation sector.

U.S. energy consumption increases through 2050, and electricity plays an increasingly large role

U.S. energy consumption increases in many end-use sectors across all AEO2023 cases. Total energy consumption, including electricity use and electricity-related losses, increases by as much as 15% from 2022 to 2050 across the AEO2023 Reference case and side cases (Figure 7). The largest increases, in percentage terms, are in the industrial sector where energy consumption increases as much as 32% and in the transportation sector where energy consumption increases as much as 8%. Energy consumption in the residential and commercial sectors are the least sensitive to changes in assumptions across cases.

Total energy consumption, including electricity use and electricity-related losses, increases by as much as 15% from 2022 to 2050 across the AEO2023 Reference case and side cases.

Figure 7.

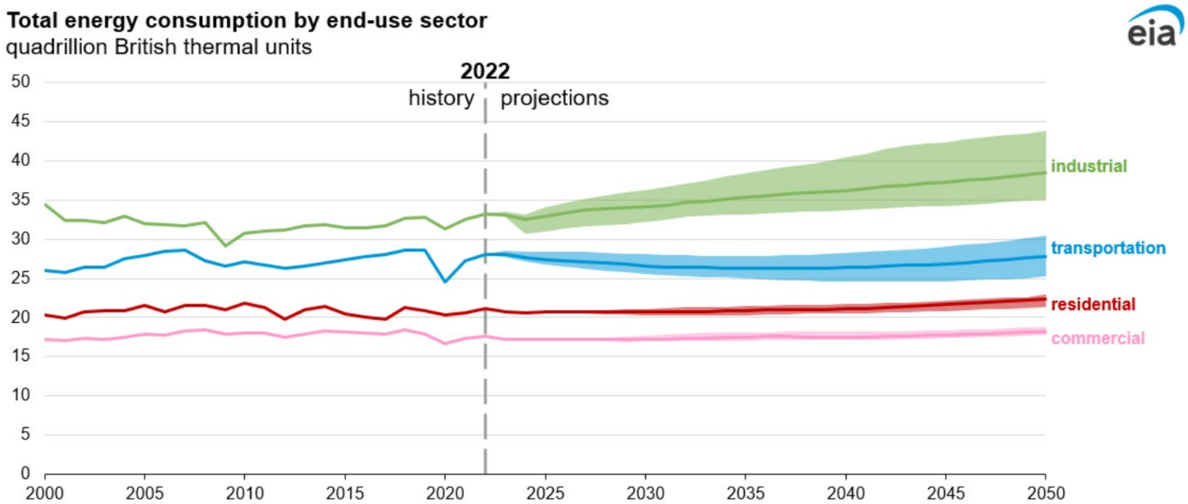

Data source: U.S. Energy Information Administration, *Annual Energy Outlook 2023* (AEO2023)
Note: Total consumption in end-use sectors includes purchased electricity and electricity-related losses. Each line represents AEO2023 Reference case projections. Shaded regions represent maximum and minimum values for each projection year across the AEO2023 Reference case and side cases.

In addition to macroeconomic growth assumptions, which affect energy consumption in all sectors, many sectors are also highly responsive to zero-carbon technology cost assumptions. Increasing energy consumption, improving end-use and electric power sector technology and efficiency, and declining costs for zero-carbon generation technologies, which, in turn, leads to cheaper electricity, all lead to increased electrification in the end-use sectors. The share of electricity in the residential and transportation sectors increase the most as demand for space cooling increases and electric vehicles gain a larger market share. The residential sector purchased 5.1 quadrillion British thermal units (quads) of electricity in 2022, and residential consumption of purchased electricity increases between about 14% and 22% from 2022 to 2050 across all cases, reaching between 5.9 and 6.3 quads. Electricity purchased for transportation reaches between about 0.6 quads and 1.3 quads in 2050, from 0.1 quads of purchased electricity in 2022, an increase of between 892% and 2,038% across all cases. Electricity purchased in the industrial sector is most influenced by economic growth assumptions, increasing by about 3%, from 3.5 quads in 2022 to about 3.6 quads in 2050 in low economic growth cases and by about 36% to 38%, to about 4.7 quads, in high economic growth cases.

Greater heating equipment efficiency reduces fossil fuel use in buildings

Despite modest growth in total energy consumption in the residential and commercial sectors, due to a growing number of households and expanding commercial floorspace, average energy intensity declines through 2050 across all cases (Figure 7 and Figure 8). Building envelope efficiency improves as states and localities adopt newer building energy codes and some existing households and commercial spaces receive additional insulation, air sealing, and other weatherization upgrades.

Figure 8.

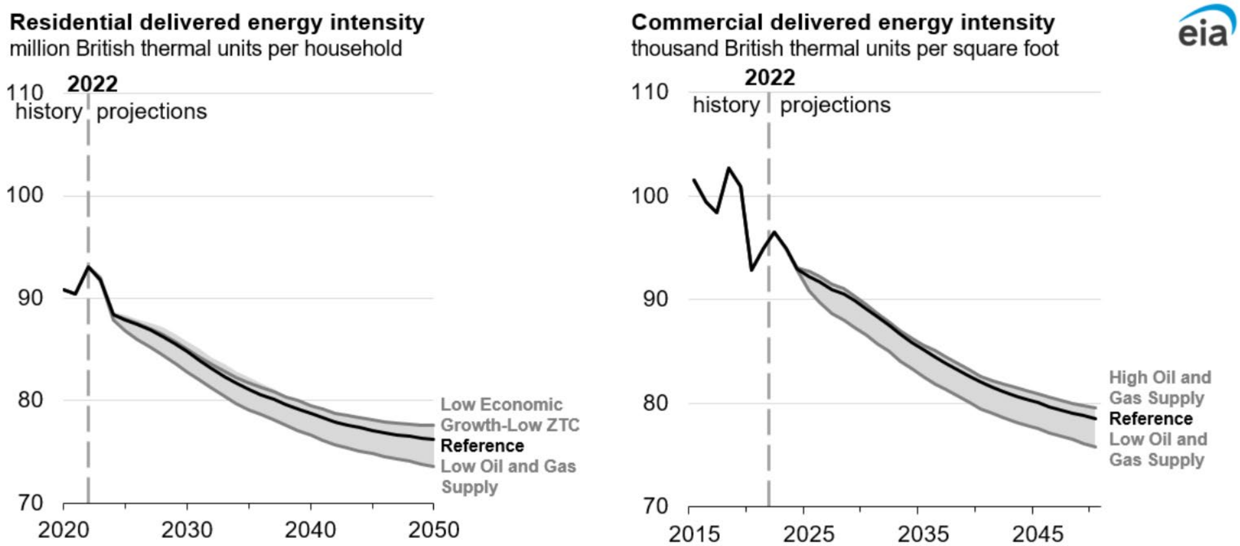

Data source: U.S. Energy Information Administration, *Annual Energy Outlook 2023* (AEO2023)
Note: Shaded regions represent maximum and minimum values for each projection year across the AEO2023 Reference case and side cases. ZTC=Zero-Carbon Technology Cost.

An established trend toward warmer winters and population shifts toward warmer and drier areas of the United States reduce energy consumption for space heating in all cases. At the same time, the established trend toward warmer summers leads to increasing electricity consumption for space cooling.

> ***Technical Note 2: Modeling growth in residential heat pump installations***
>
> *Our projections of residential heat pumps, like all major end-use equipment, begin with the census division-level stocks from our 2015 Residential Energy Consumption Survey (RECS). We use data from the most recent U.S. Census Bureau's Survey of Construction to further align recent space heating equipment shares in newly built housing units. Equipment purchase decisions account for federal and non-federal subsidies that further reduce installed costs of high-efficiency equipment such as air- and ground-source heat pumps or high-efficiency natural gas furnaces. These subsidies include national tax credits extended by the Inflation Reduction Act (IRA) and utility rebates to end users at the census-division level. Technology performance and energy prices are considered as well. Some provisions of the IRA—such as those targeting low-income households—are not explicitly included in our modeling. Refer to the Appendix for additional details.*

Natural gas-fired heating equipment, including furnaces and boilers, continue to account for the largest share of energy consumption for space heating in U.S. residential and commercial buildings across all cases throughout the projection period. Over time, older heating equipment is replaced by newer, more efficient equipment that meets updated federal minimum energy efficiency standards.

Federal and non-federal subsidies both encourage homes and businesses to adopt high-efficiency natural gas and electric equipment, including heat pumps. Electric heat pumps, including ground-source heat pumps, gain market share over the projection period, increasing from 11% of households in 2022 to between 14% and 15% of households in 2050 across all cases; however, their growth is limited by:

- A large existing market share for non-heat pump equipment that lasts a long time
- The high cost of purchasing and switching technologies, including electrical upgrades to accommodate electric heating and cooling and new ductwork when replacing boilers
- The higher price of electricity versus natural gas per million British thermal units, despite heat pump efficiency that may be multiple times higher than fossil fuel-fired equipment
- Reduced overall demand for space heating as building efficiency improves and heating degree days decrease

Electricity increasingly powers production in the iron and steel industry, decreasing energy intensity and CO_2 emissions

Steel production is an energy-intensive industry, but the choice of production technology significantly affects its energy and emission intensity. U.S. manufacturers continue to transition away from the combustion-powered, integrated steel mill process to steel produced by electric-arc furnaces, which have a lower energy intensity and make up about 68% of U.S. steel produced in 2022. Over the projection period, the share of U.S. steel produced by the electric-arc furnace process increases by 4% to 7% across the range of cases (Figure 9). The energy intensity of U.S. steel production continues to fall across all cases, declining between 12% and 21% across all cases (Figure 9). In 2018, steel production accounted for 1.3% of U.S. energy demand, and we project total energy demand for iron and steel production to fall relative to total U.S. energy demand, after peaking in 2027.

Figure 9.

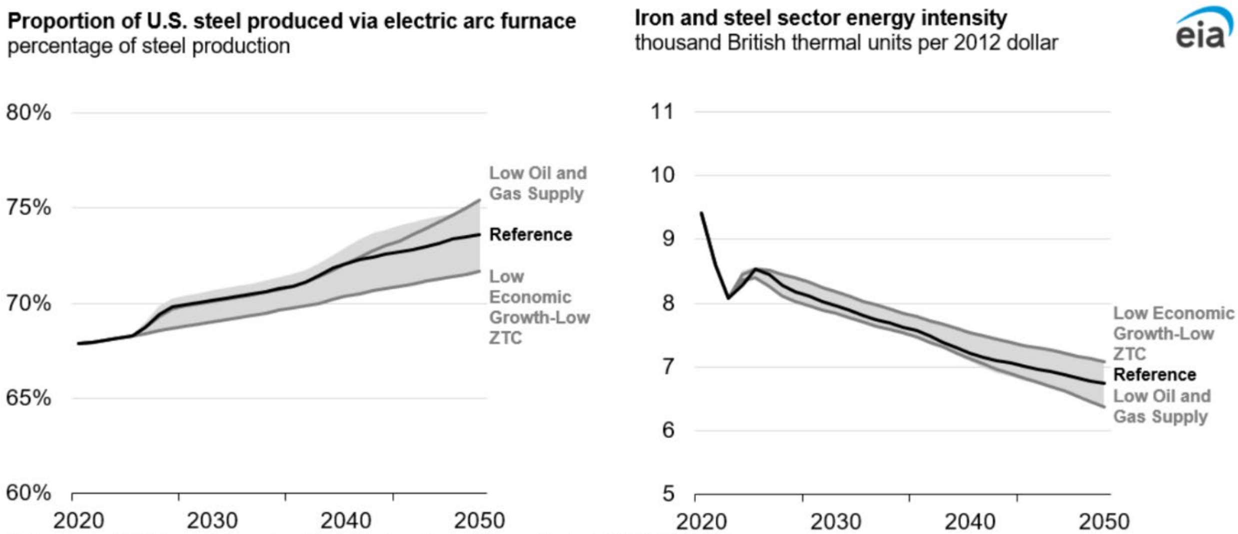

Data source: U.S. Energy Information Administration, *Annual Energy Outlook 2023* (AEO2023)
Note: All displayed data are projections. Shaded regions represent maximum and minimum values for each projection year across the AEO2023 Reference case and side cases. ZTC=Zero-Carbon Technology Cost.

Technological advancements, including electrification, for light-duty vehicles reduce energy intensity and fossil fuel use

In the transportation sector, light-duty vehicle (LDV) fuel economy increases due to rising Corporate Average Fuel Economy (CAFE) standards and electric vehicle (EV) sales. In addition to required fuel economy increases, consumer purchase decisions are also influenced by fuel prices. Consumer interest in EVs, which are significantly more efficient than internal combustion engine vehicles, and the impact EV adoption has on average light-duty vehicle fuel economy are sensitive to the price of gasoline (Figure 10).

Figure 10.

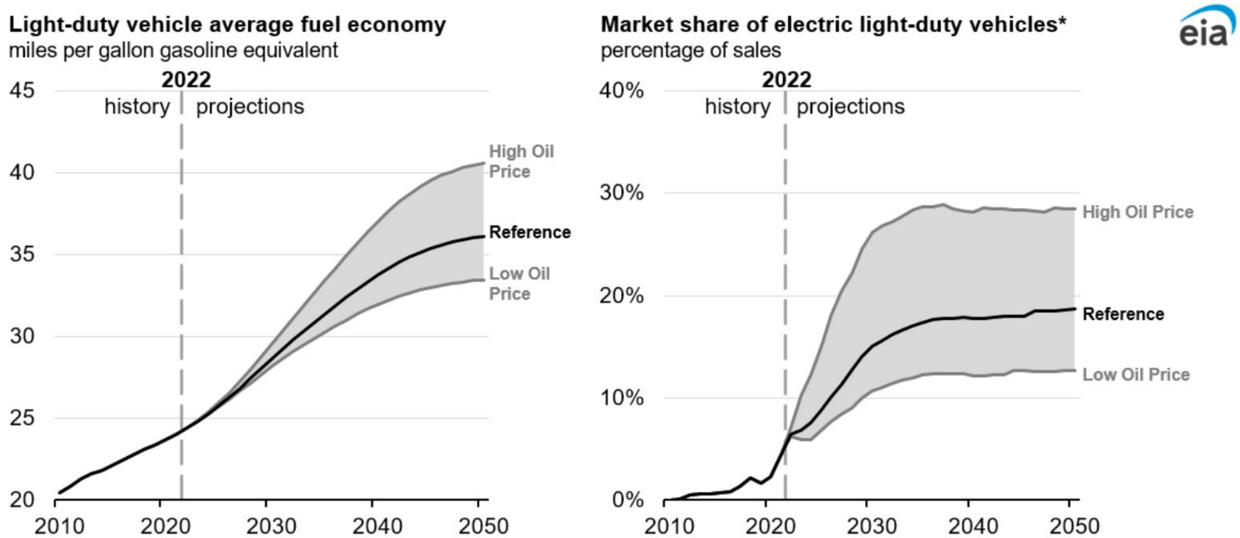

Data source: U.S. Energy Information Administration, *Annual Energy Outlook 2023* (AEO2023)
Note: *Includes battery electric and plug-in hybrid electric vehicles. Shaded regions represent maximum and minimum values for each projection year across the AEO2023 Reference case and side cases.

The updated CAFE standard, which applies to model years 2024 through 2026, significantly increases average new vehicle fuel economy requirements. By 2026, the updated CAFE standard is 28% higher than the Safer Affordable Fuel-Efficient (SAFE) standard for new vehicles it replaced, resulting in an increase from 37 miles per gallon (mpg) to 47 mpg by 2026. In addition to improved conventional vehicle fuel efficiency, EV sales increase through 2050, increasing EVs on the road. The CAFE standard, which offers credits to EV manufacturers, and decreasing battery prices help drive this increase in EV sales.

U.S. passenger vehicle-miles traveled increases steadily with population and income throughout the projection period, growing between 12% and 33% across all cases. In the Reference case, 23% more vehicle miles are traveled in 2050 than in 2022 (Figure 11). We project LDV energy consumption to fall through the early 2040s as a result of fuel economy improvements but then to rise due to increasing vehicle miles traveled for the remainder of the projection period (Figure 11).

We project LDV energy consumption to fall through the early 2040s as a result of fuel economy improvements but then to rise due to increasing vehicle miles traveled for the remainder of the projection period.

Figure 11.

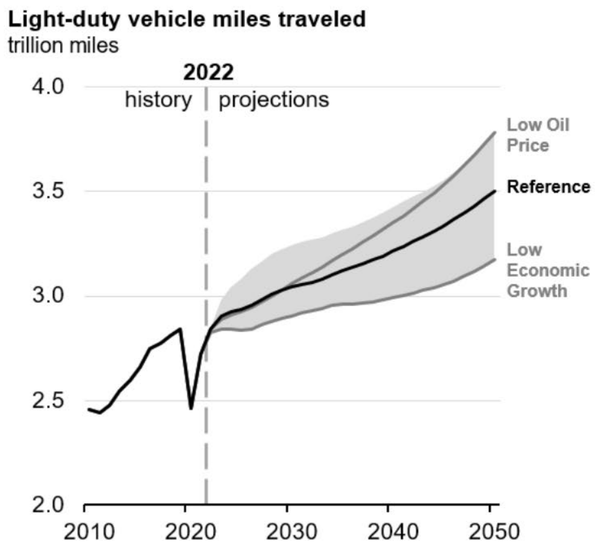

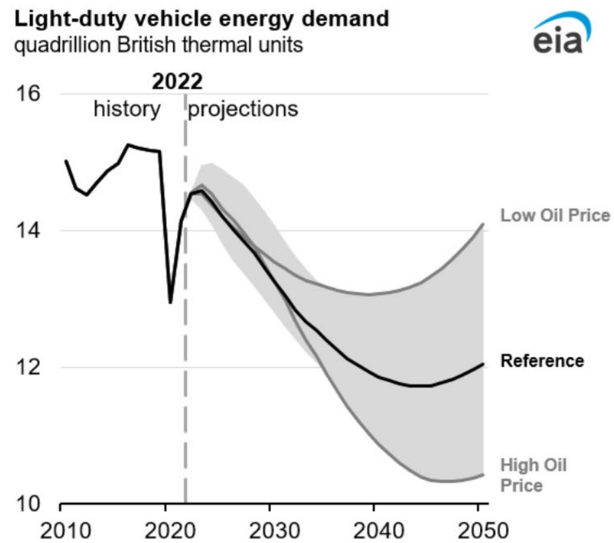

Data source: U.S. Energy Information Administration, *Annual Energy Outlook 2023* (AEO2023)
Note: Shaded regions represent maximum and minimum values for each projection year across the AEO2023 Reference case and side cases. Right hand chart includes delivered energy, specifically energy consumed on board the vehicle; it does not include losses between car and charger.

Technical Note 3: Electric vehicle (EV) deployments

Projected declines in EV vehicle component costs, along with federal and state policies that provide incentives for EV purchases or require minimum sales, drive EV sales growth in our model projection. We derive cost declines for EV powertrain components and batteries by using learning rates based on cumulative production, resulting in increased projected driving range and a continual decline in EV prices over the projection period. We derive EV sales shares at the census-division level using a consumer choice model based on preference data and calibrated to align with historical sales data. In addition to other vehicle attributes, our consumer choice model captures the impact of vehicle price, cost to drive, access to refueling, and the effect that availability of vehicle propulsion options has on consumer purchase decisions. All of these factors contribute to the attractiveness of EVs to consumers and increases EV deployment relative to internal combustion engine vehicles. We assume Corporate Average Fuel Economy standards result in technological improvements and increased EV adoption because of declining cost and favorable fuel economy credits. The clean vehicle credit in the 2022 Inflation Reduction Act, which varies from $3,750 to $7,500 per vehicle, drives additional EV sales. Our Transportation Demand Model also ensures legally enforceable state minimum EV sales requirements are met in each census division and EV prices adjust to account for tax credits at purchase. In addition, other factors, such as a rising number of charging stations, affect our EV sales projections. We base our model projections on these data, assumptions, and current enforceable laws and regulations and do not assume that state and federal stated goals for EV sales are met. These details are available in our model documentation.

3

International Demand for Petroleum and Natural Gas Drives U.S. Production, While Domestic Consumption Either Grows Slowly or Decreases

Although U.S. consumption of petroleum products remains relatively flat, international demand supports U.S. exports of petroleum and other liquids (Figure 12). The dynamics of international trade affect domestic production of natural gas and of petroleum and other liquids.

International demand drives petroleum and other liquids production

Figure 12.

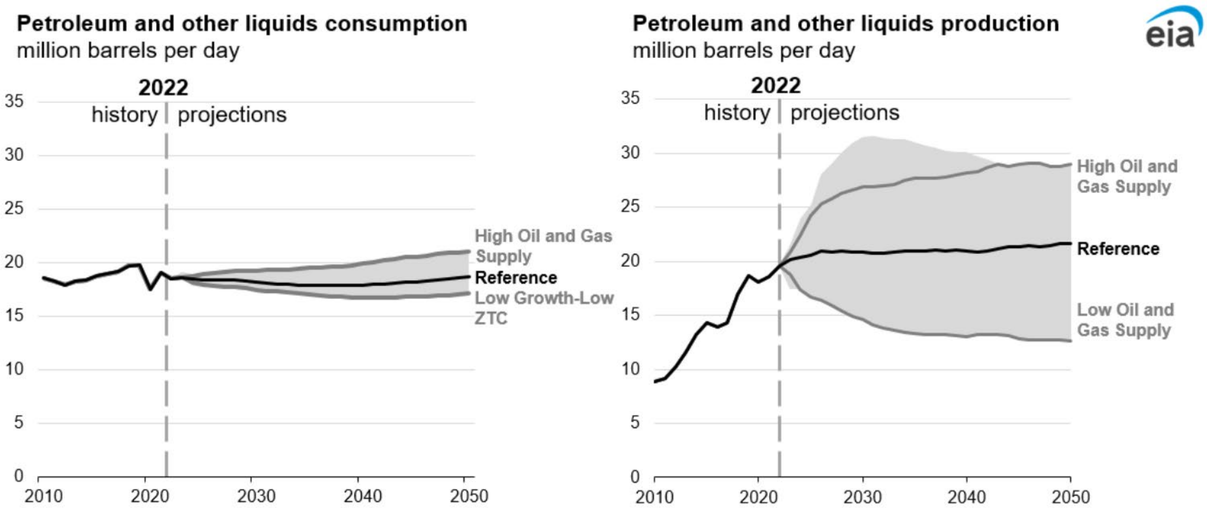

Data source: U.S. Energy Information Administration, *Annual Energy Outlook 2023* (AEO2023)
Note: Biofuels are not included in *petroleum and other liquids* production or consumption. Shaded regions represent maximum and minimum values for each projection year across the AEO2023 Reference case and side cases. ZTC=Zero-Carbon Technology Cost.

In all cases, we project that the United States will remain a net exporter of petroleum products through 2050.

Although domestic consumption of petroleum and other liquids does not increase through 2040 across most cases, U.S. petroleum and other liquids production remains high because of increased exports of finished products in response to growing international demand (Figure 13). In all cases, we project that the United States will remain a net exporter of petroleum products through 2050. In the High Oil Price case, increased production leads to the most exports among all cases over the projection period. The Low Oil Price case shows the opposite: decreased production along with the lowest export volumes.

Crude oil imports remain relatively flat in the Reference case but vary widely in the side cases (Figure 13); the Low Oil and Gas Supply case leads to the greatest level of imports throughout the forecast period while the High Oil and Gas Supply case leads to the lowest imports (Figure 13). This wide range in imports is mainly due to the tradeoff between domestic production and imports. In the Low Oil and Gas Supply case, crude oil imports increase significantly, partially to account for falling domestic crude oil production. The opposite occurs in the High Oil and Gas Supply case, in which increased domestic production balances lower crude oil imports.

Figure 13.

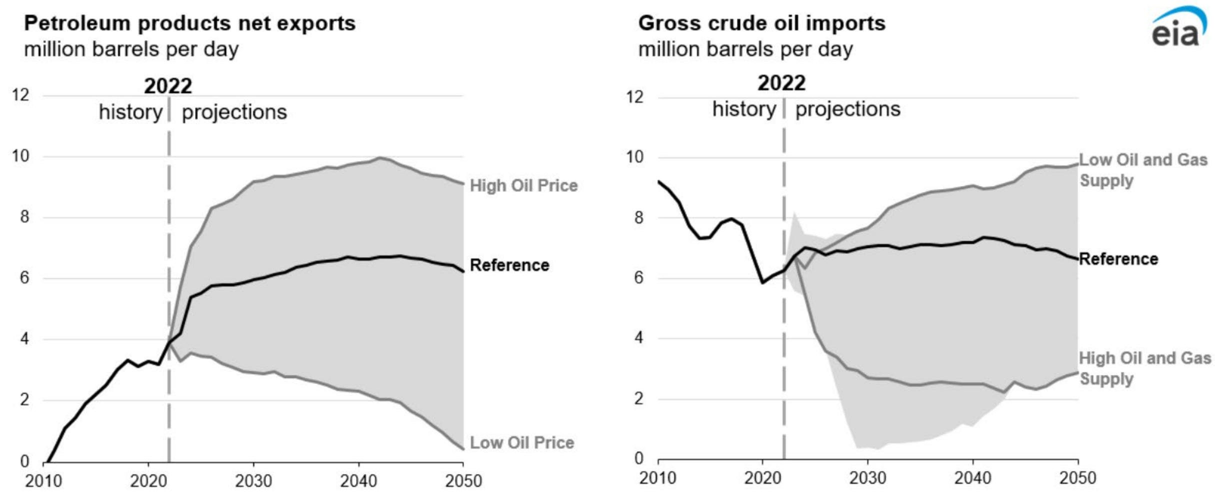

Data source: U.S. Energy Information Administration, *Annual Energy Outlook 2023* (AEO2023)
Note: Shaded regions represent maximum and minimum values for each projection year across the AEO2023 Reference case and side cases.

In the High Oil Price case, U.S. crude oil imports initially decline but begin to increase starting in 2030 because of changing trends in domestic crude oil production. In the early years, domestic crude oil production increases rapidly due to high prices. However, crude oil production begins to fall after 2030 because wells are drilled increasingly close to one another, resulting in well productivity declines. As wells are drilled closer together, they produce less crude oil and eventually become unprofitable, at which point new drilling stops. Crude oil imports decline early in the High Oil Price case as crude oil production increases; imports increase after 2030 as well productivity and crude oil production declines.

Because international demand for finished petroleum products keeps exports high, U.S. refinery runs remain strong as the U.S. refinery sector remains competitive in the global market through 2050. Refinery capacity remains relatively constant through 2050, and refinery capacity utilization remains high, at around 90% or higher, under favorable economic conditions.

Technical Note 4: Crude oil trade dynamics

Crude oil is a global commodity, and the United States participates in the global market as both an importer and exporter of crude oil and its associated products. Because of logistical, regulatory, and quality considerations, both exporting and importing petroleum often makes economic sense. For example, a refiner in the Gulf Coast may find it more profitable to export motor gasoline to Mexico rather than shipping it to the East Coast because cheaper gasoline imports from Europe may be available to the East Coast.

The chemical makeup of the imported or exported product also affects crude oil trade. The type of crude oil—light or heavy, low-sulfur (sweet) or high-sulfur (sour)—helps determine the processes that refine it into a petroleum product such as distillate fuel oil or propane. In short, the United States imports different types of crude oil to optimize production across its various refineries.

The World Oil Price path is an exogenous assumption to the model and affects domestic crude oil production and international trade. For each year of the projection period, NEMS computes the Brent crude oil price, provides a supply curve of world crude oil-like liquids, and provides supply curves for each foreign crude oil type considered. NEMS also provides, for each year of the projection period, exogenous supply and demand curves for U.S. import and export of petroleum products.

In response to Russia's full-scale invasion of Ukraine in early 2022, the United States banned petroleum imports from Russia. AEO2023 projections reflect this policy change. However, we assume that equivalent imports from other countries substitute for U.S. crude oil imports (especially unfinished oil imports) from Russia, minimizing effects on domestic markets.

Natural gas consumption in end-use sectors is variable

In the United States, electrification is displacing combustion fuels in the demand sectors. As electricity generation shifts to using more renewable and battery sources, domestic natural gas consumption for electricity generation is likely to decrease by 2050 relative to 2022, which contrasts with relatively stable growth over the past decade (Figure 14).

Figure 14.

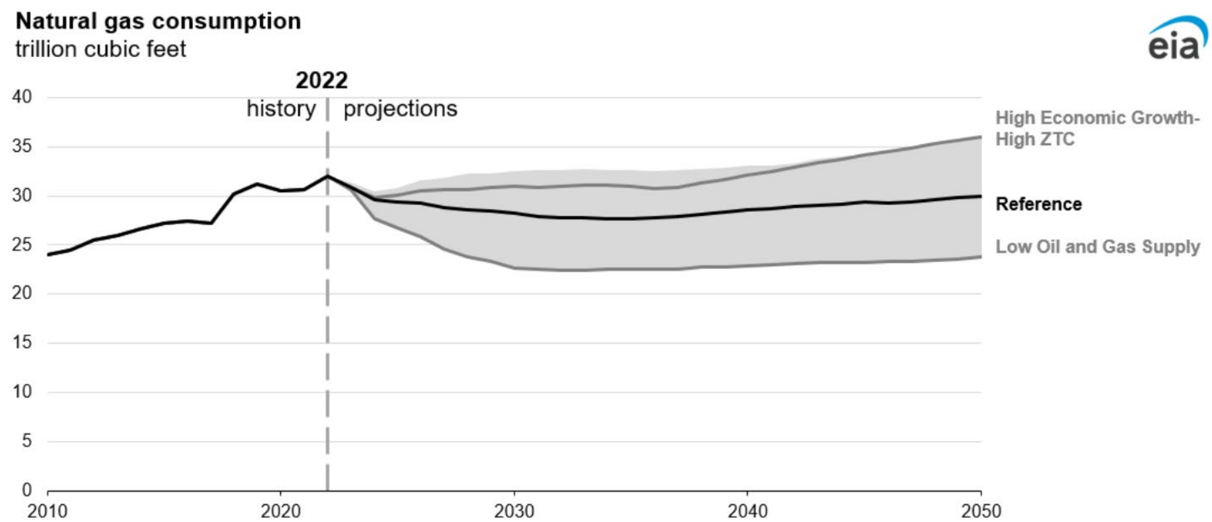

Data source: U.S. Energy Information Administration, *Annual Energy Outlook 2023* (AEO2023)
Note: Shaded regions represent maximum and minimum values for each projection year across the AEO2023 Reference case and side cases. ZTC=Zero-Carbon Technology Cost.

More natural gas is consumed in the industrial or electric power sectors than in any other sectors of the U.S. economy. Projected consumption in both sectors is very sensitive to changes in our side case assumptions, particularly in the Oil and Gas Supply cases (Figure 15). These cases, which result in the most and the least natural gas consumption in the industrial sector, vary widely due to differences in resource extraction assumptions. By 2050, natural gas consumption in the industrial sector diverges from the Reference case by 14% in the Low Oil and Gas Supply case and 18% in the High Oil and Gas Supply case.

In the electric power sector, our projections for natural gas consumption generally fall but range widely, with consumption in 2050 diverging from the Reference case by over 50% in the bounding cases.

In the electric power sector, our projections for natural gas consumption generally fall but range widely, with consumption in 2050 diverging from the Reference case by over 50% in the bounding cases (Figure 15). Natural gas consumption remains below the peak in 2022, at nearly 12 trillion cubic feet, through 2050 across all side cases except the High Economic Growth and High ZTC case. In the Low ZTC case, lower costs for renewables makes natural gas less competitive, resulting in a larger decrease in natural gas consumption compared with the Reference case. In the High Economic Growth and High ZTC case, increased economic activity drives increased end-use demand, which results in more natural gas consumption. Higher costs for renewables make natural gas a more competitive option in that case, further increasing natural gas consumption in the electric power sector.

Figure 15.

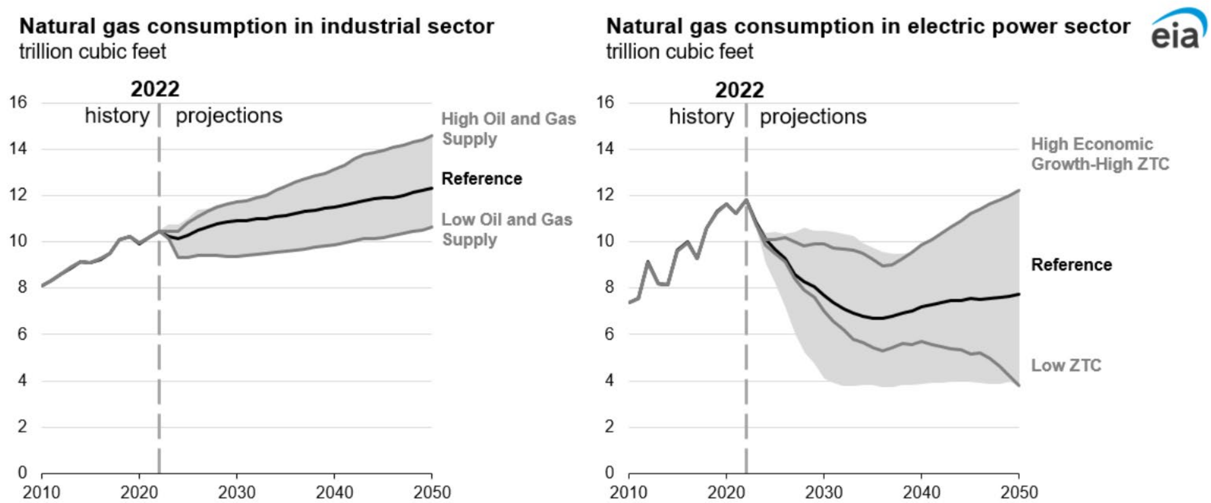

Data source: U.S. Energy Information Administration, *Annual Energy Outlook 2023* (AEO2023)
Note: Shaded regions represent maximum and minimum values for each projection year across the AEO2023 Reference case and side cases. ZTC=Zero-Carbon Technology Cost.

Under favorable economic, supply, and oil price assumptions, U.S. natural gas production continues to grow

In the Reference case, U.S. natural gas production increases by 15% from 2022 to 2050, and consumption decreases by 6% from its peak in 2022 (Figure 16). Across all cases, domestic production outpaces domestic consumption; production increases across all side cases except in the Low Oil and Gas Supply case and the Low Oil Price case.

Figure 16.

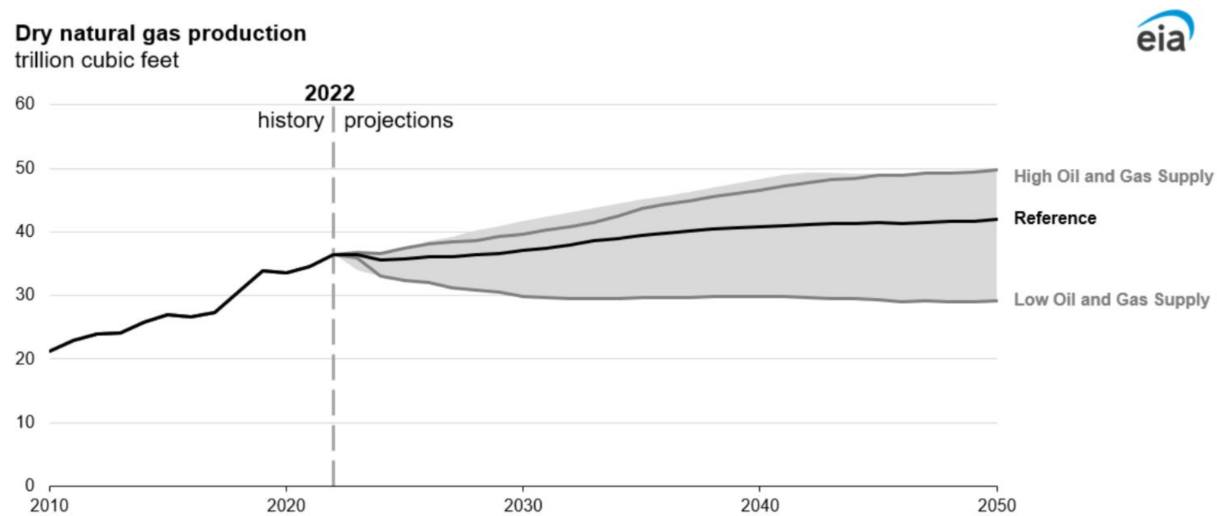

Data source: U.S. Energy Information Administration, *Annual Energy Outlook 2023* (AEO2023)
Note: Shaded regions represent maximum and minimum values for each projection year across the AEO2023 Reference case and side cases.

In some cases, exports to satisfy growing international demand for natural gas encourage growth in domestic natural gas production. A significant portion of production growth is due to liquefied natural gas (LNG) export demand, which drives the overall increase in natural gas exports (Figure 17).

Figure 17.

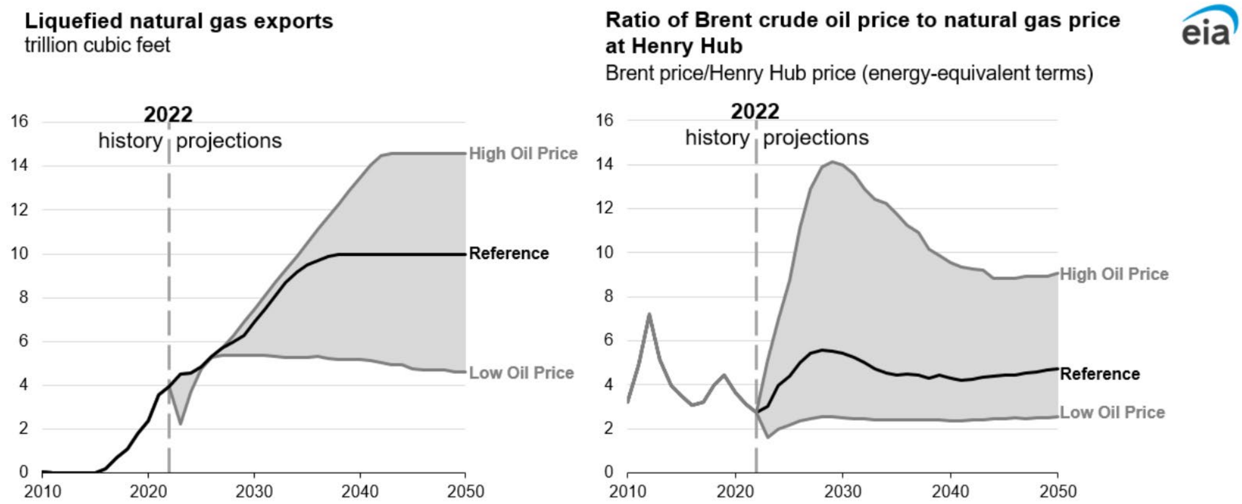

Data source: U.S. Energy Information Administration, *Annual Energy Outlook 2023* (AEO2023)
Note: Shaded regions represent maximum and minimum values for each projection year across the AEO2023 Reference case and side cases.

Historically, most LNG was traded under long-term, oil price-linked contracts because a global LNG price benchmark did not exist and because oil could substitute for natural gas in industry and for power generation, which was especially common in Asia. These factors supported highly correlated international natural gas and oil prices. With growth in more market based-LNG, the strength of the relationship between international natural gas prices and oil prices has eroded. However, we expect that future oil prices will still affect additional LNG export capacity and overall export levels. When the Brent price is high relative to the U.S. Henry Hub price, like in the High Oil Price case, building more LNG export capacity and exporting LNG are more economical than when the Brent price is lower relative to Henry Hub. In the Low Oil Price case, the Brent price is lower, and the Henry Hub price is higher, which curtails LNG exports to below current volumes in the near term and causes LNG capacity to be underutilized near the end of the projection period.

International demand for LNG exports results in rising natural gas production, favoring areas that have better access to terminals. In AEO2023, dry natural gas production grows in the Southwest, which has easy pipeline transport to the Gulf Coast, where LNG is exported. Production in the Gulf Coast also generally increases across the projection period, due to its proximity to LNG export terminals, in all cases except the Low Oil and Gas Supply case (Figure 18).

Figure 18.

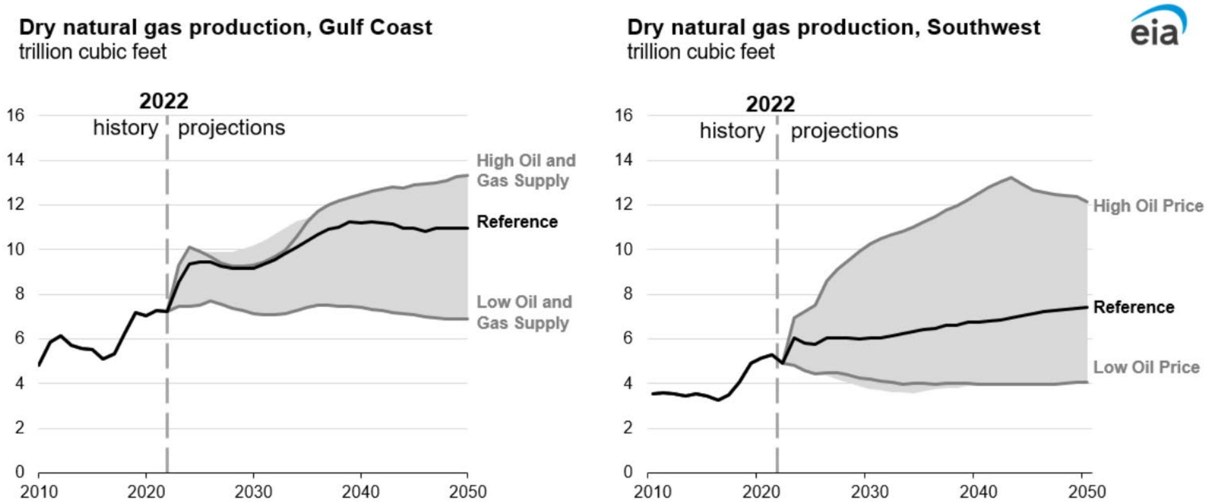

Data source: U.S. Energy Information Administration, *Annual Energy Outlook 2023* (AEO2023)
Note: Shaded regions represent maximum and minimum values for each projection year across the AEO2023 Reference case and side cases.

Associated natural gas is a major source of natural gas production

In AEO2023, shale gas and associated dissolved natural gas from oil formations are the primary sources of long-term growth of domestic natural gas production through 2050. Increased production wells in the Permian Basin (Southwest region) is the primary driver behind associated dissolved natural gas growth. Increases in shale gas production mainly comes from the Texas-Louisiana Salt Basin (Gulf Coast Region) and the Appalachian Basin (East Region).

In the High Oil Price case and High Oil and Gas Supply case, oil production growth leads to increased associated dissolved natural gas and shale production (Figure 19). The opposite occurs in the Low Oil Price case and Low Oil and Gas Supply case.

Figure 19.

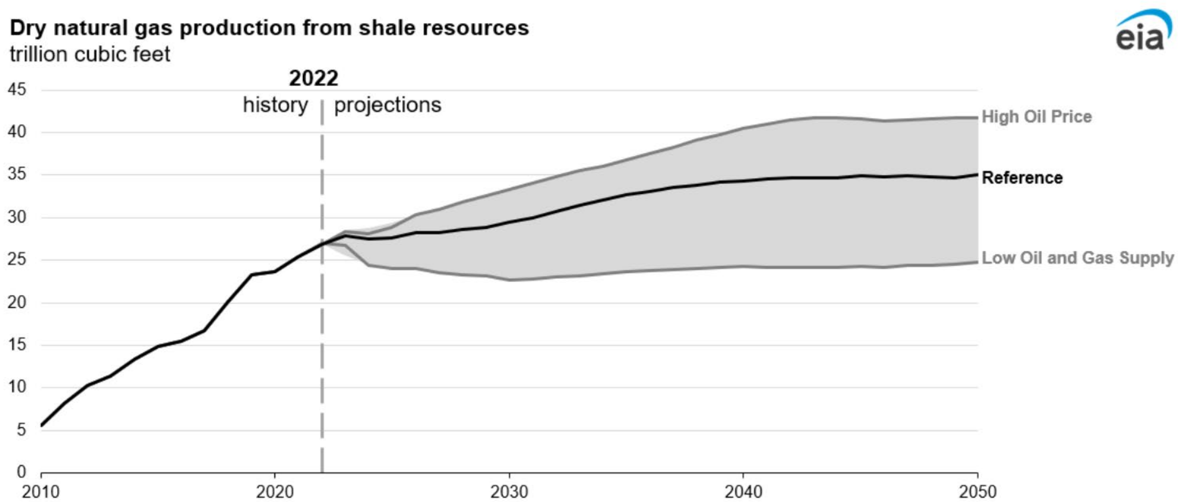

Data source: U.S. Energy Information Administration, *Annual Energy Outlook 2023* (AEO2023)
Note: Shaded regions represent maximum and minimum values for each projection year across the AEO2023 Reference case and side cases.

Discussion

Sources of uncertainty

Energy market projections are inherently uncertain because many of the events that will shape future energy markets—including developments in policy, technology, demographics, and resources—are not known. To illustrate the role of uncertainty, AEO2023 includes a baseline Reference case and several side cases that systematically vary important underlying assumptions. Many sources of uncertainty exist beyond the ones we test explicitly, including new policy, unforeseen geopolitical events, and rapid technology innovation, particularly around technologies that are in the earliest stages of development.

Policy

Our key assumptions in the Reference case provide a baseline for exploring long-term trends, based on current laws and regulations as of November 2022. These assumptions include provisions of the IRA; however, we were unable to model all provisions, as indicated in the appendix. Any future legislation would further affect technology trajectories and emissions pathways. We publish the current laws and regulations considered in the AEO2023 on the AEO website.

Geopolitical events

We account for current events that affect the energy markets with the information available at the time we prepare this publication. However, we cannot foresee future events such as wars, supply disruptions, pandemics, or other such issues that could having lasting impacts on the U.S. energy system.

Rapid technology innovation

The technologies considered in the AEO2023 include only well-documented trends in energy innovation. Additional breakthroughs not considered here might occur. Examples of the kind of breakthrough we don't consider include early-developmental-stage technologies such as hydrogen, enhanced geothermal, and fusion, as well as other technologies currently unknown or not well characterized.

Quantifying uncertainty using statistical errors from past projections

The sources of uncertainty described above, among others, result in observed values that are different than our projected values. To explore some key uncertainties, we include a number of side cases that incorporate plausible alternatives to assumptions in the Reference case. We can also develop a sense of future uncertainty by calculating the differences (or *statistical errors*[3]) between realized values and our Reference case projections from previous AEO editions. Given constantly evolving modeling techniques and a dynamic energy landscape replete with non-linear relationships, statistical errors from past projections will not necessarily provide an accurate basis for estimating uncertainty in current projections. Nevertheless, using statistical errors from past projections implicitly captures real world factors that were difficult to anticipate in past AEO editions.

[3] Here we use "error" in a statistical sense to denote the difference between projected and real-world values. Because our Reference case is not intended to serve as a forecast, deviations from reality should not be interpreted as errors.

In the 2022 edition of our *Annual Energy Outlook Retrospective Review* (AEO Retrospective), we quantified the statistical errors associated with past Reference cases over several key output metrics and projection timeframes, ranging from 1 to 15 years. Building on the work from the AEO Retrospective and following the NP2 method (a methodology detailed in a 2017 paper by researchers Lynn H. Kaack, Jay Apt, M. Granger Morgan, and Patrick McSharry), we can use statistical errors from past projections to develop a *cone of uncertainty*—similar to those used by the National Oceanic and Atmospheric Administration (NOAA) to produce hurricane path cones—which we can apply to the AEO2023 projections. Employing statistical errors from past projections along with side case projections can help us better assess the possible range of uncertainty in the AEO results.

For example, we can use the statistical errors from past AEO Reference case projections to project future uncertainty in U.S. energy-related CO_2 emissions produced by the AEO2023 Reference case until 2030 (Figure 20). Figure 20 includes two uncertainty cones for total energy-related CO_2 emissions, representing statistical error estimations where the narrower and wider cones capture 50% and 95% of the historical projection errors around the Reference case, respectively. Our Reference case projection has a wide range of future uncertainty in total energy-related CO_2 emissions, which in some instances goes beyond the bounds explored in our most extreme side cases.

Because the AEO Reference case includes only laws and regulations current at the time it is developed, past Reference case projections of total energy-related CO_2 emissions tend to be higher than actual because they don't include subsequent public policies that further reduce emissions. The uncertainty cones capture these over-projected statistical errors in total energy-related CO_2 emissions and show the possibility for lower emissions compared with our most extreme side case with the lowest total energy-related CO_2 emissions. We see the possibility of total energy-related CO_2 emissions increasing in the short term before falling in the long term, both in our High Economic Growth and High Zero-Carbon Technology Cost case and the upper 95th percentile of statistical errors from past projections.

We will continue to explore our use of this technique, as well as other ways to quantify uncertainty, in future analyses.

Figure 20.

Total energy-related carbon dioxide emissions
million metric tons

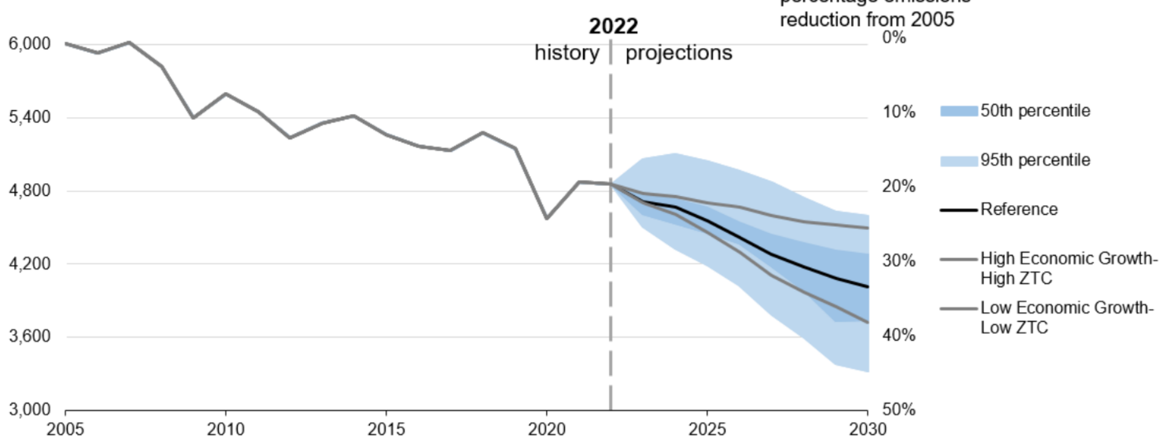

Data source: U.S. Energy Information Administration, *Annual Energy Outlook 2023* (AEO2023)
Note: Cone of uncertainty associated with total energy-related CO_2 emissions using empirical projection intervals. Historical values and AEO2023 Reference case are displayed as solid black line. The projection error density forecast by blue shaded areas. The different shades correspond to the 50th and 95th percentiles. AEO2023 envelope side cases are in solid grey lines. ZTC=Zero-Carbon Technology Cost.

Appendix

Case Descriptions

AEO2023 Reference Case

In the AEO2023 Reference case, we assess how U.S. and world energy markets would operate through 2050 under current laws and regulations as of November 2022 under evolutionary technological growth assumptions. Our key assumptions in the Reference case provide a baseline, or experimental control, for exploring long-term trends. An overview of the laws and regulations included in AEO2023 is available on the AEO website. This Appendix addresses the Inflation Reduction Act and how we incorporated it into the Reference case and side cases.

High and Low Oil Price cases

Global market balances, primarily international supply and demand factors, will drive future crude oil prices. To account for these factors, oil prices are an exogenous assumption in our analysis. In the AEO2023 High Oil Price case, the price of Brent crude oil, in 2022 dollars, reaches $190 per barrel (b) by 2050, compared with $101/b in the Reference case and $51/b in the Low Oil Price case.

High and Low Oil and Gas Supply cases

Compared with the Reference case, the High Oil and Gas Supply case assumes that the estimated ultimate recovery per well for tight oil, tight gas, or shale gas in the United States is 50% higher. Similarly, this case assumes that undiscovered resources in Alaska and the offshore Lower 48 states are 50% greater than assumed in the Reference case. Technological improvement rates that reduce costs and increase productivity of oil and natural gas production in the United States are also 50% higher than assumed in the Reference case. Conversely, the Low Oil and Gas Supply case assumes that the estimated ultimate recovery per well for tight oil, tight gas, or shale gas in the United States; the undiscovered resources in Alaska and the offshore Lower 48 states; and rates of technological improvement are all 50% lower than assumed in the Reference case.

High and Low Zero-Carbon Technology Cost cases

The High Zero-Carbon Technology Cost case and the Low Zero-Carbon Technology Cost case examine the sensitivities around capital costs for electricity-generating technologies that produce zero emissions, which include renewables, nuclear (a zero-carbon technology included in these cases for the first time in this AEO), and diurnal storage technologies. We assume capital costs decline over time from learning by doing as commercialization expands and construction and manufacturing experience accelerates. The High Zero-Carbon Technology Cost case assumes no cost reductions from learning by doing. The Low Zero-Carbon Technology Cost case assumes faster, exogenously determined technology cost declines through 2050, resulting in about a 40% cost reduction by 2050 compared with the Reference case for each zero-carbon technology. In addition, we assume fixed operating and maintenance costs will decline along with the capital cost from technology improvement. These cases replace the Low and High

Renewable Cost cases from prior AEOs and now reflect the zero-carbon technology suite, as represented in our models, which is targeted by incentives in the Inflation Reduction Act.

High and Low Economic Growth cases

The High Economic Growth case and Low Economic Growth case address the effects of economic assumptions on energy consumption modeled in the AEO2023. From 2022 to 2050, the High Economic Growth case assumes the compound annual growth rate for U.S. GDP is 2.3%, and the Low Economic Growth case assumes a 1.4% rate. By contrast, the Reference case assumes the U.S. GDP annual growth rate is 1.9% over the projection period.

Economic Growth and Zero-Carbon Technology Cost Combination cases

In addition to our eight standard core cases, we have added four combination cases for AEO2023. These cases simultaneously vary economic growth and zero-carbon technology cost assumptions. The four combinations are:

- High Economic Growth and High Zero-Carbon Technology Cost
- High Economic Growth and Low Zero-Carbon Technology Cost
- Low Economic Growth and High Zero-Carbon Technology Cost
- Low Economic Growth and Low Zero-Carbon Technology Cost

Inflation Reduction Act assumptions in the Reference case and core side cases

The Inflation Reduction Act (IRA), or Public Law 117-169, that took effect on August 16, 2022, includes energy- and climate-related provisions.[4] We reviewed the law for directives that would influence energy consumption, production, and trade in the U.S. economy as modeled in NEMS. We incorporated provisions of this law into the Reference case and side cases, unless otherwise noted. Case assumptions were frozen in mid-November 2022, and AEO2023 does not include regulatory guidance or provisions issued after that time.

This document summarizes the energy- and climate-related provisions from the IRA as incorporated into the AEO2023 Reference and side cases. This document does not cover details about provisions included in the Low and High Uptake cases, which vary the number of bonus tax credits and incentives applied to eligible technologies. Those case definitions and results are discussed in the *Issues in Focus: Inflation Reduction Act Cases in the AEO2023*. Further details about how we modeled the IRA provisions are also in the NEMS Assumptions documents. The No IRA case assumes the same economic outlook as the Reference case but excludes the IRA provisions.

All cases use the macroeconomic outlook from S&P Global IHS Markit as of September 2022.

Although all provisions of the IRA are current law, some are not explicitly included in the NEMS version used for AEO2023. We did not include these provisions for one of three reasons:

1. Guidance is not yet available on how federal agencies will implement some provisions, and without that guidance, we lack the details to analyze their effect. We will analyze these provisions in the future as we receive more clarity.
2. A number of provisions require significant modifications to NEMS that were not possible in this timeframe, and we will consider ways to include these provisions in a future outlook to the extent possible.
3. Other provisions do not align with our analytic resolution. For instance, NEMS does not model individual electricity transmission lines, and therefore, we do not model the IRA-driven impacts related to the planning or construction of transmission lines through financial appropriations in the form of assistance or loans.

Some provisions are not listed in the following table because they are not relevant to this analysis or had minor impacts to the energy system. In the *Excluded* column of Table 1, the numbers in bold correspond to one or more of the reasons listed above. The use of -- indicates that a certain column is not applicable.

---

[4] Inflation Reduction Act, Public Law 117-169, (August 16, 2022), https://www.congress.gov/bill/117th-congress/house-bill/5376.

Table 1. Included and excluded Inflation Reduction Act (IRA) provisions in NEMS

Section	Provision	Description	Included	Excluded
Title I Committee on Finance				
13101 and 13102	Extension and Modification of Credits Produced from Certain Renewable Resources Extension and Modification of Energy Tax Credit	These provisions include extensions of the Internal Revenue Service Code Section 45[i] production tax credit (PTC) and Section 48[ii] investment tax credit (ITC) for certain energy properties.	We assume the tax credit extensions and modified tax credit values. We also assume the prevailing wage and apprenticeship requirements are met by the most eligible technologies, except certain combined-heat-and-power systems, and the domestic content requirements are met by certain technologies.	We exclude certain technologies such as small-scale energy storage (called behind-the-meter storage). Further details about the technologies we model are in the NEMS Assumptions documents. We exclude the *energy communities* bonus credit. **(1,2,3)**
13103	Increase in Energy Credit for Solar and Wind Facilities Placed in Service in Connection with Low-Income Communities	This provision allows qualified solar and wind projects located in low-income communities to qualify for *environmental justice solar and wind capacity* credits.	--	**(1,3)**
13104	Extension and Modification of Credit for Carbon Oxide Sequestration	This provision extends the carbon oxide capture credit under IRS section 45Q.[iii]	We assume the tax credit extensions and modified tax credit values. We also assume the prevailing wage and apprenticeship requirements are met.	We exclude the new tax credit for direct air capture (DAC). **(2)**

Section	Provision	Description	Included	Excluded
13105	Zero-Emission Nuclear Power Production Credit	This provision creates a production credit for qualified nuclear power generation.	We assume the prevailing wage requirements are met.	--
13201	Extension of Incentives For Biodiesel, Renewable Diesel and Alternative Fuels	This provision extends the biodiesel and renewable diesel credit and an alternative fuel credit.	We extended the existing biomass-based diesel credit through 2027.	--
13202	Extension of Second Generation Biofuel Incentives	This provision extends a tax credit for second-generation biofuel production.	We extended the credit through 2027.	--
13203	Sustainable Aviation Fuel Credit	This provision creates a sustainable aviation fuel credit equal to $1.25 per gallon.	We implemented a simplified version of this credit that extends the credit through 2027	We did not assume the supplementary amount when the fuel meets certain lifecycle greenhouse gas (GHG) requirements. **(2)**
13204	Clean Hydrogen	This provision creates a new tax credit for the qualified production of clean hydrogen.	--	**(2)**
13301	Extension, Increase, and Modifications of Nonbusiness Energy Property Credit	This provision extends tax credits under IRS Section 25C[iv] for home energy efficiency improvements and modifies the tax credit for qualified energy efficiency improvements.	We assume the tax credit extensions and modified tax credit values through 2032.	We do not explicitly model service panel replacement, wiring upgrades, or home energy audits. **(3)**
13302	Residential Clean Energy Credit	This provision extends the credit under IRS Section 25D[v] for the cost of qualified residential energy efficiency expenditures and projects.	We assume the tax credit extensions and modified tax credit values, including phaseout, through 2034.	We do not explicitly model residential clean energy technologies such as residential battery storage. Further details about the

Section	Provision	Description	Included	Excluded
				technologies we model are in the NEMS Assumptions documents. **(2,3)**
13303	Energy Efficient Commercial Buildings Deduction	This provision amends IRS Section 179D[vi] and allows expenses associated with qualifying commercial building efficiency costs to be deductible expenses if they meet certain requirements.	--	**(1,3)**
13304	Extension, Increase, and Modifications of New Energy Efficient Home Credit	This provision extends Section 45L[vii] credits for new energy-efficient homes through December 31, 2032, and increases the credit if qualified projects meet prevailing wage and apprenticeship requirements.	We assume a $500–$2,500 tax credit for new properties meeting or exceeding ENERGY STAR specifications.	We do not explicitly model zero-energy ready homes ($5,000 credit), and we exclude the *energy communities* bonus credit. **(1,3)**
13401	Clean Vehicle Credit	This provision extends the Section 30D[viii] vehicle tax credit through December 31, 2032, and updates the credit value. This provision also contains vehicle assembly requirements, battery component requirements, vehicle price limits, and income limits for vehicle buyers.	We do not explicitly model this provision, but we assume the total number of vehicles that qualify for the clean vehicle tax credit based on an analysis of official U.S. government IRA expenditure estimates from the Congressional Budget Office.[ix]	--
13402	Credit for Previously-Owned Clean Vehicles	This section creates a new tax credit for used clean vehicles.	--	**(1,3)**

Section	Provision	Description	Included	Excluded
13403	Qualified Commercial Clean Vehicles	This provision provides a clean vehicle credit for vehicles not powered by internal combustion engines.	--	**(1,3)**
13404	Alternative Fuel Refueling Property Credit	This section extends and modifies a tax credit for qualified alternative-fuel refueling properties.	--	**(1,3)**
13501	Extension of the Advanced Energy Project Credit	This provision funds qualifying investments in advanced energy projects, such as facilities that manufacture electric vehicles.	--	**(1,3)**
13502	Advanced Manufacturing Production Credit	This provision provides production credits for domestic manufacturing of key components for clean energy technologies.	--	**(1,2)**
13701	Clean Electricity Production Credit	This provision creates a new production tax credit for qualified domestically produced electricity that does not emit GHG emissions.	We assume the prevailing wage and apprenticeship requirements and the domestic content requirements are met by certain technologies.	We exclude the bonus credits for qualified projects located in an *energy community*. **(1,2)**
13702	Clean Electricity Investment Credit	This provision creates a new investment tax credit for eligible clean energy technologies.	We assume the prevailing wage and apprenticeship requirements and the domestic content requirements are met by certain technologies.	We exclude the bonus credits for qualified projects located in an *energy community*. We do not model certain technologies, such as small-scale energy storage projects (called behind-the-meter storage). Further details

Section	Provision	Description	Included	Excluded
				about the technologies we model are in the NEMS Assumptions documents. **(1,2)**
13703	Cost Recovery for Qualified Facilities, Qualified Property, and Energy Storage Technology	The provision updates the definition of a *five-year property* to include facilities that qualify for the clean electricity production credit, property that qualifies for the clean energy investment tax credit, and any energy storage technology for accelerated cost recovery.	We assume the extension of the modified accelerated cost recovery system, or MACRS, for certain commercial end-use equipment and for applicable technologies in the electric power sector.	We do not explicitly model energy storage in the residential and commercial buildings sectors. Further details about the technologies we model are in the NEMS Assumptions documents. **(2,3)**
13704	Clean Fuel Production Tax Credit	This provision creates a tax credit for domestic clean fuel production, including a credit for sustainable aviation fuel, produced after December 1, 2024, and sold before December 31, 2027.	We implemented a simplified version of this credit for certain qualified fuels.	We did not model the credit values based on the lifecycle carbon emissions or emissions factor associated with qualified fuels. **(2,3)**
Part 8 13801–13802	Credit Monetization and Appropriations	These sections include provisions[x] that allow a taxpayer to transfer eligible credits to another taxpayer.	--	**(3)**
Title II Committee on Agriculture, Nutrition, and Forestry				
20001– 23005	Subtitles A–D	These sections fund the U.S. Department Forestry and U.S. Department of Agriculture for climate mitigation and restoration projects. Section 22003 focuses on	--	**(1,3)**

Section	Provision	Description	Included	Excluded
		biofuel infrastructure and agriculture product market expansion.		
Title III Committee on Banking, Housing, and Urban Affairs				
30001	Enhanced Use of Defense Production Act of 1950	This provision funds the acceleration of domestic production of clean energy technologies.	--	**(1,3)**
30002	Improving Energy Efficiency or Water Efficiency or Climate Resilience of Affordable Housing	This section funds projects that improve energy efficiency, water efficiency, or climate resilience for eligible properties.	--	**(1,3)**
Title IV Committee on Commerce, Science, and Transportation				
40007	Alternative Fuel and Low-Emission Aviation Technology Program	This section funds grants issued by the U.S. Department of Transportation for projects that produce, transport, blend, or store sustainable aviation fuel or that develop, demonstrate, or apply low-emission aviation technologies.	--	**(1)**
Title V Committee on Energy and Natural Resources				
50121	Home Energy Performance-Based, Whole-House Rebates	This section funds DOE's grants to state energy offices for rebates called Home Owner Managing Energy Savings, or HOMES.	--	**(1)**
50122	High-Efficiency Electric Home Rebate Program	This section funds DOE's financial support for state energy offices' and	--	**(1)**

Section	Provision	Description	Included	Excluded
		tribal governments' high-efficiency electric home rebate programs.		
50123	State-Based Home Energy Efficiency Contractor Training Grants	This section funds education and training for energy efficiency contractors.	--	**(3)**
50131	Assistance for Latest and Zero Building Energy Code Adoption	This section pays states and local governments to adopt the latest residential and commercial building energy codes and adopt residential and commercial building energy codes that exceed specific industry standards.	--	**(1)**
50141	Funding for DOE Loan Programs Office	This section raises the loan guarantee commitment authority to $40 billion for the DOE Title XVII Innovative Technology Loan Guarantee Program.	--	**(1)**
50142	Advanced Technology Vehicle Manufacturing	This section funds DOE's direct loans for establishing or expanding domestic manufacturing facilities for low- or no-emitting vehicles.	--	**(1)**
50143	Domestic Manufacturing Conversion Grants	This section provides grants for domestic production of electric vehicles and hydrogen fuel cell vehicles.	--	**(1)**

Section	Provision	Description	Included	Excluded
50144	Energy Infrastructure Reinvestment Financing	This section provides additional loan guarantee authority under the Energy Policy Act of 2005 for energy infrastructure that reduces air pollution.	--	**(1)**
50145	Tribal Energy Loan Guarantee Program	This provision funds the DOE's Tribal Loan Guarantee Program.	--	**(1,3)**
Part 5 50151–50153	Electric Transmission	These provisions fund DOE programs that facilitate certain transmission lines or transmission siting and planning.	--	**(1,3)**
50161	Advanced Industrial Facilities Deployment Program	This section makes about $5.8 billion available to DOE's Office of Clean Energy Demonstrations for advanced industrial technologies.	--	**(1,3)**
Part 7 50171–50173	Other Energy Matters	These sections fund the DOE laboratory infrastructure and the fabrication and enrichment facilities for special nuclear material.	--	**(1)**
50251	Leasing on the Outer Continental Shelf	This provision authorizes the U.S. Department of Interior (DOI) to conduct wind lease sales in the Outer Continental Shelf and in areas within an exclusive economic zone.	--	**(1,3)**
50261	Offshore Oil and Gas Royalty Rate	This provision increases the minimum royalty rate for new offshore fossil fuel leases.	We assume the updates to the minimum royalty rates.	--

Section	Provision	Description	Included	Excluded
50262	Mineral Leasing Act Modernization	This provision updates the onshore oil and natural gas royalty rates.	We assume the updates to the onshore oil and natural gas production royalty rates.	We exclude the adjustments to federal leases. **(3)**
50263	Royalties on All Extracted Methane	This provision modifies the royalties paid for natural gas produced on federal land and on the Outer Continental Shelf, including natural gas lost through upstream equipment.	--	**(3)**
50264	Lease Sales Under the 2017–2022 Outer Continental Shelf Leasing Program	This provision requires the completion of the 2017–2022 Outer Continental Shelf leasing program.	We assume the Outer Continental Shelf Leasing Program is completed.	--
50265	Ensuring Energy Security	This provision requires the DOI to conduct oil and natural gas lease sales annually for 10 years prior to issuing leases or rights-of-way for any new solar or wind energy projects.	--	**(3)**
Title VI Committee on Environment and Public Works				
60101	Clean Heavy-Duty Vehicles	This provision funds communities to help them replace eligible vehicles with zero-emission vehicles.	--	**(1,3)**
60103	Greenhouse Gas Reduction Fund	This section funds deployment of zero-emission technologies in low-	--	**(1,3)**

Section	Provision	Description	Included	Excluded
		income and disadvantaged communities.		
60104	Diesel Emissions Reductions	This section provides funding to identify and reduce diesel emissions from *goods movement facilities*.	--	**(1,3)**
60113	Methane Emissions Reduction Program	This section creates a methane emissions charge for qualified petroleum and natural gas systems.	--	**(1,3)**
60114	Climate Pollution Reduction Grants	This section funds the EPA's GHG air pollution implementation grants and GHG air pollution planning and implementation	--	**(1,3)**
Subtitle E 60501–60506	Transportation and Infrastructure	These sections include assistance for using low-carbon materials for constructing or altering federal buildings; for low-carbon transportation materials grants; and for a neighborhood access and equity grant program.	--	**(3)**
Title VII Committee on Homeland Security and Governmental Affairs				
70006	FEMA Building Materials Program	This section funds the Federal Emergency Management Agency's (FEMA) costs for low-carbon materials and incentives for net-zero energy projects.	--	**(3)**
Title VIII Committee on Indian Affairs				

Section	Provision	Description	Included	Excluded
80001	Tribal Climate Resilience	This section adds funds to the Bureau of Indian Affairs (BIA) for tribal climate resilience and adaptation programs.	--	**(1,3)**

---

[i] Electricity produced from certain renewable resources, etc., 26 U.S. Code § 45 (2022)
[ii] Energy credit, 26 U.S. Code § 48 (2022)
[iii] Credit for carbon oxide sequestration, 26 U.S. Code § 45Q (2022)
[iv] Energy efficient home improvement credit, 26 U.S. Code § 25C (2022)
[v] Residential clean energy credit, 26 U.S. Code § 25D (2022)
[vi] Energy efficient commercial buildings deduction, 26 U.S. Code § 179D (2022)
[vii] New energy efficient home credit, 26 U.S. Code § 45L (2022)
[viii] Clean vehicle credit, 26 U.S. Code § 30D (2022)
[ix] U.S. Congressional Budget Office, "Summary Estimated Budgetary Effects of H.R. 5376, the Inflation Reduction Act of 2022," August 5, 2022, https://www.cbo.gov/system/files/2022-08/hr5376_IR_Act_8-3-22.pdf
[x] Front Matter, 26 U.S. Code Chapter 65 § 6418 (2022)

U.S. Energy Information Administration

NATURAL GAS

OVERVIEW | DATA | ANALYSIS & PROJECTIONS | GLOSSARY › | FAQS ›

U.S. Natural Gas Exports and Re-Exports by Country

(Volumes in Million Cubic Feet, Prices in Dollars per Thousand Cubic Feet)

Period: Annual

Type - Area	Graph Clear	2017	2018	2019	2020	2021	2022	View History
Export Volumes								
Total	☐	3,153,804	3,607,841	4,657,657	5,284,678	6,652,609	6,899,616	1973-2022
Pipeline	☐	2,446,091	2,524,501	2,837,848	2,894,329	3,091,580	3,033,970	1985-2022
Canada	☐	916,380	835,982	972,519	903,520	937,124	959,630	1973-2022
Mexico	☐	1,529,711	1,688,519	1,865,329	1,990,809	2,154,457	2,074,340	1973-2022
LNG	☐	707,542	1,083,118	1,819,547	2,389,963	3,560,818	3,865,643	1985-2022
Exports	☐	707,120	1,083,118	1,819,020	2,386,944	3,560,818	3,865,643	2012-2022
By Vessel	☐	706,424	1,082,511	1,817,890	2,386,112	3,559,440	3,864,016	2012-2022
Antigua and Barbuda	☐				0	8	22	2020-2022
Argentina	☐	16,276	27,560	39,293	15,068	83,449	66,939	2015-2022
Bahamas	☐	2	137	156	257	486	489	2016-2022
Bangladesh	☐	0	0	3,419	10,660	37,734	12,663	2017-2022
Barbados	☐	200	174	211	241	297	93	2015-2022
Belgium	☐	0	0	23,897	31,946	5,584	80,245	2017-2022
Brazil	☐	17,648	35,645	54,298	111,826	307,714	71,998	2015-2022
Chile	☐	25,746	41,186	90,357	80,615	121,881	30,131	2015-2022
China	☐	103,410	90,473	6,851	214,401	453,304	96,659	2015-2022
Colombia	☐	0	5,101	6,518	4,626	2,247	5,703	2017-2022
Croatia	☐			0	3,275	36,133	77,286	2019-2022
Dominican Republic	☐	8,691	5,835	10,334	26,050	53,095	50,824	2016-2022
Egypt	☐	6,781	6,554	0	0	0	0	2016-2022
Finland	☐						329	2022-2022
France	☐	0	18,291	117,791	90,237	170,780	571,399	2017-2022
Germany	☐						7,113	2022-2022
Greece	☐	0	3,722	14,643	48,403	39,708	69,031	2017-2022
Haiti	☐	0	0	42	118	137	115	2017-2022
India	☐	20,919	57,634	91,481	124,402	196,218	122,518	2015-2022
Indonesia	☐				0	3,269	6,579	2020-2022
Israel	☐	0	3,270	0	15,834	8,906	0	2017-2022
Italy	☐	6,493	17,390	68,655	68,453	34,210	116,034	2016-2022
Jamaica	☐	0	1,303	13,892	17,052	25,276	1,516	2017-2022
Japan	☐	53,218	125,534	200,864	287,672	354,948	209,220	1973-2022
Jordan	☐	36,321	38,794	32,332	6,872	0	0	2016-2022
Kuwait	☐	20,213	9,981	10,308	17,293	34,476	57,018	2016-2022
Lithuania	☐	6,844	0	3,455	28,879	30,919	77,212	2016-2022
Malaysia	☐	0	0	3,698	0	0	0	2017-2022
Malta	☐	867	2,927	413	2,648	5,427	5,273	2016-2022
Mexico	☐	140,743	182,246	143,371	34,408	15,200	3,832	2016-2022

Netherlands	☐	3,042	12,188	81,361	85,573	174,339	378,329	2016-2022
Nicaragua	☐				0	1	0	2020-2022
Pakistan	☐	3,166	12,956	26,935	36,934	45,818	3,074	2016-2022
Panama	☐	0	6,786	10,221	12,764	8,436	13,759	2017-2022
Poland	☐	3,440	3,231	38,042	36,900	56,320	127,404	2016-2022
Portugal	☐	19,523	12,512	53,342	36,922	65,865	69,583	2015-2022
Russia	☐	0	0	0	0	0	0	2016-2022
Singapore	☐	0	3,679	31,440	28,341	20,918	22,980	2017-2022
South Korea	☐	130,185	252,223	270,025	316,227	453,483	292,732	2016-2022
Spain	☐	29,329	10,310	166,684	199,966	215,062	426,657	2016-2022
Taiwan	☐	9,004	16,731	27,397	64,363	99,350	106,738	2015-2022
Thailand	☐	3,113	0	6,635	32,622	14,548	25,988	2016-2022
Turkiye	☐	24,855	23,205	30,611	123,957	188,849	192,067	2016-2022
United Arab Emirates	☐	13,408	3,638	20,561	10,110	0	0	2015-2022
United Kingdom	☐	3,410	51,297	118,357	160,199	195,046	464,462	2016-2022
By Truck	☐	696	607	1,130	832	1,378	1,628	2012-2022
Canada	☐	5	19	25	10	128	76	2007-2022
Mexico	☐	691	587	1,105	822	1,250	1,552	1997-2022
Re-Exports	☐	422	0	526	3,019	0	0	2012-2022
Argentina	☐	0	0	0	2,164	0	0	2016-2022
Brazil	☐	0	0	0	82	0	0	2007-2022
Chile	☐							2007-2016
China	☐	0	0	0	0	0	0	2007-2022
Egypt	☐	0	0	0	0	0	0	2015-2022
India	☐	0	0	0	0	0	0	2007-2022
Japan	☐	0	0	221	387	0	0	2010-2022
Mexico	☐	0	0	0	0	0	0	2012-2022
Portugal	☐							2011-2016
South Korea	☐	0	0	0	387	0	0	2007-2022
Spain	☐	0	0	0	0	0	0	2007-2022
Turkiye	☐	0	0	0	0	0	0	2015-2022
United Kingdom	☐	0	0	305	0	0	0	2007-2022
CNG	☐	171	223	263	386	211	2	2012-2022
Canada	☐	171	223	263	386	211	2	2011-2022
Export Prices								
Average	☐	3.54	3.89	3.64	3.70	6.38	9.65	1985-2022
Pipeline	☐	3.20	3.34	2.64	2.10	4.94	6.33	1985-2022
Canada	☐	3.12	3.41	2.78	2.06	3.87	6.49	1985-2022
Mexico	☐	3.26	3.30	2.57	2.12	5.41	6.26	1985-2022
LNG	☐	4.69	5.20	5.21	5.64	7.62	12.24	1985-2022
Exports	☐	4.69	5.20	5.20	5.64	7.62	12.24	2012-2022
By Vessel	☐	4.69	5.20	5.19	5.64	7.62	12.24	2012-2022
Antigua and Barbuda	☐				--	10.80	10.80	2020-2022
Argentina	☐	4.64	6.01	5.14	5.04	6.83	13.89	2015-2022
Bahamas	☐	10.40	10.39	10.39	10.39	10.39	10.39	2016-2022
Bangladesh	☐	--	--	W	5.17	6.05	10.05	2017-2022
Barbados	☐	10.40	10.39	10.39	10.39	10.39	10.48	2015-2022
Belgium	☐	--	--	4.97	4.27	5.67	12.59	2017-2022
Brazil	☐	4.15	6.05	5.18	6.28	7.90	11.64	2015-2022
Chile	☐	5.43	4.33	4.68	5.49	7.03	10.53	2015-2022
China	☐	4.32	4.41	W	5.82	7.49	11.74	2011-2022
Colombia	☐	--	4.86	4.06	5.83	7.38	12.72	2017-2022
Croatia	☐				6.75	7.91	11.75	2020-2022

Dominican Republic	☐	4.15	3.91	4.51	5.78	7.75	12.56	2016-2022
Egypt	☐	4.93	3.27	--	--	--	--	2016-2022
Finland	☐						W	2022-2022
France	☐	--	7.03	5.33	5.17	7.34	12.48	2017-2022
Germany	☐						20.02	2022-2022
Greece	☐	--	7.62	5.90	5.86	7.61	14.52	2017-2022
Haiti	☐	--	--	10.39	10.39	10.39	10.39	2017-2022
India	☐	4.84	5.02	4.97	5.39	7.26	10.86	2015-2022
Indonesia	☐				--	8.84	11.40	2020-2022
Israel	☐	--	6.48	--	5.17	6.59	--	2017-2022
Italy	☐	3.95	6.46	4.99	5.27	6.64	11.46	2016-2022
Jamaica	☐	--	6.92	5.29	4.92	7.23	10.74	2017-2022
Japan	☐	6.13	6.86	6.55	6.38	7.80	10.73	1973-2022
Jordan	☐	4.40	4.10	3.99	5.28	--	--	2016-2022
Kuwait	☐	4.38	6.67	4.92	5.61	7.91	13.33	2016-2022
Lithuania	☐	3.84	--	W	5.17	6.98	11.14	2016-2022
Malaysia	☐	--	--	W	--	--	--	2017-2022
Malta	☐	4.70	6.70	W	5.33	7.09	8.87	2016-2022
Mexico	☐	4.93	4.70	4.53	5.02	6.08	13.43	2015-2022
Netherlands	☐	6.35	6.61	4.78	5.51	7.24	12.50	2016-2022
Nicaragua	☐				--	10.39	--	2020-2022
Pakistan	☐	3.14	5.60	6.26	4.70	7.23	W	2016-2022
Panama	☐	--	5.46	7.62	6.98	7.11	10.90	2017-2022
Poland	☐	4.26	7.12	5.72	5.13	8.10	19.74	2016-2022
Portugal	☐	5.65	5.45	5.16	5.24	8.58	10.35	2015-2022
Russia	☐	--	--	--	--	--	--	2016-2022
Singapore	☐	--	5.63	5.25	5.30	6.49	14.95	2017-2022
South Korea	☐	4.18	4.56	4.76	5.66	7.46	12.45	2016-2022
Spain	☐	4.94	4.59	5.39	5.60	8.27	11.46	2015-2022
Taiwan	☐	4.77	6.51	5.17	5.34	7.66	10.90	2015-2022
Thailand	☐	3.14	--	W	4.80	5.69	15.94	2016-2022
Turkiye	☐	4.84	5.38	5.13	5.48	8.98	11.09	2016-2022
United Arab Emirates	☐	3.87	3.46	3.99	5.91	--	--	2015-2022
United Kingdom	☐	3.87	5.77	5.32	5.78	7.79	12.06	2016-2022
By Truck	☐	8.74	8.65	9.13	8.22	11.52	13.44	2012-2022
Canada	☐	8.05	12.71	9.35	9.45	12.47	16.95	2007-2022
Mexico	☐	8.74	8.52	9.13	8.20	11.42	13.27	1992-2022
Re-Exports	☐	5.00	--	--	3.90	--	--	2012-2022
Argentina	☐	--	--	--	1.86	--	--	2015-2022
Brazil	☐	--	--	--	9.07	--	--	2007-2022
Chile	☐							2007-2016
China	☐	--	--	--	--	--	--	2007-2022
Egypt	☐	--	--	--	--	--	--	2015-2022
India	☐	--	--	--	--	--	--	2007-2022
Japan	☐	--	--	--	9.07	--	--	2010-2022
Mexico	☐	5.00	--	--	--	--	--	2012-2022
Portugal	☐							2011-2016
South Korea	☐	--	--	--	9.07	--	--	2007-2022
Spain	☐	--	--	--	--	--	--	2007-2022
Turkiye	☐	--	--	--	--	--	--	2015-2022
United Kingdom	☐	--	--	--	--	--	--	2007-2022
CNG	☐	4.76	4.69	3.98	2.55	4.13	3.09	2011-2022

Canada		4.76	4.69	3.98	2.55	4.13	3.09	2011-2022

Click on the source key icon to learn how to download series into Excel, or to embed a chart or map on your website.

- = No Data Reported; **--** = Not Applicable; **NA** = Not Available; **W** = Withheld to avoid disclosure of individual company data.

Notes: The price of LNG exports to Japan is the "landed" price, defined as received at the terminal in Japan. CNG = Compressed Natural Gas: Natural gas compressed to a pressure at or above 200-248 bar (i.e., 2900-3600 pounds per square inch) and stored in high?pressure containers. LNG re-exports are shipments of LNG to foreign countries that were previously imported, offloaded. See Definitions, Sources, and Notes link above for more information on this table.

Release Date: 4/28/2023
Next Release Date: 5/31/2023

PNAS | RESEARCH ARTICLE | EARTH, ATMOSPHERIC, AND PLANETARY SCIENCES | OPEN ACCESS

Observation-derived 2010-2019 trends in methane emissions and intensities from US oil and gas fields tied to activity metrics

Xiao Lu[a,b,c,1], Daniel J. Jacob[d,1], Yuzhong Zhang[e,f], Lu Shen[g], Melissa P. Sulprizio[d], Joannes D. Maasakkers[h], Daniel J. Varon[d], Zhen Qu[i], Zichong Chen[d], Benjamin Hmiel[j], Robert J. Parker[k,l], Hartmut Boesch[k,l], Haolin Wang[a], Cheng He[a], and Shaojia Fan[a,b,c]

Edited by Drew T. Shindell, Duke University, Durham, NC; received October 19, 2022; accepted February 17, 2023 by Editorial Board Member Akkihebbal R. Ravishankara

The United States is the world's largest oil/gas methane emitter according to current national reports. Reducing these emissions is a top priority in the US government's climate action plan. Here, we use a 2010 to 2019 high-resolution inversion of surface and satellite observations of atmospheric methane to quantify emission trends for individual oil/gas production regions in North America and relate them to production and infrastructure. We estimate a mean US oil/gas methane emission of 14.8 (12.4 to 16.5) Tg a^{-1} for 2010 to 2019, 70% higher than reported by the US Environmental Protection Agency. While emissions in Canada and Mexico decreased over the period, US emissions increased from 2010 to 2014, decreased until 2017, and rose again afterward. Increases were driven by the largest production regions (Permian, Anadarko, Marcellus), while emissions in the smaller production regions generally decreased. Much of the year-to-year emission variability can be explained by oil/gas production rates, active well counts, and new wells drilled, with the 2014 to 2017 decrease driven by reduction in new wells and the 2017 to 2019 surge driven by upswing of production. We find a steady decrease in the oil/gas methane intensity (emission per unit methane gas production) for almost all major US production regions. The mean US methane intensity decreased from 3.7% in 2010 to 2.5% in 2019. If the methane intensity for the oil/gas supply chain continues to decrease at this pace, we may expect a 32% decrease in US oil/gas emissions by 2030 despite projected increases in production.

methane | oil/gas emission | inversion | decadal trends | production activity

Significance

The United States accounts for a large share of global methane emissions from the oil/gas industry. Analysis of satellite and surface observations of atmospheric methane reveals larger-than-reported year-to-year variability of 2010 to 2019 US oil/gas methane emissions. This variability reflects trends in oil/gas production rates, number of active wells, and drilling of new wells. Emissions surged after 2017 as production increased. The methane intensity from the US oil/gas industry (methane emitted per unit methane gas produced) decreased steadily after 2010. Extension of this decreasing trend to 2030 (target date of the Global Methane Pledge) would result in a 32% decrease in US oil/gas methane emissions and 15% decrease in total anthropogenic emissions relative to 2019 despite an increase in production.

Atmospheric methane (CH_4) is a powerful climate forcer accounting for a third of the global temperature rise since the preindustrial era (1). It has a much shorter lifetime than carbon dioxide (CO_2) and 80 times higher warming potential over a 20-y horizon. Mitigation of methane emissions is critical for limiting global warming within 1.5 °C and also has cobenefits for public health and food productivity (2). Methane has a range of sources including wetlands as the major natural emitter, and agriculture (livestock, rice), waste (landfills, wastewater), and fossil fuel exploitation (coal, oil, gas) as the main anthropogenic emitters (3). Curbing methane emissions from the oil/gas industry is of particular interest due to its high feasibility and economic benefit (4–8).

The United States is the leading oil/gas methane emitter in the world according to United Nations Framework Convention on Climate Change (UNFCCC) reports, with a national emission of 8.1 Tg a^{-1} that accounts for 15% of global oil/gas methane emissions for 2019 (9). Oil and gas production in the United States increased by 137% and 88%, respectively, from 2005 to 2019 (10, 11). The US Environmental Protection Agency (EPA) reports no significant change in its methane emission inventory over that period, reflecting improved industry practices and capture of associated gas to offset increasing oil production (12). However, top-down estimates from observations of atmospheric methane indicate 0.4 to 6% a^{-1} increases in US oil/gas methane emissions over the 2006 to 2017 period (13–17) and national emissions about twice higher than given by EPA (5, 15, 16, 18, 19). Insufficient accounting of anomalously large sources (the so-called superemitters) has been blamed for at least part of the inventory underestimate (5, 20, 21), but there has been little study of the factors driving the long-term emission trend.

Here, we conduct an inverse analysis of 2010 to 2019 methane observations from satellite and surface sites over North America to determine the annual trends of emissions for different oil/gas production regions over that period. We relate the emission trends to activity metrics to identify the dominant drivers of oil/gas methane emissions. We also report trends in methane intensities, defined as the fraction of gas emitted to the atmosphere rather than taken to market, as an indicator of industry practices and of the potential to decrease emissions in the future.

Author contributions: X.L. and D.J.J. designed research; X.L. performed research; Y.Z., L.S., M.P.S., J.D.M., D.J.V., Z.Q., Z.C., B.H., R.J.P., H.B., and S.F. contributed new reagents/analytic tools; X.L., Y.Z., L.S., M.P.S., J.D.M., D.J.V., Z.Q., Z.C., B.H., H.W., and C.H. analyzed data; and X.L. and D.J.J. wrote the paper.

The authors declare no competing interest.

This article is a PNAS Direct Submission. D.T.S. is a guest editor invited by the Editorial Board.

[1]To whom correspondence may be addressed. Email: luxiao25@mail.sysu.edu.cn or djacob@fas.harvard.edu.

This article contains supporting information online at https://www.pnas.org/lookup/suppl/doi:10.1073/pnas.2217900120/-/DCSupplemental.

Published April 17, 2023.

Results

Top-Down 2010 to 2019 Estimates of Oil and Gas Methane Emissions. We quantify 2010 to 2019 annual methane emissions from the oil/gas industry by inverse analysis of atmospheric methane observations from the Greenhouse Gases Observing Satellite (GOSAT) satellite instrument (22) and the GLOBALVIEWplus CH_4 ObsPack dataset of surface (including tower) sites (23) (Fig. 1*A*), making use of the complementarity between the two observation platforms (15, 24–26). We use the continental-scale GEOS-Chem chemical transport model (27) at 0.5° × 0.625° resolution as forward model in the inversion to relate emissions to concentrations. The inversion strategy follows our previous work which examined national methane emissions from all sources for 2010 to 2017 (15), but here we extend it to 2019 with focus on the oil/gas sector and individual production regions. Emissions are optimized by drawing information from the observations and prior estimates following the Bayesian rule, where the prior estimates are from gridded versions of the national anthropogenic inventories reported to the UNFCCC (28–30) together with WetCHARTs v1.3.1 (31) for wetlands (Fig. 1*B* and *SI Appendix*, Fig. S1). The inversion is done for individual years in 2010 to 2019, updating boundary conditions over the oceans in each year with a consistent global inversion for 2010 to 2019 (25, 32, 33). The same prior emissions in North America are used for all years, effectively assuming no trend as a prior assumption. The posterior (optimal) solution for emissions on the 0.5° × 0.625° grid is obtained analytically to yield closed-form error statistics and information content, and to enable the construction of an ensemble of solutions using different inversion parameter assumptions. Posterior emission estimates from a 12-member inversion ensemble with each reporting two estimates by different sectoral attribution methods define the uncertainty range on the posterior results (*SI Appendix*, Table S1). See *Materials and Methods* for more details on inversion procedures, evaluation of posterior emissions, and uncertainty analyses.

The inversion returns yearly posterior gridded correction factors to the prior emission estimates on the 0.5° × 0.625° grid (*SI Appendix*, Fig. S2). Fig. 1*C* shows the mean 2010 to 2019 corrections for the oil/gas emission sector, based on the contribution from that sector to total prior emissions in each grid cell combined with error statistics by sector following Shen et al. (34). The inversion is able in this manner to separate oil/gas emissions and trends from those of other sectors (*Materials and Methods*). It has difficulty in separating oil and gas emissions for some regions and therefore we report combined oil/gas emissions. Fig. 2*A* quantifies oil/gas methane emissions for the 18 major production regions in North America. The 14 US regions account for, respectively, 60%

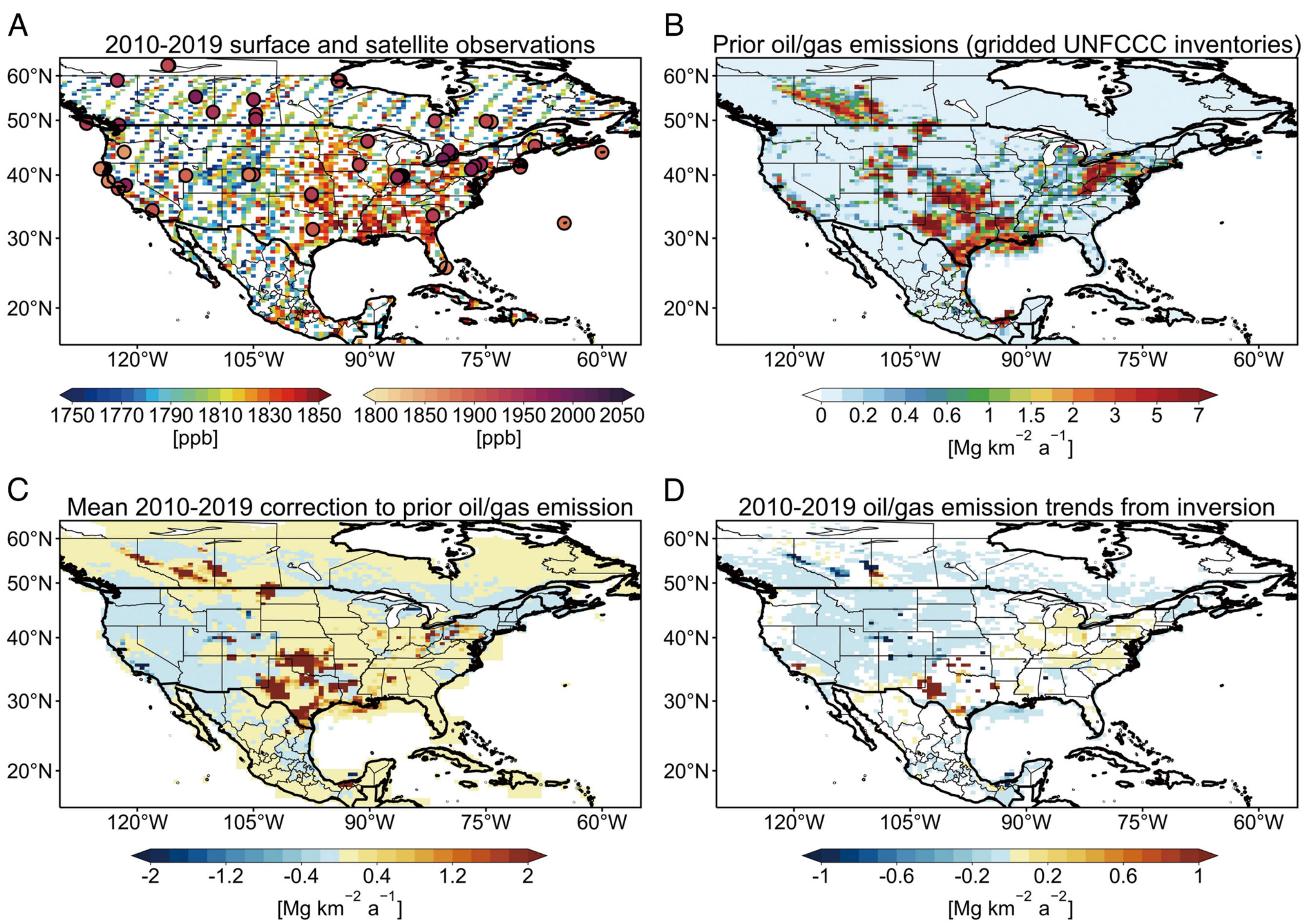

Fig. 1. Application of satellite and surface observations of atmospheric methane to quantify oil/gas emissions and 2010 to 2019 trends. Panel *A* shows mean observed surface methane mixing ratios from in situ surface and tower observations archived in the GLOBALVIEWplus CH4 ObsPack data product (circles), and dry column mixing ratios retrieved from the GOSAT satellite instrument and averaged on the 0.5° × 0.625° inversion grid. Panel *B* shows prior oil/gas emissions for the inversion from the spatially gridded versions of the US, Canada, and Mexico official national inventories reported to the United Nations Framework Convention on Climate Change (UNFCCC). Panel *C* shows the posterior corrections to mean 2010 to 2019 oil/gas methane emissions from the inversion, and Panel *D* shows the 2010 to 2019 linear trends in oil/gas emissions. The linear trends are fitted by ordinary least-squares linear regression to the inversion results for individual years. Only trends with *P-value* ≤0.34 are shown.

and 80% of the 2019 national oil and gas production, and we will see later that they largely determine the year-to-year trend in the national oil/gas emissions.

We find significant underestimation in the national inventories of 2010 to 2019 oil/gas methane emissions across North America, prominently in the central-south and midwestern US, Alberta and Saskatchewan in Canada, and the Sureste onshore oil field in Mexico. Exceptions are the Marcellus field, which is exclusively of gas production, and the Sureste offshore oil field. These results are consistent with previous top-down studies (15, 16, 19, 34–37). Our best posterior estimate of US oil/gas methane emission averaged over 2010 to 2019 is 14.8 (12.4 to 16.5 from the inversion ensemble) Tg a^{-1}, 70% higher than the most recent EPA estimate of 8.7 Tg a^{-1} for the same period (12). Our best posterior estimates for Canada and Mexico are 2.6 (2.2 to 3.3) and 1.2 (0.8 to 1.4) Tg a^{-1}, 67% and 50% higher, respectively, than their national reports. Our inversion results for individual production regions in Fig. 2*A* are generally consistent with reported estimates from field campaigns covering different time periods in 2010 to 2019 and also with an inversion from the higher-resolution TROPOspheric Monitoring Instrument (TROPOMI) satellite instrument available for 2018 to 2019 (*SI Appendix*, Table S2). Discrepancies may partly reflect differences in observing periods. Our estimate of 2010 to 2019 emissions from the Permian (2.1 Tg a^{-1}) is low compared to other top-down estimates for the post-2017 period (2.3 to 3.7 Tg a^{-1}) (19, 37–40) which may reflect in part our use of an EPA prior estimate of 0.8 Tg a^{-1} known to be too low (19, 37) and our longer time horizon.

Interpretation of 2010 to 2019 Trends in US Oil/Gas Methane Emissions. We now examine the annual trends of oil/gas methane emissions over the 2010 to 2019 period as informed by our inversion for individual years. Fig. 1*D* shows the spatial distributions of the long-term trends as obtained by ordinary least-squares linear regression, and Fig. 2*B* gives the trends for the 18 major oil/gas production regions. Trends in oil/gas emissions can be clearly separated by the inversion from trends in emissions from other sectors (*SI Appendix*, Fig. S3). We find that oil/gas emissions over the 2010 to 2019 period changed by +7% for the United States, −23% for Canada, and −60% for Mexico. There are large spatial differences in trends between US production regions. The top six US production regions with the largest emissions including the Permian, Anadarko, Marcellus, Haynesville, and Eagle Ford show increasing trends in 2010 to 2019 ranging from 0.4 to 5% a^{-1}, except for the Barnett which shows a 1.5% a^{-1} decrease. Other regions with smaller emissions generally show emission decreases. The decreasing trends in Canada may reflect the implementation of the Pan-Canadian Framework on Clean Growth and Climate Change for reducing methane released from the oil/gas sector (41). The decreasing trends in Mexico may reflect increasing utilization of associated gas from oil production (42).

Fig. 3*A* shows the year-to-year trends in US oil/gas methane emissions over the 2010 to 2019 period as optimized by the base inversion. US oil/gas emissions increased from 14.6 Tg a^{-1} in 2010 to 15.9 Tg a^{-1} in 2014, decreased to 13.6 Tg a^{-1} in 2017, and rose again to 15.6 Tg a^{-1} in 2019. This year-to-year variability is consistent across the inversion ensemble (*SI Appendix*, Fig. S4). The US EPA inventory (12) has considerably less interannual variability (8.7 ± 0.1 Tg a^{-1}, mean ± SD for 2010 to 2019). Previous top-down studies reported large oil/gas methane emission increases for the United States of 6% a^{-1} for 2008 to 2014 (43) and 3.4% a^{-1} for 2005 to 2014 (14), whereas we find 2.4% a^{-1} for 2010 to 2014. Maasakkers et al. (16) reported an increase of only 0.4% a^{-1} for 2010 to 2015, which we explain by the steep drop from 2014 to 2015. Lu et al. (15) reported an increase in oil and decrease in gas

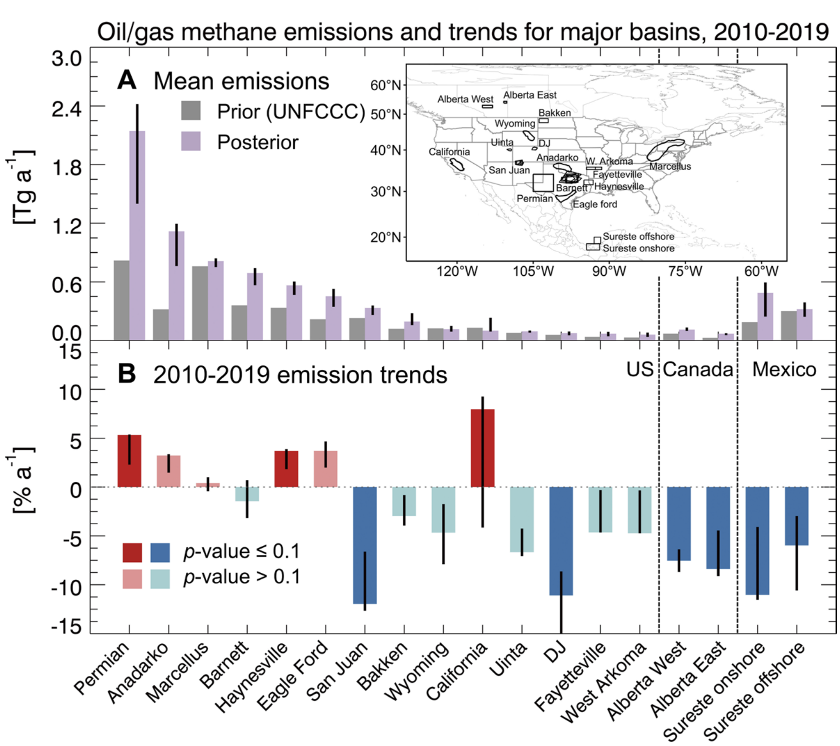

Fig. 2. Mean oil/gas methane emissions and trends for major production regions in North America, 2010 to 2019. Panel *A* shows the posterior emissions from the inversion compared to the gridded UNFCCC reports. The *Inset* panel defines the individual regions. Panel *B* shows the 2010 to 2019 emission trends inferred by ordinary least-squares linear regression on the posterior emissions for individual years. The vertical bars represent the uncertainty ranges derived from the 12-member inversion ensemble with each generating two emission estimates based on different source attribution methods, resulting in 24 estimates in total.

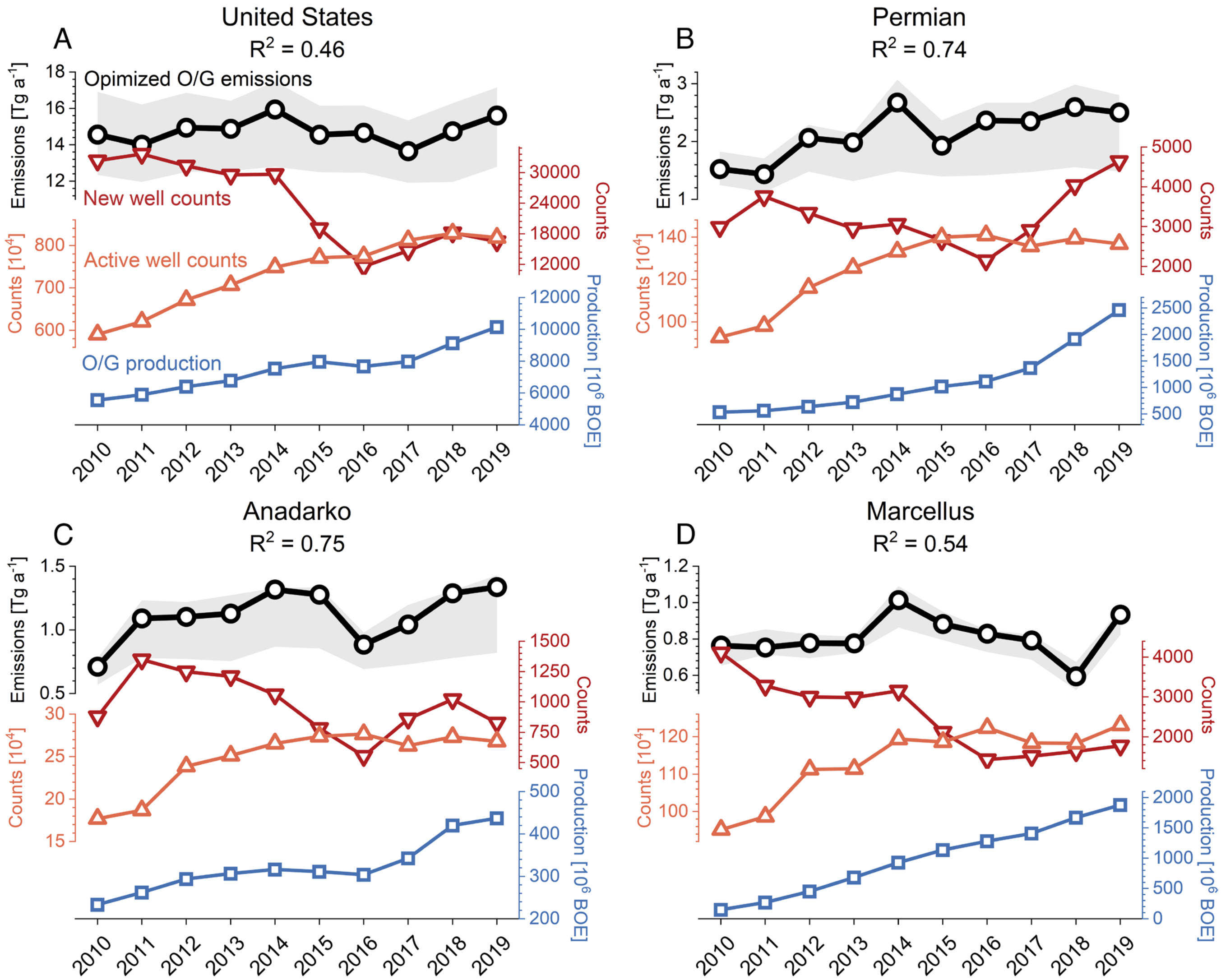

Fig. 3. 2010 to 2019 trends in oil/gas (O/G) methane emissions in the United States. Posterior emission estimates from the inversion are shown for the contiguous United States (Panel *A*) and for the three major emission regions of the Permian, Anadarko, and Marcellus (Panels *B*, *C*, and *D*) (Fig. 2). Gray shadings represent the range from the inversion ensemble; *SI Appendix*, Fig. S4 shows the trends from each ensemble member to demonstrate the consistency of the year-to-year variability across the ensemble. Also shown are trends in oil/gas production (in unit of barrel of oil equivalent, BOE), count of active wells, and count of new wells (first reported production year) from the Enverus DrillingInfo (44). These three variables are used in a multiple linear regression model to fit the posterior oil/gas emissions, with the coefficient of determination (R^2) shown as *Inset*. *SI Appendix*, Table S3 gives the detailed results for the regression model. Results for smaller oil/gas production regions are shown in *SI Appendix*, Fig. S5.

emissions for 2010 to 2017 but no significant trends for combined oil/gas emissions. The post-2017 emission surge has not been reported before to our knowledge.

We find that the interannual variability in the US oil/gas emissions can be largely explained by that in the 14 oil/gas production regions shown in Fig. 2 (R^2 = 0.74), and half can be explained by the top six regions with the largest emissions (R^2 = 0.50). We show yearly emissions for the top three production regions (Permian, Anadarko, and Marcellus) in Fig. 3 and others in *SI Appendix*, Fig. S5. The US oil/gas emission increase in 2010 to 2014 was largely driven by the Permian where emissions increased from 1.5 Tg a^{-1} in 2010 to 2.7 Tg a^{-1} in 2014 (Fig. 3*B*). The Anadarko (increasing by 0.7 Tg a^{-1}) and the Marcellus (increasing by 0.3 Tg a^{-1}) also contributed. Previous reports of large emissions in the Permian focused on the post-2017 period when TROPOMI observations became available (20, 37, 38, 40). Our inversion shows that Permian emissions were already at current high values by 2014. The national decrease in oil/gas emissions for the 2014 to 2017 period reflects a combination of trends in the Permian, Anadarko, and Marcellus (Fig. 3), while the post-2017 rebound is largely driven by the Anadarko, Marcellus, Barnett, and Haynesville. The net near-zero decadal trend of US emission in 2010 to 2019 obfuscates these subdecadal swings and spatial differences between oil/gas production regions as shown in Fig. 2*B*.

Fig. 3 further shows the relationship between the year-to-year variability in oil/gas emissions and different activity metrics. Here, we use three metrics: i) oil/gas production rate, ii) counts of active wells, and iii) counts of new wells drilled from the Enverus Drilling Info database (44). Previous aircraft-based surveys have shown strong spatial correlation of emissions with gas production and active well pad count in the Fayetteville Shale (45). Oil/gas production relates to methane emissions as high production tends to increase the number of operating facilities and the gas flowing through them. In addition, increase in production may challenge the capacity of midstream infrastructure to manage the gas flow (46). Omara et al. (47) showed that wells with low production can contribute a large proportion of oil/gas emissions, indicating that active well count number should be another predictor of oil/gas methane emissions. New wells are prone to high methane emissions due to uncontrolled emissions from exploratory drillings, a spike at well completion, and decreasing tank flash emissions during the first year of operation (48). We find that the number of new wells shows a strong correlation with the annual crude oil price from the West Texas Intermediate Cushing (WTI-Cushing) oil benchmark ($r = 0.93$) (49) and with the natural gas price from the Henry hub (https://www.eia.gov/dnav/ng/hist/rngwhhdA.htm) of ($r = 0.75$) (50). Takeaway capacity is also a possible predictor for oil/gas methane emissions as shown in a recent study of weekly emissions in Permian (51), but data are unavailable for 2010 to 2019.

We find that the three metrics of production rates, active well counts, and new well counts are complementary and together can explain 46% of the year-to-year variability of total US oil/gas emissions over the 2010 to 2019 period (Fig. 3*A*), as derived from a multiple linear regression (*SI Appendix*, Table S3). The explanatory power is higher for individual production regions, typically 60 to 80% (Fig. 3 and *SI Appendix*, Fig. S5), although the importance of each metric varies by region indicating differences in operating practices. The 2010 to 2014 increase in US oil/gas emissions by 9% was associated with a rise in oil/gas production by 34%, a rise in the number of active wells by 27%, and a sustained drilling of new wells of more than 30,000 a^{-1} over the period. All major oil/gas production regions showed similar behavior. The 2014 to 2017 drop in US oil/gas methane emissions was associated with a 60% reduction in new well development, while total oil/gas production and number of active wells remained stable. Decline in new well development was found in all major production regions (Fig. 3). This was likely driven by the drop of annual crude oil price by about 50% over the period (49).

The recent 2017 to 2019 emission surge appears to be driven by the revival of US oil/gas production which increased by 30% in this period. The number of active wells and new wells was 8% higher in 2017 to 2019 than the 2015 to 2016 mean, reflecting the upswing of oil price. The rise in oil/gas production was mostly in the Anadarko, Marcellus, and Haynesville (Fig. 3 and *SI Appendix*, Fig. S5), which accounted for most of the emission increase. Post-2017 emission increases in the Permian were weak despite large increases in oil/gas production and new well development, and this could reflect an increase in pipeline takeaway capacity (51).

Decreasing Methane Intensity from US Oil/Gas Production. Fig. 4 and *SI Appendix*, Table S4 show the magnitudes and trends of methane intensity, defined as methane emission integrated along the oil and gas supply chain per unit of methane gas production. This definition follows the US Environmental Defense Fund (EDF) (5, 46) and a number of previous studies (42, 52–54). It is similar for production regions to the methane intensity defined by the Oil and Gas Climate Initiative as upstream oil/gas emissions (from production, processing, and storage) per unit of gas marketed, since upstream emissions dominate in production regions (55). The methane intensity effectively measures the potential for reducing emissions from the oil/gas industry by marketing methane rather than emitting it. Some studies report methane intensity normalized by combined oil and gas production to estimate the amount of gas emitted per unit of total energy produced by oil/gas (40, 47, 56). The two definitions of methane intensity show similar trends (*SI Appendix*, Fig. S6). We use the first definition of methane intensity in what follows.

We derive a mean methane intensity from the US oil/gas industry of 3.1% averaged over 2010 to 2019 assuming an average methane content of 90% by volume (5). The 2010 to 2019 mean methane intensities for the eight largest US production regions (with 2010 to 2019 mean oil/gas production >100 million barrel of oil equivalent (BOE) and emission >0.2 Tg a^{-1}) vary from 1.4 to 8.8%, using reported values of methane content in natural gas for individual regions (5). The Bakken and Permian show the largest methane intensities of 8.8% and 6.3%, respectively. Both are mainly oil-producing regions where much of the by-produced gas may be vented or inefficiently flared rather than marketed (57). In comparison, gas-dominated regions such as the Marcellus, Haynesville, and Fayetteville have much lower methane intensity of less than 1.5%, reflecting a stronger motivation for these regions to capture the gas for marketing.

We find a steady decrease in the US oil/gas methane intensity of −0.13% a^{-1} ($P < 0.01$) (relative annual reduction of −0.43% a^{-1}), from 3.7% in 2010 to 2.5% in 2019. The 2017 to 2019 emission surge was driven by a large increase in production despite a continued decrease in methane intensity. 6 of the 8 largest oil/gas production regions shown in Fig. 4 have decreasing trends in methane intensity (Fig. 4*B*). Among the six smaller production regions, Denver-Julesburg also shows a decreasing trend with $P < 0.01$, while the others show insignificant trends (*SI Appendix*, Table S4). The Bakken and Permian show large methane intensity decreases of −2.3% a^{-1} and −0.53 % a^{-1}, respectively, effectively narrowing the spread of methane intensity across production regions.

The decreasing methane intensity in the United States and in the major oil/gas production regions reflects a slower increase or a decrease in oil/gas methane emissions relative to the increase in

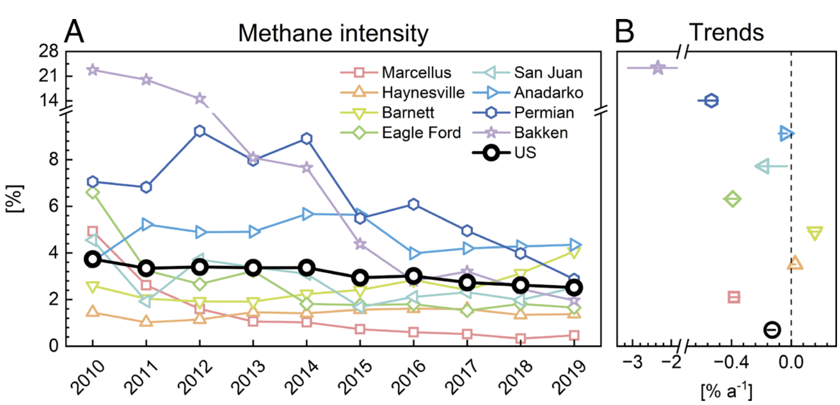

Fig. 4. 2010 to 2019 methane intensity from the US oil/gas industry. Methane intensity is defined as the total oil/gas emission per unit of gas produced. It represents the amount of methane emitted rather than used for fuel (United States) or taken to market (production regions). Panel *A* shows the year-to-year variability. Trends in Panel *B* are obtained by ordinary least-squares linear regression. Horizontal bars show the ranges from the inversion ensemble.

oil/gas production. We find that the 2010 to 2019 oil/gas methane intensity trends from all the 14 US regions of Fig. 2 are negatively correlated with their respective trends in oil/gas production ($r = -0.6$) and oil/gas production per well ($r = -0.4$) (*SI Appendix*, Table S4). Production regions with wells that are more mature and productive tend to leak less methane per unit production. Other small production regions show decreasing methane intensity even with decreasing oil/gas production and less productive wells (San Juan and Uinta).

Beyond the dominant role of production trends, we suggest that an additional driver for the decreasing methane intensity may be the US EPA's implementation of new source performance standards (NSPS) for the oil/gas sector. The NSPS proposed in 2011 (finalized form in 2012) tightened emission standards for a range of production facilities and processes including completions of hydraulically fractured gas wells, and pneumatic controllers and storage tanks from oil and gas wells (58, 59). The rules were reinforced in 2015 (finalized form in 2016) with emission standards for additional facilities and processes including hydraulically fractured oil well completions, fugitive emissions from well sites, and compressor stations (59, 60). These NSPS rules affected facilities that were constructed or modified after the date of the original proposals (2011 and 2015).

The Bakken and Permian had large methane intensities in 2010 to 2014 (8% or higher). They both show large decreases in methane intensity in 2015 (Fig. 4*A*) when the NSPS targeted emissions from the new oil production sector (60). Schneising et al. (40) previously reported a significant drop of methane intensity in Bakken from 2009 to 2011 to 2018 to 2019 and suggested that the trend may be driven by industry initiatives for leak detection and repair, replacement or upgrade of high-emitting devices, and reduction of venting or flaring. For the Permian, the US EPA's Greenhouse Gas Reporting Program indicates a 21% increase in gathering pipeline miles from its first report year in 2016 to 2019 (61), and the pipeline takeaway capacity increased by ~10% from 2018 to 2019 (earlier data are not available), indicating more effective gas capture for marketing (51). This may explain the flat emission in the Permian despite large increases in oil/gas production after 2016.

Gas-dominated production regions such as the Marcellus and Haynesville have much lower methane intensity than the Bakken and Permian and also show decreases in methane intensity over 2010 to 2019. Decreasing methane intensity in the Marcellus, the leading shale gas production region in the United States, can likely be attributed to reduced new well drilling in the second half of the decade and new regulations requiring capture of gas from the completion-venting step of hydraulic fracturing (62), though we see a rebound of new wells drilled and methane emissions in 2019 (Fig. 3*D*).

The Anadarko and Barnett stand out as the production regions with the largest methane intensities in 2019 and no significant decreases over the 2010 to 2019 period. Barnett is a mature shale production region with few new wells drilled in 2010 to 2019 (52). It shows an increase of methane intensity over 2017 to 2019 for reasons that are unclear. Persistent high methane intensity in Anadarko is consistent with findings from a previous study (40). These two regions would be attractive targets for decreasing methane emissions.

Discussion

Even with the overall decreasing trend in 2010 to 2019 methane intensity, the United States is still emitting a large amount of oil/gas methane concentrated in a few major production regions and with no sign of an actual emission decrease since production continues to increase. Our best estimate of 15.6 Tg a^{-1} for US oil/gas emissions in 2019, compared to the US EPA estimate of 8.7 Tg a^{-1}, increases the United States' contribution to global oil/gas methane emission from 15% to 28% if based on UNFCCC reports for other countries (9). The United States is committed with 121 other countries to the Global Methane Pledge, an initiative to reduce collective methane emissions by 30% below 2020 levels by 2030 (63). The US Methane Emission Reduction Action has prioritized new actions to reduce methane leaked from the oil/gas industry (64). At the same time, the US Energy Information Administration projects an increase in oil and gas production by 18% and 13%, respectively, in 2030 relative to 2020 levels in the International Energy Outlook (IEO) 2022 Reference Scenario (65). If the 2010 to 2019 decreasing trend in methane intensity shown in Fig. 4 continues at its current rate (relative annual reduction of -0.43% a^{-1}), the methane intensity would drop to 1.5% by 2030. Applying this methane intensity to the increased production in the IEO 2022 Reference Scenario and our best emission estimate of 15.6 Tg a^{-1} for 2019 indicate an US oil/gas emission of 10.6 Tg a^{-1} in 2030, 32% lower than 2019 levels, and a 15% decrease in total US anthropogenic emissions if other sectors taken from the US EPA inventory are assumed constant (12). Sustaining such a continued decrease in methane intensity may be a challenge as oil/gas fields approach maturity and wells become less productive, as is evident in the present-day Barnett (52), and development of new oil/gas fields would likely cause the methane intensity to increase. New efforts to decrease the methane intensity from oil/gas production, as outlined in the US Methane Emission Reduction Action (64), will be necessary to meet the United States' contribution to the Global Methane Pledge.

Materials and Methods

Observations of Atmospheric Methane.

In-situ observations. In-situ methane measurements are from the GLOBALVIEWplus CH_4 ObsPack product compiled by the National Oceanic and Atmospheric Administration (NOAA) Global Monitoring Laboratory (23). We use daily daytime (10 to 16 local time) methane mixing ratio at surface and tower measurement sites with continuous 10-y records in 2010 to 2019 over North America, composing a total of 73,297 data points from 47 sites.

GOSAT satellite retrievals. We use dry column methane mixing rations (XCH_4) in 2010 to 2019 from the GOSAT satellite instrument produced by the University of Leicester version 9.0 Proxy XCH_4 retrieval (22). We exclude glint data over the oceans and poleward of 60° due to seasonally biased sampling and potentially high errors. We obtain a total of 243233 GOSAT retrievals for 2010 to 2019 over North America.

Bottom-Up Emissions Used as Prior Estimates for the Inversion. We use gridded versions of the national anthropogenic methane emission inventories for the United States, Canada, and Mexico reported to the UNFCCC. Spatial allocation of these emissions by sector on a 0.1° × 0.1° grid was done by Maasakkers et al. (28) for 2012 US emissions based on the 2016 US EPA Greenhouse Gas Inventory, by Scarpelli et al. (29) for 2018 Canada emissions based on the 2020 Environment and Climate Change Canada report, and by Scarpelli et al. (30) for 2015 Mexico emissions based on the 2018 Instituto Nacional de Ecologia y Cambio Climatico report. We use the same anthropogenic emissions as prior estimates for all years in the 2010 to 2019 period, so that emission trends from the inversion are solely driven by observations.

Wetland methane emissions (*SI Appendix*, Fig. S1*D*) are from the mean of the nine highest-performance members of the WetCHARTs v1.3.1 inventory ensemble at 0.5° × 0.5° resolution (31), selected for their fit to the global GOSAT inversion results (33). We use 2010 to 2019 mean emissions by month as prior estimates in the inversion to avoid introducing prior information on interannual variability. Open fire emissions are daily values for individual years from the Global Fire Emissions Database version 4s (66). Small constant natural emissions are from Etiope et al. (67) scaled to Hmiel et al. (68) for seepages and from Fung et al. (69) for termites.

GEOS-Chem Forward Model Simulation. We use the nested version of the GEOS-Chem 12.5.0 chemical transport model (https://doi.org/10.5281/zenodo.3403111) to simulate the atmospheric methane concentrations and their sensitivity to methane emissions. The model is driven by MERRA-2 reanalysis meteorological fields (70). We conduct model simulations at 0.5° × 0.625° resolution over the North America domain (130-55°W, 15-65°N) for each individual year of 2010 to 2019, with the initial and boundary conditions at the edge of the domain archived from a global model simulation using posterior methane emissions optimized from a global inversion of GOSAT satellite observations (25, 32, 33). The boundary conditions capture the global trend of methane concentrations over the 2010 to 2019 period but may have errors in interannual variability. We therefore choose to optimize the boundary conditions in the four directions (east, west, south, and north) for individual years as state vector elements in the inversion.

Atmospheric Inverse Analysis. The inversion procedure including the design of state vector, error estimates, and optimization strategy mostly follows Lu et al. (15). We use a Gaussian mixture model (71) to generate 600 Gaussian emission functions defined by location, spread, and magnitude in the prior gridded emissions, in order to preserve high (0.5° × 0.625°) resolution for regions with strong localized emissions while smoothing the solution in regions of weak emissions. The state vector $\boldsymbol{x}$ is then defined as the emission from each of the 600 Gaussians, plus the correction to the model boundary conditions as described earlier, for a total dimension $n = 604$.

We solve the optimal estimate of $\boldsymbol{x}$ by minimizing the Bayesian cost function $J(\boldsymbol{x})$:

$$J(\boldsymbol{x}) = \left(\boldsymbol{x}-\boldsymbol{x_A}\right)^T \boldsymbol{S_A}^{-1}(\boldsymbol{x}-\boldsymbol{x_A}) + \gamma(\boldsymbol{y}-\boldsymbol{Kx})^T \boldsymbol{S_O}^{-1}(\boldsymbol{y}-\boldsymbol{Kx}), \qquad [\mathbf{1}]$$

where $\boldsymbol{x_A}$ is the prior estimate of $\boldsymbol{x}$, $\boldsymbol{S_A}$ is the prior error covariance matrix, $\boldsymbol{y}$ is the observation vector, $\boldsymbol{S_O}$ is the observation error covariance matrix, $\boldsymbol{K} = \partial \boldsymbol{y}/\partial \boldsymbol{x}$ is the Jacobian matrix representing the sensitivity of modeled methane concentrations to emissions, and γ is a regularization factor to prevent overfitting. Minimizing Eq. **1** at $\nabla_{\boldsymbol{x}} J(\boldsymbol{x}) = \boldsymbol{0}$ yields an analytical solution for the posterior state vector $\hat{\boldsymbol{x}}$, its error covariance matrix $\hat{\boldsymbol{S}}$, and the averaging kernel matrix $\boldsymbol{A}$:

$$\hat{\boldsymbol{x}} = \boldsymbol{x_A} + (\gamma \boldsymbol{K}^T \boldsymbol{S_O}^{-1}\boldsymbol{K} + \boldsymbol{S_A}^{-1})^{-1}\gamma \boldsymbol{K}^T \boldsymbol{S_O}^{-1}(\boldsymbol{y} - \boldsymbol{K}\boldsymbol{x_A}), \qquad [\mathbf{2}]$$

$$\hat{\boldsymbol{S}} = (\gamma \boldsymbol{K}^T \boldsymbol{S_O}^{-1}\boldsymbol{K} + \boldsymbol{S_A}^{-1})^{-1}, \qquad [\mathbf{3}]$$

$$\boldsymbol{A} = \frac{\partial \hat{x}}{\partial x} = \boldsymbol{I_n} - \hat{\boldsymbol{S}}\boldsymbol{S_A}^{-1}. \qquad [\mathbf{4}]$$

The inversion returns the posterior estimates of mean emissions and averaging kernel sensitivities for each Gaussian, and these values can then be mapped back to the 0.5° × 0.625° grid space.

We construct $\mathbf{K}$, $\boldsymbol{S_A}$, $\boldsymbol{S_O}$ and the regularization factor γ following Lu et al. (15). Our base inversion assumes log-normal error distribution for the prior emission magnitude of each Gaussian with a geometric SD of 2 (corresponding to a factor of 2 uncertainty). This allows us to avoid unphysical negative posterior emissions (72) and to better capture the heavy tail of the emission distribution (5, 7, 21, 73) as compared to previous studies assuming normal error distributions.

Evaluation of Posterior Estimate. We evaluate the inversion results by comparing the ability of GEOS-Chem simulations with posterior versus prior emissions to fit the observed GOSAT methane columns, the GLOBALVIEWplus CH_4 ObsPack surface/tower observations of methane concentrations, and independent ground-based methane column observations at three sites from the Total Carbon Column Observing Network (TCCON). *SI Appendix*, Fig. S7 shows that the posterior simulation with optimized emissions and trends significantly reduces the model mean bias in US surface and tower measurements from −11 ppb in the prior simulation to −6 ppb, and the rms error (rmse) from 22 to 15 ppb. We find that there is no decadal trend in the model bias relative to both in situ and GOSAT observations in the posterior simulations. The model is biased high at the three TCCON sites and this is mostly driven by the Lamont, Oklahoma site, but again there is no bias in the trend.

Attributing Posterior Emissions and Trends to Emission Sectors. Our inversion returns posterior correction factors (f_0) to the total methane emissions in individual 0.5° × 0.625° grid cells and for individual years. We apply two methods to allocate f_0 to correction factors f_i for individual sectors i in that grid cell. The first method (base estimate) derives f_i based on the fraction of sectoral emissions to the total prior emissions in the grid cell and the error statistics for that sector given in the prior US EPA emission inventory (28), following Shen et al. (34). The second method assumes that the prior sectoral distribution of emissions in the grid cell is correct and that the posterior scaling factors apply equally to all sectors in the grid cell ($f_i = f_0$).

We examined the ability of the inversion to quantify oil/gas emissions in individual production regions separately from other sources (such as livestock) in those regions. This was done by transforming the posterior full-dimension state vector $\hat{\boldsymbol{x}}$ to a reduced state vector $\hat{\boldsymbol{x}}_{\boldsymbol{red}}$, with sectoral methane emissions aggregated over the defined region as elements. We can then use the corresponding posterior error covariance matrix $\hat{\boldsymbol{S}}_{\boldsymbol{red}}$ to quantify the ability of the inversion to separate emissions from different sectors within the region. Further details on this approach are in the study by Maasakkers et al. (74). We find that we can successfully separate oil/gas emissions from other sectors in the United States and in most of the major oil/gas production regions as indicated by the small posterior error correlation coefficients for all sector pairs (*SI Appendix*, Fig. S8). However, separating oil from gas emissions can be challenging for some regions and we only report combined oil/gas methane emissions.

Uncertainty of the Posterior Estimates. Our analytical inversion returns the closed-form posterior error covariance matrix $\hat{\boldsymbol{S}}$ (Eq. **3**) which can be used to examine the uncertainty of the posterior emissions. However, $\hat{\boldsymbol{S}}$ does not reflect the uncertainty in the inversion parameters. We derive an alternative estimate of the uncertainty based on the range of posterior emissions from a 24-member inversion ensemble including different forms and values of $\boldsymbol{S_A}$, different values of the regularization parameter γ, and different sectoral attribution methods (*SI Appendix*, Table S1). Generation of this ensemble is immediate since all members use the same Jacobian matrix $\mathbf{K}$. *SI Appendix*, Fig. S9 compares the uncertainties estimated from $\hat{\boldsymbol{S}}$ and from the inversion ensemble for the year 2015. We find that the emission uncertainty defined by the range of the inversion ensemble is generally larger than the error inferred from the diagonal of $\hat{\boldsymbol{S}}$ except for small production regions, consistent with the finding in the study by Chen et al. (75). We therefore mainly use the 24-member range in the inversion ensemble to characterize uncertainty, but report uncertainty from $\hat{\boldsymbol{S}}$ where applicable (e.g., when describing a single inversion result or when uncertainty from $\hat{\boldsymbol{S}}$ is larger than the ensemble range).

SI Appendix, Fig. S4 shows the range of posterior oil/gas emissions from the 24-member ensemble (*SI Appendix*, Table S1) in the United States and the three largest basins (Permian, Anadarko, and Marcellus). We find that assuming a log-normal error distribution (inversions #1-6) for prior emission rather than a normal distribution (inversions #7-12) typically results in higher posterior emission estimates, by better capturing the observed heavy tail of the emission probability density functions. Assuming a larger prior error allows stronger upward correction of oil/gas emissions. Using a source-dependent $\boldsymbol{f_i}$ attributes more upward correction to oil/gas emissions as the oil sector has larger uncertainty in the gridded EPA emission inventory (28). Reducing the weight of GOSAT observations decreases the ability to optimize methane emissions but has relatively little impact on the magnitude. The year-to-year variability is in general consistent across the inversion ensemble.

Data, Materials, and Software Availability. Data (.csv/.nc/.sav) have been deposited in GitHub (https://github.com/luxiaoatchemsysu/Data-USoilgasCH4) (76).

ACKNOWLEDGMENTS. We acknowledge all of the data providers and laboratories that contributed to the GLOBALVIEWplus CH4 ObsPack v3.0 data product (http://doi.org/10.25925/20210401) compiled by the NOAA Global Monitoring Laboratory. We acknowledge funding from the NOAA Atmospheric Chemistry, Carbon Cycle, and Climate (AC4) Program and from the NASA Carbon Monitoring System. We thank the Japanese Aerospace Exploration Agency, National Institute for Environmental Studies, and the Ministry of Environment for the GOSAT data and their continuous support as part of the Joint Research Agreement. This research used the Alice High Performance Computing Facility at the University of Leicester for the Greenhouse Gases Observing Satellite (GOSAT) retrievals. We thank Melissa Weitz from the US EPA and Ritesh Gautam from EDF for helpful comments. X.L. would like to acknowledge funding from the National Key Research and Development Program (2022YFE0127500), Guangdong Basic and Applied Basic Research Foundation (2022A1515011554), and the National Natural Science Foundation of China (42105103). Y.Z. would like to acknowledge funding from the National Natural Science Foundation of China (42007198) and the foundation of Westlake University. R.J.P. and H.B. would like to acknowledge support from the UK National Centre for Earth Observation funded by the National Environment Research Council (NE/R016518/1 and NE/N018079/1) and the Copernicus Climate Change Service (C3S2_312a_Lot2).

Author affiliations: [a]School of Atmospheric Sciences, Sun Yat-sen University, Southern Marine Science and Engineering Guangdong Laboratory (Zhuhai), Zhuhai, Guangdong 519082, China; [b]Guangdong Provincial Observation and Research Station for Climate Environment and Air Quality Change in the Pearl River Estuary, Zhuhai, Guangdong Province 519082, China; [c]Key Laboratory of Tropical Atmosphere-Ocean System (Sun Yat-sen University), Ministry of Education, Zhuhai, Guangdong Province 519082, China; [d]School of Engineering and Applied Sciences, Harvard University, Cambridge, MA 02138; [e]Key Laboratory of Coastal Environment and Resources of Zhejiang Province, School of Engineering, Westlake University, Hangzhou, Zhejiang Province 310024, China; [f]Institute of Advanced Technology, Westlake Institute for Advanced Study, Hangzhou, Zhejiang Province 310024, China; [g]Department of Atmospheric and Oceanic Sciences, School of Physics, Peking University, Beijing 100871, China; [h]SRON Netherlands Institute for Space Research, Utrecht, the Netherlands; [i]Department of Marine, Earth, and Atmospheric Sciences, North Carolina State University, Raleigh, NC 27695; [j]Environmental Defense Fund, Washington, DC 20009; [k]National Centre for Earth Observation, Space Park Leicester, University of Leicester, Leicester LE1 7RH, UK; and [l]Department of Physics and Astronomy, Earth Observation Science, University of Leicester, Leicester LE1 7RH, UK

1. IPCC, Climate change 2021: The physical science basis. Contribution of Working Group I to the sixth assessment report of the intergovernmental panel on climate change, V. Masson-Delmotte *et al.*, Eds. (Cambridge University Press, Cambridge, United Kingdom and New York, NY, USA, 2021). In press.
2. D. Shindell *et al.*, Simultaneously mitigating near-term climate change and improving human health and food security. *Science* **335**, 183–189 (2012).
3. M. Saunois *et al.*, The global methane budget 2000–2017. *Earth Syst. Sci. Data* **12**, 1561–1623 (2020).
4. R. A. Alvarez, S. W. Pacala, J. J. Winebrake, W. L. Chameides, S. P. Hamburg, Greater focus needed on methane leakage from natural gas infrastructure. *Proc. Natl. Acad. Sci. U.S.A.* **109**, 6435–6440 (2012).
5. R. A. Alvarez *et al.*, Assessment of methane emissions from the U.S. oil and gas supply chain. *Science* **361**, 186–188 (2018).
6. T. Lauvaux *et al.*, Global assessment of oil and gas methane ultra-emitters. *Science* **375**, 557–561 (2022).
7. J. S. Rutherford *et al.*, Closing the methane gap in US oil and natural gas production emissions inventories. *Nat. Commun.* **12**, 4715 (2021).
8. I. B. Ocko *et al.*, Acting rapidly to deploy readily available methane mitigation measures by sector can immediately slow global warming. *Environ. Res. Lett.* **16**, 054042 (2021).
9. T. R. Scarpelli *et al.*, Updated global fuel exploitation inventory (GFEI) for methane emissions from the oil, gas, and coal sectors: Evaluation with inversions of atmospheric methane observations. *Atmos. Chem. Phys.* **22**, 3235–3249 (2022).
10. U.S. Energy Information Administration, Natural gas gross withdrawals and production (2022). https://www.eia.gov/dnav/ng/ng_prod_sum_a_EPG0_FPD_mmcf_a.htm.
11. U.S. Energy Information Administration, Crude oil production (2022). https://www.eia.gov/dnav/pet/pet_crd_crpdn_adc_mbbl_a.htm.
12. U.S. Environmental Protection Agency (2022) Inventory of U.S. greenhouse gas emissions and sinks: 1990-2020.
13. D. Helmig *et al.*, Reversal of global atmospheric ethane and propane trends largely due to US oil and natural gas production. *Nat. Geosci.* **9**, 490–495 (2016).
14. X. Lan *et al.*, Long-term measurements show little evidence for large increases in total U.S. methane emissions over the past decade. *Geophys. Res. Lett.* **46**, 4991–4999 (2019).
15. X. Lu *et al.*, Methane emissions in the United States, Canada, and Mexico: Evaluation of national methane emission inventories and 2010–2017 sectoral trends by inverse analysis of in situ (GLOBALVIEWplus CH4 ObsPack) and satellite (GOSAT) atmospheric observations. *Atmos. Chem. Phys.* **22**, 395–418 (2022).
16. J. D. Maasakkers *et al.*, 2010–2015 North American methane emissions, sectoral contributions, and trends: A high-resolution inversion of GOSAT observations of atmospheric methane. *Atmos. Chem. Phys.* **21**, 4339–4356 (2021).
17. J.-X. Sheng *et al.*, 2010–2016 methane trends over Canada, the United States, and Mexico observed by the GOSAT satellite: Contributions from different source sectors. *Atmos. Chem. Phys.* **18**, 12257–12267 (2018).
18. S. M. Miller *et al.*, Anthropogenic emissions of methane in the United States. *Proc. Natl. Acad. Sci. U.S.A.* **110**, 20018–20022 (2013).
19. L. Shen *et al.*, Satellite quantification of oil and natural gas methane emissions in the US and Canada including contributions from individual basins. *Atmos. Chem. Phys.* **22**, 11203–11215 (2022).
20. I. Irakulis-Loitxate *et al.*, Satellite-based survey of extreme methane emissions in the Permian basin. *Sci. Adv.* **7**, eabf4507 (2021).
21. D. Zavala-Araiza *et al.*, Reconciling divergent estimates of oil and gas methane emissions. *Proc. Natl. Acad. Sci. U.S.A.* **112**, 15597–15602 (2015).
22. R. J. Parker *et al.*, A decade of GOSAT proxy satellite CH4 observations. *Earth Syst. Sci. Data* **12**, 3383–3412 (2020).
23. K. N. Schuldt *et al.*, Multi-laboratory compilation of atmospheric methane data for the period 1983-2020: Obspack_ch4_1_GLOBALVIEWplus_v3.0_2021-05-07. NOAA Earth System Research Laboratory, Global Monitoring Laboratory (2021). Available online: https://doi.org/10.25925/20210401. Accessed 14 November 2021.
24. D. H. Cusworth *et al.*, Detecting high-emitting methane sources in oil/gas fields using satellite observations. *Atmos. Chem. Phys.* **18**, 16885–16896 (2018).
25. X. Lu *et al.*, Global methane budget and trend, 2010–2017: Complementarity of inverse analyses using in situ (GLOBALVIEWplus CH4 ObsPack) and satellite (GOSAT) observations. *Atmos. Chem. Phys.* **21**, 4637–4657 (2021).
26. A. J. Turner *et al.*, Assessing the capability of different satellite observing configurations to resolve the distribution of methane emissions at kilometer scales. *Atmos. Chem. Phys.* **18**, 8265–8278 (2018).
27. K. J. Wecht *et al.*, Spatially resolving methane emissions in California: Constraints from the CalNex aircraft campaign and from present (GOSAT, TES) and future (TROPOMI, geostationary) satellite observations. *Atmos. Chem. Phys.* **14**, 8173–8184 (2014).
28. J. D. Maasakkers *et al.*, Gridded national inventory of U.S. methane emissions. *Environ. Sci. Technol.* **50**, 13123–13133 (2016).
29. T. R. Scarpelli, D. J. Jacob, M. Moran, F. Reuland, D. Gordon, A gridded inventory of Canada's anthropogenic methane emissions. *Environ. Res. Lett.* **17**, 014007 (2021).
30. T. R. Scarpelli *et al.*, A gridded inventory of anthropogenic methane emissions from Mexico based on Mexico's national inventory of greenhouse gases and compounds. *Environ. Res. Lett.* **15**, 105015 (2020).
31. S. Ma *et al.*, Satellite constraints on the latitudinal distribution and temperature sensitivity of Wetland methane emissions. *AGU Adv.* **2**, e2021AV000408 (2021).
32. Z. Qu *et al.*, Global distribution of methane emissions: A comparative inverse analysis of observations from the TROPOMI and GOSAT satellite instruments. *Atmos. Chem. Phys.* **21**, 14159–14175 (2021).
33. Y. Zhang *et al.*, Attribution of the accelerating increase in atmospheric methane during 2010–2018 by inverse analysis of GOSAT observations. *Atmos. Chem. Phys.* **21**, 3643–3666 (2021).
34. L. Shen *et al.*, Unravelling a large methane emission discrepancy in Mexico using satellite observations. *Remote Sens. Environ.* **260**, 112461 (2021).
35. E. Chan *et al.*, Eight-year estimates of methane emissions from oil and gas operations in Western Canada are nearly twice those reported in inventories. *Environ. Sci. Technol.* **54**, 14899–14909 (2020).
36. A. M. Robertson *et al.*, New Mexico permian basin measured well pad methane emissions are a factor of 5–9 times higher than U.S. EPA estimates. *Environ. Sci. Technol.* **54**, 13926–13934 (2020).
37. Y. Zhang *et al.*, Quantifying methane emissions from the largest oil-producing basin in the United States from space. *Sci. Adv.* **6**, eaaz5120 (2020).
38. M. Liu *et al.*, A new divergence method to quantify methane emissions using observations of sentinel-5P TROPOMI. *Geophys. Res. Lett.* **48**, e2021GL094151 (2021).
39. J. McNorton *et al.*, Quantification of methane emissions from hotspots and during COVID-19 using a global atmospheric inversion. *Atmos. Chem. Phys.* **22**, 5961–5981 (2022).
40. O. Schneising *et al.*, Remote sensing of methane leakage from natural gas and petroleum systems revisited. *Atmos. Chem. Phys.* **20**, 9169–9182 (2020).
41. Environment and Climate Change Canada, Canada to reduce emissions from oil and gas industry (2017). Avaiable at https://www.canada.ca/en/environment-climate-change/news/2017/05/canada_to_reduceemissionsfromoilandgasindustry.html.
42. Y. Zhang *et al.*, Satellite-observed changes in Mexico's offshore gas flaring activity linked to oil/gas regulations. *Geophys. Res. Lett.* **46**, 1879–1888 (2019).
43. B. Franco *et al.*, Evaluating ethane and methane emissions associated with the development of oil and natural gas extraction in North America. *Environ. Res. Lett.* **11**, 044010 (2016).
44. Enverus, Drillinginfo (2021). Available at: https://app.drillinginfo.com/production.
45. S. Schwietzke *et al.*, Improved mechanistic understanding of natural gas methane emissions from spatially resolved aircraft measurements. *Environ. Sci. Technol.* **51**, 7286–7294 (2017).
46. D. R. Lyon *et al.*, Concurrent variation in oil and gas methane emissions and oil price during the COVID-19 pandemic. *Atmos. Chem. Phys.* **21**, 6605–6626 (2021).
47. M. Omara *et al.*, Methane emissions from US low production oil and natural gas well sites. *Nat. Commun.* **13**, 2085 (2022).
48. D. T. Allen *et al.*, A methane emission estimation tool (MEET) for predictions of emissions from upstream oil and gas well sites with fine scale temporal and spatial resolution: Model structure and applications. *Sci. Total Environ.* **829**, 154277 (2022).
49. U.S. Energy Information Administration, Spot prices for the West Texas Intermediate Cushing (WTI-Cushing) oil benchmark (2022). https://www.eia.gov/dnav/pet/pet_pri_spt_s1_a.htm.
50. U.S. Energy Information Administration, Henry Hub natural gas spot price (2022). https://www.eia.gov/dnav/ng/hist/rngwhhdA.htm.
51. D. J. Varon *et al.*, Continuous weekly monitoring of methane emissions from the Permian Basin by inversion of TROPOMI satellite observations. *Atmos. Chem. Phys. Discuss.* (2022).
52. F. J. Cardoso-Saldana, D. T. Allen, Projecting the temporal evolution of methane emissions from oil and gas production basins. *Environ. Sci. Technol.* **55**, 2811–2819 (2021).
53. M. Omara *et al.*, Methane emissions from natural gas production sites in the United States: Data synthesis and national estimate. *Environ. Sci. Technol.* **52**, 12915–12925 (2018).
54. J. Peischl *et al.*, Quantifying atmospheric methane emissions from the Haynesville, Fayetteville, and northeastern Marcellus shale gas production regions. *J. Geophys. Res.* **120**, 2119–2139 (2015).
55. Oil and Gas Climate Initiative OGCI (2021) Oil and gas climate initiative reporting framework (Version 3.5). Availble at https://www.ogci.com/wp-content/uploads/2021/11/OGCI_Reporting_Framework_ver_3.5_Nov_2021.pdf.
56. D. T. Allen, Atmospheric emissions and air quality impacts from natural gas production and use. *Annu. Rev. Chem. Biomol. Eng.* **5**, 55–75 (2014).
57. O. Schneising *et al.*, Remote sensing of fugitive methane emissions from oil and gas production in North American tight geologic formations. *Earth's Future* **2**, 548–558 (2014).
58. U.S. Environmental Protection Agency, Regulatory impact analysis: Final new source performance standards and amendments to the national emissions standards for hazardous air pollutants for the oil and natural gas industry (2012). https://www.regulations.gov/document/EPA-HQ-OAR-2010-0505-4544.
59. U.S. Environmental Protection Agency, Sources covered by the 2012 new source performance standards (NSPS) for VOCs and the 2016 NSPS for Methane and VOCs, by site (2016). https://www.epa.gov/sites/default/files/2016-09/documents/sources_covered_2012nsps.pdf.
60. U.S. Environmental Protection Agency, Regulatory impact analysis of the final oil and natural gas sector: Emission standards for new, reconstructed, and modified sources (2016). https://www.regulations.gov/document/EPA-HQ-OAR-2010-0505-7630.

61. U.S. Environmental Protection Agency, Annex 3.6: Methodology for estimating CH4, CO2, and N2O emissions from natural gas systems (2022).
62. X. Ren *et al.*, Methane emissions from the marcellus shale in Southwestern Pennsylvania and Northern West Virginia based on airborne measurements. *J. Geophys. Res.* **124**, 1862–1878 (2019).
63. The White House, Joint US-EU press release on the global methane pledge (2021). Available at https://www.whitehouse.gov/briefing-room/statements-releases/2021/09/18/joint-us-eu-press-release-on-the-global-methane-pledge/.
64. The White House Office of Domestic Climate Policy, U.S. Methane emissions reduction action plan (2021). Available at https://www.whitehouse.gov/wp-content/uploads/2021/11/US-Methane-Emissions-Reduction-Action-Plan-1.pdf.
65. U.S. Energy Information Administration, Annual energy outlook 2022 (2022). Available at https://www.eia.gov/outlooks/aeo/.
66. G. R. van der Werf *et al.*, Global fire emissions estimates during 1997–2016. *Earth Syst. Sci. Data* **9**, 697–720 (2017).
67. G. Etiope, G. Ciotoli, S. Schwietzke, M. Schoell, Gridded maps of geological methane emissions and their isotopic signature. *Earth Syst. Sci. Data* **11**, 1–22 (2019).
68. B. Hmiel *et al.*, Preindustrial 14CH4 indicates greater anthropogenic fossil CH4 emissions. *Nature* **578**, 409–412 (2020).
69. I. Fung *et al.*, Three-dimensional model synthesis of the global methane cycle. *J. Geophys. Res.* **96**, 13033 (1991).
70. R. Gelaro *et al.*, The modern-era retrospective analysis for research and applications, version 2 (MERRA-2). *J. Clim.* **30**, 5419–5454 (2017).
71. A. J. Turner, D. J. Jacob, Balancing aggregation and smoothing errors in inverse models. *Atmos. Chem. Phys.* **15**, 7039–7048 (2015).
72. S. M. Miller, A. M. Michalak, P. J. Levi, Atmospheric inverse modeling with known physical bounds: An example from trace gas emissions. *Geosci. Model Dev.* **7**, 303–315 (2014).
73. C. Frankenberg *et al.*, Airborne methane remote measurements reveal heavy-tail flux distribution in Four Corners region. *Proc. Natl. Acad. Sci. U.S.A.* **113**, 9734–9739 (2016).
74. J. D. Maasakkers *et al.*, Global distribution of methane emissions, emission trends, and OH concentrations and trends inferred from an inversion of GOSAT satellite data for 2010–2015. *Atmos. Chem. Phys.* **19**, 7859–7881 (2019).
75. Z. Chen *et al.*, Methane emissions from China: A high-resolution inversion of TROPOMI satellite observations. *Atmos. Chem. Phys.* **22**, 10809–10826 (2022).
76. X. Lu, Data for "Observation-derived 2010-2019 trends in methane emissions and intensities from US oil and gas fields tied to activity metrics". https://github.com/luxiaoatchemsysu/Data-USoilgasCH4. Deposited 6 January 2023.

APRIL 20, 2023

FACT SHEET: President Biden to Catalyze Global Climate Action through the Major Economies Forum on Energy and Climate

Today, President Biden will convene leaders of the Major Economies Forum on Energy and Climate (MEF) for the fourth time since taking office to galvanize efforts needed to tackle the climate crisis and keep a 1.5°C limit on warming within reach.

At today's meeting, the President will highlight new steps the United States is taking to meet its ambitious 1.5°C-aligned goal of reducing emissions 50-52 percent in 2030. The President will also announce significant new steps the United States is taking to support developing countries in taking stronger climate action – including providing $1 billion to the Green Climate Fund and requesting $500 million for the Amazon Fund and related activities – and invite other countries to join the United States and others in fully leveraging the multilateral development banks to better address global challenges, like climate change.

The President will be joined by other leaders in new efforts aimed at accelerating progress in four key areas necessary for keeping a 1.5°C limit on warming within reach, specifically:

- **Decarbonizing energy:** Announcing steps to drive down emissions in the power and transportation sectors, including scaling up of clean energy, setting ambitious 2030 zero-emission vehicle goals, and decarbonizing international shipping.

- **Ending deforestation of the Amazon and other critical forests**: Working through the Forest and Climate Leaders' Partnership to mobilize public, private, and philanthropic support.

- **Tackling potent, non-CO2 climate pollutants**: Launching a Methane Finance Sprint to cut methane emissions and accelerating hydrofluorocarbon (HFC) phasedown under the Kigali Amendment.

- **Advancing carbon management**: Partnering with countries to accelerate carbon capture, removal, use, and storage technologies through a COP 28 Carbon Management Challenge to deal with emissions that can't otherwise be avoided.

To help frame the MEF discussion, leaders will be briefed by Dr. Fatih Birol, Executive Director of the International Energy Agency (IEA), on a new report to the MEF highlighting why action in these areas between now and 2030 is critical to preserve credible pathways to limit warming to 1.5 °C by 2100.

MEF economies account for roughly 80 percent of global GDP and global greenhouse gas (GHG) emissions. Since being reconvened by President Biden in April 2021, the MEF has helped galvanize the global climate response, contributing to the progress achieved at the United Nations Climate Conferences in Glasgow (COP 26) and Sharm El-Sheikh (COP 27).

However, the most recent findings of the Intergovernmental Panel on Climate Change underscore more urgently than ever that the window for decisive action to avert the gravest consequences of climate change is quickly narrowing.

The President will highlight how the United States is addressing these four priority areas at home through measures including the Inflation Reduction Act – the largest U.S. investment ever in reducing U.S. emissions, accelerating the clean energy economy, and protecting communities from climate impacts – and how these efforts are creating good-paying jobs and building a more secure and sustainable clean energy economy.

In addition to partnering on new joint efforts, leaders are expected to announce other new steps their countries are taking to fulfill their nationally determined contributions under the Paris Agreement. The President will encourage those countries whose 2030 Paris targets are not yet aligned with keeping 1.5 °C within reach to strengthen their targets by COP 28 this November in Dubai.

Strengthening Support for Climate Action in Developing Countries

Providing $1 Billion to the Green Climate Fund

In 2021, President Biden pledged to work with Congress to quadruple U.S. climate support for developing countries to more than $11 billion a year by 2024. As part of this broader effort, today, the President will announce that the United States is providing $1 billion to the Green Climate Fund (GCF), bringing total U.S. contributions to the GCF to $2 billion.

Since 2015, the GCF has approved over $12 billion for projects across more than 125 developing countries to accelerate clean energy transitions, build resilience in the most vulnerable countries, and catalyze private investment. These projects are expected to reduce 2.5 billion tons of emissions and increase the resilience of over 900 million people. The GCF has a specific mandate to support countries particularly vulnerable to the impacts of climate change, including least developed countries, small island developing states, and African nations.

Mobilizing the Multilateral Development Banks to Usher in a New Era of Clean Growth

Following important steps taken last week by the World Bank, President Biden will encourage leaders to support a strengthened effort this year to fully leverage the capacity of the multilateral development banks (MDBs) to address global challenges, including climate change, while accelerating progress on reducing poverty and achieving the Sustainable Development Goals. The United States is working with the MDBs to evolve their visions, incentive structures, operational approaches, and financial capacity to better meet pressing global challenges.

Decarbonizing Energy

Succeeding in keeping the 1.5 °C goal within reach will require accelerating progress in key energy-related sectors, such as electric power and transportation.

Putting the Power Sector on a Path to Net Zero Emissions

Limiting warming to 1.5°C will require steep and immediate reductions in energy sector CO2 emissions, including an accelerated scale up of clean energy technologies to achieve net zero emissions by mid-century.

President Biden has set an ambitious U.S. goal of achieving a carbon pollution-free power sector by 2035 and net zero emissions economy by no later than 2050. As a result of the historic investments in the Inflation Reduction Act and Bipartisan Infrastructure Law as well as other actions the Administration is taking, the United States is on a clear path to achieve this goal, while reducing costs for consumers, lowering harmful pollutants, mitigating climate change, and creating new economic opportunities. Today, the U.S. released a new National Innovation Pathway Report, highlighting the Biden-Harris Administration's all-hands-on-deck strategy for accelerating key clean energy technology innovations. The Administration is advancing a three-pronged approach that prioritizes innovation, demonstration, and deployment to scale the technologies the United States needs to achieve its goals of a carbon pollution-free electricity sector by no later than 2035 and a net-zero emissions economy by no later than 2050.

To accelerate global progress, President Biden will invite leaders to announce steps they are taking to put their energy sectors on a path aligned with the 1.5 °C goal.

Reducing Emissions and Fossil Fuel Use by Accelerating Zero-Emission Vehicle Deployment

The transportation sector is a large and fast-growing source of greenhouse gases globally. Rapidly scaling up production and use of zero emission vehicles (ZEVs) will slash emissions, reduce oil dependence, strengthen energy security, protect economies from oil price volatility, and accelerate the phaseout of unabated fossil fuels. Faster ZEV deployment will also improve public health by reducing emissions of conventional pollutants. Thanks to technology innovations, the historic investments in the Inflation Reduction Act, and additional investments made by automakers and throughout the battery supply chain, the U.S. transportation sector is rapidly shifting towards zero emission vehicles.

The Inflation Reduction Act contains new and expanded tax credits for drivers to purchase new clean vehicles, as well as the first-ever tax credits for purchasing used clean vehicles. These tax provisions will help make clean vehicles more accessible and affordable for American families while incentivizing automakers to build secure, reliable, trusted supply chains for the critical minerals and batteries contained in those vehicles.

Last week, the U.S. Environmental Protection Agency proposed new vehicle emissions standards that would build on this progress and accelerate the ongoing transition to a clean vehicle future. The EPA projects that, under the proposed standards, electric vehicles could account for 67% of new light-duty vehicle (LDV) sales and 46% of new medium-duty vehicle sales in model year 2032. This would avoid nearly 10 billion tons of CO_2 emissions through 2055 (equivalent to nearly twice the total U.S. CO_2 emissions in 2022), save the average consumer $12,000 over the lifetime of a light-duty vehicle, reduce oil imports by approximately 20 billion barrels, and improve air quality, especially in communities that have borne the burden of polluted air.

To accelerate this transition globally, President Biden will invite leaders to join the United States in a collective goal aiming to ensure that by 2030 over 50 percent of LDVs and at least 30 percent of medium- and heavy-duty vehicles (MHDVs) sold globally will be zero-emissions vehicles (e.g., battery electric, fuel cell electric, and plug-in hybrid vehicles). Countries joining in the collective goal will set their own national 2030 LDV and MHDV market share goals by COP 28.

Decarbonizing International Shipping

Greenhouse gas emissions from the shipping sector are significant, increasing, and incompatible with limiting global temperature rise to 1.5 °C. If shipping were a "country," it would be among the top ten largest emitters. As part of the Green Shipping Challenge highlighted at last year's MEF leaders meeting, countries, ports, and companies offered more than 40 concrete announcements at COP 27 on the steps they are taking this decade to help put the shipping sector on a path to align with the 1.5 °C goal.

In July, the International Maritime Organization (IMO) will adopt a Revised IMO Greenhouse Gas Strategy to accelerate efforts to decarbonize shipping. Today, President Biden will ask leaders to join the United States in supporting the IMO's adoption of 1.5 °C-aligned goals for the sector, including a goal of zero emissions from international shipping no later than 2050.

Ending Deforestation of the Amazon and Other Critical Forests

Ending forest loss, particularly in the tropics, is vital for limiting warming to 1.5 °C. The Glasgow Leaders Declaration on Forests and Land Use calls for halting and reversing forest loss and land degradation by 2030. The United States is taking decisive action to prevent deforestation at home and abroad, as called for in the President's Executive Order on "Strengthening the Nation's Forests, Communities, and Local Economies."

Contributing to Brazil's Amazon Fund

Today, the President will announce that he will request $500 million over five years for the Amazon Fund and related activities in the context of Brazil's renewed commitment to end deforestation by 2030. The President also will call on other leaders to pledge support to the Amazon Fund.

The U.S. Development Finance Corporation is also announcing today that it is working on a $50 million debt investment in BTG Pactual's Restoration Strategy, which would help mobilize $1 billion to support the restoration of nearly 300,000 hectares of degraded lands in Brazil, Uruguay, and Chile. Conservation International will serve as the impact advisor on the pathbreaking project, which will set aside half the restored lands for permanent protection, with the other half to be managed for sustainable forestry, generating an estimated 35 million tonnes of carbon sequestration over 15 years.

Marshalling Global Action to Stop Deforestation

The Forest and Climate Leaders' Partnership (FCLP), which was launched at COP 27 and is co-led by the United States, aims to mobilize stronger action to end deforestation and to strengthen support from donor governments, philanthropy, the private sector, and multilateral finance institutions. To help protect other critical forest basins around the globe, President Biden will call on other leaders to join the United States in committing to work through the FCLP this year to coordinate and catalyze investment and support by COP 28 to advance implementation of ambitious forest, climate, and nature actions in forest countries.

To further advance the President's commitments on combatting international deforestation associated with agriculture commodity production and the reduction of global deforestation, the

U.S. government is working to identify potential approaches to address globally traded commodities associated with international deforestation as well as identify potential action to reduce global deforestation, as called for in the President's Executive Order.

Leading at Home by Strengthening America's Forests

America's forests play a key role in achieving our domestic climate goals, absorbing carbon dioxide equivalent to more than 10% of U.S. annual greenhouse gas emissions. To advance the President's commitment to strengthening America's forests, today the U.S. is announcing critical new steps to better manage our domestic forests for climate resilience, following the completion of a first-ever nationwide inventory of old and mature forests.

Tackling Potent Non-CO2 Climate Pollutants

In addition to cutting CO_2, rapid reductions of other GHG emissions are essential to keep 1.5 °C within reach. Methane and other non-CO_2 GHGs are potent climate pollutants with short atmospheric lifetimes. Rapidly reducing them would have an outsized impact on near-term warming.

Accelerating Methane Action to Reduce Global Warming by at least 0.2 degrees Celsius by 2050

Since being introduced by the United States and the European Union at the MEF leaders meeting in September 2021, 150 countries have now joined the Global Methane Pledge, with the goal of cutting anthropogenic methane emissions at least 30 percent by 2030. More than 50 countries have developed, or are developing, national methane action plans, and many new projects are underway to drive methane reductions in the key sectors of fossil energy, waste, and agriculture and food.

To support and accelerate these efforts, President Biden will invite other countries to join the United States in a new Methane Finance Sprint with the aim of scaling up methane finance, including by raising at least $200 million in new public and philanthropic donor support for developing countries by COP 28. Philanthropies have committed to dedicate $100 million in new funding through the Global Methane Hub towards the $200 million goal. To complement these efforts, the private sector and other financial institutions will also be invited to join this effort. The President also will invite leaders to report on steps their countries are taking to strengthen their national methane reduction efforts.

Expediting the Phasedown of Super-Polluting HFCs to Avoid up to Half a degree Celsius of Warming by 2100

Hydrofluorocarbons (HFCs), widely used in refrigeration and air-conditioning, are thousands of times more powerful as greenhouse gases than CO_2. In October, with bipartisan Senate support, the United States ratified the Kigali Amendment to the Montreal Protocol, which aims to phase down global production and consumption of HFCs. Other countries participating in today's MEF meeting that have ratified Kigali over the past year include Brazil, Egypt, Indonesia, Italy, and the Republic of Korea.

Full implementation of the Kigali Amendment could avoid up to half a degree of warming by 2100. According to the U.N. Environment Programme, fully seizing opportunities to improve the energy efficiency of cooling appliances alongside HFC phasedown could as much as double the Kigali Amendment's climate benefits.

To promote rapid implementation of the Kigali Amendment, President Biden will call on other countries to ratify the amendment as soon as possible, consider expedited timelines for their phasedown of HFCs, and pledge support to use the Montreal Protocol Multilateral Fund to incentivize early action on HFCs and maximize parallel cooling efficiency improvements.

Accelerating Carbon Capture and Removal Technologies

In addition to full-scale mitigation efforts – including accelerated deployment of clean energy, ending deforestation, and cutting non-CO_2 emissions – keeping a 1.5 °C warming limit within reach will require responsible deployment of carbon capture, utilization, and storage (CCUS) and carbon dioxide removal (CDR) technologies. CCUS has a critical role to play in decarbonizing the global economy, particularly the industrial sector, where process emissions are more difficult to address. Combating climate change will also require addressing legacy emissions and removing CO_2 from the ambient air, through CDR. The IEA estimates that roughly 1.2 Gt of CCUS and CDR will be needed by 2030 to limit warming to 1.5°C. If global temperature rise exceeds 1.5°C, the use of CDR to remove CO_2 from the atmosphere will be necessary to return global temperatures to 1.5 °C by the end of the century.

Dealing with Emissions that Can't Otherwise be Avoided

To accelerate these critical technologies, the Inflation Reduction Act provides tax credits of $85 per tonne of CO_2 captured and stored and $180 for every tonne of CO_2 removed through direct air capture and permanently stored. In addition, President Biden's Bipartisan Infrastructure Law included over $12 billion in investments in next-generation carbon capture, direct air capture, integrated CCUS demonstrations, and industrial emissions reduction demonstration projects, as well as CO_2 transport and storage infrastructure.

To build on these efforts, the President will invite other countries to join the Carbon Management Challenge, with the aim of unveiling at COP 28 a suite of concrete announcements and goals that will accelerate CCUS and CDR internationally.

Throughout Earth Week, President Biden, Vice President Harris and other Cabinet-level officials are holding events and announcing commitments focused on how the President's Investing in America agenda is powering an American manufacturing and clean energy boom, lowering prices, creating good-paying jobs in clean energy industries, meeting our climate goals, and advancing environmental justice and conservation.

###

APRIL 21, 2023

FACT SHEET: President Biden Signs Executive Order to Revitalize Our Nation's Commitment to Environmental Justice for All

President Biden and Vice President Harris believe that every person has a right to breathe clean air, drink clean water, and live in a healthy community – now and into the future. During his first week in office, President Biden launched the most ambitious environmental justice agenda in our nation's history. To continue delivering on that vision, today the President will sign an executive order further embedding environmental justice into the work of federal agencies to achieve real, measurable progress that communities can count on.

The Executive Order is part of the Biden-Harris Administration's whole-of-government effort to confront longstanding environmental injustices and inequities. For far too long, communities across our country have faced persistent environmental injustice through toxic pollution, underinvestment in infrastructure and critical services, and other disproportionate environmental harms often due to a legacy of racial discrimination including redlining. These communities with environmental justice concerns face even greater burdens due to climate change.

With this action, the President is working to ensure that all people – regardless of race, background, income, ability, Tribal affiliation, or zip code – can benefit from the vital safeguards enshrined in our nation's foundational environmental and civil rights laws. That means cleaner air and water, reduced risk for asthma, cancer, and other health burdens, and better access to green space, safe and affordable housing, and clean transportation.

For President Biden, protecting our planet starts with ensuring everyone lives in a safe and healthy environment. Throughout Earth Week, President Biden, Vice President Harris, and other Cabinet-level officials are holding events and announcing commitments focused on how the President's Investing in America agenda is creating good-paying clean energy jobs, lowering costs, meeting our climate goals, advancing environmental justice and conservation, and strengthening communities that for too long were left behind or left out.

The new Executive Order, *Revitalizing Our Nation's Commitment to Environmental Justice for All,* will:

- **Deepen the Biden-Harris Administration's whole-of-government commitment to environmental justice.** The new Executive Order makes clear that the pursuit of environmental justice is a duty of all executive branch agencies and should be incorporated into their missions. It also affirms that environmental justice is central to the implementation of our bedrock civil rights and environmental laws.
- **Better protect overburdened communities from pollution and environmental harms**. The Executive Order directs agencies to consider measures to address and prevent disproportionate and adverse environmental and health impacts on communities, including the cumulative impacts of pollution and other burdens like climate change. Additionally, it requires agencies to notify nearby communities in the event of a release of toxic substances from a federal facility, and to hold a public meeting to share information on resulting health risks and necessary precautions.
- **Strengthen engagement with communities and mobilize federal agencies to confront existing and legacy barriers and injustices**. Communities with environmental justice concerns have long experienced exclusion and other significant barriers to having a voice in federal decision-making. The Executive Order recognizes this reality and that racism is a fundamental driver of environmental injustice. It directs agencies to actively facilitate meaningful public participation and just treatment of all people in agency decision-making. The Executive Order also underscores the vital importance of Tribal consultation and coordination, including to strengthen nation-to-nation relationships on issues involving environmental justice.
- **Promote the latest science, data, and research, including on cumulative impacts**. The Executive Order directs agencies to identify and address gaps in science, data, and research related to environmental justice, to advance the analysis of cumulative impacts, and to make information on environmental and health concerns more publicly accessible to communities. To address the need for a coordinated strategy for identifying and filling environmental justice data and research gaps, the Executive Order establishes a new Environmental Justice Subcommittee within the National Science and Technology Council, led by the Office of Science and Technology Policy.
- **Expand interagency coordination and launch a new Office of Environmental Justice within the White House Council on Environmental Quality.** Building on Executive Order 14008, the Executive Order adds agencies to the White House Environmental Justice Interagency Council to further a whole-of-government strategy to address current and historic environmental injustice. The Executive Order also establishes the White House

Office of Environmental Justice, led by the Federal Chief Environmental Justice Officer, and tasks it with coordinating the implementation of environmental justice policy across the federal government, ensuring that federal efforts can evolve alongside our understanding of environmental justice.

- **Increase accountability and transparency in federal environmental justice policy.** The Executive Order charges federal agencies with conducting new assessments of their environmental justice efforts and developing, implementing, and periodically updating an environmental justice strategic plan. These Environmental Justice Strategic Plans and Assessments will be submitted to the White House Council on Environmental Quality (CEQ) and made public on a regular basis, including through the Environmental Justice Scorecard, a new government-wide assessment of federal agencies' efforts to advance environmental justice.
- **Honor and build on the foundation of ongoing environmental justice work.** Under the Executive Order, agencies will continue their efforts to advance environmental justice in ways that complement and deepen prior work. The Executive Order uses the term "disproportionate and adverse" as a simpler, modernized version of the phrase "disproportionately high and adverse" used in Executive Order 12898. Those phrases have the same meaning, but removing the word "high" eliminates potential misunderstanding that agencies should only be considering large disproportionate effects.

This action follows through on President Biden's promise to modernize and improve how the federal government confronts environmental injustice to address the needs of present and future generations – a promise he made following meaningful engagement with communities with environmental justice concerns and solidified in Executive Order 14008, *Tackling the Climate Crisis at Home and Abroad*. The Executive Order reflects the values, goals, and recommendations of the White House Environmental Justice Advisory Council (WHEJAC), an expert body of leaders, researchers, practitioners, and community members. In line with the WHEJAC's recommendations, the Executive Order outlines an ambitious approach to environmental justice that is informed by scientific research, high-quality data, and meaningful engagement with communities. It also reaffirms that the federal government must continue to be transparent and accountable for its actions.

The Executive Order builds on and supplements the foundational efforts of Executive Order 12898, signed by President Bill Clinton nearly 30 years ago. For the first time in our nation's history, Executive Order 12898 recognized and sought to address what community members and leaders had been saying for decades: harmful pollution disproportionally impacts low-income communities and communities of color, among other vulnerable communities.

In addition to the Executive Order, today the Biden-Harris Administration is announcing other new steps to further the President's historic commitment to environmental justice:

- **Publishing the first-ever Environmental Justice Scorecard**. The Office of Management and Budget (OMB), CEQ, and the U.S. Digital Service are publishing Phase One of the Environmental Justice Scorecard, the first government-wide assessment of federal agencies' efforts to advance environmental justice. The first version of the Scorecard establishes a baseline for tracking the federal government's efforts through 24 agencies to secure environmental justice, including to advance the Justice40 Initiative. Over time, it will show how the Administration's actions are making meaningful changes in communities. The Scorecard incorporates recommendations from the WHEJAC and feedback from the public, environmental justice stakeholders, and experts.

- **Launching the White House Campaign for Environmental Justice.** The Biden-Harris Administration is committed to ensuring that people are seeing and experiencing the impacts of the President's environmental justice agenda in their communities. To strengthen partnerships with communities that have been left behind for too long, the Administration is announcing the White House Campaign for Environmental Justice. The campaign, which is being kicked off today at the launch of the 21st Urban Waters Federal Partnership in Raleigh, North Carolina, will redouble the Biden-Harris Administration's efforts to meet people where they are and better focus agency resources and attention on the needs of marginalized and overburdened communities.

- **Announcing new Justice40 covered programs.** Through the Justice40 Initiative, the Biden-Harris Administration is reshaping hundreds of federal programs to ensure that 40 percent of the overall benefits of certain federal investments flow to disadvantaged communities. Today three additional agencies, the Department of Commerce, the National Science Foundation, and the National Aeronautics and Space Administration (NASA), announced their Justice40 covered programs. Now nearly 470 programs across nineteen federal agencies are covered under the President's Justice40 Initiative.

- **Taking new steps to combat plastic pollution in communities.** The Biden-Harris Administration recognizes that the plastic pollution crisis is an environmental justice issue, with disadvantaged communities in the U.S. and globally bearing social, economic, and public health burdens across the entire lifecycle of plastics. Today the Environmental Protection Agency is releasing a draft National Strategy on Preventing Plastic Pollution to combat the disparate impacts on communities affected by plastic from production to waste. The White House is also announcing a new Interagency Policy Committee (IPC) on Plastic Pollution and a Circular Economy. The IPC will coordinate federal efforts on plastic pollution, prioritizing public health, economic development, and equity to ensure that the benefits of acting on plastic pollution – including jobs, minimized exposure to harmful chemicals, and clean communities – are available to all.

Today's announcements build on more than two years of progress under President Biden's leadership to advance environmental justice. That progress includes:

- **Delivering on the Justice40 Initiative.** Through President Biden's Justice40 Initiative, the Administration is delivering 40 percent of the overall benefits of federal climate, clean energy, affordable and sustainable housing, clean water, and other investments to disadvantaged communities that are marginalized and overburdened by pollution. In total, hundreds of federal programs are being reimagined and transformed to meet the Justice40 goal. Agencies are using the Climate and Economic Justice Screening Tool to identify disadvantaged communities.
- **Making historic investments in environmental justice.** The President's Investing in America agenda includes historic funding for environmental justice. This week the Environmental Protection Agency released new details about the design of the $27 billion Greenhouse Gas Reduction Fund, which will leverage public investment with private capital and finance clean energy projects that reduce pollution and energy costs, increase energy security, and create good-paying jobs, especially in low-income and disadvantaged communities. Through the Bipartisan Infrastructure Law and the Inflation Reduction Act, agencies are investing billions to plug orphaned oil and gas wells, replace lead service lines, create clean energy jobs in energy communities, increase equitable access to trees and green spaces, install air monitors to screen for pollution, purchase zero-emissions school buses, and more.
- **Advancing an ambitious regulatory agenda.** The Biden-Harris Administration is advancing an ambitious regulatory agenda to protect public health and secure environmental justice. The Environmental Protection Agency is working to combat air and water pollution by proposing the first-ever national drinking water standard for PFAS, proposing to strengthen the Mercury and Air Toxics Standards, addressing elevated cancer risks with stronger standards for chemical manufacturers, and developing new health protections to reduce exposure to ethylene oxide.
- **Strengthening enforcement of environmental laws.** The Department of Justice (DOJ) is implementing a comprehensive environmental justice enforcement strategy to enhance civil and criminal enforcement of environmental violations in communities overburdened by pollution. Examples of DOJ's enforcement work include a complaint filed and interim solution reached for the court to appoint a third party to manage and stabilize the City of Jackson, Mississippi's public drinking water system, an environmental justice investigation

into the City of Houston's operations, policies and practices related to illegal dumping, and an environmental justice investigation into the wastewater disposal and infectious disease and outbreaks programs of the Alabama Department of Public Health and the Health Department of Lowndes County, Alabama.

- **Increasing technical assistance and capacity building.** In direct response to feedback from communities, the Biden-Harris Administration has established a network of assistance centers to support communities and their partners as they work to access federal resources. Last week the Administration announced 17 new Environmental Justice Thriving Communities Technical Assistance Centers to help unlock federal resources in communities across the country. The program is part of the Federal Interagency Thriving Communities Network, which is working toward a holistic government-wide framework for technical assistance and capacity building.

- **Respecting and elevating Indigenous Knowledge.** The Biden-Harris Administration has formally recognized Indigenous Knowledge as one of the many important bodies of knowledge that contributes to the scientific, technical, social, and economic advancements of the United States and our collective understanding of the natural world. The White House engaged more than a thousand individuals, organizations, and Tribal Nations to develop guidance on elevating Indigenous Knowledge in federal research, policy, and decision-making.

- **Strengthening our regulatory system for the 21st century**. Earlier this month, the Biden-Harris Administration rolled out new efforts to promote equitable and meaningful participation in the regulatory process, and OMB's Office of Information and Regulatory Affairs proposed new guidance to help agencies better account for the full range of benefits and costs of their regulatory actions. These new steps will produce a more efficient, effective regulatory review process that will help improve people's lives – from protecting children from harmful toxins to growing our economy.

For more on the Biden-Harris Administration's work to advance environmental justice, visit https://www.whitehouse.gov/environmentaljustice/.

###

APRIL 22, 2021

FACT SHEET: President Biden Sets 2030 Greenhouse Gas Pollution Reduction Target Aimed at Creating Good-Paying Union Jobs and Securing U.S. Leadership on Clean Energy Technologies

Building on Past U.S. Leadership, including Efforts by States, Cities, Tribes, and Territories, the New Target Aims at 50-52 Percent Reduction in U.S. Greenhouse Gas Pollution from 2005 Levels in 2030

Today, President Biden will announce a new target for the United States to achieve a 50-52 percent reduction from 2005 levels in economy-wide net greenhouse gas pollution in 2030 – building on progress to-date and by positioning American workers and industry to tackle the climate crisis.

The announcement – made during the Leaders Summit on Climate that President Biden is holding to challenge the world on increased ambition in combatting climate change – is part of the President's focus on building back better in a way that will create millions of good-paying, union jobs, ensure economic competitiveness, advance environmental justice, and improve the health and security of communities across America.

On Day One, President Biden fulfilled his promise to rejoin the Paris Agreement and set a course for the United States to tackle the climate crisis at home and abroad, reaching net zero emissions economy-wide by no later than 2050. As part of re-entering the Paris Agreement, he also launched a whole-of-government process, organized through his National Climate Task Force, to establish this new 2030 emissions target – known as the "nationally determined contribution" or "NDC," a formal submission to the United Nations Framework Convention on Climate Change (UNFCCC). Today's announcement is the product of this government-wide assessment of how to make the most of the opportunity combatting climate change presents.

PUSHING PROGRESS, CREATING JOBS, AND ACHIEVING JUSTICE

The United States is not waiting, the costs of delay are too great, and our nation is resolved to act now. Climate change poses an existential threat, but responding to this threat offers an opportunity to support good-paying, union jobs, strengthen America's working communities, protect public health, and advance environmental justice. Creating jobs and tackling climate change go hand in hand – empowering the U.S. to build more resilient infrastructure, expand access to clean air and drinking water, spur American technological innovations, and create good-paying, union jobs along the way.

To develop the goal, the Administration analyzed how every sector of the economy can spur innovation, unleash new opportunities, drive competitiveness, and cut pollution. The target builds on leadership from mayors, county executives, governors, tribal leaders, businesses, faith groups, cultural institutions, health care organizations, investors, and communities who have worked together tirelessly to ensure sustained progress in reducing pollution in the United States.

Building on and benefiting from that foundation, America's 2030 target picks up the pace of emissions reductions in the United States, compared to historical levels, while supporting President Biden's existing goals to create a carbon pollution-free power sector by 2035 and net zero emissions economy by no later than 2050. There are multiple paths to reach these goals, and the U.S. federal, state, local, and tribal governments have many tools available to work with civil society and the private sector to mobilize investment to meet these goals while supporting a strong economy.

SUPPORTING AMERICAN WORKERS

This target prioritizes American workers. Meeting the 2030 emissions target will create millions of good-paying, middle class, union jobs – line workers who will lay thousands of miles of transmission lines for a clean, modern, resilient grid; workers capping abandoned wells and reclaiming mines and stopping methane leaks; autoworkers building modern, efficient, electric vehicles and the charging infrastructure to support them; engineers and construction workers expanding carbon capture and green hydrogen to forge cleaner steel and cement; and farmers using cutting-edge tools to make American soil the next frontier of carbon innovation.

The health of our communities, well-being of our workers, and competitiveness of our economy requires this quick and bold action to reduce greenhouse gas emissions. We must:

- **Invest in infrastructure and innovation.** America must lead the critical industries that produce and deploy the clean technologies that we can harness today – and the ones that we will improve and invent tomorrow.
- **Fuel an economic recovery that creates jobs.** We have the opportunity to fuel an equitable recovery, expand supply chains and bolster manufacturing, create millions of good-paying,

union jobs, and build a more sustainable, resilient future.

- **Breathe clean air and drink clean water and advance environmental justice.** We can improve the health and well-being of our families and communities – especially those places too often left out and left behind.
- **Make it in America.** We can bolster our domestic supply chains and position the U.S. to ship American-made, clean energy products — like EV batteries – around the world.

MEETING THE MOMENT

The target is consistent with the President's goal of achieving net-zero greenhouse gas emissions by no later than 2050 and of limiting global warming to 1.5 degrees Celsius, as the science demands. To develop the target, the Administration:

- **Used a whole-of-government approach:** The NDC was developed by the National Climate Task Force using a whole-of-government approach, relying on a detailed bottom-up analysis that reviewed technology availability, current costs, and future cost reductions, as well as the role of enabling infrastructure. Standards, incentives, programs, and support for innovation were all weighed in the analysis. The National Climate Task Force is developing this into a national climate strategy to be issued later this year.
- **Consulted important and diverse stakeholders:** From unions that collectively bargain for millions of Americans who have built our country and work to keep it running to groups representing tens of millions of advocates and young Americans, the Administration listened to Americans across the country. This also included groups representing thousands of scientists; hundreds of governmental leaders like governors, mayors, and tribal leaders; hundreds of businesses; hundreds of schools and institutions of higher education; as well as with many specialized researchers focused on questions of pollution reduction.
- **Explored multiple pathways across the economy**: The target is grounded in analysis that explored multiple pathways for each economic sector of the economy that produces CO_2 and non-CO_2 greenhouse gases: electricity, transportation, buildings, industry, and lands.

Each policy considered for reducing emissions is also an opportunity to support good jobs and improve equity:

- The United States has set a goal to reach **100 percent carbon pollution-free electricity by 2035**, which can be achieved through multiple cost-effective pathways each resulting in meaningful emissions reductions in this decade. That means good-paying jobs deploying carbon pollution-free electricity generating resources, transmission, and energy storage and leveraging the carbon pollution-free energy potential of power plants retrofitted with carbon capture and existing nuclear, while ensuring those facilities meet robust and rigorous standards for worker, public, environmental safety and environmental justice.

- The United States can create good-paying jobs and **cut emissions and energy costs for families by supporting efficiency upgrades and electrification in buildings** through support for job-creating retrofit programs and sustainable affordable housing, wider use of heat pumps and induction stoves, and adoption of modern energy codes for new buildings. The United States will also invest in new technologies to reduce emissions associated with construction, including for high-performance electrified buildings.

- The United States can **reduce carbon pollution from the transportation sector** by reducing tailpipe emissions and boosting the efficiency of cars and trucks; providing funding for charging infrastructure; and spurring research, development, demonstration, and deployment efforts that drive forward very low carbon new-generation renewable fuels for applications like aviation, and other cutting-edge transportation technologies across modes. Investment in a wider array of transportation infrastructure, including transit, rail, and biking improvements, will make more choices available to travelers.

- The United States can **reduce emissions from forests and agriculture and enhance carbon sinks** through a range of programs and measures including nature-based solutions for ecosystems ranging from our forests and agricultural soils to our rivers and coasts. Ocean-based solutions can also contribute towards reducing U.S. emissions.

- The United States can **address carbon pollution from industrial processes** by supporting carbon capture as well as new sources of hydrogen—produced from renewable energy, nuclear energy, or waste—to power industrial facilities. The government can use its procurement power to support early markets for these very low- and zero-carbon industrial goods.

- The United States will also reduce non-CO2 greenhouse gases, including methane, hydrofluorocarbons and other potent short-lived climate pollutants. Reducing these pollutants delivers fast climate benefits.

- In addition, the United States will **invest in innovation** to improve and broaden the set of solutions as a critical complement to deploying the affordable, reliable, and resilient clean technologies and infrastructure available today.

America must act— and not just the federal government, but cities and states, small and big business, working communities. Together, we can seize the opportunity to drive prosperity, create jobs, and build the clean energy economy of tomorrow.

###

Geophysical Research Letters

RESEARCH LETTER
10.1029/2020GL088012

Key Points:
- The coseismic deformation of the 2018 Kaktovik earthquake sequence is derived from Sentinel-1 images
- Large along-strike variations in the coseismic deformation highlight the complexity of the rupture
- We propose a geological model to connect this earthquake sequence with the regional structure

Supporting Information:
- Supporting Information S1

Correspondence to:
C. Xu,
cjxu@sgg.whu.edu.cn

Citation:
Xu, G., Xu, C., Wen, Y., Xiong, W., & Valkaniotis, S. (2020). The complexity of the 2018 Kaktovik earthquake sequence in the northeast of the Brooks Range, Alaska. *Geophysical Research Letters*, *47*, e2020GL088012. https://doi.org/10.1029/2020GL088012

Received 19 MAR 2020
Accepted 8 SEP 2020
Accepted article online 21 SEP 2020

The Complexity of the 2018 Kaktovik Earthquake Sequence in the Northeast of the Brooks Range, Alaska

Guangyu Xu[1,2], Caijun Xu[1,3,4], Yangmao Wen[1,3,4], Wei Xiong[1,5], and Sotiris Valkaniotis[6]

[1]School of Geodesy and Geomatics, Wuhan University, Wuhan, China, [2]Faculty of Geomatics, East China University of Technology, Nanchang, China, [3]Key Laboratory of Geospace Environment and Geodesy, Ministry of Education, Wuhan University, Wuhan, China, [4]Key Laboratory of Geophysical Geodesy, Ministry of Natural Resources, Wuhan, China, [5]Key Laboratory of Earthquake Geodesy, Institute of Seismology, Wuhan, China, [6]Koronidos Str., 42131, Trikala, Greece

Abstract We use mainly geodetic observations to constrain the fault geometry and coseismic distribution of the 2018 Kaktovik earthquake sequence, Alaska. We find that at least three faults were activated. The earthquake sequence ruptured mainly an ESE-striking, SSW-dipping strike-slip fault and a secondary rupture on an SE-striking, SW-dipping normal fault. Slip also occurred on a small SSW-striking fault plane, which is found first in geodetic data and further verified with geological data and focal mechanism solutions. We also map 6 months of postseismic deformation and find obvious displacements in the center of the Sadlerochit Mountains. A geological model is proposed to interpret the relationship between this earthquake sequence and the regional structure. We suggest that the 2018 Kaktovik earthquake sequence may first have occurred on a fault unknown prior to the mainshock and triggered slip on both the pre-existing ramp structure below the Sadlerochit Mountains and a secondary structure.

Plain Language Summary The 2018 Kaktovik event is the largest earthquake ever to be reported and recorded within the eastern Brooks Range and presents an unprecedented opportunity to study the regional tectonic structure and crustal deformation. Here, we present a detailed investigation into the seismogenic structure of this earthquake sequence, which ruptured mainly an ESE-striking, SSW-dipping strike-slip fault and a secondary SE-striking, SW-dipping normal fault. Slip also occurred on a small SSW-striking fault plane, which is found first in the geodetic data and further verified with seismic and geological data. Perhaps the most striking discovery from the InSAR observations of the Kaktovik earthquake sequence is that most of the displacement occurred on a fault whose existence was unknown prior to the earthquake sequence: a blind fault with no surface expression; additionally, a conjugate fault structure could have been triggered in this earthquake sequence. To explain the different orientations and kinematics of the two main ruptures (Faults 1 and 2), we use a ramp structure with variable geometry for the main fault zone: The first rupture has a higher dip and more strike-slip, while the second rupture has a lower dip and a dominant normal component.

1. Introduction

The Brooks Range of northern Alaska, which formed during the Mesozoic convergence of the continental Arctic Alaska terrane, is the northernmost and westernmost manifestation of the fold and thrust belt of the North American Cordilleran (Harris, 2004; Young, 2004). Numerous investigations have focused on the central Brooks Range due to its proximity to the trans-Alaska pipeline and the Dalton Highway (Mull & Adams, 1989). The northeastern Brooks Range is characterized predominantly by Cenozoic anticlinoria with cores of sub-Mississippian rocks (Wallace & Hanks, 1990). These regional anticlinoria are expressed as a series of northward-displaced, fault-bend folded horses. Furthermore, a passive-proof duplex that is deformed into kilometer-scale detachment folds can also be identified in the fold and thrust belt of the northeastern Brooks Range (Homza & Wallace, 1997). Situated in the northernmost extent of the Brooks Range, the Sadlerochit Mountains lie close to the Arctic continental margin and feature thrust faults and two anticlines (O'Sullivan & Wallace, 2002). Two major structure-tectonic units are identified around the Sadlerochit Mountains area: (1) major folds and reverse faults striking EW and (2) shallow detached folds and thrust faults striking NE. The NE-striking features may be regionally extensive, while the EW-striking structures are restricted to within the mountain range (Leiggi & Russell, 1985).

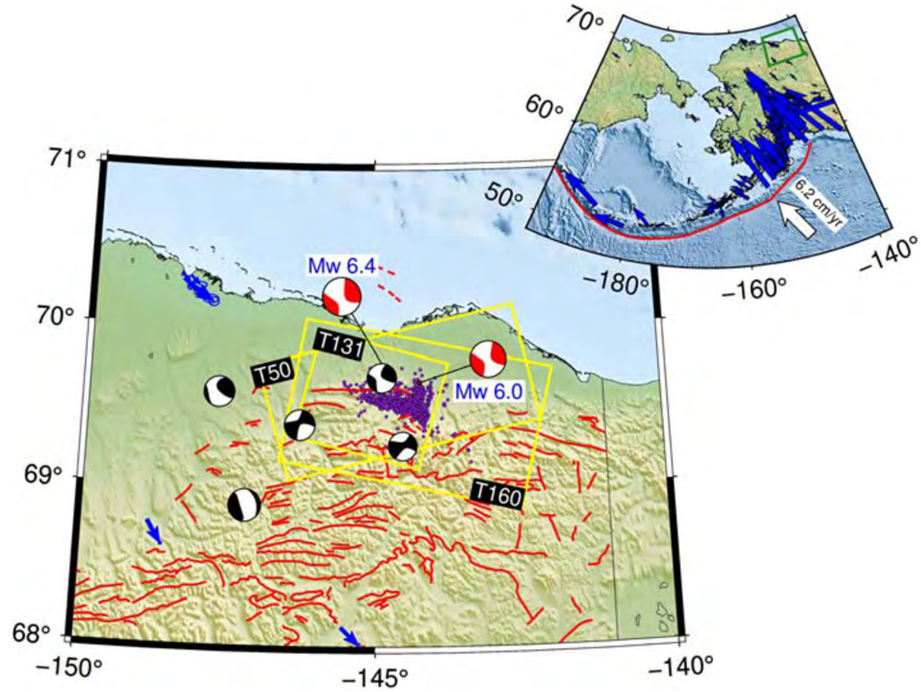

Figure 1. Tectonic background of the 12 August 2018 Kaktovik earthquake sequence. The yellow rectangles outline the spatial coverage of the SAR data used in this study. The black beach balls denote historical earthquakes from the GCMT catalog (Dziewonski et al., 1981). The red beach balls are the mainshock (Mw 6.4) and the largest aftershock (Mw 6.0) from the GCMT catalog. The purple dots represent USGS-recorded aftershocks for the period from 12 August 2018 to 31 November 2018. Red lines are major Quaternary and pre-Quaternary faults modified from Plafker et al. (1994), Koechler et al. (2012), and Koechler (2013). The blue arrows represent the interseismic GPS velocities (Herring et al., 2016). The green box in the inset map outlines the area in Figure 1, and the red line in the inset map represents the Aleutian Megathrust.

On 12 August 2018 (14:58:53 UTC), a Mw 6.4 earthquake struck northeast of the Brooks Range in Alaska, approximately 84 km southwest of Kaktovik (hereafter the Kaktovik earthquake) (Figure 1). The epicenter was in the remote Sadlerochit Mountains, approximately 40 km south of the Beaufort Sea coast. The focal mechanism reported by the United States Geological Survey (USGS) identified a predominant strike-slip mechanism with two possible nodal planes (striking north or east). This earthquake sequence initiated a vigorous aftershock sequence, including a Mw 6.0 earthquake (the second largest ever recorded northeast of the Brooks Range) 37 km southeast of the mainshock. Table S1 in the supporting information shows the information of 16 aftershocks, three of them were normal faulting events, while the others were strike-slip events. To date, no injuries or damage have been reported. This event marks the largest earthquake ever reported to occur within the eastern Brooks Range and presents an unprecedented opportunity to study the regional tectonic structure and crustal deformation. In this context, Gaudreau et al. (2019) used Interferometric Synthetic Aperture Radar (InSAR) data as a constraint in their inversion of the possible fault geometry for the Kaktovik earthquake sequence and found that a model involving two strike-slip faults can provide a good visual fit for the observed coseismic deformation.

In this study, we map the coseismic deformation associated with the Kaktovik earthquake sequence, Alaska, with three tracks of Sentinel-1 SAR data and evaluate the early postseismic deformation in the first 6 months. The 2.5D displacement field of the Kaktovik earthquake sequence is further decomposed from the combination of ascending and descending track interferograms. Large EW variations in the quasi-vertical displacement highlight the kinematic complexities of this earthquake sequence. The interferometric signals reveal that, in addition to the displacements due to slip on two subsurface faults, there are also displacement discontinuities relative to a small surface fault rupture at the center of the main deformation area. Using line-of-sight (LOS) displacements from the three tracks of interferograms, we invert the data for a model that can offer useful information on the characteristics of the earthquake

10.1029/2020GL088012

sequence. Finally, we evaluate the triggered rupture of a conjugate fault structure, explore the deformation mechanism during the early postseismic period, and discuss the relationship between the derived seismogenic faults and regional structure.

2. InSAR and InSAR Time Series

2.1. Data Processing Strategy

During the 2018 Kaktovik earthquake sequence, the Sentinel-1 satellites recorded ground displacements from space. Three tracks (ascending track 50, descending track 131, and descending track 160) were traversed by Sentinel-1 in Interferometric Wide Swath (IWS) Terrain Observation with Progressive Scans (TOPS) mode covering the 2018 Kaktovik earthquake epicenter area (Table S2). The TOPS data contain three swaths, with every swath including several bursts, which can provide a 250 km coverage area. In this study, we use only Swaths 1 and 2 (Bursts 1–4), Swath 1 (Bursts 5–10), and Swaths 2 and 3 (Bursts 6–10) from tracks 50, 131, and 160, respectively, to construct the coseismic deformation map. The GAMMA software is used to process the Sentinel-1 SAR data (Wegmüller et al., 2016). The detailed data processing steps can be found in the supporting information.

The Kaktovik earthquake sequence occurred in the Sadlerochit Mountains region, which has a rugged topography; therefore, topography-correlated atmospheric signals are relatively strong in the interferograms, especially in the Ignek Valley area. To remove the topography-correlated atmospheric delay, a digital elevation model (DEM)-dependent correction is applied (e.g., Feng et al., 2018; Wen et al., 2016). We first estimate a linear ramp in the interferogram by employing a plane fitting function, $d_{los}(x, y) = ax + by$, where a and b are linear coefficients of the coordinates (x, y) and are deducted from the InSAR data to remove the residual orbital error (e.g., Sudhaus & Jónsson, 2009; Wen et al., 2013). We then estimate the standard deviations of the LOS observations on the three tracks using a 1-D covariance function with observations in the far-field where no deformation signal can be recognized (Parsons et al., 2006) (Table S2).

2.2. Coseismic Deformation

The wrapped coseismic LOS displacements of the three tracks show a complex fringe pattern corresponding to the earthquake rupture sequence, which may cut across the Sadlerochit Mountains (Figure 2). The overall deformation pattern is consistent with an ESE-striking strike-slip fault. There is a clear boundary between the negative and positive LOS displacements, but this boundary is not quasi-linear. Rather, the boundary is somewhat curvilinear, especially in the eastern Sadlerochit Mountains. The opposite pattern of LOS displacements on the ascending and descending track interferograms suggests that the majority of the deformation was horizontal ground movement, which is consistent with the surface motions driven by a strike-slip fault (e.g., Jiang et al., 2013). The range of LOS displacements in the three track images is −13.12 to 21.45 cm for ascending track 50, −26.64 to 14.93 cm for descending track 131, and −28.22 to 17.68 cm for descending track 160. A prominent feature of the displacement field is observed in the southeastern Sadlerochit Mountains, where the LOS displacement shows the same sign (negative) in a small area, which implies the presence of a strong vertical displacement component therein. There are multiple lobes in the three track images, which may indicate that multiple faults may have been activated during the Kaktovik earthquake sequence; this would mean that the present deformation map constitutes the joint contribution of several events. We should note that the observed InSAR data represent only the cumulative displacements of the coseismic slip during the mainshock, several large aftershocks, and early afterslip.

We obtain the 2.5D displacement field (Fujiwara et al., 2000) of the Kaktovik earthquake sequence by decomposing the ascending and descending InSAR measurements (see Text S2). The retrieved quasi-vertical displacements present significant lateral variation with three district deformation areas, which overlap mainly within the eastward movement area (Figure S2b). These three deformation areas exhibit small uplift (approximately 10.2 cm) in a strip west of the main deformation area, similar uplift (approximately 11.4 cm) in a circular area at the center, and substantial subsidence (22 cm) to the east. From the 2-D displacements along profile CD (Figure S2d), the deformation in the vertical direction transforms from uplift to subsidence at a distance of 40 km. Beyond 52 km, the ground shows eastward movement, which opposes the westward deformation direction at distances of less than 52 km. These large variations in the vertical displacement indicate a complex geometric fault-zone (detailed analysis can be found in Text S2).

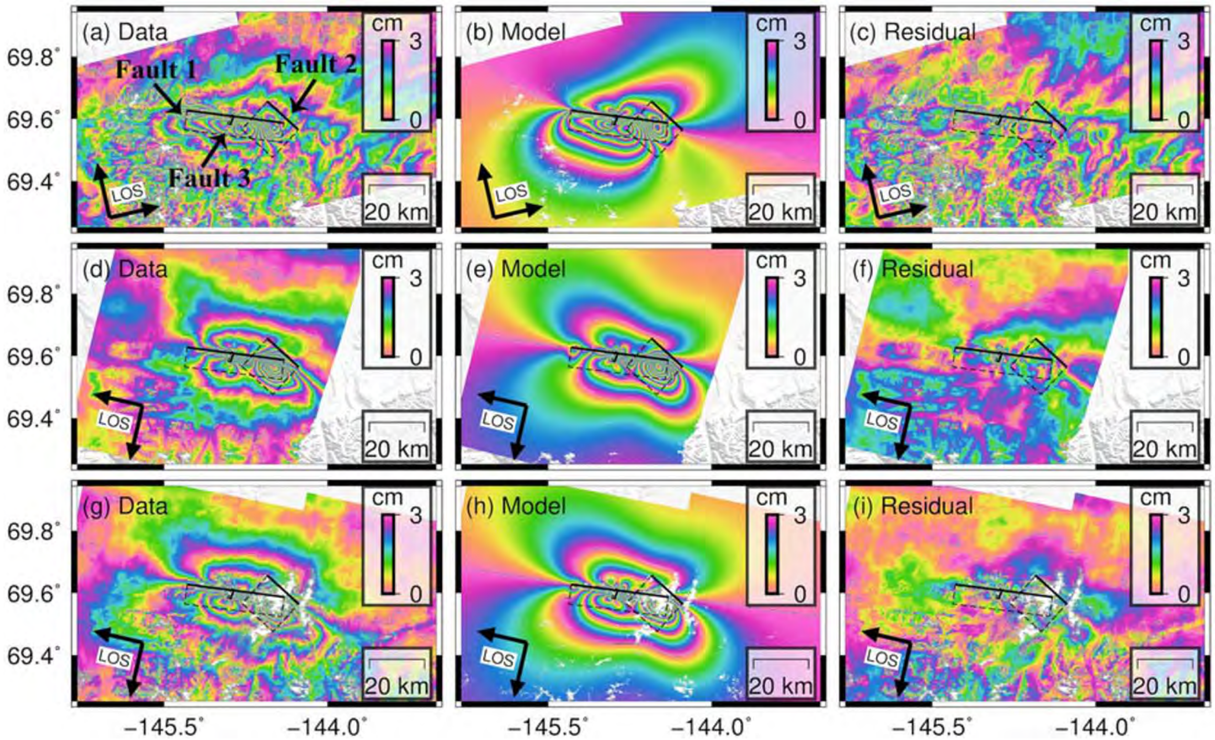

Figure 2. Optimal three-fault distributed slip model of the Kaktovik earthquake sequence. (a, d, g) Observed interferograms of ascending track 50, descending track 131, and descending track 160. (b, e, h) Model interferograms of ascending track 50, descending track 131, and descending track 160. (c, f, i) Residual interferograms of ascending track 50, descending track 131, and descending track 160. Black rectangles show the location of surface projection of extended faults.

2.3. Early Postseismic Deformation

To evaluate the early postseismic deformation following the 2018 Kaktovik earthquake sequence, InSAR time series of the first 6 months after the mainshock was constructed using the same processing approach described above. Our data set consists of 17 and 19 Sentinel-1 images from ascending track 50 and descending track 131, respectively (Table S3). We select the interferograms based on the length of the perpendicular baselines (<200 m) (Figure S3) and then invert the interferogram network to assess the phase evolution employing the small baseline method integrated in the MintPy package (Fattahi & Amelung, 2013, 2016; Zhang et al., 2019). We use the ERA5 model (Dee et al., 2011) to correct the delay of stratified tropospheric (Jolivet et al., 2014) and topographic residuals.

Due to the topography and weather conditions, large areas of incoherence are identified in most interferograms during the first 6 months of acquisition following the 2018 Kaktovik earthquake sequence, except in the Sadlerochit Mountains. The postseismic interferograms from the ascending and descending tracks clearly show surface strain occurring in the region with the greatest coseismic deformation gradient (Figure S4). Approximately, we find an ~2 cm postseismic displacement at the center of the Sadlerochit Mountains (Figure S4). The opposite pattern of postseismic LOS displacements between the ascending and descending tracks suggests that the majority of the postseismic deformation was composed of horizontal ground movement (Figure S4). In the following, we explore the dominant mechanism responsible for the postseismic deformation (see Text S4 and section 4.3).

3. Coseismic Slip Model Constrained by Geodetic Data

Based on dislocation in an elastic half space (Okada, 1985), we invert the available InSAR measurements for a detailed slip model for the Kaktovik earthquake sequence. Details of the inversion procedure are described in the supporting information (Text S3). We adopt a combined structure comprising one buried ESE-striking, SSW-dipping main strike-slip fault, one buried SE-striking, SW-dipping secondary normal fault, and a small SSW-striking strike-slip fault. The slip on the small SSW-striking strike-slip fault plane is found first in the geodetic data and further verified with seismic and geological data. We suspect that the slip on the secondary fault may have occurred on the plane of a pre-existing thrust structure due to the consistency of the fault position between the inversion results and the regional structure (see section 4.2).

The detailed configuration of the three-fault model (Table S8) consists of a hitherto hidden or "blind" strike-slip fault crossing the Sadlerochit Mountains, a secondary normal slipping fault whose SE-striking surface trace is close to the eastern edge of the first mapped fault, and a small strike-slip fault whose surface trace is almost perpendicular to that of the first mapped fault (Figure 2). The geometries of these three faults appear likely to intersect and interact at depth. The main fault is derived mainly from the InSAR data, and the secondary fault is constrained by both InSAR data and focal mechanisms, while the third fault is derived from the joint analysis of InSAR, focal mechanism, and geological data (see section 4.1 and Text S5). We also compare the coseismic slip models estimated in this study with those reported by other researchers (see Text S6). For example, compared with the two strike-slip fault model of Gaudreau et al. (2019), our three-fault model can provide more details of the earthquake sequence.

The best-fitting model shows that the majority of slip occurred between 3 and 8 km on the main strike-slip fault with a maximum slip of 1.4 m; in addition, there was a concentrated slip patch on the secondary normal fault, and slip reached the surface on the small strike-slip fault. The total geodetic moment released by this earthquake sequence amounts to 8.05×10^{18} N m, assuming a rigidity of 30 GPa.

4. Discussion

4.1. The Camp 263 Fault: Triggered Slip on a Secondary Structure

From the InSAR results, an NNE–SSW fault rupture with a length of 4–6 km can be identified in the Sadlerochit Mountains (Figure 3). We name this fault the Camp 263 fault (corresponding to Fault 3 in section 3); this name corresponds to a small stream that crosses the fault in the USGS topographic map. We adopt this name because it is the only toponym identified in the vicinity of the fault. We use the published geological map by Robinson et al. (1989) and detailed IFSAR (5 m) and ArcticDEM (2 m) digital surface models (Figure 3) for fault analysis and evaluation.

Another fault (F) strikes parallel to the Camp 263 fault. The Camp 263 and F faults are almost vertical (i.e., the fault trace is almost linear, an indication of a high dip angle) (Figure 3). Due to the high dip angle, the dip orientation is ambiguous: the fault could dip either east or west. Due to mapping simplification or other constraints, the trace of the F fault on the geological map is not incompatible with a high-angel east-dipping fault, which is one possible orientation from the inversion results. The F fault has a small apparent displacement, which is evident from the lack of significant variation in geological formation thicknesses along the fault and the small displacements of contact markers (Figure 3). Using local bed markers along the fault traces, we interpret that the Camp 263 fault exhibits more displacement than the F fault. This is mostly attributed to left-lateral strike-slip movement; geological map criteria mostly account for the older stage of fault activity and may not necessarily agree with recent reactivation.

Fault scarps are not truly visible in the morphology at the upper part of the map. The uneven distribution of morphologically preserved scarps is an indication of the older age of faults (preceding the present-day stress regime); parts of the fault scarps are eroded due to Quaternary glacial activity, and other parts show differential erosion and variable preservation due to the changes in the bedrock lithology. Furthermore, from the map, the fault traces do not significantly vary across local stream bends (no major horizontal displacement). There are few indicators of possible recent fault reactivations during the latest Pleistocene–Holocene (some fresh fault scarps are visible), but we do not expect significant morphological imprints, as the fault would have a very small slip rate (<0.05–0.1 mm/yr). At such rate, erosion/deposition and other forces would exceed fault displacement, leaving few to no surface expressions of recent fault activity.

A significant amount of left-lateral strike-slip at the surface implies that the Camp 263 fault was activated during the 2018 Kaktovik earthquake sequence. The Camp 263 fault is almost conjugate to the main nearly EW-striking fault rupture. A similar rupture pattern was proposed for the 2019 Ridgecrest earthquake sequence, in which two orthogonal faults were ruptured sequentially (Barnhart et al., 2019; Feng et al., 2020). Coseismic slip on the Camp 263 fault can be explained either as slip on a secondary fault plane

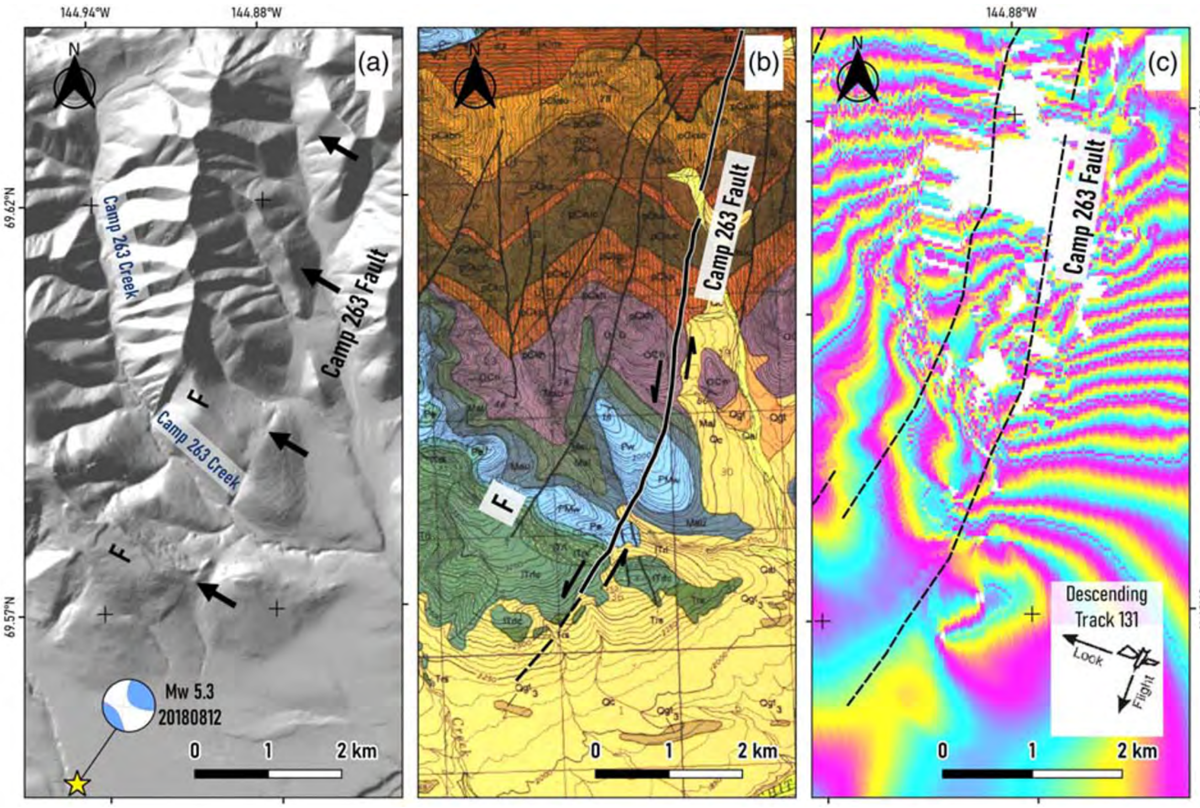

Figure 3. (a) Relief map (from the ArcticDEM 2 m DEM) of the 12 August surface slip. The Camp 263 fault scarp is marked with black arrows. A subparallel fault, the F fault is visible ~1–1.5 km to the west of the Camp 263. The star at the southwest corner marks the USGS epicenter of the Mw 5.3 aftershock (focal mechanism from the USGS). Camp 263 creek runs SE-NW crossing the Camp 263 fault scarp (blue label). (b) Detailed view of the Robinson et al. (1989) geological map with the mapped traces of the Camp 263 fault and the F fault. (c) Coseismic interferogram (descending track 131) with a major discontinuity along the Camp 263 fault.

adjacent to the main fault or as the possible shallow rupture of an aftershock. The USGS catalog includes a Mw 5.3 aftershock 1 hr after the mainshock (12 August 2018, 16:02:08 UTC) close to the Camp 263 fault (Figure 3). Although the hypocentral depth is given as 18.4 km, we cannot exclude a possible shallower depth due to velocity model uncertainties that could account for the local rupture patch along the Camp 263 fault.

4.2. Geological Model of the Kaktovik Earthquake Sequence

Perhaps the most striking discovery made from the InSAR observations of the Kaktovik earthquake sequence is that the majority of the displacement in this sequence occurred on a fault whose existence was unknown prior to the earthquake sequence: a blind fault with no surface expression; additionally, a conjugate fault structure could have been triggered during this earthquake sequence. The absence of clear geomorphic indicators, such as features near the main fault or offset drainage channels, can be ascribed to several factors. The lack of a strong vertical component in the fault motion, as evidenced by the almost pure right-lateral fault rake obtained for the main fault in our source parameter inversion, would suggest that the topographic signature due to a single earthquake would be on the order of a few centimeters, and therefore, hundreds of earthquake cycles would be needed to build topography. Additionally, Quaternary glaciation activity or any recent minor morphotectonic features of the Alaskan North Slope have probably been erased and/or covered with glacial sediments.

After thoroughly examining the geological maps (there is a rich collection of published and unpublished geological and structural maps available through the digital archive of the Alaska Division of Geological & Geophysical Surveys), the findings of previous studies, and our InSAR results, we establish the first geological model for this earthquake sequence (Figures 3 and 4). The dominant geomorphic feature in the area seems to be a major EW-striking fault zone that rotates NW-SE farther to the east. The surface expression of

10.1029/2020GL088012

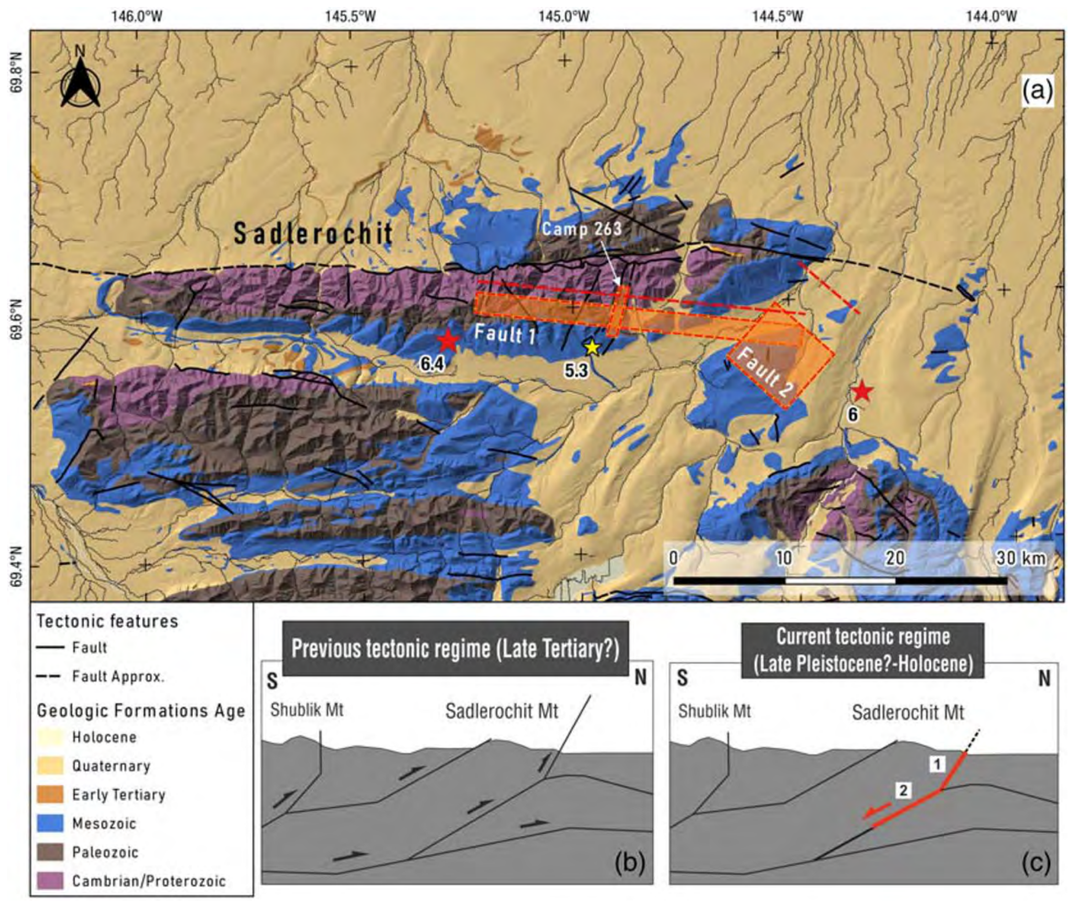

Figure 4. Simplified geologic map of the Sadlerochit Mountains area (a) with the fault models from inversion as overlay (horizontal projection with red polygons, estimated surface projection with red dashed lines). Geological formations and faults (black lines) from Robinson et al. (1989). Below a simplified tectonic sketch of the Sadlerochit Mountains area subsurface structure, based on O'Sullivan and Wallace (2002). In panel (b), the previous state is displayed with contractional structures formed (thrusts and ramps). A proposed model for the current stress regime is displayed in panel (c), with thick red lines representing the 12 August 2018 slip surfaces along a pre-existing ramp structure below Sadlerochit Mountains.

this fault is not continuous, as it might be covered by recent (Quaternary) sediments (we mark this fault zone with a bold line and arrows in Figure 4). This fault zone is inherited from the older tectonic regime (thrust ramps and reverse faults), while pre-existing fault planes are reactivated under the new stress regime with different kinematics. The different orientations and kinematics of the two main ruptures (Faults 1 and 2) can be explained by using a ramp structure with variable geometry for the main fault zone: The first rupture has a higher dip and more strike-slip, while the second rupture has a lower dip and a dominant normal component (Figure 4). The existence of Fault 2 is consistent with the north-south extension along the northern Alaska margin. We also find that the derived position of Fault 2 is consistent with the old thrust structure, which suggests that normal slip during this earthquake sequence may have occurred on the old thrust plane. The tectonic of the Sadlerochit Mountains area may have experienced a transition from compression (Late Tertiary?) to extension (Late Tertiary?-Holocene) (Figure 4). The triggered Fault 3 (the Camp 263 fault) is an old structure in the Sadlerochit Mountains; therefore, the rupture of Fault 3 may have been caused by a Mw 5.3 aftershock with focal mechanisms similar to our inversion results.

4.3. Afterslip During the Early Postseismic Period

We process the first 6 months of InSAR postseismic data (after the mainshock) to evaluate early postseismic deformation. Our results show transient postseismic deformation close to the surface projection of the main fault. Either afterslip or poroelastic rebound may potentially dominate the early postseismic period

(Feng et al., 2018). Therefore, we calculate the deformation of potential poroelastic rebound using Poisson ratios of 0.1 and 0.25 for drained and undrained crustal rocks, respectively, in a homogenous crust (Feng et al., 2018). Considering that the modeled poroelastic deformation shows an opposite deformation pattern compared with the postseismic InSAR observations (Figure S5), we suggest that the afterslip mechanism is the main contributor to the early postseismic displacements. To explore the afterslip distribution during the early postseismic period, we perform a kinematic inversion using the cumulative displacement during the observation period. Our preferred afterslip model shows a good agreement with the postseismic observations (Figure S6). The model shows that the maximum afterslip reaches up to 0.15 m, and the majority of the afterslip distribution occurs immediately updip of the main coseismic rupture (Figure S6). The complementary relationship between afterslip and coseismic slip may imply complex frictional properties in downdip of the seismogenic fault.

5. Conclusion

In this study, we use mainly geodetic observations supplemented with geological and seismic observations to constrain the fault geometry and slip distribution of the 2018 Kaktovik earthquake sequence. Our results demonstrate that at least three faults were involved in the earthquake sequence. The most striking discovery made from the InSAR observations of the Kaktovik earthquake sequence is that the majority of the displacement in the event occurred on a fault whose existence was unknown prior to the earthquake sequence: a blind fault with no surface expression; a SSW-striking fault rupture (the Camp 263 fault) with a length of 4–6 km can be identified in the Sadlerochit Mountains. We invert the postseismic deformation in the first 6 months following the mainshock and find a complementary relationship between the afterslip and coseismic slip. The geological model (a ramp structure with variable geometry for the main fault zone) proposed in this study can effectively connect the 2018 Kaktovik earthquake sequence with the regional tectonic structure. Our study shows that multisource observations can provide comprehensive constraints on the fault geometry associated with the 2018 earthquake sequence and slip distribution.

Data Availability Statement

The Sentinel-1 SAR data are downloaded from the Sentinel-1 Scientific Data Hub (https://scihub.copernicus.eu).

Acknowledgments
We thank the editor Gavin Hayes and two anonymous reviewers for their valuable comments, which greatly improved this manuscript. Figures in this study are mainly prepared by using the Generic Mapping Tools (Wessel & Smith, 1998). We thank Dr. Élyse Gaudreau for sharing her slip model and her patient reply to our questions about this earthquake sequence. This work is co-supported by the National Natural Science Foundation of China Innovation Group Project (No. 41721003), the National Key R&D Program of China under Grant Nos. 2018YFC1503604 and 2019YFC1509204, the National Natural Science Foundation of China under Grant Nos. 41774011 and 41604079, the DAAD Thematic Network Project (DAAD 57421148), and the Key Laboratory of Geospace Environment and Geodesy, Ministry of Education, Wuhan University (No. 17-02-09).

References

Barnhart, W. D., Hayes, G. P., & Gold, R. D. (2019). The July 2019 Ridgecrest, California, earthquake sequence: Kinematics of slip and stressing in cross-fault ruptures. *Geophysical Research Letters*, *46*, 11,859–11,867. https://doi.org/10.1029/2019GL084741

Dee, D. P., Uppala, S. M., Simmons, A. J., Berrisford, P., Poli, P., Kobayashi, S., et al. (2011). The ERA-Interim reanalysis: Configuration and performance of the data assimilation system. *Quarterly Journal of the Royal Meteorological Society*, *137*(656), 553–597. https://doi.org/10.1002/qj.828

Dziewonski, A. M., Chou, T. A., & Woodhouse, J. H. (1981). Determination of earthquake source parameters from waveform data for studies of global and regional seismicity. *Journal of Geophysical Research*, *86*, 2825–2852. https://doi.org/10.1029/JB086iB04p02825

Fattahi, H., & Amelung, F. (2013). DEM error correction in InSAR time series. *IEEE Transactions on Geoscience and Remote Sensing*, *51*(7), 4249–4259. https://doi.org/10.1109/TGRS.2012.2227761

Fattahi, H., & Amelung, F. (2016). InSAR observations of strain accumulation and fault creep along the Chaman fault system, Pakistan and Afghanistan. *Geophysical Research Letters*, *43*, 8399–8406. https://doi.org/10.1002/2016GL070121

Feng, W. P., Samsonov, S., Almeida, R., Yassaghi, A., Li, J. H., Qiu, Q., et al. (2018). Geodetic constraints of the 2017 Mw 7.3 Sarpol Zahab, Iran earthquake, and its implications on the structure and mechanics of the northwest Zagros thrust-fold belt. *Geophysical Research Letters*, *45*, 6853–6861. https://doi.org/10.1029/2018GL078577

Feng, W. P., Samsonov, S., Qiu, Q., Wang, Y. Q., Zhang, P. Z., Li, T., & Zheng, W. J. (2020). Orthogonal fault rupture and rapid postseismic deformation following 2019 Ridgecrest, California earthquake sequence revealed from geodetic observations. *Geophysical Research Letters*, *47*, e2019GL086888. https://doi.org/10.1029/2019GL086888

Fujiwara, S., Nishimura, T., Murakami, M., Nakagawa, H., Tobita, M., & Rosen, P. A. (2000). 2.5-D surface deformation of M6.1 earthquake near Mt Iwate detected by SAR interferometry. *Geophysical Research Letters*, *27*(14), 2049–2052. https://doi.org/10.1029/1999GL011291

Gaudreau, É., Nissen, E. K., Bergman, E. A., Benz, H. M., Tan, F., & Karasözen, E. (2019). The August 2018 Kaktovik earthquakes: Active tectonics in northeastern Alaska revealed with InSAR and seismology. *Geophysical Research Letters*, *46*, 14,412–14,420. https://doi.org/10.1029/2019GL085651

Harris, R. (2004). Tectonic evolution of the Brooks Range ophiolite, northern Alaska. *Tectonophysics*, *392*(1–4), 143–163. https://doi.org/10.1016/j.tecto.2004.04.021

Herring, T. A., Melbourne, T. I., Murray, M. H., Floyd, M. A., Szeliga, W. M., King, R. W., et al. (2016). Plate Boundary Observatory and related networks: GPS data analysis methods and geodetic products. *Reviews of Geophysics*, *54*, 759–808. https://doi.org/10.1002/2016RG000529

Homza, T. X., & Wallace, W. K. (1997). Detachment folds with fixed hinges and variable detachment depth, northeastern Brooks Range, Alaska. *Journal of Structural Geology*, *19*(3–4), 337–354. https://doi.org/10.1016/S0191-8141(96)00118-6

Jiang, G. Y., Xu, C. J., Wen, Y. M., Liu, Y., Yin, Z., & Wang, J. J. (2013). Inversion for coseismic slip distribution of the 2010 Mw 6.9 Yushu earthquake from InSAR data using angular dislocations. *Geophysical Journal International*, *194*(2), 1011–1022. https://doi.org/10.1093/gji/ggt141

Jolivet, R., Agram, P. S., Lin, N. Y., Simons, M., Doin, M., Peltzer, G., & Li, Z. H. (2014). Improving InSAR geodesy using global atmospheric models. *Journal of Geophysical Research: Solid Earth*, *119*, 2324–2341. https://doi.org/10.1002/2013JB010588

Koechler, R. D. (2013). Quaternary faults and folds (QFF): Alaska Division of Geological & Geophysical Surveys Digital Data Series 3. Retrieved from http://maps.dggs.alaska.gov/qf; http://doi.org/10.14509/24956

Koechler, R. D., Farrell, R. E., Burns, P. A. C., & Combellick, R. A. (2012). Quaternary faults and folds in Alaska—A digital database. In R. D. Koehler (Ed.), *Quaternary Faults and Folds (QFF)* (Vol. 141, p. 31). Fairbanks, Alaska: Alaska Division of Geological & Geophysical Surveys. https://doi.org/10.14509/23944

Leiggi, P. A., & Russell, B. J. (1985). Style and age of tectonism of the Sadlerochit Mountains to Franklin Mountains, Arctic National Wildlife Refuge (ANWR), Alaska. *AAPG Bulletin*, *69*, 668. https://doi.org/10.1306/AD462687-16F7-11D7-8645000102C1865D

Mull, C. G., & Adams, K. E. (1989). Dalton Highway, Yukon River to Prudhoe Bay, Alaska. In *Bedrock geology of the eastern Koyuhuk basin, central Brooks Range and Arctic Slope: Alaska Division of Geological and Geophysical Surveys, Guidebook 7* (Vol. *2*, pp. 1–327).

Okada, Y. (1985). Surface deformation due to shear and tensile faults in a half-space. *Bulletin of the Seismological Society of America*, *85*, 1135–1154.

O'Sullivan, P. B., & Wallace, W. K. (2002). Out-of-sequence, basement-involved structures in the Sadlerochit Mountains region of the Arctic National Wildlife Refuge, Alaska: Evidence and implications from fission-track thermochronology. *Geological Society of America Bulletin*, *114*(11), 1356–1378. https://doi.org/10.1130/0016-7606(2002)114<1356:OOSBIS>2.0.CO;2

Parsons, B., Wright, T., Rowe, P., Andrews, J., Jackson, J., Walker, R., et al. (2006). The 1994 Sefidabeh (eastern Iran) earthquake revisited: New evidence from satellite radar interferometry and carbonate dating about the growth of an active fold above a blind thrust fault. *Geophysical Journal International*, *164*(1), 202–217. https://doi.org/10.1111/j.1365-246X.2005.02655.x

Plafker, G., Gilpin, L. M., & Lahr, J. C. (1994). *Neotectonic map of Alaska: The geology of Alaska*. Boulder, CO: Geological Society of America. Retrieved from http://www.dggs.alaska.gov/pubs/id/22331

Robinson, M. S., Decker, J. E., Clough, J. G., Reifenstuhl, R. R., Bakke, A. A., Dillon, J. T., et al. (1989). *Geology of the Sadlerochit and Shublik Mountains, Arctic National Wildlife Refuge, northeastern Alaska* (Alaska Division of Geological & Geophysical Surveys Professional Report 100, 1 sheet, scale 1:63,360). https://doi.org/10.14509/2281

Sudhaus, H., & Jónsson, S. (2009). Improved source modelling through combined use of InSAR and GPS under consideration of correlated data errors: Application to the June 2000 Kleifavatn earthquake, Iceland. *Geophysical Journal International*, *176*(2), 389–404. https://doi.org/10.1111/j.1365-246X.2008.03989.x

Wallace, W. K., & Hanks, C. L. (1990). Structural provinces of the northeastern Brooks Range, Arctic National Wildlife Refuge, Alaska. *AAPG Bulletin*, *74*, 1100–1118. https://doi.org/10.1306/0C9B2425-1710-11D7-8645000102C1865D

Wegmüller, U., Werner, C., Strozzi, T., Wiesmann, A., Frey, O., & Santoro, M. (2016). Sentinel-1 support in the GAMMA software. *Procedia Computer Science*, *100*, 1305–1312. https://doi.org/10.1016/j.procs.2016.09.246

Wen, Y. M., Xu, C. J., Liu, Y., & Jiang, G. Y. (2016). Deformation and source parameters of the 2015 Mw 6.5 earthquake in Pishan, western China, from Sentinel-1A and ALOS-2 data. *Remote Sensing*, *8*, 134. https://doi.org/10.3390/rs8020134

Wen, Y. M., Xu, C. J., Liu, Y., Jiang, G. Y., & He, P. (2013). Coseismic slip in the 2010 Yushu earthquake (China), constrained by wide-swath and strip-map InSAR. *Natural Hazards and Earth System Sciences*, *13*(1), 35–44. https://doi.org/10.5194/nhess-13-35-2013

Wessel, P., & Smith, W. H. F. (1998). New, improved version of generic mapping tools released. *Eos, Transactions of the American Geophysical Union*, *79*(47), 579. https://doi.org/10.1029/98EO00426

Young, L. E. (2004). A geologic framework for mineralization in the Western Brooks Range, Alaska. *Economic Geology*, *99*(7), 1281–1306. https://doi.org/10.2113/gsecongeo.99.7.1281

Zhang, Y. J., Fattahi, H., & Amelung, F. (2019). Small baseline InSAR time series analysis: Unwrapping error correction and noise reduction. *Computational Geosciences*, *133*, 104331. https://doi.org/10.1016/j.cageo.2019.104331

References From the Supporting Information

Atzori, S., Hunstad, I., Chini, M., Salvi, S., Tolomei, C., Bignami, C., et al. (2009). Finite fault inversion of DInSAR coseismic displacement of the 2009 L'Aquila earthquake (central Italy). *Geophysical Research Letters*, *36*, L15305. https://doi.org/10.1029/2009GL039293

Bagnardi, M., & Hooper, A. (2018). Inversion of surface deformation data for rapid estimates of source parameters and uncertainties: A Bayesian approach. *Geochemistry, Geophysics, Geosystems*, *19*, 2194–2211. https://doi.org/10.1029/2018GC007585

Fan, Q. B., Xu, C. J., Yi, L., Liu, Y., Wen, Y. M., & Yin, Z. (2017). Implication of adaptive smoothness constraint and Helmert variance component estimation in seismic slip inversion. *Journal of Geodesy*, *91*(10), 1163–1177. https://doi.org/10.1007/s00190-017-1015-0

Farr, T. G., Rosen, P. A., Caro, E., Crippen, R., Duren, R., Hensley, S., et al. (2007). The shuttle radar topography mission. *Reviews of Geophysics*, *45*, RG2004. https://doi.org/10.1029/2005RG000183

Fialko, Y., Simons, M., & Agnew, D. (2001). The complete (3-D) surface displacement field in the epicentral area of the 1999 Mw 7.1 Hector Mine earthquake, California, from space geodetic observations. *Geophysical Research Letters*, *28*(16), 3063–3066. https://doi.org/10.1029/2001GL013174

Frietsch, M., Ferreira, A. M. G., Funning, G. J., & Weston, J. (2019). Multiple fault modelling combining seismic and geodetic data: The importance of simultaneous subevent inversions. *Geophysical Journal International*, *218*(2), 958–976. https://doi.org/10.1093/gji/ggz205

Fukushima, Y., Cayol, V., Durand, P., & Massonnet, D. (2010). Evolution of magma conduits during the 1998–2000 eruptions of Piton de la Fournaise volcano, Réunion Island. *Journal of Geophysical Research*, *115*, B10204. https://doi.org/10.1029/2009JB007023

Funning, G. J., Parsons, B., Wright, T. J., Jackson, J. A., & Fielding, E. J. (2005). Surface displacements and source parameters of the 2003 Bam (Iran) earthquake from Envisat advanced synthetic aperture radar imagery. *Journal of Geophysical Research*, *110*, B09406. https://doi.org/10.1029/2004JB003338

Goldstein, R. M., & Werner, C. L. (1998). Radar interferogram filtering for geophysical applications. *Geophysical Research Letters*, *25*(21), 4035–4038. https://doi.org/10.1029/1998GL900033

Goldstein, R. M., Zebker, H. A., & Werner, C. L. (1988). Satellite radar interferometry: Two-dimensional phase unwrapping. *Radio Science*, *23*(4), 713–720. https://doi.org/10.1029/RS023i004p00713

Hastings, W. K. (1970). Monte Carlo sampling methods using Markov chains and their applications. *Biometrika*, *57*(1), 97–109. https://doi.org/10.1093/biomet/57.1.97

Jónsson, S., Zebker, H., Segall, P., & Amelung, F. (2002). Fault slip distribution of the 1999 Mw 7.1 Hector Mine, California, earthquake, estimated from satellite radar and GPS measurements. *Bulletin of the Seismological Society of America*, *92*, 1377–1389. https://doi.org/10.1785/0120000922

Lohman, R. B., & Simons, M. (2005). Some thoughts on the use of InSAR data to constrain models of surface deformation: Noise structure and data downsampling. *Geochemistry, Geophysics, Geosystems*, *6*, Q01007. https://doi.org/10.1029/2004GC000841

Scheiber, R., & Moreira, A. (2000). Coregistration of interferometric SAR images using spectral diversity. *IEEE Transactions on Geoscience and Remote Sensing*, *38*(5), 2179–2191. https://doi.org/10.1109/36.868876

Wright, T. J., Parsons, B. E., Jackson, J. A., Haynes, M., Fielding, E. J., England, P. C., & Clarke, P. J. (1999). Source parameters of the 1 October 1995 Dinar (Turkey) earthquake from SAR interferometry and seismic bodywave modelling. *Earth and Planetary Science Letters*, *172*(1–2), 23–37. https://doi.org/10.1016/S0012-821X(99)00186-7

Xu, C. J., Ding, K. H., Cai, J. Q., & Grafarend, E. W. (2009). Methods of determining weight scalling factors for geodetic-geophysical joint inversion. *Journal of Geodynamics*, *47*(1), 39–46. https://doi.org/10.1016/j.jog.2008.06.005

Xu, C. J., Gong, Z., & Niu, J. M. (2016). Recent developments in seismological geodesy. *Geod. Geodyn*, *7*(3), 157–164. https://doi.org/10.1016/j.geog.2016.04.009